frontiers | Research Topics

The molecular mechanisms of epilepsy and potential therapeutics

Edited by
Tobias Engel, Hermona Soreq and Gary Patrick Brennan

Published in
Frontiers in Molecular Neuroscience

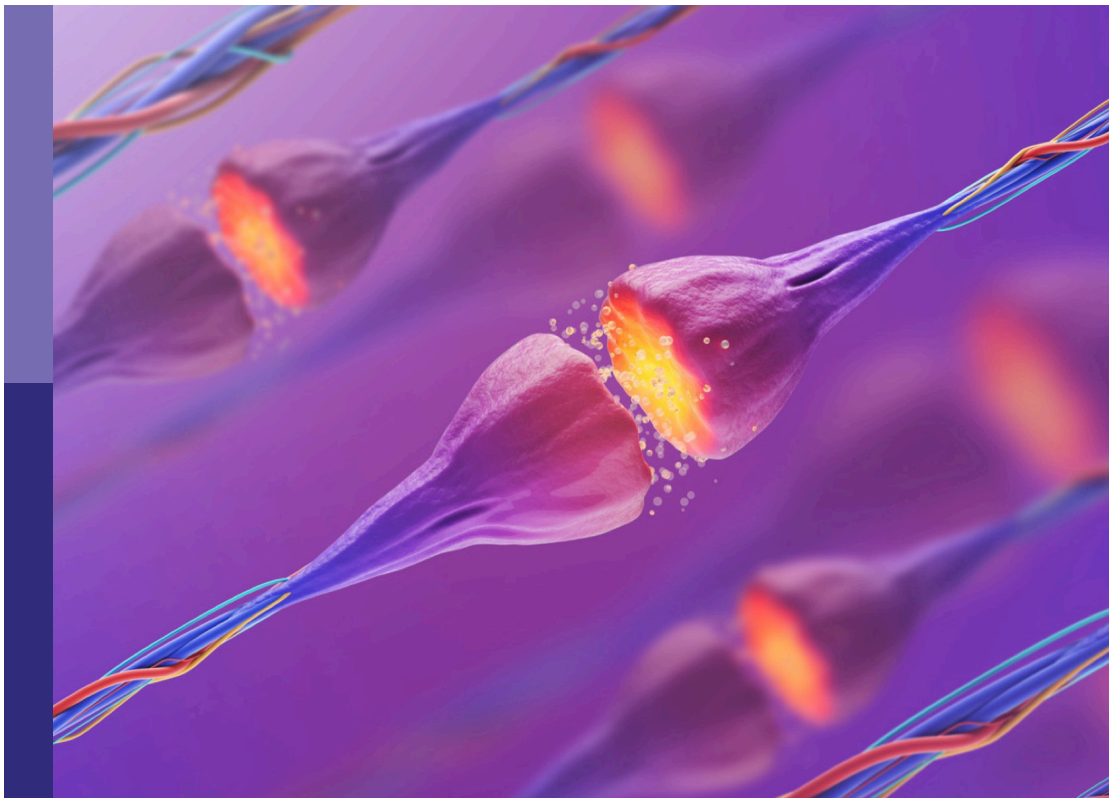

ISSN 1664-8714
ISBN 978-2-83250-969-2
DOI 10.3389/978-2-83250-969-2

About Frontiers

Frontiers is more than just an open access publisher of scholarly articles: it is a pioneering approach to the world of academia, radically improving the way scholarly research is managed. The grand vision of Frontiers is a world where all people have an equal opportunity to seek, share and generate knowledge. Frontiers provides immediate and permanent online open access to all its publications, but this alone is not enough to realize our grand goals.

Frontiers journal series

The Frontiers journal series is a multi-tier and interdisciplinary set of open-access, online journals, promising a paradigm shift from the current review, selection and dissemination processes in academic publishing. All Frontiers journals are driven by researchers for researchers; therefore, they constitute a service to the scholarly community. At the same time, the *Frontiers journal series* operates on a revolutionary invention, the tiered publishing system, initially addressing specific communities of scholars, and gradually climbing up to broader public understanding, thus serving the interests of the lay society, too.

Dedication to quality

Each Frontiers article is a landmark of the highest quality, thanks to genuinely collaborative interactions between authors and review editors, who include some of the world's best academicians. Research must be certified by peers before entering a stream of knowledge that may eventually reach the public - and shape society; therefore, Frontiers only applies the most rigorous and unbiased reviews. Frontiers revolutionizes research publishing by freely delivering the most outstanding research, evaluated with no bias from both the academic and social point of view. By applying the most advanced information technologies, Frontiers is catapulting scholarly publishing into a new generation.

What are Frontiers Research Topics?

Frontiers Research Topics are very popular trademarks of the *Frontiers journals series*: they are collections of at least ten articles, all centered on a particular subject. With their unique mix of varied contributions from Original Research to Review Articles, Frontiers Research Topics unify the most influential researchers, the latest key findings and historical advances in a hot research area.

Find out more on how to host your own Frontiers Research Topic or contribute to one as an author by contacting the Frontiers editorial office: frontiersin.org/about/contact

The molecular mechanisms of epilepsy and potential therapeutics

Topic editors

Tobias Engel — Royal College of Surgeons in Ireland, Ireland
Hermona Soreq — Hebrew University of Jerusalem, Israel
Gary Patrick Brennan — University College Dublin, Ireland

Citation

Engel, T., Soreq, H., Brennan, G. P., eds. (2022). *The molecular mechanisms of epilepsy and potential therapeutics*. Lausanne: Frontiers Media SA.
doi: 10.3389/978-2-83250-969-2

Table of contents

frontiers | Frontiers in Molecular Neuroscience

TYPE Editorial
PUBLISHED 22 November 2022
DOI 10.3389/fnmol.2022.1064121

OPEN ACCESS

EDITED BY
Marco I. Gonzalez,
University of California, Davis,
United States

REVIEWED BY
Andreia Cristina Karklin Mortensen,
Drexel University, United States

*CORRESPONDENCE
Tobias Engel
tengel@rcsi.ie

†These authors have contributed equally to this work

SPECIALTY SECTION
This article was submitted to Brain Disease Mechanisms, a section of the journal Frontiers in Molecular Neuroscience

RECEIVED 07 October 2022
ACCEPTED 14 November 2022
PUBLISHED 22 November 2022

CITATION
Engel T, Brennan GP and Soreq H (2022) Editorial: The molecular mechanisms of epilepsy and potential therapeutics.
Front. Mol. Neurosci. 15:1064121.
doi: 10.3389/fnmol.2022.1064121

Editorial: The molecular mechanisms of epilepsy and potential therapeutics

Tobias Engel[1,2*†], Gary P. Brennan[2,3†] and Hermona Soreq[4,5†]

[1]Department of Physiology and Medical Physics, Royal College of Surgeons in Ireland, University of Medicine and Health Sciences, Dublin, Ireland, [2]FutureNeuro, SFI Research Centre for Chronic and Rare Neurological Diseases, RCSI University of Medicine and Health Sciences, Dublin, Ireland, [3]UCD School of Biomolecular and Biomedical Science, UCD Conway Institute, University College Dublin, Dublin, Ireland, [4]The Edmond & Lily Safra Center for Brain Sciences, The Hebrew University of Jerusalem, Jerusalem, Israel, [5]The Alexander Silberman Institute of Life Sciences, The Hebrew University of Jerusalem, Jerusalem, Israel

KEYWORDS

epilepsy, epileptogenesis, brain, therapy, anti-seizure medication (ASM)

Editorial on the Research Topic
The molecular mechanisms of epilepsy and potential therapeutics

Epilepsy comprises a heterogeneous group of brain diseases, which all share in common an enduring predisposition to generate seizures. With an incidence of 1–2%, epilepsy is one of the most common chronic brain diseases affecting people of all ages, which in addition to exacting an enormous toll on human potential is also one of the most costly neurological diseases in terms of healthcare and societal costs (Allers et al., 2015). Major challenges in the management of epilepsy include treatment complexity, social disadvantages (e.g., unemployment, stigma), an up to 3-fold increased risk of premature mortality and the presence of numerous co-morbidities such as depression and anxiety (Moshe et al., 2015; Loscher, 2019; Thijs et al., 2019; Shlobin and Sander, 2022). Known causes of epilepsy include genetic abnormalities such as *de novo* mutations and/or a precipitating injury (e.g., traumatic brain injury (TBI), infection, stroke, tumors). In the majority of cases, the underlying causes remain, elusive (Pitkanen and Engel, 2014; Klein et al., 2018). Epileptogenesis, a pathological process transforming a normal healthy brain into an epileptic brain, is characterized by multiple pathological changes within the brain such as acute and ongoing cell death, aberrant synaptic reorganization and neurogenesis, blood-brain barrier (BBB) disruption, and inflammation among many others (Pitkanen et al., 2015). First-line treatment for epilepsy is based on anti-seizure medications (ASM) that are mainly focused on targeting synaptic transmissions and ion channels. Other treatment options include invasive surgery, nerve stimulation and ketogenic diet. Current ASMs in clinical use are, however, only effective in 70% of patients, show no significant impact on disease progression, and may cause serious side effects. Therefore, there remains a pressing need for the identification of treatments with a non-classical mechanism of action, which impact upon disease progression and show efficacy in refractory patients. Pathological changes occurring in the brain during

the development of epilepsy remain incompletely understood. In order to design much needed new treatment strategies, we must, however, understand precisely which changes contribute to epileptogenesis and what causes these changes. The goal of this Research Topic was to provide an up-to-date summary of the diverse and complex molecular mechanisms that contribute to epilepsy pathology ranging from inflammatory cells and their role in pathogenesis to the development to post-traumatic epilepsy resulting from TBI.

The outcome volume of this Research Topic comprises eleven articles containing five original research articles and six reviews, including two mini-reviews. The original research article by Schlabitz et al. analyzed changes in gene expression due to epileptiform activity in *in vitro* models of seizures using rodent and human brain slices, which show that *in vitro* seizure models represent a suitable tool to investigate gene expression. Using organotypic hippocampal slice cultures from mice expressing enhanced green fluorescent protein (eGFP) in differentiated granule cells treated with kainic acid, Orcinha et al. show that that the protein Reelin is essential for the maintenance of granular cell lamination in the dentate gyrus and that granule cell dispersion, a pathological hallmark of epilepsy, is the result of a local Reelin deficiency. Using a lithium-pilocarpine status epilepticus rat model, Liu B. et al. investigated the contribution of the gap junction blocker carbenoxolone on dynamic changes in the spectral power of ripples and fast ripples. Their data show that rats pre-treated with carbenoxolone present reduced expression of the gap-junction protein connexin-43, as well as suppressed formation of pathological high-frequency oscillations; thereby providing further evidence of the BBB's impact on epilepsy. Liu R. et al. investigated the effects of imbalanced Na^+-K^+-$2Cl^-$ (NKCC1) and K^+-Cl^- (KCC2) co-transporters on γ-aminobutyric acidergic (GABAergic) neurotransmission in human focal cortical dysplasia (FCD). The main conclusions of their study is that an imbalanced function of NKCC1 and KCC2 may affect chloride ion homeostasis in neurons and alter GABAergic inhibitory action, thereby contributing to epileptogenesis in FCDs. Finally, Drexel and Sperk investigated whether seizure-induced over-expression of Neuropeptide Y (NPY) contributes to epileptic tolerance by using an animal model based on selective inhibition of GABA release from parvalbumin-containing basket cells in the subiculum/sector CA1. Their results show that NPY overexpression, induced *via* spontaneous recurrent seizures, contributes to epileptic tolerance possibly *via* its actions on the presynaptic Y2 receptor.

In the review article written by Chen et al. the role of interleukin-4 and its impact on glial changes, occurring during epileptogenesis, is discussed as well as its potential as a target for the treatment of epilepsy. Sharma et al. provided a review about mechanisms and risk factors underlying post-traumatic epilepsy with a particular focus on the contribution of neuroinflammatory mediators and immune response factors to the development of epilepsy following TBI and current and novel treatments and management strategies for the prevention of post-traumatic epilepsy. Chen et al. provided a comprehensive review about the latest findings on the possible mechanisms of how N-methyl-D-aspartate receptors contribute to seizures and epilepsy. Mueller et al. provided a general introduction to Designer Receptors Exclusively Activated by Designer Drugs (DREADDs) and how this technique may be applied as treatments for epilepsy. Finally, Wang and Zhao discussed in a mini-review the roles of microRNAs treatments and diagnostic targets for epilepsy and Shaimardanova et al. discussed in another mini-review the potential of gene and cell therapy in epilepsy.

In summary, this Research Topic summarizes and provides new evidence at several different levels relating to its topic and provides useful updates to the readers.

Author contributions

All authors listed have made a substantial, direct, and intellectual contribution to the work and approved it for publication.

Acknowledgments

We thank all authors for their contribution to this Research Topic and we would like also to acknowledge the work of reviewers whose constructive comments contributed to improve the quality of the articles.

Conflict of interest

The authors declare that the research was conducted in the absence of any commercial or financial relationships that could be construed as a potential conflict of interest.

Publisher's note

References

Allers, K., Essue, B. M., Hackett, M. L., Muhunthan, J., Anderson, C. S., Pickles, K., et al. (2015). The economic impact of epilepsy: a systematic review. *BMC Neurol*. 15, 245. doi: 10.1186/s12883-015-0494-y

Klein, P., Dingledine, R., Aronica, E., Bernard, C., Blümcke, I., Boison, D., et al. (2018). Commonalities in epileptogenic processes from different acute brain insults: do they translate? *Epilepsia* 59, 37–66. doi: 10.1111/epi.13965

Loscher, W. (2019). The holy grail of epilepsy prevention: preclinical approaches to antiepileptogenic treatments. *Neuropharmacology* 167, 107605. doi: 10.1016/j.neuropharm.04011

Moshe, S. L., Perucca, E., Ryvlin, P., and Tomson, T. (2015). Epilepsy: new advances. *Lancet* 385, 884–898. doi: 10.1016/S0140-6736(14)60456-6

Pitkanen, A., and Engel, J. Jr. (2014). Past and present definitions of epileptogenesis and its biomarkers. *Neurotherapeutics* 11, 231–241. doi: 10.1007/s13311-014-0257-2

Pitkanen, A., Lukasiuk, K., Dudek, F. E., and Staley, K. J. (2015). Epileptogenesis. *Cold Spring Harb. Perspect. Med*. 5, a022822. doi: 10.1101/cshperspect.a022822

Shlobin, N. A., and Sander, J. W. (2022). Learning from the comorbidities of epilepsy. *Curr. Opin. Neurol*. 35, 175–180. doi: 10.1097/WCO.0000000000001010

Thijs, R. D., Surges, R., O'Brien, T. J., and Sander, J. W. (2019). Epilepsy in adults. *Lancet* 393, 689–701. doi: 10.1016/S0140-6736(18)32596-0

frontiers in Molecular Neuroscience

REVIEW
published: 04 September 2020
doi: 10.3389/fnmol.2020.554547

Interleukin 4 Affects Epilepsy by Regulating Glial Cells: Potential and Possible Mechanism

Lu Chen[1], Lin Zhu[1], Di Lu[2], Zhe Wu[3], Yanbing Han[1], Puying Xu[1], Lvhua Chang[1†] and Qian Wu[1*†]*

[1]Department of Neurology, First Affiliated Hospital, Kunming Medical University, Kunming, China, [2]Biomedicine Engineering Research Centre, Kunming Medical University, Kunming, China, [3]Department of Psychology, The First People's Hospital of Yunnan Province, Kunming, China

Epilepsy is a chronic brain dysfunction induced by an abnormal neuronal discharge that is caused by complicated psychopathologies. Recently, accumulating studies have revealed a close relationship between inflammation and epilepsy. Specifically, microglia and astrocytes are important inflammatory cells in the central nervous system (CNS) that have been proven to be related to the pathogenesis and development of epilepsy. Additionally, interleukin 4 (IL-4) is an anti-inflammatory factor that can regulate microglia and astrocytes in many aspects. This review article focuses on the regulatory role of IL-4 in the pathological changes of glial cells related to epilepsy. We additionally propose that IL-4 may play a protective role in epileptogenesis and suggest that IL-4 may be a novel therapeutic target for the treatment of epilepsy.

Keywords: interleukin 4, epilepsy, microglia, astrocytes, cognition

OPEN ACCESS

Edited by:
Marie-Eve Tremblay, University of Victoria, Canada

Reviewed by:
Caghan Kizil, Helmholtz-Gemeinschaft Deutscher Forschungszentren (HZ), Germany
Eva Maria Jimenez-Mateos, Trinity College Dublin, Ireland

***Correspondence:**
Lvhua Chang
changluh@aliyun.com
Qian Wu
qian.wu.neuro@gmail.com

†These authors have contributed equally to this work

Received: *22 April 2020*
Accepted: *19 August 2020*
Published: *04 September 2020*

Citation:
Chen L, Zhu L, Lu D, Wu Z, Han Y, Xu P, Chang L and Wu Q (2020) Interleukin 4 Affects Epilepsy by Regulating Glial Cells: Potential and Possible Mechanism. Front. Mol. Neurosci. 13:554547. doi: 10.3389/fnmol.2020.554547

INTRODUCTION

Epilepsy is a chronic neurological disease characterized by recurrent seizures. There are 65 million people worldwide that currently suffer from epilepsy, 80% of whom live in developing countries. Furthermore, recurrent seizures and related cognitive impairments lead to a significant social and economic burden (Beghi, 2020). At present, it is thought that disorders in synaptic structure and neuronal excitability might be involved in epileptogenesis (González et al., 2019).

Abbreviations: CKs, Cytokines; IL-1β, interleukin-1β; IL-4, Interleukin 4; IL4Rα, interleukin 4 receptor alpha; γc, r chain; IL-13Rα1, interleukin 13 receptor α1; IFN-γ, Interferon γ; TNF-α, tumor necrosis factor-α; MHC II, major histocompatibility complex II; SE, status epilepticus; FS, febrile seizures; CORT, corticosterone; PGE2, prostaglandin E2; 5-HT, serotonin; NE, norepinephrine; JAK, Janus kinase; IRS, Insulin receptor substrate protein; PI3K, Phosphoinositide-3 kinase; AKT, Protein kinase B; STAT6, Signal transducer and activator of transcription factor; mTOR, Mammalian target of rapamycin; P2Y1, Purinergic Receptor 1; EAE, experimental allergic encephalomyelitis; MOGp, myelin oligodendrocyte glycoprotein; MSCs, mesenchymal stem cells; CPZ, Cuprizone; KA, Kainic acid; EEG, electroencephalographic; LPS, lipopolysaccharide; MTLE-HS, mesial temporal lobe epilepsy with hippocampal sclerosis; ADP, adenosine diphosphate; PPARγ, peroxisome proliferator activated receptor γ; AD, Alzheimer's disease; MTLE, mesial temporal lobe epilepsy; HS, hippocampal sclerosis; RE, Rasmussen's encephalitis; HMGB-1, High mobility group box-1 protein; DAMP, Damage Associated Molecular Patterns; NF-κB, nuclear factor-kB; NLRP3, NOD-like receptor with pyrin domain containing-3; OLCs, oligodendroglia-like cells; GRE, glioma-associated epilepsy; LGG, low-grade gliomas; GBM, glioblastoma; HIF-1α, hypoxia-inducible factor-1; AED, antiepileptic drugs; MWM, Morris water maze; BNDF, brain-derived neurotrophic factor; SPR, surface plasmon resonance.

Moreover, the inflammatory and immune responses in the early stage of human brain development have been proven to result in several neuropsychiatric diseases and dysfunctions such as autism, schizophrenia, cerebral palsy, epilepsy, cognitive disorders, depression, et cetera (Mahfoz and Shahzad, 2019). Accumulating evidence has recently verified that neurons and endothelial cells of the blood-brain barrier (BBB), activated microglia and astrocytes contribute to neuroinflammation in animal models with epilepsy. Furthermore, the inflammatory cascade and its related processes play important roles in epileptogenesis and epilepsy-related cognitive impairment (Vezzani et al., 2019). For instance, after epileptic injury [such as neurotrauma, stroke, central nervous system (CNS) infection], status epilepticus (SE), febrile seizures (FS) and recurrent seizures, glial cells are activated and subsequently followed by the release of large amounts of cytokines (CKs), chemokines, and the activation of downstream reactions that eventually worsen the onset of primary seizures or cause secondary seizures (Vezzani et al., 2013). Also, several pro-inflammatory CKs, such as interleukin 1β (IL-1β) and tumor necrosis factor-α (TNF-α), are involved in decreasing the seizure threshold and leading to epileptogenesis (Iori et al., 2016). Interleukin 4 (IL-4) is an anti-inflammatory cytokine that has been proven to reduce the activation of various immunocompetent cells such as macrophages, monocytes, and neutrophils by inhibiting the production of pro-inflammatory CKs (IL-1, TNF, etc.; Standiford et al., 1990; Te Velde et al., 1990; Wertheim et al., 1993). In the CNS, Park et al. (2015) also found that IL-4 could inhibit IL-1β-induced depression-like behavior, modulate the metabolism of corticosterone (CORT), prostaglandin E2 (PGE2), serotonin (5-HT), norepinephrine (NE) and other hormones and neurotransmitters in a rat disease model.

Currently, many studies are focusing on the relationship between IL-4 and epilepsy. In a study of 82 Iranian FS children aged 6 months to 6 years old, Zare-Shahabadi et al. (2015) evaluated allele and genotype frequencies of three single-nucleotide polymorphisms of the IL-4 gene. This work found that, compared to controls, the level of IL4-590/C allele and TCC haplotype was higher and the frequencies of GCC, TTT, TTC haplotypes, and that the IL-4 (-590) TC, IL-4 (-33) TC genotypes were lower in epilepsy patients. This study illustrated that the IL-4 gene changes in FS patients and may make individuals more susceptible to the disease (Zare-Shahabadi et al., 2015). However, Tsai et al. (2002) detected IL-4 intron three gene polymorphism in 51 FS and 43 epileptic children from Taiwan and found that there was no significant difference between patients with healthy children. Therefore, they concluded that the association of IL-4 polymorphisms with FS and epilepsy of children does not exist (Tsai et al., 2002). Both experiments use polymerase chain reaction monitoring, which may cause different results due to the patient's ethnicity and different detection sites, alleles, and genotypes. Moreover, Ha et al. (2018) tested IL-4 levels in 50 FS patients within 1 h of a seizure and found that IL-4 levels were higher in those patients who had fever without seizures. Similarly, in the serum of 22 out of 100 patients with epilepsy, IL-4 was significantly increased within 24 h of seizures. During the seizure-free period, the level of IL-4 could be reduced from 18.8 to 0% of the pre-seizure period (**Table 1**). These results all point to the concept that the increase of anti-inflammatory cytokine IL-4 may be a natural defense mechanism as the body responds to injury. On the other hand, due to the multimodal effect of CKs, IL-4 can play an anti-inflammatory or pro-inflammatory function in different environments (Sinha et al., 2008). For example, Li et al. (2017) found that in mice, spontaneous recurrent seizures induced by the intraperitoneal injection of pilocarpine, which up-regulates IL-4, can rescue microglial phenotypes, reduce the frequency, duration and severity of spontaneous recurrent seizures, and improve cognitive dysfunction. Thus, IL-4 likely plays an important role in epileptogenesis and the physiopathology of epilepsy. The current review aims to elaborate on the possible role of IL-4 in epileptogenesis, epileptic development, and epilepsy-related cognitive impairment.

IL-4

Overview

IL-4 is a pleiotropic cytokine mainly produced by activated T lymphocytes, especially Th2 cells, mast cells, and basophils. Isakson et al. (1982) found that a cytokine can promote B

TABLE 1 | IL-4, glial cells, and epilepsy.

Epilepsy	Interleukin 4 (IL-4) related mechanism	Glial cell targets	Epilepsy related outcome	Research model
FS	IL-4 polymorphisms	-	-	Human
Partial seizure	IL-4 increase	-	-	Human
TLE	IL-13 increase	M2 polarization of Microglia/macrophages; M1 inhibition	- - Reduced frequency, duration, and severity of spontaneous epilepsy	KA-induced mice Lithium-pilocarpine induced rats
SE	IL-4 increase; IL-1β increase	M1, M2 M1 inhibition	Reduce frequency, duration, and severity of spontaneous Recurrent seizures; improve Cognitive dysfunction	Human KA-induced mice Pilocarpine-induced mice
	HMGB1-mediated pathway	Astrogliosis, microgliosis		Pilocarpine-induced Wistar rats
Intractable epilepsy	IL-4 increase	Astrocytic hypertrophy and proliferation	Inhibited the mitogenic effect of TNF on astrocytes	Non-neoplastic human astrocytes

cell proliferation, which was successfully cloned in 1986 and eventually named IL-4 (Isakson et al., 1982). Although the IL-4 cDNA sequence in human beings contains 153 amino acid residues, it can only produce secreted IL-4 proteins containing 129 amino acid residues. The spherical hydrophobic core of secreted IL-4 contains three disulfide bonds and four α-helices (Powers et al., 1992). After the addition of N-chain oligosaccharides, this core produces different molecular weights that include 15, 18, and 19 kDa. Essentially, secreted IL-4 mainly functions as follows: (1) driving Th2 cell differentiation to produce more IL-4, and then promoting the release of other Th2 anti-inflammatory CKs such as IL-5 and IL-13; (2) inhibiting the production of pro-inflammatory CKs such as TNF-α, interferon γ (IFN-γ), and IL-17; and (3) promoting B cell proliferation and differentiation and up-regulating the expression of major histocompatibility complex II (MHC II) molecules, IL-4R and CD23 on B cells (Lu et al., 2015).

IL4-Related Signaling Pathways

There are two types of IL4 receptors, Type I and Type II. Type I receptors are a kind of heterodimer receptor that was formed by IL-4 receptor α (IL4Rα) and common r chain (γc) chains and are mainly expressed on the surface of hematopoietic cells. Type II receptors contain the IL4Rα and IL-13 receptor α1 (IL-13Rα1) and are expressed on the surface of non-hematopoietic cells (Sequeida et al., 2020). The binding of IL-4 to its receptor leads to the activation of the Janus kinase (JAK) family and the phosphorylation of IL4Rα. Three signaling pathways are related to the activation of the JAK family: (1) insulin receptor substrate protein (IRS)/Phosphoinositide-3 kinase (PI3K)/Protein kinase B (AKT) pathway. Activated JAK3 can stimulate IRS tyrosine phosphorylation and provide binding sites to those signaling molecules which contain the SH2 domain, such as P85. Then, the combination of P85 and IRS can activate PI3K and its downstream signaling molecules such as AKT, and finally affect cell proliferation and differentiation. (2) Signal transduction and activation of the transcription factor (STAT6) pathway. STAT6 forms a homomeric dimer by JAKs phosphorylation which is then transported to the nucleus initiates IL4/IL13 gene transcription and regulates the expression of genes such as CD23 (Keegan et al., 2018). (3) Mammalian target of rapamycin (mTOR) signaling pathway. mTOR is a critically synergistic protein that aids IL-4 in activating STAT6 to the greatest extent and ultimately regulates the differentiation of Th2 cells (Delgoffe et al., 2009). In short, IL-4 regulates the growth and development of T cells through a variety of molecular signal pathways, but its specific mechanism remains unknown (**Figure 1**).

Besides, IL-4 can also abnormally activate STAT3 in glioblastoma (GBM) cells, which are related to the expression of IL-13Rα2 (Rahaman et al., 2005). In most cases, STAT3 mediates pro-IL-6 and anti-IL-10 signals (Pfitzner et al., 2004). It was reported that pilocarpine-induced SE can activate the JAK/STAT signaling pathway, especially STAT3 (Xu et al., 2011). Similarly, Zhang et al. (2019) found that STAT3 was overexpressed in 169 children suffering from epilepsy, suggesting that it is associated with the risk of epilepsy and drug resistance to epilepsy (Li et al., 2020). By inhibiting STAT3 gene transcription, the frequency of seizures can be reduced (Grabenstatter et al., 2014).

IL-4, IL-13, and Epileptogenesis

IL-4 and IL-13 are related CKs that may activate similar downstream signaling pathways and exert molecular regulatory effects (Athari, 2019). IL-13Rα1 can specifically bind to IL-13 through its critical binding unit D1 domain. This can lead IL-13 to play an important role in the pathogenesis of bronchial asthma by acting on epithelial cells and fibroblasts (Ito et al., 2009). Moreover, Umeshita-Suyama et al. found that IL-4 and IL-13 induced STAT3 activation in B cells with high expression of IL-13Rα1 (Umeshita-Suyama et al., 2000). IL-13Rα2 is another receptor of IL-13; Andrews et al. (2013) used surface plasmon resonance (SPR) analysis to show that IL-13Rα2 does not bind IL-4, nor does it affect the binding of IL-4 to IL-4Rα. These authors also used EBAS-2B cell lines (human bronchial epithelium) to prove that IL-13Rα2 overexpression weakened IL-4 and IL-13-mediated STAT6 phosphorylation. Furthermore, IL-13Rα2 without cytoplasmic domain continued to weaken the IL-13-mediated signaling pathway but did not affect the IL-4 mediated STAT6 signaling pathway (Andrews et al., 2013).

Studies have shown that IL-13 also may be involved in the regulation of the inflammatory process of the CNS, however, whether this regulatory role is protective or disruptive is controversial. In a study on experimental allergic encephalomyelitis (EAE) induced by myelin oligodendrocyte glycoprotein (MOGp), Barik et al. (2017) found that the ability of Th17 cells from IL-13Rα1–deficient ($13R^{-/-}$) mice to transform into Th1 cells was reduced, and the sensitivity to Treg inhibition was also reduced. HR ($13R^{-/-}$) mice were more susceptible to EAE and developed early-onset and more severe disease. These observations indicated that IL-13 can control immune-mediated CNS inflammation (Barik et al., 2017). Le Blon et al. (2016) transplanted mesenchymal stem cells (MSCs)/IL-13 into a Cuprizone (CPZ) mouse model and found that IL-13 released by grafted MSC was able to trigger the alternate activation of macrophages and microglia related to MSC transplantation. IL-13 was also found to reduce the inflammation and demyelination induced by CPZ through its direct effect or the combined effect with the alternate activation of macrophages/microglia, indicating that IL-13 has protective effects on CPZ-induced neuroinflammation (Le Blon et al., 2016). Some studies have found that the CPZ mouse model showed tonic-clonic seizures, intermittent ictal spikes, and frequent spike discharge. Accordingly, CPZ models have also been used to study pathology and/or therapy for epilepsy (Praet et al., 2014). However, after transplanting MSCs/IL-13 into mice hippocampi and then inducing epilepsy by Kainic acid (KA) 1 week later, Ali et al. (2017) found that transplantation had no significant influence on the duration, frequency, and onset of seizures, or their electroencephalographic (EEG) dynamics. Hence, they claimed that the injection of MSCs/IL-13 into the hippocampus might not have a direct protective effect on SE or chronic epilepsy. Nevertheless, as an indirect mechanism, MSCs/IL-13 was found to optimize the hippocampal niche,

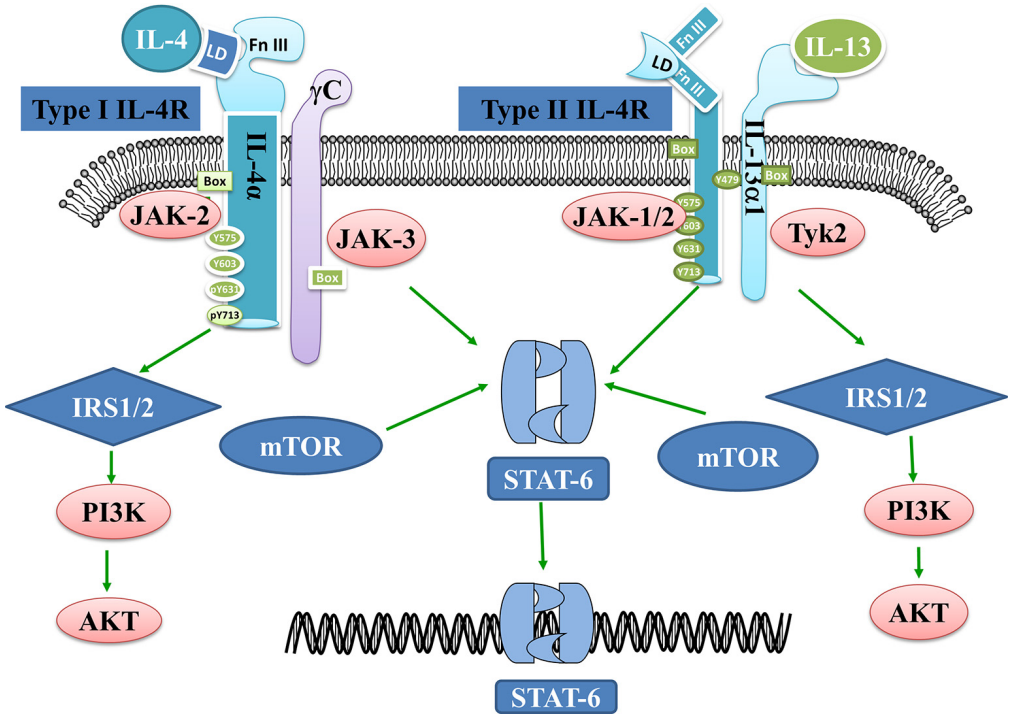

FIGURE 1 | Interleukin 4 (IL-4)- and IL-13-related signaling pathways. IL-4 binds to Type I receptors and then activates the IRS1/2-P13K-AKT and STAT6 pathways. mTOR is a prime synergistic protein that helps IL-4 to maximally activate STAT6. IL-13 on the other hand binds to Type II receptors and activates JAK1/2 and Tykine2 (tyrosinekinase2), which in turn activates the IRS1/2-P13K-AKT or STAT6 pathways.

outside of the lesion site, by inducing M2 polarization of microglia/macrophages (**Table 1**, Ali et al., 2017). Several aspects, such as the difference in the transplanted cell line, transplantation methods, grafting sites and EEG monitoring time might lead to different or even contrary results. On the one hand, MSC grafts and epilepsy may result in large astrocyte scars which can physically obstruct IL-13 from reaching the hippocampus. On the other hand, neuroinflammation associated with MSC transplantation may counteract the protective effect of IL-13 on inflammation. Therefore, whether IL-13 has a protective effect on the pathophysiology of epilepsy is still controversial, and more powerful evidence is needed for verification.

IL-4, GLIAL CELLS, AND EPILEPSY

IL-4, Epilepsy, and Microglial Phenotypic Transformation

Microglia and astrocytes are the main inflammatory cells in the nervous system. Glia-mediated inflammation induced by various brain insults can promote seizures and epileptogenesis (**Figure 2**), especially when the inflammation is difficult to control (Eyo et al., 2017). Microglia are highly adaptable glial cells that, during development, recognize and phagocytose apoptotic neurons, prune synapses, modulate the differentiation and migration of neural precursor cells, regulate neurogenesis, and improve neuron survival. In the mature brain, microglia play an important role in general cognitive function, learning and memory, neuroplasticity, and synaptic plasticity (Hammond et al., 2018). Moreover, microglia can regulate the release of anti-inflammatory and pro-inflammatory factors. During brain and niche damage, microglia can be activated through morphological changes or molecular modifications, which can activate a protective response to inflammation in the CNS (Tay et al., 2017). Interestingly, microglia can exhibit different activation subtypes—M1, M2a, M2b, M2c—according to environmental changes and exogenous stimuli. The M1 phenotype is mainly induced by lipopolysaccharides (LPS) and IFN-γ; the M2a phenotype by IL-4 and IL-13; the M2b phenotype by the immune complex toll-like receptor and IL-1R agonist; the M2c phenotype by IL-10 and glucocorticoids (Franco and Fernández-Suárez, 2015).

RNA sequencing analysis showed that microglial phenotypes varied according to their response function in patients who suffered from mesial temporal lobe epilepsy with hippocampal sclerosis (MTLE-HS; Morin-Brureau et al., 2018). For example, in CA1/CA3 after epilepsy, microglial cells could reduce neuron density by regulating MHCII overexpression and their shapes. Furthermore, increased adenosine diphosphate (ADP) can induce microglial migrative behavior by expressing purinergic receptor 1 (P2Y1; De Simone et al., 2010), enhance tissue repair, promote vascular reconstruction and strengthen the BBB by expressing IL-10 and its related transcription factors. In different epilepsy models, microglia phenotypes undergo similar transformations. In a study of the Cstb$^{-/-}$

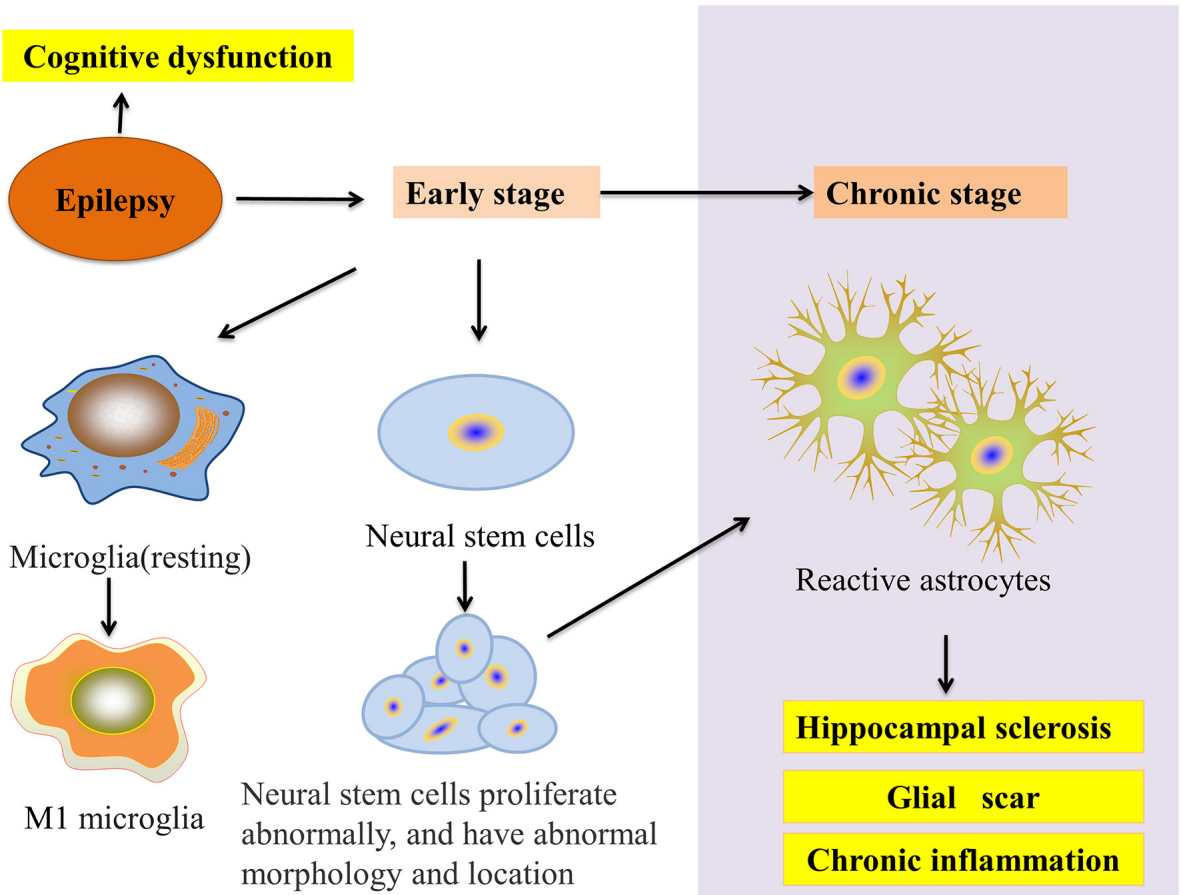

FIGURE 2 | Glial cells and epilepsy pathology. In the early stage of epilepsy, microglial cells transform into the M1 phenotype and neural stem cell (NSC) disorders appear in proliferation, migration, and integration. In chronic epilepsy, neurogenesis gradually decreases to a halt. NSCs start transforming into reactive astrocytes and finally accelerate HS. Moreover, these processes result in the epilepsy-induced inhibition of autophagy and cognitive impairment.

mouse, an animal model for progressive myoclonus epilepsy of Unverricht–Lundborg type (EPM1), Okuneva et al. (2015) found that the proportion of pro-inflammatory M1 and anti-inflammatory M2 microglia was higher than that of the control group. Additionally, in pre-symptomatic Cstb$^{-/-}$ mice, M1/M2 polarization is skewed towards the M2 type at postnatal day 14 (P14). At P30, however, this ratio reversed to skew towards M1, which is a time point related to the onset of myoclonus. This phenomenon indicates that M2 microglia attempt to support neurons that may be dysfunctional and prevent further damage, however, may fail to maintain this function (Okuneva et al., 2015). Benson et al. (2015) compared microglial polarization in pilocarpine-induced SE and kainic acid-induced SE. In the acute phase, both M1 and M2 marker expression was increased in the pilocarpine model, while M1 in the KA model increased. This difference may be due to the more frequent seizures in the KA model. Consequently, acute M1 upregulation post-SE can play an important role in epileptogenesis (Benson et al., 2015). In a rat lithium-pilocarpine model of TLE, Wang et al. (2015) found that M1 microglial cells maintained a high level at 7 and 14 days after SE. Subsequently, they proved that the second generation of tetracycline-minocycline can effectively inhibit M1 microglia activation, mitigate SE induced brain inflammation, and reduce the frequency, duration, and severity of spontaneous epilepsy (Wang et al., 2015). Hence, correcting phenotypic deviations when the microglia phenotype balance changes will help improve the prognosis of epilepsy.

The interleukins IL-10, IL-13, and IL-4 are essential modulators of neuroinflammation by promoting the polarization of M2-like microglia (Michels et al., 2014). In an epilepsy mouse model, Li et al. (2017) found that M1 and M1-associated cytokine IL-1β rapidly increased to the peak value 1 day after SE, and fell to normal levels in 3 weeks. On the other hand, IL-4 was unchanged in the early epileptic stages and gradually increased over the following 2 weeks. However, the percentage of M2 exhibited an immediate drop on the first day after SE and then gradually increased at 3 weeks after SE. Nevertheless, based on the intraperitoneal injection of IL-4 (100 ng/mouse) 5 h before and 4 days after pilocarpine-induced SE, Li et al. (2017) found that IL-4 inhibited the early increase of M1. By contrast, except for the first day after IL-4 injection, M2 did

not show a substantial sustained increase after SE. Therefore, Li et al. (2017) considered the reduced damage and inflammation due to early inhibition of M1 which may inhibit the subsequent increase in M2. This study first indicated that IL-4 can affect the inflammatory process of epilepsy by regulating microglial phenotypes (**Table 1**, Li et al., 2017).

Additionally, in a stroke model, early intracerebral injection of IL-4 was able to inhibit M1 activation while enhancing M2 microglial activation and promoting neuro-functional recovery (Yang et al., 2016). Knock-out STAT6 mice led to the down-regulation of IL-4 and STAT6/Arg1 (arginase 1), which stimulates the transformation of microglia and macrophages into pro-inflammatory phenotypes and result in the reduction of dead/dying neuron clearance in the lesion area, augmentation of brain inflammation, increase of neuronal death, and eventually poor long-term prognoses (Cai et al., 2019). In an Alzheimer's diseases (AD) mouse model, IL-4 did induce a robust M2a phenotype (Latta et al., 2015), and rather induced autophagy vacuole formation and microglial autophagy flux generation, increased uptake and degradation of Amyloid-β (Aβ), inhibited the Aβ deposition induced autophagy flux blockade, and returned autophagy flux to a normal level (Tang et al., 2019). Based on the above results, IL-4 can likely regulate the microglia to the anti-inflammatory M2 phenotype, enhance the phagocytosis of apoptotic neurons, and play a protective role in many neurological diseases such as epilepsy, stroke, and AD. Additionally, epidemiological studies have shown that the risk of epilepsy among brain-infected survivors is 7–9% in developed countries and is much higher in developing countries (Ramantani and Holthausen, 2017). Neuronal excitability secondary to pro-inflammatory signals caused by CNS infection is an important mechanism for epileptogenesis (Singhi, 2011). Stroke is responsible for approximately 10% of all seizures and 55% of new seizures in the elderly. Early epilepsy after stroke is caused by local metabolic disorders, without changing the neural network and late epilepsy by acquired epilepsy susceptibility (Feyissa et al., 2019). Furthermore, in patients over 65 years of age, neurodegenerative diseases account for approximately 10% of all new seizures, recurrent cases of which also aggravate the decline in cognitive function (Friedman et al., 2012). The accumulation of Aβ peptides in the brain of AD patients can cause synaptic degeneration and remodeling of neuronal circuits, leading to neuronal hyperexcitability. As a result, epilepsy is highly correlated with neurological diseases such as infections, stroke, and AD (Garg et al., 2018). Nevertheless, the specific mechanism of IL-4 in epileptogenesis needs to be further studied.

IL-4, Epilepsy, and Astrocytes

Astrocytes account for about one-third of brain cells and can provide structural, metabolic, and homeostatic support for neurons (Shigetomi et al., 2019). After infection, trauma, ischemia, and neurodegenerative disease, astrocytes are activated, and in severe cases, reactive astrocytes progressively enlarge, proliferate, and form marked scars (Sofroniew, 2009).

In vivo and *in vitro* experiments investigating epilepsy have revealed that reactive astrocyte proliferation and glial scar formation are common pathological changes. In a KA-induced mouse model of medial temporal lobe epilepsy (MTLE), Muro-García et al. found that at 1 week after epilepsy, neural stem cells (NSCs) began transforming into reactive NSCs that would gradually inhibit neurogenesis and transform into reactive astrocytes. Even more, at 6 weeks post-seizure, hippocampal neurogenesis completely stopped, and reactive astrocytes induced hippocampal sclerosis (HS) and chronic inflammation. Moreover, drug-resistant MTLE patients were found to have inhibited neurogenesis, reactive astrocyte proliferation, and HS (Muro-García et al., 2019). Interestingly, in both mitochondrial epilepsy (a type of epilepsy that is extremely difficult to treat and has a poor prognosis due to mutations in mitochondrial DNA) and Rasmussen's encephalitis (RE; a type of epilepsy with chronic brain inflammation), patients experienced astrocyte apoptosis and loss (Bauer et al., 2007; Chan et al., 2019). Above all, reactive astrocytes play an important role in epileptogenesis and epileptic development. Based on these results, intervention in reactive astrocytes may become a new target for epilepsy treatment.

Early in 1993, in an adult human glial cell line-derived from epilepsy white matter, Estes et al. (1993) confirmed that IL-4 down-regulated the DNA synthesis and proliferation of astrocytes and inhibited the mitogenic effect of TNF on astrocytes by anti-IL-4 antibody. Moreover, in an AD model, IL4/STAT6 signaling hurt astrocyte survival *in vivo* (Mashkaryan et al., 2020), and *in vitro*, IL-4 rescued the impairment of proliferation and neurogenic ability of primary human cortical astrocytes by Aβ42-induced *via* IL-4/STAT6 pathway (Papadimitriou et al., 2018). On the other hand, Brodie et al. (1998) found that astrocytes express IL-4R *in vivo* but do not secrete IL-4. Furthermore, after being treated with IL-4, the activation of astrocytes was inhibited, NO, and iNOS content caused by LPS stimulation was decreased, and TNF-α secretion was reduced. These results indicate that IL-4 may act as an immunosuppressive factor in the CNS during inflammation (Brodie et al., 1998). Also, high mobility group box-1 protein (HMGB-1), an important damage-associated molecular pattern (DAMP), has been shown to induce dendrite loss and neurodegeneration *via* nuclear factor-κB (NF-κB) signaling activation. The release of NF-κB in human patients and models of epileptic seizures are often accompanied by reactive gliosis and neurodegeneration. In a model of pilocarpine-induced SE Wistar rats, Rosciszewski et al. (2019) found that blocking the HMGB1-mediated signaling pathway was beneficial to reduce reactive astrogliosis, microgliosis and neurodegenerative changes after SE. Furthermore, in glial cultures obtained from cerebral cortices of C57BL/6 mice treated with different concentrations of HMGB1, Yao et al. (2019) elucidated that IL4 could activate PPARγ *via* the STAT6 singling pathway and inhibit NF-kB activation, significantly reducing the formation of the HMGB1-mediated NOD-like receptor with pyrin domain containing-3 (NLRP3) inflammasome complex in astrocytes (**Table 1**). Additionally, Garg et al. (2009) found that IFN-γ protected the ability of murine astrocytes to clear extracellular glutamate *in vitro* and undergo oxidative stress and that IL-4 has no effect at any concentration that was tested (10–100 ng/ml).

When IL-4 and IFN-γ were co-administered, IL-4 reduced the clearance of glutamate by IFN-γ. However, IL-4 avoided the harmful effects of excessively strong IFN-γ by increasing the neuroprotective thiol and lactic acid secretion and inhibiting the release of Th1 CKs (Garg et al., 2009). In summary, IL-4 can regulate reactive astrocytes and play a protective role against neuroinflammation through the IL-4/STAT6 signaling pathway. However, whether IL-4 has protective effects on reactive astrocyte hyperplasia and inflammation caused by epilepsy needs further verification.

Oligodendrocytes are myeloid cells in the CNS, which must undergo a complex and precise process of proliferation, migration, differentiation, and myelination, and finally form an insulating sheath (Bradl and Lassmann, 2010). In 30 patients who underwent surgical resection for intractable focal epilepsy, Sakuma et al. (2014) found that compared with control cases, the number of oligodendroglia-like cells (OLCs) in refractory focal epilepsy specimens of children increased, OLCs increased in the gray matter and the junction of gray/white matter to white matter. Zhang et al. (2019) further confirmed that IL-4 has a direct beneficial effect on the differentiation of oligodendrocytes through the PPARγ axis, however, at present, the effect of IL-4 on the increase of post-epileptic OLCs lacks relevant evidence.

The IL4/IL4R Axis in the Treatment of Glioma and Glioma-Related Epilepsy

Gliomas are the most common primary CNS brain tumors and include astrocytomas, oligodendrogliomas, and ependymomas that originate in astroglial cells, oligodendrocyte cells, ependymal cells or cancer stem cells (Zhu et al., 2012). Increasing evidence suggests that the growth of gliomas stimulate seizures, while seizure activity may also contribute to tumor growth (Yang et al., 2016). Symptomatic seizure activity secondary to gliomas is referred to as glioma-associated epilepsy (GRE). The epileptogenesis of GRE involves multiple factors, including tumor location, degree of differentiation, tumor microenvironment, and specific genetic changes (Liang et al., 2019). In 65–90% of low-grade gliomas (LGG), epilepsy is the most common first symptom. Furthermore, seizure control is often the most important predictor of quality-of-life in patients with recurrent LGG (Dunn-Pirio et al., 2018). Compared to standard antiepileptic medications, effectively inhibiting the development of gliomas is more conducive to control the onset of glioma-related seizures (Samudra et al., 2019). Moreover, Zhu et al. (2012) indicated that CKs play a critical role in glioma diagnosis, prognosis, and therapy.

From 100 histologically confirmed adult Iraq patients with glioma blood samples, Shamran et al. (2014) suggested that the C allele of the SNP S503P in the IL-4R and the T allele of the SNP C-33T in the IL-4 gene may have a protective role against glioma development. Compared with normal brain tissues, IL-4R is overexpressed in GBM; based on this phenomenon, Rand et al. (2000) developed a cytotoxin targeting IL-4R and cpIL4-PE, which can mediate extensive necrosis of gliomas without obvious toxicity to healthy adjacent brain tissue. Joshi et al. (2001) demonstrated that human brain tumors *in situ* also overexpressed IL-4R and that most GBM primary cell cultures were found to be highly sensitive to cpIL4-PE, but not to normal astrocytes or neuronal cell lines. Hence, these results confirmed that the differential expression of IL-4R may offer an attractive target of IL-4 cytotoxin for brain tumor therapy (Joshi et al., 2001). In recent years, tumor drugs have targeted AP1, a new glioma affinity peptide that specifically binds to IL-4R and exhibits the highest therapeutic effect on glioma (Sun et al., 2017). Moreover, early in 2000, Liu et al. (2000) revealed that IL-4α receptors in non-neoplastic astrocytes derived from human brain specimens of patients with epilepsy were expressed similar to malignant astrocytoma (**Table 1**). Therefore, IL-4R may also be a new target for glioma-associated epilepsy treatment.

Additionally, STAT6 is an important target protein of IL-4 that likely regulates the microenvironment of tumor cell growth, inhibits tumor invasion, and reduces tumor proliferation and differentiation (Rahaman et al., 2005; Hammond et al., 2018). Both in human glioma tissue and glioblastoma cells (U87MG and U373MG), Park et al. (2019) found that CpG islands in the STAT6 promoter were hypermethylated by DNA methyltransferase which ultimately led to the down-regulated and even silenced expression of STAT6. Furthermore, under hypoxic conditions, the decrease of STAT6 could activate the mTOR signaling pathway, promote hypoxia-inducible factor-1 (HIF-1α) protein synthesis, and eventually enhance the viability and anti-apoptotic ability of tumor cells. Using DNA methyltransferase inhibitors, such as five-azacitidine and decitabine, to restore STAT6 expression in STAT6-silenced gliomas can increase tumor cell death, which would provide a new treatment (Park et al., 2019). Interestingly, in glioblastoma cells (U251, T98G, and A172), Rahaman et al. found that IL-4 induced the abnormal activation of STAT3 in GBM cells, but not in normal human astrocytes. These results indicate that IL-13Rα2, a decoy receptor for IL-13, negatively regulates STAT6 activation and positively regulates IL-4R/IL-13R-mediated STAT3 activation in GBM cells. Moreover, this work also demonstrated that the IL-13Rα2-mediated activation of STAT3 did not need a direct physical interaction between IL-13Rα2 and STAT3 (Rahaman et al., 2005). Thus, as IL-4 induces a similar response in intractable epilepsy and glioma, IL-4/IL4R-STAT6 may be a potential therapeutic target for glioma-related epilepsy but requires future studies.

IL-4, EPILEPSY AND COGNITIVE FUNCTION

The temporal lobe is thought to influence cognition and memory, especially in the spatial domain. Chronic recurrent temporal lobe epilepsy can lead to dramatic cognitive impairment (Chauvière, 2020). Many reports have found that children with epilepsy have high levels of cognitive disorders, which is mainly influenced by the etiology, time of seizures, frequency of interictal epileptiform discharges, and the adverse reactions of antiepileptic drugs (AED) or surgery (Moosa and Wyllie, 2017). A recent registration study of 6,635 children with epilepsy in Norway showed that 17.0% have intellectual disabilities, 21.3% have mental developmental disabilities, and 7.5% have unexplained developmental delays (Aaberg et al., 2016). In children who have

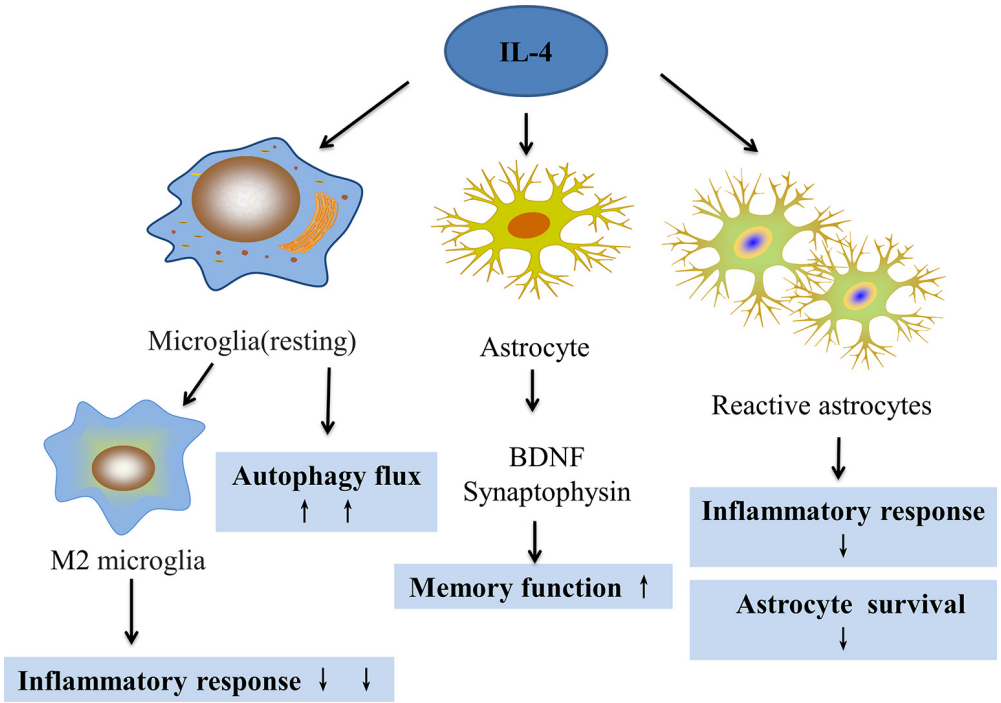

FIGURE 3 | The effect of IL-4 on microglia and astrocytes. IL-4 can regulate microglial transformation into the M2 phenotype to reduce inflammation, increase autophagy flux, and improve autophagy. IL-4 can also increase the expression of BDNF and synaptophysin in astrocytes, which can improve memory. IL-4 can also reduce the proliferation of reactive astrocytes and reduce the inflammatory response.

had seizures at least once in the past year or used AEDs, 40% had an IQ less than 70 and 24% under 50 (Reilly et al., 2015). Cognitive impairment imposes a serious burden on patients and families and therefore, early improvement of cognitive impairment will help improve the patients' quality-of-life.

A recent study discovered that IL-4 is beneficial to cognition. In the meninges of Morris water maze (MWM)-trained mice, CD4+ T cells were activated and produced more IL-4 than untrained controls. IL-$4^{-/-}$ mice exhibited severe cognitive impairment and the level of pro-inflammatory CKs was increased. Subsequently, the bone marrow of these IL-$4^{-/-}$ mice was transplanted into wild-type mice, which also showed severe cognitive impairment and revealed a marked pro-inflammatory skew in meningeal myeloid cells. On the other hand, injecting wild-type mouse T cells into IL-$4^{-/-}$ mice could significantly improve cognitive function and ameliorated the pro-inflammatory tendency of meningeal cells. Derecki et al. (2010) also found IL-4 increased brain-derived neurotrophic factor (BNDF) mRNA levels in astrocytes. Wild type mice that were tested in the MWM appeared to accumulate IL-4 and IL-13 in their meninges and BDNF in the hippocampus continued to rise. Overall, both IL-4 and IL-13 deficiency in the brains of these mice could damage spatial learning. Consequently, both IL-4 and IL-13 are involved in cognitive function by stimulating astrocytes from the meninges and hippocampus (Brombacher et al., 2017). Additionally, in the hippocampus of aged Sprague-Dawley male rats, the level of BDNF and synaptophysin is reduced, pro-inflammatory cytokine (IL-1β and IL-6) to be released, and cognitive dysfunction present. Treatment with IL-4 reversed BDNF and synaptophysin expression promoted the transformation of microglia to the M2 phenotype, downregulated the expression of IL-1β and IL-6, and improved the behavioral performance (Li et al., 2017).

BDNF and synaptophysin regulated by astrocytes are both important for cognitive processes. BDNF can regulate neuroplasticity, including long-term potentiation, synaptogenesis, and neurogenesis, all of which are related to learning and memory (Leal et al., 2017). Specifically, synaptophysin plays a crucial role in the regulation of synaptic plasticity that, when disordered, can result in the cognitive decline of AD (Valtorta et al., 2004). Nowadays, several studies have shown that IL-4 might have potential neuroprotective effects on cognition by regulating BDNF and synaptophysin. Nevertheless, this concept still requires further studies to show whether IL-4 can act as a cognitive protector in epilepsy-related cognitive impairment.

SUMMARY

Increasing evidence has revealed that inflammation and epilepsy exhibit complex interactions. Microglia and astrocytes are the main inflammatory cells in the nervous system that are involved in the pathogenesis of epilepsy. This pathogenesis includes activating M1 microglia, releasing pro-inflammatory factors, and stimulating the proliferation of reactive astrocytes that form glial scars and cause hippocampal sclerosis. IL-4 is an

important anti-inflammatory cytokine that has an important regulatory effect on the above response processes of glial cells (**Figure 3**). Furthermore, IL-4/STAT6 might be an important pathway for regulating multiple aspects of the activated glial pathology. Additionally, IL-4 can affect the prognosis of gliomas, which are closely related to epilepsy, and improve cognitive function. Moreover, in the adult zebrafish brain, Bhattarai et al. (2016) found that IL-4 regulated neurogenesis, especially NSC proliferation through the STAT6 pathway, and also promoted neural stem cell proliferation and neurogenesis by inhibiting tryptophan metabolism. These events reduce serotonin production and up-regulate BDNF (Bhattarai et al., 2020). Whether in animal models with epilepsy or patients with temporal lobe epilepsy, neurogenesis was reported to be involved in epileptogenesis and epilepsy outcomes (Chen et al., 2019). Consequently, IL-4 very likely plays an important role in the development of epilepsy by regulating neuron-glial interactions.

AUTHOR CONTRIBUTIONS

LChen, LZ, DL, ZW, and PX contributed to the conception and design of the study. LChen to the writing of the article. QW and YH were responsible for funding. YH contributed to revising the article. LChang and QW were responsible for scientific consultation at all stages, the conceptualization of the study, and revision of the article.

FUNDING

This work was supported by the National Natural Science Foundation of China (81601134, 81660228), Yunnan Applied Basic Research Projects [2017FE468 (-144)], Program for Science and Technology Innovation Team in Yunnan Province (2018HC008), supported by Yunnan Health Training Project of High-Level Talents, and also supported by China Scholarship Council.

REFERENCES

Aaberg, K. M., Bakken, I. J., Lossius, M. I., Lund Søraas, C., Håberg, S. E., Stoltenberg, C., et al. (2016). Comorbidity and childhood epilepsy: a nationwide registry study. *Pediatrics* 138:e20160921. doi: 10.1542/peds.2016-0921

Ali, I., Aertgeerts, S., Le Blon, D., Bertoglio, D., Hoornaert, C., Ponsaerts, P., et al. (2017). Intracerebral delivery of the M2 polarizing cytokine interleukin 13 using mesenchymal stem cell implants in a model of temporal lobe epilepsy in mice. *Epilepsia* 58, 1063–1072. doi: 10.1111/epi.13743

Andrews, A. L., Nordgren, I. K., Campbell-Harding, G., Holloway, J. W., Holgate, S. T., Davies, D. E., et al. (2013). The association of the cytoplasmic domains of interleukin 4 receptor alpha and interleukin 13 receptor alpha 2 regulates interleukin 4 signaling. *Mol. Biosyst.* 9, 3009–3014. doi: 10.1039/c3mb70298g

Athari, S. S. (2019). Targeting cell signaling in allergic asthma. *Signal. Transduct. Target. Ther.* 4:45. doi: 10.1038/s41392-019-0079-0

Barik, S., Ellis, J. S., Cascio, J. A., Miller, M. M., Ukah, T. K., Cattin-Roy, A. N., et al. (2017). IL-4/IL-13 heteroreceptor influences Th17 cell conversion and sensitivity to regulatory T cell suppression to restrain experimental allergic encephalomyelitis. *J. Immunol.* 199, 2236–2248. doi: 10.4049/jimmunol.1700372

Bauer, J., Elger, C. E., Hans, V. H., Schramm, J., Urbach, H., Lassmann, H., et al. (2007). Astrocytes are a specific immunological target in Rasmussen's encephalitis. *Ann. Neurol.* 62, 67–80. doi: 10.1002/ana.21148

Beghi, E. (2020). The epidemiology of epilepsy. *Neuroepidemiology* 54, 185–191. doi: 10.1159/000503831

Benson, M. J., Manzanero, S., and Borges, K. (2015). Complex alterations in microglial M1/M2 markers during the development of epilepsy in two mouse models. *Epilepsia* 56, 895–905. doi: 10.1111/epi.12960

Bhattarai, P., Cosacak, M. I., Mashkaryan, V., Demir, S., Popova, S. D., Govindarajan, N., et al. (2020). Neuron-glia interaction through Serotonin-BDNF-NGFR axis enables regenerative neurogenesis in Alzheimer's model of adult zebrafish brain. *PLoS Biol.* 18:e3000585. doi: 10.1371/journal.pbio.3000585

Bhattarai, P., Thomas, A. K., Cosacak, M. I., Papadimitriou, C., Mashkaryan, V., Froc, C., et al. (2016). IL4/STAT6 signaling activates neural stem cell proliferation and neurogenesis upon amyloid-β42 aggregation in adult zebrafish brain. *Cell Rep.* 17, 941–948. doi: 10.1016/j.celrep.2016.09.075

Bradl, M., and Lassmann, H. (2010). Oligodendrocytes: biology and pathology. *Acta Neuropathol.* 119, 37–53. doi: 10.1007/s00401-009-0601-5

Brodie, C., Goldreich, N., Haiman, T., and Kazimirsky, G. (1998). Functional IL-4 receptors on mouse astrocytes: IL-4 inhibits astrocyte activation and induces NGF secretion. *J. Neuroimmunol.* 81, 20–30. doi: 10.1016/s0165-5728(97)00154-9

Brombacher, T. M., Nono, J. K., De Gouveia, K. S., Makena, N., Darby, M., Womersley, J., et al. (2017). IL-13-mediated regulation of learning and memory. *J. Immunol.* 198, 2681–2688. doi: 10.4049/jimmunol.1601546

Cai, W., Dai, X., Chen, J., Zhao, J., Xu, M., Zhang, L., et al. (2019). STAT6/Arg1 promotes microglia/macrophage efferocytosis and inflammation resolution in stroke mice. *JCI Insight* 4:e131355. doi: 10.1172/jci.insight.131355

Chan, F., Lax, N. Z., Voss, C. M., Aldana, B. I., Whyte, S., Jenkins, A., et al. (2019). The role of astrocytes in seizure generation: insights from a novel *in vitro* seizure model based on mitochondrial dysfunction. *Brain* 142, 391–411. doi: 10.1093/brain/awy320

Chauvière, L. (2020). Potential causes of cognitive alterations in temporal lobe epilepsy. *Behav. Brain Res.* 378:112310. doi: 10.1016/j.bbr.2019.112310

Chen, L., Wang, Y., and Chen, Z. (2019). Adult neurogenesis in epileptogenesis: an update for preclinical finding and potential clinical translation. *Curr. Neuropharmacol.* 18, 464–484. doi: 10.2174/1570159X17666191118142314

Delgoffe, G. M., Kole, T. P., Zheng, Y., Zarek, P. E., Matthews, K. L., Xiao, B., et al. (2009). The mTOR kinase differentially regulates effector and regulatory T cell lineage commitment. *Immunity* 30, 832–844. doi: 10.1016/j.immuni.2009.04.014

Derecki, N. C., Cardani, A. N., Yang, C. H., Quinnies, K. M., Crihfield, A., Lynch, K. R., et al. (2010). Regulation of learning and memory by meningeal immunity: a key role for IL-4. *J. Exp. Med.* 207, 1067–1080. doi: 10.1084/jem.20091419

De Simone, R., Niturad, C. E., De Nuccio, C., Ajmone-Cat, M. A., Visentin, S., and Minghetti, L. (2010). TGF-β and LPS modulate ADP-induced migration of microglial cells through P2Y1 and P2Y12 receptor expression. *J. Neurochem.* 115, 450–459. doi: 10.1111/j.1471-4159.2010.06937.x

Dunn-Pirio, A. M., Woodring, S., Lipp, E., Herndon, J. E. II., Healy, P., Weant, M., et al. (2018). Adjunctive perampanel for glioma-associated epilepsy. *Epilepsy Behav. Case Rep.* 10, 114–117. doi: 10.1016/j.ebcr.2018.09.003

Estes, M. L., Iwasaki, K., Jacobs, B. S., and Barna, B. P. (1993). Interleukin-4 down-regulates adult human astrocyte DNA synthesis and proliferation. *Am. J. Pathol.* 143, 337–341.

Eyo, U. B., Murugan, M., and Wu, L. J. (2017). Microglia-neuron communication in epilepsy. *Glia* 65, 5–18. doi: 10.1002/glia.23006

Feyissa, A. M., Hasan, T. F., and Meschia, J. F. (2019). Stroke-related epilepsy. *Eur. J. Neurol.* 26:18–e13. doi: 10.1111/ene.13813

Franco, R., and Fernández-Suárez, D. (2015). Alternatively activated microglia and macrophages in the central nervous system. *Prog. Neurobiol.* 131, 65–86. doi: 10.1016/j.pneurobio.2015.05.003

Friedman, D., Honig, L. S., and Scarmeas, N. (2012). Seizures and epilepsy in Alzheimer's disease. *CNS Neurosci. Ther.* 18, 285–294. doi: 10.1111/j.1755-5949.2011.00251.x

Garg, N., Joshi, R., and Medhi, B. (2018). Cracking novel shared targets between epilepsy and Alzheimer's disease: need of the hour. *Rev. Neurosci.* 29, 425–442. doi: 10.1515/revneuro-2017-0064

Garg, S. K., Kipnis, J., and Banerjee, R. (2009). IFN-γ and IL-4 differentially shape metabolic responses and neuroprotective phenotype of astrocytes. *J. Neurochem.* 108, 1155–1166. doi: 10.1111/j.1471-4159.2009.05872.x

González, O. C., Krishnan, G. P., Timofeev, I., and Bazhenov, M. (2019). Ionic and synaptic mechanisms of seizure generation and epileptogenesis. *Neurobiol. Dis.* 130:104485. doi: 10.1016/j.nbd.2019.104485

Grabenstatter, H. L., Del Angel, Y. C., Carlsen, J., Wempe, M. F., White, A. M., Cogswell, M., et al. (2014). The effect of STAT3 inhibition on status epilepticus and subsequent spontaneous seizures in the pilocarpine model of acquired epilepsy. *Neurobiol. Dis.* 62, 73–85. doi: 10.1016/j.nbd.2013.09.003

Ha, J., Choi, J., Kwon, A., Kim, K., Kim, S. J., Bae, S. H., et al. (2018). Interleukin-4 and tumor necrosis factor-alpha levels in children with febrile seizures. *Seizure* 58, 156–162. doi: 10.1016/j.seizure.2018.04.004

Hammond, T. R., Robinton, D., and Stevens, B. (2018). Microglia and the brain: complementary partners in development and disease. *Annu. Rev. Cell. Dev. Biol.* 34, 523–544. doi: 10.1146/annurev-cellbio-100616-060509

Iori, V., Frigerio, F., and Vezzani, A. (2016). Modulation of neuronal excitability by immune mediators in epilepsy. *Curr. Opin. Pharmacol.* 26, 118–123. doi: 10.1016/j.coph.2015.11.002

Isakson, P. C., Puré, E., Vitetta, E. S., and Krammer, P. H. (1982). T cell-derived B cell differentiation factor(s). Effect on the isotype switch of murine B cells. *J. Exp. Med.* 155, 734–748. doi: 10.1084/jem.155.3.734

Ito, T., Suzuki, S., Kanaji, S., Shiraishi, H., Ohta, S., Arima, K., et al. (2009). Distinct structural requirements for interleukin-4 (IL-4) and IL-13 binding to the shared IL-13 receptor facilitate cellular tuning of cytokine responsiveness. *J. Biol. Chem.* 284, 24289–24296. doi: 10.1074/jbc.m109.007286

Joshi, B. H., Leland, P., Asher, A., Prayson, R. A., Varricchio, F., and Puri, R. K. (2001). *In situ* expression of interleukin-4 (IL-4) receptors in human brain tumors and cytotoxicity of a recombinant IL-4 cytotoxin in primary glioblastoma cell cultures. *Cancer Res.* 61, 8058–8061.

Keegan, A. D., Zamorano, J., Keselman, A., and Heller, N. M. (2018). IL-4 and IL-13 receptor signaling from 4PS to insulin receptor substrate 2: there and back again, a historical view. *Front. Immunol.* 9:1037. doi: 10.3389/fimmu.2018.01037

Latta, C. H., Sudduth, T. L., Weekman, E. M., Brothers, H. M., Abner, E. L., Popa, G. J., et al. (2015). Determining the role of IL-4 induced neuroinflammation in microglial activity and amyloid-β using BV2 microglial cells and APP/PS1 transgenic mice. *J. Neuroinflammation* 12:41. doi: 10.1186/s12974-015-0243-6

Leal, G., Bramham, C. R., and Duarte, C. B. (2017). BDNF and hippocampal synaptic plasticity. *Vitam. Horm.* 104, 153–195. doi: 10.1016/bs.vh.2016.10.004

Le Blon, D., Guglielmetti, C., Hoornaert, C., Quarta, A., Daans, J., Dooley, D., et al. (2016). Intracerebral transplantation of interleukin 13-producing mesenchymal stem cells limits microgliosis, oligodendrocyte loss and demyelination in the cuprizone mouse model. *J. Neuroinflammation* 13:288. doi: 10.1186/s12974-016-0756-7

Li, Z., Liu, F., Ma, H., White, P. F., Yumul, R., Jiang, Y., et al. (2017). Age exacerbates surgery-induced cognitive impairment and neuroinflammation in Sprague-Dawley rats: the role of IL-4. *Brain Res.* 1665, 65–73. doi: 10.1016/j.brainres.2017.04.004

Li, T., Zhai, X., Jiang, J., Song, X., Han, W., Ma, J., et al. (2017). Intraperitoneal injection of IL-4/IFN-γ modulates the proportions of microglial phenotypes and improves epilepsy outcomes in a pilocarpine model of acquired epilepsy. *Brain Res.* 1657, 120–129. doi: 10.1016/j.brainres.2016.12.006

Li, Y. Z., Zhang, L., Liu, Q., Bian, H. T., and Cheng, W. J. (2020). The effect of single nucleotide polymorphisms of STAT3 on epilepsy in children. *Eur. Rev. Med. Pharmacol. Sci.* 24, 837–842. doi: 10.26355/eurrev_202001_20067

Liang, S., Fan, X., Zhao, M., Shan, X., Li, W., Ding, P., et al. (2019). Clinical practice guidelines for the diagnosis and treatment of adult diffuse glioma-related epilepsy. *Cancer Med.* 8, 4527–4535. doi: 10.1002/cam4.2362

Liu, H., Prayson, R. A., Estes, M. L., Drazba, J. A., Barnett, G. H., Bingaman, W., et al. (2000). *In vivo* expression of the interleukin 4 receptor alpha by astrocytes in epilepsy cerebral cortex. *Cytokine* 12, 1656–1661. doi: 10.1006/cyto.2000.0773

Lu, R., Zhang, J., Sun, W., Du, G., and Zhou, G. (2015). Inflammation-related cytokines in oral lichen planus: an overview. *J. Oral Pathol. Med.* 44, 1–14. doi: 10.1111/jop.12142

Mahfoz, A. M., and Shahzad, N. (2019). Neuroinflammation impact in epileptogenesis and new treatment strategy. *Behav. Pharmacol.* 30, 661–675. doi: 10.1097/fbp.0000000000000513

Mashkaryan, V., Siddiqui, T., Popova, S., Cosacak, M. I., Bhattarai, P., Brandt, K., et al. (2020). Type 1 interleukin-4 signaling obliterates mouse astroglia *in vivo* but not *in vitro*. *Front. Cell Dev. Biol.* 8:114. doi: 10.3389/fcell.2020.00114

Michels, M., Danielski, L. G., Dal-Pizzol, F., and Petronilho, F. (2014). Neuroinflammation: microglial activation during sepsis. *Curr. Neurovasc. Res.* 11, 262–270. doi: 10.2174/1567202611666140520122744

Moosa, A. N. V., and Wyllie, E. (2017). Cognitive outcome after epilepsy surgery in children. *Semin. Pediatr. Neurol.* 24, 331–339. doi: 10.1016/j.spen.2017.10.010

Morin-Brureau, M., Milior, G., Royer, J., Chali, F., Leduigou, C., Savary, E., et al. (2018). Microglial phenotypes in the human epileptic temporal lobe. *Brain* 141, 3343–3360. doi: 10.1093/brain/awy276

Muro-García, T., Martín-Suárez, S., Espinosa, N., Valcárcel-Martín, R., Marinas, A., Zaldumbide, L., et al. (2019). Reactive disruption of the hippocampal neurogenic niche after induction of seizures by injection of kainic acid in the amygdala. *Front. Cell Dev. Biol.* 7:158. doi: 10.3389/fcell.2019.00158

Okuneva, O., Körber, I., Li, Z., Tian, L., Joensuu, T., Kopra, O., et al. (2015). Abnormal microglial activation in the Cstb(−/−) mouse, a model for progressive myoclonus epilepsy, EPM1. *Glia* 63, 400–411. doi: 10.1002/glia.22760

Papadimitriou, C., Celikkaya, H., Cosacak, M. I., Mashkaryan, V., Bray, L., Bhattarai, P., et al. (2018). 3D culture method for Alzheimer's disease modeling reveals interleukin-4 rescues Aβ42-induced loss of human neural stem cell plasticity. *Dev. Cell* 46, 85.e8–101.e8. doi: 10.1016/j.devcel.2018.06.005

Park, H. J., Shim, H. S., An, K., Starkweather, A., Kim, K. S., and Shim, I. (2015). IL-4 inhibits IL-1β-induced depressive-like behavior and central neurotransmitter alterations. *Mediators Inflamm.* 2015:941413. doi: 10.1155/2015/941413

Park, S. J., Kim, H., Kim, S. H., Joe, E. H., and Jou, I. (2019). Epigenetic downregulation of STAT6 increases HIF-1α expression *via* mTOR/S6K/S6, leading to enhanced hypoxic viability of glioma cells. *Acta Neuropathol. Commun.* 7:149. doi: 10.1186/s40478-019-0798-z

Pfitzner, E., Kliem, S., Baus, D., and Litterst, C. M. (2004). The role of STATs in inflammation and inflammatory diseases. *Curr. Pharm. Des.* 10, 2839–2850. doi: 10.2174/1381612043383638

Powers, R., Garrett, D. S., March, C. J., Frieden, E. A., Gronenborn, A. M., and Clore, G. M. (1992). Three-dimensional solution structure of human interleukin-4 by multidimensional heteronuclear magnetic resonance spectroscopy. *Science* 256, 1673–1677. doi: 10.1126/science.256.5064.1673

Praet, J., Guglielmetti, C., Berneman, Z., Van Der Linden, A., and Ponsaerts, P. (2014). Cellular and molecular neuropathology of the cuprizone mouse model: clinical relevance for multiple sclerosis. *Neurosci. Biobehav. Rev.* 47, 485–505. doi: 10.1016/j.neubiorev.2014.10.004

Rahaman, S. O., Vogelbaum, M. A., and Haque, S. J. (2005). Aberrant Stat3 signaling by interleukin-4 in malignant glioma cells: involvement of IL-13Rα2. *Cancer Res.* 65, 2956–2963. doi: 10.1158/0008-5472.can-04-3592

Ramantani, G., and Holthausen, H. (2017). Epilepsy after cerebral infection: review of the literature and the potential for surgery. *Epileptic Disord.* 19, 117–136. doi: 10.1684/epd.2017.0916

Rand, R. W., Kreitman, R. J., Patronas, N., Varricchio, F., Pastan, I., and Puri, R. K. (2000). Intratumoral administration of recombinant circularly permuted interleukin-4-Pseudomonas exotoxin in patients with high-grade glioma. *Clin. Cancer Res.* 6, 2157–2165.

Reilly, C., Atkinson, P., Das, K. B., Chin, R. F., Aylett, S. E., Burch, V., et al. (2015). Cognition in school-aged children with "active" epilepsy: a population-based study. *J. Clin. Exp. Neuropsychol.* 37, 429–438. doi: 10.1080/13803395.2015.1024103

Rosciszewski, G., Cadena, V., Auzmendi, J., Cieri, M. B., Lukin, J., Rossi, A. R., et al. (2019). Detrimental effects of HMGB-1 require microglial-astroglial interaction: implications for the status epilepticus -induced

neuroinflammation. *Front. Cell. Neurosci.* 13:380. doi: 10.3389/fncel.2019.00380

Sakuma, S., Halliday, W. C., Nomura, R., Ochi, A., and Otsubo, H. (2014). Increased population of oligodendroglia-like cells in pediatric intractable epilepsy. *Neurosci. Lett.* 566, 188–193. doi: 10.1016/j.neulet.2014.03.002

Samudra, N., Zacharias, T., Plitt, A., Lega, B., and Pan, E. (2019). Seizures in glioma patients: an overview of incidence, etiology and therapies. *J. Neurol. Sci.* 404, 80–85. doi: 10.1016/j.jns.2019.07.026

Sequeida, A., Castillo, A., Cordero, N., Wong, V., Montero, R., Vergara, C., et al. (2020). The Atlantic salmon interleukin 4/13 receptor family: structure, tissue distribution and modulation of gene expression. *Fish Shellfish Immunol.* 98, 773–787. doi: 10.1016/j.fsi.2019.11.030

Shamran, H. A., Hamza, S. J., Yaseen, N. Y., Al-Juboory, A. A., Taub, D. D., Price, R. L., et al. (2014). Impact of single nucleotide polymorphism in IL-4, IL-4R genes and systemic concentration of IL-4 on the incidence of glioma in Iraqi patients. *Int. J. Med. Sci.* 11, 1147–1153. doi: 10.7150/ijms.9412

Shigetomi, E., Saito, K., Sano, F., and Koizumi, S. (2019). Aberrant calcium signals in reactive astrocytes: a key process in neurological disorders. *Int. J. Mol. Sci.* 20:996. doi: 10.3390/ijms20040996

Singhi, P. (2011). Infectious causes of seizures and epilepsy in the developing world. *Dev. Med. Child Neurol.* 53, 600–609. doi: 10.1111/j.1469-8749.2011.03928.x

Sinha, S., Patil, S. A., Jayalekshmy, V., and Satishchandra, P. (2008). Do cytokines have any role in epilepsy? *Epilepsy Res.* 82, 171–176. doi: 10.1016/j.eplepsyres.2008.07.018

Sofroniew, M. V. (2009). Molecular dissection of reactive astrogliosis and glial scar formation. *Trends Neurosci.* 32, 638–647. doi: 10.1016/j.tins.2009.08.002

Standiford, T. J., Strieter, R. M., Chensue, S. W., Westwick, J., Kasahara, K., and Kunkel, S. L. (1990). IL-4 inhibits the expression of IL-8 from stimulated human monocytes. *J. Immunol.* 145, 1435–1439.

Sun, Z., Yan, X., Liu, Y., Huang, L., Kong, C., Qu, X., et al. (2017). Application of dual targeting drug delivery system for the improvement of anti-glioma efficacy of doxorubicin. *Oncotarget* 8, 58823–58834. doi: 10.18632/oncotarget.19221

Tang, R. H., Qi, R. Q., and Liu, H. Y. (2019). Interleukin-4 affects microglial autophagic flux. *Neural Regen. Res.* 14, 1594–1602. doi: 10.4103/1673-5374.255975

Tay, T. L., Savage, J. C., Hui, C. W., Bisht, K., and Tremblay, M. (2017). Microglia across the lifespan: from origin to function in brain development, plasticity and cognition. *J. Physiol.* 595, 1929–1945. doi: 10.1113/jp272134

Te Velde, A. A., Huijbens, R. J., Heije, K., De Vries, J. E., and Figdor, C. G. (1990). Interleukin-4 (IL-4) inhibits secretion of IL-1 β, tumor necrosis factor alpha and IL-6 by human monocytes. *Blood* 76, 1392–1397. doi: 10.1182/blood.v76.7.1392.1392

Tsai, F. J., Chou, I. C., Hsieh, Y. Y., Lee, C. C., Lin, C. C., and Tsai, C. H. (2002). Interleukin-4 intron 3 polymorphism is not related to susceptibility to febrile seizures. *Pediatr. Neurol.* 27, 271–274. doi: 10.1016/s0887-8994(02)00434-4

Umeshita-Suyama, R., Sugimoto, R., Akaiwa, M., Arima, K., Yu, B., Wada, M., et al. (2000). Characterization of IL-4 and IL-13 signals dependent on the human IL-13 receptor alpha chain 1: redundancy of requirement of tyrosine residue for STAT3 activation. *Int. Immunol.* 12, 1499–1509. doi: 10.1093/intimm/12.11.1499

Valtorta, F., Pennuto, M., Bonanomi, D., and Benfenati, F. (2004). Synaptophysin: leading actor or walk-on role in synaptic vesicle exocytosis? *Bioessays* 26, 445–453. doi: 10.1002/bies.20012

Vezzani, A., Balosso, S., and Ravizza, T. (2019). Neuroinflammatory pathways as treatment targets and biomarkers in epilepsy. *Nat. Rev. Neurol.* 15, 459–472. doi: 10.1038/s41582-019-0217-x

Vezzani, A., Friedman, A., and Dingledine, R. J. (2013). The role of inflammation in epileptogenesis. *Neuropharmacology* 69, 16–24. doi: 10.21236/ada583972

Wang, N., Mi, X., Gao, B., Gu, J., Wang, W., Zhang, Y., et al. (2015). Minocycline inhibits brain inflammation and attenuates spontaneous recurrent seizures following pilocarpine-induced status epilepticus. *Neuroscience* 287, 144–156. doi: 10.1016/j.neuroscience.2014.12.021

Wertheim, W. A., Kunkel, S. L., Standiford, T. J., Burdick, M. D., Becker, F. S., Wilke, C. A., et al. (1993). Regulation of neutrophil-derived IL-8: the role of prostaglandin E2, dexamethasone and IL-4. *J. Immunol.* 151, 2166–2175.

Xu, Z., Xue, T., Zhang, Z., Wang, X., Xu, P., Zhang, J., et al. (2011). Role of signal transducer and activator of transcription-3 in up-regulation of GFAP after epilepsy. *Neurochem. Res.* 36, 2208–2215. doi: 10.1007/s11064-011-0576-1

Yang, J., Ding, S., Huang, W., Hu, J., Huang, S., Zhang, Y., et al. (2016). Interleukin-4 ameliorates the functional recovery of intracerebral hemorrhage through the alternative activation of microglia/macrophage. *Front. Neurosci.* 10:61. doi: 10.3389/fnins.2016.00061

Yao, X., Jiang, Q., Ding, W., Yue, P., Wang, J., Zhao, K., et al. (2019). Interleukin 4 inhibits high mobility group box-1 protein-mediated NLRP3 inflammasome formation by activating peroxisome proliferator-activated receptor-γ in astrocytes. *Biochem. Biophys. Res. Commun.* 509, 624–631. doi: 10.1016/j.bbrc.2018.11.145

Zare-Shahabadi, A., Soltani, S., Ashrafi, M. R., Shahrokhi, A., Zoghi, S., Pourakbari, B., et al. (2015). Association of IL4 single-nucleotide polymorphisms with febrile seizures. *J. Child Neurol.* 30, 423–428. doi: 10.1177/0883073814551389

Zhang, Q., Zhu, W., Xu, F., Dai, X., Shi, L., Cai, W., et al. (2019). The interleukin-4/PPARγ signaling axis promotes oligodendrocyte differentiation and remyelination after brain injury. *PLoS Biol.* 17:e3000330. doi: 10.1155/1751

Zhu, V. F., Yang, J., Lebrun, D. G., and Li, M. (2012). Understanding the role of cytokines in glioblastoma multiforme pathogenesis. *Cancer Lett.* 316, 139–150. doi: 10.1016/j.canlet.2011.11.001

Conflict of Interest: The authors declare that the research was conducted in the absence of any commercial or financial relationships that could be construed as a potential conflict of interest.

frontiers in Molecular Neuroscience

REVIEW
published: 23 February 2021
doi: 10.3389/fnmol.2021.612073

Neuropathophysiological Mechanisms and Treatment Strategies for Post-traumatic Epilepsy

*Shaunik Sharma, Grant Tiarks, Joseph Haight and Alexander G. Bassuk**

Medical Laboratories, Department of Pediatrics, University of Iowa, Iowa City, IA, United States

Traumatic brain injury (TBI) is a leading cause of death in young adults and a risk factor for acquired epilepsy. Severe TBI, after a period of time, causes numerous neuropsychiatric and neurodegenerative problems with varying comorbidities; and brain homeostasis may never be restored. As a consequence of disrupted equilibrium, neuropathological changes such as circuit remodeling, reorganization of neural networks, changes in structural and functional plasticity, predisposition to synchronized activity, and post-translational modification of synaptic proteins may begin to dominate the brain. These pathological changes, over the course of time, contribute to conditions like Alzheimer disease, dementia, anxiety disorders, and post-traumatic epilepsy (PTE). PTE is one of the most common, devastating complications of TBI; and of those affected by a severe TBI, more than 50% develop PTE. The etiopathology and mechanisms of PTE are either unknown or poorly understood, which makes treatment challenging. Although anti-epileptic drugs (AEDs) are used as preventive strategies to manage TBI, control acute seizures and prevent development of PTE, their efficacy in PTE remains controversial. In this review, we discuss novel mechanisms and risk factors underlying PTE. We also discuss dysfunctions of neurovascular unit, cell-specific neuroinflammatory mediators and immune response factors that are vital for epileptogenesis after TBI. Finally, we describe current and novel treatments and management strategies for preventing PTE.

Keywords: traumatic brain injury, post-traumatic epilepsy, excitotoxicity, neuroinflammation, oxidative stress, neurodegeneration, immune response, clinical management

OPEN ACCESS

Edited by:
Tobias Engel,
Royal College of Surgeons in Ireland, Ireland

Reviewed by:
Edward Haig Beamer,
Royal College of Surgeons in Ireland, Ireland
Fernando Peña-Ortega,
National Autonomous University of Mexico, Mexico

***Correspondence:**
Alexander G. Bassuk
alexander-bassuk@uiowa.edu

Received: *30 September 2020*
Accepted: *26 January 2021*
Published: *23 February 2021*

Citation:
Sharma S, Tiarks G, Haight J and Bassuk AG (2021) Neuropathophysiological Mechanisms and Treatment Strategies for Post-traumatic Epilepsy. Front. Mol. Neurosci. 14:612073. doi: 10.3389/fnmol.2021.612073

INTRODUCTION

More than 3 million people in United States suffer a TBI each year. Among these cases, 80% are mild, 10% moderate, and about 10% severe, accounting for ∼300,000 hospitalizations and ∼50,000 fatalities, annually (Maas et al., 2017). Many traumatic brain injuries cause long-term disabilities, cognitive decline, psychiatric illness, and post-traumatic disorders. About 35% of TBI result from falls, 17% from motor vehicle accidents, and 10% from assaults, while in 21% of the cases, the cause was not recorded (Ding et al., 2016; Centers for Disease Control and Prevention, 2019). Incidence rates are higher in both males and females up to 9 years of age, during teen years, and towards the end of life (>74 years of age). Approximately, 2% of U.S. population live with long-lasting disabilities

stemming from TBI; and is one of the single greatest causes of deaths and permanent disability in people under the age of 45 (Maas et al., 2017). The total estimated annual cost for TBI treatment is over $56.3 billion (Faul and Coronado, 2015; Maas et al., 2017). Currently, no available therapies can limit secondary injury or foster repair and regeneration.

Traumatic brain injury can trigger seizures and account for 4% of epilepsy cases (Gupta et al., 2014). New-onset symptomatic epilepsy in adolescents and young adults is most often caused by developmental disorders, infections, skull fracture, intracranial hemorrhage, and subarachnoid or subdural hemorrhage. In contrast, amongst older populations, intracranial hematoma, strokes and tumors are more common causes (Mahler et al., 2015). More than 50% of people develop PTE after severe TBI. According to the American Academy of Neurology, severe TBI is defined as the condition in which a person stays in coma for longer than 24 h post-injury or requires a neurosurgical intervention. Among those who develop epilepsy after severe TBI, nearly 40% experience their first seizure within 6 months of injury, 50–60% within a year and about 80% in the later years of life (Annegers et al., 1998; Agrawal et al., 2006; Pohlmann-Eden et al., 2006; Ding et al., 2016).

Traumatic brain injury is the third most common cause of all epilepsies and results from either direct (primary) or indirect (secondary) damage to brain parenchyma (Kaur and Sharma, 2018; Fordington and Manford, 2020). Trauma or brain injury results in both focal and diffuse injury to the central nervous system (CNS) that can trigger epileptogenesis (Shlosberg et al., 2010; Webster et al., 2017). Focal injuries usually cause contusion, hemorrhage, infarction, and necrosis, causing cortical scarring that effects synaptic plasticity and recovery. On the other hand, diffuse injury leads to axonal shearing, microvasculature damage, release of inflammatory mediators, and free radical overload (Greenfield et al., 2008; Mckee and Daneshvar, 2015). These injuries sabotage vulnerable neuronal populations and white matter tracts; and reactive gliosis that follow neuroinflammation (Wang et al., 2008; Lamar et al., 2014). Later, secondary injury mechanisms reorganize the neural circuits and disrupt brain homeostasis, with the degree of secondary damage largely depending on the severity of primary damage. A mild injury may deteriorate and remodel neural circuits to a lesser extent, whereas a severe insult not only reorganizes neural networks but also cause long-term degenerative changes that results in neuropsychiatric conditions, and cognitive and behavioral deficits (Burda et al., 2016; Ladak et al., 2019). For instance, the release of glutamate after severe head injury causes excitotoxic cell death via excessive calcium release, and generation of free radicals such as reactive oxygen and nitrogen species (ROS/RNS), which elicit an oxidative response against the mitochondria. Further, the recruitment of glial cells and peripheral immune cells (such as leucocytes and macrophages) aggravate the neuroinflammatory response by secreting cytokines. This enhanced proinflammatory response, combined with endothelial ROS, deteriorates the blood-brain barrier (BBB) integrity (Rosenfeld et al., 2012). These combined mechanisms of primary and secondary insults commence a vicious cycle of neurodegenerative events that persist for months to years, executing permanent degenerative changes in the brain (**Figure 1**). This review highlights cellular and molecular mechanisms that promote seizures, epileptogenesis and epilepsy after TBI. We also discuss the role of immune system, contribution of glial cells, long-term consequences of TBI and therapeutic strategies for managing PTE.

MOLECULAR MECHANISMS OF POST-TRAUMATIC EPILEPSY

Hyperexcitability/Excitotoxicity and BBB Breakdown in TBI

Hyperexcitability/Excitotoxicity

After TBI, excitotoxicity in the brain is generally caused by an increase in extracellular glutamate. Under physiological conditions, glutamate is taken up by astrocytes and converted into glutamine which is then shuttled back to neurons as an alternative energy source (Dienel, 2014). However, excess glutamate overloads astrocytes' capacity to remove glutamate from the extracellular space (ECS), triggering an enormous Ca^{2+} and Na^{+} influx and K^{+} efflux (Tehse and Taghibiglou, 2019). This resulting ionic imbalance depolarizes the postsynaptic cell membrane, causing a long-lasting increase in excitatory post-synaptic potential. Altered calcium signaling after TBI activates nitric oxide synthase (NOS), proteases, and lipases that trigger cell signaling cascades linked to excitotoxicity and cell death (Weber, 2012; Jarrahi et al., 2020). Elevations in nitric oxide (NO) levels interferes with mitochondrial bioenergetics leading to energy depletion, further adding oxidative stress in neurons. The changes in mitochondrial bioenergetics initiate the release of cytochrome-c- activating caspases, that cause inflammation-induced apoptosis (Adam-Vizi and Starkov, 2010; Rowley and Patel, 2013; Puttachary et al., 2015). Compromise to mitochondrial integrity after TBI elicits the release of ROS/RNS, which deteriorates membrane lipids, proteins, and DNA, and downregulates the expression of glutamate transporters such as GLT-1 and GLAST promoting cellular excitotoxicity (Trotti et al., 1998; Abdul-Muneer et al., 2015; Chen et al., 2020). TBI-induced ATP depletion cause loss of Na^{+}/K^{+} ion concentration gradient across the plasma membrane due to dysfunctional Na^{+}/K^{+}-ATPase, and leads to excitotoxicity-induced cell stress (Lima et al., 2008). In addition to dysfunctional Na^{+}/K^{+}-ATPase induced excitotoxicity, cell death via lysis or apoptosis also releases cytoplasmic glutamate in ECS after TBI (Zhang et al., 2005). These two forms of glutamate release cause a continual domino effect of cellular excitability that elevates extracellular glutamate concentration in the injured brain.

Numerous *in vivo* studies on rodent models of TBI have reported an increased glutamate levels in the brain of injured mice, 1–2 days post-injury (Hinzman et al., 2010; Guerriero et al., 2015). *Ex vivo* studies on brain slices using extracellular field potential recordings have reported elevations in excitatory inputs and evoked synaptic connections between dentate granule cells with mossy fibers, when stimulated with glutamate photostimulation in controlled cortical impact (CCI) model

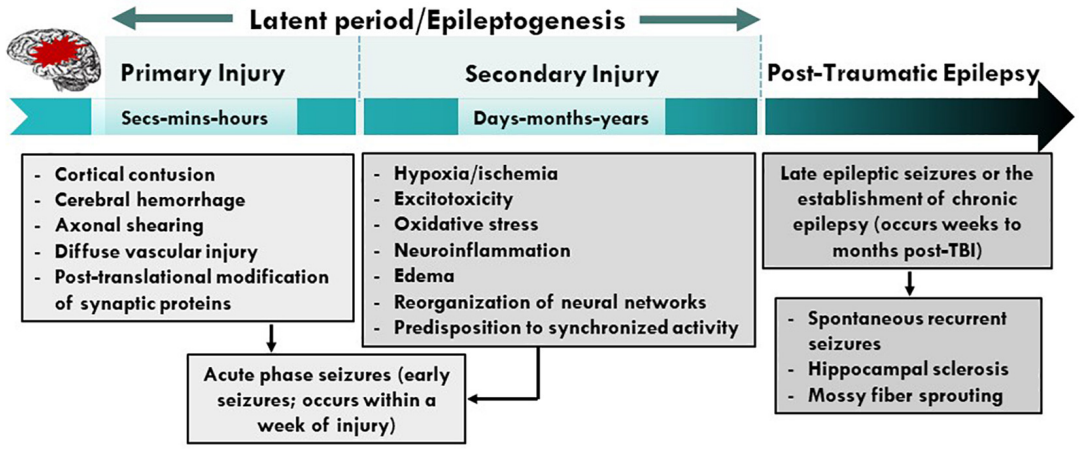

FIGURE 1 | Pathophysiological basis of epileptogenesis following TBI. Complex and multifaceted events triggered during primary injury contribute to secondary injury. These primary and secondary events, which take place over months or years, represent a period of epileptogenesis. Changes such as post-translational modifications of synaptic proteins, reorganization of neural circuits and production and activation of neuroinflammatory molecules/pathways result in PTE. PTE is a progressive process which is a result of mossy fiber sprouting, hippocampal sclerosis, neuroinflammation, neurodegeneration and SRS. PTE, post-traumatic epilepsy; SRS, spontaneous recurrent seizures.

(Hunt et al., 2010). Similar studies, using FRET-based glutamate sensors on hippocampal slices, also reported enhanced cortical excitability and glutamatergic signaling, and increased spread of perforant-path stimulation evoked depolarization in brain slices of CCI and weight drop animals, 2–4 weeks post-injury (Golarai et al., 2001; Cantu et al., 2015). These and other studies confirmed that increase in glutamate response after injury modulate neuronal microcircuits that correlates with an increase in epileptiform activity adjacent to the site of injury.

Blood-Brain Barrier Breakdown in TBI

Blood-brain barrier disruption has a well-recognized role in the pathophysiology of CNS diseases; and understanding the anatomy and physiology of the neurovascular unit in health and disease is critical for advancing translational research into the clinics. Many studies demonstrated that BBB integrity is lost in CNS diseases such as meningitis, encephalitis, Alzheimer disease, Parkinson's disease, multiple sclerosis, and epilepsy. Damage to the components of neurovascular unit (NVU) such as endothelial cells, after TBI, can impair BBB. Dysfunctional endothelial cell signaling and activation of the immune cell response stimulates the release of proinflammatory mediators, such as ROS, matrix metalloproteinases (MMPs), bradykinins, prostaglandins, cytokines, tachykinins, and excitatory amino acids (Paudel et al., 2019). The formation of intercellular adhesion molecule 1 and vascular cell adhesion protein 1/ERM complex with integrin, via Rac1, releases NADPH oxidase (enzyme involved in oxidative stress) in the endothelial cells generating ROS (Cerutti and Ridley, 2017; Jarrahi et al., 2020). Elevations in ROS levels stimulate the release of MMP-2 and 9 causing damage to tight and gap junction proteins such as occludins, claudins and connexin-43. A further rise in oxidative stress activates focal adhesion kinase, a non-receptor tyrosine kinase, and heat-shock protein 27, that results in receptor endocytosis and stress fiber formation within the cell (Hemphill et al., 2011; Cerutti and Ridley, 2017; Jarrahi et al., 2020). In addition, vascular endothelial growth factor stimulated increase in Src increases phosphorylation of VE-cadherins via serine/threonine-protein kinase, which results in receptor endocytosis. Concurrently, an increase in intracellular calcium activates calcium/calmodulin complex that generates endothelial nitric oxide synthase (eNOS). Rise in eNOS levels inhibits the transcription of claudin-5 and occludin, further increasing BBB permeability (Badaut et al., 2015; Andrews et al., 2016; Cerutti and Ridley, 2017) (**Figure 2**). An activation of inflammation and the immune response triggers a heightened neuronal response, stimulating neurotransmitter release from the endothelial cells via activation of the central-mediated hypothalamic-pituitary-adrenal axis (Licinio and Frost, 2000; Silverman et al., 2005; Burfeind et al., 2016). These deleterious events initiate multiple signaling transduction pathways, causing changes in BBB permeability and activation of signaling enzymes, such as kinases, to regulate calcium mobilization and gene expression. This affects the transport characteristics of proteins located on endothelial cells, promoting excitotoxicity (Dalal et al., 2020). Therefore, changes in BBB permeability and enhanced endothelial paracellular leak (due to tight junction protein modifications) alter the volume regulators that control BBB homeostasis. This alters tight junction proteins, leading to reorganization and remodeling of the cytoskeletal proteins disrupting brain homeostasis (Stamatovic et al., 2008; Burda et al., 2016).

After TBI, loss in BBB integrity is primarily due to the release of excitotoxic factors by injured neurons and activated glial cells. These factors drive blood cell chemotaxis and their transmigration into the brain. Enhanced leukocyte infiltration and invasion of CNS parenchyma generates a cytokine storm which induces neuronal injury. Infiltration of leukocytes also increases accumulation of intracellular fluid

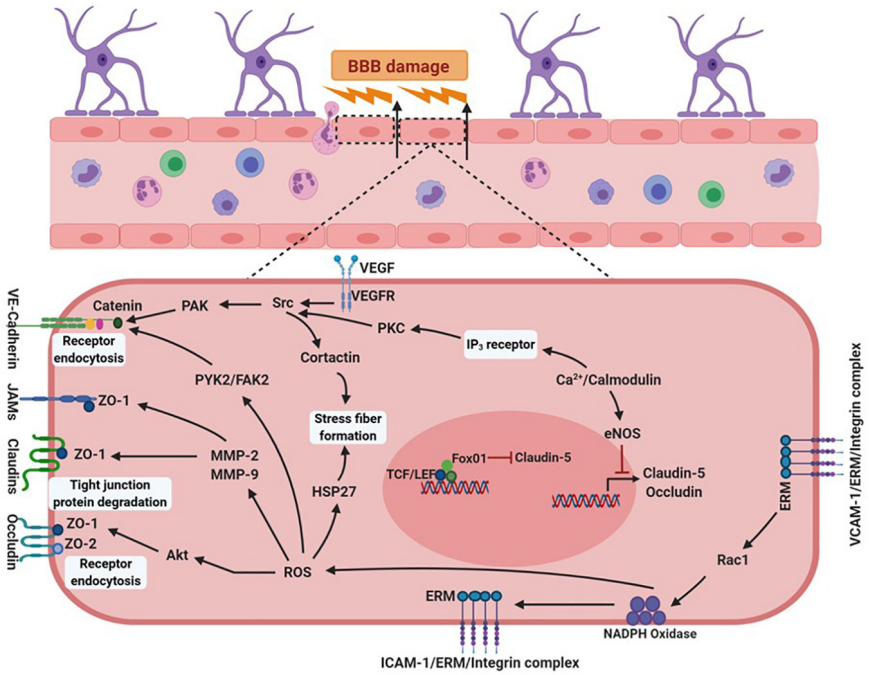

FIGURE 2 | Vascular endothelial signaling after brain injury. In a brain inflicted with traumatic injury, inflammatory conditions stimulate signaling pathways in the cells of NVU. Cytokines TNFα and IL-1 released from blood cells activate receptors present on the vascular lumen near the sites of inflammation. These cytokines upregulate expression of selectins, chemokines, and integrin ligands like ICAM-1 and VCAM-1 on the surface of the endothelial cells, causing increased production of NADPH oxidase. Elevations in NADPH oxidase-mediated release of ROS degrades tight and gap junction proteins such as occludins, claudins and connexins, by generating excessive amounts of Akt and MMPs (MMP-2 and MMP-9). Oxidative stress enhances the production of FAK2, that damages adhesion molecules, cadherins. Alternatively, increased calcium inside the cell activates IP_3 receptors resulting in increased PKC production, which in turn generates PAK via phosphorylation of Src kinase. PAK is also activated by Src phosphorylation via the activation of VEGF receptors. These events collectively damage cadherins compromising integrity of cellular junctions. Elevations in calcium levels also produces eNOS, which blocks claudin-5 and occluding transcription. These events cause BBB breakdown, allowing increased migration of peripheral immune cells into the central nervous system. NVU, neurovascular unit; ICAM-1, intercellular adhesion molecule 1; VCAM-1, vascular cell adhesion protein 1; MMPs, matrix metallopeptidase; FAK2, focal adhesion kinase 2. Figure created with BioRender.com and R&D Systems.

and capillary pressure causing turnover in the transendothelial volume. This can lead to traumatic brain edema exemplifying a transcytosis response to injury (Castejon, 1984; Scallan et al., 2010). Additionally, concurrent modifications take place in glial cells that drive morphological and molecular changes in order to attain reactive morphology. Increased proinflammatory secretions from neurons and reactive glial cells facilitate recruitment of additional immune cells, such as neutrophils and monocytes, from the periphery further modulating brain activity by increasing proinflammatory receptor expression on their surface. The binding of molecules released by neighboring glial cells and injured neurons cause activation of these receptors, exacerbating neuronal excitotoxicity (Medzhitov, 2008; Aronica et al., 2012; Burda and Sofroniew, 2014; Sanz and Garcia-Gimeno, 2020). Increased blood immune cell infiltration and dysfunctional neuro-glia crosstalk cause further rise in cytokine storm, therefore damaging BBB and its components (**Figure 3**).

Pericytes in traumatic brain injury

Traumatic brain injury can have deleterious effects on the neurovascular unit (NVU). Pericytes, an important component of NVU found in capillaries around the brain and other regions, play an important role in the maintenance of BBB, angiogenesis, regulation of blood flow and immune cell movement in the brain (Brown et al., 2019). After brain injury, dysfunctions in pericyte signaling results in the loss of pericyte–endothelium interactions, allowing easy passage for neurotoxins from the blood to enter brain. *In vivo* studies on the mouse model of TBI have reported reduced expression of pericyte markers, platelet-derived growth factor-B (PDGF-B), NG2 and CD13, 24 h post lateral fluid percussion injury (LFPI). Reduction in these markers also corresponds to a decrease in tight and gap junction proteins (Bhowmick et al., 2019). Alterations in these proteins cause increased water permeability in the brain due to a substantial changes in aquaporin (AQP4) expression around the perivascular region. These studies also reported higher expression of calcium binding protein and a reactive astrocyte marker, S100β, and neuron-specific enolase in the blood samples of TBI animals (Bhowmick et al., 2019). Using two different adult viable pericyte deficiency mouse strains with variable degrees of pericyte loss, Bell et al. (2010) demonstrated that pericyte loss during neurodegenerative conditions can influence brain capillary density, resting cerebral blood flow, blood flow responses to brain activation and blood brain integrity to serum proteins, and blood derived cytotoxic and neurotoxic molecules. Using *in vivo* multiphoton microscopy on mouse

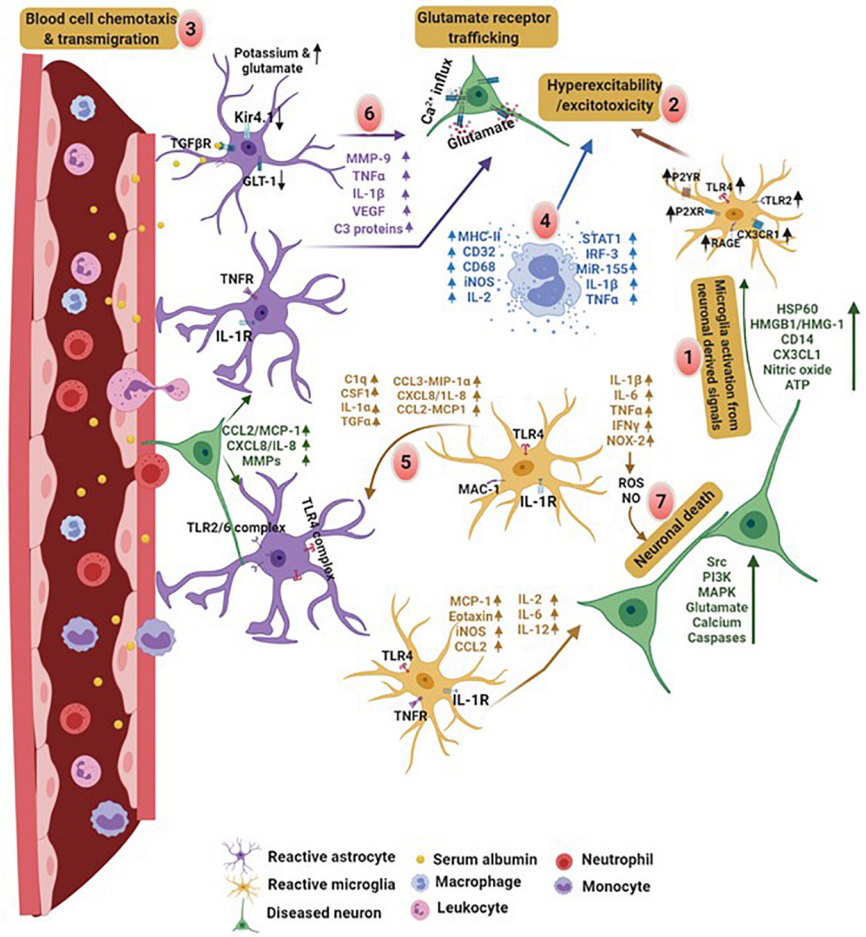

FIGURE 3 | Comprised BBB integrity and neuro-glia crosstalk in PTE. Proinflammatory factors released by damaged neurons and glial cells initiate a vicious cycle of inflammation in the brain. **(1)** Brain injury results in an early activation of microglia and stimulate production of cytokines and expression of DAMPs associated receptors on their surface, leading to neuronal excitability. **(2)** Increased cellular hyperexcitability due to molecules released by reactive glia and neurons promote, **(3)** blood cell chemotaxis and transmigration into the brain. Disruption in BBB leads to brain infiltration of immune cells from the blood releasing **(4)** proinflammatory factors and promoting excitotoxicity. **(5)** Later, activated microglia release signals that bind to the receptors on astrocytes. **(6)** Serum albumin induced activation of astrocytes impairs potassium channel and glutamate transporter. In addition, activated astrocytes release proinflammatory factors which exacerbates neuronal hyperexcitability. **(7)** These factors collectively or on their own cause neurodegeneration. Cytokine mediated crosstalk between astrocyte-microglia and neuro-glia induces hyperexcitability and neuronal cell death. In contrast, molecules derived from neurons, such as HSP60, HMGB1, CD14, CX3CL1, and ATP, cause microglia activation leading to excitotoxicity. Monocytes and leukocytes also release cytokines at this point. This creates an activation cycle which causes release of additional inflammatory molecules triggering cytokine storm in the brain. Discharge of molecules like MHCII, complementary proteins, proinflammatory interleukins, iNOS, transcription factors and microRNAs by macrophages, cause excitotoxicity in neurons. These molecules promote neurodegeneration and initiate neuroinflammatory pathways lowering the seizure threshold. HSP60, heat shock proteins; HMGB1, high mobility group box 1; CD14, cluster of differentiation 14; CX3CL1, chemokine (C-X3-C motif) ligand 1; ATP, adenosine 5′-triphosphate; iNOS, inducible nitric oxide synthase. Figure created with BioRender.com (2020). Retrieved from https://app.biorender.com/biorender-templates.

lines expressing PDGFRβ^{+} exclusively on pericytes, the same group further reported a significant reduction in the length of perfused capillaries that corresponded to a reduction in cerebral blood flow volume (Bell et al., 2010). BBB disruption after TBI causes dysfunction in pericyte-endothelium interaction and increase in toxic accumulation of serum derived proteins in the brain. Using time-lapse imaging of a low-molecular weight 40 KDa TMR-Dextran, studies have reported diminished brain capillary perfusion and changes in vascular permeability in PDGFRβ$^{-/-}$deficient mice. Golgi histological analysis of neuronal structure and function revealed progressive loss of dendritic spines and significant structural abnormalities in CA1 region of hippocampus in PDGFRβ heterozygous mice at 8 and 16 months of age, supporting a crucial role of pericytes in neurovasculature (Bell et al., 2010). Studies on mouse models of TBI have shown diminished pericyte-endothelium interactions showing reduced oxygenation in ipsilateral and contralateral areas of the somatosensory cortex, as well as other regions of the brain, during early stages of TBI (Johnstone et al., 2014; Zehendner et al., 2015; Ichkova et al., 2020).

Using acute brain slices and vascular staining, studies reported changes in neurovascular reactivity and morphological variations in the blood vessels of mice, 1 and 30 days post-injury (dpi). These changes reversed during early and late stages, revealing time-dependent alterations in the neurovasculature and dysfunction in oxygenation and vascular coupling (Ichkova et al., 2020). The results from these and other studies suggest that neurodegenerative changes develop following a primary vascular insult which impairs pericyte–endothelium interactions. Disruption in pericyte signaling alters brain microcirculation causing diminished brain capillary perfusion. This leads to chronic perfusion stress and cellular and molecular alterations of BBB, which includes, changes in transport functions of endothelium, loss of pericytes, decrease in cerebral blood flow, loss of vascular reactivity, changes in vascular morphology, alterations in glial metabolic rate and oxygen deficiency in tissues. These post traumatic brain injury events lead to cellular excitotoxicity and chronic neurodegeneration (Bell et al., 2010; Wu et al., 2020).

Oxidative Stress and Neurodegeneration

Oxidative Stress

Mitochondrial dysfunction has long been recognized as a key source of oxidative stress in epilepsy. Emerging evidence suggests that acute seizures induce oxidative stress, and as a result of initial insult, the process of epileptogenesis begins to dominate the brain (Patel, 2004; Liang and Patel, 2006). During oxidative stress, deleterious changes in mitochondria include altered mitochondrial membrane potential, enhanced nicotinamide adenine dinucleotide phosphate (NADPH) production, impairment of electron transport chain complex 1, 3, and 4, rise in mitochondrial ROS, and mitochondrial DNA damage (Dexter et al., 1989; Cini and Moretti, 1995; Chuang et al., 2004; Kann et al., 2005; Chuang, 2010). These changes in mitochondrial activity cause progressive dysfunction, aligning with a common theme of epileptogenesis as a series of degenerative events that triggers a vicious cycle of oxidative stress and neurodegeneration, ultimately leading to PTE (Vezzani et al., 2011).

Free Radicals of Oxygen and Nitrogen

Free radicals are generated by oxidation and reduction reactions of electrons during hemolytic cleavage, when the bond is broken in such a way that the pair of electrons is shared equally by both the separating fragments. These separating fragments may carry one or more unpaired electrons, which makes free radicals highly reactive in nature. Free radicals are chemically unstable molecules that cause cellular and mitochondrial DNA fragmentation (Lobo et al., 2010; Cardenas-Rodriguez et al., 2013; Ozcan and Ogun, 2015). As a result of oxidative damage, alterations in morphological and functional properties of proteins and lipids takes place. This further impacts cellular and mitochondrial DNA, and cross-link base pairs and cause genetic mutations (Emerit et al., 2004; Waldbaum and Patel, 2010; Ramalingam and Kim, 2012). Free radical species of oxygen and nitrogen include superoxide anion, hydroxyl radical (OH), peroxyl and alkoxyl radicals, hydrogen peroxide (H_2O_2), peroxynitrite, nitroxyl anion, nitrogen dioxide and nitrate/nitrite (Cheeseman and Slater, 1993; Ozcan and Ogun, 2015; Puttachary et al., 2015). An excessive generation of these radicals within the cell causes oxidative stress.

Free Radical Production and Oxidative Stress

Oxidative stress is a biochemical state when an excessive production of ROS/RNS cause damage to the cell membranes and proteins, as well as to cellular and mitochondrial genomes (Cardenas-Rodriguez et al., 2013). Majority of oxygen and nitrogen-centered free radicals are generated from interactions between NO and molecular oxygen (O_2). NO is produced from the substrate L-arginine, with the help of a co-factor NADPH and O_2, and enzyme nitric oxide synthase (NOS). In the cytoplasmic membrane, superoxides are primarily generated by NADPH oxidase, after an electron transfer from NADPH to O_2. These superoxides are also generated by the action of O_2 on xanthine oxidase. Under normal physiological conditions, superoxides are converted into H_2O_2 by the action of superoxide dismutase, which is then broken down into water and oxygen (with the help of catalase and glutathione peroxidase). Degradation of superoxide dismutase promotes enhanced production of highly reactive peroxynitrites ($ONOO^-$), a powerful oxidizing agent, which results in increased ROS production, DNA, proteins and lipids oxidation and loss of ion channel dysfunction (Halliwell, 1999; Puttachary et al., 2015). Increased superoxide in a cell cause oxidative burst promoting oxidative damage by exacerbating inflammation, enhancing redox signaling and proinflammatory gene regulation (Agledal et al., 2010). Moreover, impairment of catalase and peroxides promote formation of hypochlorous acid from H_2O_2 by reacting with Cl^-, NO^{2-} and phenols. This causes cell death by destabilizing calcium homeostasis. Alternatively, H_2O_2 can also undergo Fenton and Haber–Weiss reaction to form OH radicals (a harmful free radical of oxygen with high reactivity and a short half-life) which results in proteins and lipid peroxidation, mitochondrial DNA damage and depletion of antioxidant enzymes (Bae et al., 2011; Puttachary et al., 2015).

The metabolic regulation and signaling of redox enzymes, such as NADPH oxidase, lipoxygenase and endoperoxide synthase is exceedingly altered after TBI. At basal levels, NADPH oxidase (NOX-2) is expressed widely in the brain where it plays an important role in learning, memory consolidation, innate immunity, phagocytic activity and apoptosis (Infanger et al., 2006; Aguiar et al., 2012; Eastman et al., 2020). However, under pathological conditions, such as in PTE, NADPH oxidase generates greater amounts of superoxide ions, triggering neuroinflammation and neurodegeneration, as evidenced by various animal models of TBI and chemoconvulsant-induced TLE (Ferreira et al., 2013; Angeloni et al., 2015; Ma et al., 2017; Eastman et al., 2020). For instance, Li et al. (2019) on the chemical induced brain injury model of mice, reported the accumulation of oxidative stress factors such as lipid ROS and 4-hydroxy-2-nonenal (4-HNE) adducts in the somatosensory cortex and hippocampal HT22 cells, 12–36 h post-injury. The same group also discussed the involvement of oxidative enzyme 12/15 lipoxygenase (12/15-LOX) associated ferroptosis in a trauma induced neuronal damage, that corresponds to reduced

cell viability and glutathione peroxidase 4 activity in the cortex of mice and in hippocampal cultures (Li et al., 2019). 12/15 LOX plays an important role in modulating oxidative stress and increase post-traumatic seizures by generating oxidized phospholipids (Chinnici et al., 2005). In a study on the rat model of LFPI, Saraiva et al. (2012) demonstrated that an increased levels of thiobarbituric acid and protein carbonylation contents in the brain increased seizure and spiking activity, within a week after injury (Saraiva et al., 2012). These and other studies provide a strong evidence and the significance of synergistic interactions between the redox enzymes in maintaining TBI-induced oxidative stress. In addition, detrimental role of prostaglandin-endoperoxide synthase, such as cyclooxygenase (COX-2) have also widely been reported in various clinical and experimental models of TBI and epilepsy. COX-2 upregulates ROS by producing prostaglandins (specifically, F2 and H), and stimulate astrocytes to produce proinflammatory cytokines which signals for oxidative stress-mediated neuronal death (Madrigal et al., 2006; Hickey et al., 2007; Rojas et al., 2014). COX-2 also initiates inflammatory response in immune cells such as neutrophils and alters tissue homeostasis (Ricciotti and FitzGerald, 2011). Interactions between NOS and COX-2, after brain injury, can affect neocortical development by creating pathological milieu (Kaufmann et al., 1997). Studies on immature rats have reported enhanced COX-2 expression after TBI, that corresponds to an increased NOS and prostaglandin synthesis. Studies have shown that increased lesion size after TBI, corresponds with an increased COX-2 expression, that leads to impaired cognitive deficits in rats (Hickey et al., 2007). These studies demonstrate that the accumulation of oxidative stress factors, after TBI, cause increased cytokine levels, NO metabolites, oxidative enzymes, protein carbonylation contents, SRS and memory deficits over time- which altogether may lead to PTE (**Table 1**). Inhibition of these enzymes have been shown to prevent cognitive deficits, motor dysfunctions, cerebral edema, cerebral perfusion rate, neurodegeneration and neuroinflammation, in many clinical and animal models (Madrigal et al., 2006; Zhang et al., 2012; Ferreira et al., 2013; Liu et al., 2016; Li et al., 2019). Therefore, targeting these molecules can provide neuroprotection against TBI-induced epileptogenesis.

Neurodegeneration

Depending on the molecular mechanisms affected, neuronal cell death in TBI is classified as either physiologic or excitotoxic. Physiologic cell death is due to injuries that initiate cellular events such as mitochondrial swelling and nuclear membrane/cytoplasm rupture, whereas, excitotoxic cell death occurs a few hours after injury and causes chromatin agglutination and DNA fragmentation, but maintains an intact nuclear membrane (Stoica and Faden, 2010; Ladak et al., 2019). These intrinsic forms of cell death are primarily regulated by calcium release and enzyme-based regulators such as phospholipases, proteases, endonucleases, caspases, death-inducible complexes and pro-apoptotic proteins (Kögel and Prehn, 2000-2013; Broker et al., 2005; Raja et al., 2018). After TBI, the release of caspase-3 and caspase-12 disrupts the balance between pro-apoptotic and anti-apoptotic proteins, drawing the cell toward neurodegeneration and inflammation-induced apoptosis (Knoblach et al., 2002; Li and Yuan, 2008). Caspase-3 cleaves a specific serine-threonine protein kinase called PKCδ, causing its phosphorylation and activation. The activation of the NOX enzyme complex, either on its own or via TNFα, also increases PKCδ production. PKCδ trips the MAP kinase cascade, which allows NFκB to translocate into the nucleus, and transcriptionally activate proinflammatory genes (Sharma et al., 2018). PKCδ also regulates NOS expression and stimulates its release from reactive microglia and neurons, promoting lipid peroxidation by producing 4-HNE and malondialdehyde from hydroxyl radicals via a Fenton reaction (Puttachary et al., 2015; Sharma et al., 2018). 4-HNE impairs astrocytic proteins, such as glutamate transporter (GLT-1) which enhances free glutamate in the ECS. Free glutamate binds to NMDAR, causing NMDAR trafficking and calcium overload, free radical production, activation of $gp91^{phox}$ (heme-binding subunit of NADPH oxidase) and, ultimately, cell-membrane protein degradation and cell death (Reyes et al., 2012; Pecorelli et al., 2015; Sharma et al., 2018). These events are progressive in nature and drive long-term neurodegenerative changes in the brain over time (**Figure 4**).

Physiological and structural evidence of dendritic loss, modulation of spine density and hippocampal sclerosis have widely been associated with increased seizure susceptibility after TBI (Golarai et al., 2001; Gao et al., 2011; Winston et al., 2013). There are numerous reports on the unilateral or bilateral loss of neurons in hilus and CA3 of hippocampus, progressive mossy fiber sprouting (MFS) in the inner molecular layer of DG and hyperexcitability in DG circuitry, several weeks after TBI (Lowenstein et al., 1992; Diaz-Arrastia et al., 2000; Golarai et al., 2001)-observations that were consistent with human PTE cases (Diaz-Arrastia et al., 2000). EEG and MRI studies on patients with intractable epilepsy, who suffered TBI, showed dysfunctions in temporal lobe as characterized by increased epileptiform spiking, dendritic spine remodeling, reactive gliosis and poor neuropsychologic response. These morphological changes in hippocampus were associated with MFS and hippocampal sclerosis (Diaz-Arrastia et al., 2000). Numerous studies on the rodent models of TBI have reported a strong association between dentate granule cell hyperexcitability and enhanced MFS with hippocampal sclerosis. These studies also demonstrated intense glial reactivity, DG hyperexcitability and neuronal loss in hilus of DG (Golarai et al., 2001; Kharatishvili et al., 2006; Hunt et al., 2009, 2010). Long-term persistent hyperexcitability in DG cause alterations in hippocampal pyramidal cell dendrites, that leads to reduction in spine density or spine loss (Jiang et al., 1998). Abnormalities in dendritic spines promote hyperexcitable circuits which directly influences neuronal excitability. The changes in number and morphology of spines are related to alterations in LTP and LTD, which can have a significant effect on the cognition (Wong and Guo, 2013). In PTE patients, the loss of dendritic spines has been observed in the pyramidal layers of hippocampus and in the granule cell layer of DG (Isokawa and Levesque, 1991; Wong, 2005). Dendritic atrophy, arborization, changes in dendritic length and even varicose swelling of dendrites were reported in some cases (Multani et al., 1994; Isokawa, 1998; Wong, 2005). Animal studies have

TABLE 1 | Biomarkers of TBI-induced epileptogenesis.

Experimental model	Specie, age, strain	Injury mechanism	Biomarkers analyzed	Time-points markers observed (post-TBI)	Region/s analyzed	Effects on brain physiology/ mechanism/outcome	References
Lateral Fluid Percussion Injury	Rat, P32–35, Sprague Dawley	10 ms pressure pulse of 3.75–4 atm	GFAP; Cellular necrosis; Neocortical hyperexcitability; Epileptiform activity; SRS	• Gliosis and cellular necrosis: 6–16 weeks • Cortical hyperexcitability: 8–10 weeks • Epileptiform activity: 2–10 weeks • SRS: 2–8 weeks	Frontal-parietal and parietal-temporal neocortex; Thalamus	• Intense glial reactivity and neuronal depletion in neocortex and thalamus • Neocortical hyperexcitability in frontal, parietal I and II areas	D'Ambrosio et al., 2004
Lateral Fluid Percussion Injury	Rat, 305–390 g, Sprague Dawley	21–23 ms pressure pulse of 2.6–3.3 atm	Neuronal loss; MFS; Behavioral seizures; Epileptiform activity; SRS	• Hippocampal cell loss and MFS: 10–12 months • SRS: 8–52 weeks	Frontal and parietal cortex; Hippocampus	• Ipsilateral loss of dentate hilar neurons • Enhanced MFS in ipsilateral hippocampus • Increased behavior seizure severity • 50% animals developed epilepsy after severe injury	Kharatishvili et al., 2006
Rostral parasagittal FPI	Rat, P33–35, Sprague Dawley	10 ms pressure pulse of 3.25–3.5 atm	GFAP; Neuronal loss; Thalamic calcification; CA3 hyperexcitability; SRS	• Gliosis and neuronal loss: 2–4 weeks and 7 months • SRS: 2–8 months	Hippocampus; Thalamus; Temporal neocortex; Frontal-parietal cortex	• Increased glial immunoreactivity and neuronal depletion • Progressive shrinkage of ipsilateral hippocampus (hippocampal atrophy) and temporal neocortex with loss of laminar features • Increased bilateral seizures in hippocampus and cortical discharges over time	D'Ambrosio et al., 2005
Controlled Cortical Impact/Lateral Fluid Percussion Injury with PTZ	Mice, 10–11 weeks, C57BL/6S	CCI: Cortical compression at 0.5 mm depth at 5 m/sec velocity and 100 ms duration; FPI: 21–23 ms pressure pulse of 2.9 atm; 50 mg/kg PTZ (i.p.) 6 months post-CCI or FPI	Cortical contusion/lesion; MFS; Hippocampal neurodegeneration; Electrographic activity; SRS	• Cortical contusion, hippocampal neurodegeneration and MFS: 6–9 months • Epileptiform discharges and SRS: 6–9 months	Frontal Cortex; Hippocampus	• Cortical lesion injury extended through all layers of cortex • Higher hippocampal neurodegeneration in granule cell layer, hilus, CA3 and CA1 • MFS more apparent septally than temporally • Increased epileptiform discharges, seizure susceptibility and SRS	Bolkvadze and Pitkänen, 2012
Controlled Cortical Impact	Mice, 8 weeks, CD-1	Cortical compression at 2 mm depth at 5 m/sec velocity and 100 ms duration	phospho S6; 4EBP1; STAT3; FJB; MFS; SRS	• phospho S6: 3, 6, 24 h, 3 days, 1 week, 2 weeks • 4EBP1: 3 days • STAT3: 6 h, 3 days • FJB: 3 days • MFS: 5 and 16 weeks • SRS: 10–16 weeks	Neocortex; Hippocampus	• Hyperactivation of mTORC1 pathway • Increased neuronal degeneration and MFS • Increased PTS frequency during early phases of disease progression	Guo et al., 2013

(Continued)

TABLE 1 | Continued

Experimental model	Specie, age, strain	Injury mechanism	Biomarkers analyzed	Time-points markers observed (post-TBI)	Region/s analyzed	Effects on brain physiology/ mechanism/outcome	References
Lateral Fluid Percussion Injury	Rat, 8–9 weeks, Long-Evans	Percussion wave of 2.3 atm	GFAP; GLT-1; SRS	• Gliosis and GLT-1: 7 days • SRS: 12 weeks	Neocortex	• Suppression of GLT-1i • Increased GFAP expression and PTS frequency	Goodrich et al., 2013
Fluid Percussion Injury with PTZ	Rat, 250–300 g, Wistar	10–15 ms pressure pulse of 3.53 atm; 35 mg/kg PTZ (i.p.) 4–8 days post-TBI	TBARS; Protein carbonyl content; Na+-K+-ATPase activity; Early seizures	• TBARS and carbonyl content: 4 and 8 days • Na+-K+-ATPase activity: 3 and 7 days • Early seizures: 4–8 days	Parietal CTX	• Increased oxidative damage due to lipid and protein oxidation • Increased seizures and spiking activity	Saraiva et al., 2012
Lateral Fluid Percussion Injury	Rat, 305–390 g, Sprague Dawley	21–23 ms pressure pulse of 2.64–3.11 atm	Cortical lesion; FJB	• Cortical lesion: 12 months • FJB: 14 days	Cortex; Hippocampus	• Extensive degeneration and atrophy in injured cortex • Reduced cortical volume	Kharatishvili and Pitkänen, 2010
Human sTBI	Males, 18–65 years old	Severe TBI with Glasgow Coma Scale Score 4–8	GFAP; IL-6; S100β; NSE; TNFα; Estrogen; Progesterone	• Gliosis and IL-6: 8 h and 1 week • NSE: 1 week	Serum	• Increased gliosis and IL-6 over time in patients with severe TBI • High GFAP and IL-6 levels	Raheja et al., 2016
Human TBI	Males and females, 1 month- 13 year old	Based on lesion area and other demographic and clinical features	HMGB1; IL-1β; S100β; GFAP; AACT; Epileptiform discharges	• HMGB1, IL-1β, S100β & gliosis: within 24 h and 1 week after seizure onset • Epileptiform discharges: 6, 12, and 18 months	Serum	• Higher HMGB1, IL-1β, S100β and gliosis; • Abnormal EEG with epileptiform waves associated with increased HMGB1 and IL-1β levels	Zhu et al., 2018
$FeCl_3$-induced injury	Male, 18–22 g, C57BL/6J	Stereotaxic injection of 50 mM $FeCl_3$ in somatosensory cortex	Lipid ROS; 4-HNE adducts; PTGS2; GPX4; 12/15 LOX	• Lipid ROS, 4-HNE adducts, PTGS2, GPX4, 12/15 LOX: 12–36 h	Somatosensory cortex; Hippocampal HT22 cells	• 12/15-LOX associated ferroptosis dependent Fe-Cl_3-induced neuronal damage • Reduced cell viability & GPX4 activity • Increased ferroptotic inducers (lipid ROS, 4-HNE and PTGS2 mRNA)	Li et al., 2019
Controlled Cortical Impact	Rat, 2–11 month, Sprague Dawley	Cortical compression at 2.8 mm depth at 4 m/s velocity and 100 ms duration	$GABA_AR$ α1, α4, γ2 & δ subunits; NR2B; GluR1; HSP70 and HSP90; NeuN; SRS	• $GABA_AR$ α4 and δ subunit, NR2B and HSP70: 5–9 months • SRS: 3–9 months	Cerebral cortex; Hippocampus	• Reinforced hyperexcitability and seizure susceptibility after $GABA_AR$ modulation • Altered NR2B, HSP70 and GluR1 expression • Tissue loss and necrotic cavity formation in right ipsilateral hemisphere • Morphological changes in ipsilateral hippocampus	Kharlamov et al., 2011

(Continued)

TABLE 1 | Continued

Experimental model	Specie, age, strain	Injury mechanism	Biomarkers analyzed	Time-points markers observed (post-TBI)	Region/s analyzed	Effects on brain physiology/ mechanism/outcome	References
Controlled Cortical Impact	Mice, 8–10 weeks, CD-1	Cortical compression at 1 mm depth at 5 m/s velocity and 200 ms duration	AQP4; Kir4.1; GFAP; SRS	• AQP4 and Kir4.1: 30 and 60 days in cortex • Gliosis: 14, 30, 60, and 90 days • SRS: 14–90 days	Frontal cortex; Hippocampus	• Mislocalized and dysregulated perivascular AQP4 associated astrocytic swelling • Decreased ECS and increased ephatic interactions	Szu et al., 2020
Fluid Percussion Injury with/without KA	Rat, 297 g, Sprague Dawley	Pulse pressure of 2.3 atm	Cell loss; 2DG/FDG; ^{14}C-AIB	• Cell loss: 7 days • 2DG/FDG (glucose metabolism): 75 min • ^{14}C-AIB (BBB permeability): 70 min	Hippocampus; Plasma	• Increased ipsilateral ICMRglc after double insult paradigm • Enhanced regional BBB permeability • Hippocampal cell loss and damage	Zanier et al., 2003
Lateral Fluid Percussion Injury	Rat, 4 weeks, Wistar	Pulse pressure of 2.0–2.2 atm	fEPSP from DG cells; GluA1 and GluA2; MAP2; GFAP; IBA1; CD45; CD3; CD4; GR-1; OX42; SRS	• MAP2, gliosis and IBA1: 24 h • DG hyperexcitability, GluA1 and GluA2: 7 days • CD45, CD3, and CD4: 5–6 days • SRS: 12–15 weeks	Hippocampus; Brain slices; Primary hippocampal neurons	• DG granule cell AMPAR based network excitability • Increased seizure susceptibility by TLR4 signaling in neurons • Neuronal loss	Korgaonkar et al., 2020
Lateral Fluid Percussion Injury	Mice, 8 weeks, C57BL/6J	12–16 ms pressure pulse of 1.5 atm	CD3e; CD4; CD19; CD8; MHC II; CLIP; FJC; GFAP	• CLIP: 24 h • FJC and gliosis: 3 days post-injury	Parietal CTX; Brain leukocytes; Intestinal lymphocytes	• Enhanced astrocytic response in perilesion cortex • Increased CLIP-dependent neurodegeneration via CD74 cleavage • Increased brain immune cell infiltration after MIF-binding • CD74 and MIF-dependent astrocyte activation	Newell-Rogers et al., 2020
Controlled Cortical Impact with/without PTZ	Rat, 250–280 g, Wistar	Cortical compression at 2 mm depth at 4.5 m/s velocity and 150 ms duration; 30 mg/kg PTZ (i.p.) 24 h post-TBI	Brain contusion; IL-1β; TNF-α	• Brain contusion • IL-1β and TNF-α : 4 and 12 h	Hippocampus	• Accelerated rate of kindled seizure acquisition • Increased TNF-α and IL-1β overexpression • Increased neuroinflammation and neural damage	Eslami et al., 2015
Controlled Cortical Impact with electrical kindling	Rat, 9 weeks, Wistar	Cortical compression at 2 mm depth at 4.5 m/s velocity and 150 ms duration; Electrical kindling (50 μA at 5-min intervals).	Cortical lesion volume; TNF-α	• Cortical contusion and TNF-α: 24 h	Parietal cortex	• Increased seizure duration directly correlated to increased TNF-α levels	Hesam et al., 2018

(Continued)

TABLE 1 | Continued

Experimental model	Specie, age, strain	Injury mechanism	Biomarkers analyzed	Time-points markers observed (post-TBI)	Region/s analyzed	Effects on brain physiology/ mechanism/outcome	References
Parasagittal Fluid Percussion Injury with PTZ	Rat, 294–384 g, Sprague Dawley	Pulse pressure of 1.9–2.1 atm; 30 mg/kg PTZ (i.p.) 2 weeks post-TBI	Cortical lesion volume; NeuN	• Cortical contusion and cortical and hippocampal neuronal cell loss: 2 weeks	Cortex; Hippocampus	• Increased cortical contusion and volume • Neuronal depletion in parietal cortex and hippocampus	Bao et al., 2011
Controlled Cortical Impact with PTZ	Mice, P21, C57BL/6J	Cortical compression at 1.2–1.73 mm depth at 4–4.5 m/s velocity and 150 ms duration; 30–50 mg/kg PTZ (i.p.)	Cortical lesion volume; IL-1R1; IL1-1β; GFAP; Vimentin; ZnT3; NeuN; IBA1; SRS	• Tissue deformation and volumetric loss: 6 months • ZnT3: 2 weeks and 3 months • IL-1β: 2–12 h and 1–14 days • IL-1R1 and Vimentin: 1 day • GFAP: 1 day, 14 days, and 6 months • SRS: 4–5 months	Cortex; Hippocampus; Corpus Callosum; Serum	• Abnormal hippocampal MFS at lesion epicenter • Robust hippocampal gliosis • Long-term structural reorganization in DG • IL-1R/IL-1β mediated post-traumatic alterations in network excitability • Cortical tissue loss	Semple et al., 2017
Closed Head Injury with Electroconvulsive Shock	Mice, 20–25 g, CD-1	2 mm steel tip impounder at 6 m/s velocity and impact depth 3.2 mm	GFAP; S100β; IBA1; NeuN; MT-1 and MT-2	• Gliosis, S100β, IBA1 and MTT: 8 days • GFAP and S100β: 14 days	Hippocampus	• Increased neurobehavioral impairment due to increased gliosis and metallothionein levels • Greater neurological injury after enhanced astrocytic release of MTT • Increased seizure susceptibility associated with greater glial activation and cytokine response	Chrzaszcz et al., 2010
Closed Head Injury with PTZ	Mice, 6–8 weeks, C57BL/6J	5–7 mm impactor at 7.14 m/s velocity during 100 ms period; 10 mg/kg PTZ (i.p.) 3 days post-TBI	GABA potential; NKCC1; KCC2; TGF-β2; NeuN; GFAP	• Reversal potential of $GABA_A$ currents: 3 days • NKCC1 and TGFβ: 3 h, 1, 3, and 7 days • Gliosis; 3 days	Cortex; Hippocampus; Cortical Brain Slices	• Astrocytic TGFβ involved in neuronal upregulation of NKCC1 • Increased early PTS through NKCC1 mediated hyperexcitability • Increased seizure severity by TGFβ mediated NKCC1 expression	Wang et al., 2017
Weight Drop with PTZ	Rats, 250–400 g, Sprague Dawley	20 g weight dropped from 20 cm height; 30 mg/kg PTZ (i.p.) 15 weeks post-TBI	Neuronal loss and degeneration; FJB; pEPSP	• Cell loss: 2–27 weeks • Neurodegeneration: 1–5 days and 2 and 8 weeks • MFS: 15 weeks • DG excitability: 2–3 weeks and 14–15 weeks	Somatosensory cortex; Hippocampus; Brain Slices	• Gross cell loss and neurodegeneration in hippocampal CA3 over time • Atrophy of ipsilateral hilus and reproducible damage to somatosensory cortex • Long-term persistent DG hyperexcitability	

(Continued)

TABLE 1 | Continued

Experimental model	Specie, age, strain	Injury mechanism	Biomarkers analyzed	Time-points markers observed (post-TBI)	Region/s analyzed	Effects on brain physiology/ mechanism/outcome	References
						• Increased spread of depolarization evoked by perforant-path stimulation in slices	
						• Bilateral development of MFS with unilateral loss of bilaterally projecting hilar neurons	Golarai et al., 2001
Controlled Cortical Impact	Mice, 28–35 g, CD-1	Cortical compression at 1 mm depth at 3.5 m/s velocity and 400 ms duration	Glutamate stimulation/EPSC; MFS; Dentate granule cell excitation; SRS	• MFS and EPSC: 8–12 weeks • SRS: 6–10 weeks	Hippocampus; Brain Slices	• Increased DG excitatory input • Evoked synaptic connections between granule cells with MFS in slices	Hunt et al., 2010
Controlled Cortical Impact with/without PTZ	Mice, 12–14 weeks, C57BL/6J	Cortical compression at 0.5 mm depth at 5 m/s velocity and 100 ms duration; 30 mg/kg PTZ (i.p.) 15 weeks post-TBI	Cortical degeneration and lesion; MMP-9; Epileptiform activity	• Cortical degeneration: 1, 7, 14, and 30 days • Cortical lesion: 14 weeks • MMP-9: 10–60 min, 2–6 h, 1–30 days • Epileptiform activity: 12 weeks	Somatosensory cortex; Hippocampus	• Somatosensory cortex degeneration and long-term motor function • MMP-9 mediated structural changes and increased seizure susceptibility over time • MMP-9 dependent increased lesion volume	Pijet et al., 2018
Fluid Percussion Injury with PTZ	Mice, 23–28 g, C57BL/6J	12–16 ms pressure pulse of 1.5–1.7 atm; 30 mg/kg PTZ (i.p.) 30 days post-TBI	Cortical lesion; Neurodegeneration; GFAP; IBA1	• Cortical lesion, neurodegeneration, gliosis: 1, 3, 7, and 30 days	Cortex; Hippocampus	• Glial scarring and robust glial response early after injury • Increased neurodegeneration associated with increased gliosis • Persistent necrosis in the region surrounding the impact zone	Mukherjee et al., 2013
Controlled Cortical Impact	Mice, 25–30 g, CD-1	Cortical compression at 0.5–1 mm depth at 3.5 m/s velocity and 400 ms duration	MFS; EPSP; SRS	• MFS: 7 and 42–71 days • DG excitability and SRS: 42–71 days	Hippocampus; Brain Slices	• Axonal reorganization at early and later stages of injury proximal to the lesion • Spontaneous epileptiform activity in slices with robust MFS • Interval-specific changes in paired-pulse ratio associated with MFS • Unprovoked seizures due to injury-induced structural changes	Hunt et al., 2009
Weight Drop with/without Pilocarpine	Mice, 8 weeks, C57BL/6J	50 g weight dropped from 80 cm height; 250–350 mg/kg pilocarpine (i.p.) 24 h post-TBI	Thrombin; IL-1β; TNF-α; HPRT; Factor X	• Thrombin; IL-1β; TNF-α; HPRT; Factor X: 24 h	Hippocampus	• Enhanced thrombin activity related to PTS • Increased inflammatory markers, HPRT and Factor X, correlated with seizure severity	Ben Shimon et al., 2020

*SRS, spontaneous recurrent seizures; MFS, mossy fiber sprouting; PTS, post-traumatic seizures; ECS, extracellular space. * Only the time-points of biomarkers with increased activity after TBI are described in the table.*

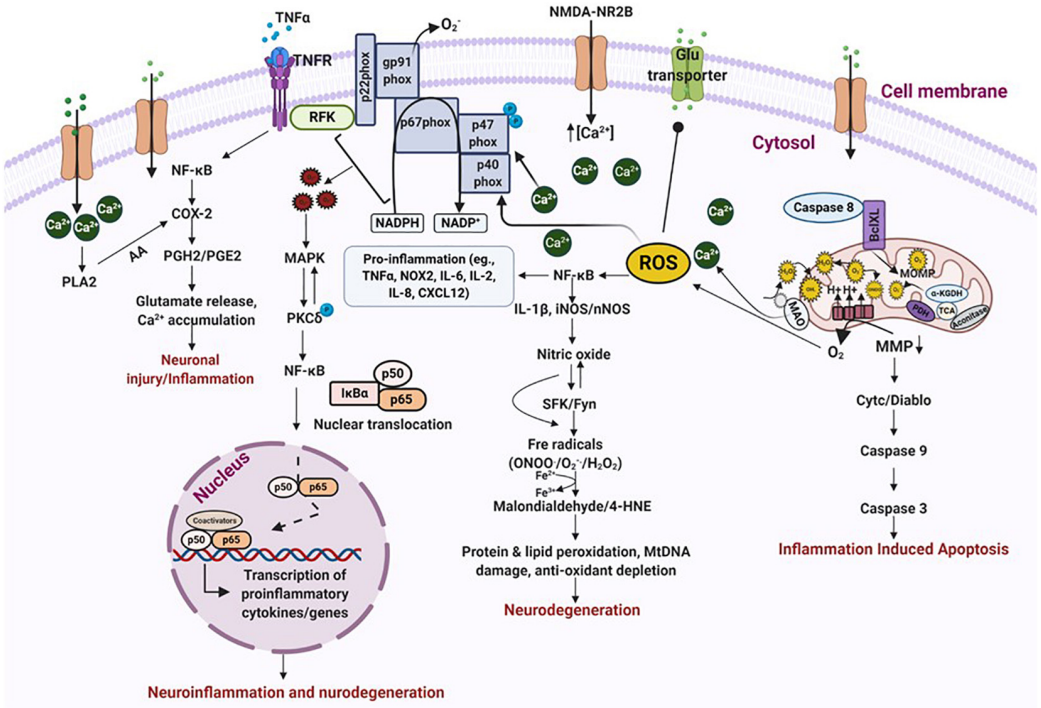

FIGURE 4 | Oxidative stress leads to neurodegeneration and neuroinflammation. ROS/RNS incites a multitude of different events that leads to oxidative stress and neurodegeneration. Binding of TNFα to its receptor triggers activation of transcription factors which stimulate the release of prostaglandins and cause neuronal injury via excessive calcium release. An inflammatory stimulus also activates NOX enzymes, either on its own or via TNFα, which produces exorbitant amounts of free radicals of oxygen and nitrogen. This results in peroxidation of proteins and lipids, DNA damage and depletion of anti-oxidant proteins, ultimately causing neurodegeneration. These events also impair mitochondrial bioenergetics leading to inflammation induced apoptosis. Increased calcium influx, due to NMDAR trafficking, also triggers NOX activation and blocks glutamate transporters causing excitotoxic cell death. Increased accumulation of free radicals activates MAP kinase which in turn activates PKCδ. PKCδ phosphorylation promotes transcription of proinflammatory proteins either directly or through NF-κB activation. All these events finally resolve into neuroinflammation and neurodegeneration. ROS/RNS, reactive oxygen/nitrogen species; NOX, nicotinamide adenine dinucleotide phosphate oxidase; MAP, mitogen-activated protein kinase; PKCδ, protein kinase C delta. Figure created with BioRender.com.

not only provided a strong evidence for dendritic alterations after TBI, but also provided insights into the cellular and molecular mechanisms involved in such changes. It has been reported that changes in the neural circuits after TBI, and during early post-traumatic seizures can cause spine remodeling due to increased MMP-7 and 9 through NMDA-mediated receptor activation (Bilousova et al., 2006; Pijet et al., 2019). This alters neuromodulation resulting in excitotoxicity-induced neuronal death in the brain (Wong, 2005). For instance, experiments with GABA antagonist on hippocampal slice cultures revealed an increased spine loss in CA3 layer of hippocampus. This was partially reversed by an application of glutamate antagonist. Furthermore, application of glutamate agonist also caused loss of these spines due to NMDA-induced glutamate excitotoxicity due to activation of calcium-dependent enzymes, which degraded cytoskeletal structures (Müller et al., 1993; Jiang et al., 1998). Therefore, these studies strongly supports the role of NMDA receptors in dendritic spine loss and abnormalities that can be reversed using NMDAR modulators, suggesting the role of glutamate excitotoxicity in dendritic spine remodeling after TBI.

Numerous studies point to immunoregulatory molecules as master regulators of inflammation after injury. In cases of severe traumatic brain injuries, immunoregulators activate multiple signaling pathways that drives chronic microglial and immune response, and cause neurodegeneration (Loane et al., 2014). Interferons (IFNs) are among those pleiotropic signaling protein molecules that play a significant role in promoting neuroinflammation and neurodegeneration following PTE. IFNs are potent immune system activators and can act in an autocrine fashion to induce type I-IFN-driven inflammation and disease (Trinchieri, 2012; Uggenti and Crow, 2018). Type I IFNs play an important role in microglial activation and neurodegeneration, especially in the aging brain; and neutralization of such interferons alleviates cognitive deficits and slows down aging (Baruch et al., 2014). Recently, interest has been developed in identifying the DNA sensors responsible for IFN activation. An example of one such sensor is the cGAS-STING pathway. cGAS belongs to the nucleotidyltransferase family that activates STING by binding to DNA, which induces enormous amounts of type I IFN, driving neurodegeneration (Abdullah et al., 2018; Uggenti and Crow, 2018). In their CCI model, James Barret's group recently reported increased cGAS and STING levels in the brain of juvenile mice, 3 days post-TBI. Using gene expression studies, they further reported enhanced mRNA expression of

IFN-β and interferon regulatory factors such as IRF1, IRF4, and IRF7- factors that regulate amplification of type I IFNs in microglia. These studies show that microglia expressing high levels of IFNAR, following TBI, achieve reactive morphology and activation, and can prove to be a crucial target for IFNAR related diseases. Higher IFNAR expression subsequently increases production of TNF-α, NOX2, CCL5, and IL-1β mRNA, promoting cell death by driving synaptic and dendritic loss in neurons. In contrast, knocking out IFNAR and IFN-β has been shown to reverse these effects in the cortex and hippocampus of the mice (Karve et al., 2016; Barrett et al., 2020). Further, through behavioral studies, Barrett et al. (2020) demonstrated that knocking out *IFN*-β gene significantly improves motor and cognitive performance in the experimental subjects (Barrett et al., 2020). Moreover, several studies suggest that targeting IFN can prevent lesion volume, increase neuronal density, reduce the cytokine storm, decrease microglial activation and leucocyte infiltration, and limit neurodegeneration in the brain (Biliau, 2006; Mathur et al., 2017; Ta et al., 2019). Therefore, therapies targeting IFNAR can prove to be beneficial in treating TBI-associated neurological conditions. These therapeutic strategies can include using caspase inhibitors; cyclic dipeptides (to slow down cytochrome *c* release); use of pharmacological compounds (blocks cell cycle activators); progesterone and erythropoietin treatment (for edema and proinflammatory cytokine release); and statins (for governing Akt and slowing down microglial activation) (Ucciferri et al., 2007; Tayel et al., 2013; Zhu et al., 2013; Dejager et al., 2014).

Neuroinflammation

Neuroinflammation in the brain is triggered by factors such as microbial infections, accumulation of toxic metabolites, traumatic brain and spinal cord injury, and tissue damage and malfunction. Acute inflammation, after TBI, activate molecules and signaling mechanisms that attempts to restore the body's disrupted equilibrium by balancing inflammatory and resolution pathways. If these events are not controlled in time, they progress into a chronic stage, eliciting deleterious effects on the brain. The key molecules that regulate inflammation at this stage are granulocytes, platelets, prostaglandins, and cytokines released by lymphocytes, macrophages, microglia and stressed neurons. Their secretions cause intracellular modifications to recreate an unstable cellular microenvironment that disrupts cellular and molecular communications between cells (Herz et al., 2017; Davies et al., 2019; Scanlon, 2019).

Numerous studies on rodent models of epileptogenesis have reported on the post-TBI role of inflammatory mediators, prostaglandins and cytokines IL-1β and TNFα, in the hippocampus and other regions of the brain (Patel et al., 2017; Serhan, 2017). IL-1β, an immune cell mediator and IL-1RI ligand, has been associated with modulation of various neurological functions and in diseases. IL-1β increases NMDAR-mediated calcium release through the activation of Src family kinases (SFKs) (Viviani et al., 2003; Salter and Kalia, 2004). NMDAR are regulated by SFKs, especially by Fyn (Salter and Kalia, 2004). Substantial evidence suggests the link between increased IL-1β-NMDAR-SFK interactions in numerous neurological conditions influencing neuronal functions and enhancing neuronal excitability (Vezzani et al., 1999; Fogal and Hewett, 2008). Studies on hippocampal neurons have demonstrated that neurons exposed to IL-1β exhibit greater glutamatergic excitation and calcium release through NMDAR component, which induces excitotoxic cell death (Viviani et al., 2003). Interaction of IL-1β with IL-1R results in the recruitment of adaptor protein MYD88, which further recruits TRAF6 or IRAK I and II. The MYD88-TRAF6/IRAK I and II complex phosphorylates MAP kinase, causing NF-kB translocation into the nucleus, promoting transcription of proinflammatory genes (O'neill, 1995; Vezzani et al., 2011; Lalitha et al., 2018). These proinflammatory genes are primarily involved in cell death and survival, reorganization of molecular networks, plasticity, synaptogenesis and aberrant neurogenesis- events that takes place simultaneously with epileptogenesis (Vezzani et al., 2011). Activation of IL-1β/IL1R also promotes release of TNFα from astrocytes and glial cells. In contrast, toll-like receptor (TLR) activation stimulates TNFα expression as has been demonstrated in many experimental models of TBI (Yu and Zha, 2012; Shi et al., 2019). TNFα modulates neuronal excitability perhaps by internalizing inhibitory $GABA_A$ receptors (Stellwagen et al., 2005; Stück et al., 2012; Pribiag and Stellwagen, 2013). TNFα binding to its receptor activates the TRADD complex and PI3 kinase, resulting in NF-κB activation modulating apoptosis and inflammation (Ermolaeva et al., 2008; Ting and Bertrand, 2016; Holbrook et al., 2019). TNFα activation also increases COX-2 production in response to injury, which is followed by an increase in PGE2 synthesis. Activation of these events cause glutamate accumulation and increases calcium load in the cell exacerbating neuroinflammation (**Figure 4**).

IL-1β and TNFα are undoubtedly the most well studied and widely known mediators of inflammation following TBI. Exuberant amount of work is underway, in both animal and human models, to target these molecules and prevent neurological outcomes related to TBI. For instance, in a mouse model of blast-injury, IL-1β antagonist Anakinra, has been shown to reduce gliosis, retinal degeneration and neuronal dysfunction (Evans et al., 2020). Another IL-1β synthesis inhibitor, VX-765, delayed seizure onset, duration and the number of SRS in chemoconvulsant induced experimental model of epilepsy (Maroso et al., 2011). In a study on TNFα inhibitors, C7 and SGT11, on a mice model of midline FPI, Rowe et al. (2018) reported significant improvements in cognitive deficits and sensorimotor function tasks (Rowe et al., 2018). Therefore, these studies provide strong evidence on the roles of IL-1β and TNFα inhibitors in modulating TBI-induced inflammation, and improving neurocognitive deficits, linked to TBI.

The role of prostaglandins in the animal models of TBI and in epileptogenesis is well known. Prostaglandins are produced by the action of COX-2 on arachidonic acid, which can be converted into five different prostanoids by the action of specific enzymes, depending on cellular conditions and their requirements. Prostanoids activate 11 receptors that primarily play a role in smooth muscle relaxation and contraction. Depending on the type of receptors and ligands activated, prostaglandins can play a significant role in various physiological

and pathological conditions (Jiang et al., 2013; Rojas et al., 2014; Du et al., 2016; Eastman et al., 2020). Numerous studies showed high concentrations of prostaglandins in the brains of human patients and animals with temporal lobe epilepsy (TLE) (Takemiya et al., 2006; Jiang et al., 2013; Rojas et al., 2014; Rana and Musto, 2018). Excess prostaglandins modulate calcium mobilization and cAMP activity, inducing neuronal injury and defects in neuronal plasticity (Hein and O'Banion, 2009; Figueiredo-Pereira et al., 2015; Kang et al., 2017). For example, during febrile seizures, inflammation in the hypothalamic neurons modulate systemic inflammatory response by recruiting prostaglandins from the system (Berg et al., 1998; Zetterström et al., 1998). This enhances EP1/EP2 receptor trafficking, stimulates COX-2 production, and increase prostaglandins within the brain, thereby reducing the threshold for seizures (Gatti et al., 2002). So far, multiple clinical trials of prostaglandin inhibitors for controlling febrile seizures have been largely contradictory: for e.g., patients treated with aspirin therapy had fewer seizures on day two of monitoring, whereas randomized placebo-controlled ibuprofen treatment, in children with febrile seizures, failed to prevent spontaneous recurrent seizures (SRS) (Godfred et al., 2013). An overproduction of prostaglandins and cytokines, along with the recruitment of other disease-causing molecules (such as platelet activating factors, MMPs and TLRs) trigger cellular damage, decrease long-term potentiation, elongate dendritic spines, increase production of forkhead transcription factor 3, modulate voltage-dependent ion channels, and impair BBB leukocyte-endothelium interactions (causing a leaky BBB) (Anderson and Delgado, 2008; Vezzani et al., 2012, 2015; Rana and Musto, 2018). Enhanced production of these molecules and the events they trigger lowers the seizure threshold post-injury and increases the brain's susceptibility to PTE.

IMMUNE RESPONSE AFTER TBI

Immune cells play important roles in regulating normal functions of the brain, such as neurogenesis, cognition, aging, translation, formation of neural circuits, and stress responses. When this system stops functioning well, disease manifests. Therefore, it is essential to understand the functions of the immune system, to be able to evaluate its role as a repair mechanic that can be optimized, or a disease promoter that should be suppressed. The local inflammation surrounding an injured tissue is pivotal for its recovery. Although sometimes inflammation runs out of control, suppressing it may impact the normal functions of the system. Several studies report that circulating immune cells are vital for CNS protection and repair (Louveau et al., 2015; Morimoto and Nakajima, 2019; Norris and Kipnis, 2019). Blood macrophages are initially activated at the site of injury, and are generally anti-inflammatory and not proinflammatory in nature, challenging the notion of a strictly proinflammatory role for macrophages, post-injury (Popovich et al., 1996). These macrophages are reparative and alternate between an activated or M2 morphology (Rapalino et al., 1998). Rapalino et al. (1998) reported that animals injected with these macrophages, at the site of injury, recovered their locomotor activity and formed less scar tissue. Studies on a TBI chimeric mouse models of neurological diseases have addressed the need for the recruitment of monocytes/blood macrophages to fight progression of the disease, that follows post-injury. These studies proposed that blood macrophages degrade amyloid-β, elevate IL-10 levels, downregulate TNFα, and boost levels of growth factors, such as IGF-1, in the brain, which attenuates neuropathology (Shechter et al., 2009; Hu et al., 2012; Hsieh et al., 2013; Zyśk et al., 2019). Other studies argued that not only do macrophages have a reparative role, but so do circulating *T*-lymphocytes after injury (especially $CD4^+$ lymphocytes) (Rapalino et al., 1998; Shechter et al., 2009). For instance, elevating the levels of myelin-recognizing T cells, after TBI, is protective and supports recovery, enhances neurogenesis, improves cognition and provides better protection and the ability to cope with stressful conditions (Mckee and Lukens, 2016; Krämer et al., 2019). It is notable that these protective T cells are different from those that cause autoimmune diseases, in terms of their antigen affinity and regulation. These studies validate an indirect role of T cells in maintaining brain homeostasis by regulating hippocampal neurogenesis, maintaining brain plasticity, enhancing cognition, and controlling the stress response.

Immune cells such as microglia (inflammatory microglia) initiate debris disposal after injury, whereas anti-inflammatory microglia initiate healing in response to sterile inflammation. During severe injury, if microglia cannot clear the debris, macrophages from the blood (or healing macrophages) enter the brain, and terminate the microglial response by releasing high amounts of IL-10. Resident microglia and blood macrophages have different functions in protecting the brain from neuroinflammation and behave differently, in a time-dependent manner. The infiltrating blood macrophages support cell survival and renewal after injury, whereas their depletion causes loss of cells (Shechter et al., 2009). Importantly, immune system activation does not always exacerbate the injury response and cause chronic inflammation. If the activated microglia can return to normal, then inflammation resolves itself; if not, however, they can trigger a systemic immune response. Therefore, it is crucial to understand whether the nature of the inflammation is local or systemic when employing anti-inflammatory therapies. In contrast to systemic inflammation, suppressing local inflammation may prove to be the more beneficial option.

The inflammation conundrum in neurodegenerative diseases occurs in the backdrop of ineffective recruitment or a dysfunctional immune system; it varies with model, strain, sex, region of the brain affected, severity and time of insult, age, etc. After an initial infection, the number of T cells remains steady for a long period of time and then declines; and when their number crosses a critical threshold, disease is manifested. The drop of T lymphocytes over time, as reported by Ho et al. (1995), is a very dynamic process, since immediately after infection T cells furiously regenerate themselves. The inflammatory response then kicks in to regenerate more T cells to fight the infection. When

this process is exhausted, the disease is evinced (Ho et al., 1995). Researchers recently discovered that the brain is not as immune privileged as previously thought. In fact, CD4 T cells are present around leptomeninges, blood vessels and glia limitans, where they secrete immune signals into the CSF that bathes the brain; and these cells populate the brain meninges right around the time when all of the synaptic remodeling events are taking place, thereby exacerbating inflammation (Rauch, 2004; Koronyo et al., 2015; Pasciuto et al., 2020). In addition to this neuroinflammatory component, PTE also has a peripheral immune element, as the periphery too gets inflamed by the TBI-activated innate and adaptive responses. After traumatic injury, studies have reported a significant activation of immune cells, such as B cells, CD3+, CD4+, and CD8+ T cells, Tregs, and γδ-T cells in spleen as detected through flow cytometry. Evidence of innate and adaptive responses to injury were also observed in other tissues, such as the GI tract and liver (Tobin et al., 2014; Bai et al., 2017). For instance, PCR-arrays tracking cytokine expression showed increase in mRNA for chemokines, such as MCP-1, in the liver and gut, and proliferation of γδ-T cells (Tobin et al., 2014). Researchers are now beginning to realize that cytokines, for the most part, are not made by the neurons and astrocytes but by immune cells and microglia, which populate the entire body including the developing brain, and communicate with resident macrophages to promote tissue remodeling and cleanup (Röszer, 2015; Sridharan et al., 2015; Wynn and Vannella, 2016; Kumar, 2019). Interestingly, in a recent study on maternal immune activation, it was observed that maternal immune activation (from infection or autoimmune predisposition) induces T-cells to release IL-6 and IL-17. IL-17 can cross the placenta and cause cortical malformation and behavioral abnormalities in the baby (Choi et al., 2016; Wong and Hoeffer, 2018). Together, these studies conclusively support a crucial role for our immune system in health, and in the maintenance of inflammation after TBI.

CONTRIBUTION OF ASTROCYTES AND MICROGLIA TO PTE

Role of Microglia in TBI/PTE

Microglia are the resident immune cells that play an important role in immune surveillance of the CNS. Based on their morphology and activation, microglia have various subpopulation forms in the CNS. These subtypes include M0, M2a, M2b, M2c, M2d, and M1 (Franco and Fernandez-Suarez, 2015). M2 microglia have anti-inflammatory properties and play a significant role in maintenance of CNS homeostasis and plasticity, synaptic pruning, removal of pathogens through phagocytosis, neural development, regulating neurotransmitter release, neurogenesis, release of neurotrophic factors and tissue/synaptic remodeling. Microglia are acquisitively sensitive to changes in their local microenvironment. They dramatically change their phenotype and upregulate number of diverse cell-surface antigens. These microglia are typically referred to as M1 microglia. M1 microglia are in the hyper-activated state and can be amoeboid or rod-shaped. They promote immune cell recruitment into the CNS (such as Th1 and Th17), where they release proinflammatory cytokines, chemokines such as CCL2 and CCL20, and monocyte chemoattractant protein-1 and eotaxin. Under such circumstances, microglia stimulate iNOS production, trigger generation and release of ROS/RNS, activate the complementary proteins, and increase COX-2 production to produce prostaglandins (Streit et al., 2004; Dheen et al., 2007; Franco and Fernandez-Suarez, 2015).

During TBI, M1 microglia express several receptors on its surface as a result of either neural injury-derived damage-associated molecular patterns (DAMPs) or due to astrocytic secretions, that bind onto these receptors. Many of these receptors are a family of pathogen recognition receptors, such as TLRs, that recruit adapter proteins and initiate complex cascade of signaling events which regulate transcriptional events and inflammation. In response to DAMPs, and factors released by damaged neurons, astrocytes and immune cells, microglia drastically changes its morphology, proliferate, move along chemotactic gradience, express surface molecules for signaling, carry out cytotoxic attack on neurons and increase increase proinflammatory secretions. Activation of proinflammatory receptors and their downstream products, when released, either causes neural injury or modulate astrocytic activity, causing an A1 phenotype (Sharma and Naidu, 2016; Clark et al., 2019; Wofford et al., 2019). For instance, primary astrocyte-activating signals released by microglia include IL-1, TNFα, and C1q (Liddelow and Barres, 2017; Clark et al., 2019). These cytokines and complement proteins cause structural and functional changes in astrocytes. Reactive astrocytes disassemble synaptic connections between neurons and release neurotoxins that degenerates mature neurons and oligodendrocytes in CNS after TBI (Liddelow et al., 2017). Astrocytes, likewise microglia, also express high levels of proinflammatory receptors, which similarly alter microglial and neuronal activity. The crosstalk between astrocytes, microglia, and neurons causes degradation of the extracellular matrix (Hevin) and metabolic proteins (ADAMTs), triggers leukocyte mediated inflammatory responses (TREM2, complement proteins), promotes neutrophil chemotaxis (complement proteins), recruits immune cells (purinergic receptors), stimulates cell lysis, enhances production of miRNAs, disrupts lipid homeostasis and cell membranes (nuclear receptors), and impairs synaptogenesis (SPARC) (**Figure 5**). This cross-coupling between neuroglia induce changes in glial physiology causing long-term neurodegenerative changes after TBI, promoting epileptogenesis resulting in PTE (Smith, 2013; Izzy et al., 2019). Increased inflammasome binding onto TLRs, during the first few days post-injury is one of the major drivers of neuroinflammation that triggers epileptogenesis (O'Brien et al., 2020). In addition to the above events, microglial pruning of synapses is increased very early in the disease progression; as a result, the loss of synaptic density due to an increase in the phagocytic capacity of microglia could perhaps be an important factor that promotes epileptogenesis after TBI (Andoh et al., 2019).

The signals and response modifiers in microglial activation can be triggered and modified by several factors based on the cellular origin, chemical structure and signaling. These include structures of infectious agents, immunoglobulins/immune

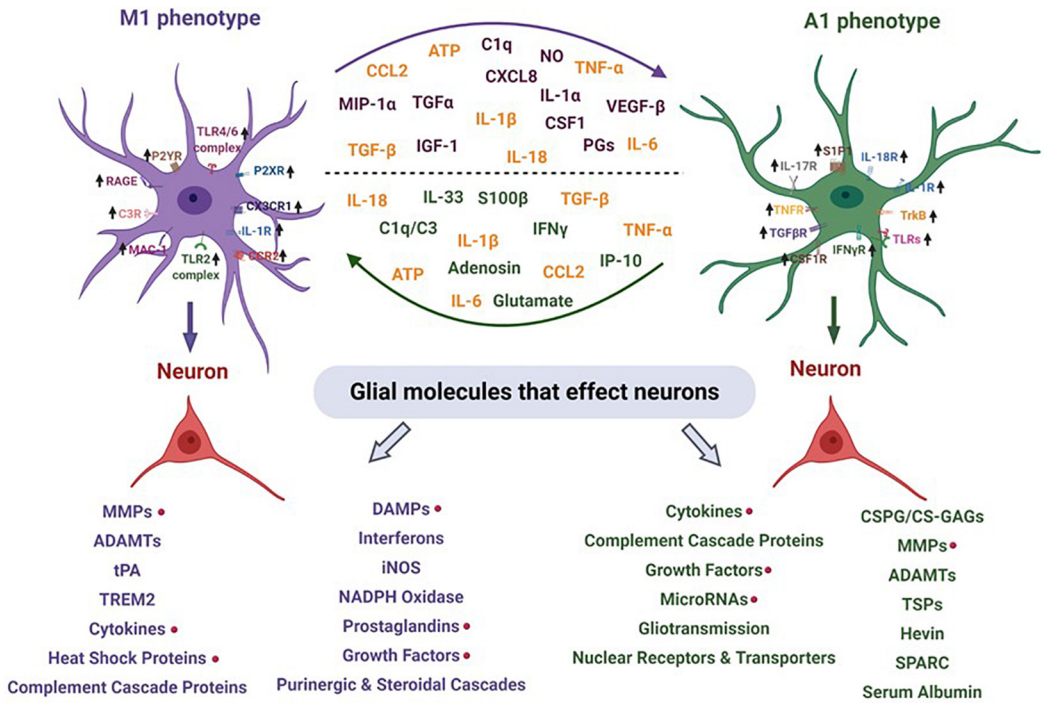

FIGURE 5 | Crosstalk between reactive microglia, reactive astrocytes and neurons during neuroinflammation. During inflammation, microglia and astrocytes achieve M1 and A1 like morphology. M1-like microglia, also known as reactive microglia, secrete multiple factors that modulate astrocytic functions by binding onto their receptors. Likewise, astrocytes too secrete molecules that bind onto microglia and modulate their activities. Molecules in purple are released by microglia and induce A1 phenotype in astrocytes and/or modulate astrocytic activity. Molecules in green are released by astrocytes and modulate microglia activity and/or forms reactive microglia. Molecules in orange are released by both astrocytes and microglia, co-regulating each other's activities. Molecules released by these cells also effect neurons (in red). Beneath neurons are molecules (in purple) that microglia secrete which cause neuronal damage. In green are molecules secreted by astrocytes that cause neurodegeneration. Red dots next to purple and green text indicate molecules released by neurons that alter microglia and astrocytic activities. Some of the receptors on M1 microglia such as TLR4/6 complex, RAGE, CX3CR1, P2YR and P2XR cause microglia activation due to neural injury-derived DAMPs.

complexes, complement system, cytokines, neurotrophic factors, proteins and peptides, and neurotransmission related compounds and ions such as ATP, purines and glutamate. Many of these molecules, and associated signaling events, are also released after TBI, which perhaps play a crucial role in the pathogenesis of PTE (Wofford et al., 2019). Signals emitted by neighboring resident cells or by immune cells from the periphery shape profiles of induced genes and functions in microglia. Studies have shown that activation of certain types of cytokines such as IFNγ, IL-1β, and TNFα after TBI, drives proinflammatory microglial response with increased expression of IL-12, supporting the role of immune cell (such as Th1) mediated reactions in regulating M1 state of microglia. These signals, in turn, influence the cocktail of chemoattractive factors to organize for a change in the composition of infiltrates to instruct the engagement of neutrophils, monocytes and distinct T-cell subpopulations (Hanisch and Kettenmann, 2007). Indeed, there are multiple reports of the phenotypic shifts in macrophages and microglia *in vitro* and *in vivo*, and cytokines produced by T-cell subtypes such as IFNγ are primarily known for this change. These series of events can orchestrate inflammatory reactions in response to traumatic insult (Hanisch and Kettenmann, 2007). Furthermore, time lapse images of microglia, after TBI, have revealed immediate microglial response to the focal injury. They undergo a rapid phenotypic change and form a bulbous body that extend towards the ablation site forming a spherical containment releasing 'on' signals (Davalos et al., 2005). On signals are inducible factors and includes a range of chemokines, but also neurotransmitters such as purines and glutamate. A prominent feature of reactive microglia is the high expression of receptors for purines and their wide range of responses to receptor activation, which have been reported in numerous experimental models TBI (Davalos et al., 2005; Jackson et al., 2016; Frenguelli, 2019). For instance, single focal injection of ATP in mice induced a localized response of activated microglia with higher P2Y6 and P2Y12 receptor expression, may support the role of purine receptors in TBI induced epileptogenesis (Davalos et al., 2005; Kumaria et al., 2008; Jackson et al., 2016).

The exciting development in microglia research in terms of origin and progenitors of microglia, their population and stability or turnover under normal and diseased conditions, their contribution to the maturation and support of neuronal development and glial functions, their protective and harmful actions in diseases and the options of therapeutic interventions by silencing or enhancing functions, will help to answer several

key questions and help in understanding their role more clearly in health and disease.

Astrocytes and Their Role in TBI/PTE

Astrocytes, first identified by Virchow in 1846 as a glue filling the interstitial fluid, are star-shaped cells in the CNS that play an important role in maintaining brain homeostasis. Astrocytes use their "astrocytic end-feet" to support the metabolic demands of neurons by supplying nutrients from the blood vessels (Cui et al., 2012). They make 'tripartite synapses' with pre- and post-synaptic neurons, to integrate synaptic function by means of neurotransmitters and gliotransmitter release (Cui et al., 2012). Neuroactive molecules of astrocytes, such as $_D$-serine, GABA, and adenosine triphosphate (ATP), regulate neuronal functions such as synaptic activity by inducing long-term depression and long-term potentiation, mediate tonic inhibition through Best1 ion channels, inhibit proinflammatory molecules (such as TNFα), assist GABA transporters in a calcium-independent manner and regulate sleep homeostasis, synaptic plasticity, and memory formation (Panatier et al., 2006; Haskó et al., 2008; Lee et al., 2010; Yoon et al., 2011; Fossat et al., 2012).

Astrocytes regulate neuronal functions under normal physiological conditions, but under pathological conditions, astrocytes phenotypically change in response to their microenvironment and become reactive during inflammation (Cui et al., 2012; Pekny and Pekna, 2016). After TBI, reactive astrocytes undergo morphological changes, that corresponds to changes in their functional and molecular properties. These alterations include dysfunctional potassium and glutamate buffering, modulation of aquaporins and adenosine activity, disturbances in gap junctions, disruption of glutamate-glutamine cycle, impairment of cysteine-glutamate antiporter system and mutations in potassium channel genes (Lewerenz et al., 2013; Burda et al., 2016; Zhou et al., 2020). Series of these events over time, results in the accumulation of neurotoxic molecules in the brain and cause BBB disruption. The damage to the BBB promotes extravasation of serum albumin into the brain (Puttachary et al., 2016). Serum albumin in the brain binds to TGFβ receptors on astrocytes, which phosphorylates Alk5 mediated SMAD2/3 complex and p-38 MAPK. This causes SMAD2/3 translocation into the nucleus activating transcription of proinflammatory genes promoting TGFβ and IL-6 production (Milikovsky et al., 2017). In numerous studies on rodent models of TBI, it has been reported that extravasation of serum albumin cause impairment of potassium buffering and glutamate reuptake by downregulating Kir4.1 potassium channels and glutamate transporters (Ranaivo et al., 2012; Weissberg et al., 2015; Zhou et al., 2020). This elevates extracellular K^+ and glutamate concentration, and cause hyperexcitability (Puttachary et al., 2016; Steinhäuser et al., 2016). Infiltration of peripheral immune cells (such as T cells and monocytes) after BBB breakdown signals the release of complementary proteins. Up-regulation in complementary proteins promote leukocyte chemotaxis and migration at the lesion site (Cho, 2019). Many complement cascade genes are profoundly upregulated in the reactive astrocytes and neurons after TBI. They play an important roles in activating numerous pathological pathways involved in synaptic loss, increased synaptic pruning, impairment of neuromelanin clearance, increased stress in endoplasmic reticulum, decreased phagocytosis by dendritic cells, modulation in neurite outgrowth and regulating control of growth factors (Daglas and Adlard, 2018; Hammad et al., 2018; Cho, 2019). In response to proinflammatory insult, reactive astrocytes also produce an unknown factor called protein-X, which triggers the production and shedding of the complement components by neurons (Shi et al., 2010). Excessive tagging of neurons by activated complement proteins and their recognition by complement receptors or reactive microglia results in phagocytosis and removal of synapses, and eventually neuronal death.

The combination of aforementioned damaged signals and their relative concentrations most likely determine the type of astrogliosis experienced by astrocytes in different regions surrounding the initial insult zone. On a cellular level, insult to the brain such as TBI results in hypertrophy of astroglial processes and significant increase in astrocytic cytoskeleton (Sofroniew and Vinters, 2010; Burda et al., 2016; Steinhäuser et al., 2016; Chen et al., 2020). Brain damage very rapidly turns most of the astroglial cells into GFAP expressing reactive astrocytes. Both GFAP and vimentin are critically important for the development of reactive astrocytes. Severe stress in astroglia energetics leads to subsequent loss of ion homeostasis that triggers enormous amounts of glutamate in ECS. The astroglial involvement in controlling brain glutamate concentration is double edged. Upon severe injury, astrocytes may turn from being the sink for glutamate to being the main source of the latter. Astrocytes can release glutamate by several mechanisms which are triggered in PTE. First, the reversal of glutamate transporters can be caused by ATP depletion accompanied with an increase in intracellular Na^+ concentration and cell depolarization. Second, elevation of cytoplasmic Ca^{2+} concentration in astrocytes, that follows traumatic injury, may trigger the release of glutamate stored in vesicles. Third, acidosis and lowering extracellular Ca^{2+} concentration may open glutamate-permeable hemichannels. Fourth, ATP released in higher concentrations by dying and disintegrating neurons can open astrocytic $P2X_7$ purinoceptors which allows glutamate release. Fifth, brain oedema post-TBI can activate volume-sensitive channels which too allows the passage of glutamate.

Excess glutamate in the extracellular space disrupts the cysteine/glutamate antiporter system (CGS), a key anti-oxidant system in astrocytes that imports oxidized cysteine into the cell in exchange for glutamate. CGS regulates movement of amino acids in to and out of the cell, depending on the cellular requirements, and regulates the immune system, resistance against anti-cancer drugs, protection against carcinogenesis, cellular redox homeostasis, and modulates memory and behavior. In astrocytes, the intracellular concentration of cysteine (in its reduced form) is generally lower than glutamate (Lewerenz et al., 2013). Cysteine is an important substrate for the production of glutathione; and, inside the cell, oxidized cystine is reduced to form glutathione through the help of enzyme thioredoxin reductase 1 (Mandal et al., 2010; Lewerenz et al., 2013). Post-TBI, dysfunctional CGS upsets the balance between anti-oxidant and oxidants, causing oxidative stress as a result of glutamate

excitotoxicity (Koza and Linseman, 2019). During inhibition of CGS, glutathione levels decline. Once glutathione depletion reaches a critical level, ROS production increases. This does not cause cell death immediately but instead facilitates the activation of signaling pathways and ultimately culminates in cell death. Therefore, neuroprotective compounds that generally are not beneficial during chronic stages of the disease can have favorable outcomes when administered at early time-points (when ROS concentration is gradually increasing, post injury) (Maher and Schubert, 2000; Lewerenz et al., 2013). Modulation in CGS levels have been reported in many neurodegenerative conditions. The increase in CGS in these conditions could primarily be due to an increased glutamate accumulation and release (Chung et al., 2005; Pampliega et al., 2011). This rise in extracellular glutamate is a result of downregulation of the excitatory amino acid transporter (EAAT) that balances CGS-mediated glutamate release. Therefore, specifically targeting glutamate by inhibiting CGS, can be an alternate approach for treating TBI related disorders as it aims to balance glutamate release into the ECS with glutamate uptake by EAATs. Drugs that protect from glutamate excitotoxicity act mainly through these mechanisms and inhibit excitotoxic effects of CGS by increasing glutathione synthesis modulating glutamate release (Lewerenz et al., 2013).

After TBI, initiation of secondary insult mechanisms can trigger epileptogenesis. If primary mechanisms are not controlled on time, they can cause long-term cellular and molecular alterations in astrocytes, leading to serious neurological consequences over time. For instance, astrocytic dysfunction can result in disruption of homeostatic regulation of brain volume and water content levels, causing edema. This can result in increased intracranial pressure, changes in extracellular osmotic pressure and compression damage to neural tissues (Dearden, 1992; Jha et al., 2019). After TBI, astrocytes are unable to remove excess water due to damage to their water channels, called aquaporins. Aquaporins have been widely studied as drivers of pathogenesis in epilepsy and other neurodegenerative conditions. Mutations in aquaporin 4 disrupt fluid osmolarity and potassium homeostasis (Heuser et al., 2010; Binder et al., 2012; Nagelhus and Ottersen, 2013). Although the role of gap junction dysregulation in epilepsy is still controversial, some studies have demonstrated an anti-epileptic role of gap junctions during astrocytic coupling. According to the spatial buffering concept, astrocytes pass excess K^+ ions between their networks, reducing K^+ concentration in the ECS. Dysfunctions in gap junction proteins, such as connexins, have been reported to increase cellular hyperexcitability and cause seizures. For instance, studies on $Cx30^{-/-}$ mice reported increased neuronal depolarization and lower seizure threshold with disturbances in potassium and glutamate clearance in astrocytes, causing astrocytic swelling (Wallraff et al., 2006; Steinhäuser et al., 2016). Damage to aquaporins and rapid swelling of astrocytes after injury is accompanied by a significant increase in astroglial surface area. Astroglial swelling can trigger numerous secondary effects that can exacerbate the brain damage. In particular, swelling of perivascular astrocytes and astrocyte endfeet may compress brain vessels and limit circulation. Swelling of astrocytes can result in the opening of volume regulated ion channels permeable to glutamate and other excitatory amino acids exacerbating excitotoxic cell death (Sun et al., 2003; Tran et al., 2010). Therefore, the functional and molecular changes in astrocytes, after TBI, promote epileptogenesis suggesting their role in the development of PTE.

LONG-TERM CONSEQUENCES OF TBI/PTE

The possibility of developing PTE, after post-traumatic seizures, is generally higher and so increases the risk of long-term consequences of TBI. These consequences depend on the severity of injury and the region of the brain affected. For instance, the odds of developing long-term implications diminish if the injury is a mild or moderate closed-head one, in contrast to a severe closed-head injury (Naalt et al., 1999; McCullagh and Feinstein, 2003). The closed-head TBI causes bleeding or intracranial hematoma which raises the risk of lasting impact on the brain. Recently, a 30 years followup study conducted in Sweden on patients with TBI, reported that all survivors of TBI, whether moderate or severe, developed dementia within 30 years of injury (Himanen et al., 2006). Moreover, studies on Vietnam War veterans, over the span of 40 years, revealed that treating with anti-convulsants during the acute phase of injury controlled severity and frequency of early seizures, whereas later treatments with anti-convulsants did not prevent the onset of PTE (Raymont et al., 2011). Over 40% of troops that suffer TBI develop PTE in their lifetime, with lasting effects including confusion, cognitive deficits, depression, and anxiety disorders. Long-term follow-up studies on veterans also revealed that about 18% of veterans experienced their first seizure after 15 years of injury (most had seizures after 1–5 years) and about two-thirds are on life-long medications (Raymont et al., 2010, 2011). Interestingly, having a family history of epilepsy or a genetic predisposition adds to the risk of developing PTE after brain injury. The genes involved mainly control plasticity, modulate levels of neurotransmitters, control ion channels, and regulate immune functions (Swartz et al., 2006; Raymont et al., 2010).

After TBI, the incidence of PTE increases and some patients are notoriously difficult to treat due to challenges in long-term follow up and therapeutics (Garga and Lowenstein, 2006; Schmidt et al., 2014; Szaflarski et al., 2014). Video-EEG monitoring and MRI studies on patients with PTE reported that approximately one quarter of the patients develop mesial temporal sclerosis and predicted the development of neocortical lesions on other half of the patients, at some stage in life; whereas, the vast majority of the cases develop focal epilepsy (Gupta et al., 2014). Swartz et al. reported that, of 200 consecutive temporal lobectomies performed on TBI survivors, 21 cases were of PTE, and about 50% of these cases had hippocampal sclerosis characterized by neuronal loss primarily in the hilar region of DG (Swartz et al., 2006). Moreover, a CEEG and PET scanning on 16 TBI patients revealed that ∼28% of these patients had non-convulsive seizures (NCS) over 7 days after injury and one had R temporal NCS during PET while comatosed (Vespa et al., 2010). Further, the same study reported the patients who had

seizures several days after injury developed hippocampal atrophy, ipsilateral to the seizure, which was possibly why some develop PTE later in life (Vespa et al., 2010). High-resolution analysis of the brain (through diffusion tensor imaging of the perforant path) revealed that the white matter tracts that are either afferent and efferent to the hippocampus are particularly sensitive to shearing and stretching forces (Wang et al., 2008). This indicates that, at least in some cases, the mechanism of epileptogenesis results from a deafferentation or disconnection of the hippocampus from the long-term synaptic connections which develops over time.

Repeated TBI can alter neural circuits and lead to long-term degenerative changes in the brain and periphery. For instance, chronic traumatic encephalopathy (CTE; a neurological deterioration due to accumulation of hyperphosphorylated tau) causes release of TDP43 (transactive response DNA binding protein), which forms neurofibrillary tangles and increases oxidative stress. TDP43 is produced in high amounts, which affects the anti-oxidant enzyme SOD-1 and causes protein misfolding, damaging the BBB (Pokrishevsky et al., 2012). The breakdown of the BBB may persist for many months or years, gradually causing damage over time. The BBB disruption results in local inflammation which ultimately resolves into epileptogenesis (Tomkins et al., 2011; Vezzani et al., 2012). In the periphery, the cardiac complications of PTE cause morbidity and mortality due to enhanced cardiac contractility, high blood pressure, and production of myocardial ROS. The increased cardiac contractility results in sympathetic storm that causes arrhythmias, high blood pressure, reduced heart rate variability, and the manifestation of congenital heart problems. It also raises plasma catecholamine production, further damaging the myocardium (Shanlin et al., 1988). Elevated catecholamine enhances oxidative load in myocardial tissues, disrupting the balance between oxidants and anti-oxidants. This diminishes NO bioavailability in the heart, affecting general circulation and regulation of blood pressure (Larson et al., 2012).

Generally, after penetrating or severe closed TBI, altered homeostatic mechanisms generate the first seizure, usually a generalized seizure with focal onset, and a late seizure that is a partial complex seizure. A better understanding of the molecular mechanisms that cause these seizures and epilepsies is imperative for development of better drugs and treatments. Moreover, greater understanding of the brain's immune system is also necessary to identify the causal mechanisms of long-term PTE-related consequences.

THERAPEUTIC INTERVENTION AND MANAGEMENT

Management of brain injury focuses primarily on preventing signs of secondary injury. Currently, no therapies are available for permanently treating TBI-related injuries, although more than 20 drugs are available to treat epilepsy (however one-third of epilepsy patients are refractory to these drugs) (Dalic and Cook, 2016; Hogan, 2018). Moreover, over 40 failed drugs have been tested in the clinical trials against epilepsy in the past decade, most of which were ion channel targets. The failure of these compounds to treat PTE could perhaps be due to the complexity of PTE and the new unknown mechanisms that regulate epileptogenesis after TBI (Temkin, 2001; Varvel et al., 2014). Therefore, it is important to investigate novel non-neuronal targets/mechanisms other than ion channels, such as enzymes, glial cells, neurovascular components, oxidative stress molecules, and nuclear proteins (**Table 2**).

No existing treatments can prevent the long-lasting neurodegenerative changes in PTE, but targeting free radicals during the acute phase of inflammation might prove to be more effective. For example, increased levels of NADPH oxidase after TBI damages mitochondria and other organelles (Bordt and Polster, 2014; Angeloni et al., 2015; Ma et al., 2017). Pharmacological inhibitors of free radicals such as NOX, peroxides, peroxynitrites/nitrates, hypochlorites, phenols and prostanoid antagonists can modulate free radical production and suppress inflammation (Cheng et al., 2012; Korkina et al., 2016; Ma et al., 2017; Smith et al., 2019). Studies have shown that inhibition or genetic ablation of NADPH oxidase improves outcomes in terms of neurodegeneration, oxidative stress mediated mitochondrial dysfunction, gliosis, and increases neurogenesis (Cheng et al., 2012; Altenhöfer et al., 2015; Hirano et al., 2015; Maqbool et al., 2020). In contrast to reducing pro-oxidant levels, increasing anti-oxidants can be a useful, alternate therapy for preventing long-term changes in the brain post-TBI. Inhibitors of conventional targets, such as COX-2, IFN, and prostaglandin, can also help in combating poor outcomes. Interestingly, the chronic PTE signature is quite similar to the IFN signature, in terms of activation of neurodegenerative mechanisms; and inactivating type I IFN with αIFNAR-infusion therapy can block IFNα/IFNβ signaling, lowers expression of inflammatory mediators, diminishes neurodegeneration, and attenuates inflammation. Moreover, an ICV infusion of αIFNAR significantly improves cognitive deficits, motor functions, upregulates neuroprotective genes, and reduces lesion volume (Barrett et al., 2020).

Inhibiting hippocampal neurogenesis after TBI can be a viable therapeutic option for preventing mesial TLE. In most cases, the process of neurogenesis in the hippocampus after injury benefits the brain and allows for recovery of memory and normal behavior (Parent, 2002; Sun, 2014; Redell et al., 2020). Some of that repair may be imperfect and show synaptic reorganization of neural networks, which can create circuitry that is epileptogenic. These considerations show the need for caution and careful design of strategies that target aberrant neurogenesis and synaptogenesis, while leaving the neurogenesis and synaptogenesis that are important for recovery in place.

In terms of treatment and management, controlling swelling and preventing hypoxia or ischemia can prove to be another effective therapy. If, at a certain point, intracranial pressure (ICP) rises dramatically with an increase in intracranial volume, then the brain swells substantially. Preventing this is important because the degree of ICP directly correlates with cerebral perfusion pressure (CPP), the key pressure required by brain, in terms of delivery of oxygen and other nutrients. As ICP

TABLE 2 | Novel therapeutic interventions that may have potential to impact the outcome of TBI-induced epileptogenesis.

Treatment	Model	Specie, age, strain	Dosage regimen	Targets/suggested mechanism of action	Region/Tissue analyzed	Outcome/effects	References
ISO1	Lateral Fluid Percussion Injury	Mice, 8 weeks, C57BL/6J	10 mg/kg (i.p.) (single dose), 30 min post-injury	• Macrophage migration inhibitory factor (MIF) antagonist • Inhibits MIF binding to CD74 and prevents its cleavage and activation • Inhibits TNFα and reduces gliosis	Parietal CTX; Brain leukocytes; Intestinal lymphocytes	• Decreased astrocyte activation and B cell brain infiltration • Elevation of splenic B cells • Inhibition of γδT cells' increase in gut	Newell-Rogers et al., 2020
Baicalein	$FeCl_3$-induced injury	Male, 18–22 g, C57BL/6J	50 and 100 mg/kg (i.p.) (single dose), 30 min prior to injury	• Positive allosteric modulator of $GABA_A$ receptor • Inhibitor of CYP2C9 and prolyl endopeptidase • Inhibits lipoxygenases	Somatosensory cortex; Hippocampal HT22 cells	• Reduced number and duration of seizures • Reduction in $FeCl_3$-induced PTS • Inhibition of 12/15-LOX-mediated lipid peroxidation by • antagonizing ferroptosis • Neuroprotection against FAC-induced HT22 cell damage	Li et al., 2019
Ceftriaxone	Lateral Fluid Percussion Injury	Rat, 8–9 weeks, Long-Evans	200 mg/kg (i.p.) for 7 days (once daily), 30 min post-TBI	• Third-generation cephalosporin antibiotic, also anti-microbial in nature • Inhibits mucopeptide synthesis in bacterial cell wall by binding to carboxypeptidases, endopeptidases, and transpeptidases	Neocortex	• Reduced seizures • Restoration of GLT-1 expression and reduced gliosis in lesioned cortex • Attenuation of PTS	Goodrich et al., 2013
Creatinine	Fluid Percussion Injury with PTZ	Rat, 250–300 g, Wistar	300 mg/kg (oral) for 3–7 days (once daily), 30 min post-TBI	• Neuroprotective, anti-inflammatory and cardioprotective actions • Inhibits JAK/STAT1 signal transmission by inhibiting interaction of IFNγ receptors with JAK2	Parietal CTX	• No change in susceptibility to seizures • Protection against protein carbonylation and TBARS after neuronal damage • No effect on convulsive parameters	Saraiva et al., 2012
Ketogenic diet	Fluid Percussion Injury with Flurothyl-induced seizures	Rat, 8 weeks, Sprague Dawley	Bio-Serv F3666 diet for 9 weeks, started 3 weeks prior to TBI	• High fat low carbohydrate diet, effective against drug-resistant epilepsy • Generates ketone bodies- which has anti-convulsive properties • Increases GABA, NPY, adenosine and reduces glutamate	Hippocampus	• Primarily anticonvulsive but not antiepileptogenic • Increased latency to myoclonic jerks at 9 weeks • Protection against hippocampal lesion volume and cell loss • Reduced gliosis and MFS	Schwartzkroin et al., 2010

(Continued)

TABLE 2 | Continued

Treatment	Model	Specie, age, strain	Dosage regimen	Targets/suggested mechanism of action	Region/Tissue analyzed	Outcome/effects	References
Apocynin	Lateral Fluid Percussion Injury	Mice, 28–32 g, Swiss	0.05, 0.5, and 5 mg/kg (subcut) (single dose), 30 min and 24 h post-TBI	• NADPH-oxidase inhibitor • Reduces pro-inflammatory cytokine production, neutrophil infiltration, ICAM-1 and P-selectin expression, PAR and nitrotyrosine formation, and MAPK activation	Cortex	• Attenuation of IL-1β, TNFα, NO metabolites and water content levels • Reduced oxidative damage (protein carbonyl, lipoperoxidation) • Reduced cortical lesion volume • Reduced secondary brain damage and improved cognition	Ferreira et al., 2013
Minozac	Closed Head Injury with Electroconvulsive Shock	Mice, 20–25 g, CD-1	5 mg/kg (i.p.) (two doses), 3 and 6 h post-TBI	• Selective inhibitor of proinflammatory cytokine by activated glia • More potency towards IL-1β, TNFα, and IL-6	Hippocampus	• Reduced seizure • susceptibility and neuronal injury by suppressing cytokine elevation • Diminished astrocyte activation and metallothionein expression • Improved neurobehavioral task performance	Chrzaszcz et al., 2010
Monophosphoryl Lipid A (MPL) and Pam3Cys	Controlled Cortical Impact with electrical kindling	Rat, 9 weeks, Wistar	1 μg/1 μl/rat MPL and Pam3Cys (intracerebroventricular injection) in lateral ventricle, 5 days prior to TBI	• Toll-like receptor agonists and potent stimulator of T-cells and antibody responses • Affects adaptive immune responses via specific interactions with B cells • Activators of monocytes and macrophages	Parietal cortex	• Reduced acceleration of epileptogenesis caused by trauma • Reduction in TNFα levels • No change in the speed of kindling and duration of kindled seizure parameters • Prevented decrease in seizure threshold	Hesam et al., 2018
Pyrroloquinoline Quinone (PQQ)	Controlled Cortical Impact	Rat, 8–9 weeks, Sprague Dawley	5, 7, and 10 mg/kg (i.p.) (single dose for 3 days) prior to TBI	• Superoxide scavenger and prevents oxidative changes • Inhibits glutamate decarboxylase and protects against NMDAR mediated neurotoxicity • Increases nerve growth factor synthesis	Cortex; Hippocampus	• Reduced oxidative stress induced neuronal death • Diminished cortical lesion volume • Reduced destruction, disordered arrangement and abnormal nuclear morphology in CA2 • Improved spatial memory and learning performance • Enhanced β-1,4-GalT-I and -V expression and 4-GlcNAc in microglia and neurons	Zhang et al., 2012
Rapamycin	Controlled Cortical Impact	Mice, 8 weeks, CD-1	6 mg/kg (i.p.) (single dose for 4 weeks), 1 h post-TBI	• Specifically inhibits mTOR by forming immunosuppresive complex with FKBP-12 • Inhibits T-cell activation and proliferation that occurs in response to proinflammatory cytokine stimulation	Neocortex; Hippocampus	• Reversed hyperactivation of mTORC1 pathway • Decreased neuronal • degeneration and mossy fiber sprouting • Reduced seizure frequency and rate of developing PTE	Guo et al., 2013

(Continued)

TABLE 2 | Continued

Treatment	Model	Specie, age, strain	Dosage regimen	Targets/suggested mechanism of action	Region/Tissue analyzed	Outcome/effects	References
SR141716A/ Rimonabant	Lateral Fluid Percussion Injury	Rat, P21–22, Wistar	1 and 10 mg/kg (i.p.) (single dose), 2 and 20 min post-TBI	• Selective CB1 antagonist and a dual inhibitor of ACAT • Alters cell cycle distribution and produces G2/M cell cycle arrest • Modulates RANTES and MCP-1 levels • Attenuates and controls neutrophils, monocytes and PDGF levels	Cortex	• Reduced post-traumatic hyperexcitability • Attenuation in long term increase in seizure susceptibility • Increased seizure latency and reduction in cumulative duration of seizures	Echegoyen et al., 2009
Trametinib	Controlled Cortical Impact	Mice, C57BL.6J	1 mg/kg (oral) (single dose for 7 days), 2 h post-TBI	• Highly specific and potent MEK1/2 inhibitor • Inhibits cell proliferation, activates autophagy and induces apoptosis	Cortex; Primary microglia culture	• Rescued oligodendrocytes and decreased infiltrating microglial density • Reduced microglial activation and proinflammatory cytokines • Inhibition of microglial MEK/ERK signaling cascade activation • Improved cognitive functions	Huang et al., 2020
DHEAS (Dehydroepian-drosterone Sulfate)	Weight Drop	Mice, 30–40 g, ICR	20 mg/kg (subcut) (once a week), 7 days post-TBI	• Androgen receptor antagonist and estrogen receptor agonist	Frontal cortex; Hippocampus	• Improved long-term cognitive and behavioral deficits	Milman et al., 2007
Atipamezole	Lateral Fluid Percussion Injury	Rat, 12 weeks, Sprague-Dawley	1 mg/kg (i.p.) followed by 100 μg/kg/h (subcut) (for 9 weeks), 30 min post-TBI	• α2-adrenergic receptor antagonist • Reverses analgesia by blocking norepinephrine feedback inhibition on nociceptors	Cortex; Hippocampus	• Reduced seizure susceptibility • Improved cognitive performance	Nissinen et al., 2017
Gabapentin	Undercut cortex model	Rat, P30, Sprague-Dawley	100 mg/kg (subcut) (thrice a day for 2 days) and 120 mg/kg/d (subcut) (13–15 days), 1 h post-TBI	• Inhibits L-type calcium channel and thrombospondin-induced excitatory synapses formation • Acts on adenosine receptors and voltage-gated potassium channels	Cortex; Brain slices	• Reduced posttraumatic hyperexcitability • Decreased incidence of evoked epileptiform discharges in cortical slices • Reduced expression of neurofilament and GFAP immunoreactivity • Reduced frequency of spontaneous and miniature EPSCs on layer V pyramidal neurons	Li et al., 2012
Sodium selenate	Lateral Fluid Percussion Injury	Rat, Adult Long-Evans	1 mg/kg (subcut) (for 12 weeks), after TBI	• Acts as an antioxidant via actions of selenoproteins for protection against oxidative stress • Acts as a catalyst for the production of thyroid hormone • Activates PP2A and decreases p-tau	Cortex; Hippocampus; Amygdala	• Suppressed epileptogenesis and reduced seizure frequency • Upregulation of PP2A and increased PR55 expression • Decreased tau phosphorylation and neurodegeneration	Liu et al., 2016

rises, CPP drops, and as with it the delivery of nutrients and oxygen decelerates having deleterious effects on the brain. This can further affect cerebral blood flow, reducing oxygen content in the blood (Bouzat et al., 2013; Kinoshita, 2016). Therefore, it is important to develop techniques that will sustain cerebral blood at an appropriate level—keeping CPP up without increasing ICP—to prevent permanent infarction from TBI (Zauner et al., 2002). Strategies for lowering ICP may include stepwise medical management or surgical options (like placing a ventricular drain for CSF) or employing strategies that would increase the intracranial vault size (like decompressive craniotomy). Medical management therapies can include normothermia, normoglycemia, targeting blood pressure, maintaining oxygen and carbon dioxide saturation levels, eliminating hyponatremia, decreasing cerebral metabolic demand/rate, increasing the mean arterial pressure to enhance CPP, and use of vasopressors such as norepinephrine and dopamine to prevent edema (Vespa et al., 1998; Hutchinson et al., 2002; Sookplung et al., 2011).

Prophylactic use of antiepileptic drugs (AEDs) can reduce the risk of early post-traumatic seizures but not the later ones. PTE perhaps represents the ideal model to study the mechanisms of epileptogenesis and develop therapies for epilepsy. Over the last several years it has become clear that, properly chosen, cases of PTE can successfully be treated with surgical interventions. Approximately 60% of the surgical cases of PTE end up being Engel class I, ∼20% Engel class II; and about 80% had favorable surgical outcomes. Gupta et al. (2014) reported that patients with mesial temporal sclerosis, as an epilepsy syndrome, have 92% class I and II outcomes. The lesional cases, from both frontal and temporal, and non-lesional cases were somewhat less favorable (Gupta et al., 2014). In contrast, the outcome of surgical intervention depended on the seizure-onset localization zone. The surgical intervention is not generally recommended in most cases of PTE, as seizure foci can be difficult to localize due to technical issues, such as craniotomies and breach rhythms. Patients with severe TBI may have undergone craniotomy, which may cause breath rhythms (special EEG rhythms that can be artifacts or misguide diagnosis). Moreover, patients with severe TBI may have diffuse cerebral or axonal injury evident on EEG recording as multiple epileptic foci that can overlap with localization of eloquent brain regions (Hakimian et al., 2012). Therefore, it is important to carefully select surgical candidates, as the patient with severe TBI may be at greater risk of surgical complications due to their structural damage or scar tissue and adhesion formation. For these reasons, other adjunctive treatment options such as stimulation of the vagus nerve, responsive nerve, and anterior nerve should be considered.

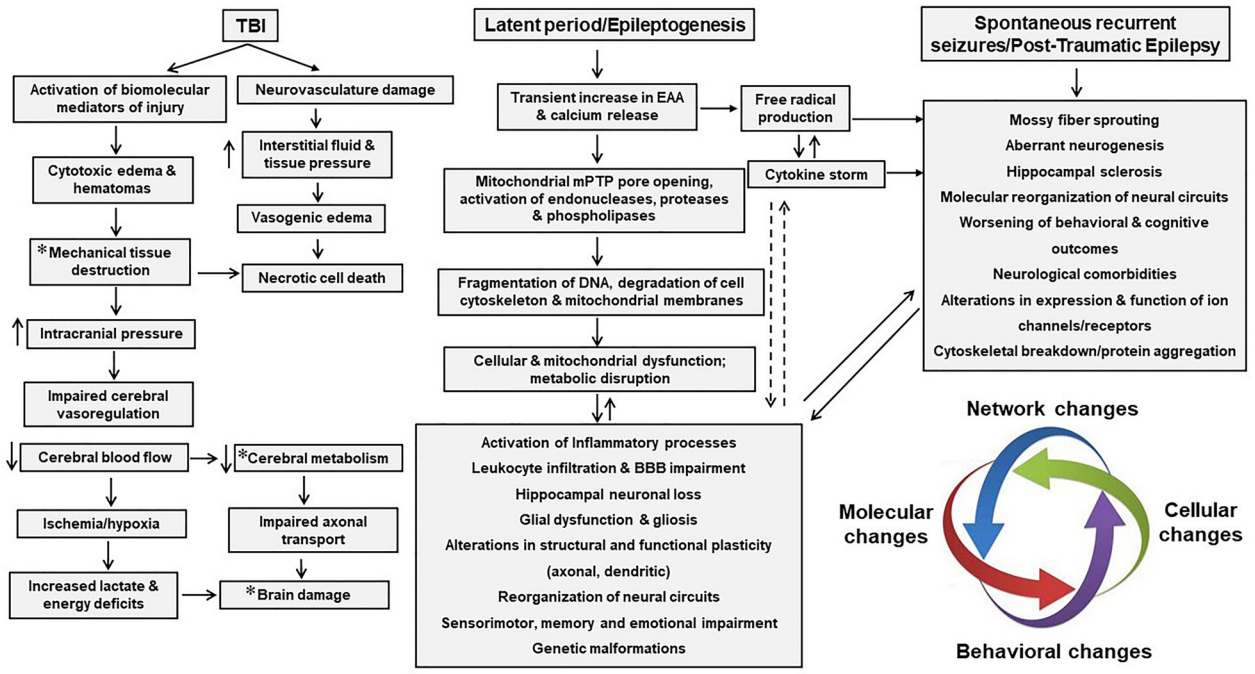

FIGURE 6 | Pathophysiological cascades of events from TBI to PTE. A series of cellular and molecular events overwhelms the brain following TBI. TBI induces neurovascular damage and activates biomolecular mediators of injury. This neurovascular damage leads to vasogenic edema and necrotic cell death, while biomolecular mediators lead to necrotic cell death and brain damage. TBI also induces structural damage that leads to cerebral edema and decreases cerebral blood flow, causing acute neurological damage. In addition, cytokines and other molecules released in the extracellular space trigger free radical production in neurons and glial cells, promotes neuronal excitability, and neuronal death. Alterations in mitochondrial bioenergetics, fragmentation of DNA and structural proteins, and activation of neuroinflammatory pathways cause structural and functional changes in the brain that accompany recurrent post-epileptic seizures. All these events, after TBI, are interwoven and rely on other altered cellular and molecular events which exacerbates post-epileptic seizures. Asterisk represents changes that can also lead to secondary damage either directly or indirectly.

Medical treatment for PTE can be similar to that for other epilepsies, with the caveat that unnecessary treatment with AEDs may impair neurorehabilitation. There is no evidence that treatment with AEDs or anti-convulsants will be beneficial in cases of moderate to severe TBI; however, some evidence suggests AEDs could possibly reduce the incidence of post-traumatic seizure if administered during the acute phase of injury. One study conducted by Hernandez (1997) showed that treating patients with phenytoin during the acute phase lowers the incidence of early post-traumatic seizures from 14.2 to 3.6%. Yet continuing AED treatment beyond the acute phase has never been shown to change the prognosis for the ultimate development of epilepsy (Hernandez, 1997). Recently, levetiracetam (LEV) has gained popularity in the treatment of PTE, as LEV does not cause the same side effects and has lower cytotoxic effects than other AEDs. Even though no randomized controlled trials have been done, comparative studies show the efficacy of LEV seems slightly better than standard AEDs, and with fewer side-effects. On the downside, observational studies report that LEV is not effective in reducing PTE risk, so it is generally not recommended beyond 7 days post-injury (Szaflarski et al., 2010). As an alternate to LEV, sodium channel blockers are an ideal option, but some of these blockers do not appear to be effective against PTE. For example, Dilantin blocks early seizures but it is not regarded as an effective anti-epileptogenic agent (Szaflarski et al., 2010). Although not every sodium channel blocker has been tested in PTE models, additional replacement therapies are required to treat PTE. These alternate therapies must rely on things like blocking inflammation, promoting BBB repair, or perhaps promoting the integrity of damaged axonal pathways to prevent persistent brain inflammation. Therefore, the goal of developing anti-epileptogenic compounds should be tied to these strategies to promote integrity, resilience, and recovery of neural structures.

CONCLUDING REMARKS

Four key elements—excitotoxicity, neuroinflammation, oxidative stress, and neurodegeneration—are the primary pathognomonic mechanisms responsible for PTE; and it is well known that TBI initiate cycles of neuroinflammatory events that elicit the oxidative stress response tripping a series of events and cycles that exacerbate the acute stage and lead to chronic conditions (**Figure 6**). The goal of this review is to understand the mechanisms of epileptogenesis after TBI and identify, develop, and validate therapeutic strategies to prevent PTE. In this regard, we can make several key conclusions: (1) the primary source of cellular excitotoxicity after TBI is elevation in extracellular glutamate, increased immune cell infiltration and crosstalk between glial cells and neurons governed mainly through cytokine and chemokine networks; (2) the initial immune response to injury is beneficial and, it works to counterbalance the disequilibrium in the system; (3) Impairment of mitochondria due to an excessive generation of ROS/RNS is a continuous process during epileptogenesis, and is associated with inflammation and neurodegeneration; (4) pro-inflammatory cytokines, and chemokines are the key players released by invading blood cells, microglia, astrocytes, and neurons; (5) over-production of cytokines, lipids, and chemokines over long periods of time triggers cell death; (6) invasion by leukocytes and activated microglia leads to tissue damage at later stages.

Post-traumatic epilepsy is phenotypically heterogenous in humans and it is important to understand this phenotypic heterogeneity to develop antiepileptogenic therapies. Both focal and diffuse mechanisms can result in PTE, and approximately 25–30% of PTE cases are associated with mesial temporal sclerosis. Although surgery is an alternate option, it is generally not recommended, so AEDs remain the first line of treatment. Yet, AEDs are not very effective in treating PTE, but are rather used to treat the symptoms without improving the underlying condition. Patients receiving AEDs often require lifelong AED treatment and some develop severe side effects over time. Furthermore, failure to control epileptic seizures can also lead to increased mortality, reduced quality of life, comorbidity, and depression. In spite of the many AEDs available, a little progress has been made in preventing the onset of new types of epilepsies. Moreover, repurposing anti-seizure drugs to prevent the onset of epilepsy has been entirely unsuccessful up to now.

Understanding epilepsy as a network disorder suggests early phases of epileptogenesis should be targeted before the imbalance spreads to other regions of the brain. This, however, is not as simple as it seems because many of the candidate compounds being investigated have multiple effects and target multiple pathways. These pathways can be different in humans and animal models, which devalues the translational significance of the latter and highlights the importance of designing experiments with the right timing, dosage, and targets, and with appropriate animal models (Smith, 2016; Saletti et al., 2019). Moreover, it is important to define targets with variable injury mechanics and to vary treatments at particular time-points. Ultimately, a clearer understanding of the molecular mechanisms of epilepsy will allow development of truly novel therapeutic targets for PTE.

AUTHOR CONTRIBUTIONS

SS reviewed the literature, wrote and edited manuscript, and prepared the tables and figures. GT and JH edited the manuscript. AB conceived the idea, and reviewed and edited manuscript. All the authors contributed to the manuscript revision, read, and approved the submitted version.

ACKNOWLEDGMENTS

The authors would like to thank Neha Pandya for editing and making figures.

REFERENCES

Abdullah, A., Zhang, M., Frugier, T., Bedoui, S., Taylor, J. M., and Crack, P. J. (2018). STING-mediated type-I interferons contribute to the neuroinflammatory process and detrimental effects following traumatic brain injury. *J. Neuroinflamm.* 15:323. doi: 10.1186/s12974-018-1354-7

Abdul-Muneer, P. M., Chandra, N., and Haorah, J. (2015). Interactions of oxidative stress and neurovascular inflammation in the pathogenesis of traumatic brain injury. *Mol. Neurobiol.* 51, 966–979. doi: 10.1007/s12035-014-8752-3

Adam-Vizi, V., and Starkov, A. A. (2010). Calcium and mitochondrial reactive oxygen species generation: how to read the facts. *J. Alzheimer Dis.* 20(Suppl. 2), S413–S426. doi: 10.3233/JAD-2010-100465

Agledal, L., Niere, M., and Ziegler, M. (2010). The phosphate makes a difference: cellular functions of NADP. *Redox Rep.* 15, 2–10. doi: 10.1179/174329210X12650506623122

Agrawal, A., Timothy, J., Pandit, L., and Manju, M. (2006). Post-traumatic epilepsy: an overview. *Clin. Neurol. Neurosurg.* 108, 433–439. doi: 10.1016/j.clineuro.2005.09.001

Aguiar, C. C. T., Almeida, A. B., Araújo, P. V. P., Abreu, R. N. D. C. D., Chaves, E. M. C., Vale, O. C. D., et al. (2012). Oxidative stress and epilepsy: literature review. *Oxid. Med. Cell. Longev.* 2012:795259. doi: 10.1155/2012/795259

Altenhöfer, S., Radermacher, K. A., Kleikers, P. W., Wingler, K., and Schmidt, H. H. (2015). Evolution of NADPH oxidase inhibitors: selectivity and mechanisms for target engagement. *Antioxid. Redox Signal.* 23, 406–427. doi: 10.1089/ars.2013.5814

Anderson, P., and Delgado, M. (2008). Endogenous anti-inflammatory neuropeptides and pro-resolving lipid mediators: a new therapeutic approach for immune disorders. *J. Cell. Mol. Med.* 12, 1830–1847. doi: 10.1111/j.1582-4934.2008.00387.x

Andoh, M., Ikegaya, Y, and Koyama, R. (2019). Synaptic pruning by microglia in epilepsy. *J. Clin. Med.* 8:2170. doi: 10.3390/jcm8122170

Andrews, A. M., Lutton, E. M., Merkel, S. F., Razmpour, R., and Ramirez, S. H. (2016). Mechanical injury induces brain endothelial-derived microvesicle release: implications for cerebral vascular injury during traumatic brain injury. *Front. Cell. Neurosci.* 10:43. doi: 10.3389/fncel.2016.00043

Angeloni, C., Prata, C., Vieceli Dalla Sega, F., Piperno, R., and Hrelia, S. (2015). Traumatic brain injury and NADPH oxidase: a deep relationship. *Oxid. Med. Cell. Longev.* 2015:370312. doi: 10.1155/2015/370312

Annegers, J. F., Hauser, W. A., Coan, S. P., and Rocca, W. A. (1998). A population-based study of seizures after traumatic brain injuries. *New Engl. J. Med.* 338, 20–24. doi: 10.1056/NEJM199801013380104

Aronica, E., Ravizza, T., Zurolo, E., and Vezzani, A. (2012). Astrocyte immune responses in epilepsy. *Glia* 60, 1258–1268. doi: 10.1002/glia.22312

Badaut, J., Ajao, D., Sorensen, D., Fukuda, A., and Pellerin, L. (2015). Caveolin expression changes in the neurovascular unit after juvenile traumatic brain injury: Signs of blood-brain barrier healing? *Neuroscience* 285, 215–226. doi: 10.1016/j.neuroscience.2014.10.035

Bae, Y. S., Oh, H., Rhee, S. G., and Yoo, Y. D. (2011). Regulation of reactive oxygen species generation in cell signaling. *Mol. Cells* 32, 491–509. doi: 10.1007/s10059-011-0276-3

Bai, R., Gao, H., Han, Z., Huang, S., Ge, X., Chen, F., et al. (2017). Flow cytometric characterization of T-cell subsets and microglia after repetitive mild traumatic brain injury in rats. *Neurochem. Res.* 42, 2892–2901. doi: 10.1007/s11064-017-2310-0

Bao, Y. H., Bramlett, H. M., Atkins, C. M., Lotocki, G., Alonso, O. F., Dietrich, W. D., et al. (2011). Post-traumatic seizures exacerbate histopathological damage after fluid-percussion brain injury. *J. Neurotrauma* 28, 35–42. doi: 10.1089/neu.2010.1383

Barrett, J. P., Henry, R. J., Shirey, K. A., Doran, S. J., Makarevich, O. D., Ritzel, R. M., et al. (2020). Interferon-β plays a detrimental role in experimental traumatic brain injury by enhancing neuroinflammation that drives chronic neurodegeneration. *J. Neurosci.* 40, 2357–2370. doi: 10.1523/JNEUROSCI.2516-19.2020

Baruch, K., Deczkowska, A., David, E., Castellano, J. M., Miller, O., Kertser, A., et al. (2014). Aging-induced type I interferon response at the choroid plexus negatively affects brain function. *Science* 346, 89–93. doi: 10.1126/science.1252945

Bell, R. D., Winkler, E. A., Sagare, A. P., Singh, I., Larue, B., Deane, R., et al. (2010). Pericytes control key neurovascular functions and neuronal phenotype in the adult brain and during brain aging. *Neuron* 68, 409–427. doi: 10.1016/j.neuron.2010.09.043

Ben Shimon, M., Shavit-Stein, E., Altman, K., Pick, C. G., and Maggio, N. (2020). Thrombin as key mediator of seizure development following traumatic brain injury. *Front. Pharmacol.* 10:1532. doi: 10.3389/fphar.2019.01532

Berg, A. T., Darefsky, A. S., Holford, T. R., and Shinnar, S. (1998). Seizures with fever after unprovoked seizures: an analysis in children followed from the time of a first febrile seizure. *Epilepsia* 39, 77–80. doi: 10.1111/j.1528-1157.1998.tb01277.x

Bhowmick, S., D'Mello, V., Caruso, D., Wallerstein, A., and Abdul-Muneer, P. M. (2019). Impairment of pericyte-endothelium crosstalk leads to blood-brain barrier dysfunction following traumatic brain injury. *Exp. Neurol.* 317, 260–270. doi: 10.1016/j.expneurol.2019.03.014

Biliau, A. (2006). Interferon: the pathways of discovery I. molecular and cellular aspects. *Cytokine Growth Fact. Rev.* 17, 381–409. doi: 10.1016/j.cytogfr.2006.07.001

Bilousova, T. V., Rusakov, D. A., Ethell, D. W., and Ethell, I. M. (2006). Matrix metalloproteinase-7 disrupts dendritic spines in hippocampal neurons through NMDA receptor activation. *J. Neurochem.* 97, 44–56. doi: 10.1111/j.1471-4159.2006.03701.x

Binder, D. K., Nagelhus, E. A., and Ottersen, O. P. (2012). Aquaporin-4 and epilepsy. *Glia* 60, 1203–1214. doi: 10.1002/glia.22317

Bolkvadze, T., and Pitkänen, A. (2012). Development of post-traumatic epilepsy after controlled cortical impact and lateral fluid-percussion-induced brain injury in the mouse. *J. Neurotrauma* 29, 789–812. doi: 10.1089/neu.2011.1954

Bordt, E. A., and Polster, B. M. (2014). NADPH oxidase- and mitochondria-derived reactive oxygen species in proinflammatory microglial activation: a bipartisan affair? *Free Rad. Biol. Med.* 76, 34–46. doi: 10.1016/j.freeradbiomed.2014.07.033

Bouzat, P., Sala, N., Payen, J.-F., and Oddo, M. (2013). Beyond intracranial pressure: optimization of cerebral blood flow, oxygen, and substrate delivery after traumatic brain injury. *Ann. Intens. Care* 3:23. doi: 10.1186/2110-5820-3-23

Broker, L. E., Kruyt, F. A., and Giaccone, G. (2005). Cell death independent of caspases: a review. *Clin. Cancer Res.* 11, 3155–3162. doi: 10.1158/1078-0432.CCR-04-2223

Brown, L. S., Foster, C. G., Courtney, J., King, N. E., Howells, D. W., and Sutherland, B. A. (2019). Pericytes and neurovascular function in the healthy and diseased brain. *Front. Cell. Neurosci.* 13:282. doi: 10.3389/fncel.2019.00282

Burda, J. E., Bernstein, A. M., and Sofroniew, M. V. (2016). Astrocyte roles in traumatic brain injury. *Exper. Neurol.* 275, 305–315. doi: 10.1016/j.expneurol.2015.03.020

Burda, J. E., and Sofroniew, M. V. (2014). Reactive gliosis and the multicellular response to CNS damage and disease. *Neuron* 81, 229–248. doi: 10.1016/j.neuron.2013.12.034

Burfeind, K. G., Michaelis, K. A., and Marks, D. L. (2016). The central role of hypothalamic inflammation in the acute illness response and cachexia. *Semin. Cell Dev. Biol.* 54, 42–52. doi: 10.1016/j.semcdb.2015.10.038

Cantu, D., Walker, K., Andresen, L., Taylor-Weiner, A., Hampton, D., Tesco, G., et al. (2015). Traumatic brain injury increases cortical glutamate network activity by compromising GABAergic control. *Cereb. Cortex* 25, 2306–2320. doi: 10.1093/cercor/bhu041

Cardenas-Rodriguez, N., Huerta-Gertrudis, B., Rivera-Espinosa, L., Montesinos-Correa, H., Bandala, C., Carmona-Aparicio, L., et al. (2013). Role of oxidative stress in refractory epilepsy: evidence in patients and experimental models. *Intern. J. Mol. Sci.* 14, 1455–1476. doi: 10.3390/ijms14011455

Castejon, O. J. (1984). Formation of transendothelial channels in traumatic human brain edema. *Pathol. Res. Pract.* 179, 7–12. doi: 10.1016/S0344-0338(84)80054-0

Centers for Disease Control and Prevention (2019). *Surveillance Report of Traumatic Brain Injury-Related Emergency Department Visits, Hospitalizations, and Deaths—United States, 2014.* Available online at: https://www.cdc.gov/traumaticbraininjury/pdf/TBI-Surveillance-Report-508.pdf (accessed August 15, 2020).

Cerutti, C., and Ridley, A. J. (2017). Endothelial cell-cell adhesion and signaling. *Exp. Cell Res.* 358, 31–38. doi: 10.1016/j.yexcr.2017.06.003

Cheeseman, K. H., and Slater, T. F. (1993). An introduction to free radical biochemistry. *Br. Med. Bull.* 49, 481–493. doi: 10.1093/oxfordjournals.bmb.a072625

Chen, Y., Qin, C., Huang, J., Tang, X., Liu, C., Huang, K., et al. (2020). The role of astrocytes in oxidative stress of central nervous system: a mixed blessing. *Cell Prolifer.* 53:12781. doi: 10.1111/cpr.12781

Cheng, G., Kong, R. H., Zhang, L. M., and Zhang, J. N. (2012). Mitochondria in traumatic brain injury and mitochondrial-targeted multipotential therapeutic strategies. *Br. J. Pharmacol.* 167, 699–719. doi: 10.1111/j.1476-5381.2012.02025.x

Chinnici, C. M., Yao, Y., Ding, T., Funk, C. D., and Praticò, D. (2005). Absence of 12/15 lipoxygenase reduces brain oxidative stress in apolipoprotein E-deficient mice. *Am. J. Pathol.* 167, 1371–1377. doi: 10.1016/S0002-9440(10)61224-2

Cho, K. (2019). Emerging Roles of Complement Protein C1q in Neurodegeneration. *Aging Dis.* 10:652. doi: 10.14336/ad.2019.0118

Choi, G. B., Yim, Y. S., Wong, H., Kim, S., Kim, H., Kim, S. V., et al. (2016). The maternal interleukin-17a pathway in mice promotes autism-like phenotypes in offspring. *Science* 351, 933–939. doi: 10.1126/science.aad0314

Chrzaszcz, M., Venkatesan, C., Dragisic, T., Watterson, D. M., and Wainwright, M. S. (2010). Minozac treatment prevents increased seizure susceptibility in a mouse "two-hit" model of closed skull traumatic brain injury and electroconvulsive shock-induced seizures. *J. Neurotrauma* 27, 1283–1295. doi: 10.1089/neu.2009.1227

Chuang, T.-C., Chang, A. Y. W., Lin, J.-W., Hsu, S.-P., and Chan, S. H. H. (2004). Mitochondrial dysfunction and ultrastructural damage in the hippocampus during kainic acid-induced status epilepticus in the rat. *Epilepsia* 45, 1202–1209. doi: 10.1111/j.0013-9580.2004.18204.x

Chuang, Y. C. (2010). Mitochondrial dysfunction and oxidative stress in seizure-induced neuronal cell death. *Acta Neurol. Taiwa.* 19, 3–15.

Chung, R. S., McCormack, G. H., King, A. E., West, A. K., and Vickers, J. C. (2005). Glutamate induces rapid loss of axonal neurofilament proteins from cortical neurons in vitro. *Exper. Neurol.* 193, 481–488. doi: 10.1016/j.expneurol.2005.01.005

Cini, M., and Moretti, A. (1995). Studies on lipid peroxidation and protein oxidation in the aging brain. *Neurobiol. Aging* 16, 53–57. doi: 10.1016/0197-4580(95)80007-e

Clark, D. P., Perreau, V. M., Shultz, S. R., Brady, R. D., Lei, E., Dixit, S., et al. (2019). Inflammation in traumatic brain injury: roles for toxic A1 astrocytes and microglial-astrocytic crosstalk. *Neurochem. Res.* 44, 1410–1424. doi: 10.1007/s11064-019-02721-8

Cui, H., Kong, Y., and Zhang, H. (2012). Oxidative stress, mitochondrial dysfunction, and aging. *J. Signal Transd.* 2012:646354.

Daglas, M., and Adlard, P. A. (2018). The involvement of iron in traumatic brain injury and neurodegenerative disease. *Front. Neurosci.* 12:981. doi: 10.3389/fnins.2018.00981

Dalal, P. J., Muller, W. A., and Sullivan, D. P. (2020). Endothelial cell calcium signaling during barrier function and inflammation. *Am. J. Pathol.* 190, 535–542. doi: 10.1016/j.ajpath.2019.11.004

Dalic, L., and Cook, M. J. (2016). Managing drug-resistant epilepsy: challenges and solutions. *Neuropsychiatr. Dis. Treat.* 12, 2605–2616. doi: 10.2147/NDT.S84852

D'Ambrosio, R., Fairbanks, J. P., Fender, J. S., Born, D. E., Doyle, D. L., and Miller, J. W. (2004). Post-traumatic epilepsy following fluid percussion injury in the rat. *Brain* 127, 304–314. doi: 10.1093/brain/awh038

D'Ambrosio, R., Fender, J. S., Fairbanks, J. P., Born, D. E., Doyle, D. L., Miller, J. W., et al. (2005). Progression from frontal-parietal to mesial-temporal epilepsy after fluid percussion injury in the rat. *Brain* 128, 174–188. doi: 10.1093/brain/awh337

Davalos, D., Grutzendler, J., Yang, G., Kim, J. V., Zuo, Y., Jung, S., et al. (2005). ATP mediates rapid microglial response to local brain injury in vivo. *Nat. Neurosci.* 8, 752–758. doi: 10.1038/nn1472

Davies, C. L., Patir, A., and McColl, B. W. (2019). Myeloid cell and transcriptome signatures associated with inflammation resolution in a model of self-limiting acute brain inflammation. *Front. Immunol.* 10:1048. doi: 10.3389/fimmu.2019.01048

Dearden, N. M. (1992). "Brain edema and raised intracranial pressure after head injury," in *Yearbook of Intensive Care and Emergency Medicine Yearbook of Intensive Care and Emergency Medicine*, ed. J. L. Vincent (Berlin: Springer), 537–552. doi: 10.1007/978-3-642-84734-9_52

Dejager, L., Vandevyver, S., Ballegeer, M., Van Wonterghem, E., An, L. L., Riggs, J., et al. (2014). Pharmacological inhibition of type I interferon signaling protects mice against lethal sepsis. *J. Infect. Dis.* 209, 960–970. doi: 10.1093/infdis/jit600

Dexter, D. T., Carter, C. J., Wells, F. R., Javoy-Agid, F., Agid, Y., Lees, A., et al. (1989). Basal lipid peroxidation in substantia nigra is increased in Parkinson's disease. *J. Neurochem.* 52, 381–389. doi: 10.1111/j.1471-4159.1989.tb09133.x

Dheen, S. T., Kaur, C., and Ling, E.-A. (2007). Microglial activation and its implications in the brain diseases. *Curr. Med. Chem.* 14, 1189–1197. doi: 10.2174/092986707780597961

Diaz-Arrastia, R., Agostini, A., Frol, A. B., Mickey, B., Fleckenstein, J., Bigio, E., et al. (2000). Neurophysiologic and neuroradiologic features of intractable epilepsy after traumatic brain injury in adults. *Arch. Neurol.* 57, 1611–1616. doi: 10.1001/archneur.57.11.1611

Dienel, G. A. (2014). Lactate shuttling and lactate use as fuel after traumatic brain injury: metabolic considerations. *J. Cereb. Blood Flow Metab.* 34, 1736–1748. doi: 10.1038/jcbfm.2014.153

Ding, K., Gupta, P. K., and Diaz-Arrastia, R. (2016). "Ch. 14 Epilepsy after traumatic brain injury," in *Translational Research in Traumatic Brain Injury*, eds D. Laskowitz and G. Grant (Boca Raton, FL: CRC Press).

Du, Y., Kemper, T., Qiu, J., and Jiang, J. (2016). Defining the therapeutic time window for suppressing the inflammatory prostaglandin E2 signaling after status epilepticus. *Expert Rev. Neurotherapeut.* 16, 123–130. doi: 10.1586/14737175.2016.1134322

Eastman, C. L., D'Ambrosio, R., and Ganesh, T. (2020). Modulating neuroinflammation and oxidative stress to prevent epilepsy and improve outcomes after traumatic brain injury. *Neuropharmacology* 172:107907. doi: 10.1016/j.neuropharm.2019.107907

Echegoyen, J., Armstrong, C., Morgan, R. J., and Soltesz, I. (2009). Single application of a CB1 receptor antagonist rapidly following head injury prevents long-term hyperexcitability in a rat model. *Epilepsy Res.* 85, 123–127. doi: 10.1016/j.eplepsyres.2009.02.019

Emerit, J., Edeas, M., and Bricaire, F. (2004). Neurodegenerative diseases and oxidative stress. *Biomed. Pharmacother.* 58, 39–46. doi: 10.1016/j.biopha.2003.11.004

Ermolaeva, M. A., Michallet, M., Papadopoulou, N., Utermöhlen, O., Kranidioti, K., Kollias, G., et al. (2008). Function of TRADD in tumor necrosis factor receptor 1 signaling and in TRIF-dependent inflammatory responses. *Nat. Immunol.* 9, 1037–1046. doi: 10.1038/ni.1638

Eslami, M., Sayyah, M., Soleimani, M., Alizadeh, L., and Hadjighassem, M. (2015). Lipopolysaccharide preconditioning prevents acceleration of kindling epileptogenesis induced by traumatic brain injury. *J. Neuroimmunol.* 289, 143–151. doi: 10.1016/j.jneuroim.2015.11.003

Evans, L. P., Woll, A. W., Wu, S., Todd, B. P., Hehr, N., Hedberg-Buenz, A., et al. (2020). Modulation of post-traumatic immune response using the IL-1 receptor antagonist anakinra for improved visual outcomes. *J. Neurotrauma* 37, 1463–1480. doi: 10.1089/neu.2019.6725

Faul, M., and Coronado, V. (2015). Epidemiology of traumatic brain injury. *Handb. Clin. Neurol.* 127, 3–13. doi: 10.1016/B978-0-444-52892-6.00001-5

Ferreira, A. P., Rodrigues, F. S., Della-Pace, I. D., Mota, B. C., Oliveira, S. M., Velho Gewehr Cde, C., et al. (2013). The effect of NADPH-oxidase inhibitor apocynin on cognitive impairment induced by moderate lateral fluid percussion injury: role of inflammatory and oxidative brain damage. *Neurochem. Int.* 63, 583–593. doi: 10.1016/j.neuint.2013.09.012

Figueiredo-Pereira, M. E., Rockwell, P., Schmidt-Glenewinkel, T., and Serrano, P. (2015). Neuroinflammation and J2 prostaglandins: linking impairment of the ubiquitin-proteasome pathway and mitochondria to neurodegeneration. *Front. Mol. Neurosci.* 7:104. doi: 10.3389/fnmol.2014.00104

Fogal, B., and Hewett, S. J. (2008). Interleukin-1β: a bridge between inflammation and excitotoxicity? *J. Neurochem.* 106, 1–23. doi: 10.1111/j.1471-4159.2008.05315.x

Fordington, S., and Manford, M. (2020). A review of seizures and epilepsy following traumatic brain injury. *J. Neurol.* 267, 3105–3111. doi: 10.1007/s00415-020-09926-w

Fossat, P., Turpin, F. R., Sacchi, S., Dulong, J., Shi, T., Rivet, J. M., et al. (2012). Glial D-serine gates NMDA receptors at excitatory synapses in prefrontal cortex. *Cereb. Cortex* 22, 595–606. doi: 10.1093/cercor/bhr130

Franco, R., and Fernandez-Suarez, D. (2015). Alternatively activated microglia and macrophages in the central nervous system. *Prog. Neurobiol.* 131, 65–86. doi: 10.1016/j.pneurobio.2015.05.003

Frenguelli, B. G. (2019). The purine salvage pathway and the restoration of cerebral ATP: implications for brain slice physiology and brain injury. *Neurochem. Res.* 44, 661–675. doi: 10.1007/s11064-017-2386-6

Gao, X., Deng, P., Xu, Z. C., and Chen, J. (2011). Moderate traumatic brain injury causes acute dendritic and synaptic degeneration in the hippocampal dentate Gyrus. *PLoS One* 6:e024566. doi: 10.1371/journal.pone.0024566

Garga, N., and Lowenstein, D. H. (2006). Posttraumatic epilepsy: a major problem in desperate need of major advances. *Epilepsy Curr.* 6, 1–5. doi: 10.1111/j.1535-7511.2005.00083.x

Gatti, S., Vezzani, A., and Bartfai, T. (2002). "Mechanisms of fever and febrile seizures: putative role of the interleukin-1 system," in *Febrile Seizures*, eds T. Z. Baram and S. Shinnar (Cambridge, MA: Academic Press), 169–188. doi: 10.1016/B978-012078141-6/50014-7

Godfred, R. M., Parikh, M. S., Haltiner, A. M., Caylor, L. M., Sepkuty, J. P., and Doherty, M. J. (2013). Does aspirin use make it harder to collect seizures during elective video-EEG telemetry? *Epilepsy Behav.* 27, 115–117. doi: 10.1016/j.yebeh.2012.12.031

Golarai, G., Greenwood, A. C., Feeney, D. M., and Connor, J. A. (2001). Physiological and structural evidence for hippocampal involvement in persistent seizure susceptibility after traumatic brain injury. *J. Neurosci.* 21, 8523–8537. doi: 10.1523/JNEUROSCI.21-21-08523.2001

Goodrich, G. S., Kabakov, A. Y., Hameed, M. Q., Dhamne, S. C., Rosenberg, P. A., and Rotenberg, A. (2013). Ceftriaxone treatment after traumatic brain injury restores expression of the glutamate transporter, GLT-1, reduces regional gliosis, and reduces post-traumatic seizures in the rat. *J. Neurotrauma* 30, 1434–1441. doi: 10.1089/neu.2012.2712

Greenfield, J. G., Love, S., Louis, D. N., and Perry, A. (2008). *Greenfield's Neuropathology*, 8th Edn. London: Hodder Arnold.

Guerriero, R. M., Giza, C. C., and Rotenberg, A. (2015). Glutamate and GABA imbalance following traumatic brain injury. *Curr. Neurol. Neurosci. Rep.* 15:27. doi: 10.1007/s11910-015-0545-1

Guo, D., Zeng, L., Brody, D. L., and Wong, M. (2013). Rapamycin attenuates the development of posttraumatic epilepsy in a mouse model of traumatic brain injury. *PLoS One* 8:e64078. doi: 10.1371/journal.pone.0064078

Gupta, P. K., Sayed, N., Ding, K., Agostini, M. A., Van Ness, P. C., Yablon, S., et al. (2014). Subtypes of post-traumatic epilepsy: clinical, electrophysiological, and imaging features. *J. Neurotrauma* 31, 1439–1443. doi: 10.1089/neu.2013.3221

Hakimian, S., Kershenovich, A., Miller, J. W., Ojemann, J. G., Hebb, A. O., D'Ambrosio, R., et al. (2012). Long-term outcome of extratemporal resection in posttraumatic epilepsy. *Neurosurg. Focus* 32:E10. doi: 10.3171/2012.1.FOCUS11329

Halliwell, B. (1999). Antioxidant defence mechanisms: from the beginning to the end (of the beginning). *Free Rad. Res.* 31, 261–272. doi: 10.1080/10715769900300841

Hammad, A., Westacott, L., and Zaben, M. (2018). The role of the complement system in traumatic brain injury: a review. *J. Neuroinflamm.* 15:24. doi: 10.1186/s12974-018-1066-z

Hanisch, U., and Kettenmann, H. (2007). Microglia: active sensor and versatile effector cells in the normal and pathologic brain. *Nat. Neurosci.* 10, 1387–1394. doi: 10.1038/nn1997

Haskó, G., Linden, J., Cronstein, B., and Pacher, P. (2008). Adenosine receptors: therapeutic aspects for inflammatory and immune diseases. *Nat. Rev. Drug Discov.* 7, 759–770. doi: 10.1038/nrd2638

Hein, A. M., and O'Banion, M. K. (2009). Neuroinflammation and memory: the role of prostaglandins. *Mol. Neurobiol.* 40, 15–32. doi: 10.1007/s12035-009-8066-z

Hemphill, M. A., Dabiri, B. E., Gabriele, S., Kerscher, L., Franck, C., Goss, J. A., et al. (2011). A possible role for integrin signaling in diffuse axonal injury. *PLoS One* 6:e022899. doi: 10.1371/journal.pone.0022899

Hernandez, T. D. (1997). Preventing post-traumatic epilepsy after brain injury: weighing the costs and benefits of anticonvulsant prophylaxis. *Trends Pharmacol. Sci.* 18, 59–62. doi: 10.1016/S0165-6147(97)89801-X

Herz, J., Filiano, A. J., Smith, A., Yogev, N., and Kipnis, J. (2017). Myeloid cells in the central nervous system. *Immunity* 46, 943–956. doi: 10.1016/j.immuni.2017.06.007

Hesam, S., Khoshkholgh-Sima, B., Pourbadie, H. G., Babapour, V., Zendedel, M., and Sayyah, M. (2018). Monophosphoryl lipid A and Pam3Cys prevent the increase in seizure susceptibility and epileptogenesis in rats undergoing traumatic brain injury. *Neurochem. Res.* 43, 1978–1985. doi: 10.1007/s11064-018-2619-3

Heuser, K., Nagelhus, E. A., Taubøll, E., Indahl, U., Berg, P. R., Lien, S., et al. (2010). Variants of the genes encoding AQP4 and Kir4.1 are associated with subgroups of patients with temporal lobe epilepsy. *Epilepsy Res.* 88, 55–64. doi: 10.1016/j.eplepsyres.2009.09.023

Hickey, R. W., Adelson, P. D., Johnnides, M. J., Davis, D. S., and Yu, Z. (2007). Cyclooxygenase-2 activity following traumatic brain injury in the developing rat. *Pediatr. Res.* 62, 271–276. doi: 10.1203/pdr.0b013e3180db2902

Himanen, L., Portin, R., Isoniemi, H., Helenius, H., Kurki, T., and Tenovuo, O. (2006). Longitudinal cognitive changes in traumatic brain injury: a 30-year follow-up study. *Neurology* 66, 187–192. doi: 10.1212/01.wnl.0000194264.60150.d3

Hinzman, J. M., Thomas, T. C., Burmeister, J. J., Quintero, J. E., Huettl, P., Pomerleau, F., et al. (2010). Diffuse brain injury elevates tonic glutamate levels and potassium-evoked glutamate release in discrete brain regions at two days post-injury: an enzyme-based microelectrode array study. *J. Neurotrauma* 27, 889–899. doi: 10.1089/neu.2009.1238

Hirano, K., Chen, W. S., Chueng, A. L., Dunne, A. A., Seredenina, T., Filippova, A., et al. (2015). Discovery of GSK2795039, a novel small molecule NADPH Oxidase 2 inhibitor. *Antioxid. Redox Signal.* 23, 358–374. doi: 10.1089/ars.2014.6202

Ho, D. D., Neumann, A. U., Perelson, A. S., Chen, W., Leonard, J. M., and Markowitz, M. (1995). Rapid turnover of plasma virions and CD4 lymphocytes in HIV-1 infection. *Nature* 373, 123–126. doi: 10.1038/373123a0

Hogan, E. (2018). Drug resistant epilepsy and new AEDs: two perspectives. *Epilepsy Curr.* 18, 304–306. doi: 10.5698/1535-7597.18.5.304

Holbrook, J., Lara-Reyna, S., Jarosz-Griffiths, H., and McDermott, M. (2019). Tumour necrosis factor signalling in health and disease. *F1000Research* 8:F1000FacultyRev-111. doi: 10.12688/f1000research.17023.1

Hsieh, C. L., Kim, C. C., Ryba, B. E., Niemi, E. C., Bando, J. K., Locksley, R. M., et al. (2013). Traumatic brain injury induces macrophage subsets in the brain. *Eur. J. Immunol.* 43, 2010–2022. doi: 10.1002/eji.201243084

Hu, X., Li, P., Guo, Y., Wang, H., Leak, R. K., Chen, S., et al. (2012). Microglia/macrophage polarization dynamics reveal novel mechanism of injury expansion after focal cerebral ischemia. *Stroke* 43, 3063–3070. doi: 10.1161/strokeaha.112.659656

Huang, Y., Li, Q., Tian, H., Yao, X., Bakina, O., Zhang, H., et al. (2020). MEK inhibitor trametinib attenuates neuroinflammation and cognitive deficits following traumatic brain injury in mice. *Am. J. Transl. Res.* 12, 6351–6365.

Hunt, R. F., Scheff, S. W., and Smith, B. N. (2009). Posttraumatic epilepsy after controlled cortical impact injury in mice. *Exp. Neurol.* 215, 243–252. doi: 10.1016/j.expneurol.2008.10.005

Hunt, R. F., Scheff, S. W., and Smith, B. N. (2010). Regionally localized recurrent excitation in the dentate gyrus of a cortical contusion model of posttraumatic epilepsy. *J. Neurophysiol.* 103, 1490–1500. doi: 10.1152/jn.00957.2009

Hutchinson, P. J., Gupta, A. K., Fryer, T. F., Al-Rawi, P. G., Chatfield, D. A., Coles, J. P., et al. (2002). Correlation between cerebral blood flow, substrate delivery, and metabolism in head injury: a combined microdialysis and triple oxygen positron emission tomography study. *J. Cereb. Blood Flow Metab.* 22, 735–745. doi: 10.1097/00004647-200206000-00012

Ichkova, A., Rodriguez-Grande, B., Zub, E., Saudi, A., Fournier, M. L., Aussudre, J., et al. (2020). Early cerebrovascular and long-term neurological modifications ensue following juvenile mild traumatic brain injury in male mice. *Neurobiol. Dis.* 2020:104952. doi: 10.1016/j.nbd.2020.104952

Infanger, D. W., Sharma, R. V., and Davisson, R. L. (2006). NADPH oxidases of the brain: distribution, regulation, and function. *Antioxid. Redox Signal.* 8, 1583–1596. doi: 10.1089/ars.2006.8.1583

Isokawa, M. (1998). Remodeling dendritic spines in the rat pilocarpine model of temporal lobe epilepsy. *Neurosci. Lett.* 258, 73–76. doi: 10.1016/s0304-3940(98)00848-9

Isokawa, M., and Levesque, M. F. (1991). Increased NMDA responses and dendritic degeneration in human epileptic hippocampal neurons in slices. *Neurosci. Lett.* 132, 212–216. doi: 10.1016/0304-3940(91)90304-c

Izzy, S., Liu, Q., Fang, Z., Lule, S., Wu, L., Chung, J. Y., et al. (2019). Time-dependent changes in microglia transcriptional networks following traumatic brain injury. *Front. Cell. Neurosci.* 13:307. doi: 10.3389/fncel.2019.00307

Jackson, E. K., Boison, D., Schwarzschild, M. A., and Kochanek, P. M. (2016). Purines: Forgotten mediators in traumatic brain injury. *J. Neurochem.* 137, 142–153. doi: 10.1111/jnc.13551

Jarrahi, A., Braun, M., Ahluwalia, M., Gupta, R. V., Wilson, M., Munie, S., et al. (2020). Revisiting traumatic brain injury: from molecular mechanisms to therapeutic interventions. *Biomedicines* 8:389. doi: 10.3390/biomedicines8100389

Jha, R. M., Kochanek, P. M., and Simard, J. M. (2019). Pathophysiology of cerebral edema in traumatic brain injury. *Neuropharmacology* 145, 230–246. doi: 10.1016/j.neuropharm.2018.08.004

Jiang, J., Quan, Y., Ganesh, T., Pouliot, W. A., Dudek, F. E., and Dingledine, R. (2013). Inhibition of the prostaglandin receptor EP2 following status epilepticus reduces delayed mortality and brain inflammation. *Proc. Natl. Acad. Sci. U.S.A.* 110, 3591–3596. doi: 10.1073/pnas.1218498110

Jiang, M., Lee, C. L., Smith, K. L., and Swann, J. W. (1998). Spine loss and other persistent alterations of hippocampal pyramidal cell dendrites in a model of early-onset epilepsy. *J. Neurosci.* 18, 8356–8368. doi: 10.1523/jneurosci.18-20-08356.1998

Johnstone, V. P., Shultz, S. R., Yan, E. B., O'Brien, T. J., and Rajan, R. (2014). The acute phase of mild traumatic brain injury is characterized by a distance-dependent neuronal hypoactivity. *J. Neurotrauma* 31, 1881–1895. doi: 10.1089/neu.2014.3343

Kang, X., Qiu, J., Li, Q., Bell, K. A., Du, Y., Jung, D. W., et al. (2017). Cyclooxygenase-2 contributes to oxidopamine-mediated neuronal inflammation and injury via the prostaglandin E2 receptor EP2 subtype. *Sci. Rep.* 7:9459. doi: 10.1038/s41598-017-09528-z

Kann, O., Kovács, R., Njunting, M., Behrens, C. J., Otáhal, J., Lehmann, T. N., et al. (2005). Metabolic dysfunction during neuronal activation in the ex vivo hippocampus from chronic epileptic rats and humans. *Brain* 128, 2396–2407. doi: 10.1093/brain/awh568

Karve, I. P., Zhang, M., Habgood, M., Frugier, T., Brody, K. M., Sashindranath, M., et al. (2016). Ablation of Type-1 IFN signaling in hematopoietic cells confers protection following traumatic brain injury. *eNeuro* 3:ENEURO.0128-15.2016. doi: 10.1523/ENEURO.0128-15.2016

Kaufmann, W. E., Worley, P. F., Taylor, C. V., Bremer, M., and Isakson, P. C. (1997). Cyclooxygenase-2 expression during rat neocortical development and in Rett syndrome. *Brain Dev.* 19, 25–34. doi: 10.1016/s0387-7604(96)00047-2

Kaur, P., and Sharma, S. (2018). Recent advances in pathophysiology of traumatic brain injury. *Curr. Neuropharmacol.* 16, 1224–1238. doi: 10.2174/1871530318666180423121833

Kharatishvili, I., Nissinen, J. P., McIntosh, T. K., and Pitkänen, A. (2006). A model of posttraumatic epilepsy induced by lateral fluid-percussion brain injury in rats. *Neuroscience* 140, 685–697. doi: 10.1016/j.neuroscience.2006.03.012

Kharatishvili, I., and Pitkänen, A. (2010). Association of the severity of cortical damage with the occurrence of spontaneous seizures and hyperexcitability in an animal model of posttraumatic epilepsy. *Epilepsy Res.* 90, 47–59. doi: 10.1016/j.eplepsyres.2010.03.007

Kharlamov, E. A., Lepsveridze, E., Meparishvili, M., Jiang, Q., Zhao, M., Hu, F., et al. (2011). Alterations of GABA(A) and glutamate receptor subunits and heat shock protein in rat hippocampus following traumatic brain injury and in posttraumatic epilepsy. *Epilepsy Res.* 95, 20–34. doi: 10.1016/j.eplepsyres.2011.02.008

Kinoshita, K. (2016). Traumatic brain injury: pathophysiology for neurocritical care. *J. Intens. Care* 4:29. doi: 10.1186/s40560-016-0138-3

Knoblach, S. M., Nikolaeva, M., Huang, X., Fan, L., Krajewski, S., Reed, J. C., et al. (2002). Multiple caspases are activated after traumatic brain injury: evidence for involvement in functional outcome. *J. Neurotrauma* 19, 1155–1170. doi: 10.1089/08977150260337967

Kögel, D. and Prehn, J.H.M (2000-2013). "Caspase-independent cell death mechanisms," in *Madame Curie Bioscience Database [Internet]*, (Austin, TX: Landes Bioscience). Available online at: https://www.ncbi.nlm.nih.gov/books/NBK6197/

Korgaonkar, A. A., Li, Y., Sekhar, D., Wang, J., Zhao, K., Zhang, H., et al. (2020). Toll-like Receptor 4 signaling in neurons enhances calcium-permeable α-Amino-3-Hydroxy-5-Methyl-4-isoxazolepropionic acid receptor currents and drives post-traumatic epileptogenesis. *Ann. Neurol.* 87, 497–515. doi: 10.1002/ana.25698

Korkina, L., Ozben, T., and Saso, L. (2016). Modulation of oxidative stress: pharmaceutical and pharmacological aspects. *Oxid. Med. Cell. Longev.* 2016:6023417. doi: 10.1155/2016/6023417

Koronyo, Y., Salumbides, B. C., Sheyn, J., Pelissier, L., Li, S., Ljubimov, C., et al. (2015). Therapeutic effects of glatiramer acetate and grafted $CD115^{+}$ monocytes in a mouse model of Alzheimer's disease. *Brain* 138, 2399–2422. doi: 10.1093/brain/awv150

Koza, L., and Linseman, D. A. (2019). Glutathione precursors shield the brain from trauma. *Neural Regen. Res.* 14:1701. doi: 10.4103/1673-5374.257520

Krämer, T. J., Hack, N., Brühl, T. J., Menzel, L., Hummel, R., Griemert, E.-V., et al. (2019). Depletion of regulatory T cells increases T cell brain infiltration, reactive astrogliosis, and interferon-γ gene expression in acute experimental traumatic brain injury. *J. Neuroinflamm.* 16:163. doi: 10.1186/s12974-019-1550-0

Kumar, V. (2019). "Macrophages: the potent immunoregulatory innate immune cells," in *Macrophage at the Crossroads of Innate and Adaptive Immunity*, ed. K. H. Bhat (London: IntechOpen), doi: 10.5772/intechopen.88013

Kumaria, A., Tolias, C. M., and Burnstock, G. (2008). ATP signalling in epilepsy. *Purinerg. Signal.* 4, 339–346. doi: 10.1007/s11302-008-9115-1

Ladak, A. A., Enam, S. A., and Ibrahim, M. T. (2019). A review of the molecular mechanisms of traumatic brain injury. *World Neurosurg.* 131, 126–132. doi: 10.1016/j.wneu.2019.07.039

Lalitha, S., Minz, R. W., and Medhi, B. (2018). Understanding the controversial drug targets in epilepsy and pharmacoresistant epilepsy. *Rev. Neurosci.* 29, 333–345. doi: 10.1515/revneuro-2017-0043

Lamar, C. D., Hurley, R. A., Rowland, J. A., and Taber, K. H. (2014). Post-traumatic epilepsy: review of risks, pathophysiology, and potential biomarkers. *J. Neuropsychiatry Clin. Neurosci.* 26, 4–113. doi: 10.1176/appi.neuropsych.260201

Larson, B. E., Stockwell, D. W., Boas, S., Andrews, T., Wellman, G. C., Lockette, W., et al. (2012). Cardiac reactive oxygen species after traumatic brain injury. *J. Surg. Res.* 173, e73–e81. doi: 10.1016/j.jss.2011.09.056

Lee, S., Yoon, B. E., Berglund, K., Oh, S. J., Park, H., Shin, H. S., et al. (2010). Channel-mediated tonic GABA release from glia. *Science* 330, 790–796. doi: 10.1126/science.1184334

Lewerenz, J., Hewett, S. J., Huang, Y., Lambros, M., Gout, P. W., Kalivas, P. W., et al. (2013). The cystine/glutamate antiporter system xc- in health and disease: from molecular mechanisms to novel therapeutic opportunities. *Antioxid. Redox Signal.* 18, 522–555. doi: 10.1089/ars.2011.4391

Li, H., Graber, K. D., Jin, S., McDonald, W., Barres, B. A., and Prince, D. A. (2012). Gabapentin decreases epileptiform discharges in a chronic model of neocortical trauma. *Neurobiol. Dis.* 48, 429–438. doi: 10.1016/j.nbd.2012.06.019

Li, J., and Yuan, J. (2008). Caspases in apoptosis and beyond. *Oncogene* 27, 6194–6206. doi: 10.1038/onc.2008.297

Li, Q., Li, Q. Q., Jia, J. N., Sun, Q. Y., Zhou, H. H., Jin, W. L., et al. (2019). Baicalein exerts neuroprotective effects in $FeCl_3$-induced posttraumatic epileptic seizures *via* suppressing ferroptosis. *Front. Pharmacol.* 10:638. doi: 10.3389/fphar.2019.00638

Liang, L. P., and Patel, M. (2006). Seizure-induced changes in mitochondrial redox status. *Free Rad. Biol. Med.* 40, 316–322. doi: 10.1016/j.freeradbiomed.2005.08.026

Licinio, J., and Frost, P. (2000). The neuroimmune-endocrine axis: pathophysiological implications for the central nervous system cytokines and hypothalamus-pituitary-adrenal hormone dynamics. *Braz. J. Med. Biol. Res.* 33, 1141–1148. doi: 10.1590/s0100-879x2000001000003

Liddelow, S. A., and Barres, B. A. (2017). Reactive astrocytes: production, function, and therapeutic potential. *Immunity* 46, 957–967. doi: 10.1016/j.immuni.2017.06.006

Liddelow, S. A., Guttenplan, K. A., Clarke, L. E., Bennett, F. C., Bohlen, C. J., Schirmer, L., et al. (2017). Neurotoxic reactive astrocytes are induced by activated microglia. *Nature* 541, 481–487. doi: 10.1038/nature21029

Lima, F. D., Souza, M. A., Furian, A. F., Rambo, L. M., Ribeiro, L. R., Martignoni, F. V., et al. (2008). Na^+, K^+-ATPase activity impairment after experimental traumatic brain injury: relationship to spatial learning deficits and oxidative stress. *Behav. Brain Res.* 193, 306–310. doi: 10.1016/j.bbr.2008.05.013

Liu, S. J., Zheng, P., Wright, D. K., Zhou, H. H., and Mao, X. Y. (2016). Sodium selenate retards epileptogenesis in acquired epilepsy models reversing changes in protein phosphatase 2A and hyperphosphorylated tau. *Brain* 139, 1919–1938. doi: 10.1093/brain/aww116

Loane, D. J., Kumar, A., Stoica, B. A., Cabatbat, R., and Faden, A. I. (2014). Progressive neurodegeneration after experimental brain trauma: association with chronic microglial activation. *J. Neuropatho. Exper. Neurol.* 73, 14–29. doi: 10.1097/NEN.0000000000000021

Lobo, V., Patil, A., Phatak, A., and Chandra, N. (2010). Free radicals, antioxidants and functional foods: impact on human health. *Pharm. Rev.* 4:118. doi: 10.4103/0973-7847.70902

Louveau, A., Harris, T. H., and Kipnis, J. (2015). Revisiting the mechanisms of CNS immune privilege. *Trends Immunol.* 36, 569–577. doi: 10.1016/j.it.2015.08.006

Lowenstein, D. H., Thomas, M. J., Smith, D. H., and McIntosh, T. K. (1992). Selective vulnerability of dentate hilar neurons following traumatic brain injury: a potential mechanistic link between head trauma and disorders of the hippocampus. *J. Neurosci.* 12, 4846–4853. doi: 10.1523/JNEUROSCI.12-12-04846.1992

Ma, M. W., Wang, J., Zhang, Q., Wang, R., Dhandapani, K. M., Vadlamudi, R. K., et al. (2017). NADPH oxidase in brain injury and neurodegenerative disorders. *Mol. Neurodegen.* 12:7. doi: 10.1186/s13024-017-0150-7

Maas, A., Menon, D. K., Adelson, P. D., Andelic, N., Bell, M. J., Belli, A., et al. (2017). Traumatic brain injury: integrated approaches to improve prevention, clinical care, and research. *Lancet Neurol.* 16, 987–1048. doi: 10.1016/S1474-4422(17)30371-X

Madrigal, J. L., García-Bueno, B., Caso, J. R., Pérez-Nievas, B. G., and Leza, J. C. (2006). Stress-induced oxidative changes in brain. *CNS Neurol. Disord. Drug Targets* 5, 561–568. doi: 10.2174/187152706778559327

Maher, P., and Schubert, D. (2000). Signaling by reactive oxygen species in the nervous system. *Cell. Mol. Life Sci.* 57, 1287–1305. doi: 10.1007/pl00000766

Mahler, B., Carlsson, S., Andersson, T., Adelöw, C., Ahlbom, A., and Tomson, T. (2015). Unprovoked seizures after traumatic brain injury: a population-based case-control study. *Epilepsia* 56, 1438–1444. doi: 10.1111/epi.13096

Mandal, P. K., Seiler, A., Perisic, T., Kölle, P., Canak, A. B., Förster, H., et al. (2010). System xc- and thioredoxin reductase 1 cooperatively rescue glutathione deficiency. *J. Biol. Chem.* 285, 22244–22253. doi: 10.1074/jbc.M110.121327

Maqbool, A., Watt, N. T., Haywood, N., Viswambharan, H., Skromna, A., Makava, N., et al. (2020). Divergent effects of genetic and pharmacological inhibition of Nox2 NADPH oxidase on insulin resistance-related vascular damage. *Am. J. Physiol. Cell Physiol.* 319, C64–C74. doi: 10.1152/ajpcell.00389.2019

Maroso, M., Balosso, S., Ravizza, T., Jiang, G. L., Wang, F., Xue, Y., et al. (2011). Interleukin-1β biosynthesis inhibition reduces acute seizures and drug resistant chronic epileptic activity in mice. *Neurotherapeutics* 8, 304–315. doi: 10.1007/s13311-011-0039-z

Mathur, V., Burai, R., Vest, R. T., Bonanno, L. N., Lehallier, B., Zardeneta, M. E., et al. (2017). Activation of the STING-dependent Type I interferon response reduces microglial reactivity and neuroinflammation. *Neuron* 96, 1290–1302.e6. doi: 10.1016/j.neuron.2017.11.032

McCullagh, S., and Feinstein, A. (2003). Outcome after mild traumatic brain injury: an examination of recruitment bias. *J. Neurol. Neurosurgery Psychiatry* 74, 39–43. doi: 10.1136/jnnp.74.1.39

Mckee, A. C., and Daneshvar, D. H. (2015). The neuropathology of traumatic brain injury. *Handb. Clini. Neurol.* 127, 45–66. doi: 10.1016/B978-0-444-52892-6.00004-0

Mckee, C. A., and Lukens, J. R. (2016). Emerging roles for the immune system in traumatic brain injury. *Front. Immunol.* 7:556. doi: 10.3389/fimmu.2016.00556

Medzhitov, R. (2008). Origin and physiological roles of inflammation. *Nature* 454, 428–435. doi: 10.1038/nature07201

Milikovsky, D. Z., Weissberg, I., Kamintsky, L., Lippmann, K., Schefenbauer, O., Frigerio, F., et al. (2017). Electrocorticographic dynamics as a novel biomarker in five models of epileptogenesis. *J. Neurosci.* 37, 4450–4461. doi: 10.1523/JNEUROSCI.2446-16.2017

Milman, A., Zohar, O., Maayan, R., Weizman, R., and Pick, C. G. (2007). DHEAS repeated treatment improves cognitive and behavioral deficits after mild traumatic brain injury. *Eur. Neuropsychopharmacol.* 18, 181–187. doi: 10.1016/j.euroneuro.2007.05.007

Morimoto, K., and Nakajima, K. (2019). Role of the immune system in the development of the central nervous system. *Front. Neurosci.* 13:916. doi: 10.3389/fnins.2019.00916

Mukherjee, S., Zeitouni, S., Cavarsan, C. F., and Shapiro, L. A. (2013). Increased seizure susceptibility in mice 30?days after fluid percussion injury. *Front. Neurol.* 4:28. doi: 10.3389/fneur.2013.00028

Müller, M., Gähwiler, B. H., Rietschin, L., and Thompson, S. M. (1993). Reversible loss of dendritic spines and altered excitability after chronic epilepsy in hippocampal slice cultures. *Proc. Natl. Acad. Sci. U.S.A.* 90, 257–261. doi: 10.1073/pnas.90.1.257

Multani, P., Myers, R. H., Blume, H. W., Schomer, D. L., and Sotrel, A. (1994). Neocortical dendritic pathology in human partial epilepsy: a quantitative Golgi study. *Epilepsia* 35, 728–736. doi: 10.1111/j.1528-1157.1994.tb02503.x

Naalt, J., vander Zomeren, A. H., van Sluiter, W. J., and Minderhoud, J. M. (1999). One year outcome in mild to moderate head injury: the predictive value of acute injury characteristics related to complaints and return to work. *J. Neurol. Neurosurgery Psychiatry* 66, 207–213. doi: 10.1136/jnnp.66.2.207

Nagelhus, E. A., and Ottersen, O. P. (2013). Physiological roles of aquaporin-4 in brain. *Physiol. Rev.* 93, 1543–1562. doi: 10.1152/physrev.00011.2013

Newell-Rogers, M. K., Rogers, S. K., Tobin, R. P., Mukherjee, S., and Shapiro, L. A. (2020). Antagonism of macrophage migration inhibitory factory (MIF) after traumatic brain injury ameliorates astrocytosis and peripheral lymphocyte activation and expansion. *Int. J. Mol. Sci.* 21:7448. doi: 10.3390/ijms21207448

Nissinen, J., Andrade, P., Natunen, T., Hiltunen, M., Malm, T., Kanninen, K., et al. (2017). Disease-modifying effect of atipamezole in a model of post-traumatic epilepsy. *Epilepsy Res.* 136, 18–34. doi: 10.1016/j.eplepsyres.2017.07.005

Norris, G. T., and Kipnis, J. (2019). Immune cells and CNS physiology: microglia and beyond. *J. Exper. Med.* 216, 60–70. doi: 10.1084/jem.20180199

O'Brien, W. T., Pham, L., Symons, G. F., Monif, M., Shultz, S. R., and Mcdonald, S. J. (2020). The NLRP3 inflammasome in traumatic brain injury: potential as a biomarker and therapeutic target. *J. Neuroinflamm.* 17:104. doi: 10.1186/s12974-020-01778-5

O'neill, L. A. (1995). Towards an understanding of the signal transduction pathways for interleukin 1. *Biochim. Biophys. Acta Mol.Cell Res.* 1266, 31–44. doi: 10.1016/0167-4889(94)00217-3

Ozcan, A., and Ogun, M. (2015). "Biochemistry of reactive oxygen and nitrogen species," in *Basic Principles and Clinical Significance of Oxidative Stress*, ed. S. J. T. Gowder (London: IntechOpen), doi: 10.5772/61193

Pampliega, O., Domercq, M., Soria, F. N., Villoslada, P., Rodríguez-Antigüedad, A., and Matute, C. (2011). Increased expression of cystine/glutamate antiporter in multiple sclerosis. *J. Neuroinflamm.* 8:63. doi: 10.1186/1742-2094-8-63

Panatier, A., Theodosis, D. T., Mothet, J. P., Touquet, B., Pollegioni, L., Poulain, D. A., et al. (2006). Glia-derived D-serine controls NMDA receptor activity and synaptic memory. *Cell* 125, 775–784. doi: 10.1016/j.cell.2006.02.051

Parent, J. M. (2002). The role of seizure-induced neurogenesis in epileptogenesis and brain repair. *Epilepsy Res.* 50, 179–189. doi: 10.1016/s0920-1211(02)00078-5

Pasciuto, W., Burton, O. T., Roca, C. P., Lagou, V., Rajan, W. D., Theys, T., et al. (2020). Microglia require CD4 T cells to complete the fetal-to-adult transition. *Cell* 182, 625–640. doi: 10.1016/j.cell.2020.06.026

Patel, D. C., Wallis, G., Dahle, E. J., McElroy, P. B., Thomson, K. E., Tesi, R. J., et al. (2017). Hippocampal TNFα signaling contributes to seizure generation in an infection-induced mouse model of limbic epilepsy. *eNeuro* 4:ENEURO.0105-17.2017. doi: 10.1523/ENEURO.0105-17.2017

Patel, M. (2004). Mitochondrial dysfunction and oxidative stress: cause and consequence of epileptic seizures. *Free Rad. Biol. Med.* 37, 1951–1962. doi: 10.1016/j.freeradbiomed.2004.08.021

Paudel, Y. N., Semple, B. D., Jones, N. C., Othman, I., and Shaikh, M. F. (2019). High mobility group box 1 (HMGB 1) as a novel frontier in epileptogenesis: from pathogenesis to therapeutic approaches. *J. Neurochem.* 151, 542–557. doi: 10.1111/jnc.14663

Pecorelli, A., Natrella, F., Belmonte, G., Miracco, C., Cervellati, F., Ciccoli, L., et al. (2015). NADPH oxidase activation and 4-hydroxy-2-nonenal/aquaporin-4 adducts as possible new players in oxidative neuronal damage presents in drug-resistant epilepsy. *Biochim. Biophys. Acta* 1852, 507–519. doi: 10.1016/j.bbadis.2014.11.016

Pekny, M., and Pekna, M. (2016). Reactive gliosis in the pathogenesis of CNS diseases. *Biochim. Biophys. Acta* 1862, 483–491. doi: 10.1016/j.bbadis.2015.11.014

Pijet, B., Stefaniuk, M., and Kaczmarek, L. (2019). MMP-9 contributes to dendritic spine remodeling following traumatic brain injury. *Neural Plast.* 2019, 1–12. doi: 10.1155/2019/3259295

Pijet, B., Stefaniuk, M., Kostrzewska-Ksiezyk, A., Tsilibary, P. E., Tzinia, A., and Kaczmarek, L. (2018). Elevation of MMP-9 levels promotes epileptogenesis after traumatic brain injury. *Mol. Neurobiol.* 55, 9294–9306. doi: 10.1007/s12035-018-1061-5

Pohlmann-Eden, B., Beghi, E., Camfield, C., and Camfield, P. (2006). The first seizure and its management in adults and children. *BMJ* 332, 339–342. doi: 10.1136/bmj.332.7537.339

Pokrishevsky, E., Grad, L. I., Yousefi, M., Wang, J., Mackenzie, I. R., and Cashman, N. R. (2012). Aberrant localization of FUS and TDP43 is associated with misfolding of SOD1 in amyotrophic lateral sclerosis. *PLoS One* 7:e35050. doi: 10.1371/journal.pone.0035050

Popovich, P. G., Stokes, B. T., and Whitacre, C. C. (1996). Concept of autoimmunity following spinal cord injury: possible roles for T lymphocytes in the traumatized central nervous system. *J. Neurosci. Res.* 45, 349–363.

Pribiag, H., and Stellwagen, D. (2013). TNF-α downregulates inhibitory neurotransmission through protein phosphatase 1-dependent trafficking of GABA(A) receptors. *J. Neurosci.* 33, 15879–15893. doi: 10.1523/JNEUROSCI.0530-13.2013

Puttachary, S., Sharma, S., Stark, S., and Thippeswamy, T. (2015). Seizure-induced oxidative stress in temporal lobe epilepsy. *Biomed. Res. Intern.* 2015:745613. doi: 10.1155/2015/745613

Puttachary, S., Sharma, S., Verma, S., Yang, Y., Putra, M., Thippeswamy, A., et al. (2016). 1400W, a highly selective inducible nitric oxide synthase inhibitor is a potential disease modifier in the rat kainate model of temporal lobe epilepsy. *Neurobiol. Dis.* 93, 184–200. doi: 10.1016/j.nbd.2016.05.013

Raheja, A., Sinha, S., Samson, N., Windisch, M., Hutter-Paier, B., Jolkkonen, J., et al. (2016). Serum biomarkers as predictors of long-term outcome in severe traumatic brain injury: analysis from a randomized placebo-controlled Phase II clinical trial. *J. Neurosurg.* 125, 631–641. doi: 10.3171/2015.6.JNS15674

Raja, M., Chowdhury, J., and Radosevich, J. A. (2018). "Role of phospholipases in cell death," in *Apoptosis and Beyond: The Many Ways Cells Die*, ed. J. Radosevich (Hoboken, NJ: Wiley), 395–410.

Ramalingam, M., and Kim, S. J. (2012). Reactive oxygen/nitrogen species and their functional correlations in neurodegenerative diseases. *J. Neural Transm.* 119, 891–910. doi: 10.1007/s00702-011-0758-7

Rana, A., and Musto, A. E. (2018). The role of inflammation in the development of epilepsy. *J. Neuroinflamm.* 15:144. doi: 10.1186/s12974-018-1192-7

Ranaivo, H. R., Hodge, J. N., Choi, N., and Wainwright, M. S. (2012). Albumin induces upregulation of matrix metalloproteinase-9 in astrocytes via MAPK and reactive oxygen species-dependent pathways. *J. Neuroinflamm.* 9:68. doi: 10.1186/1742-2094-9-68

Rapalino, O., Lazarov-Spiegler, O., Agranov, E., Velan, G. J., Yoles, E., Fraidakis, M., et al. (1998). Implantation of stimulated homologous macrophages results in partial recovery of paraplegic rats. *Nat. Med.* 4, 814–821. doi: 10.1038/nm0798-814

Rauch, U. (2004). Extracellular matrix components associated with remodelling processes in brain. *Cell. Mol. Life Sci.* 61, 2031–2045. doi: 10.1007/s00018-004-4043-x

Raymont, V., Salazar, A., Krueger, F., and Grafman, J. (2011). "Studying injured minds"-the Vietnam head injury study and 40 years of brain injury research. *Front. Neurol.* 2:15. doi: 10.3389/fneur.2011.00015

Raymont, V., Salazar, A. M., Lipsky, R., Goldman, D., Tasick, G., and Grafman, J. (2010). Correlates of posttraumatic epilepsy 35 years following combat brain injury. *Neurology* 75, 224–229. doi: 10.1212/WNL.0b013e3181e8e6d0

Redell, J. B., Maynard, M. E., Underwood, E. L., Vita, S. M., Dash, P. K., and Kobori, N. (2020). Traumatic brain injury and hippocampal neurogenesis: Functional implications. *Exper. Neurol.* 331:113372. doi: 10.1016/j.expneurol.2020.113372

Reyes, R. C., Brennan, A. M., Shen, Y., Baldwin, Y., and Swanson, R. A. (2012). Activation of neuronal NMDA receptors induces superoxide-mediated oxidative stress in neighboring neurons and astrocytes. *J. Neurosci.* 32, 12973–12978. doi: 10.1523/JNEUROSCI.1597-12.2012

Ricciotti, E., and FitzGerald, G. A. (2011). Prostaglandins and inflammation. *Arterioscler. Thromb. Vasc. Biol.* 31, 986–1000. doi: 10.1161/ATVBAHA.110.207449

Rojas, A., Jiang, J., Ganesh, T., Yang, M. S., Lelutiu, N., Gueorguieva, P., et al. (2014). Cyclooxygenase-2 in epilepsy. *Epilepsia* 55, 17–25. doi: 10.1111/epi.12461

Rosenfeld, J. V., Maas, A. I., Bragge, P., Morganti-Kossmann, M. C., Manley, G. T., and Gruen, R. L. (2012). Early management of severe traumatic brain injury. *Lancet* 380, 1088–1098. doi: 10.1016/S0140-6736(12)60864-2

Röszer, T. (2015). Understanding the mysterious M2 macrophage through activation markers and effector mechanisms. *Med. Inflamm.* 2015:816460. doi: 10.1155/2015/816460

Rowe, R. K., Harrison, J. L., Zhang, H., Hesson, D. P., O'Hara, B. F., Greene, M. I., et al. (2018). Novel TNF receptor-1 inhibitors identified as potential therapeutic candidates for traumatic brain injury. *J. Neuroinflamm.* 15:154. doi: 10.1186/s12974-018-1200-y

Rowley, S., and Patel, M. (2013). Mitochondrial involvement and oxidative stress in temporal lobe epilepsy. *Free Rad. Biol. Med.* 62, 121–131. doi: 10.1016/j.freeradbiomed.2013.02.002

Saletti, P. G., Ali, I., Casillas-Espinosa, P. M., Semple, B. D., Lisgaras, C. P., Moshe, S. L., et al. (2019). In search of antiepileptogenic treatments for post-traumatic epilepsy. *Neurobiol. Dis.* 123, 86–99. doi: 10.1016/j.nbd.2018.06.017

Salter, M. W., and Kalia, L. V. (2004). Src kinases: a hub for NMDA receptor regulation. *Nat. Rev. Neurosci.* 5, 317–328. doi: 10.1038/nrn1368

Sanz, P., and Garcia-Gimeno, M. A. (2020). Reactive Glia inflammatory signaling pathways and epilepsy. *Intern. J. Mol. Sci.* 21:4096. doi: 10.3390/ijms21114096

Saraiva, A. L., Ferreira, A. P., Silva, L. F., Wilcock, D. M., Goulding, D., Neltner, J. H., et al. (2012). Creatine reduces oxidative stress markers but does not protect against seizure susceptibility after severe traumatic brain injury. *Brain Res. Bull.* 87, 180–186. doi: 10.1016/j.brainresbull.2011.10.010

Scallan, J., Huxley, V. H., and Korthuis, R. J. (2010). "Capillary fluid exchange: Regulation functions and pathology," in *Colloquium Lectures on Integrated Systems Physiology: From Molecules to Function*, eds D. N. Granger and J. P. Granger (San Rafael, CA: Morgan & Claypool Publishers).

Scanlon, S. T. (2019). A myeloid cell atlas of neuroinflammation. *Science* 363, 360–362. doi: 10.1126/science.363.6425.360-l

Schmidt, D., Friedman, D., and Dichter, M. A. (2014). Anti-epileptogenic clinical trial designs in epilepsy: issues and options. *Neurotherapeutics* 11, 401–411. doi: 10.1007/s13311-013-0252-z

Schwartzkroin, P. A., Wenzel, H. J., Lyeth, B. G., Watterson, D. M., and Van, E. L. J. (2010). Does ketogenic diet alter seizure sensitivity and cell loss following fluid percussion injury? *Epilepsy Res.* 92, 74–84. doi: 10.1016/j.eplepsyres.2010.08.009

Semple, B. D., O'Brien, T. J., Gimlin, K., Casillas-Espinosa, P. M., Webster, K. M., Petrou, S., et al. (2017). Interleukin-1 receptor in seizure susceptibility after traumatic injury to the pediatric brain. *J. Neurosci.* 37, 7864–7877. doi: 10.1523/JNEUROSCI.0982-17.2017

Serhan, C. N. (2017). Treating inflammation and infection in the 21st century: new hints from decoding resolution mediators and mechanisms. *FASEB J.* 31, 1273–1288. doi: 10.1096/fj.201601222R

Shanlin, R. J., Sole, M. J., Rahimifar, M., Tator, C. H., and Factor, S. M. (1988). Increased intracranial pressure elicils hypertension, increased sympathetic activity, electrocardiographic abnormalities and myocardial damage in rats. *J. Am. Coll. Cardiol.* 12, 727–736. doi: 10.1016/s0735-1097(88)80065-2

Sharma, S., Carlson, S., Puttachary, S., Sarkar, S., Showman, L., Putra, M., et al. (2018). Role of the Fyn-PKCδ signaling in SE-induced neuroinflammation and epileptogenesis in experimental models of temporal lobe epilepsy. *Neurobiol. Dis.* 110, 102–121. doi: 10.1016/j.nbd.2017.11.008

Sharma, S. K., and Naidu, G. (2016). The role of danger-associated molecular patterns (DAMPs) in trauma and infections. *J. Thorac. Dis.* 8, 1406–1409. doi: 10.21037/jtd.2016.05.22

Shechter, R., London, A., Varol, C., Raposo, C., Cusimano, M., Yovel, G., et al. (2009). Infiltrating blood-derived macrophages are vital cells playing an anti-inflammatory role in recovery from spinal cord injury in mice. *PLoS Med.* 6:e1000113. doi: 10.1371/journal.pmed.1000113

Shi, H., Hua, X., Kong, D., Stein, D., and Hua, F. (2019). Role of toll-like receptor mediated signaling in traumatic brain injury. *Neuropharmacology* 145, 259–267. doi: 10.1016/j.neuropharm.2018.07.022

Shi, W., Zhao, W., Shen, A., Shao, B., Wu, X., Yang, J., et al. (2010). Traumatic brain injury induces an up-regulation of Hs1-associated protein X-1 (Hax-1) in rat brain cortex. *Neurochem. Res.* 36, 375–382. doi: 10.1007/s11064-010-0332-y

Shlosberg, D., Benifla, M., Kaufer, D., and Friedman, A. (2010). Blood-brain barrier breakdown as a therapeutic target in traumatic brain injury. *Nat. Rev. Neurol.* 6, 393–403. doi: 10.1038/nrneurol.2010.74

Silverman, M. N., Pearce, B. D., Biron, C. A., and Miller, A. H. (2005). Immune modulation of the hypothalamic-pituitary-adrenal (HPA) axis during viral infection. *Viral Immunol.* 18, 41–78. doi: 10.1089/vim.2005.18.41

Smith, B. N. (2016). How and why study posttraumatic epileptogenesis in animal models? *Epilepsy Curr.* 16, 393–396. doi: 10.5698/1535-7511-16.6.393

Smith, C. (2013). Review: the long-term consequences of microglial activation following acute traumatic brain injury. *Neuropathol. Appl. Neurobiol.* 39, 35–44. doi: 10.1111/nan.12006

Smith, R. E., Ozben, T., and Saso, L. (2019). Modulation of oxidative stress: pharmaceutical and pharmacological aspects 2018. *Oxid. Med. Cell. Longev.* 2019:6380473. doi: 10.1155/2019/6380473

Sofroniew, M. V., and Vinters, H. V. (2010). Astrocytes: biology and pathology. *Acta Neuropathol.* 119, 7–35. doi: 10.1007/s00401-009-0619-8

Sookplung, P., Siriussawakul, A., Malakouti, A., Sharma, D., Wang, J., Souter, M. J., et al. (2011). Vasopressor use and effect on blood pressure after severe adult traumatic brain injury. *Neurocrit Care* 15, 46–54. doi: 10.1007/s12028-010-9448-9

Sridharan, R., Cameron, A. R., Kelly, D. J., Kearney, C. J., and O'Brien, F. J. (2015). Biomaterial based modulation of macrophage polarization: a review and suggested design principles. *Mater. Today* 18, 313–325. doi: 10.1016/j.mattod.2015.01.019

Stamatovic, S. M., Keep, R. F., and Andjelkovic, A. V. (2008). Brain endothelial cell-cell junctions: how to "open" the blood brain barrier. *Curr. Neuropharmacol.* 6, 179–192. doi: 10.2174/157015908785777210

Steinhäuser, C., Grunnet, M., and Carmignoto, G. (2016). Crucial role of astrocytes in temporal lobe epilepsy. *Neuroscience* 323, 157–169. doi: 10.1016/j.neuroscience.2014.12.047

Stellwagen, D., Beattie, E. C., Seo, J. Y., and Malenka, R. C. (2005). Differential regulation of AMPA receptor and GABA receptor trafficking by tumor necrosis factor-alpha. *J. Neurosci.* 25, 3219–3228. doi: 10.1523/JNEUROSCI.4486-04.2005

Stoica, B. A., and Faden, A. I. (2010). Cell death mechanisms and modulation in traumatic brain injury. *Neurotherapeutics* 7, 3–12. doi: 10.1016/j.nurt.2009.10.023

Streit, W. J., Mrak, R. E., and Griffin, W. S. T. (2004). Microglia and neuroinflammation: a pathological perspective. *J. Neuroinflamm.* 1, 1–4. doi: 10.1186/1742-2094-1-14

Stück, E. D., Christensen, R. N., Huie, J. R., O'Brien, T. J., Rajan, R., Shultz, S. R., et al. (2012). Tumor necrosis factor alpha mediates GABA(A) receptor trafficking to the plasma membrane of spinal cord neurons in vivo. *Neural Plast.* 2012:261345. doi: 10.1155/2012/261345

Sun, D. (2014). The potential of endogenous neurogenesis for brain repair and regeneration following traumatic brain injury. *Neural Regen. Res.* 9, 688–692. doi: 10.4103/1673-5374.131567

Sun, M., Honey, C. R., Berk, C., Wong, N. L., and Tsui, J. K. (2003). Regulation of aquaporin-4 in a traumatic brain injury model in rats. *J. Neurosurg.* 98, 565–569. doi: 10.3171/jns.2003.98.3.0565

Swartz, B. E., Houser, C. R., Tomiyasu, U., Walsh, G. O., DeSalles, A., Rich, J. R., et al. (2006). Hippocampal cell loss in posttraumatic human epilepsy. *Epilepsia* 47, 1373–1382. doi: 10.1111/j.1528-1167.2006.00602.x

Szaflarski, J. P., Nazzal, Y., and Dreer, L. E. (2014). Post-traumatic epilepsy: current and emerging treatment options. *Neuropsychiatr. Dis. Treat.* 10, 1469–1477. doi: 10.2147/NDT.S50421

Szaflarski, J. P., Sangha, K. S., Lindsell, C. J., and Shutter, L. A. (2010). Prospective, randomized, single-blinded comparative trial of intravenous levetiracetam versus phenytoin for seizure prophylaxis. *Neurocrit. Care* 12, 165–172. doi: 10.1007/s12028-009-9304-y

Szu, J. I., Chaturvedi, S., Patel, D. D., and Binder, D. K. (2020). Aquaporin-4 dysregulation in a controlled cortical impact injury model of posttraumatic epilepsy. *Neuroscience* 428, 140–153. doi: 10.1016/j.neuroscience.2019.12.006

Ta, T., Dikmen, H. O., Schilling, S., Chausse, B., Lewen, A., Hollnagel, J., et al. (2019). Priming of microglia with IFN-γ slows neuronal gamma oscillations in situ. *Proc. Natl. Acad. Sci. U.S.A.* 116, 4637–4642. doi: 10.1073/pnas.1813562116

Takemiya, T., Maehara, M., Matsumura, K., Yasuda, S., Sugiura, H., and Yamagata, K. (2006). Prostaglandin E2 produced by late induced COX-2 stimulates hippocampal neuron loss after seizure in the CA3 region. *Neurosci. Res.* 56, 103–110. doi: 10.1016/j.neures.2006.06.003

Tayel, S. S., Helmy, A. A., Ahmed, R., Esmat, G., Hamdi, N., and Abdelaziz, A. I. (2013). Progesterone suppresses interferon signaling by repressing TLR-7 and MxA expression in peripheral blood mononuclear cells of patients infected with hepatitis C virus. *Archiv. Virol.* 158, 1755–1764. doi: 10.1007/s00705-013-1673-z

Tehse, J., and Taghibiglou, C. (2019). The overlooked aspect of excitotoxicity: glutamate-independent excitotoxicity in traumatic brain injuries. *Eur. J. Neurosci.* 49, 1157–1170. doi: 10.1111/ejn.14307

Temkin, N. R. (2001). Antiepileptogenesis and seizure prevention trials with antiepileptic drugs: meta-analysis of controlled trials. *Epilepsia* 42, 515–524. doi: 10.1046/j.1528-1157.2001.28900.x

Ting, A. T., and Bertrand, M. (2016). More to life than NF-κB in TNFR1 Signaling. *Trends Immunol.* 37, 535–545. doi: 10.1016/j.it.2016.06.002

Tobin, R. P., Mukherjee, S., Kain, J. M., Rogers, S. K., Henderson, S. K., Motal, H. L., et al. (2014). Traumatic brain injury causes selective, CD74-dependent peripheral lymphocyte activation that exacerbates neurodegeneration. *Acta Neuropathol. Commun.* 2, 1–10. doi: 10.1186/s40478-014-0143-5

Tomkins, O., Feintuch, A., Benifla, M., Cohen, A., Friedman, A., and Shelef, I. (2011). Blood-brain barrier breakdown following traumatic brain injury: a possible role in posttraumatic epilepsy. *Cardiovasc. Psychiatry Neurol.* 2011:765923. doi: 10.1155/2011/765923

Tran, N. D., Kim, S., Vincent, H. K., Rodriguez, A., Hinton, D. R., Bullock, M. R., et al. (2010). Aquaporin-1-mediated cerebral edema following traumatic brain injury: effects of acidosis and corticosteroid administration. *J. Neurosurg.* 112, 1095–1104. doi: 10.3171/2009.8.jns081704

Trinchieri, G. (2012). Cancer and inflammation: an old intuition with rapidly evolving new concepts. *Annu. Rev. Immunol.* 30, 677–706. doi: 10.1146/annurev-immunol-020711-075008

Trotti, D., Danbolt, N. C., and Volterra, A. (1998). Glutamate transporters are oxidant-vulnerable: a molecular link between oxidative and excitotoxic neurodegeneration? *Trends Pharmacol. Sci.* 19, 328–334. doi: 10.1016/s0165-6147(98)01230-9

Ucciferri, C., Falasca, K., Mancino, P., De Tullio, D., Pizzigallo, E., and Vecchiet, J. (2007). High dose of erythropoietin in management of interferon/ribavirin induced anemia. *Hepatogastroenterology* 54, 2181–2183.

Uggenti, C., and Crow, Y. J. (2018). Taking the STING out of inflammation. *Nat. Rev. Rheumatol.* 14, 508–509. doi: 10.1038/s41584-018-0071-z

Varvel, N. H., Jiang, J., and Dingledine, R. (2014). Candidate drug targets for prevention or modification of epilepsy. *Annu. Rev. Pharmacol. Toxicol.* 55, 229–247. doi: 10.1146/annurev-pharmtox-010814-124607

Vespa, P., Prins, M., Ronne-Engstrom, E., Caron, M., Shalmon, E., Hovda, D. A., et al. (1998). Increase in extracellular glutamate caused by reduced cerebral perfusion pressure and seizures after human traumatic brain injury: a microdialysis study. *J. Neurosurg.* 89, 971–982. doi: 10.3171/jns.1998.89.6.0971

Vespa, P. M., McArthur, D. L., Xu, Y., Eliseo, M., Etchepare, M., Dinov, I., et al. (2010). Nonconvulsive seizures after traumatic brain injury are associated with hippocampal atrophy. *Neurology* 75, 792–798. doi: 10.1212/WNL.0b013e3181f07334

Vezzani, A., Conti, M., Luigi, A. D., Ravizza, T., Moneta, D., Marchesi, F., et al. (1999). Interleukin-1β immunoreactivity and microglia are enhanced in the rat hippocampus by focal kainate application: functional evidence for enhancement of electrographic seizures. *J. Neurosci.* 19, 5054–5065. doi: 10.1523/jneurosci.19-12-05054.1999

Vezzani, A., French, J., Bartfai, T., and Baram, T. Z. (2011). The role of inflammation in epilepsy. *Nat. Rev. Neurol.* 7, 31–40. doi: 10.1038/nrneurol.2010.178

Vezzani, A., Friedman, A., and Dingledine, R. J. (2012). The role of inflammation in epileptogenesis. *Neuropharmacology* 69, 16–24. doi: 10.1016/j.neuropharm.2012.04.004

Vezzani, A., Fujinami, R. S., White, H. S., Preux, P., Blümcke, I., Sander, J. W., et al. (2015). Infections, inflammation and epilepsy. *Acta Neuropathol.* 131, 211–234. doi: 10.1007/s00401-015-1481-5

Viviani, B., Bartesaghi, S., Gardoni, F., Beynon, S., Schmidt, S. F., Kaye, A. H., et al. (2003). Interleukin-1beta enhances NMDA receptor-mediated intracellular calcium increase through activation of the Src family of kinases. *J. Neurosci.* 23, 8692–8700. doi: 10.1523/JNEUROSCI.23-25-08692.2003

Waldbaum, S., and Patel, M. (2010). Mitochondria, oxidative stress, and temporal lobe epilepsy. *Epilepsy Res.* 88, 23–45. doi: 10.1016/j.eplepsyres.2009.09.020

Wallraff, A., Köhling, R., Heinemann, U., Theis, M., Willecke, K., and Steinhäuser, C. (2006). The impact of astrocytic gap junctional coupling on potassium buffering in the hippocampus. *J. Neurosci.* 26, 5438–5447. doi: 10.1523/JNEUROSCI.0037-06.2006

Wang, F., Wang, X., Shapiro, L. A., Sun, M., Semple, B. D., Ozturk, E., et al. (2017). NKCC1 up-regulation contributes to early post-traumatic seizures and increased post-traumatic seizure susceptibility. *Brain Struct. Funct.* 222, 1543–1556. doi: 10.1007/s00429-016-1292-z

Wang, J. Y., Bakhadirov, K., Devous, M. D., Abdi, H., McColl, R., Moore, C., et al. (2008). Diffusion tensor tractography of traumatic diffuse axonal injury. *Archiv. Neurol.* 65, 619–626. doi: 10.1001/archneur.65.5.619

Weber, J. T. (2012). Altered calcium signaling following traumatic brain injury. *Front. Pharmacol.* 3:60. doi: 10.3389/fphar.2012.00060

Webster, K. M., Sun, M., Crack, P., O'Brien, T. J., Shultz, S. R., and Semple, B. D. (2017). Inflammation in epileptogenesis after traumatic brain injury. *J. Neuroinflamm.* 14, 1–17. doi: 10.1186/s12974-016-0786-1

Weissberg, I., Wood, L., Kamintsky, L., Vazquez, O., Milikovsky, D. Z., Alexander, A., et al. (2015). Albumin induces excitatory synaptogenesis through astrocytic TGF-β/ALK5 signaling in a model of acquired epilepsy following blood-brain barrier dysfunction. *Neurobiol. Dis.* 78, 115–125. doi: 10.1016/j.nbd.2015.02.029

Winston, C. N., Chellappa, D., Wilkins, T., Barton, D. J., Washington, P. M., Loane, D. J., et al. (2013). Controlled cortical impact results in an extensive loss of dendritic spines that is not mediated by injury-induced amyloid-beta accumulation. *J. Neurotrauma* 30, 1966–1972. doi: 10.1089/neu.2013.2960

Wofford, K. L., Loane, D. J., and Cullen, D. K. (2019). Acute drivers of neuroinflammation in traumatic brain injury. *Neural. Regen. Res.* 14, 1481–1489. doi: 10.4103/1673-5374.255958

Wong, H., and Hoeffer, C. (2018). Maternal IL-17A in autism. *Exper. Neurol.* 299, 228–240. doi: 10.1016/j.expneurol.2017.04.010

Wong, M. (2005). Modulation of dendritic spines in epilepsy: cellular mechanisms and functional implications. *Epilepsy Behav.* 7, 569–577. doi: 10.1016/j.yebeh.2005.08.007

Wong, M., and Guo, D. (2013). Dendritic spine pathology in epilepsy: cause or consequence? *Neuroscience* 251, 141–150. doi: 10.1016/j.neuroscience.2012.03.048

Wu, Y., Wu, H., Guo, X., Pluimer, B., and Zhao, Z. (2020). Blood-brain barrier dysfunction in mild traumatic brain injury: evidence from preclinical murine models. *Front. Physiol.* 11:1030. doi: 10.3389/fphys.2020.01030

Wynn, T. A., and Vannella, K. M. (2016). Macrophages in tissue repair, regeneration, and fibrosis. *Immunity* 44, 450–462. doi: 10.1016/j.immuni.2016.02.015

Yoon, B. E., Jo, S., Woo, J., Lee, J. H., Kim, T., Kim, D., et al. (2011). The amount of astrocytic GABA positively correlates with the degree of tonic inhibition in hippocampal CA1 and cerebellum. *Mol. Brain* 4:42. doi: 10.1186/1756-6606-4-42

Yu, Z.-Q., and Zha, J.-H. (2012). Genetic ablation of toll-like receptor 2 reduces secondary brain injury caused by cortical contusion in mice. *Ann. Clin. Lab. Sci.* 42, 26–33.

Zanier, E. R., Lee, S. M., Vespa, P. M., Giza, C. C., and Hovda, D. A. (2003). Increased hippocampal CA3 vulnerability to low-level kainic acid following lateral fluid percussion injury. *J. Neurotrauma* 20, 409–420. doi: 10.1089/089771503765355496

Zauner, A., Daugherty, W. P., Bullock, M. R., and Warner, D. S. (2002). Brain oxygenation and energy metabolism: part I-biological function and pathophysiology. *Neurosurgery* 51, 289–302. doi: 10.1227/00006123-200208000-00003

Zehendner, C. M., Sebastiani, A., Hugonnet, A., Bischoff, F., Luhmann, H. J., and Thal, S. C. (2015). Traumatic brain injury results in rapid pericyte loss followed by reactive pericytosis in the cerebral cortex. *Sci. Rep.* 5:13497. doi: 10.1038/srep13497

Zetterström, M., Lundkvist, J., Malinowski, D., Eriksson, G., and Bartfai, T. (1998). Interleukin-1-mediated febrile responses in mice and inter-leukin-1 beta activation of NFB in mouse primary astrocytes, involves the interleukin-1 receptor accessory protein. *Eur. Cytokine Netw.* 9, 131–138.

Zhang, L., Liu, J., Cheng, C., Yuan, Y., Yu, B., Shen, A., et al. (2012). The neuroprotective effect of pyrroloquinoline quinone on traumatic brain injury. *J. Neurotrauma* 29, 851–864. doi: 10.1089/neu.2011.1882

Zhang, X., Chen, Y., Jenkins, L. W., Kochanek, P. M., and Clark, R. S. B. (2005). Bench-to-bedside review: apoptosis/programmed cell death triggered by traumatic brain injury. *Crit. Care* 9, 66–75. doi: 10.1186/cc2950

Zhou, Y., Shao, A., Yao, Y., Tu, S., Deng, Y., and Zhang, J. (2020). Dual roles of astrocytes in plasticity and reconstruction after traumatic brain injury. *Cell Commun. Signal.* 18:62. doi: 10.1186/s12964-020-00549-2

Zhu, M., Chen, J., Guo, H., Ding, L., Zhang, Y., and Xu, Y. (2018). High mobility group Protein B1 (HMGB1) and Interleukin-1β as prognostic biomarkers of epilepsy in children. *J. Child Neurol.* 33, 909–917. doi: 10.1177/0883073818801654

Zhu, Q., Li, N., Han, Q., Zhang, P., Yang, C., Zeng, X., et al. (2013). Statin therapy improves response to interferon alfa and ribavirin in chronic hepatitis C: a systematic review and meta-analysis. *Antiv. Res.* 98, 373–379. doi: 10.1016/j.antiviral.2013.04.009

Zyśk, M., Clausen, F., Aguilar, X., Sehlin, D., Syvänen, S., and Erlandsson, A. (2019). Long-term effects of traumatic brain injury in a mouse model of Alzheimer's disease. *J. Alzheimers Dis.* 72, 161–180. doi: 10.3233/jad-190572

Conflict of Interest: The authors declare that the research was conducted in the absence of any commercial or financial relationships that could be construed as a potential conflict of interest.

frontiers in Molecular Neuroscience

MINI REVIEW
published: 12 March 2021
doi: 10.3389/fnmol.2021.650372

MicroRNA Dysregulation in Epilepsy: From Pathogenetic Involvement to Diagnostic Biomarker and Therapeutic Agent Development

*Jialu Wang and Jiuhan Zhao**

Department of Neurology, First Affiliated Hospital of China Medical University, Shenyang, China

Epilepsy is the result of a group of transient abnormalities in brain function caused by an abnormal, highly synchronized discharge of brain neurons. MicroRNA (miRNA) is a class of endogenous non-coding single-stranded RNA molecules that participate in a series of important biological processes. Recent studies demonstrated that miRNAs are involved in a variety of central nervous system diseases, including epilepsy. Although the exact mechanism underlying the role of miRNAs in epilepsy pathogenesis is still unclear, these miRNAs may be involved in the inflammatory response in the nervous system, neuronal necrosis and apoptosis, dendritic growth, synaptic remodeling, glial cell proliferation, epileptic circuit formation, impairment of neurotransmitter and receptor function, and other processes. Here, we discuss miRNA metabolism and the roles of miRNA in epilepsy pathogenesis and evaluate miRNA as a potential new biomarker for the diagnosis of epilepsy, which enhances our understanding of disease processes.

Keywords: microRNA, epilepsy, pathogenesis, biomarker, diagnosis, therapy

OPEN ACCESS

Edited by:
Hermona Soreq,
Hebrew University of Jerusalem, Israel

Reviewed by:
Gürsel Caliskan,
Otto von Guericke University Magdeburg, Germany
Gerald Seifert,
University Hospital Bonn, Germany

***Correspondence:**
Jiuhan Zhao
cmu_zhaojh@126.com

Received: *07 January 2021*
Accepted: *23 February 2021*
Published: *12 March 2021*

Citation:
Wang J and Zhao J (2021) MicroRNA Dysregulation in Epilepsy: From Pathogenetic Involvement to Diagnostic Biomarker and Therapeutic Agent Development. Front. Mol. Neurosci. 14:650372. doi: 10.3389/fnmol.2021.650372

INTRODUCTION

Epilepsy is the result of a group of transient abnormalities in brain function caused by an abnormal, highly synchronous discharge of brain neurons. Its clinical manifestations mainly include recurrent convulsions and changes in consciousness, which seriously affect the work, daily activities, and physical and mental health of those afflicted with this disorder (Henshall, 2014). There are about 50,000,000 cases of epilepsy worldwide, with approximately 9,000,000 cases in China. Changes in multiple gene patterns in the brain result in the variations in cellular protein metabolism observed in the brain tissue of patients with epilepsy. The pathological mechanism of this disorder has not been clearly defined, and the processes related to neuronal apoptosis, glial regeneration, and the inflammatory response and the molecular mechanisms involved in the multiple links in the genetic information chain (e.g., gene translation, transcription, and post-transcription modification) require further investigation. Thus far, almost all transcriptional and post-transcriptional regulatory mechanisms have been shown to function abnormally during the onset of epilepsy (the process of a normal brain becoming epileptic), including classical transcription factors and epigenetic modifications (Becker et al., 2002; McClelland et al., 2011; Miller-Delaney et al., 2015; Brennan and Henshall, 2018).

MicroRNA (miRNA) is an endogenous non-coding gene that plays a role in post-transcriptional regulation and gene expression in advanced eukaryotes. Its main mode of action is to inhibit mRNA

expression by identifying a complementary ribonucleotide sequence in the 3′-untranslated region (UTR) of the target messenger RNA (mRNA). Each miRNA may correspond to mRNAs encoded by hundreds of genes at the same time. Most miRNAs exhibit strictly regulated expression patterns, usually tissue-specific or even cell-specific, highlighting the importance of miRNAs in the time, space, and development stages of specific gene expression patterns. miRNAs can act as negative regulators of mRNAs that mediate gene expression (Uğurel et al., 2016). Therefore, the upregulation of miRNA may downregulate their target mRNA and the expression of the genetic information encoded by these mRNAs. The miRNAs of the nervous system form a complex gene regulatory network, which contains not only normal physiological regulatory information but also abundant neurobiological information related to neurological diseases (Christensen and Schratt, 2009).

In recent years, the emergence of gene chip technology has further explored the relationship between miRNA and epilepsy, as well as the treatment and prognosis of epilepsy (Henshall et al., 2016). Nervous system miRNAs are mainly involved in inflammatory responses, neuronal necrosis and apoptosis, dendritic growth, pathological circuit re-formation, glial cell proliferation, the formation of epileptic networks, impaired neurotransmitter release and receptor function. In short, a series of pathological changes in the nervous system eventually form a repeated excitatory cycle in the hippocampus, leading to the occurrence and development of epilepsy (Alsharafi et al., 2015; Pitkänen et al., 2016). In this review, the role of epilepsy-related pathological mechanisms and the regulatory involvement of miRNAs will be discussed to provide a new understanding of the early diagnosis and treatment of this disorder.

miRNAS: EXPRESSION, PRODUCTION AND MECHANISMS

MicroRNAs are small single stranded RNAs of about 22 nucleotides in length. miRNAs are widely distributed in animals, plants, fungi, and other multicellular eukaryotes. They are highly conserved in evolution and mainly located in non-coding regions of the genome. Although they do not encode proteins, miRNAs participate in important physiological and pathological processes. miRNAs can complement and pair with the 3′-UTR region of target gene mRNA, resulting in mRNA degradation or inhibition of translation. Thus, they can regulate up to 30% of protein expression after transcription (Bartel, 2004; He and Hannon, 2004; Bushati and Cohen, 2007).

Most miRNA promoters are recognized by RNA polymerase II (Pol II), and the initial miRNA transcription products must undergo splicing and polyadenylation (Winter et al., 2009). The initial transcription product, called primary miRNA (pri-miRNA), is about 1000 bp in size (Zeng et al., 2005). In the nucleus, the endonuclease RNase III-type protein Drosha cuts the double strand at the base of the pri-miRNA. The stem-loop intermediate with a phosphate group at the 5′-end of 60–100 bp and a dinucleotide overhang at the 3′-end is the precursor miRNA (pre-miRNA). Drosha is a non-specific RNase that cannot recognize pri-miRNA for specific cleavage and must form a complex with DGCR8 (Pasha) in animals. Specifically, the pri-RNA substrate is recognized by the double-stranded RNA binding site on DGCR8, and then Drosha cleaves the RNA 11 bp from the recognition point to generate the pre-miRNA (Chendrimada et al., 2005; Yeom et al., 2006). Next, Exportin-5, a transport protein on the nuclear membrane, binds to the pre-miRNA by recognizing the protruding dinucleotide structure at the 3′-end of the pre-miRNA, exporting it into the cytoplasm with the help of Ran-GTP. In the cytoplasm, the pre-miRNA is recognized by Dicer. The double strand of the spirochete is cut around the two helical corners from the stem-loop, resulting in a double-stranded RNA of 19–23 nucleotides that is similar in structure to small interfering RNA (siRNA). The mature miRNA comes from one arm of the pre-miRNA, and the other arm produces a fragment of the same length as the miRNA, namely miRNA*. Finally, RNA helicase acts on the miRNA* duplex and undergoes a chain selection process. One strand of the miRNA* of the double RNA is degraded, and the other becomes the mature miRNA, which enters the RNA-induced silencing complex (RISC) (Chendrimada et al., 2007).

MicroRNAs are partially complementary to the 3′-UTR sequences of their target mRNAs. Target mRNA stability is not affected by the binding of miRNA; however, mRNA expression after translation initiation is inhibited. miRNAs can inhibit the extension or termination of translation or degrade newly synthesized peptide chains from ribosomes (Bazzini et al., 2012). Recent studies have shown that miRNAs are susceptible to various forms of RNA editing, including adenosine-to-inosine (A-to-I) RNA editing. The editing of miRNAs has a profound impact on the set of target genes that they can regulate. This type of modification can greatly expand the number of potential targets a single miRNA family can regulate and change our understanding of the role of miRNAs in homeostasis and disease environments (Zhang et al., 2006; Kawahara et al., 2007).

THE ROLE OF miRNAs IN EPILEPSY PATHOGENESIS

The exact etiology of epilepsy is still controversial. Its pathogenesis may be closely related to neuronal cell apoptosis, pathological circuit re-formation, glial fibroblast proliferation and inflammatory response (Chang and Lowenstein, 2003; Vezzani et al., 2011), and miRNAs may be involved in the occurrence and development of epilepsy by regulating these pathological processes (Cattani et al., 2016; Wang T. et al., 2017; Korotkov et al., 2020). The potential mechanisms of miRNA imbalance and the different roles of miRNAs in epilepsy pathogenesis are discussed below to highlight potential biomarkers and therapeutic developments (**Figure 1**).

Neuroinflammation and miRNA

Cerebral tissue injury in patients with epilepsy can promote the release of inflammatory factors and induce inflammatory reactions. These inflammatory factors (e.g., interleukin-1 [IL-1], interferon-α [INF-α], and tumor necrosis factor-α [TNF-α])

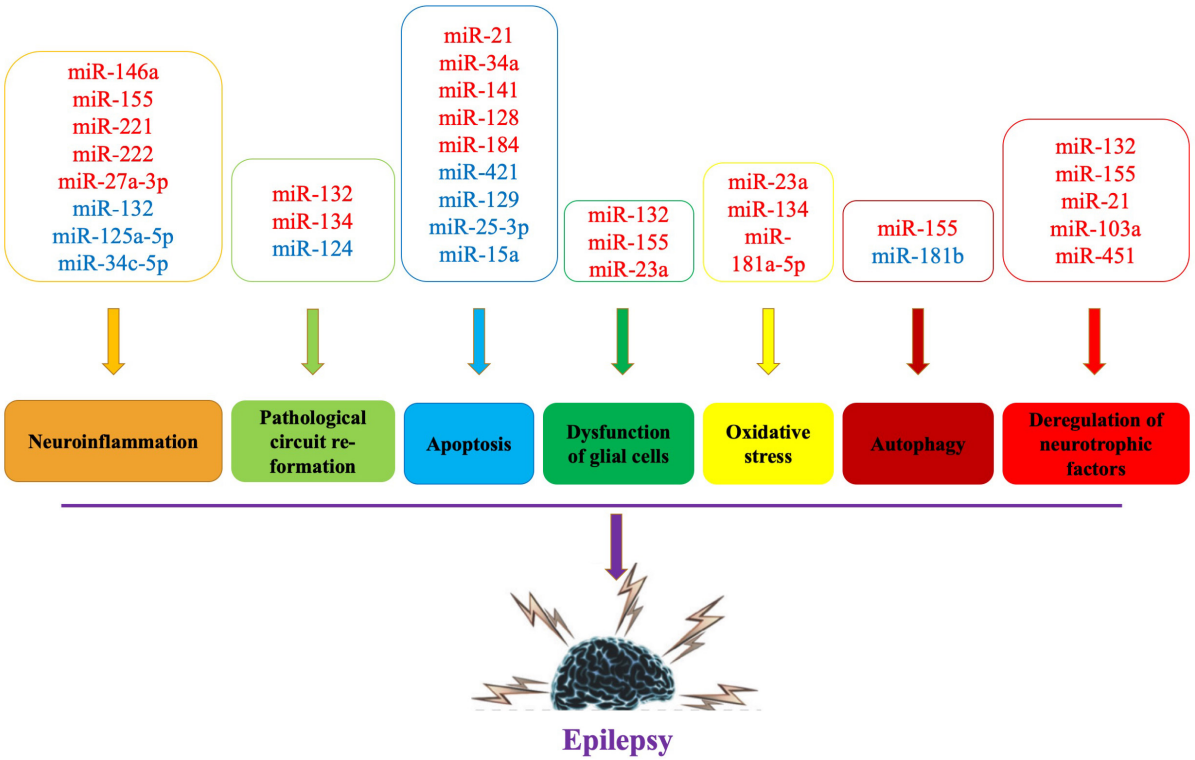

FIGURE 1 | Pathogenic mechanisms and related miRNAs of epilepsy. Red words indicate the upregulated miRNAs and blue words indicate the downregulated miRNAs.

can destroy the blood-brain barrier and aggravate damage to the nervous system and also excite neurons and promote repeated seizures (Vezzani et al., 2016, 2019; Rana and Musto, 2018).

In patients with drug-resistant epilepsy, miR-34c-5p was significantly downregulated, which might upregulate high mobility group protein (HMGB1) and IL-1β expression (Fu et al., 2020). Therefore, the authors of the study pointed out that decreased miR-34c-5p levels might exacerbate neuroinflammation in drug-resistant epilepsy and aggravate hippocampal neuron loss in epileptogenesis.

Toll-like receptor 4 (TLR4) is an important immune receptor involved in the development of epileptic inflammation by regulating the expression of nuclear factor-κB (NF-κB), tumor necrosis factor receptor-related factor 6, and IL-1 receptor-related kinase 1 (Kan et al., 2019). Elevated expression of IL-1, IL-6, and INF-α in epileptic foci demonstrates that inflammation is indeed closely related to the occurrence and development of epilepsy (Vezzani et al., 2008; Zhou et al., 2017). miR-146a regulates the expression of NF-κB, IL-1, and INF-α at the post-transcriptional level and affects the inflammatory reaction after an epileptic seizure. Increased miR-146a levels in the epileptic brain may alleviate inflammation, suggesting that miR-146a may be a target for disease treatment (Aronica et al., 2010; Tao et al., 2017; Zhang et al., 2018). In preclinical models of epilepsy, miR-146a also plays an important role in the TLR4 signaling pathway. After a seizure, TLR4 receptors are activated, and NF-κB enters the nucleus for activation. Activated NF-κB can upregulate the expression of miR-146a, IL-1, and INF-α. The increased miR-146a can suppress the activity of NF-κB, thereby reducing the production of IL-1 and INF-α and the inflammatory reaction caused by epilepsy (Boldin et al., 2011; Wang X. et al., 2018). In the refractory temporal lobe epilepsy (TLE) rat model, miR-146a increased the epilepsy susceptibility by reducing complement factor H. Thus, reducing the differential expression of miR-146a induced by epilepsy might reduce the occurrence of epilepsy (He et al., 2016). Enhanced miR-146a expression upregulated IL-1β in chronic TLE by downregulating complement factor H. Therefore, modulating the miR-146a-complement factor H-IL-1β loop circuit might be a novel therapeutic strategy for TLE (Li et al., 2018). miR-146a was up-regulated in the rat/mouse models. However, considering the differences in its downstream regulated target genes, miR-146a as a target for the treatment of epilepsy needs further study.

miR-155 is also associated with the regulation of inflammatory pathways in epilepsy. In children with chronic TLE, the expression levels of both miR-155 and TNF-α are increased. The increased TNF-α levels act as a feedback loop to regulate miR-155 expression. Thus, these two molecules interact to mediate the inflammatory process (Ashhab et al., 2013). Ashhab et al. (2013) confirmed that the expression levels of miR-155 and TNF-α were increased in children with chronic TLE, and miR-155 could increase TNF-α expression to enhance the inflammatory response.

The expression of miR-27a-3p is significantly increased in the hippocampus of epileptic rats (Lu et al., 2019). A miR-27a-3p inhibitor could effectively reduce IL-1β, IL-6, and TNF-α levels and neuronal apoptosis in the hippocampus of these rats (Lu et al., 2019). In contrast, expression of miR-125a-5p is downregulated in the hippocampus of pentylenetetrazol-induced epileptic rats (Liu Q. et al., 2019). Overexpression of miR-125a-5p attenuated epilepsy and decreased inflammatory factor levels in the hippocampus by suppressing calmodulin-dependent protein kinase IV (CAMK4), suggesting that miR-125a-5p might represent a novel treatment for epilepsy (Liu Q. et al., 2019). Lipopolysaccharide (LPS) treatment downregulated miR-132 levels *in vitro* (Ji et al., 2018). Overexpression of miR-132 reduced LPS-induced inflammatory injury, decreased the phosphorylated levels of kinases in the NF-κB and MEK/ERK pathways, and attenuated LPS-induced inflammatory cell injury by targeting tumor necrosis factor receptor-associated factor 6 (TRAF6) (Ji et al., 2018).

To conclude, dysregulated miRNA expression may be involved in epilepsy pathogenesis by regulating the expression of inflammatory factors (e.g., IL-1, INF-α, and TNF-α). Importantly, miR-146a may not only regulate inflammatory factors involved in the onset of epilepsy but may also be a biomarker for diagnosing epilepsy and an important therapeutic target.

Apoptosis and miRNA

Recurrent epileptic seizures can cause neuronal apoptosis, and the decrease in cell number can reorganize the synapses between neurons and form abnormal synaptic loops that promote epilepsy recurrence (Henshall and Simon, 2005). Tivnan et al. (2011) were the first to demonstrate an association between miR-34 and apoptosis by reducing MAP3K9 mRNA and protein levels. After an epileptic seizure, the body upregulates the expression of pro-apoptotic miRNA and downregulates the expression of anti-apoptotic miRNA to increase cell apoptosis, which affects the occurrence and development of epilepsy (Hu et al., 2012).

miR-21 can inhibit cell apoptosis (Wang K. et al., 2017). miR-21 expression in the hippocampus is increased several hours after a seizure, which might reduce the inhibitory effect on the 3′ UTR region of the neurotrophin-3 and promote cell apoptosis (Peng et al., 2013). Risbud et al. (2011) demonstrated that the hippocampal miR-21 levels increased significantly from 2 days to 3 weeks in epileptic rats. They also found that the active protein of caspase-3 related to apoptosis signal transmission and the number of apoptotic cells also increased. Therefore, the mechanism underlying the role of miR-21 in epilepsy may be by activating pro-apoptotic genes to promote neuronal apoptosis.

miR-34a is an evolutionarily conserved pro-apoptotic miRNA that can be upregulated by activated p53. Hu et al. (2012) reported that miR-34a expression levels are increased in post-status epileptic rats. They showed that miR-34a was upregulated during seizure-induced neuronal death or apoptosis, and targeting miR-34a was neuroprotective and abrogated the increase in activated caspase-3 protein. miR-141 expression is also upregulated in patients with epilepsy. *In vitro*, miR-141 overexpression induces nerve cell apoptosis, suppresses proliferation, induces caspase-3/9, Bax and p53 expression, and reduces silent information regulator 1 protein expression (Liu D. et al., 2019). miR-128 expression is increased in rats with lithium chloride-induced epilepsy. Chen et al. (2019) demonstrated that miR-128 overexpression promoted nerve cell apoptosis, increased p53, Bax, and cytochrome c protein expression, and enhanced caspase-3/9 activity. Therefore, anti-miR-128 may be neuroprotective against epilepsy through the SIRT1/p53/caspase signaling pathway.

In addition to the role of pro-apoptotic miRNAs in epilepsy, some anti-apoptotic miRNAs are also differentially expressed and involved in the pathological mechanism of epilepsy. miR-184 is an apoptosis regulator that is upregulated in the CA3 subfield of the mouse hippocampus (McKiernan et al., 2012). McKiernan et al. (2012) showed that miR-184 had anti-apoptotic effects, which might be achieved by regulating the Numblike gene. miR-421 is downregulated in hippocampal neurons of epileptic mice. MYD88 is a target of miR-421. This miRNA could inhibit apoptosis and autophagy in hippocampal neurons in epileptic mice by downregulating the TLR/MYD88 pathway (Wen et al., 2018).

miR-129 expression is decreased in hippocampal neurons in epileptic rats (Wu et al., 2018). Wu et al. (2018) suggested that c-Fos was a potential target gene for miR-129, which could inhibit proliferation and apoptosis of hippocampal neurons in rats by repressing c-Fos expression through inhibiting the MAPK signaling pathway.

miR-25-3p is associated with oxidative stress and apoptosis. Li et al. (2020) found that miR-25-3p was downregulated concomitant with upregulated OXSR1 expression in the hippocampus of KA-treated rats. miR-15a expression is also downregulated in TLE tissues. Upregulated miR-15a significantly suppresses the apoptosis rate in epileptic cells. In addition, Fan et al. (2020) demonstrated that miR-15a directly targets GFAP. Thus, miR-15a upregulation might inhibit cell apoptosis and the inflammation in TLE by targeting GFAP, providing a potential therapeutic target for the treatment of TLE.

In general, the available data suggest that different miRNAs participate in epilepsy pathogenesis or protect neurons by regulating the level of apoptosis. Modulation of these differentially expressed miRNAs may provide new strategies for the treatment of epilepsy.

Glial Cell Dysfunction and miRNA

Glial cells have supportive and protective effects on neurons, and they are mainly involved in the material metabolism of neurons. Their dysfunction may be an important cause of epilepsy. For example, dysfunction of glial cells may interfere with glutamate homeostasis and uptake, resulting in overexcitation of neurons and, eventually, epilepsy (Jimenez-Mateos et al., 2015). Reactive glial cells are also believed to contribute to the development of epilepsy by regulating brain inflammation and extracellular matrix (ECM) remodeling (Korotkov et al., 2020). miR-132 is one of the most commonly upregulated miRNAs in animal TLE models. Korotkov et al. (2020) demonstrated that the miR-132 expression is increased in the human epileptogenic hippocampus, particularly in glial cells. By transfecting miR-132 into human

primary astrocytes, the expression of pro-epileptogenic COX-2, IL-1β, TGF-β2, CCL2, and MMP3 were decreased, suggesting that modulating miR-132 expression in astrocytes might be a potential therapeutic target warranting further investigation (Korotkov et al., 2020).

miR-155 is abundantly expressed in glial cells, and its expression is significantly increased in the brain tissue of epilepsy patients and kainate (KA)-induced epileptic mice. Fu et al. (2019) noted that abnormal proinflammatory cytokine expression and microglia morphology could be changed by silencing miR-155. In addition, a miR-155 antagomir may reduce microglia-impaired neuron excitability and attenuate KA-induced epilepsy by inhibiting microglia activation (Fu et al., 2019). Moreover, inhibition of miR-155 could also attenuate MMP3 overexpression after IL-1β stimulation in astrocytes, suggesting a possible strategy to prevent epilepsy via the modulation of glial cells and reduction of inflammation (Korotkov et al., 2018).

miR-23a is another miRNA for which increased expression is observed in the hippocampus of epileptic rats. Song et al. (2011) demonstrated that miR-23a had an effect on glial cell apoptosis. When miR-23a was inhibited, the expression of its target genes (STK4 and caspases) was increased, leading to increased glial cell apoptosis. Therefore, miR-23a might participate in the development of epilepsy by promoting glial cell proliferation and blocking glial cell apoptosis (Song et al., 2011).

Pathological Circuit Re-formation and miRNA

The synapse is a special structure composed of the neuronal cell body, axon, and dendrite. An external signal stimulates the growth of dendritic spines and synapse formation. Pathological circuit re-formation refers to abnormal synaptic connections caused by brain tissue damage. The pathological neural circuit formed by this remodeling may lead to recurrent epilepsy (Janz et al., 2017). Previous studies have suggested that some miRNAs affect neuron development and pathological circuit re-formation by regulating protein synthesis, covalently modifying existing proteins, and reusing membrane receptors after epileptic seizures (Cattani et al., 2016).

miR-132 is involved in pathological circuit re-formation and the regulation of dendritic spines. Studies have also found that miR-132 expression is increased in children with TLE, speculating that increased miR-132 levels might affect pathological circuit re-formation and neuronal apoptosis through the regulation of P250GAP and promote the occurrence of epilepsy (Jimenez-Mateos et al., 2011; Scott et al., 2012). This miRNA was first discovered by Nudelman et al. (2010), who observed that the upregulation of miR-132 expression could increase neuronal activity in a rat model of pilocarpine-induced epilepsy. Through a series of complex signal transduction, miR-132 could inhibit the production of GTPase activating protein (P250GAP), thereby affecting the pathological circuit re-formation of hippocampal neurons (Nudelman et al., 2010). Moreover, increasing miR-132 expression in hippocampal neurons could induce pathological circuit re-formation, while inhibiting its expression would have the opposite effect (Wayman et al., 2008).

miR-124 is a brain-specific miRNA that was originally believed to be a key regulator of neuronal differentiation and nervous system development. It is extremely abundant in the brain and can regulate the growth of neuronal synapses. miR-124 also plays an important role in epilepsy. Wang W. et al. (2016) found that miR-124 expression was decreased in patients with epilepsy and rats after drug induced-seizures. CAMP response element-binding protein1 (CREB1) is a key regulator in epileptogenesis (Wang W. et al., 2016). miR-124 directly targets the 3′ UTR of the CREB1 gene to repress CREB1 expression and abrogate the-epileptic effect (Wang W. et al., 2016). The EPAC protein is a guanine nucleotide exchange factor that acts as an intracellular receptor for cyclic adenylate. Yang et al. (2012) found that a mutation in the mouse EPAC gene caused abnormal synaptic transmission, which reduced the spatial and social learning ability of mice. However, the silencing of miR-124 restored the cognitive function of the mice, suggesting that miR-124 was closely associated with pathological circuit re-formation and could further affect the cognitive function of epileptic mice (Yang et al., 2012).

miR-134 is a brain-specific, activity-regulated miRNA that has been implicated in the control of dendritic spine morphology (Jimenez-Mateos et al., 2012). miR-134 expression is upregulated in experimental epilepsy models and the human disease. Inhibition of miR-134 expression could reduce the number of neuronal spines and degree of pathological damage to brain tissue after an epileptic seizure (Jimenez-Mateos et al., 2012).

Autophagy and miRNA

The relationship between autophagy and epilepsy has not been fully clarified. Some studies suggest that autophagy may induce epilepsy through the mammalian target of rapamycin (mTOR) pathway or abnormal glycogen accumulation. Some miRNAs may affect the onset of epilepsy by regulating the process of autophagy. For example, miR-34a negatively regulates autophagy and is up-regulated after epileptic status. However, autophagy is activated after recurrent neonatal convulsions, suggesting that miR-34a may play an important role in the excitatory toxicity induced by neonatal convulsions (Gan et al., 2015).

miR-155 induces autophagy through mTOR, and this effect is more obvious in the young mouse status epilepticus model, which strongly suggests the existence of this hypothetical pathway in epilepsy (Wan et al., 2014).

miR-181b expression is decreased in juvenile KA-induced epileptic rats (Wang et al., 2019). Wang et al. demonstrated that TLR4 is a direct target of miR-181b. This miRNA can inhibit the P38/JNK signaling pathway by targeting TLR4, thereby attenuating autophagy of KA-induced epileptic juvenile rats (Wang et al., 2019).

Furthermore, as mentioned above, miR-421 could inhibit the apoptosis and autophagy of hippocampal neurons in epilepsy mice by down−regulating the TLR/MyD88 pathway (Wen et al., 2018).

Oxidative Stress and miRNA

Oxidative stress caused by excessive free radical release is involved in the pathological processes of many

neurodegenerative diseases. However, the relationship between oxidative stress and epilepsy has only recently been recognized. Accumulating evidence demonstrates that oxidative stress is a key factor in not only the consequences of epilepsy but may also be involved in the disease pathogenesis. An impaired antioxidant system, mitochondrial dysfunction, and activation of the arachidonic acid pathway may be the main underlying causes of epilepsy pathogenesis. Oxidative stress affects the expression levels of multiple miRNAs, and, conversely, miRNAs could regulate many genes involved in the oxidative stress response. Both oxidative stress and miRNA regulatory networks influence processes of neurological diseases, including epilepsy (Konovalova et al., 2019).

miR-23a is one of the most common miRNAs involved in hippocampal neuronal injuries and spatial memory impairment in an experimental model of TLE. Zhu et al. (2019) found that miR-23a was upregulated in the hippocampus after status epilepticus (SE) in KA-induced TLE mice. In addition, this change in miR-23a expression was accompanied by hippocampal oxidative damage. Furthermore, hippocampal oxidative stress and neuronal injuries could be significantly improved by inhibiting miR-23a expression with miR-23a antagomirs. Thus, targeting miR-23a in the epileptic brain might provide a novel strategy for protecting against hippocampal neuronal injuries in TLE patients (Zhu et al., 2019).

Previous studies revealed the neuroprotective effect of miR-134 antagomirs, which could reduce ischemic injury and cause prolonged seizure suppression (Huang et al., 2014). It was reported that miR-134 levels were significantly upregulated in rat brain after KA-induced SE (Gao et al., 2019). A miR-134 antagonist could suppress lesion-induced endoplasmic reticulum stress and apoptosis-related CHOP expression. Gao et al. (2019) suggested silencing of miR-134 could modulate the epileptic phenotype by upregulating CREB, which might be a promising intervention for the treatment of epilepsy.

The miR-181a-5p expression levels are increased in a lithium-pilocarpine model of epilepticus in immature rats. Inhibition of miR-181a-5p might protect the hippocampus against the damage from an epileptic seizure through various mechanisms, including oxidative stress. Moreover, inhibition of miR-181a-5p could exert a seizure-suppressing effect via SIRT1 upregulation, suggesting a potential role for the miR-181a-5p/SIRT1 pathway in the development of temporal lobe epilepsy (Kong et al., 2020).

Deregulation of Neurotrophic Factors and miRNA

Brain-derived neurotrophic factor (BDNF) and its receptor tropomyosin-related kinase B (TrkB) are involved in the pathophysiology observed with epilepsy. In recent years, the miRNAs that may be involved in BDNF-mediated epilepsy have received increasing attention. miR-155 expression levels were higher in epilepsy patients compared to the normal controls. Moreover, Duan et al. (2018) also demonstrated that miR-155 contributes to the occurrence of epilepsy through the PI3K/Akt/mTOR signaling pathway. Xiang et al. (2015) found a dramatic upregulation of miR-132 and BDNF mRNA expression in the hippocampal neuronal culture model of SE. In addition, their results suggested that miR-132 promotes epileptogenesis by regulating BDNF/TrkB signaling. In contrast, neurotrophin-3 mRNA levels decrease in the hippocampus following SE, concurrent with an increase in miR-21. Thus, the miR-21 levels in cultured hippocampal neurons are inversely correlated with neurotrophin-3 mRNA levels, and miR-21 is a candidate for regulating neurotrophin-3 signaling in the hippocampus following status epilepticus (Risbud et al., 2011).

miR-103a expression is increased in an epileptic rat model induced by lithium chloride-pilocarpine treatment. miR-103a inhibitors induced BDNF expression, increased the number of surviving neurons, and decreased the number of apoptotic neurons (Zheng et al., 2019). miR-451 is also upregulated in KA-induced epilepsy models, and miR-451 knockout improved the pathological changes in the hippocampus. In addition, miR-451 knockout might inhibit the apoptosis of hippocampal neurons. Glial cell line-derived neurotrophic factor (GDNF) is a target gene of miR-451. GDNF overexpression reversed the effect of miR-451 on KA-induced brain injury and neuronal apoptosis (Weng et al., 2020).

miRNAs AS BIOMARKERS OF EPILEPSY

For most epilepsy patients, clinicians can give a timely and correct diagnosis through patient history and clinical manifestations. Effective biomarkers can help to make the correct diagnosis and epilepsy classification and provide an opportunity to develop targeted therapy for epilepsy. Genetic biomarkers, such as the gamma-aminobutyric acid (GABA) receptor gene, 5-hydroxy tryptamine (5-HT) receptor gene, sodium channel voltage-gated type I-alpha (SCN1A) gene, aquaporin-4 (AQP4), and inwardly rectifying potassium channel (Kir4.1) gene, and inflammatory biomarkers (e.g., IL-2, IL-6, and TNF-α) may offer help in diagnosing epilepsy (Symonds et al., 2017). However, the application of these biomarkers is limited as some results are inconsistent and lack diagnostic specificity.

MicroRNA can affect the synthesis and molecular structure of a variety of proteins, and changes in miRNA expression levels and activity may affect cellular functions (Krol et al., 2010). Indeed, miRNA expression via oligonucleotides can easily lead to widespread gene expression changes (Bajan and Hutvagner, 2020). These properties make miRNAs useful epilepsy biomarkers and potential new therapeutic targets (**Supplementary Table 1**). Avansini et al. (2017) performed high-throughput sequencing analysis on plasma miRNA from 14 mesial TLE (MTLE) and 13 focal cortical dysplasia (FCD) samples along with 16 normal controls. They found that miR-134 was significantly downregulated in the plasma of MTLE patients, suggesting that decreased hsa-miR-134 expression could be a potential non-invasive biomarker to support the diagnosis of patients with MTLE. Other potential circulating biomarkers are miR-145, miR-181c, miR-199a, and miR-1183, which were overexpressed in the blood of patients with MTLE with hippocampal sclerosis (MTLE-HS) (Antônio et al., 2019). Serum miR-328-3p is also an important peripheral biomarker

for the diagnosis of MTLE-HS with high area under the curve (AUC) values when comparing controls to Engel I (90.3%). For predicting the surgical prognosis of MTLE-HS patients, miR-654-3p had statistical power as a peripheral biomarker (AUC = 73.6%) to differentiate Engel I from Engel III-IV patients (Ioriatti et al., 2020). Wang et al. (2015b) used Illumina HiSeq2000 sequencing to screen for differentially expressed miRNAs in the serum of 30 epilepsy patients and 30 healthy controls. They found that miR-106b-5p had the highest diagnostic value for epilepsy, with a sensitivity of 80.3% and a specificity of 81.2%, suggesting that miR-106b-5p could be used as a non-invasive diagnostic biomarker for epilepsy (Wang et al., 2015b). An et al. (2016) recruited 90 epilepsy patients (57 cases of generalized seizures, 33 cases of focal seizures) and 90 healthy controls for their study that used a PCR method to detect the expression levels of four epilepsy-related miRNAs (miR-106b, miR-146a, miR-194-5p, and miR-301a) in serum. Compared to the control group, serum miR-106b, miR-146a, and miR-301a were significantly upregulated in the epilepsy group, while miR-194-5p was significantly downregulated. In addition, serum miR-106b and miR-146a expression levels were positively correlated with the severity of epilepsy. The combined detection of these two miRNAs in serum had better sensitivity and specificity for the prediction of epilepsy (An et al., 2016).

miR-129-2-3p is upregulated in the temporal cortex and plasma of patients with refractory TLE (Sun Y. et al., 2016). With increasing epilepsy frequency, miR-129-2-3p expression levels are also upregulated, and the prognosis of patients with epilepsy is also poor. Therefore, plasma miR-129-2-3p may be used as a potential non-invasive biomarker for early detection and clinical prognosis evaluation for refractory TLE (Sun Y. et al., 2016). In contrast, miR-145-5p expression levels in plasma are significantly downregulated in patients with refractory TLE. This decreased expression is positively correlated with the age of onset and frequency of epilepsy (Shen et al., 2019). Sun J. et al. (2016) found that the expression levels of miR-30a, miR-378, miR-106b, and miR-15a in the serum of patients with epilepsy were upregulated compared to the levels observed during the inter-seizure period. Among these miRNAs, miR-30a was positively correlated with seizure frequency but had no significant correlation with sex, age, and medical history (Sun J. et al., 2016). miR-4521 is upregulated in the brain tissue and serum of refractory epilepsy patients. Serum miR-4521 levels may represent a potential diagnostic biomarker for FCD with refractory epilepsy (Wang X. et al., 2016). Another study with FCD patients found that the expression of miR-323a-5p was significantly elevated in the cortex and plasma of FCD patients with refractory epilepsy, suggesting that abnormal miR-323a-5p expression could be used to monitor treatment responses in patients with FCD (Che et al., 2017). Serum of miR-146a and miR-155 levels are also significantly upregulated in genetic generalized epilepsy patients. Martins-Ferreira et al. (2020) suggested that the combined serum levels of miR-132, miR-146a, and miR-155 could discriminate between genetic generalized epilepsy patients and controls with high specificity and sensitivity.

Some circulating miRNAs have been associated with drug-resistant epilepsy. Wang et al. (2015a) used Illumina HiSeq2000 sequencing technology to analyze the differential expression of serum miRNAs in 30 drug-resistant epilepsy patients and 30 drug-sensitive epilepsy patients. miR-301a-3p is the most valuable biomarker for the identification of drug-resistant epilepsy to date. Multiple regression analysis showed that downregulated miR-301a-3p expression represents a potential biomarker for the diagnosis of drug-resistant epilepsy, with a sensitivity of 81.5% and specificity of 81.2% (Wang et al., 2015a). Leontariti et al. (2020) demonstrated that miR-134 and miR-146a serum levels were elevated in patients with drug-resistant epilepsy. These levels represented a significantly higher risk of developing drug-resistant epilepsy.

So far, new biomarkers for the diagnosis of epilepsy are still being evaluated. The expression changes of various miRNAs identified by expression profiling of circulating miRNA have been confirmed in epilepsy patients (Antônio et al., 2019; Brennan et al., 2020). There is evidence that epilepsy is associated with the expression changes observed in the circulating miRNAs. The inclusion of more cases and consistent studies of circulating miRNA detection techniques could enhance the potential of using miRNAs as biomarkers for epilepsy.

miRNA-BASED THERAPEUTIC APPROACHES FOR EPILEPSY

With the continuous deepening of the research on the mechanism of miRNAs involved in epilepsy pathogenesis, the idea of miRNA-targeted intervention to prevent or delay the occurrence of epilepsy is valuable. Because a single miRNA can simultaneously regulate multiple pathways, targeting a single miRNA may affect many cell processes and, thus, be an effective intervention strategy following epileptogenic injury. Many preclinical studies have demonstrated the function of miRNAs and their potential to treat acute or chronic epilepsy. The path of clinical transformation has begun. So far, miRNA-based therapies have been well-tolerated and have yielded therapeutic effects in preclinical studies (**Supplementary Table 2**).

Vagus nerve stimulation (VNS) has proven to be a safe and effective treatment for refractory epilepsy. This procedure could activate neuronal and astrocyte a7nAchR and inhibit the apoptotic and oxidant stress responses. Jiang et al. (2015) suggested that miR-210 plays an important role in the antioxidant stress and anti-apoptosis responses induced by VNS, indicating that the miR-210 is a potential mediator of VNS-induced neuroprotection against I/R injury. miR-137 is an extremely rich miRNA in the central nervous system and is believed to be closely associated with synaptic plasticity. In the pilocarpin-induced epileptic mouse model, miR-137 overexpression induced by intrahippocampal injection of a specific Agomir prolonged the latency period of spontaneously recurring seizures and reduced the severity of epilepsy (Wang W. et al., 2018). miR-135a silencing in an experimental temporal lobe epilepsy model reduced seizure activity at the spontaneous recurrent seizure stage by regulating Mef2 proteins, which are key regulators of excitatory synapse density (Vangoor et al., 2019). By Nissl staining, miR-134

silencing significantly reduced the loss of CA3 pyramidal neurons and abnormal mossy fiber germination. In addition, EEG and behavioral analysis showed that miR-134 antagonists had a palliative effect on experimental epileptic seizures. These results suggested that silencing miR-134 regulated epileptic phenotypes by upregulating its target gene CREB (Gao et al., 2019).

Silencing miR-132 inhibited the aberrant formation of dendritic spines and chronic spontaneous seizures in a lithium-pilocarpine-induced epileptic mouse model (Yuan et al., 2016). Experiments with cultured epileptic neurons suggesting that miR-132 silencing exerted a neuroprotective effect through the miR-132/p250GAP/Cdc42 pathway (Yuan et al., 2016). miR-204 directly targets and downregulates TrkB protein in various diseases (Xiang et al., 2016). Xiang et al. (2016) suggested that miR-204 overexpression caused anti-epileptogenic effects by regulating TrkB and its downstream ERK1/2-CREB signaling pathway. Moreover, Zheng et al. (2016) demonstrated that miR-219 plays a crucial role in suppressing seizures in experimental epilepsy models via modulating the CaMKII/NMDA receptor pathway, and miR-219 supplementation may be a potential anabolic strategy for ameliorating epilepsy. Furthermore, Qi et al. (2020) found that miR-494 overexpression could repress RIPK1, which inactivates the NF-κB signaling pathway, acceleration of cell proliferation, and suppression of apoptosis in hippocampal neurons of epileptic rats, attenuating neuronal injury and epilepsy development.

In mouse models of epilepsy, attempts have been made to control epilepsy by regulating the expression of miR-146a. Tao et al. (2017) found that intranasal delivery of miR-146a mimics could improve epilepsy onset and hippocampal damage in the acute phase of lithium-pilocarpine-induced epilepsy by modulating the expression of inflammatory factors. Intracerebroventricular injection of miR-146a could also relieve epilepsy in an immature rat model of lithium-pilocarpine-induced status epilepticus (Wang X. et al., 2018).

In general, multiple miRNAs are potential therapeutic targets for the treatment of epilepsy; however, there are still some challenges to their clinical application. First, previous studies have mostly been performed only in a single model or species. Thus, the results may need to be verified in models representing different etiologies or in larger animals. Secondly, it is necessary to understand the mechanism of miRNA-targeted therapy. However, the establishment of these mechanisms is limited to a small number of studies, and the mechanisms have rarely been verified *in vivo*. Thirdly, the safety of oligonucleotides that target brain miRNAs needs to be extensively evaluated in preclinical studies.

CONCLUSION

Emerging studies have shown that miRNAs are key gene regulation factors in epilepsy pathogenesis. Indeed, miR-146a and miR-155 might be critical miRNAs involved in this disease. Expression differences of circulating miRNAs may be useful biomarkers for diagnosing, evaluating prognosis, and predicting treatment response. Differentially expressed miRNAs can be used to identify changes in the molecular structure and cellular pathways in epilepsy patients and represent possible treatment targets. However, the results of multiple studies on miRNA as biomarkers for epilepsy diagnosis need to be unified. Regulating pathological genes and interfering with other pathogenic mechanisms can produce therapeutic effects. Thus, the development of effective miRNA therapeutics holds great promise for potential therapeutic strategies for epilepsy.

AUTHOR CONTRIBUTIONS

JW and JZ drafted and revised the manuscript. JZ drafted and modified the figures and tables. Both authors approved the final version of the manuscript and agreed to be accountable for all aspects of the work to ensure that questions related to the accuracy or integrity of any part of the work are appropriately investigated and resolved.

SUPPLEMENTARY MATERIAL

The Supplementary Material for this article can be found online at: https://www.frontiersin.org/articles/10.3389/fnmol.2021.650372/full#supplementary-material

REFERENCES

Alsharafi, W. A., Xiao, B., Abuhamed, M. M., and Luo, Z. (2015). miRNAs: biological and clinical determinants in epilepsy. *Front. Mol. Neurosci.* 8:59. doi: 10.3389/fnmol.2015.00059

An, N., Zhao, W., Liu, Y., Yang, X., and Chen, P. (2016). Elevated serum miR-106b and miR-146a in patients with focal and generalized epilepsy. *Epilepsy Res.* 127, 311–316. doi: 10.1016/j.eplepsyres.2016.09.019

Antônio, L. G. L., Freitas-Lima, P., Pereira-Da-Silva, G., Assirati, J. A. Jr., Matias, C. M., Cirino, M. L. A., et al. (2019). Expression of MicroRNAs miR-145, miR-181c, miR-199a and miR-1183 in the Blood and Hippocampus of Patients with Mesial Temporal Lobe Epilepsy. *J. Mol. Neurosci.* 69, 580–587. doi: 10.1007/s12031-019-01386-w

Aronica, E., Fluiter, K., Iyer, A., Zurolo, E., Vreijling, J., Van Vliet, E. A., et al. (2010). Expression pattern of miR-146a, an inflammation-associated microRNA, in experimental and human temporal lobe epilepsy. *Eur. J. Neurosci.* 31, 1100–1107. doi: 10.1111/j.1460-9568.2010.07122.x

Ashhab, M. U., Omran, A., Kong, H., Gan, N., He, F., Peng, J., et al. (2013). Expressions of tumor necrosis factor alpha and microRNA-155 in immature rat model of status epilepticus and children with mesial temporal lobe epilepsy. *J. Mol. Neurosci.* 51, 950–958. doi: 10.1007/s12031-013-0013-9

Avansini, S. H., De Sousa Lima, B. P., Secolin, R., Santos, M. L., Coan, A. C., Vieira, A. S., et al. (2017). MicroRNA hsa-miR-134 is a circulating biomarker for mesial temporal lobe epilepsy. *PLoS One* 12:e0173060. doi: 10.1371/journal.pone.0173060

Bajan, S., and Hutvagner, G. (2020). RNA-Based Therapeutics: From Antisense Oligonucleotides to miRNAs. *Cells* 9:137. doi: 10.3390/cells9010137

Bartel, D. P. (2004). MicroRNAs: genomics, biogenesis, mechanism, and function. *Cell* 116, 281–297. doi: 10.1016/S0092-8674(04)00045-5

Bazzini, A. A., Lee, M. T., and Giraldez, A. J. (2012). Ribosome profiling shows that miR-430 reduces translation before causing mRNA decay in zebrafish. *Science* 336, 233–237. doi: 10.1126/science.1215704

Becker, A. J., Chen, J., Paus, S., Normann, S., Beck, H., Elger, C. E., et al. (2002). Transcriptional profiling in human epilepsy: expression array and single cell

real-time qRT-PCR analysis reveal distinct cellular gene regulation. *Neuroreport* 13, 1327–1333. doi: 10.1097/00001756-200207190-00023

Boldin, M. P., Taganov, K. D., Rao, D. S., Yang, L., Zhao, J. L., Kalwani, M., et al. (2011). miR-146a is a significant brake on autoimmunity, myeloproliferation, and cancer in mice. *J. Exp. Med.* 208, 1189–1201. doi: 10.1084/jem.20101823

Brennan, G. P., and Henshall, D. C. (2018). microRNAs in the pathophysiology of epilepsy. *Neurosci. Lett.* 667, 47–52. doi: 10.1016/j.neulet.2017.01.017

Brennan, G. P., Bauer, S., Engel, T., Jimenez-Mateos, E. M., Del Gallo, F., Hill, T. D. M., et al. (2020). Genome-wide microRNA profiling of plasma from three different animal models identifies biomarkers of temporal lobe epilepsy. *Neurobiol. Dis.* 144:105048. doi: 10.1016/j.nbd.2020.105048

Bushati, N., and Cohen, S. M. (2007). microRNA functions. *Annu. Rev. Cell Dev. Biol.* 23, 175–205. doi: 10.1146/annurev.cellbio.23.090506.123406

Cattani, A. A., Allene, C., Seifert, V., Rosenow, F., Henshall, D. C., and Freiman, T. M. (2016). Involvement of microRNAs in epileptogenesis. *Epilepsia* 57, 1015–1026. doi: 10.1111/epi.13404

Chang, B. S., and Lowenstein, D. H. (2003). Epilepsy. *N. Engl. J. Med.* 349, 1257–1266. doi: 10.1056/NEJMra022308

Che, N., Zu, G., Zhou, T., Wang, X., Sun, Y., Tan, Z., et al. (2017). Aberrant Expression of miR-323a-5p in Patients with Refractory Epilepsy Caused by Focal Cortical Dysplasia. *Genet. Test Mol. Biomark.* 21, 3–9. doi: 10.1089/gtmb.2016.0096

Chen, D. Z., Wang, W. W., Chen, Y. L., Yang, X. F., Zhao, M., and Yang, Y. Y. (2019). miR-128 is upregulated in epilepsy and promotes apoptosis through the SIRT1 cascade. *Int. J. Mol. Med.* 44, 694–704. doi: 10.3892/ijmm.2019.4223

Chendrimada, T. P., Finn, K. J., Ji, X., Baillat, D., Gregory, R. I., Liebhaber, S. A., et al. (2007). MicroRNA silencing through RISC recruitment of eIF6. *Nature* 447, 823–828. doi: 10.1038/nature05841

Chendrimada, T. P., Gregory, R. I., Kumaraswamy, E., Norman, J., Cooch, N., Nishikura, K., et al. (2005). TRBP recruits the Dicer complex to Ago2 for microRNA processing and gene silencing. *Nature* 436, 740–744. doi: 10.1038/nature03868

Christensen, M., and Schratt, G. M. (2009). microRNA involvement in developmental and functional aspects of the nervous system and in neurological diseases. *Neurosci. Lett.* 466, 55–62. doi: 10.1016/j.neulet.2009.04.043

Duan, W., Chen, Y., and Wang, X. R. (2018). MicroRNA-155 contributes to the occurrence of epilepsy through the PI3K/Akt/mTOR signaling pathway. *Int. J. Mol. Med.* 42, 1577–1584. doi: 10.3892/ijmm.2018.3711

Fan, Y., Wang, W., Li, W., and Li, X. (2020). miR-15a inhibits cell apoptosis and inflammation in a temporal lobe epilepsy model by downregulating GFAP. *Mol. Med. Rep.* 22, 3504–3512. doi: 10.3892/mmr.2020.11388

Fu, H., Cheng, Y., Luo, H., Rong, Z., Li, Y., Lu, P., et al. (2019). Silencing MicroRNA-155 Attenuates Kainic Acid-Induced Seizure by Inhibiting Microglia Activation. *Neuroimmunomodulation* 26, 67–76. doi: 10.1159/000496344

Fu, M., Tao, J., Wang, D., Zhang, Z., Wang, X., Ji, Y., et al. (2020). Downregulation of MicroRNA-34c-5p facilitated neuroinflammation in drug-resistant epilepsy. *Brain Res.* 1749:147130. doi: 10.1016/j.brainres.2020.147130

Gan, J., Qu, Y., Li, J., Zhao, F., and Mu, D. (2015). An evaluation of the links between microRNA, autophagy, and epilepsy. *Rev. Neurosci.* 26, 225–237. doi: 10.1515/revneuro-2014-0062

Gao, X., Guo, M., Meng, D., Sun, F., Guan, L., Cui, Y., et al. (2019). Silencing MicroRNA-134 Alleviates Hippocampal Damage and Occurrence of Spontaneous Seizures After Intraventricular Kainic Acid-Induced Status Epilepticus in Rats. *Front. Cell Neurosci.* 13:145. doi: 10.3389/fncel.2019.00145

He, F., Liu, B., Meng, Q., Sun, Y., Wang, W., and Wang, C. (2016). Modulation of miR-146a/complement factor H-mediated inflammatory responses in a rat model of temporal lobe epilepsy. *Biosci. Rep.* 36:e00433. doi: 10.1042/BSR20160290

He, L., and Hannon, G. J. (2004). MicroRNAs: small RNAs with a big role in gene regulation. *Nat. Rev. Genet.* 5, 522–531. doi: 10.1038/nrg1379

Henshall, D. C. (2014). MicroRNA and epilepsy: profiling, functions and potential clinical applications. *Curr. Opin. Neurol.* 27, 199–205. doi: 10.1097/WCO.0000000000000079

Henshall, D. C., and Simon, R. P. (2005). Epilepsy and apoptosis pathways. *J. Cereb. Blood Flow Metab.* 25, 1557–1572. doi: 10.1038/sj.jcbfm.9600149

Henshall, D. C., Hamer, H. M., Pasterkamp, R. J., Goldstein, D. B., Kjems, J., Prehn, J. H. M., et al. (2016). MicroRNAs in epilepsy: pathophysiology and clinical utility. *Lancet Neurol.* 15, 1368–1376. doi: 10.1016/S1474-4422(16)30246-0

Hu, K., Xie, Y. Y., Zhang, C., Ouyang, D. S., Long, H. Y., Sun, D. N., et al. (2012). MicroRNA expression profile of the hippocampus in a rat model of temporal lobe epilepsy and miR-34a-targeted neuroprotection against hippocampal neurone cell apoptosis post-status epilepticus. *BMC Neurosci.* 13, 115. doi: 10.1186/1471-2202-13-115

Huang, Y., Guo, J., Wang, Q., and Chen, Y. (2014). MicroRNA-132 silencing decreases the spontaneous recurrent seizures. *Int. J. Clin. Exp. Med.* 7, 1639–1649.

Ioriatti, E. S., Cirino, M. L. A., Lizarte Neto, F. S., Velasco, T. R., Sakamoto, A. C., Freitas-Lima, P., et al. (2020). Expression of circulating microRNAs as predictors of diagnosis and surgical outcome in patients with mesial temporal lobe epilepsy with hippocampal sclerosis. *Epilepsy Res.* 166:106373. doi: 10.1016/j.eplepsyres.2020.106373

Janz, P., Savanthrapadian, S., Häussler, U., Kilias, A., Nestel, S., Kretz, O., et al. (2017). Synaptic Remodeling of Entorhinal Input Contributes to an Aberrant Hippocampal Network in Temporal Lobe Epilepsy. *Cereb. Cortex* 27, 2348–2364. doi: 10.1093/cercor/bhw093

Ji, Y. F., Wang, D., Liu, Y. R., Ma, X. R., Lu, H., and Zhang, B. A. (2018). MicroRNA-132 attenuates LPS-induced inflammatory injury by targeting TRAF6 in neuronal cell line HT-22. *J. Cell Biochem.* 119, 5528–5537. doi: 10.1002/jcb.26720

Jiang, Y., Li, L., Tan, X., Liu, B., Zhang, Y., and Li, C. (2015). miR-210 mediates vagus nerve stimulation-induced antioxidant stress and anti-apoptosis reactions following cerebral ischemia/reperfusion injury in rats. *J. Neurochem.* 134, 173–181. doi: 10.1111/jnc.13097

Jimenez-Mateos, E. M., Arribas-Blazquez, M., Sanz-Rodriguez, A., Concannon, C., Olivos-Ore, L. A., Reschke, C. R., et al. (2015). microRNA targeting of the P2X7 purinoceptor opposes a contralateral epileptogenic focus in the hippocampus. *Sci. Rep.* 5:17486. doi: 10.1038/srep17486

Jimenez-Mateos, E. M., Bray, I., Sanz-Rodriguez, A., Engel, T., Mckiernan, R. C., Mouri, G., et al. (2011). miRNA Expression profile after status epilepticus and hippocampal neuroprotection by targeting miR-132. *Am. J. Pathol.* 179, 2519–2532. doi: 10.1016/j.ajpath.2011.07.036

Jimenez-Mateos, E. M., Engel, T., Merino-Serrais, P., Mckiernan, R. C., Tanaka, K., Mouri, G., et al. (2012). Silencing microRNA-134 produces neuroprotective and prolonged seizure-suppressive effects. *Nat. Med.* 18, 1087–1094. doi: 10.1038/nm.2834

Kan, M., Song, L., Zhang, X., Zhang, J., and Fang, P. (2019). Circulating high mobility group box-1 and toll-like receptor 4 expressions increase the risk and severity of epilepsy. *Braz. J. Med. Biol. Res.* 52:e7374. doi: 10.1590/1414-431x20197374

Kawahara, Y., Zinshteyn, B., Sethupathy, P., Iizasa, H., Hatzigeorgiou, A. G., and Nishikura, K. (2007). Redirection of silencing targets by adenosine-to-inosine editing of miRNAs. *Science* 315, 1137–1140. doi: 10.1126/science.1138050

Kong, H., Wang, H., Zhuo, Z., Li, Z., Tian, P., Wu, J., et al. (2020). Inhibition of miR-181a-5p reduces astrocyte and microglia activation and oxidative stress by activating SIRT1 in immature rats with epilepsy. *Lab. Invest.* 100, 1223–1237. doi: 10.1038/s41374-020-0444-1

Konovalova, J., Gerasymchuk, D., Parkkinen, I., Chmielarz, P., and Domanskyi, A. (2019). Interplay between MicroRNAs and Oxidative Stress in Neurodegenerative Diseases. *Int. J. Mol. Sci.* 20:6055. doi: 10.3390/ijms20236055

Korotkov, A., Broekaart, D. W. M., Banchaewa, L., Pustjens, B., Van Scheppingen, J., Anink, J. J., et al. (2020). microRNA-132 is overexpressed in glia in temporal lobe epilepsy and reduces the expression of pro-epileptogenic factors in human cultured astrocytes. *Glia* 68, 60–75. doi: 10.1002/glia.23700

Korotkov, A., Broekaart, D. W. M., Van Scheppingen, J., Anink, J. J., Baayen, J. C., Idema, S., et al. (2018). Increased expression of matrix metalloproteinase 3 can be attenuated by inhibition of microRNA-155 in cultured human astrocytes. *J. Neuroinflamm.* 15:211. doi: 10.1186/s12974-018-1245-y

Krol, J., Loedige, I., and Filipowicz, W. (2010). The widespread regulation of microRNA biogenesis, function and decay. *Nat. Rev. Genet.* 11, 597–610. doi: 10.1038/nrg2843

Leontariti, M., Avgeris, M., Katsarou, M. S., Drakoulis, N., Siatouni, A., Verentzioti, A., et al. (2020). Circulating miR-146a and miR-134 in predicting drug-resistant

epilepsy in patients with focal impaired awareness seizures. *Epilepsia* 61, 959–970. doi: 10.1111/epi.16502

Li, R., Wen, Y., Wu, B., He, M., Zhang, P., Zhang, Q., et al. (2020). MicroRNA-25-3p suppresses epileptiform discharges through inhibiting oxidative stress and apoptosis via targeting OXSR1 in neurons. *Biochem. Biophys. Res. Commun.* 523, 859–866. doi: 10.1016/j.bbrc.2020.01.050

Li, T. R., Jia, Y. J., Ma, C., Qiu, W. Y., Wang, Q., Shao, X. Q., et al. (2018). The role of the microRNA-146a/complement factor H/interleukin-1β-mediated inflammatory loop circuit in the perpetuate inflammation of chronic temporal lobe epilepsy. *Dis. Model Mech.* 11:dmm031708. doi: 10.1242/dmm.031708

Liu, D., Li, S., Gong, L., Yang, Y., Han, Y., Xie, M., et al. (2019). Suppression of microRNA-141 suppressed p53 to protect against neural apoptosis in epilepsy by SIRT1 expression. *J. Cell Biochem.* 120, 9409–9420. doi: 10.1002/jcb.28216

Liu, Q., Wang, L., Yan, G., Zhang, W., Huan, Z., and Li, J. (2019). MiR-125a-5p Alleviates Dysfunction and Inflammation of Pentylenetetrazol-induced Epilepsy Through Targeting Calmodulin-dependent Protein Kinase IV (CAMK4). *Curr. Neurovasc. Res.* 16, 365–372. doi: 10.2174/1567202616666190906125444

Lu, J., Zhou, N., Yang, P., Deng, L., and Liu, G. (2019). MicroRNA-27a-3p Downregulation Inhibits Inflammatory Response and Hippocampal Neuronal Cell Apoptosis by Upregulating Mitogen-Activated Protein Kinase 4 (MAP2K4) Expression in Epilepsy: In Vivo and In Vitro Studies. *Med. Sci. Monit.* 25, 8499–8508. doi: 10.12659/MSM.916458

Martins-Ferreira, R., Chaves, J., Carvalho, C., Bettencourt, A., Chorão, R., Freitas, J., et al. (2020). Circulating microRNAs as potential biomarkers for genetic generalized epilepsies: a three microRNA panel. *Eur. J. Neurol.* 27, 660–666. doi: 10.1111/ene.14129

McClelland, S., Flynn, C., Dubé, C., Richichi, C., Zha, Q., Ghestem, A., et al. (2011). Neuron-restrictive silencer factor-mediated hyperpolarization-activated cyclic nucleotide gated channelopathy in experimental temporal lobe epilepsy. *Ann. Neurol.* 70, 454–464. doi: 10.1002/ana.22479

McKiernan, R. C., Jimenez-Mateos, E. M., Sano, T., Bray, I., Stallings, R. L., Simon, R. P., et al. (2012). Expression profiling the microRNA response to epileptic preconditioning identifies miR-184 as a modulator of seizure-induced neuronal death. *Exp. Neurol.* 237, 346–354. doi: 10.1016/j.expneurol.2012.06.029

Miller-Delaney, S. F., Bryan, K., Das, S., Mckiernan, R. C., Bray, I. M., Reynolds, J. P., et al. (2015). Differential DNA methylation profiles of coding and non-coding genes define hippocampal sclerosis in human temporal lobe epilepsy. *Brain* 138, 616–631. doi: 10.1093/brain/awu373

Nudelman, A. S., Dirocco, D. P., Lambert, T. J., Garelick, M. G., Le, J., Nathanson, N. M., et al. (2010). Neuronal activity rapidly induces transcription of the CREB-regulated microRNA-132, in vivo. *Hippocampus* 20, 492–498. doi: 10.1002/hipo.20646

Peng, J., Omran, A., Ashhab, M. U., Kong, H., Gan, N., He, F., et al. (2013). Expression patterns of miR-124, miR-134, miR-132, and miR-21 in an immature rat model and children with mesial temporal lobe epilepsy. *J. Mol. Neurosci.* 50, 291–297. doi: 10.1007/s12031-013-9953-3

Pitkänen, A., Löscher, W., Vezzani, A., Becker, A. J., Simonato, M., Lukasiuk, K., et al. (2016). Advances in the development of biomarkers for epilepsy. *Lancet Neurol.* 15, 843–856. doi: 10.1016/S1474-4422(16)00112-5

Qi, Y., Qian, R., Jia, L., Fei, X., Zhang, D., Zhang, Y., et al. (2020). Overexpressed microRNA-494 represses RIPK1 to attenuate hippocampal neuron injury in epilepsy rats by inactivating the NF-κB signaling pathway. *Cell Cycle* 19, 1298–1313. doi: 10.1080/15384101.2020.1749472

Rana, A., and Musto, A. E. (2018). The role of inflammation in the development of epilepsy. *J. Neuroinflamm.* 15:144. doi: 10.1186/s12974-018-1192-7

Risbud, R. M., Lee, C., and Porter, B. E. (2011). Neurotrophin-3 mRNA a putative target of miR21 following status epilepticus. *Brain Res.* 1424, 53–59. doi: 10.1016/j.brainres.2011.09.039

Scott, H. L., Tamagnini, F., Narduzzo, K. E., Howarth, J. L., Lee, Y. B., Wong, L. F., et al. (2012). MicroRNA-132 regulates recognition memory and synaptic plasticity in the perirhinal cortex. *Eur. J. Neurosci.* 36, 2941–2948. doi: 10.1111/j.1460-9568.2012.08220.x

Shen, C. H., Zhang, Y. X., Zheng, Y., Yang, F., Hu, Y., Xu, S., et al. (2019). Expression of plasma microRNA-145-5p and its correlation with clinical features in patients with refractory epilepsy. *Epilepsy Res.* 154, 21–25. doi: 10.1016/j.eplepsyres.2019.04.010

Song, Y. J., Tian, X. B., Zhang, S., Zhang, Y. X., Li, X., Li, D., et al. (2011). Temporal lobe epilepsy induces differential expression of hippocampal miRNAs including let-7e and miR-23a/b. *Brain Res.* 1387, 134–140. doi: 10.1016/j.brainres.2011.02.073

Sun, J., Cheng, W., Liu, L., Tao, S., Xia, Z., Qi, L., et al. (2016). Identification of serum miRNAs differentially expressed in human epilepsy at seizure onset and post-seizure. *Mol. Med. Rep.* 14, 5318–5324. doi: 10.3892/mmr.2016.5906

Sun, Y., Wang, X., Wang, Z., Zhang, Y., Che, N., Luo, X., et al. (2016). Expression of microRNA-129-2-3p and microRNA-935 in plasma and brain tissue of human refractory epilepsy. *Epilepsy Res.* 127, 276–283. doi: 10.1016/j.eplepsyres.2016.09.016

Symonds, J. D., Zuberi, S. M., and Johnson, M. R. (2017). Advances in epilepsy gene discovery and implications for epilepsy diagnosis and treatment. *Curr. Opin. Neurol.* 30, 193–199. doi: 10.1097/WCO.0000000000000433

Tao, H., Zhao, J., Liu, T., Cai, Y., Zhou, X., Xing, H., et al. (2017). Intranasal Delivery of miR-146a Mimics Delayed Seizure Onset in the Lithium-Pilocarpine Mouse Model. *Mediat. Inflamm.* 2017:6512620. doi: 10.1155/2017/6512620

Tivnan, A., Tracey, L., Buckley, P. G., Alcock, L. C., Davidoff, A. M., and Stallings, R. L. (2011). MicroRNA-34a is a potent tumor suppressor molecule in vivo in neuroblastoma. *BMC Cancer* 11:33. doi: 10.1186/1471-2407-11-33

Uğurel, E., Şehitoğlu, E., Tüzün, E., Kürtüncü, M., Çoban, A., and Vural, B. (2016). Increased complexin-1 and decreased miR-185 expression levels in Behçet's disease with and without neurological involvement. *Neurol. Sci.* 37, 411–416. doi: 10.1007/s10072-015-2419-3

Vangoor, V. R., Reschke, C. R., Senthilkumar, K., Van De Haar, L. L., De Wit, M., Giuliani, G., et al. (2019). Antagonizing Increased miR-135a Levels at the Chronic Stage of Experimental TLE Reduces Spontaneous Recurrent Seizures. *J. Neurosci.* 39, 5064–5079. doi: 10.1523/JNEUROSCI.3014-18.2019

Vezzani, A., Balosso, S., and Ravizza, T. (2019). Neuroinflammatory pathways as treatment targets and biomarkers in epilepsy. *Nat. Rev. Neurol.* 15, 459–472. doi: 10.1038/s41582-019-0217-x

Vezzani, A., French, J., Bartfai, T., and Baram, T. Z. (2011). The role of inflammation in epilepsy. *Nat. Rev. Neurol.* 7, 31–40. doi: 10.1038/nrneurol.2010.178

Vezzani, A., Fujinami, R. S., White, H. S., Preux, P. M., Blümcke, I., Sander, J. W., et al. (2016). Infections, inflammation and epilepsy. *Acta Neuropathol.* 131, 211–234. doi: 10.1007/s00401-015-1481-5

Vezzani, A., Ravizza, T., Balosso, S., and Aronica, E. (2008). Glia as a source of cytokines: implications for neuronal excitability and survival. *Epilepsia* 49(Suppl. 2), 24–32. doi: 10.1111/j.1528-1167.2008.01490.x

Wan, G., Xie, W., Liu, Z., Xu, W., Lao, Y., Huang, N., et al. (2014). Hypoxia-induced MIR155 is a potent autophagy inducer by targeting multiple players in the MTOR pathway. *Autophagy* 10, 70–79. doi: 10.4161/auto.26534

Wang, J., Tan, L., Tan, L., Tian, Y., Ma, J., Tan, C. C., et al. (2015a). Circulating microRNAs are promising novel biomarkers for drug-resistant epilepsy. *Sci. Rep.* 5:10201. doi: 10.1038/srep10201

Wang, J., Yu, J. T., Tan, L., Tian, Y., Ma, J., Tan, C. C., et al. (2015b). Genome-wide circulating microRNA expression profiling indicates biomarkers for epilepsy. *Sci. Rep.* 5:9522. doi: 10.1038/srep09522

Wang, K., Bei, W. J., Liu, Y. H., Li, H. L., Chen, S. Q., Lin, K. Y., et al. (2017). miR-21 attenuates contrast-induced renal cell apoptosis by targeting PDCD4. *Mol. Med. Rep.* 16, 6757–6763. doi: 10.3892/mmr.2017.7426

Wang, L., Song, L. F., Chen, X. Y., Ma, Y. L., Suo, J. F., Shi, J. H., et al. (2019). MiR-181b inhibits P38/JNK signaling pathway to attenuate autophagy and apoptosis in juvenile rats with kainic acid-induced epilepsy via targeting TLR4. *CNS Neurosci. Ther.* 25, 112–122. doi: 10.1111/cns.12991

Wang, T., Cai, Z., Hong, G., Zheng, G., Huang, Y., Zhang, S., et al. (2017). MicroRNA-21 increases cell viability and suppresses cellular apoptosis in non-small cell lung cancer by regulating the PI3K/Akt signaling pathway. *Mol. Med. Rep.* 16, 6506–6511. doi: 10.3892/mmr.2017.7440

Wang, W., Guo, Y., He, L., Chen, C., Luo, J., Ma, Y., et al. (2018). Overexpression of miRNA-137 in the brain suppresses seizure activity and neuronal excitability: A new potential therapeutic strategy for epilepsy. *Neuropharmacology* 138, 170–181. doi: 10.1016/j.neuropharm.2018.06.010

Wang, W., Wang, X., Chen, L., Zhang, Y., Xu, Z., Liu, J., et al. (2016). The microRNA miR-124 suppresses seizure activity and regulates CREB1 activity. *Expert Rev. Mol. Med.* 18:e4. doi: 10.1017/erm.2016.3

Wang, X., Sun, Y., Tan, Z., Che, N., Ji, A., Luo, X., et al. (2016). Serum MicroRNA-4521 is a Potential Biomarker for Focal Cortical Dysplasia with Refractory Epilepsy. *Neurochem. Res.* 41, 905–912. doi: 10.1007/s11064-015-1773-0

Wang, X., Yin, F., Li, L., Kong, H., You, B., Zhang, W., et al. (2018). Intracerebroventricular injection of miR-146a relieves seizures in an immature rat model of lithium-pilocarpine induced status epilepticus. *Epilepsy Res.* 139, 14–19. doi: 10.1016/j.eplepsyres.2017.10.006

Wayman, G. A., Davare, M., Ando, H., Fortin, D., Varlamova, O., Cheng, H. Y., et al. (2008). An activity-regulated microRNA controls dendritic plasticity by down-regulating p250GAP. *Proc. Natl. Acad. Sci. U S A.* 105, 9093–9098. doi: 10.1073/pnas.0803072105

Wen, X., Han, X. R., Wang, Y. J., Wang, S., Shen, M., Zhang, Z. F., et al. (2018). MicroRNA-421 suppresses the apoptosis and autophagy of hippocampal neurons in epilepsy mice model by inhibition of the TLR/MYD88 pathway. *J. Cell Physiol.* 233, 7022–7034. doi: 10.1002/jcp.26498

Weng, N., Sun, J., Kuang, S., Lan, H., He, Q., Yang, H., et al. (2020). MicroRNA-451 Aggravates Kainic Acid-induced Seizure and Neuronal Apoptosis by Targeting GDNF. *Curr. Neurovasc. Res.* 17, 50–57. doi: 10.2174/1567202617666191223150510

Winter, J., Jung, S., Keller, S., Gregory, R. I., and Diederichs, S. (2009). Many roads to maturity: microRNA biogenesis pathways and their regulation. *Nat. Cell Biol.* 11, 228–234. doi: 10.1038/ncb0309-228

Wu, D. M., Zhang, Y. T., Lu, J., and Zheng, Y. L. (2018). Effects of microRNA-129 and its target gene c-Fos on proliferation and apoptosis of hippocampal neurons in rats with epilepsy via the MAPK signaling pathway. *J. Cell Physiol.* 233, 6632–6643. doi: 10.1002/jcp.26297

Xiang, L., Ren, Y., Cai, H., Zhao, W., and Song, Y. (2015). MicroRNA-132 aggravates epileptiform discharges via suppression of BDNF/TrkB signaling in cultured hippocampal neurons. *Brain Res.* 1622, 484–495. doi: 10.1016/j.brainres.2015.06.046

Xiang, L., Ren, Y., Li, X., Zhao, W., and Song, Y. (2016). MicroRNA-204 suppresses epileptiform discharges through regulating TrkB-ERK1/2-CREB signaling in cultured hippocampal neurons. *Brain Res.* 1639, 99–107. doi: 10.1016/j.brainres.2016.02.045

Yang, Y., Shu, X., Liu, D., Shang, Y., Wu, Y., Pei, L., et al. (2012). EPAC null mutation impairs learning and social interactions via aberrant regulation of miR-124 and Zif268 translation. *Neuron* 73, 774–788. doi: 10.1016/j.neuron.2012.02.003

Yeom, K. H., Lee, Y., Han, J., Suh, M. R., and Kim, V. N. (2006). Characterization of DGCR8/Pasha, the essential cofactor for Drosha in primary miRNA processing. *Nucleic Acids Res.* 34, 4622–4629. doi: 10.1093/nar/gkl458

Yuan, J., Huang, H., Zhou, X., Liu, X., Ou, S., Xu, T., et al. (2016). MicroRNA-132 Interact with p250GAP/Cdc42 Pathway in the Hippocampal Neuronal Culture Model of Acquired Epilepsy and Associated with Epileptogenesis Process. *Neural. Plast.* 2016:5108489. doi: 10.1155/2016/5108489

Zeng, Y., Yi, R., and Cullen, B. R. (2005). Recognition and cleavage of primary microRNA precursors by the nuclear processing enzyme Drosha. *EMBO J.* 24, 138–148. doi: 10.1038/sj.emboj.7600491

Zhang, B., Pan, X., Cobb, G. P., and Anderson, T. A. (2006). Plant microRNA: a small regulatory molecule with big impact. *Dev. Biol.* 289, 3–16. doi: 10.1016/j.ydbio.2005.10.036

Zhang, H., Qu, Y., and Wang, A. (2018). Antagonist targeting microRNA-146a protects against lithium-pilocarpine-induced status epilepticus in rats by nuclear factor-κB pathway. *Mol. Med. Rep.* 17, 5356–5361. doi: 10.3892/mmr.2018.8465

Zheng, H., Tang, R., Yao, Y., Ji, Z., Cao, Y., Liu, Z., et al. (2016). MiR-219 Protects Against Seizure in the Kainic Acid Model of Epilepsy. *Mol. Neurobiol.* 53, 1–7. doi: 10.1007/s12035-014-8981-5

Zheng, P., Bin, H., and Chen, W. (2019). Inhibition of microRNA-103a inhibits the activation of astrocytes in hippocampus tissues and improves the pathological injury of neurons of epilepsy rats by regulating BDNF. *Cancer Cell Int.* 19:109. doi: 10.1186/s12935-019-0821-2

Zhou, H., Wang, N., Xu, L., Huang, H., and Yu, C. (2017). The efficacy of gastrodin in combination with folate and vitamin B12 on patients with epilepsy after stroke and its effect on HMGB-1. IL-2 and IL-6 serum levels. *Exp. Ther. Med.* 14, 4801–4806. doi: 10.3892/etm.2017.5116

Zhu, X., Zhang, A., Dong, J., Yao, Y., Zhu, M., Xu, K., et al. (2019). MicroRNA-23a contributes to hippocampal neuronal injuries and spatial memory impairment in an experimental model of temporal lobe epilepsy. *Brain Res. Bull.* 152, 175–183. doi: 10.1016/j.brainresbull.2019.07.021

Conflict of Interest: The authors declare that the research was conducted in the absence of any commercial or financial relationships that could be construed as a potential conflict of interest.

frontiers in Molecular Neuroscience

ORIGINAL RESEARCH
published: 30 March 2021
doi: 10.3389/fnmol.2021.643763

Spatiotemporal Correlation of Epileptiform Activity and Gene Expression *in vitro*

Sophie Schlabitz[1], Laura Monni[1], Alienor Ragot[1], Matthias Dipper-Wawra[1], Julia Onken[2], Martin Holtkamp[1,3] and Pawel Fidzinski[1,3,4]*

[1] Charité – Universitätsmedizin Berlin, Corporate Member of Freie Universität Berlin, Humboldt-Universität zu Berlin, and Berlin Institute of Health, Department of Neurology with Experimental Neurology, Clinical and Experimental Epileptology, Berlin, Germany, [2] Charité – Universitätsmedizin Berlin, Corporate Member of Freie Universität Berlin, Humboldt-Universität zu Berlin, and Berlin Institute of Health, Department of Neurosurgery, Berlin, Germany, [3] Epilepsy-Center Berlin-Brandenburg, Institute for Diagnostics of Epilepsy, Berlin, Germany, [4] Charité – Universitätsmedizin Berlin, Corporate Member of Freie Universität Berlin, Humboldt-Universität zu Berlin, and Berlin Institute of Health, NeuroCure Cluster of Excellence, Neuroscience Research Center, Berlin, Germany

Epileptiform activity alters gene expression in the central nervous system, a phenomenon that has been studied extensively in animal models. Here, we asked whether also *in vitro* models of seizures are in principle suitable to investigate changes in gene expression due to epileptiform activity and tested this hypothesis mainly in rodent and additionally in some human brain slices. We focused on three genes relevant for seizures and epilepsy: FOS proto-oncogene (*c-Fos*), inducible cAMP early repressor (*Icer*) and mammalian target of rapamycin (*mTor*). Seizure-like events (SLEs) were induced by 4-aminopyridine (4-AP) in rat entorhinal-hippocampal slices and by 4-AP/8 mM potassium in human temporal lobe slices obtained from surgical treatment of epilepsy. SLEs were monitored simultaneously by extracellular field potentials and intrinsic optical signals (IOS) for 1–4 h, mRNA expression was quantified by real time PCR. In rat slices, both duration of SLE exposure and SLE onset region were associated with increased expression of *c-Fos* and *Icer* while no such association was shown for *mTor* expression. Similar to rat slices, *c-FOS* induction in human tissue was increased in slices with epileptiform activity. Our results indicate that irrespective of limitations imposed by *ex vivo* conditions, *in vitro* models represent a suitable tool to investigate gene expression. Our finding is of relevance for the investigation of human tissue that can only be performed *ex vivo*. Specifically, it presents an important prerequisite for future studies on transcriptome-wide and cell-specific changes in human tissue with the goal to reveal novel candidates involved in the pathophysiology of epilepsy and possibly other CNS pathologies.

Keywords: epileptiform activity *in vitro*, 4-aminopyridine, intrinsic optical signals, gene expression, *c-Fos*, *Icer*, *mTor*, cell death

OPEN ACCESS

Edited by:
Hermona Soreq,
Hebrew University of Jerusalem, Israel

Reviewed by:
Nibha Mishra,
Takeda Oncology, United States
Logan James Voss,
Waikato District Health Board, New Zealand

****Correspondence:***
Sophie Schlabitz
sophie.schlabitz@charite.de

Received: *18 December 2020*
Accepted: *03 March 2021*
Published: *30 March 2021*

Citation:
Schlabitz S, Monni L, Ragot A, Dipper-Wawra M, Onken J, Holtkamp M and Fidzinski P (2021) Spatiotemporal Correlation of Epileptiform Activity and Gene Expression in vitro. Front. Mol. Neurosci. 14:643763. doi: 10.3389/fnmol.2021.643763

INTRODUCTION

According to the World Health Organization, diseases of the central nervous system represent a major health risk for the world population (World Health Organization, 2006). To address this risk appropriately and to pursue new therapeutic options, it is critical to understand diverse and often complex molecular mechanisms leading to pathology. For decades, basic research in neurobiology together with disease-specific animal models served as a framework to understand fundamental mechanisms of neurological disorders. This effort led to many useful insights, however, the translational and predictive value of animal models has remained limited (Löscher, 2017). In recent years, this gap between animal models and clinical application has received increasing attention. Consequently, more effort has been put into models that reflect the clinical setting more closely and into novel strategies to increase reproducibility in basic research, aiming for improvement of translation (Bauer et al., 2017).

One of the possibilities to bridge differences between animal models and clinical neurology is to use human tissue-derived *ex vivo* models and to investigate functional disease mechanisms in a species-specific manner. So far, the approaches include the use of resected specimen from brain surgery procedures, investigation of post mortem tissue (Verwer et al., 2002) and the recently evolving field of brain organoids (Di Lullo and Kriegstein, 2017). With the exception of brain organoids, functional investigation of human-derived CNS tissue is constrained by the naturally limited life span of *ex vivo* samples. The recent development of organotypic cultures is a promising advance to overcome this conundrum, however, as of now it still poses challenges associated with low reproducibility and large protocol variety (Jones et al., 2016). According to a recent study on disease burden (GBD 2015 Neurological Disorders Collaborator Group, 2017), epilepsy constitutes one of the most common neurological diseases with a prevalence between 0.5 and 1.0% in the developed world (Fiest et al., 2017). Up to one third of individuals afflicted with epilepsy suffer from pharmacoresistance (Chen et al., 2018). Although numerous *in vivo* and *in vitro* animal models established throughout the years increased our knowledge about disease mechanisms, many questions including how to address pharmacoresistance remain unanswered (Becker, 2018). Recent technological advances in the field of transcriptomics and single cell analysis (Becker et al., 2002; Guelfi et al., 2019) made it possible to discover novel disease-specific genetic alterations in epilepsy. Importantly, these findings include not only monogenetic mutations as singular causative factors. Also, seizure-related modulation of gene expression and gene editing as well as epigenetic modulation during epileptogenesis have been reported (Kobow and Blümcke, 2018).

Modulation of gene expression is mostly studied *in vivo*. However, for obvious reasons such approach is not possible in human tissue – in this case only *ex vivo* studies on resected tissue would be possible. To our knowledge, it is not known whether or to what degree *in vitro* models can recapitulate changes in gene expression observed under *in vivo* conditions. Here, in a proof-of-principle study, we aimed to assess the general, species-independent suitability of *in vitro* models of acute seizures to investigate changes in gene expression due to epileptiform activity. In a first step in that direction, we aimed to test our hypothesis mainly in rat tissue, for which modulation of gene expression due to epileptiform activity has been studied *in vivo* before. In addition, we extended our studies to some human slices. We focused on three genes relevant for seizures and epilepsy: FOS proto-oncogene (*c-Fos*), inducible cAMP early repressor (*Icer*), and mammalian target of rapamycin (*mTor*). Expression of these genes and/or the involved pathways has been described before to be positively modulated by seizure activity and, in case of *Icer* and *mTor*, also to be involved in epileptogenesis (Lund et al., 2008; Porter et al., 2008; Szyndler et al., 2009; Zeng et al., 2009; Huang et al., 2010; Barros et al., 2015).

MATERIALS AND METHODS

Rat Slice Preparation

All animal procedures were conducted according to the German Animal Welfare Act as well as the European Directive 2010/63/EU for animal experiments and were approved by the Institutional Animal Welfare Officer and the responsible local authority (Landesamt für Gesundheit und Soziales, Berlin, Germany, T0336/12). Institutional security procedures were followed. Experiments were performed using combined hippocampal-entorhinal cortex (EC) slices from rats as previously reported (Heuzeroth et al., 2019) with some modifications. The study design is represented in **Figure 1**. Briefly, adult male Wistar-Han rats (220–240 g) were deeply anesthetized by inhalation of isoflurane (4% in 100% O_2) and then decapitated. Their brains were rapidly removed and placed into ice-cold N-methyl-D-glucamine (NMDG) containing artificial cerebrospinal fluid (NMDG-aCSF) (Ting et al., 2014). Equimolar replacement of sodium by NMDG leads to decreased permeation of ions via neuronal membranes and subsequent reduced cell swelling (Hille, 1971). Carbogenated NMDG-aCSF (95% O_2, 5% CO_2) contained (in mM): NMDG (93), KCl (2.5), NaH_2PO_4 (1.2), $NaHCO_3$ (30), $MgSO_4$ (10), $CaCl_2$ (0.5), glucose (25), HEPES (20), sodium l-ascorbate (5), thiourea (2), and sodium pyruvate (3). Horizontal slices (400 μm) enclosing the hippocampal formation (H), the entorhinal cortex (EC), and adjacent parts of the temporal cortex (TC) were cut using a vibratome (Vibroslicer VT1200S, Leica, Wetzlar, Germany). From each rat brain, 15 slices were collected and assigned in an alternating manner to three groups, five slices each: (1) basal group to determine initial gene expression; (2) control group to investigate effects of slicing and storage; and (3) intervention group in which epileptiform activity was induced. Slices of the control and intervention group were individually placed in an interface chamber and continuously perfused (1.5–2.0 ml/min) with prewarmed (35°C) and carbogenated aCSF (95% O_2, 5% CO_2, pH 7.4), containing (in mM): NaCl (129), KCl (3), NaH_2PO_4 (1.25), $NaHCO_3$ (21), $MgSO_4$ (1.8), $CaCl_2$ (1.6), and glucose (10). During storage and experiments, warmed, humified carbogen was directed over the slice surface. All slices were

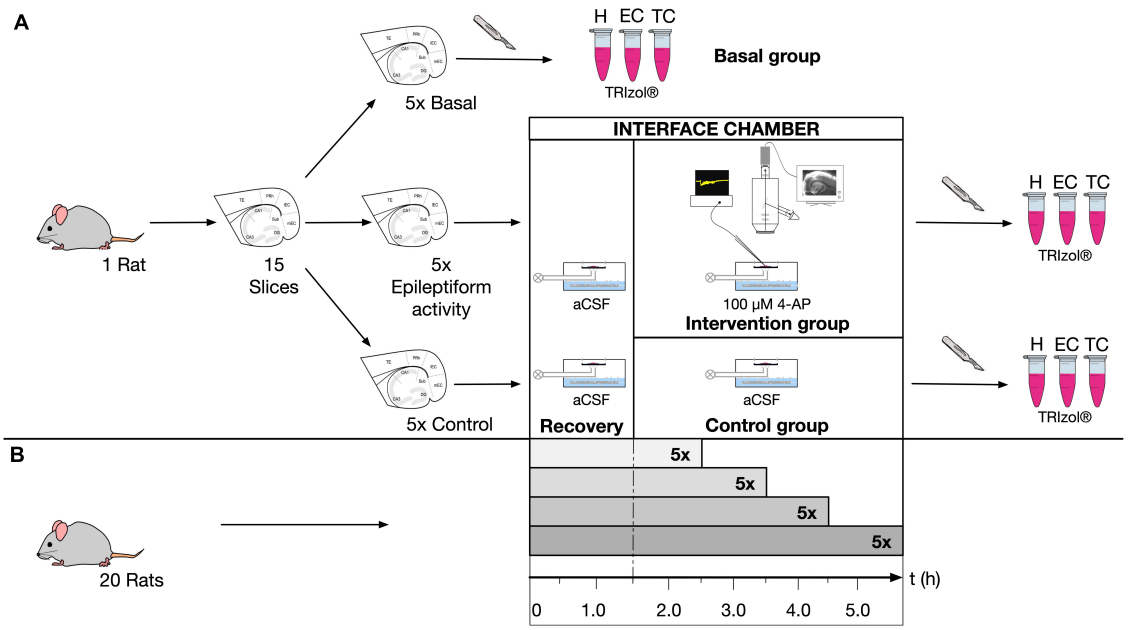

FIGURE 1 | Study design for rat tissue. **(A)** Chronological sequence of each experiment: rat brain preparation; allocation of 15 horizontal slices to three different groups (basal, control and intervention); recovery of 10 slices (control and intervention group) for 1.5 h in an interface chamber with incubation in carbogenated aCSF (95% O_2, 5% CO_2, pH 7.4); induction of epileptiform activity by 100 µM 4-AP in five slices (intervention group) and recording of field potentials as well as intrinsic optical signals; five control slices in aCSF for same amount of time; microdissection of slices into hippocampus (H), entorhinal cortex (EC), and temporal cortex (TC) and subsequent cell lysis of pooled tissue in TRIzol before RT-qPCR. **(B)** Procedure was performed with 20 rats in total; five rats were assigned to each 4-AP treatment duration of 1, 2, 3, or 4 h.

allowed to recover 1.5 h after preparation. In the intervention group, seizure-like events (SLEs) were induced by 100 µM 4-aminopyridine (4-AP, Sigma, Munich, Germany), which non-selectively blocks voltage-dependent potassium channels, augments presynaptic calcium influx (Mathie et al., 1998) and enhances synaptic transmission (Perreault and Avoli, 1991). *In vitro* addition of 4-AP to aCSF results in long lasting ictal-like discharges considered as correspondent to focal to bilateral seizures *in vivo* (Avoli et al., 2002). The intervention group was treated with 4-AP for either 1, 2, 3, or 4 h, while the control slices remained in aCSF for the same amount of time. This procedure was performed with 20 rats in total and five rats were assigned to each treatment duration.

Human Slice Preparation

Brain temporal lobe tissue was obtained from surgical treatment of epilepsy in five female donor patients (age at resection: 21–58 years) diagnosed with mesial temporal lobe epilepsy (mTLE). The experimental protocol was approved by the local Ethics Committee (EA2/111/14) in agreement with the Declaration of Helsinki. Written informed consent was given by all patients before surgery. Cortex specimens were collected in the operating room, immediately immersed in cold (∼4°C) carbogenated NMDG-aCSF (95% O_2, 5% CO_2). The same solution was used for transportation and tissue processing, which took in total up to 2 h. 400 µm-thick slices were then sectioned and assigned as basal, control and intervention as described above. Before start of experiments, slices recovered in standard aCSF for 5 h. After the stabilization period, on average three slices per patient were further incubated for the duration of 4 h in standard aCSF (control) or with aCSF containing 8 mM potassium and 100 µM 4-AP (pH 7.4) (intervention) to examine the effects of slicing and storage and epileptiform activity on gene expression, respectively. In human brain slices, the application of neither 4-AP alone nor 10 or 12 mM potassium is sufficient to induce epileptiform activity (Gabriel et al., 2004). Therefore, SLEs were evoked by applying a combination of high potassium (8 mM) and 4-AP (100 µM), while adjusting the increased osmolarity of aCSF by lowering the concentration of NaCl from 129 to 124 mM (Kraus et al., 2019).

Electrophysiological and Optical Recordings

Epileptiform activity was monitored by local field potential recordings in 20 selected slices of the intervention group (one slice per rat and three slices per human sample). To control for the influence of the slice position, rat slices were classified to different locations along the dorsoventral axis defined as ventral (−7.6 to −6.8 mm ventrally from bregma), medial (−6.4 to −5.6 mm), and dorsal (−5.2 to −4.4 mm) (see also Paxinos and Watson, 1998). Extracellular field potentials were measured with glass electrodes (filled with 150 mM NaCl, electrode resistance 1–2 MΩ). In rats, one electrode was placed in layer IV or V of the lateral EC, the second electrode was positioned in the stratum pyramidale of the hippocampal CA1 region. In

human tissue, SLEs were recorded for at least 40 min with one electrode placed on the superficial cortical layers of human slices (layers II/III, 200–700 μm from pial surface) (Köhling and Avoli, 2006). Electrophysiological signals were acquired with a custom-made amplifier (10×) connected to an A/D interface (Micro 1401 mk II, Cambridge Electronic Design Limited, Cambridge, United Kingdom). Data were recorded with Spike2 and Signal (versions 7.00 and 3.07, respectively, Cambridge Electronic Design Limited, Cambridge, United Kingdom) and analyzed using custom-written algorithms in MATLAB (R2014b, MathWorks, Natick, MA, United States). SLEs were identified using the following criteria: (1) field potential decrease > 0.3 mV, (2) duration of field potential shift > 10 s and (3) superimposition by ripple-like discharges during negative field potential shift.

Intrinsic optical imaging was employed in each electrophysiologically recorded slice according to previous reports (Weissinger et al., 2017). In brief, slices were positioned on a transparent membrane (0.4 μm Millicell culture plate inserts, Millipore, Bedford MA, United States) and homogeneously illuminated from below by a halogen cold light source (KL 1500, Schott, Wiesbaden, Germany) and a curved glass rod (Ø 8 mm). Images were received using an upright binocular microscope (MS 5, Leica, Bensheim, Germany) with a 4× objective, a monocular phototube (Leica, Bensheim, Germany) and a CCD camera (8 bit, Sanyo, Osaka, Japan). In-house macros for ImageJ 1.51m9 (Wayne Rasband National Institutes of Health, United States) and MATLAB software were applied for the processing of the images. 8-bit video signals were converted at a 10 MHz ratio into 320 × 240-pixel images employing a frame-grabber board (pciGrabber-4plus, Phytec, Mainz, Germany). Images were only saved when triggered by the experimenter in case ictal activity became apparent in the electrophysiological recording. Using a circular data buffer, the first image was captured 5–10 s before the onset of the SLE, the recording continued for 50–180 s depending on the duration of the electrophysiologically recorded ictal event. The time course of light transmittance was calculated for each SLE as difference in light transmittance (ΔT) between a given image and the control image (mean of the first 20 images in each series recorded before start of ictal activity), and expressed as percentage of the control image transmittance ($\Delta T/T$). During ictal events, $\Delta T/T$ typically ranged from 1.0 to 7.5% whereas background noise never exceeded 1.0%. The amplitude during SLEs is expressed as max($\Delta T/T$). Optical imaging also enabled us to detect spreading depolarizations (SDs) associated with decreased light transmittance (Müller and Somjen, 1999). In regions displaying SD, ΔT/T decreased in the range of −1.0 to −9.2%. Changes of light transmittance over time provided insight into onset, direction and evolution of both ictal activity and SDs in the entire slice. Using squared regions of interests (ROI) sized 20 × 20 pixels each, the optical signal was quantified separately for the anatomical regions (H, EC, and TC) assigned to later gene expression analysis. Optical signals were considered significantly associated with a SLE when the increase of light transmittance was above a threshold of >1.0% and with a SD when the decrease of light transmittance was <−1.0%. The onset of SLE activity was determined by the first region where transmittance increase above threshold was observed. For calculation of the SLE area, every pixel within a given anatomical region that reached at least 1% ΔT/T in > 9 subsequent images during one SLE was considered to be involved in this SLE. The SLE area was calculated for each region separately and expressed as percentage of the total area for a given anatomical region.

RNA Extraction and Reverse Transcription

All investigated rat slices were microdissected into H, EC and TC in order to separately quantify mRNA levels within these brain areas. In human cortical slices, microdissection was aimed to separate the seizure onset region (named "onset site" group) determined by electrophysiology and optical imaging from the rest of the slice (named "rest" group). Basal slices were snap frozen in liquid nitrogen and stored at −80°C immediately after preparation while slices from the intervention and control groups were frozen immediately after the assigned experimental time period (1–4 h in rat and 4 h in human slices). To obtain sufficient amounts of mRNA, tissue from different slices within one experiment but the same anatomical region and group was pooled. Pooled tissue was lyzed in 1 ml TRIzol (Invitrogen AG, Carlsbad, United States). Tissue homogenization and cell lysis were facilitated by highspeed shaking (50 Hz) with stainless steel beads for 10 min (TissueLyser LT, Qiagen N.V., Venlo, Netherlands). Based on the acid guanudinium thiocyanate-phenol-chloroform extraction method, chloroform (200 μl) was added to the sample to isolate RNA (Chomczynski and Sacchi, 1987). Phase separation was conducted by centrifugation (15 min at 12,000 × *g* and 4°C) and subsequent precipitation of RNA by incubation with 500 μl isopropanol for 10 min and 3.5 μl Recombinant RNasin Ribonuclease Inhibitor (Promega, Fitchburg, WI, United States) resuspended RNA in 25.0 μl nuclease-free water. Additional RNA purification was accomplished by refilling the remaining volume to 200 μl and adding an equal volume of Roti-Phenol/Chloroform/Isoamyl alcohol (Carl Roth, Karlsruhe, Germany). Following short-time centrifugation (5 min), the RNA containing aqueous phase was treated with 200 μl chloroform to remove residual phenol from the solution. RNA was then recovered by overnight precipitation with 550 μl ethanol (96%) and 6 μl ammonium acetate (10 M) at −20°C and dissolved in 16 μl nuclease-free water. Concentration of total RNA was determined by measuring the optical density at 260 nm with NanoDrop 2000 Spectrophotometer (Thermo Fisher Scientific Inc., Waltham, MA, United States) and ranged from 143.5 to 738.5 ng/μl per rat sample and from 71.4 to 2,224.2 ng/μl per human sample. Purity was checked using the 260/230 nm as well as the 260/280 nm ratios (accepted values > 1.8). First strand cDNA synthesis was carried out using moloney murine leukemia virus reverse transcriptase (M-MLV RT, Promega, Fitchburg, WI, United States) according to the manufacturer's instructions with several modifications. In brief, a mixture of 15.0 μl diluted, purified RNA (2.0 μg for rat sample, 0.5 μg for human sample), 1.5 μl random hexamers (100 μM, Roche, Basel, Switzerland) and 1.5 μl dNTPs (10 mM each, Roche, Basel, Switzerland) was incubated at 65°C for 5 min. The

mixture was then assembled with a prepared reaction volume, consisting of: 2.0 µl M-MLV-RT (200 U/µl), 5.0 µl M-MLV RT Reaction Buffer (Promega, Fitchburg, WI, United States), 0.5 µl Recombinant RNasin Ribonuclease Inhibitor (40 U/µl) and 0.5 µl DTT (100 mM, Promega, Fitchburg, WI, United States). Reverse transcription mixture was successively incubated as follows: 5 min at 21°C, 60 min at 37°C, 15 min at 70°C. To assess genomic DNA contamination in the RNA preparation, a minus RT-control was included in each quantitative reverse transcription PCR (RT-qPCR) experiment. cDNA samples were stored at −20°C until further analysis.

Primer Design and Efficiency

Quantitative PCR (qPCR) primer design was based on mRNA sequences from the RefSeq database[1]. Specificity was verified using the Primer-BLAST program[2]. Primers were synthesized by EUROFINS genomics (Ebersberg, Germany). In addition to electrophoresis in 1% agarose gel, PCR products were also verified by sanger sequencing (EUROFINS). In case of rat *c-Fos*, sequences were adapted from published data (Barros et al., 2015), while in case of the human *c-FOS*, the primer pair was designed *de novo* using Primer-Blast. The *Icer* primers amplificated two of three possible transcript variants of CREM (2, 5). The optimal annealing temperature, the amplification efficiency and R^2 of the standard curve were determined for each primer pair (**Table 1**) and calculated as follow. PCR efficiency of each primer pair was evaluated by performing a dilution series of the target assay and standard curve analysis of the *Cq* data points using MS excel. The slope of the standard curve ($E = [10^{(-1/m)}] - 1$ with E = amplification efficiency, m = slope) was used to calculate the amplification efficiency, which ranged from 0.88 to 1.

NormFinder Analysis

The NormFinder algorithm was used to assess expression stability in a set of candidate genes and to identify the most suitable reference gene for RT-qPCR analysis (Andersen et al., 2004). For rat tissue, five candidate reference genes were selected based on literature: beta-actin (*Actb*), tyrosine 3-monooxygenase/tryptophan 5-monooxygenase activation protein (*Ywhaz*), hypoxanthine phosphoribosyltransferase 1 (*Hprt1*), receptor expression-enhancing protein 5 (*Reep5*), and TATA box binding protein (*Tbp*) (Sadangi et al., 2017). NormFinder analysis was separately performed for the three anatomical ROI (H, EC, and TC). To consider all experimental conditions, gene expression was determined in two independent samples of the following nine groups: basal; control 1, 2, 3, and 4 h; 4-AP 1, 2, 3, and 4 h. For human tissue, three candidate genes were selected: *ACTB*, *TBP* and ribosomal protein L13A (*RPL13A*) (Vandesompele et al., 2002; Rydbirk et al., 2016). NormFinder analysis was performed considering all four experimental conditions and examined in two independent samples of the following groups: basal, control, onset site and rest. NormFinder MS Excel application was used to calculate both the intra- and intergroup variation expressed as standard deviation. Candidate genes with a standard deviation > 0.25 were excluded from the subsequent determination of gene stability value, the remaining candidate genes were ranked according to their gene stability value with increasing values implying less stability.

Quantitative PCR

Quantitative PCR was conducted using the LightCycler 480 II (Roche Diagnostics International AG, Rotkreuz, Switzerland). The reaction assay contained 10 µl LightCycler 480 SYBR Green I Master (Roche Diagnostics International AG, Rotkreuz, Switzerland), 1 µl of forward and reverse primers (0.5 µM each), 1 µl of template cDNA and was diluted by 8 µl H_2O to a final volume of 20 µl. In the case of primer pairs of the human genes, the quantities of forward and reverse primers were lowered to 0.6 µl (0.3 µM each) for *c-FOS* and 0.4 µl (0.2 µM each) for *ACTB* and *RPL13A*, in order to improve their amplification efficiency. All assays included a minus RT-control to verify previous DNase digestion as well as a negative control without cDNA (NTC), to reveal any non-specific amplification, and were replicated twice. Each PCR reaction was pre-incubated at 95°C for 10 min followed by 45 amplification cycles with the following sequence: melting at 95°C for 5 s, annealing at a primer specific temperature for 10 s, elongation at 72°C for 15 s and quantification at a primer specific temperature for 1 s. After the amplification, melt curve analysis was run with the following sequence: denaturation at 95°C for 30 s, annealing at 70°C for 30 s, followed by the acquisition increasing the temperature to 95°C at a transition rate of 0.11°C/s in continuous mode. Relative quantification of mRNA levels was done using the efficiency-adjusted "delta-delta Ct method" (Pfaffl, 2001). According to this approach, we calculated fold induction of our selected genes relative to basal gene expression:

$$Ratio\left(\frac{GOI}{RG}\right) = \frac{E_{GOI}^{\triangle Cq_{GOI}(mean\ of\ basal\ Cq-x)}}{E_{RG}^{\triangle Cq_{RG}(mean\ of\ basal\ Cq-y)}}$$

with GOI = gene of interest, RG = reference gene, E = amplification efficiency, Cq = quantification cycle, x = individual Cq of gene of interest, y = individual Cq of reference gene.

To determine the actual effect of 4-AP induced epileptiform activity on gene expression, the ratio of 4-AP to control was calculated.

Cell Death Assay

To evaluate the spatiotemporal profile of slice viability, we performed fluorescent staining with propidium iodide (PI), an indicator of cell death (Buskila et al., 2014). 41 brain slices were taken from three rats and alternatingly assigned to the following groups: basal, control 1 h, control 4 h, 4-AP 1 h and 4-AP 4 h. At the end of each experiment, slices were exposed to PI (1 µg/ml) in carbogenated aCSF for 1 h. In 4-AP treated slices, 4-AP (100 µM) was also added to the staining solution. Following PI staining, slices were fixed by paraformaldehyde (4%) in phosphate buffered saline (0.2 M) for 30 min and subsequently incubated in DAPI (2 µg/ml) for 10 min. Images were acquired using an inverted

[1] www.ncbi.nlm.nih.gov

[2] www.ncbi.nlm.nih.gov/tools/primer-blast/index.cgi

TABLE 1 | Genes and corresponding oligonucleotide primer sequences for qPCR.

Gene	Species	Transcript variants	GenBank reference	5′-3′sequence	Amplicon length (bp)	PCR efficiency (%)	R^2	Annealing temperature (°C)	Quantification temperature (°C)	C_q of NTC
c-Fos	rat		NM_022197	F - ACGGAGAATCCGAAGGGAAAGGAA R - TCTGCAACGCAGACTTCTCGTCTT	125	88	0.9988	62	80	ND
Icer	rat	2 5 6	NM_017334 NM_001271102 NM_001271245	F - CTTTATTTTGGACTGTGGTACGGC R - AGTAGGAGCTCGGATCTGGTAA	161 125 207	100	0.991	61	79	40.00
mTor	rat		NM_019906	F - CGGAGAGAGGCCATCCGAGT R - ACGGCGGGGTAGAACTCGTC	209	100	0.9966	64	82	36.91
Ywhaz	rat		NM_013011	F - TTGAGCAGAAGACGGAAGGT R - GAAGCATTGGGGATCAAGAA	135	90	0.9995	58	79	36.77
Actb	rat		NM_031144	F - ACCCACACTGTGCCCATCTA R - GCCACAGGATTCCATACCCA	341	88	0.9959	68	80	35.77
Tbp	rat		NM_001004198	F - CCTTCACCAATGACTCCTATG R - TGGATTGTTCTTCACTCTTGGC	273	100	0.9908	62	80	ND
Hprt1	rat		NM_012583	F - TTGTTGGATATGCCCTTGACT R - CCGCTGTCTTTTAGGCTTTG	105	92	0.9944	60	75	34.79
Reep5	rat		NM_001108888	F - CTGATAGGTTTCGGATACCCA R - GACTCGTGCTTCAGGAAGATGG	269	91	0.9979	68	80	38.27
c-FOS	human		NM_005252	F - TGGCGTTGTGAAGACCATGA R - AGTTGGTCTGTCTCCGCTTG	189	90	0.998	60	81	38.41
RPL13A	human		NM_012423	F - CCTGGAGGAGAAGAGGAAAGAGA R - TTGAGGACCTCTGTGTATTTGTCAA	341	94	0.9939	60	77	ND
ACTB	human		NM_001101	F - ACCCACACTGTGCCCATCTAC R - GCCACAGGACTCCATGCCCA	125	88	0.9986	66	84	ND
TBP	human		NM_003339	F - GCCCGAAACGCCGAATATAA R - AATCAGTGCCGTGGTTCGTG	81	91	0.999	58	77	38.22

Gene name, species of the gene and corresponding primer pair, transcript variants, GenBank reference and sequence of the primers are listed. The table shows also the length of the amplicon for each primer pair. Amplification efficiency and R^2 from the standard curve were calculated as described in materials and methods section. Annealing temperature and quantification temperature specific for each primer pair are also listed. F, forward primer; R, reverse primer; bp, base pair; NTC, no template control; ND, not detectable (>40 Cq).

confocal microscope (LSM 700, Zeiss, Oberkochen, Germany) at 20× magnification. DAPI signals were obtained at 470 nm by laser excitation at 405 nm, while PI signals were measured at 617 nm upon excitation at 555 nm. *Z* plane image stacks were acquired at intervals of 2.47 μm beginning at the surface up to 40–50 mm depth. Images were visualized using ZEN software and processed using ImageJ 1.51m9. DAPI and PI/DAPI positive cells were counted in the somata containing areas of the hippocampal formation (st. granulosum of dentate gyrus, st. pyramidale of CA3, CA1 and subiculum) and two cortical depths (layer I–III and layer IV–VI of the EC and TC, respectively) in a visual field sized 500 × 300 μm. Slice viability was assessed as the ratio between PI positive and DAPI positive (dead/total) cells for each investigated region.

Data Analysis and Statistics

Raw image data were analyzed with ImageJ 1.51m9, MATLAB and MS Excel. Statistical analysis and processing of graphs were performed using GraphPad Prism 5 or 7 (GraphPad Software, La Jolla, CA, United States). All data were first tested for normality distribution with D'Agostino and Pearson omnibus normality test. If the evaluation of normality was not possible due to too small sample size, Kruskal–Wallis non-parametric test was used. To assess statistical significance between groups, continuous variables were examined using ordinary one-way ANOVA with multiple comparisons (normally distributed data) or Kruskal–Wallis test (non-normally distributed data or small sample size) and *post-hoc* Tukey's or Dunnett's multiple comparison of individual groups. Values of $p < 0.05$ were considered statistically significant. All data analyzed by parametric tests are expressed as mean ± standard deviation while data analyzed by non-parametric tests are shown as median ± interquartile range. OmniGraffle 7 (The Omni Group, Seattle, WA, United States) was used as graphical software to process images.

RESULTS

Properties of 4-AP Induced SLEs in Acute Rat Brain Slices

Epileptiform activity due to 4-AP treatment was induced in 100 rat slices (five slices per animal). Local field potentials were recorded in 20 selected slices and yielded 572 SLEs. In the lateral EC, SLE activity started on average 18.0 min (±7.5 min) after 4-AP onset and maintained a stable frequency throughout the entire 4 h incubation period. SLEs displayed the following electrophysiological properties: incidence median 0.24 ± 0.09/min in EC and 0.22 ± 0.05/min in CA1; amplitude median 0.81 ± 0.52 mV in EC and 0.62 ± 0.29 mV in CA1; duration median 50.54 ± 28.39 s in EC and 51.88 ± 40.31 s in CA1 (**Figure 2**). SLE activity never occurred in slices incubated in standard aCSF. In five ventral slices with respect to the dorsoventral axis, the 4-AP induced activity differed such that no separate SLE but rather a persistent epileptiform activity was observed in the course of the experiment (**Supplementary Figure 1**). These slices were excluded from further electrophysiological analysis. Simultaneous to electrophysiological recordings, the spatiotemporal evolution of SLEs was monitored by IOS within the entire slice (**Figure 3A**). Each SLE was assessed for onset and propagation region, respectively. SLE onset in the TC was observed in 61.1% of SLEs followed by 27.4% in the EC and 0.0% in the H (median numbers). In addition to single regions, 57 SLEs (10.0%) in 13 slices had a multiregional onset in anatomical regions distant from each other. The onset region was dependent on the slice origin with respect to the dorsoventral axis such that hippocampal onset almost exclusively occurred in ventral slices while TC and EC onset was more frequent in medial and dorsal slices. Regarding propagation, 49 SLEs (8.6%) in nine slices stayed limited to the onset region while the remaining (>90%) SLEs propagated at least to one neighboring region. The vast majority of SLEs propagated within neocortical regions and invaded hippocampal structures only to a minor degree (6.7%), and, similar to onset, mainly in ventral slices. Propagation to the TC and EC was frequently observed in dorsal and medial slices, respectively. SLE extent assessed by comparing the affected area with the total size of a given region revealed the largest expansion of epileptiform activity in the TC (68.8%) followed by the EC (68.1%). In line with the low rate of onset and propagation, expansion of SLEs within the hippocampus was low (34.0%) and involved in most of the cases the subiculum as previously reported (Heuzeroth et al., 2019). All SLEs were associated with an increase in light transmittance with the maximum in the TC ($\Delta T/T$ = 2.94%) followed by the EC ($\Delta T/T$ = 2.23%) and the H ($\Delta T/T$ = 1.98%). Summary of optical results is given in **Figures 3B–G**. Overall, the TC stood out such that it presented as the most frequent onset region, displayed the largest intraregional expansion and showed the maximal increase of light transmittance.

Spreading Depolarizations

Increasing excitability not only decreases the threshold for SLEs but also for spreading depolarizations (SDs) that reflect a propagation of neuronal silencing due to loss of ion homeostasis and a depolarization block (Dreier, 2011). Electrophysiologically, SDs are distinguished from SLEs by their massive amplitude, duration > 1 min and subsequent block of interictal activity. 16.5% of SLEs were associated with simultaneous SDs. No preferred region of SD occurrence could be detected (median numbers, **Figure 3H**). The relative SD expansion within a given anatomical region was smaller than SLE expansion and showed no significant interregional difference (**Figure 3I**). In IOS recordings, SDs led to a marked decrease of light transmittance which was pronounced in the TC ($\Delta T/T = -1.77\%$) followed by EC ($\Delta T/T = -1.27\%$) and H ($\Delta T/T = -1.19\%$) (**Figure 3J**).

Cell Death Assay

Neuronal activity in acute brain slices can be recorded up to 8 h after slice preparation. Within this time frame, occurrence of cell death with impact on gene expression and neuronal activity is likely (Buskila et al., 2014) and needs to be considered. To

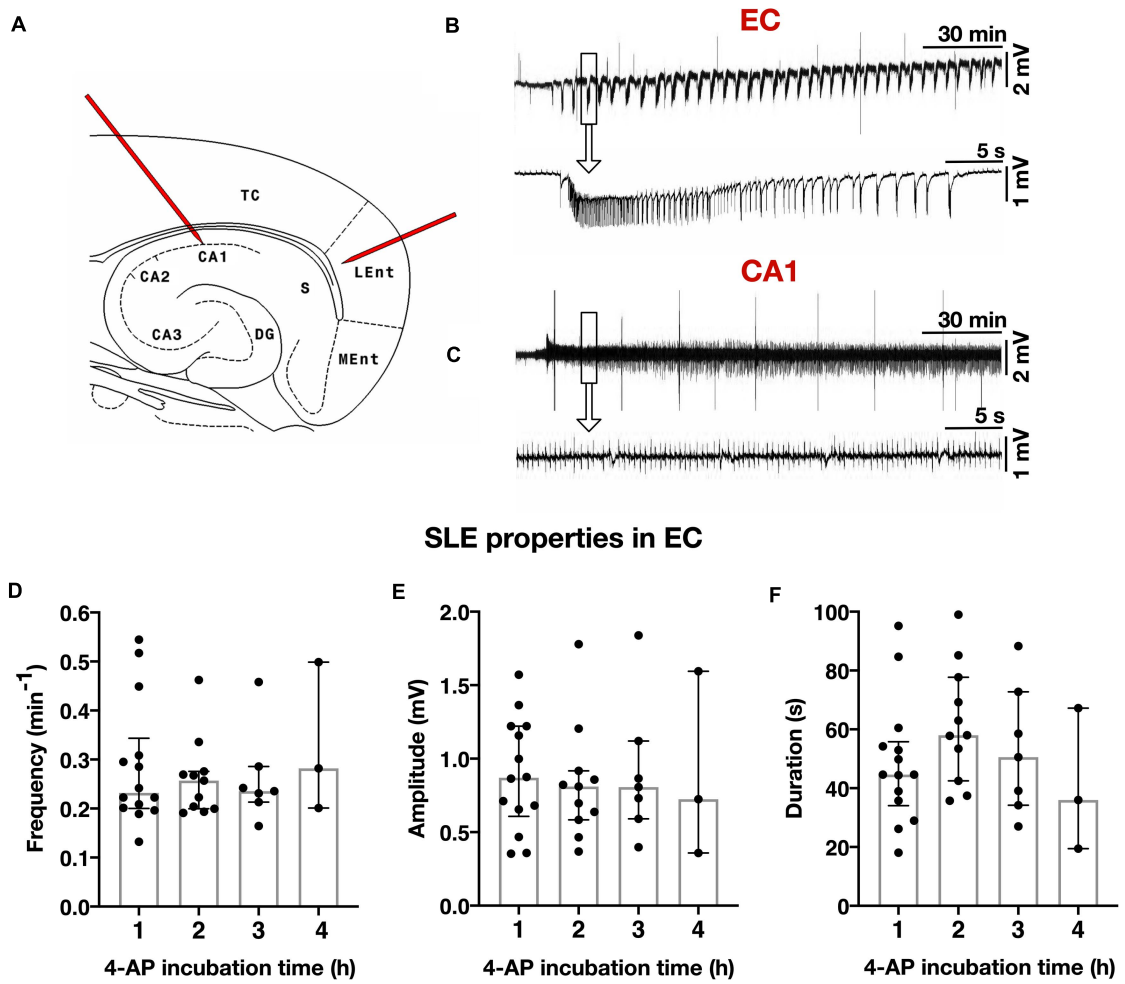

FIGURE 2 | Electrophysiological recordings in rat slices. **(A)** Schematic drawing of a combined hippocampal-entorhinal cortex slice with localization of two extracellular recording electrodes in layer IV/V of the lateral EC and stratum pyramidale of the hippocampal CA1 region, respectively. TC = temporal cortex, LEnt = lateral entorhinal cortex, MEnt = medial entorhinal cortex, S = subiculum, CA1–3 = hippocampal cornu ammonis, DG = dentate gyrus. **(B)** Exemplary trace of local field potentials in the EC during a 4 h experiment with stable occuring seizure-like events (SLEs). Single SLE marked in rectangle with enlarged presentation below. Monomorphic configuration of SLE with an initial sharp transient superimposed by a tonic and then clonic-like phase. **(C)** Representative recording of simultaneous interictal spikes in hippocampal CA1 during the same experimental period, enlarged depiction in the lower trace. **(D–F)** SLE properties in the EC remain stable as demonstrated by similar frequency **(D)**, amplitude **(E)**, and duration **(F)** for each treatment duration in a total number of $n = 20$ slices (five slices for each 4-AP treatment duration of 1, 2, 3, or 4 h). Scatter plots represent individual recordings for 4-AP treatment duration of 1–4 h, superimposed boxes show median ± interquartile range.

assess the impact of cell death on our results, we performed combined PI and DAPI staining in acute brain slices stored for different time periods. In all investigated brain regions, cell death increased time-dependently under 4-AP treatment as well as control conditions (**Figure 4**): In basal slices not subjected to storage, the rate of cell death ranged between 3.4% (±8.8%) in the superficial TC layers and 11.6% (±4.5%) in the dentate gyrus. Upon incubation for 4 h (5.5 h when including recovery), the extent of cell death markedly increased. In the hippocampus it varied between 14.8% (±5.4%) in subiculum and 39.0% (±17.1%) in dentate gyrus. In neocortical regions, incubation increased the rate of cell death in deep as well as superficial layers (layer I-III: 15.9% in EC; 9.7% in TC, layer IV-VI: 24.9% in EC; 25.5% in TC). No differences were observed when comparing 4-AP treatment and control, suggesting that 4-AP and the associated epileptiform activity do not increase processes leading to cell death. 4-AP treatment even tended to reduce the cell death rate within the 4 h intervention period when compared to time-matched controls.

Reference Gene Identification

To identify a reference gene not dependent on neuronal activity or storage duration, we compared *Actb*, *Ywhaz*, *Hprt1*, *Reep5*, and *Tbp*. *Cq* variability did not differ across investigated regions (H: 19.1–32.8; EC: 19.5–29.8; TC: 19.6–31.5) (**Supplementary Figure 2A**). In all investigated regions, *Actb* was the most abundantly expressed gene and *Tbp* showed the lowest gene expression (**Supplementary Figure 2B**). In order to obtain a

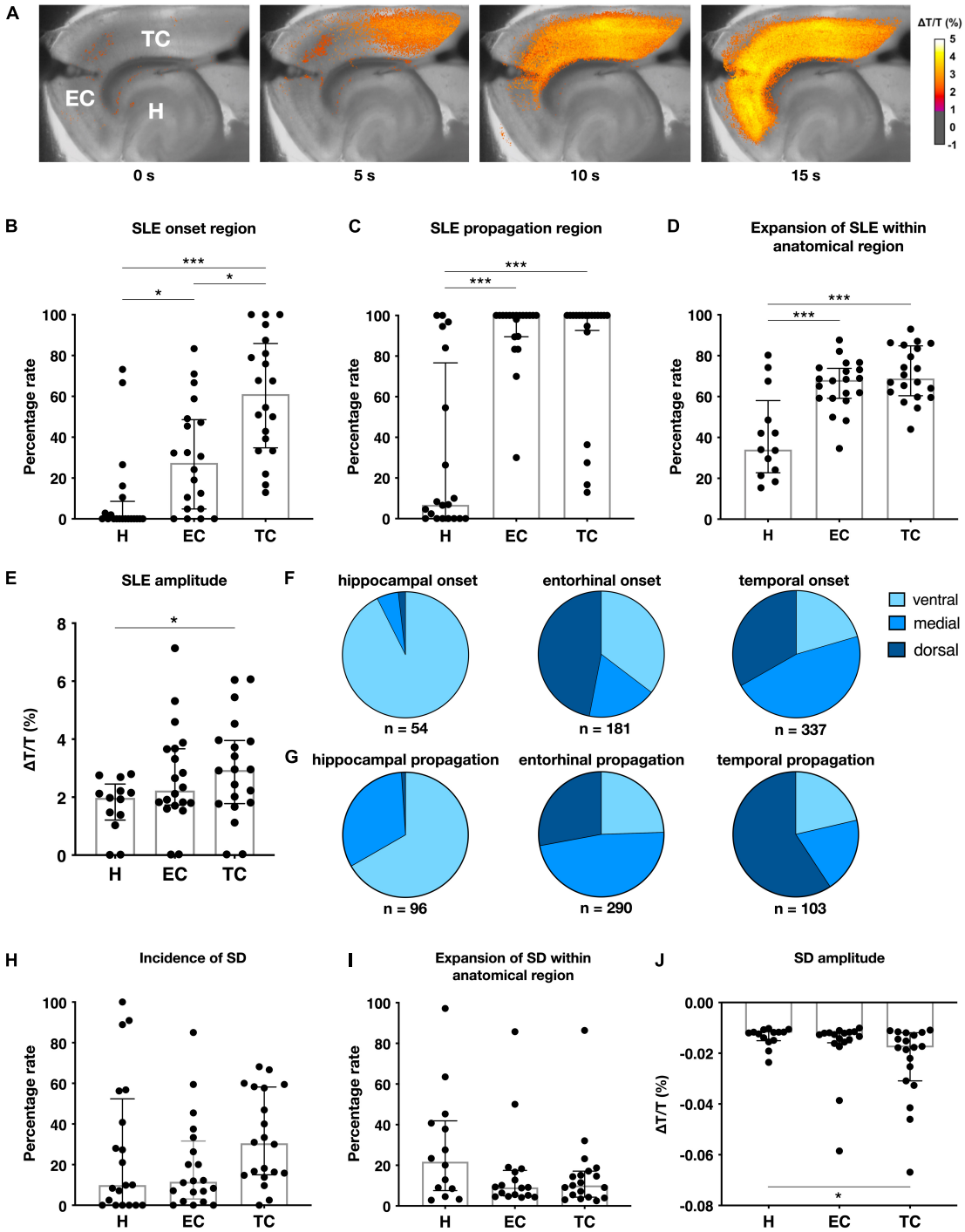

FIGURE 3 | Intrinsic optical imaging (IOS) in rat slices. **(A)** Color-coded SLE amplitude ($\Delta T/T$) over time during an exemplary SLE generated in the temporal cortex and propagating to the entorhinal cortex without further invading the hippocampal formation. Characteristics of SLEs **(B–E)** and spreading depolarizations (SDs) **(H–J)** measured by IOS in $n = 20$ slices (five slices for each 4-AP treatment duration of 1, 2, 3, or 4 h), scatter plots represent means of individually recorded slices, superimposed boxes show median ± interquartile range (*$p < 0.05$, ***$p < 0.001$). **(F–G)** SLE origin is influenced by the anatomical slice origin (dorsoventral axis) separated in ventral (−7.6 to −6.8 mm ventrally from bregma), medial (−6.4 to −5.6 mm) and dorsal (−5.2 to −4.4 mm) regions.

more robust stability ranking, the NormFinder algorithm was applied to calculate the gene stability value M based on standard deviation expressed intra- and intergroup variation (Andersen et al., 2004). Reference genes with standard deviation > 0.25 (*Reep5* in H and *Tbp* in TC) were excluded. Among the remaining candidates, *Ywhaz* turned out to be the most stably expressed

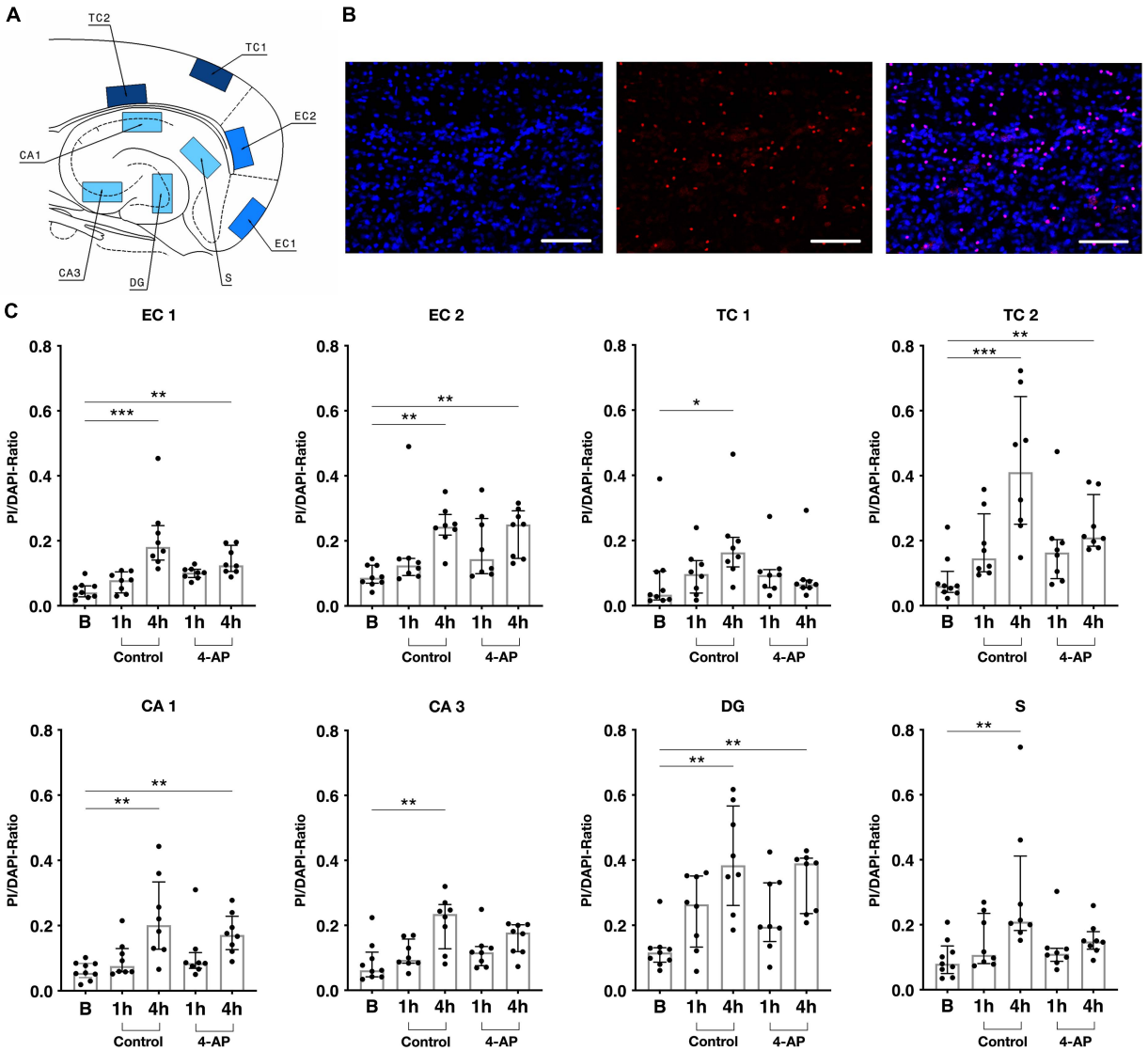

FIGURE 4 | Cell death assay for rat slices. **(A)** Schematic depiction of a rat slice with eight visual fields (500 × 300 μm) in which cells were counted: two layers of each entorhinal (EC1 and EC2) and temporal cortex (TC1 and TC2) as well as subiculum (S), CA1, C3 and dentate gyrus (DG). **(B)** Exemplary images acquired by an inverted confocal microscope (20× magnification, merged *Z* plane image stack), left: DAPI staining (2 μg/ml), in center: PI staining (1 μg/ml), right: merged. Scale bar 100 μm. **(C)** Slice viability measured as ratio of PI (dead) and DAPI (total) positive cells in $n = 41$ slices (9 × basal, 8 × control 1 h, 8 × control 4 h, 8 × 4-AP 1 h, 8 × 4-AP 4 h). Scatter plots represent PI/DAPI-Ratio of individually stained slices, superimposed boxes show median ± interquartile range (*$p < 0.05$, **$p < 0.01$, ***$p < 0.001$).

gene across all groups (stability value M: H 0.069; EC 0.09; TC 0.071) (**Supplementary Figure 2C**) and was therefore used as the reference gene for qPCR in the following experiments.

Gene Expression Analysis

Investigation of activity-dependent gene expression in rat brain slices was performed for the genes *c-Fos*, *Icer*, and *mTor* referenced to *Ywhaz* expression as stated above. In basal slices immediately processed after the slice procedure, relative *c-Fos* expression varied between regions with the lowest expression in the H and the highest expression in the TC (median *c-Fos/Ywhaz*: $H = 0.0033$, EC = 0.0080, TC = 0.0134). Basal *c-Fos* mRNA levels were positively correlated with the duration of the brain slice preparation (**Supplementary Figure 3**). In comparison to basal values, incubation in aCSF markedly increased *c-Fos* gene expression. This increase was strongest after 1 h of incubation (corresponding to 2.5 h when including recovery) and most distinctive in the H (median fold induction of 69.5 relative to basal) followed by the EC (median fold increase of 20.1) and the TC (median fold increase of 7.8). Compared to 1 h, incubation for longer intervals (2–4 h or 3.5–5.5 h including recovery) resulted in weaker *c-Fos* expression which was negatively correlated with incubation time (**Figure 5**). In 4-AP treated slices, a similar time course of *c-Fos* expression with the strongest increase

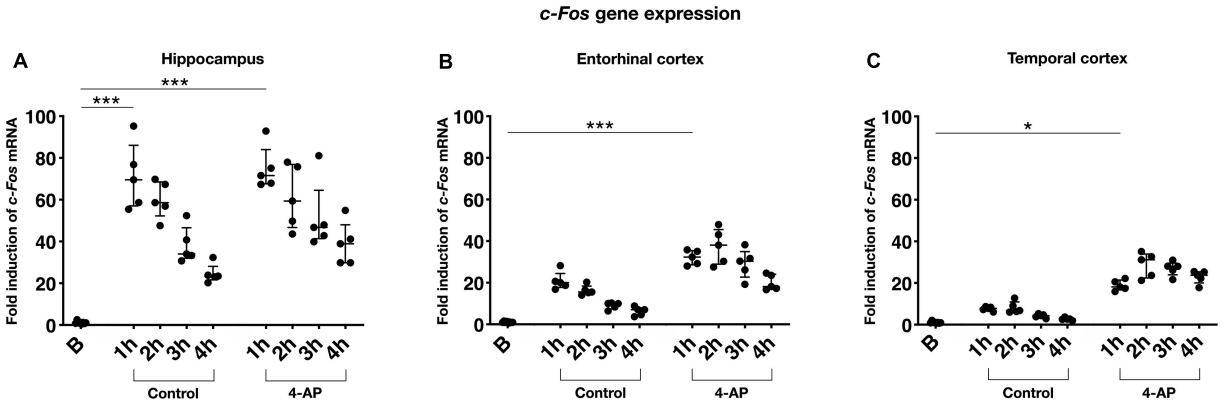

FIGURE 5 | Activity and time dependent *c-Fos* gene expression in rat slices. Induction of *c-Fos* mRNA relative to basal gene expression in **(A)** Hippocampus, **(B)** Entorhinal cortex, and **(C)** Temporal cortex, respectively. All investigated conditions are represented: control slices (control), 4-AP treated slices (4-AP) with experimental duration of 1, 2, 3 or 4 h. For relative quantification in RT-qPCR, *Ywhaz* was used as reference gene. Scatter plots show means of individual rats ($n = 20$) since tissue was pooled before RT-qPCR, superimposed lines represent median ± interquartile range ($^*p < 0.05$, $^{***}p < 0.001$).

after 1 h of incubation and subsequent decrease was observed. Strikingly, when comparing *c-Fos* expression in 4-AP treated slices to time-matched controls, *c-Fos* expression was consistently higher in the intervention group (**Figure 5**). Correlation of the duration of intervention and *c-Fos* expression revealed a time-dependent increase of *c-Fos* mRNA that largely differed across examined brain regions (**Figure 6A**). In the hippocampus, 4-AP treatment increased *c-Fos* mRNA levels only marginally with a (non-significant) slope of 0.19 while significant slopes of 0.64 ($p < 0.05$) and 2.18 ($p < 0.01$) were observed in the EC and TC, respectively. The spatiotemporal pattern of *Icer* expression was similar to *c-Fos* but showed a weaker increase. In all investigated regions of basal slices, *Icer* mRNA levels were low when compared to *c-Fos* mRNA (median *Icer/Ywhaz* $H = 0.0002$, EC = 0.0003, TC = 0.0003). Reflecting the effect of slice preparation and storage, *Icer* gene expression was also induced in control slices. In contrast to *c-Fos*, the strongest increase of *Icer* mRNA levels was observed in control slices incubated in aCSF for 3 h (median fold induction relative to basal: H 15.1; EC 15.0; TC 6.3) (**Supplementary Figures 4A–C**). Comparing *Icer* expression between 4-AP and control, slices revealed a region and time-dependent increase of *Icer* mRNA in 4-AP treated slices (**Figure 6B**): while in the H and the EC, 4-AP treatment had only a marginal effect, it clearly induced an increase in *Icer* expression in the TC with a significant slope of 0.41 (p-value 0.0271). In basal slices, *mTor* mRNA did not largely differ between the investigated regions (median *mTor/Ywhaz* $H = 0.0137$, EC = 0.0151, TC = 0.0145). Interestingly, in all investigated regions, a weak, time-dependent decrease of *mTor* expression in both control and 4-AP treated slices was observed. In the EC and TC, the decrease of *mTor* mRNA levels got significant in 4-AP treated slices after 4 h (**Supplementary Figures 4D–F**). Compared to time-matched control slices, 4-AP induced epileptiform activity did not show any effect on *mTor* gene expression.

So far, our data demonstrated that gene expression of all examined genes depends on the duration of storage and in case of *c-Fos* and *Icer* additionally to the chosen condition (control/intervention). Gene expression was also associated with the pattern of epileptiform activity: in case of *c-Fos*, the 4-AP induced increase of gene expression and the rate of SLE onset were positively correlated with highest values in the TC and lowest values in the H (**Figure 6C**). This positive correlation was also observed between *c-Fos* expression and the intraregional SLE expansion and the maximum increase of IOS intensity (**Figures 6D–E**). Similar effects could be confirmed for *Icer* (**Figures 6C–E**), albeit to a weaker extent. Naturally, no such correlation was observed for *mTor* that did not show changes in gene expression.

Gene Expression Analysis in Human Tissue

In human tissue, the NormFinder algorithm revealed *RPL13A* as the most stable gene (stability values M: *RPL13A* 0.068; *ACTB* 0.07; *TBP* 0.115) (**Supplementary Figure 5**) and therefore employed as reference gene for the following qPCR experiments. To identify the region of seizure onset in human slices, we likewise performed electrophysiological recordings combined with optical imaging (**Figure 7A**). During 4 h of application, SLEs (**Figure 7B**) were recorded for a minimum of 40 min to identify the seizure onset site. In a significant proportion of investigated slices, the onset site varied in the course of the experiment. In these slices, the area with the highest number of SLE onsets was assigned as the onset region and further processed. qPCR revealed that *c-FOS* expression increased both during 4 h storage in standard aCSF (control) and epileptogenic aCSF (intervention). Similar to rat slices, the relative increase of *c-FOS* in the intervention group was higher compared to control and basal conditions (Kruskal–Wallis test, p-value 0.0031; Dunnet's *post hoc* test, Basal vs. Onset + Rest p-value < 0.01). Values from onset site and the remaining slice were pooled as no difference in *c-FOS* expression could be detected between these regions. As depicted in **Figure 7C**, in slices subjected to

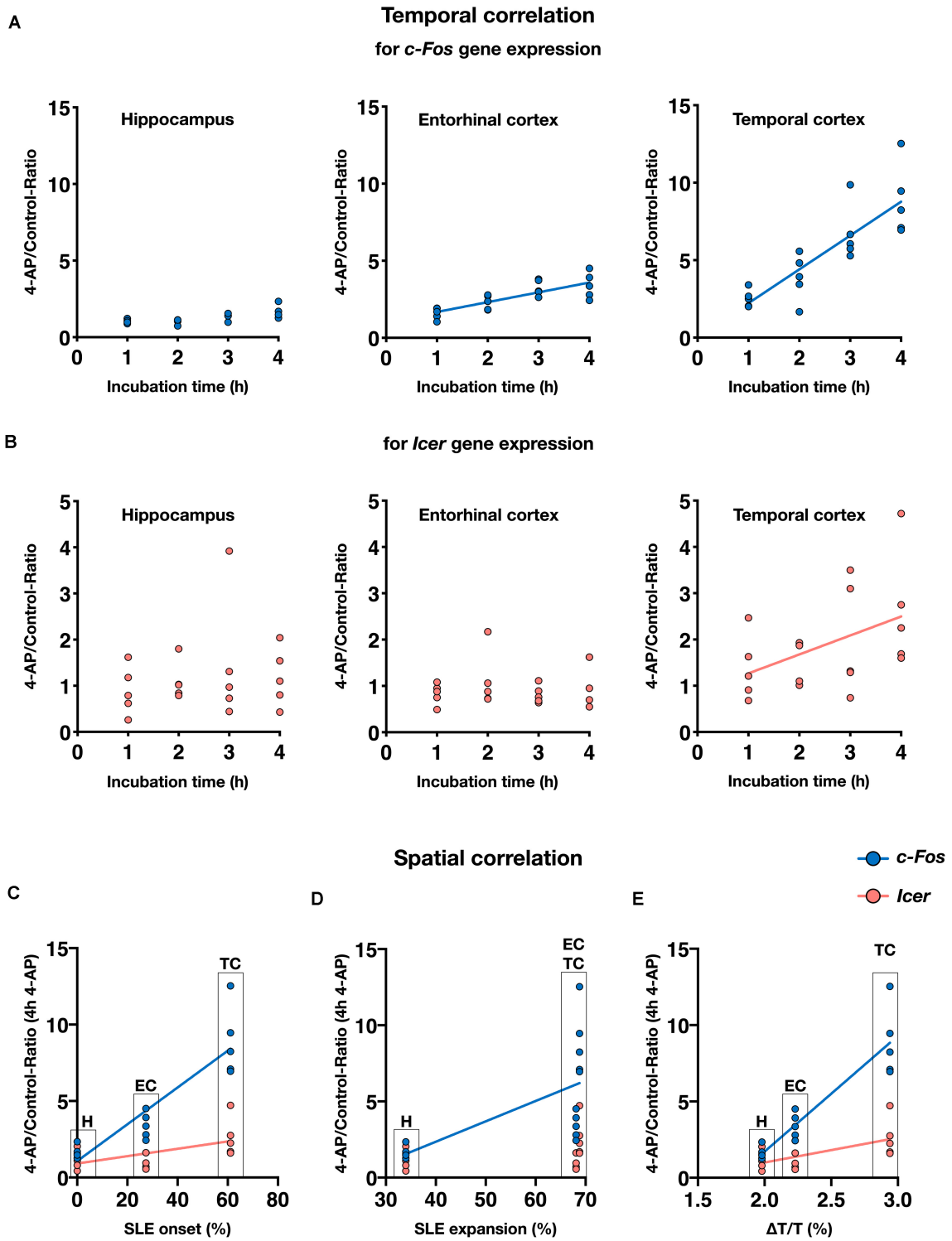

FIGURE 6 | Spatiotemporal correlation of epileptiform activity and gene expression in rat slices. Summary of results from rat slices demonstrating spatial and temporal dependence of *c-Fos* and *Icer* expression. **(A,B)** Scatter plots show means of mRNA expression ratios of 4-AP vs. control from individual rats (n = 20) and different incubation intervals for hippocampus (H), entorhinal cortex (EC), and temporal cortex (TC), respectively. Regression lines show significant temporal correlation between 4-AP exposure and *c-Fos* **(A)** or *Icer* expression **(B)**. **(C–E)** Spatial dependence of gene expression following 4-AP treatment duration of 4 h (n = 5) shown by spatial parameters such as rate of SLE onset **(C)**, SLE expansion within anatomical region **(D)** as well as SLE amplitude **(E)**. Note that data in C-E are presented as median and do not sum up to 100%.

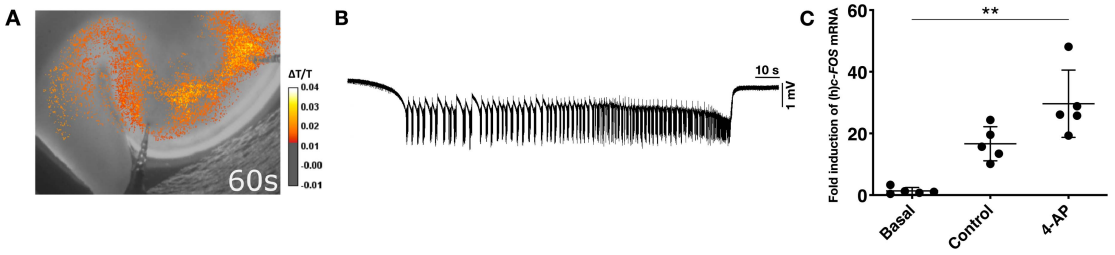

FIGURE 7 | Activity-dependent *c-FOS* expression in human slices. **(A)** Example of a typical IOS image of a SLE in a human cortex slice at 60 s after start. **(B)** Example of an electrophysiological trace showing a SLE recorded in human cortical layers II/III upon application of aCSF containing 8 mM potassium and 100 μM 4-AP. **(C)** Scatter plots showing *c-FOS* expression fold changes relative to basal condition. All data are normalized to the reference gene *RPL13A* and expressed as median ± interquartile range. *c-FOS* expression in slices displaying SLE activity is higher when compared to basal condition (**$p < 0.01$, $n = 5$).

seizure-like activity, *c-FOS* expression was increased 26.1-fold relative to basal conditions. In contrast, control slices incubated with standard aCSF showed a median fold-increase of *c-FOS* expression of 15.7.

DISCUSSION

In the present proof-of-principle study, we investigated the association between neuronal activity and gene expression in acute brain slice preparations, mainly from rodents. For the activity-dependent genes *c-Fos* and *Icer*, we found a positive spatiotemporal correlation between gene expression and epileptiform activity while no correlation was found for *mTor*. Increases induced by neuronal activity could be differentiated from increases inherent to slice preparation, temperature variations and incubation time. We were able to partly reproduce the results on *c-Fos* mRNA increase observed in rat slices in human brain slice preparations from epilepsy surgery.

The highest correlation between gene expression and epileptiform activity was observed in case of *c-Fos*, its expression is well established as a marker of neuronal activity (Willoughby et al., 1995; Mihály et al., 2001; Szyndler et al., 2009; Barros et al., 2015). As an immediate early gene within the family of inducible transcription factors, *c-Fos* is involved in regulating cellular responses including differentiation, plasticity and cell degeneration (Chiu et al., 1988; Pennypacker et al., 1994). Proconvulsant stimuli result in an increase of *c-Fos* mRNA as well as c-FOS protein in rat brains *in vivo* (Barros et al., 2015; Yang et al., 2019). A regional and persistent induction of *c-FOS* gene expression was also found in human epileptic neocortex regardless of the underlying pathology (Rakhade et al., 2005). So far, only little data exists about *c-Fos* induction in brain slices (Massamiri et al., 1994), and this work suffered from technical limitations as changes in *c-Fos* expression were assessed semiquantitatively using southern blots without accounting for differences between subregions and impact of exposure time.

With a weaker extent than *c-Fos*, SLE activity was also associated with increased *Icer* mRNA. *Icer* is a member of cAMP-dependent transcription factors (*Crem* = cAMP response element modulator). Electroconvulsive seizures *in vivo* increased *Crem* and *Icer* mRNA in rat brains with a maximum at 1 h after seizures and with a most prominent increase in the dentate gyrus and deep layers of cerebral cortex (Fitzgerald et al., 1996). In a different model using pilocarpine-induced status epilepticus in rats, *Icer* mRNA assessed in the dentate gyrus peaked at 6 h and declined to control levels after 1 week (Lund et al., 2008). Interestingly, phosphorylation of cAMP response element-binding protein (CREP) that is assumed to positively affect *ICER* gene expression was regionally increased in seizure onset zone of human neocortex measured following epilepsy surgery (Rakhade et al., 2005), suggesting that involvement of the *CREM/ICER* pathways is likely in the pathophysiology of human epilepsy. Several studies support the idea that activation of the *ICER* pathway upon seizures represents an adaptive mechanism aiming to reduce excess neuronal activity. *Crem/Icer* null mutant mice suffered from more frequent seizures following status epilepticus than their control littermates (Porter et al., 2008), and overexpression of *Icer* negatively regulated neuronal plasticity (Kojima et al., 2008). By revealing a positive correlation of *Icer* expression and epileptiform activity, we were able to reproduce these results *in vitro* specifically in the TC.

Finally, we investigated gene expression of *mTOR*, a member of a complex regulatory pathway modulating proliferation and neuronal activity. In patients with tuberous sclerosis complex suffering from severe and treatment-resistant epilepsy, the *mTOR* pathway is hyperactivated due to mutations in TSC1 and TSC2 genes (Overwater et al., 2019). In these patients, treatment with *mTOR* inhibitors such as everolimus reduced seizure frequency in up to 40% of individuals (French et al., 2016). Apart from tuberous sclerosis complex, the involvement of the *mTor* pathway in structural epilepsy was shown in several animal models (Huang et al., 2010; Zhang and Wong, 2012; Wang et al., 2018), including chronic models induced by kainate and pilocarpine. Importantly, the acute phase of *mTor* activation seems to be directly driven by epileptiform activity. Pentylenetetrazole (PTZ)-induced seizures caused a transient *mTor* activation in rat hippocampus and neocortex starting by 1 h and returning to baseline by 16 h after seizure onset (Zhang and Wong, 2012). Activation of the *mTor* pathway is believed to occur by protein phosphorylation rather than gene activation (Zeng et al., 2009; Zhang and Wong, 2012).

In our study, we did not find evidence for additional activation of *mTor* gene expression by epileptiform activity. Rather conversely, *mTor* expression seems to be negatively affected by *in vitro* storage as demonstrated by decreased *mTor* mRNA levels in the entorhinal and temporal cortex.

The results from our cell death assay based on PI/DAPI staining imply that the 4-AP *in vitro* model represents a suitable tool to examine gene expression *in vitro*. Although cell death expectedly increased with increasing incubation intervals, we did not observe spatial or temporal differences between control and intervention groups. Interestingly, 4-AP treatment for 4 h tended to decrease the cell death rate when compared to time-matched controls. Previous studies demonstrated that preconditioning with 4-AP for 48 h protects rat cellular granule neuron culture against excitotoxicity by a number of stressors (glutamate, NMDA and 3-nitropropionic acid) (Smith et al., 2009). The results are consistent with an earlier investigation of 4-AP induced protection of hippocampal and cortical neuron culture (Hardingham et al., 2002; Tauskela et al., 2008). Overall, exposure to 4-AP or other proconvulsant agents such as the $GABA_A$-receptor antagonist bicuculline, seems to be involved in neuroprotection (Hardingham et al., 2002; Tauskela et al., 2008), although the exact mechanisms remain unclear.

In our approach, we aimed to systematically overcome previous technical limitations by using various internal controls, applying quantitative means to measure gene expression and comparing different regions within a slice as well as different exposure times to the applied proconvulsant. As an acute *in vitro* model of seizures, we used 4-AP as in this model epileptiform activity remains stable over hours. We could clearly detect spatial differences demonstrated by the highest increase of *c-Fos* expression in the TC, the most frequent onset region for SLEs, while in the hippocampus, only a marginal increase in *c-Fos* mRNA was observed. This correlation applied also to the intraregional SLE expansion and activity-dependent increase of light transmittance.

Our work poses several limitations. According to previous reports, hippocampal slice preparation causes a remarkable induction of *c-Fos* mRNA within 6 h when compared to intact hippocampus (Taubenfeld et al., 2002). We confirmed these results with a hippocampal *c-Fos* mRNA increase up to 70-fold while increase in the entorhinal and temporal cortex was much lower. We assume that structural differences between the investigated regions including strong reciprocal connectivity in the hippocampus renders the latter more sensitive to the transient but massive neuronal activation during slice preparation. This high sensitivity with massive *c-Fos* increase in basal hippocampal slices presents a limiting factor as gene expression is not unlimited. It seems rpossible that strong initial hippocampal *c-Fos* increase made a further increase upon SLE induction less likely. This aspect together with the low incidence of SLEs in the hippocampal formation might explain the weak effects of SLE activity on hippocampal gene expression. The artificial, *in vitro* setting presents a general limitation that cannot be easily overcome. Gene expression observed *in vitro* might largely differ from the natural *in vivo* situation. Therefore, future observations from human samples investigated *in vitro* need to be interpreted with caution.

In human slices, *c-FOS* expression correlated with epileptiform activity, but we did not find increased expression in the onset zone, most likely due a high variability of the SLE onset and consequently probable imprecise definition. This onset variability as compared to rat tissue is likely due to the overall variability of human tissue obtained from different patients with consequent impact on the activity *in vitro* (Andersson et al., 2016; Wickham et al., 2018; Kraus et al., 2019) and also due to differences in tissue or different slicing angles (Kraus et al., 2020). All these variables not only influence neuronal survival and network excitability, but also could have affected gene expression. Finally, the infrequent availability and low number of human samples allowed only for a limited analysis and also precluded detailed comparison with rat tissue.

The discussed limitations need to be considered in future studies. In case of human tissue, however, using an *ex vivo* approach remains without alternatives. Overall, our results indicate that irrespective of limitations mostly imposed by *ex vivo* conditions, *in vitro* models in general represent a suitable tool for the investigation of gene expression by epileptiform activity. As an outlook, transcriptome-wide approaches including spatial transcriptomics as well as investigation of single cell profiles might reveal novel candidates involved in the human pathophysiology of epilepsy and possibly other CNS pathologies.

DATA AVAILABILITY STATEMENT

All datasets generated for this study are included in the manuscript and/or the **Supplementary Files**.

ETHICS STATEMENT

The studies involving human participants were reviewed and approved by Charité-Universitätsmedizin Berlin (EA2/111/14). The patients/participants provided their written informed consent to participate in this study. The animal study was reviewed and approved by the Institutional Animal Welfare Officer and the responsible local authority (Landesamt für Gesundheit und Soziales Berlin, T0336/12).

AUTHOR CONTRIBUTIONS

SS, PF, and MH contributed to the conception and design of the study. SS performed and analyzed all experiments in rat brain slices, including electrophysiological and optical recordings, cell death assay, qPCR, and NormFinder analysis. MH selected the patients for operation. JO operated the patients. LM performed and analyzed all measurements in the human tissue. MD-W and PF contributed to the data analysis and statistics. SS, LM, and PF wrote the manuscript, which all authors edited and finalized. All authors contributed to the article and approved the submitted version.

FUNDING

We acknowledge support from the German Research Foundation (DFG) and the Open Access Publication Fund of Charité – Universitätsmedizin Berlin.

ACKNOWLEDGMENTS

We would like to thank the Department of Neuropathology for facilitating the use of brain temporal lobe tissues upon epilepsy surgery, namely Dr. Arend Koch. We also thank Mandy Marbler-Pötter and Claudia Muselmann-Genschow (Department of Neurology with Experimental Neurology) for excellent technical assistance.

SUPPLEMENTARY MATERIAL

The Supplementary Material for this article can be found online at: https://www.frontiersin.org/articles/10.3389/fnmol.2021.643763/full#supplementary-material

Supplementary Figure 1 | Persistent epileptiform activity in ventral rat slices. Exemplary electrophysiological recording of 4-AP induced persistent epileptiform activity in the EC observed ventral rat slices (−7.6 to −6.8 mm from bregma) in contrast to separate SLEs in medial and dorsal slices.

Supplementary Figure 2 | Reference gene identification for rat slices. **(A)** Mean quantification value (*Cq*) and standard deviation of five reference genes determined in two independent samples for each condition (basal; control 1, 2, 3, and 4 h; 4-AP 1, 2, 3, and 4 h; $n = 18$). Values obtained from the three rat brain regions processed: hippocampus, entorhinal cortex and temporal cortex. **(B)** *Cq* of five candidate reference genes in all conditions across the three regions investigated (hippocampus, *H*, entorhinal cortex, EC, and temporal cortex, TC). The box chart indicates the first and the third interquartile range. The vertical line across the box indicates the median, while the lower and upper dashes show the minimum and maximum values. **(C)** Expression stability values (*M*) of the five candidate reference genes evaluated by NormFinder. A lower stability value indicates a more stable expression. *Reep5* in hippocampus and *Tbp* in temporal cortex showed a standard deviation > 0.25, so they were excluded from the determination of the stability value.

Supplementary Figure 3 | Gene expression of *c-Fos* in basal rat slices. Duration of brain slice procedure (from decapitation to cell lysis in TRIzol) positively correlated with basal *c-Fos* mRNA levels. Relative to the reference gene Ywhaz, *c-Fos* expression in basal slices was highest in temporal cortex (TC) followed by entorhinal cortex (EC) and hippocampus (H) in decreasing order.

Supplementary Figure 4 | Gene expression of *Icer* and *mTor* in rat slices. Fold induction of *Icer* **(A–C)** and *mTor* **(D–F)** relative to basal gene expression in hippocampus, entorhinal, and temporal cortex, respectively. All investigated conditions are represented: control slices (control) and 4-AP treated slices (4-AP) with experimental duration of 1, 2, 3, or 4 h. For relative quantification in RT-qPCR, *Ywhaz* was used as reference gene. Scatter plots show means of individual rats ($n = 20$) since tissue was pooled before RT-qPCR, superimposed graphs represent median ± interquartile range ($^*p < 0.05$, $^{**}p < 0.01$, $^{***}p < 0.001$).

Supplementary Figure 5 | Reference gene identification for human slices. **(A)** Mean quantification value (*Cq*) and standard deviation of three reference genes determined in two independent samples for each condition considered for human samples (basal, control, onset site, rest of slice; $n = 8$). **(B)** *Cq* of three candidate reference genes in all conditions. The box chart indicates the first and the third interquartile range. The vertical line across the box indicates the median, while the lower and upper dashes show the minimum and maximum values. **(C)** Expression stability values (*M*) of the three candidate reference genes evaluated by NormFinder. A lower stability value indicates a more stable expression.

REFERENCES

Andersen, C. L., Jensen, J. L., and Ørntoft, T. F. (2004). Normalization of real-time quantitative reverse transcription-PCR data: a model-based variance estimation approach to identify genes suited for normalization, applied to bladder and colon cancer data sets. *Cancer Res.* 64, 5245–5250. doi: 10.1158/0008-5472.CAN-04-0496

Andersson, M., Avaliani, N., Svensson, A., Wickham, J., Pinborg, L. H., Jespersen, B., et al. (2016). Optogenetic control of human neurons in organotypic brain cultures. *Sci. Rep.* 6:24818. doi: 10.1038/srep24818

Avoli, M., D'Antuono, M., Louvel, J., Köhling, R., Biagini, G., Pumain, R., et al. (2002). Network and pharmacological mechanisms leading to epileptiform synchronization in the limbic system in vitro. *Prog. Neurobiol.* 68, 167–207. doi: 10.1016/S0301-0082(02)00077-1

Barros, V. N., Mundim, M., Galindo, L. T., Bittencourt, S., Porcionatto, M., and Mello, L. E. (2015). The pattern of c-Fos expression and its refractory period in the brain of rats and monkeys. *Front. Cell.* Neurosci. 9:72. doi: 10.3389/fncel.2015.00072

Bauer, S., van Alphen, N., Becker, A., Chiocchetti, A., Deichmann, R., Deller, T., et al. (2017). Personalized translational epilepsy research — novel approaches and future perspectives: part II: experimental and translational approaches. *Epilepsy Behav.* 76, 7–12. doi: 10.1016/j.yebeh.2017.06.040

Becker, A. J. (2018). Review: animal models of acquired epilepsy: insights into mechanisms of human epileptogenesis. *Neuropathol. Appl. Neurobiol.* 44, 112–129. doi: 10.1111/nan.12451

Becker, A. J., Chen, J., Paus, S., Normann, S., Beck, H., Elger, C. E., et al. (2002). Transcriptional profiling in human epilepsy: expression array and single cell real-time qRT-PCR analysis reveal distinct cellular gene regulation. *NeuroReport* 13, 1327–1333. doi: 10.1097/00001756-200207190-00023

Buskila, Y., Breen, P. P., Tapson, J., van Schaik, A., Barton, M., and Morley, J. W. (2014). Extending the viability of acute brain slices. *Sci. Rep.* 4:5309. doi: 10.1038/srep05309

Chen, Z., Brodie, M. J., Liew, D., and Kwan, P. (2018). Treatment outcomes in patients with newly diagnosed epilepsy treated with established and new antiepileptic drugs a 30-year longitudinal cohort study. *JAMA Neurol.* 75, 279–286. doi: 10.1001/jamaneurol.2017.3949

Chiu, R., Boyle, W. J., Meek, J., Smeal, T., Hunter, T., and Karin, M. (1988). The c-fos protein interacts with c-Jun AP-1 to stimulate transcription of AP-1 responsive genes. *Cell* 54, 541–552. doi: 10.1016/0092-8674(88)90076-1

Chomczynski, P., and Sacchi, N. (1987). Single-step method of RNA isolation by acid guanidinium thiocyanate-phenol-chloroform extraction. *Anal. Biochem.* 162, 156–159. doi: 10.1016/0003-2697(87)90021-2

Di Lullo, E., and Kriegstein, A. R. (2017). The use of brain organoids to investigate neural development and disease. *Nat. Rev. Neurosci.* 18, 573–584. doi: 10.1038/nrn.2017.107

Dreier, J. P. (2011). The role of spreading depression, spreading depolarization and spreading ischemia in neurological disease. *Nat. Med.* 17, 439–447. doi: 10.1038/nm.2333

Fiest, K. M., Sauro, K. M., Wiebe, S., Patten, S. B., Kwon, C. S., Dykeman, J., et al. (2017). Prevalence and incidence of epilepsy: a systematic review and meta-analysis of international studies. *Neurology* 88, 296–303. doi: 10.1212/WNL.0000000000003509

Fitzgerald, L. R., Vaidya, V. A., Terwilliger, R. Z., and Duman, R. S. (1996). Electroconvulsive seizure increases the expression of CREM (Cyclic AMP response element modulator) and ICER (Inducible cyclic AMP early repressor) in Rat Brain. *J. Neurochem.* 66, 429–432. doi: 10.1046/j.1471-4159.1996.66010429.x

French, J. A., Lawson, J. A., Yapici, Z., Ikeda, H., Polster, T., Nabbout, R., et al. (2016). Adjunctive everolimus therapy for treatment-resistant focal-onset

seizures associated with tuberous sclerosis (EXIST-3): a phase 3, randomised, double-blind, placebo-controlled study. *Lancet* 388, 2153–2163. doi: 10.1016/S0140-6736(16)31419-2

Gabriel, S., Njunting, M., Pomper, J. K., Merschhemke, M., Sanabria, E. R. G., Eilers, A., et al. (2004). Stimulus and potassium-induced epileptiform activity in the human dentate gyrus from patients with and without hippocampal sclerosis. *J. Neurosci.* 24, 10416–10430. doi: 10.1523/JNEUROSCI.2074-04.2004

GBD 2015 Neurological Disorders Collaborator Group (2017). Global, regional, and national burden of neurological disorders during 1990–2015: a systematic analysis for the global burden of disease study 2015. *Lancet Neurol.* 16, 877–897. doi: 10.1016/S1474-4422(17)30299-5

Guelfi, S., Botia, J. A., Thom, M., Ramasamy, A., Perona, M., Stanyer, L., et al. (2019). Transcriptomic and genetic analyses reveal potential causal drivers for intractable partial epilepsy. *Brain* 142, 1616–1630. doi: 10.1093/brain/awz074

Hardingham, G. E., Fukunaga, Y., and Bading, H. (2002). Extrasynaptic NMDARs oppose synaptic NMDARs by triggering CREB shut-off and cell death pathways. *Nat. Neurosci.* 5, 405–414. doi: 10.1038/nn835

Heuzeroth, H., Wawra, M., Fidzinski, P., Dag, R., and Holtkamp, M. (2019). The 4-aminopyridine model of acute seizures in vitro elucidates efficacy of new antiepileptic drugs. *Front. Neurosci.* 13:677. doi: 10.3389/fnins.2019.00677

Hille, B. (1971). The permeability of the sodium channel to organic cations in myelinated nerve. *J. Gen. Physiol.* 58, 599–619. doi: 10.1085/jgp.58.6.599

Huang, X., Zhang, H., Yang, J., Wu, J., McMahon, J., Lin, Y., et al. (2010). Pharmacological inhibition of the mammalian target of rapamycin pathway suppresses acquired epilepsy. *Neurobiol. Dis.* 40, 193–199. doi: 10.1016/j.nbd.2010.05.024

Jones, R. S. G., da Silva, A. B., Whittaker, R. G., Woodhall, G. L., and Cunningham, M. O. (2016). Human brain slices for epilepsy research: pitfalls, solutions and future challenges. *J. Neurosci. Methods* 260, 221–232. doi: 10.1016/j.jneumeth.2015.09.021

Kobow, K., and Blümcke, I. (2018). Epigenetics in epilepsy. *Neurosci. Lett.* 667, 40–46. doi: 10.1016/j.neulet.2017.01.012

Köhling, R., and Avoli, M. (2006). Methodological approaches to exploring epileptic disorders in the human brain in vitro. *J. Neurosci. Methods* 155, 1–19. doi: 10.1016/j.jneumeth.2006.04.009

Kojima, N., Borlikova, G., Sakamoto, T., Yamada, K., Ikeda, T., Itohara, S., et al. (2008). Inducible cAMP early repressor acts as a negative regulator for kindling epileptogenesis and long-term fear memory. *J. Neurosci.* 28, 6459–6472. doi: 10.1523/JNEUROSCI.0412-08.2008

Kraus, L., Hetsch, F., Schneider, U. C., Radbruch, H., Holtkamp, M., Meier, J. C., et al. (2019). Dimethylethanolamine decreases epileptiform activity in acute human hippocampal slices in vitro. *Front. Mol. Neurosci.* 12:209. doi: 10.3389/fnmol.2019.00209

Kraus, L., Monni, L., Schneider, U. C., Onken, J., Spindler, P., Holtkamp, M., et al. (2020). Preparation of acute human hippocampal slices for electrophysiological recordings. *J. Vis. Exp.* 159, 1–9. doi: 10.3791/61085

Löscher, W. (2017). Animal models of seizures and epilepsy: past, present, and future role for the discovery of antiseizure drugs. *Neurochem. Res.* 42, 1873–1888. doi: 10.1007/s11064-017-2222-z

Lund, I. V., Hu, Y., Raol, Y. S. H., Benham, R. S., Faris, R., Russek, S. J., et al. (2008). BDNF selectively regulates GABAA receptor transcription by activation of the JAK/STAT pathway. *Sci. Signal.* 1:ra9. doi: 10.1126/scisignal.1162396

Massamiri, T., Khrestchatisky, M., and Ben-Ari, Y. (1994). Induction of c-fos mRNA expression in an in vitro hippocampal slice model of adult rats after kainate but not γ-aminobutyric acid or bicuculline treatment. *Neurosci. Lett.* 166, 73–76. doi: 10.1016/0304-3940(94)90843-5

Mathie, A., Wooltorton, J. R. A., and Watkins, C. S. (1998). Voltage-activated potassium channels in mammalian neurons and their block by novel pharmacological agents. *Gen. Pharmacol.* 30, 13–24. doi: 10.1016/S0306-3623(97)00034-7

Mihály, A., Szakács, R., Bohata, C., Dobó, E., and Krisztin-Péva, B. (2001). Time-dependent distribution and neuronal localization of c-fos protein in the rat hippocampus following 4-aminopyridine seizures. *Epilepsy Res.* 44, 97–108. doi: 10.1016/S0920-1211(01)00190-5

Müller, M., and Somjen, G. G. (1999). Intrinsic optical signals in rat hippocampal slices during hypoxia-induced spreading depression-like depolarization. *J. Neurophysiol.* 82, 1818–1831. doi: 10.1152/jn.1999.82.4.1818

Overwater, I. E., Rietman, A. B., van Eeghen, A. M., and de Wit, M. C. Y. (2019). Everolimus for the treatment of refractory seizures associated with tuberous sclerosis complex (TSC): Current perspectives. *Ther. Clin. Risk Manag.* 15, 951–955. doi: 10.2147/TCRM.S145630

Paxinos, G., and Watson, C. (1998). *The Rat Brain in Stereotaxic Coordinates*, 4th Edn. San Diego, CA: Academic Press.

Pennypacker, K. R., Thai, L., Hong, J. S., and McMillian, M. K. (1994). Prolonged expression of AP-1 transcription factors in the rat hippocampus after systemic kainate treatment. *J. Neurosci.* 14, 3998–4006. doi: 10.1523/jneurosci.14-07-03998.1994

Perreault, P., and Avoli, M. (1991). Physiology and pharmacology of epileptiform activity induced by 4-aminopyridine in rat hippocampal slices. *J. Neurophysiol.* 65, 771–785. doi: 10.1152/jn.1991.65.4.771

Pfaffl, M. W. (2001). A new mathematical model for relative quantification in real-time RT-PCR. *Nucleic Acids Res.* 29, 2002–2007. doi: 10.1093/nar/29.9.e45

Porter, B. E., Lund, I. V., Varodayan, F. P., Wallace, R. W., and Blendy, J. A. (2008). The role of transcription factors cyclic-AMP responsive element modulator (CREM) and inducible cyclic-AMP early repressor (ICER) in epileptogenesis. *Neuroscience* 152, 829–836. doi: 10.1016/j.neuroscience.2007.10.064

Rakhade, S. N., Yao, B., Ahmed, S., Asano, E., Beaumont, T. L., Shah, A. K., et al. (2005). A common pattern of persistent gene activation in human neocortical epileptic foci. *Ann. Neurol.* 58, 736–747. doi: 10.1002/ana.20633

Rydbirk, R., Folke, J., Winge, K., Aznar, S., Pakkenberg, B., and Brudek, T. (2016). Assessment of brain reference genes for RT-qPCR studies in neurodegenerative diseases. *Sci. Rep.* 6:37116. doi: 10.1038/srep37116

Sadangi, C., Rosenow, F., and Norwood, B. A. (2017). Validation of reference genes for quantitative gene expression analysis in experimental epilepsy. *J. Neurosci. Res.* 95, 2357–2366. doi: 10.1002/jnr.24089

Smith, A. J., Tauskela, J. S., Stone, T. W., and Smith, R. A. (2009). Preconditioning with 4-aminopyridine protects cerebellar granule neurons against excitotoxicity. *Brain Res.* 1294, 165–175. doi: 10.1016/j.brainres.2009.07.061

Szyndler, J., Maciejak, P., Turzyñska, D., Sobolewska, A., Taracha, E., and Skórzewska, A. (2009). Mapping of c-Fos expression in the rat brain during the evolution of pentylenetetrazol-kindled seizures. *Epilepsy Behav.* 16, 216–224. doi: 10.1016/j.yebeh.2009.07.030

Taubenfeld, S. M., Stevens, K. A., Pollonini, G., Ruggiero, J., and Alberini, C. M. (2002). Profound molecular changes following hippocampal slice preparation: loss of AMPA receptor subunits and uncoupled mRNA/protein expression. *J. Neurochem.* 81, 1348–1360. doi: 10.1046/j.1471-4159.2002.00936.x

Tauskela, J. S., Fang, H., Hewitt, M., Brunette, E., Ahuja, T., Thivierge, J. P., et al. (2008). Elevated synaptic activity preconditions neurons against an in vitro model of ischemia. *J. Biol. Chem.* 283, 34667–34676. doi: 10.1074/jbc.M805624200

Ting, J. T., Daigle, T. L., Chen, Q., and Feng, G. (2014). Acute brain slice methods for adult and aging animals: application of targeted patch clamp analysis and optogenetics. *Methods Mol. Biol.* 1183, 221–242. doi: 10.1007/978-1-4939-1096-0_14

Vandesompele, J., de Preter, K., Pattyn, F., Poppe, B., van Roy, N., de Paepe, A., et al. (2002). accurate normalization of real-time quantitative RT-PCR data by geometric averaging of multiple internal control genes. *Genome Biol.* 3, 1–11. doi: 10.1186/gb-2002-3-7-research0034

Verwer, R. W. H., Hermens, W. T. J. M. C., Dijkhuizen, P. A., Brake, O. T., Baker, R. E., Salehi, A., et al. (2002). Cells in human postmortem brain tissue slices remain alive for several weeks in culture. *FASEB J.* 16, 54–60. doi: 10.1096/fj.01-0504com

Wang, F., Chen, F., Wang, G., Wei, S., Fang, F., Kang, D., et al. (2018). Rapamycin provides anti-epileptogenic effect in a rat model of post-traumatic epilepsy via deactivation of mTOR signaling pathway. *Exp. Ther. Med.* 15, 4763–4770. doi: 10.3892/etm.2018.6004

Weissinger, F., Wawra, M., Fidzinski, P., Elsner, M., Meierkord, H., Holtkamp, M., et al. (2017). Dentate gyrus autonomous ictal activity in the status epilepticus rat model of epilepsy. *Brain Res.* 1658, 1–10. doi: 10.1016/j.brainres.2016.12.030

Wickham, J., Brödjegård, N. G., Vighagen, R., Pinborg, L. H., Bengzon, J., Woldbye, D. P. D., et al. (2018). Prolonged life of human acute hippocampal slices from temporal lobe epilepsy surgery. *Sci. Rep.* 8:4158. doi: 10.1038/s41598-018-22554-9

Willoughby, J. O., Mackenzie, L., Medvedev, A., and Hiscock, J. J. (1995). Distribution of Fos-positive neurons in cortical and subcortical structures after picrotoxin-induced convulsions varies with seizure type. *Brain Res.* 683, 73–87. doi: 10.1016/0006-8993(95)00366-X

World Health Organization (2006). *WHO, Neurological Disorders: Public Health Challenges, 1. Nervous System Diseases. 2. Public Health. 3. Cost of Illness. I.* Switzerland: WHO Press.

Yang, H., Shan, W., Zhu, F., Yu, T., Fan, J., Guo, A., et al. (2019). C-Fos mapping and EEG characteristics of multiple mice brain regions in pentylenetetrazol-induced seizure mice model. *Neurol. Res.* 41, 749–761. doi: 10.1080/01616412.2019.1610839

Zeng, L. H., Rensing, N. R., and Wong, M. (2009). The mammalian target of rapamycin signaling pathway mediates epileptogenesis in a model of temporal lobe epilepsy. *J. Neurosci.* 29, 6964–6972. doi: 10.1523/JNEUROSCI.0066-09.2009

Zhang, B., and Wong, M. (2012). Pentylenetetrazole-induced seizures cause acute, but not chronic, mTOR pathway activation in rat. *Epilepsia* 53, 506–511. doi: 10.1111/j.1528-1167.2011.03384.x

Conflict of Interest: The authors declare that the research was conducted in the absence of any commercial or financial relationships that could be construed as a potential conflict of interest.

frontiers in Molecular Neuroscience

ORIGINAL RESEARCH
published: 13 August 2021
doi: 10.3389/fnmol.2021.730811

Reelin Is Required for Maintenance of Granule Cell Lamination in the Healthy and Epileptic Hippocampus

Catarina Orcinha[1†], Antje Kilias[2†], Enya Paschen[1,3], Marie Follo[4] and Carola A. Haas[1,5]*

[1] Experimental Epilepsy Research, Department of Neurosurgery, Medical Center – University of Freiburg, Faculty of Medicine, University of Freiburg, Freiburg im Breisgau, Germany, [2] Biomicrotechnology, Department of Microsystems Engineering (IMTEK), University of Freiburg, Freiburg im Breisgau, Germany, [3] Faculty of Biology, University of Freiburg, Freiburg im Breisgau, Germany, [4] Lighthouse Core Facility, Department of Internal Medicine I, Medical Center – University of Freiburg, Faculty of Medicine, University of Freiburg, Freiburg im Breisgau, Germany, [5] Center for Basics in NeuroModulation, Faculty of Medicine, University of Freiburg, Freiburg im Breisgau, Germany

OPEN ACCESS

Edited by:
Lars Klimaschewski,
Medical University of Innsbruck, Austria

Reviewed by:
Stephan Wolfgang Schwarzacher,
Goethe University Frankfurt, Germany
Lars Fester,
Friedrich-Alexander-Universität Erlangen-Nürnberg, Germany

***Correspondence:**
Carola A. Haas
carola.haas@uniklinik-freiburg.de

†Present address:
Catarina Orcinha,
Department of Internal Medicine I, Hematology, Oncology and Stem Cell Transplantation, Medical Center – University of Freiburg, Faculty of Medicine, University of Freiburg, Freiburg im Breisgau, Germany
Antje Kilias,
Institute for Physiology I, Systemic and Cellular Neurophysiology, Faculty of Medicine, University of Freiburg, Freiburg im Breisgau, Germany

Specialty section:
This article was submitted to Brain Disease Mechanisms, a section of the journal Frontiers in Molecular Neuroscience

Received: 25 June 2021
Accepted: 26 July 2021
Published: 13 August 2021

Citation:
Orcinha C, Kilias A, Paschen E, Follo M and Haas CA (2021) Reelin Is Required for Maintenance of Granule Cell Lamination in the Healthy and Epileptic Hippocampus. Front. Mol. Neurosci. 14:730811. doi: 10.3389/fnmol.2021.730811

One characteristic feature of mesial temporal lobe epilepsy is granule cell dispersion (GCD), a pathological widening of the granule cell layer in the dentate gyrus. The loss of the extracellular matrix protein Reelin, an important positional cue for neurons, correlates with GCD formation in MTLE patients and in rodent epilepsy models. Here, we used organotypic hippocampal slice cultures (OHSC) from transgenic mice expressing enhanced green fluorescent protein (eGFP) in differentiated granule cells (GCs) to monitor GCD formation dynamically by live cell video microscopy and to investigate the role of Reelin in this process. We present evidence that following treatment with the glutamate receptor agonist kainate (KA), eGFP-positive GCs migrated mainly toward the hilar region. In the hilus, Reelin-producing neurons were rapidly lost following KA treatment as shown in a detailed time series. Addition of recombinant Reelin fragments to the medium effectively prevented the KA-triggered movement of eGFP-positive GCs. Placement of Reelin-coated beads into the hilus of KA-treated cultures stopped the migration of GCs in a distance-dependent manner. In addition, quantitative Western blot analysis revealed that KA treatment affects the Reelin signal transduction pathway by increasing intracellular adaptor protein Disabled-1 synthesis and reducing the phosphorylation of cofilin, a downstream target of the Reelin pathway. Both events were normalized by addition of recombinant Reelin fragments. Finally, following neutralization of Reelin in healthy OHSC by incubation with the function-blocking CR-50 Reelin antibody, GCs started to migrate without any direction preference. Together, our findings demonstrate that normotopic position of Reelin is essential for the maintenance of GC lamination in the dentate gyrus and that GCD is the result of a local Reelin deficiency.

Keywords: dentate granule cells, hippocampus, granule cell dispersion, epilepsy, Reelin

INTRODUCTION

Reelin is a key regulator of neuronal positioning during mammalian brain development, acting as a possible stopping signal (Dulabon et al., 2000; Chai et al., 2009; Sekine et al., 2011). Additionally, Reelin it is also important for synaptic function, plasticity and memory formation in the adult brain (for review see Herz and Chen, 2006; D'Arcangelo, 2014; Jossin, 2020). During development of

telencephalic structures, such as the cerebral cortex and the hippocampus, Reelin is synthesized by early born Cajal-Retzius (CR) cells, later mainly by interneurons (Alcántara et al., 1998; Pesold et al., 1998). Reelin is a large glycoprotein, which is secreted into the extracellular matrix, where it is proteolytically cleaved into smaller isoforms, an important prerequisite for activation of target cells (Jossin et al., 2004, 2007; Tinnes et al., 2011; 2013). Cleavage of Reelin can occur at two sites: N-terminally between the second and the third repeat, and C-terminally between the sixth and seventh repeat, generating five isoforms depending on the protease in action (Lambert de Rouvroit et al., 1999; Jossin et al., 2004; Sato et al., 2016). However, which Reelin fragment is required for the normal Reelin signaling is still a matter for debate. Some research shows that the so-called central Reelin fragment, consisting of repeats 3–6 (R3-6), is imperative for receptor activation (D'Arcangelo et al., 1999; Jossin et al., 2004; Lee and D'Arcangelo, 2016), whilst other results demonstrate that the N-terminal (Nakajima et al., 1997; Dulabon et al., 2000) or C-terminal (Nakano et al., 2007) portion of the Reelin molecule is significant.

The canonical Reelin pathway involves binding of Reelin to lipoprotein receptors, the very-low-density lipoprotein receptor (VLDLR) and the apolipoprotein E receptor 2 (ApoER2), leading to tyrosine phosphorylation of the intracellular adaptor protein Disabled-1 (Dab1). Since VLDLR and ApoER2 lack core kinase activity, this is compensated for by the recruitment of Src family kinases. It results in the subsequent activation of downstream effectors, which target the actin and microtubule cytoskeleton (D'Arcangelo et al., 1999; Howell et al., 1999; Tissir and Goffinet, 2003; Stolt and Bock, 2006; Jossin and Goffinet, 2007; Leemhuis and Bock, 2011; Bock and May, 2016). Recently, it was reported that Reelin also interacts genetically and biochemically with ephrin/EphB receptors (Sentürk et al., 2011; Bouché et al., 2013). Ephrin/EphB and Reelin signaling share several downstream effector molecules and there is considerable overlap in the processes regulated by ephrinB/EphB and Reelin, showing that these molecules help mediate Reelin signaling outcomes (reviewed in Niethamer and Bush, 2019).

Dysregulation of Reelin signaling has been associated with several brain disorders such as autism, schizophrenia, bipolar disorder, depression, Alzheimer's disease and epilepsy (reviewed in Ishii et al., 2016; Devinsky et al., 2018; Armstrong et al., 2019). The pathoetiologies of these conditions have been associated with aberrant brain cytoarchitecture, impaired synapse formation and stability and improper neuronal migration, most likely caused by a loss of Reelin. False neuronal positioning is particularly observed in mesial temporal lobe epilepsy (MTLE), typified by recurrent focal seizures and Ammon's horn sclerosis (Thom, 2014). The latter is characterized by neuronal loss and often by granule cell dispersion (GCD), a malpositioning of dentate granule cells (GCs) (Houser, 1990; Haas et al., 2002).

There is evidence that a loss of Reelin is involved GCD formation, since the Reelin-deficient *reeler* mouse (D'Arcangelo et al., 1995; Hirotsune et al., 1995) shows a disorganized granule cell layer (GCL), reminiscent of GCD (Frotscher et al., 2003). Moreover, GCD formation has been shown to be accompanied by a loss of Reelin-producing neurons in the hippocampus of MTLE patients (Haas et al., 2002; Liu et al., 2020) and in rodent epilepsy models (Heinrich et al., 2006; Gong et al., 2007; Antonucci et al., 2008; Duveau et al., 2011; Orcinha et al., 2016). A local rescue of GC lamination has been achieved *in vivo* by infusion of recombinant Reelin into the mouse hippocampus during epileptogenesis (Müller et al., 2009) and *in vitro* by addition of recombinant Reelin in kainate (KA)-treated organotypic hippocampal slice cultures (OHSC; Orcinha et al., 2016). Conversely, neutralization of Reelin in the healthy mouse hippocampus by infusion of the function-blocking CR-50 antibody caused a local widening of the GCL (Heinrich et al., 2006). GCD can be induced *in vitro* in OHSCs by KA application (Tinnes et al., 2011, 2013; Chai et al., 2014). In this *in vitro* model, differentiated GCs have been shown to migrate via somal translocation (Murphy and Danzer, 2011; Chai et al., 2014), but so far the precise mechanism has remained unclear.

In the present study, we used KA-treated OHSC from transgenic mice expressing enhanced green fluorescent protein (eGFP) in differentiated GCs (1) to monitor the movement behavior of individual GCs in detail by live cell video microscopy, (2) to investigate which part of the Reelin molecule is efficient in GCD rescue, (3) whether the site of the Reelin loss matters, and (4) whether Reelin is needed for the maintenance of lamination in the healthy hippocampus. We present evidence that differentiated GCs actively migrate toward the Reelin-free hilar region and this motility can be prevented by application of the recombinant N-terminal or the central Reelin fragment. In addition, we show that placement of Reelin-coated beads into the hilus significantly stops the aberrant migration of GCs after KA exposure, and that neutralization of Reelin by the CR-50 antibody causes locomotion of GCs in healthy OHSC.

MATERIALS AND METHODS

Animals

Experiments were performed with transgenic Thy1-eGFP mice, in which eGFP is expressed under the control of the Thy1 promoter in a subpopulation of differentiated GCs in the dentate gyrus (RRID: IMSR_JAX:007788, M-line, C57BL/6 background, Feng et al., 2000). Mice were bred at the Center for Experimental Models and Transgenic Service (CEMT), University of Freiburg, and kept in a 12 h light/dark cycle at room temperature (RT) with food and water *ad libitum*. All animal procedures were handled according to the guidelines of the European Community's Council Directive of 22 September 2010 (2010/63/EU) and were approved by the regional council (Regierungspräsidium Freiburg).

Organotypic Hippocampal Slice Cultures (OHSC)

Seven- or eight-days-old (P7-P8) male and female Thy1-eGFP mouse pups were used for OHSC preparation as described previously (Gerlach et al., 2016; Orcinha et al., 2016). In brief, brains were rapidly removed from the skull after decapitation under isoflurane (Abbott) anesthesia. The hippocampi were dissected and sliced (400 μm) perpendicular to the longitudinal

axis of the hippocampus using a McIlwain tissue chopper. Only slices from the mid portion of each hippocampus were used. The slices were placed onto culture inserts (Millicell cell culture inserts, RRID:SCR_015799, Merck) and transferred to 6-well plates with 1 mL of incubation medium (pH 7.2) per well containing 50% minimal essential medium (MEM, Gibco), 25% basal medium Eagle (BME, Gibco), 25% heat-inactivated horse serum (Gibco) supplemented with 0.65% glucose (Braun) and 2 mM glutamate (Gibco). OHSC were incubated as static cultures (Stoppini et al., 1991) in 5% CO_2 at 37°C for at least 7 days *in vitro* (DIV) to allow full eGFP expression (Chai et al., 2014) which was checked using an inverted epifluorescence microscope (Olympus CKX41 with U-RFL-T, Olympus). Incubation medium was changed every second day.

Live Cell Imaging

Organotypic hippocampal slice cultures were prepared as described above and cultivated for 7 – 18 DIV for the different live cell imaging experiments. Immediately before imaging, OHSC were handled as follows: (1) to monitor the migration behavior of individual GCs, OHSC were treated with KA (10 μM; Tocris) for 45 min, followed by addition of fresh medium with or without recombinant Reelin fragments (1 nM); Reelin fragments were produced as previously described in Orcinha et al. (2016); (2) to study the influence of Reelin in normotopic position within the dentate gyrus, OHSC were treated with KA (10 μM) for 45 min followed by addition of fresh medium, and placement of Reelin-coated fluorescent microspheres into the hilus (see below); and (3) to neutralize endogenous Reelin, the monoclonal CR-50 antibody (8 μg/mL; MBL Int. Corp) or normal mouse IgG (8 μg/mL; Santa Cruz) was added to fresh medium. In all control experiments, OHSC were cultured in fresh medium, only.

For live cell imaging, a laser scanning confocal microscope (Zeiss LSM 880) was used equipped with a multiline Argon 488 nm scanning laser. OHSC were securely placed in a stage enclosed in an aerated chamber at 37°C with humidified atmosphere containing 5% CO_2, and were imaged along the *z*-axis with a spacing of 7 μm using a 20× objective (Plan Apochromat NA 0.8), at 45 min intervals over a period of 8 h (stack acquisition between each interval took roughly 15 min). The lowest laser power setting was used to avoid photo bleaching and associated photo damage. At the end of the imaging period, the confocal z-stacks obtained for each time point were converted to a maximum projection image using the Zen 2 lite software (Zeiss) and exported as TIFF-files for further analysis.

Analysis of Migration Behavior

To assess the migration pattern and direction of individual eGFP-positive GCs, a custom Matlab® software script (Matlab R2017b, RRID:SCR_001622, The-MathWorks) was applied. The confocal image stacks obtained at the different time points were imported into the analysis script and individual eGFP-positive GCs were automatically detected and numbered (**Supplementary Figures 1A,B**). Only cells with a diameter of approximately 10 μm and visible throughout all raw images were flagged by the function trackCells in the custom script. Taking into account the scaling factor (conversion from pixel to μm), cell motility was quantified by calculating (1) the total path length (**Supplementary Figure 1C**, totalDist) over 8 h and (2) the effective migration distance (**Supplementary Figure 1C**, effectDist) as the length of the resulting vector between start and end point (**Supplementary Figure 1C**, start and finish). These values were also used to calculate the directionality ratio as the quotient of effective distance and total path length according to Gorelik and Gautreau (2014) (**Supplementary Figure 1C**). If the neuron had a straight trajectory, this ratio was close to 1.0 (0.80 – 1.0). If the values were smaller (<0.80), a frequent change in direction had occurred. To analyze the migration direction, the border between hilus and GCL (white dotted line in **Supplementary Figure 1A**) or between microspheres and GCL (white dotted line in **Supplementary Figure 1B**) were marked and the distance of the start and end point to the hilus/microsphere – GCL border was calculated. Cells with a reduced distance to the border [$H_{distance}(t = 0\ h) - H_{distance}(t = 8\ h)$] were considered to migrate toward the hilus, whereas cells with an increased distance in relation to the hilus-GCL/microsphere border moved toward the molecular layer (ML).

Preparation of Reelin-Coated Fluorescent Microspheres

For the application of Reelin into the hilus of OHSC, red fluorescent latex beads (10 μL; Lumafluor Inc.) were incubated with recombinant full-length (FL) Reelin (1 nM) overnight at 4°C with mild agitation. Then, microspheres were centrifuged, the supernatant was removed, and the remaining beads were resuspended in 5 μL of sterile saline as previously described (Dulabon et al., 2000). A 0.8 nL bead solution (uncoated or Reelin-coated) was placed into the hilus of each OHSC using a programmable nanoliter injector (Nanoject III, Drummond) with a glass pipet fixed to a micromanipulator. Due to the broad bandwidth of the fluorophore used to produce the red beads, it was possible to detect them easily during the live cell imaging experiments using the green channel (see **Supplementary Figure 2**).

Immunohistochemistry

For the time course analysis of Reelin expression following KA application, OHSC were treated with KA (10 μM) for 45 min followed by incubation in fresh medium. Slices were fixed at 0 (immediately after KA treatment), 1, 2, 3, 4, 6, and 8 h post-KA with 4% paraformaldehyde (PFA, Roth) in 0.1 M phosphate buffer (PB; pH 7.4; 4 h at RT) and subsequently rinsed several times in PB. Immunolabeling for Reelin was performed using a free-floating protocol (Orcinha et al., 2016). After pre-treatment (0.25% Triton X-100, 10% normal serum in PB, 2 h at RT), slices were incubated (0.1% Triton X-100, 1% normal serum in PB, 24 h at RT) with a mouse monoclonal anti-Reelin antibody (G10, 1:1.000, Millipore, Cat# MAB5364, RRID: AB_2179313). Antibody binding was visualized by incubation with a goat anti-mouse Cy5-conjugated secondary antibody (1:400, RRID: AB_2338714, Jackson ImmunoResearch Laboratories) in the dark

(6 h at RT) and counterstained with DAPI (4′,6-diamidino-2-phenylindole; 1:10.000, Roche). Whole slices were dried on glass slides, coverslipped with anti-fading mounting medium (DAKO, Sigma Aldrich, United States) and stored in the dark at 4°C.

Quantification of Reelin-Immunofluorescence in OHSC

Immunolabeled slices were analyzed with an epifluorescence microscope (Axio Imager 2 with ZEN blue software, Zeiss) and photomicrographs were taken with a 10-fold objective (Plan Apochromat, NA 0.45). Exposure times were kept constant to allow comparison between individual slices. To quantify fluorescence intensity of Reelin signals in the hilus, photomicrographs were converted to grayscale and the signal intensity was quantified as integrated density using the ImageJ software (ImageJ, RRID: SCR_003070). The regions of interest were manually outlined with the polygon selection tool. Values were corrected by background subtraction: integrated density – (measured area × mean background signal). Background was measured in each picture in a small region close to the area of interest and without Reelin signal. The mean background was calculated for each experiment and for the area of the hilus.

Western Blot Analysis

Eight – ten OHSC per animal and treatment were pooled and placed in 200 μL of lysis buffer (50 mM Tris pH 8.0, 150 mM NaCl, 1% Triton, supplemented with protease inhibitor cocktail cOmplete^{TM} and phosphatase inhibitor tablets PhosSTOP^{TM} (Roche Diagnostics). The samples were homogenized, the protein suspension was shaken for 15 min at 4°C and the insolubilized fraction was removed by centrifugation at 12,500 rpm for 10 min at 4°C. The supernatant was collected, and protein concentration was quantified using the Bicinchoninic Acid Assay (BCA) kit (Pierce). The protein concentration was determined following the instructions described in the manual. For the colorimetric measurement, the absorbance was read at 562 nm using bovine serum albumin (BSA) as standard.

For electrophoresis, 20 μg of total protein per lane were mixed with loading buffer. The samples were size-fractionated by standard sodium dodecyl sulfate – polyacrylamide gel electrophoresis (NuPAGE^{TM}, 4–12% Bis-Tris gel, Invitrogen) and transferred to polyvinylidene difluoride membranes (Roche Diagnostics). Membranes were blocked with I-Block (Tropix) or 5% BSA (for phosphorylated cofilin) in Tris-buffered saline with Tween-20 (TBST) for 1 h, washed with TBST and incubated overnight at 4°C with the following primary antibodies: rabbit polyclonal anti-Dab1 (1:1.000; Abcam), rabbit monoclonal anti-GAPDH (1:10.000; Clone 14C10; Cell Signaling) and rabbit polyclonal anti-p-cofilin (Ser3) (1:1.000; Cell Signaling). After several washing steps, the membranes were incubated with goat anti-rabbit alkaline-phosphatase-conjugated secondary antibody (1:10.000; Tropix) for 1 h at RT or overnight at 4°C and CDP Star (Tropix) was used as substrate for chemiluminescent detection by the Fusion FX Western Blot Imaging System (Vilber Lourmat).

Quantification of Western blot signals was attained with ImageJ software and GAPDH density was used as the loading control. In brief, images were opened with the ImageJ software and the color was inverted so that the bands turned black. The bands of interest were marked with the rectangle tool and the band intensity was measured with the "Gels" function available in the software. The band intensity peaks were plotted and the peaks were separated using the line tool. The area under each peak was measured and the size of the peak was indicated as percent of the total size of all of the highlighted peaks. The peak percentage of each analyzed protein was divided by the peak percentage of the respective loading control to give the relative percent of expression for each protein and each condition. These values were normalized to the control band and the relative value for the control group was always set as 100%. The experiments were repeated at least three times for each condition.

Statistical Analysis

All values were expressed as mean ± standard deviation. All statistical analysis was performed with GraphPad Prism 7 software (RRID: SCR_002798). Differences between groups were tested for statistical significance (Unpaired student's *t*-test or one-way ANOVA with Tukey's multiple comparison test). Significance levels were set to $^{*}P < 0.05$, $^{**}P < 0.01$, $^{***}P < 0.001$.

RESULTS

Migration Behavior of eGFP-Positive Granule Cells in OHSC After KA Treatment

First, we investigated the migration behavior of individual eGFP-positive GCs in KA-challenged OHSC in real time by life microscopy. To this end, OHSC were prepared from Thy1-eGFP mice, in which eGFP is expressed exclusively in differentiated dentate GCs (Chai et al., 2014; Orcinha et al., 2016) and were cultured for 7 days. OHSC were exposed to 10 μM KA for 45 min, followed by incubation in fresh medium and live cell imaging with a laser scanning confocal microscope (**Figures 1A,B**). Confocal stacks were acquired every hour over a period of 8 h and were evaluated offline by a custom script. The individual eGFP-positive GCs were automatically detected throughout the GCL and their position was tracked with respect to a manually drawn border between the hilus and GCL over the whole observation period (**Supplementary Figure 1**). The differences in motility were quantified by calculating (1) the total length of the traveled path over 8 h, (2) the effective distance of migration as the length of the vector between start ($t = 0$ h) and end point ($t = 8$ h), and (3) the directionality ratio (see in detail in "Materials and Methods").

Granule cells showed a significantly higher motility after KA treatment ($n = 20$ slices, 868 cells) when compared to control conditions ($n = 23$ slices, 548 cells) (**Figures 1A,B**), evident from an increased effective distance (in μm: controls: 3.065 ± 1.358; KA: 8.075 ± 2.975; unpaired *t*-test: $P < 0.001$). In contrast to controls (**Figure 1C**; Pearson correlation coefficient $r = -0.04558$; ns with $P = 0.2525$), almost all analyzed GCs migrated after KA treatment regardless of their position within

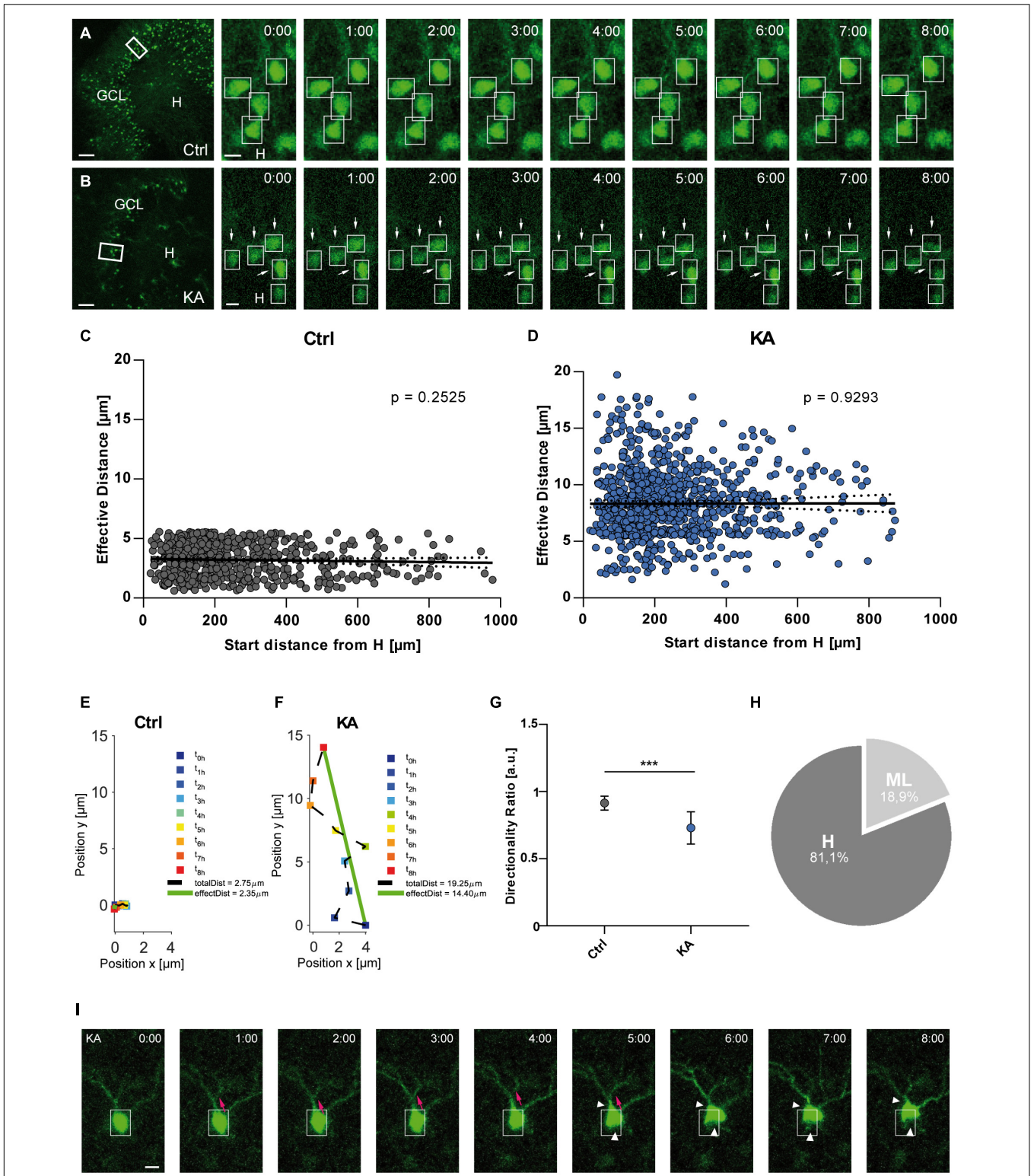

FIGURE 1 | EGFP-positive GCs migrate preferentially toward the hilus after KA treatment. Live cell imaging of individual eGFP-labeled GCs in control OHSC and after exposure to KA over a period of 8 h. **(A,B)** Representative confocal micrographs of nine imaging time points are shown for each condition. Left panel: overview; white frame indicates the area shown at high magnification on the right. Tracked cells are marked by white frames. **(A)** Untreated control. GCs do not change position. **(B)** Treatment with 10 µM KA for 45 min. GCs with high motility are indicated by arrows. Scale bars: 80 µm for overview; 10 µm for high magnifications. **(C,D)** Quantitative evaluation of migration distances of individual GCs in controls (**C**; *n* = 23 slices, 548 cells) and in KA-treated OHSC (**D**; *n* = 20 slices, 868 cells).

(Continued)

FIGURE 1 | Continued
Each slice was from a different animal. In contrast to controls **(C)**, almost all GCs change their positions after KA treatment **(D)** and travel mainly toward the hilus regardless of their initial position in the GCL. **(E,F)** Graphs showing the representative behavior of an individual, tracked neuron in a control **(E)** and a KA-treated OHSC **(F)**. Cell motility was assessed by calculating both the total length of the traveled path over 8 h (black dashed line = total distance) and the effective distance of the migration as the length of the resulting vector (green solid line) between start (t = 0 h) and end point (t = 8 h). Note the meandering way of migration in the KA group. **(G)** Diagram showing the directionality ratio (defined as ratio of total to effective distance). GCs from KA-treated slices have a lower directionality ratio than controls since they undergo requent changes in direction. **(H)** Relative distribution of GCs traveling toward the hilus (81.1%) or molecular layer (18.9%) in KA-treated OHSC. Unpaired student's t-test (***$P < 0.001$). **(I)** Morphological changes following KA application. Representative GC from a KA-exposed culture imaged for 8 h. There is a clear change in the shape of the soma (white arrow heads) and migration of the soma into a dendritic branch (magenta arrows). Scale bar: 5 μm. GCL, granule cell layer; H, hilus; Ctrl, control.

the GCL (**Figure 1D**; Pearson correlation coefficient $r = 0.00288$; ns with $P = 0.9293$). We also found different populations of GCs: some traveled longer distances than others and a small population of neurons did not change their position. Analysis of the migration behavior revealed that GCs in KA-treated OHSCs did not move straight ahead, but were meandering, indicated by a reduced directionality ratio (0.7295 ± 0.1201) (**Figures 1E–G**). If a neuron has a straight trajectory, this ratio is close to 1.0 (0.8 – 1.0), if there are frequent changes in direction, the ratio is below 0.8. In addition, many GCs (81.1%) in KA-treated slices migrated in the direction of the hilus, whereas only a minority (18.9%) headed toward the molecular layer (**Figure 1H**). The constant, small values of effective distance in control OHSC were interpreted as adjustments to the environment.

Interestingly, the soma shape of migrating GCs was altered as the movement progressed over the 8 h after KA treatment (**Figure 1I**). The soma of the GCs appeared to move up toward one dendritic branch (magenta arrows, **Figure 1I**), then shifted to another one by retraction of the cell body (white arrow heads, **Figure 1I**), gradually displacing the soma. GCs in control slices did not show any morphological changes.

Time Course of Reelin Expression in OHSC Following KA Treatment

To probe the role of Reelin loss in the migratory behavior of GCs following KA exposure, we performed a detailed time course analysis of Reelin expression in OHSC following KA treatment. As before, OHSC were exposed to 10 μM KA for 45 min and were immediately fixed with PFA (0 h time point) or incubated in fresh medium followed by fixation at 1, 2, 3, 4, 6, and 8 h post-KA treatment. Slices were immunolabeled for Reelin and signals were quantified by densitometry (**Figure 2**). Control slices were handled in parallel for the corresponding time points, but since the Reelin signal was consistent in all controls, data were pooled (**Figure 2A**).

In control OHSC, many brightly labeled Reelin-positive neurons were present at the hippocampal fissure (HF) and less abundantly distributed in the hilus, consistent with previous reports (Tinnes et al., 2011; Orcinha et al., 2016). In KA-treated OHSC, many Reelin-immunolabeled neurons remained at the hippocampal fissure, but in the hilus the number of Reelin-positive neurons decreased rapidly between 0 and 8 h post-KA treatment when compared with controls (**Figures 2B–H**). Densitometric evaluation revealed a significant loss of the Reelin signal in the hilus already at the end of the KA treatment (0 h), which progressed over the next 3 h. After 4 h, all Reelin-immunolabeled neurons had disappeared from the hilus and no significant differences were found between 4, 6, and 8 h after KA exposure: controls: 17.9 ± 2.36 (n = 21 slices); 0 h: 14.07 ± 1.24 (n = 6 slices); 1 h: 9.24 ± 1.92 (n = 7 slices); 2 h: 8.3 ± 1.15 (n = 8 slices); 3 h: 5.44 ± 0.79 (n = 9 slices); 4 h: 1.16 ± 0.34 (n = 9 slices); 6 h: 0.72 ± 0.32 (n = 5 slices); 8 h: 0.45 ± 0.32 (n = 9 slices); ANOVA: $P < 0.001$; Tukey's post-test: $P < 0.001$; **Figure 2I**). In parallel, we observed morphological changes in the Reelin-expressing neurons in the hilus, they appeared shrunken right after KA exposure, until the 3 h time point (**Figure 2A'–E'**).

This detailed time course showed that Reelin-expressing neurons were rapidly lost (within 3 h) in the hilus following KA treatment, whereas Reelin-synthetizing neurons at the hippocampal fissure survived.

Influence of Recombinant Reelin Fragments on KA-Induced Motility of eGFP-Labeled GCs

So far, we found that in KA-treated OHSC most GCs migrated toward the hilus, where Reelin-expressing neurons were lost within 3 h after KA exposure. If the Reelin loss indeed plays a role in the migration process, addition of exogenous Reelin should influence it. Therefore, we added recombinant Reelin fragments, specifically N-terminal and the central fragment (R3-6, N-R2, N-R6), to the medium after KA treatment and followed GCs by live cell imaging for 8 h.

As before, KA treatment alone caused a significantly increased motility of eGFP-positive GCs when compared to controls (**Figures 3A,B,F**). In contrast, GCs, although treated with KA, did not migrate in the presence of recombinant Reelin fragments: R3-6 (n = 12 slices, 470 cells), N-R2 (n = 9 slices, 284 cells) and N-R6 (n = 7 slices, 228 cells) (**Figures 3C–F**). All three fragments significantly prevented the movement of GCs (in μm: R3-6: 3.448 ± 1.157; N-R2: 3.778 ± 0.9103; N-R6: 3.372 ± 1.108; KA vs. KA+R3-6, KA+N-R2 and KA+NR-6; ANOVA: $P < 0.001$; Tukey's post-test: $P < 0.001$; **Figure 3F**). Also, the directionality ratio was increased after incubation with recombinant Reelin fragments (R3-6: 0.869 ± 0.07; N-R2: 0.835 ± 0.10; N-R6: 0.863 ± 0.08) reaching values similar to controls (0.914 ± 0.05), in contrast to slices exposed to KA alone (Ctrl vs. KA+R3-6, KA+N-R2 and KA+NR-6, ns. KA vs. KA+R3-6, KA+N-R2 and KA+NR-6; ANOVA: $P < 0.001$; Tukey's post-test: $P < 0.001$) (**Figure 3G**). These results indicate that all applied Reelin fragments were able to stop the KA-mediated migration of eGFP-positive GCs,

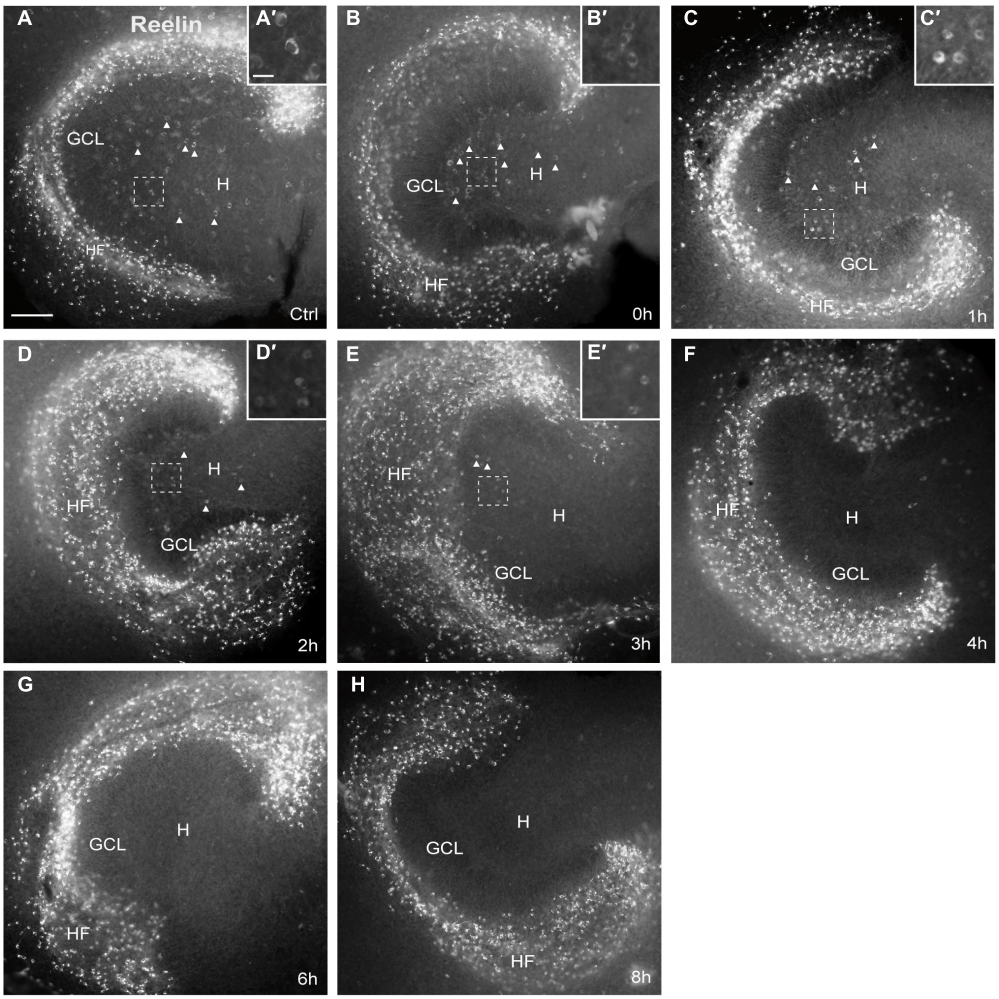

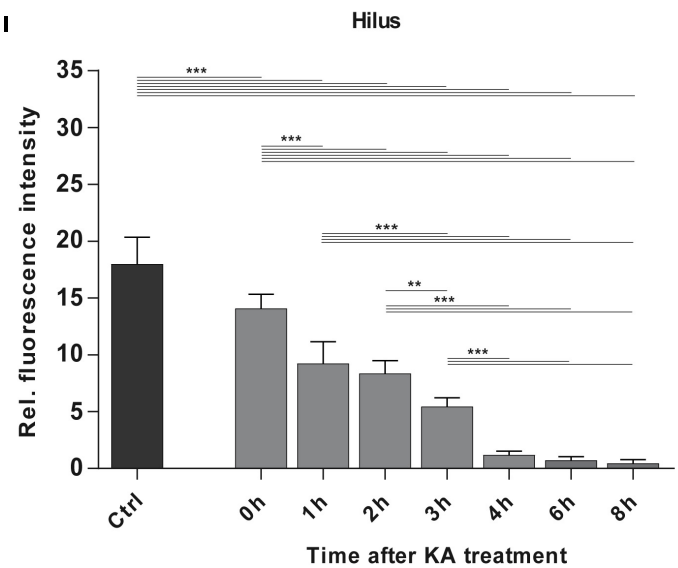

FIGURE 2 | Time course of KA-induced loss of Reelin-expressing neurons in the hilus. Representative images of whole OHSC immunolabeled for Reelin are shown. Small insets show high magnification of Reelin-expressing interneurons in the area of the hilus indicated by the dashed white frame **(A'–E')**. **(A)** In control slices

(Continued)

FIGURE 2 | Continued
(n = 21 slices), many Reelin-positive Cajal-Retzius cells are present at the hippocampal fissure, and large Reelin-immunopositive interneurons **(A')** in the hilus (arrow heads). **(B–H)** Slices were fixed at **(B)** 0 h (=45 min after KA) (n = 6 slices), **(C)** 1 h (n = 7 slices), **(D)** 2 h (n = 8 slices), **(E)** 3 h (n = 9 slices), **(F)** 4 h (n = 9 slices), **(G)** 6 h (n = 5 slices), and **(H)** 8 h (n = 9 slices) after KA application. Reelin-positive cells are completely lost in the hilus at 4 h after treatment, whereas Reelin-expressing neurons at the hippocampal fissure survive throughout all time points. Note the morphological change of the Reelin-expressing interneurons in the hilus between 0 and 3 h **(B'–E')** which appear shrunken. **(I)** Densitometric quantification of the Reelin signal in the hilus in controls and after KA treatment. Note the fast and continuous decline of the Reelin signal within the first 3 h after treatment. One-way ANOVA, followed by Tukey's Multiple Comparison (**P < 0.01; ***P < 0.001). GCL, granule cell layer; H, hilus; HF, hippocampal fissure. Scale bar: 100 μm for overview, 20 μm for insets.

supporting the role for Reelin as a positional signal for GCs in the hippocampus.

Placement of Reelin-Coated Beads Into the Hilus of KA-Treated OHSC

Next, we aimed at addressing the question whether the localization of the exogenous Reelin source matters. To this end, we used fluorescent beads with or without recombinant Reelin, placed them with the help of a micromanipulator into the hilus of healthy or KA-treated OHSC and performed life cell imaging for 8 h as described before. Following imaging, individual eGFP-positive GCs were automatically detected in confocal image stacks and their positions were tracked with respect to a manually drawn border between the beads and the GCL (**Supplementary Figure 1**).

First, we assessed whether application of fluorescent beads had any effect when present in control OHSCs (**Figures 4A,B**). There was no difference in the effective distance of eGFP-positive neurons when uncoated beads (n = 6 slices, 77 cells) or Reelin-coated beads (n = 7 slices, 89 cells) were placed into the hilus of control slices (**Figure 4E**) (in μm: uncoated beads: 2.537 ± 1.518; Reelin-coated beads: 2.456 ± 1.178; Ctrl+uncoated beads vs. Ctrl+Reelin-coated beads, ns; Tukey's post-test: P = 0.9937). Moreover, placement of uncoated beads into KA-treated OHSC did not affect the significantly increased motility of GCs (**Figures 4C,E**) (n = 4 slices, 70 cells; 8.527 ± 2.69 μm; Ctrl+uncoated beads and Ctrl+Reelin-coated beads vs. KA+uncoated beads, ANOVA: P < 0.001; Tukey's post-test: P < 0.001). Interestingly, when Reelin-coated beads were placed into the hilus of KA-treated OHSC (n = 5 slices, 68 cells), the movement of GCs was significantly reduced when compared to GCs from KA-treated slices with uncoated beads (**Figures 4D,E**) (4.596 ± 2.32 μm; KA+uncoated beads vs. KA+Reelin-coated beads, ANOVA: P < 0.001; Tukey's post-test: P < 0.001), but did not reach control levels (Ctrl+uncoated beads and Ctrl+Reelin-coated beads vs. KA+Reelin-coated beads, ANOVA: P < 0.001; Tukey's post-test: P < 0.001).

The directionality ratio showed a lower value in GCs of OHSC exposed to KA with uncoated beads (0.695 ± 0.14) when compared with GCs from untreated slices with uncoated beads or with Reelin-coated beads (Ctrl+uncoated beads: 0.909 ± 0.06; Ctrl+Reelin-coated beads: 0.876 ± 0.08; Ctrl+uncoated beads and Ctrl+Reelin-coated beads vs. KA+uncoated beads, ANOVA: P < 0.001; Tukey's post-test: P < 0.001). However, in KA-treated OHSC with Reelin-coated beads, the ratio was similar to controls (0.885 ± 0.10; Ctrl+uncoated beads and Ctrl+Reelin-coated vs. KA+Reelin-coated beads, ns; KA+uncoated beads vs. KA+Reelin-coated beads, ANOVA: P < 0.001; Tukey's post-test: P < 0.001) (**Figure 4F**). Moreover, as anticipated, there was no correlation between the effective migration distance and the start distance from the beads in both control groups (**Figures 4G,H**) and in the KA+uncoated beads group (**Figure 4I**). In contrast, in KA-treated OHSC with Reelin-coated beads, there was a positive correlation (Pearson correlation coefficient r = 0.7461; P < 0.001) between the effective migration distance and the initial position from the beads (**Figure 4J**). This means that GCs closer to the Reelin source did not change their position significantly (values similar to controls) while more distant GCs did, indicating a concentration-dependent effect of Reelin. Apparently, the Reelin-coated beads created a Reelin gradient to which GCs responded in a distance-dependent manner: keeping them in place when sufficient Reelin was sensed but making them move when Reelin concentration was low.

Effect of KA Application on Intracellular Components of the Reelin Signaling Machinery

Based on the described observations, we aimed at investigating potential effects of KA on the Reelin signal transduction pathway. Dentate GCs express Reelin receptors and the intracellular adaptor protein Dab1 and maintain their expression under epileptic conditions as shown in MTLE patients (Haas et al., 2002) and rodent epilepsy models (Gong et al., 2007; Müller et al., 2009). Activation of the Reelin signal transduction pathway depends on phosphorylation of Dab1 (Howell et al., 1999) and further downstream of cofilin (Chai et al., 2009).

Hence, we investigated intracellular signaling components of the canonical Reelin pathway after KA treatment. OHSC were treated with KA for 45 min, followed by washout, and incubation with or without recombinant Reelin fragments for 8 h. Subsequently, Dab1 and phosphorylated cofilin (p-cofilin) levels were detected by Western blot analysis and densitometrically quantified (**Figure 5**).

Kainate treatment resulted in significantly elevated Dab1 levels synthesis (% of control: 153.9 ± 43.34; n = 3) when compared to controls (Ctrl vs. KA. ANOVA: P < 0.001; Tukey's post-test: P = 0.014; n = 8). Noteworthy, the incubation with the different Reelin fragments resulted equally in a drop of Dab1 levels, significantly different from KA slices (% of controls: controls: 100%; R3-6 (n = 4): 64.76 ± 7.786%; N-R6 (n = 3): 67.94 ± 6.63%; N-R2 (n = 4): 56.16 ± 3.029%; ANOVA: P < 0.001; KA vs. R3-6: Tukey's post-test: P = 0.0005; Ctrl

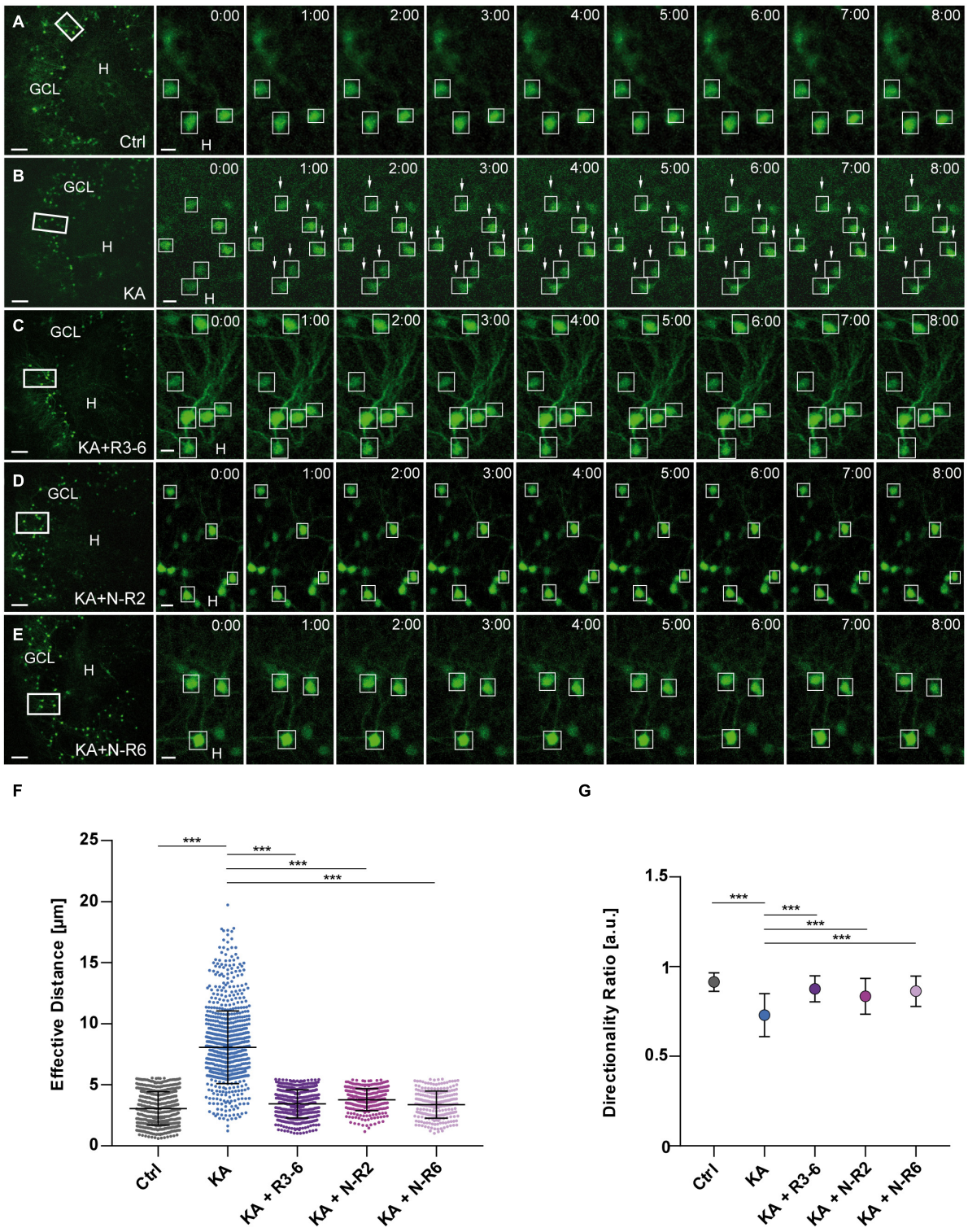

FIGURE 3 | KA-induced migration of differentiated GCs is prevented by recombinant Reelin fragments. **(A–E)** Live cell imaging of individual eGFP-positive GCs was performed over a period of 8 h, and migration distances of automatically selected cells were assessed. Representative confocal micrographs of nine imaging time points are shown for each condition. Left panel: overview; white frame indicates the area shown at high magnification on the right. Tracked cells are marked by white frames. **(A)** Untreated control (n = 23 slices, 548 cells). GCs do not change their position. In all experiments, each slice derived from a different animal. **(B)** Treatment of OHSC with 10 µM KA for 45 min (n = 20 slices, 868 cells). GCs with high motility are indicated by arrows.

(Continued)

FIGURE 3 | Continued
(C–E) Treatment of OHSC with 10 μM KA for 45 min, followed by incubation with fresh medium and subsequent application of recombinant Reelin fragments (each 1 nM). **(C)** R3-6 (n = 12 slices, 470 cells), **(D)** N-R2 (n = 9 slices, 284 cells), and **(E)** N-R6 (n = 7 slices, 228 cells). There is no migration of GCs in cultures treated with Reelin fragments. **(F)** Quantitative evaluation of migration distances of individual GCs. KA-treated GCs migrate, but migration can be prevented by application of the different recombinant Reelin fragments. **(G)** Diagram showing the directionality ratio. GCs from KA-treated slices show a reduced directionality ratio when compared to controls. Following application of the different recombinant Reelin fragments, directionality ratio of GCs reach control values. One-way ANOVA, followed by Tukey's Multiple Comparison Test (***$P < 0.001$; Ctrl vs. KA + R3-6, Ctrl vs. KA + N-R2 and Ctrl vs. KA + N-R6 show no significant difference). GCL, granule cell layer; H, hilus. Scale bars: 80 μm for overview; 10 μm for high magnifications.

vs. N-R6: Tukey's post-test: $P = 0.0007$; KA vs. N-R2: Tukey's post-test: $P = 0.0002$).

The levels of p-cofilin were significantly reduced after KA exposure (% of controls: 57.24 ± 20.17%; Ctrl vs. KA. ANOVA: $P = 0.0051$; Tukey's post-test: $P = 0.0452$). As shown in **Figure 5C**, this effect was abolished after the incubation with the recombinant Reelin fragments N-R6 and N-R2, with values similar to controls (controls: 100%; N-R6: 128.2 ± 9.231%; N-R2: 111.2 ± 41.72%; ANOVA: $P = 0.0051$; Ctrl vs. N-R2: Tukey's post-test: $P = 0.9434$; Ctrl vs. N-R6: Tukey's post-test: $P = 0.4598$). No difference was found between post-KA treatment and incubation with the central fragment R3-6 (R3–6: 78.69 ± 38.37%; KA vs. R3-6; Tukey's post-test: $P = 0.6924$).

Together, these findings show that the loss of Reelin post-KA treatment caused an increase of Dab1 and decrease of p-cofilin levels reminiscent of the *reeler* phenotype (Chai et al., 2009) and addition of Reelin to the culture medium reversed these effects.

Migration Behavior of eGFP-Positive GCs After Neutralization of Reelin

Finally, we tested the effect of Reelin neutralization in healthy OHSC by application of the function-blocking CR-50 antibody known to block Reelin function *in vivo* and *in vitro* (Ogawa et al., 1995; Nakajima et al., 1997; Heinrich et al., 2006). OHSC from Thy1-eGFP mice were incubated with normal medium (control), normal mouse IgG or CR-50 followed by live cell imaging for 8 h (**Figures 6A–C**). Normal mouse IgG was used as a negative control to confirm the specificity of the CR-50 antibody and for ruling out non-specific Fc receptor binding (Burry, 2011). As before, individual eGFP-positive GCs were automatically detected throughout the GCL and their position was tracked with respect to a manually drawn border between the hilus and GCL (**Supplementary Figure 1**).

Granule cells became motile in the presence of CR-50 (**Figure 6C**) with a significantly increased effective distance when compared to controls (**Figure 6D**) [in μm: Ctrl: 2.95 ± 1.22 (n = 15 slices, 183 cells); IgG: 3.221 ± 0.93 (n = 2 slices, 38 cells); CR-50: 9.602 ± 3.78 (n = 10 slices, 254 cells); Ctrl vs. IgG, ns with $P = 0.8564$; Ctrl and IgG vs. CR-50, ANOVA: $P < 0.001$; Tukey's post-test: $P < 0.001$). Interestingly, the directionality ratio was close to 1 (**Figure 6E**) (Ctrl: 0.869 ± 0.06; IgG: 0.871 ± 0.07; CR-50: 0.883 ± 0.09; ANOVA: ns with $P = 0.2280$) portraying a straight migration behavior in the presence of CR-50 (**Figure 6F**). No correlation was found between the start distance from the hilus and the effective distance of eGFP-positive neurons after incubation with CR-50. Almost all cells traveled long distances regardless of their initial position in the deep or superficial GCL (**Figure 6G**) and without any preference in migration direction (**Figure 6H**). In addition, changes occurred in the soma as the neurons shift position (**Figure 6I**). As observed in **Figure 1I**, the soma of the GCs moved up into the apical dendrite (magenta arrows, **Figure 6I**). In this particular case, there is no retraction of the cell body, only change in shape (white arrow heads, **Figure 6I**), and the soma continues moving into the dendritic branch. Altogether, these data clearly show that ubiquitous neutralization of Reelin by the CR-50 antibody caused a non-directional migration of eGFP-positive GCs indicating that Reelin is necessary to maintain GC lamination in the healthy hippocampus.

DISCUSSION

The main findings of the present study are as follows: KA treatment caused a rapid and complete loss of Reelin-producing hilar neurons. Upon KA challenge, eGFP-positive GCs actively migrated toward the Reelin-poor hilar region. This migration was effectively prevented by application of recombinant N-terminal or central Reelin fragments. Placement of Reelin-coated beads into the hilus of KA-treated cultures slowed the migration of GCs in a distance-dependent manner. In addition, we found that KA treatment impaired the Reelin signal transduction pathway by accumulation of Dab1 and reduced phosphorylation of cofilin. Importantly, neutralization of Reelin in healthy OHSC lead to a non-directed movement of GCs underlining the importance of Reelin for maintenance of GC lamination.

GCs Preferentially Migrate Toward the Reelin-Poor Hilus Following KA Challenge

In the adult dentate gyrus, GCs form a densely packed layer. Under epileptic conditions, the lamination can dissolve resulting in GCD, as observed in MTLE patients (Houser, 1990; Haas et al., 2002; Fahrner et al., 2007) and in the intrahippocampal KA mouse model (Bouilleret et al., 1999; Heinrich et al., 2006; Häussler et al., 2012; Janz et al., 2017). Since neurogenesis is lost in the dentate gyrus following KA injection (Kralic et al., 2005; Heinrich et al., 2006; Nitta et al., 2008; Häussler et al., 2012), it was assumed that differentiated GCs undergo GCD (Chai et al., 2014). Here, we demonstrate in OHSC by live cell microscopy that eGFP-labeled, differentiated GCs become motile in response to KA exposure. The migrating GCs altered their soma shape over the observation period: the nuclei of the GCs moved up toward one dendritic branch followed by a shift to another one, thereby

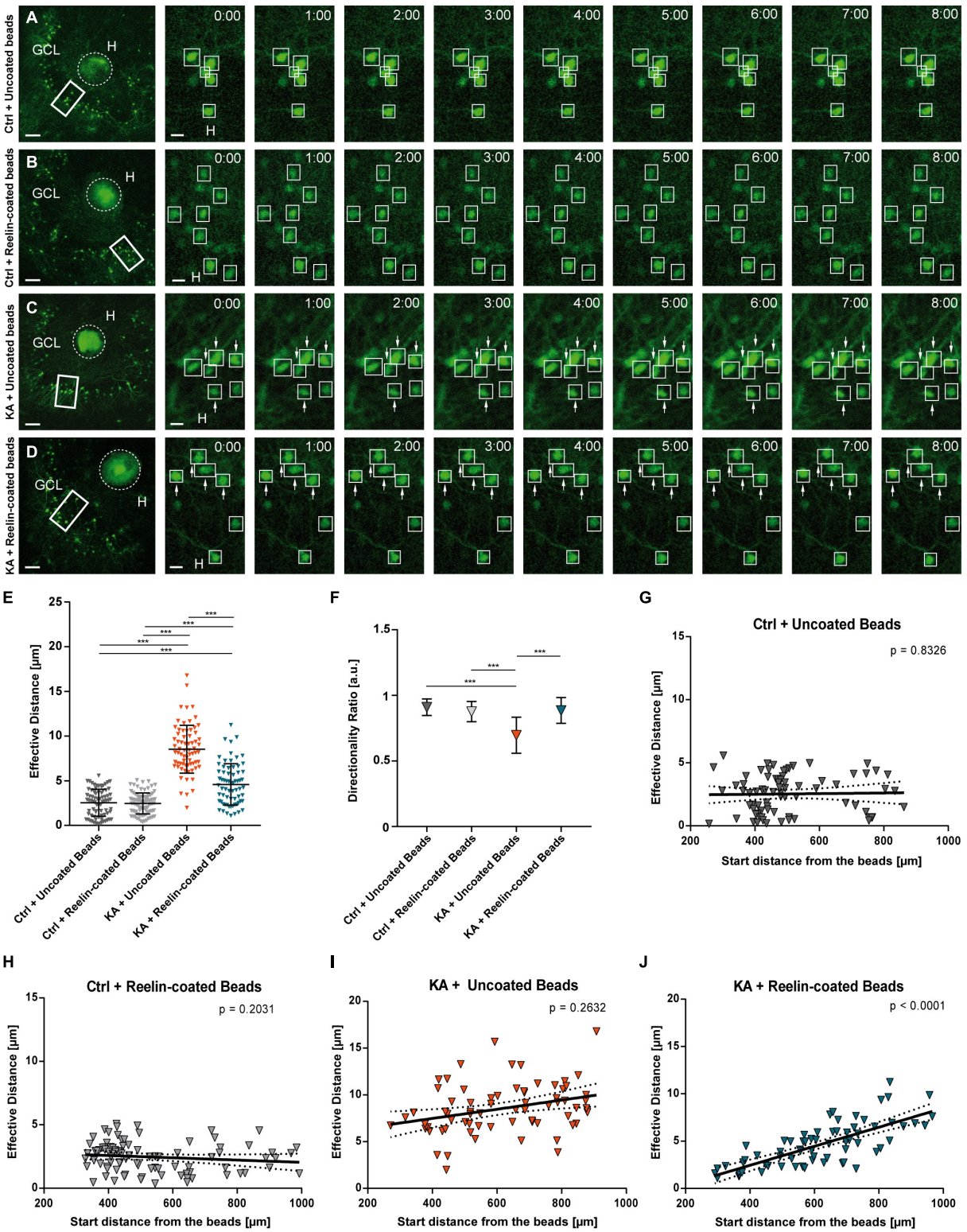

FIGURE 4 | Placement of Reelin-coated beads into the hilus stops KA-induced migration. Live cell imaging of individual eGFP-positive GCs was performed over a period of 8 h, and migration distances of automatically selected neurons were assessed. Cell motility was determined by calculating both the total length of the traveled path over 8 h and the effective migration distance as the length of the resulting vector between start (t = 0 h) and end point (t = 8 h). The border between the beads and GCL was marked and the distance was calculated between the start and end point of the cells to this border. **(A–D)** Representative confocal micrographs

(Continued)

FIGURE 4 | Continued
of nine imaging time points are shown for each condition. Left panel: overview; white frame indicates the area shown at high magnification on the right. Tracked cells are marked by white frames and GCs with high motility are indicated by arrows. OHSC were treated with 10 μM KA for 45 min, followed by placement of beads. Uncoated fluorescent beads **(A,C)** or Reelin-coated **(B,D)** were positioned into the hilus. Each slice derived from a different animal **(A)** Control + uncoated beads (n = 6 slices, 77 cells). **(B)** Control + Reelin-coated beads (n = 7 slices, 89 cells). **(C)** KA + uncoated beads (n = 4 slices, 70 cells). **(D)** KA + Reelin-coated beads (n = 5 slices, 68 cells). **(E)** Quantitative evaluation of migration distances of individual GCs. Under control conditions with uncoated and with Reelin-coated beads, GCs do not change position. KA induces migration of GCs but this is strongly reduced by placement of Reelin-coated beads. **(F)** Diagram showing the directionality ratios of the different groups. Note that GCs of the KA + uncoated bead group have lower values than the two control groups. GCs of KA-treated OHSC with Reelin-coated beads present a ratio similar to controls. **(G–J)** Quantitative evaluation of migration distances of individual GCs in relation to their start distance from the beads. **(G)** Control + uncoated beads, **(H)** Control + Reelin-coated beads, **(I)** KA + uncoated beads. Note that in these group there is no correlation between effective migration distance and start distance from the beads of tracked GCs. **(J)** KA + Reelin-coated beads. A positive correlation (Pearson correlation coefficient r = 0.7461) between the initial position and the migration behavior of the eGFP-positive cells is apparent. One-way ANOVA followed by Tukey's Multiple Comparison Test (***$P < 0.001$). GCL, granule cell layer; H, hilus. Scale bars: 80 μm for overview; 10 μm for high magnifications.

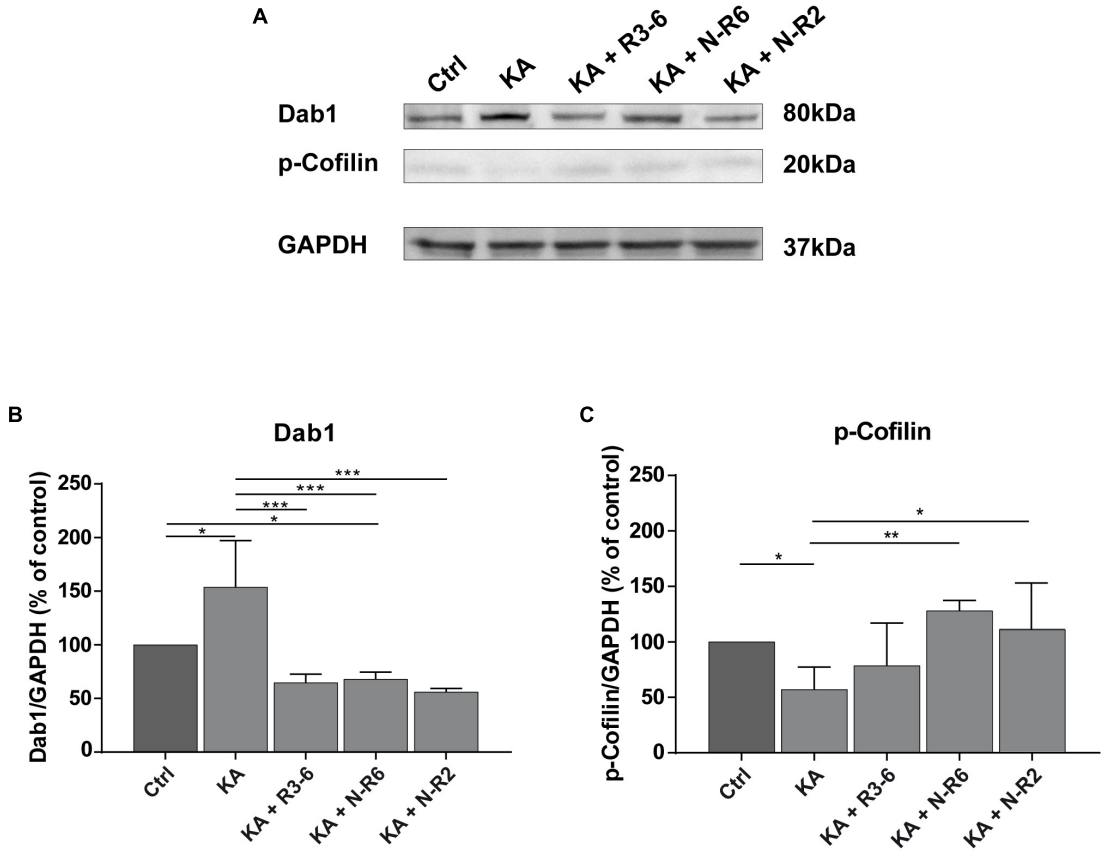

FIGURE 5 | Addition of recombinant Reelin fragments restores KA-mediated alterations of Reelin signaling components. Quantitative Western blot analysis for Dab1, p-cofilin was performed with extracts from control OHSC (n = 8 animals, 8–10 slices/animal), OHSC treated with 10 μM KA for 45 min (n = 3 animals, 8–10 slices/animal) and OHSC exposed to KA followed by incubation with fresh medium and subsequent application of recombinant Reelin fragments: R3-6 (n = 4 animals, 8–10 slices/animal), N-R6 (n = 3 animals, 8–10 slices/animal) and N-R2 (n = 4 animals, 8–10 slices/animal). **(A)** Representative Western blot for Dab1 and p-cofilin. GAPDH was used as a loading control. **(B,C)** Densitometric evaluation of **(B)** Dab1, **(C)** p-cofilin. Treatment with KA results in a significant upregulation of Dab1 synthesis and reduction of phosphorylated cofilin levels in tissue extracts. Subsequent incubation with the different recombinant Reelin fragments restores Dab1 and p-cofilin levels. One-way ANOVA followed by Tukey's Multiple Comparison Test (*$P < 0.05$; **$P < 0.01$; ***$P < 0.001$). Molecular weights are shown in kilodalton.

gradually displacing the soma mainly in the direction of the hilus. These observations suggest that the migration of mature GCs described here relies on nuclear movement in line with previous studies describing somal translocation as a novel mechanism of GCs undergoing dispersion (Murphy and Danzer, 2011; Chai et al., 2014). Somal translocation is a mechanism of migratory neurons during brain development, involving the translocation of the nucleus and perisomatic cytoplasm into a leading process (Rakic, 1972; Métin et al., 2008). This migration mode does not require a radial glia scaffold (Miyata et al., 2001; Morest and Silver, 2003), since it is only used by neurons migrating short distances (Nadarajah et al., 2001). Accordingly, in our

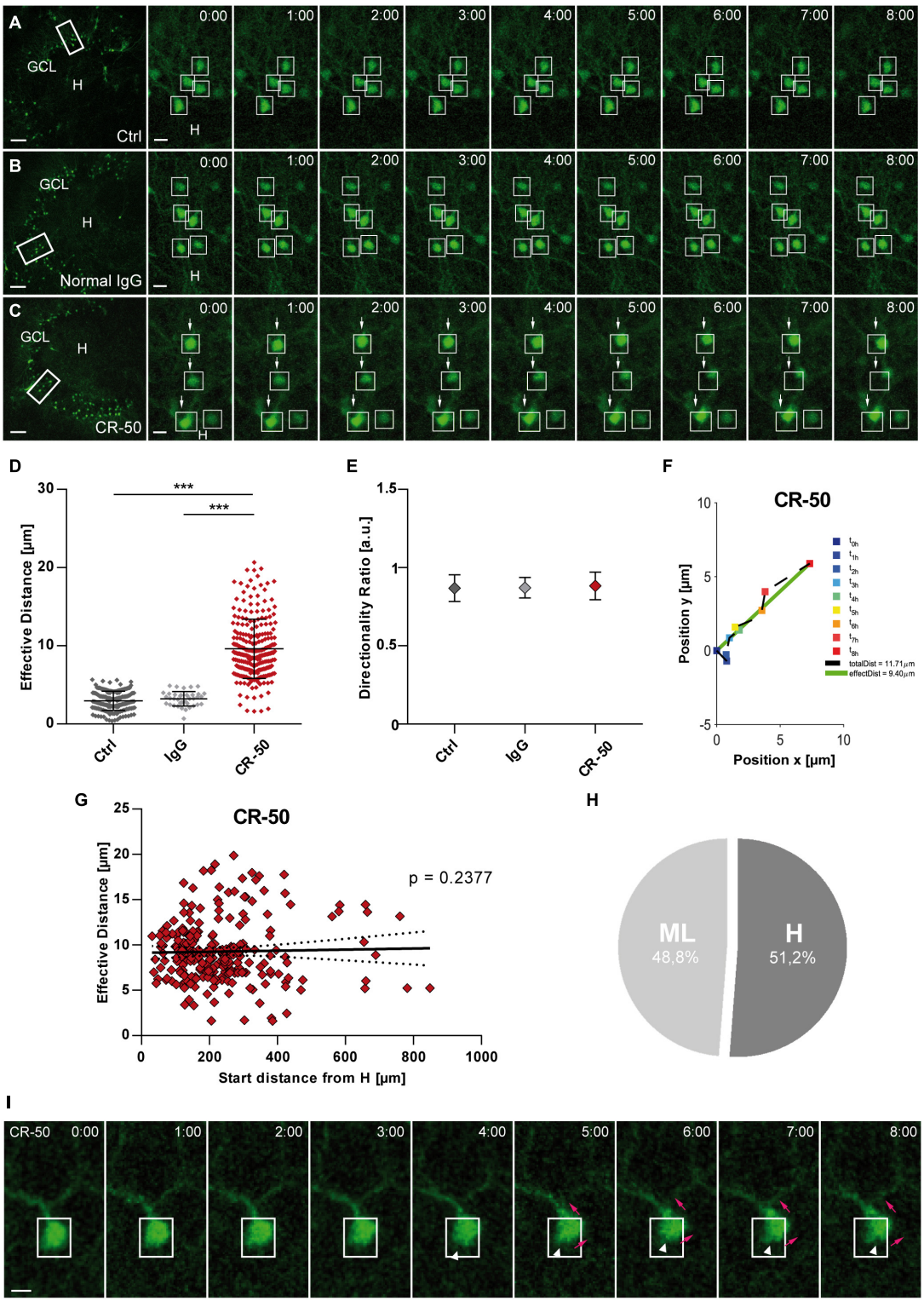

FIGURE 6 | Neutralization of Reelin in the healthy hippocampus leads to migration of mature granule cells. Live cell imaging of individual eGFP-positive GCs was performed over a period of 8 h, and migration distances of automatically selected cells were assessed. **(A–C)** Representative confocal micrographs of nine imaging time points are shown for each condition. Left panel: overview; white frame indicates the area shown at high magnification on the right. Tracked cells are marked by white frames. **(A)** Untreated control. GCs do not change position. **(B)** OHSC incubated with normal mouse IgG (8 µg/mL). As in controls, there is no neuronal displacement. **(C)** OHSC incubated with neutralizing CR-50 antibody (8 µg/mL). GCs with high motility are indicated by arrows. **(D)** Comparison of effective

(Continued)

FIGURE 6 | Continued
migration distances of individual GCs between groups: controls (n = 15 slices; 183 cells), normal mouse IgG (n = 2 slices, 38 cells) and CR-50 (n = 10; 254 cells). Under control conditions and with normal mouse IgG, GCs do not change position. In contrast, incubation with the CR-50 antibody strongly induces migratory behavior as indicated by strongly increased effective distances. **(E)** Diagram showing the directionality ratio. All three groups show similar values. **(F)** Graph showing the path of one representative neuron after incubation with the CR-50 antibody. Cell motility was assessed by calculating both the total length of the traveled path over 8 h (black dashed line = total distance) and the effective distance of the migration as the length of the resulting vector (green solid line) between start (t = 0 h) and end point (t = 8 h). Note that the path of this neuron is straight without any changes in direction. **(G)** Graph showing that there is no correlation between effective migration distance and start distance from the hilus of tracked GCs. All cells change their positions and travel regardless of their position in the GCL. **(H)** Relative distribution of cells traveling toward the hilus (51.2%) or molecular layer (48.8%) in OHSC incubated with CR-50 antibody. To differentiate the migration direction, the border between the hilus and GCL was marked and the distance of the start and end point of the cells to this border was calculated Cells that reduce their distance to the border over time [$H_{distance}$ (t = 0 h) – $H_{distance}$ (t = 8 h), positive values] are considered migrating toward the hilus. Cells showing an increase in distance (negative values) moved toward the ML. One-way ANOVA, followed by Tukey's Multiple Comparison Test (***$P < 0.001$; Ctrl vs. Normal IgG show no significance). Scale bars: 80 μm for overview; 10 μm for high magnifications. **(I)** Representative GC from an OHSC treated with CR-50 and imaged over a period of 8 h, as described above. Note the change in the soma shape as the neuron shifts position (white arrow heads), the soma moves into an apical dendrite (magenta arrows). Scale bar: 5 μm. GCL, granule cell layer; H, hilus.

study the differentiated GCs traveled short distances at a slow speed (approximately 1 μm/h). In contrast, during development of the dentate gyrus, the migration speed of newly born GCs is much faster (approximately 10 μm/h), and requires a radial glial scaffold (Wang et al., 2018). Previous studies addressing migration during brain development have uncovered that the actin cytoskeleton is required for nuclear movement, involving F-actin and the myosin II motor (actomyosin), creating pulling (He et al., 2010) and pushing forces (Martini and Valdeolmillos, 2010). He et al. (2010) found that the leading tip of migrating neurons pulls the soma forward through myosin II dynamics in an actin-dependent manner, depicting a growth cone-like structure, which we did not observe. In contrast, pushing forces can be created by actomyosin contraction at the rear of the soma of a migrating neuron (Shieh et al., 2011), comparable with the results from our live cell imaging experiments. It is possible that pushing forces, acting without directional pulling forces, explain the slow migration rate and the "winding" soma of the GCs in our system.

By tracking the path of individual neurons, we could show that the majority of GCs (81.1%) moved in the direction of the hilus following a meandering path as if they were actively searching for a positional cue. In fact, Reelin-producing, hilar neurons started to degenerate already at 45 min after KA exposure and were completely lost within 4 h, resulting in an area devoid of Reelin as shown by our detailed time series of Reelin expression. Therefore, we assume that most GCs moved speci?cally to the direction of the Reelin-free hilar area, whereas only about 20% traveled in the opposite direction toward the molecular layer where Reelin-expressing neurons did not degenerate in response to KA exposure. It is possible that a functional inactivation of Reelin by impaired proteolytic processing (Tinnes et al., 2011) plays a role in the migration of GCs toward the molecular layer. Tinnes et al. (2011) showed that in KA-treated OHSC Reelin secreted by Cajal-Retzius cells is abnormally processed, leading to the production of high molecular weight Reelin unable to diffuse through the tissue and to activate enough Reelin receptors on GCs (Jossin et al., 2007; Tinnes et al., 2011).

The selective vulnerability of Reelin-positive hilar neurons has been described before in rodent epilepsy models (Gong et al., 2007; Orcinha et al., 2016) and *in vitro* in OHSC following KA exposure (Tinnes et al., 2011; Chai et al., 2014; Orcinha et al., 2016), but nobody performed such a detailed time course analysis showing death of hilar Reelin-positive cells already within 45 min after KA treatment. The observed differential survival capacity of hilar interneurons and Cajal-Retzius cells is most likely due to a lack of KA receptors on the latter, since only hilar interneurons, but not Cajal-Retzius cells, respond to KA treatment with c-Fos induction (Tinnes et al., 2011).

Presence of Recombinant Reelin Fragments Stop KA-Induced Motility of GCs

Reelin is a key regulator of neuronal migration, delivering a signal to migrating neurons instructing them to assume their correct position during development (Tissir and Goffinet, 2003; Hirota and Nakajima, 2017; Jossin, 2020). Reelin-deficient *reeler* mice studies revealed faulty lamination in several brain structures as well as GC positioning defects in the hippocampus (D'Arcangelo et al., 1995, D'Arcangelo, 2014; Frotscher et al., 2003; Tissir and Goffinet, 2003; Zhao et al., 2004). These findings established a role for Reelin in stabilizing the lamination of the dentate gyrus. Here, we show that addition of the recombinant N-terminal Reelin fragments N-R2 and N-R6 and central Reelin fragment R3-6 to the medium of KA-treated OHSC were equally effective in preventing KA-induced migration of GCs toward the Reelin-free hilus. These data confirm and extend previous results showing that addition of the central Reelin fragment R3-6 stopped KA-induced GC migration in OHSC (Orcinha et al., 2016). R3-6 and N-R6 can activate the Reelin signaling cascade via the canonical pathway involving VLDR and ApoER2 receptors (Jossin et al., 2004; Koie et al., 2014), whereas the N-terminal fragment NR-2 has been shown to interact specifically with the extracellular domains of the EphB transmembrane proteins, inducing receptor clustering and activation of EphB signaling, independently of ApoER2 and VLDLR (Bouché et al., 2013). Reelin can also activate phosphorylation of Dab1 via binding to ephrin B proteins which are expressed on hippocampal neurons (Sentürk et al., 2011). In addition to stopping KA-induced migration of differentiated GCs, the Reelin recombinant fragments were also effective in rescuing the downstream signaling components of Reelin as shown by our quantitative Western blot analysis. They reverted the accumulation of Dab1,

known to occur in the absence of Reelin (Rice et al., 1998; Bock and Herz, 2003) and reestablished the phosphorylation of cofilin, necessary for downstream effects of Reelin (Chai et al., 2009; Frotscher et al., 2017).

The effect we observed in our OHSC strongly supports the proposed hypothesis that Reelin has a positional cue function in the dentate gyrus that is impaired in the presence of KA, and small fragments derived from the Reelin molecule were capable of rescuing GCD. Similarly, the importance of Reelin for correct positioning of dentate granule cells was shown by Gong et al. (2007), who found that exogenous Reelin had a positive effect in recovering normal migration and integration of late-born GCs in dentate gyrus explants from epileptic mice. In contrast, in a recent study, quantitative analysis of interneuron-specific Reelin knockout in adult mice did not reveal structural changes in the dentate gyrus, when compared to wild type mice (Pahle et al., 2020). Interestingly, these authors showed that the number of Reelin-expressing CR cells was significantly increased in interneuron-specific knockout mice. It was proposed to be a compensatory process for the loss of Reelin-expressing interneurons experienced in these knockout mice during development, resulting in an organized GC layer. As previously shown, this compensatory mechanism is not present in the mature hippocampus, after KA treatment (Duveau et al., 2011; Orcinha et al., 2016). In our conditions, Reelin that is secreted by CR cells is abnormally processed, leading to the production of high molecular weight Reelin isoforms (Tinnes et al., 2011) unable to diffuse through the tissue. This fails to activate enough Reelin receptors present in GCs (Jossin et al., 2007; Tinnes et al., 2011), entailing migration of mature GCs and resulting in GCD. Therefore, we speculate that the observed increase in Reelin expression in the hands of Pahle et al. (2020) was enough for the maintenance of the layering in the adult dentate gyrus. In addition, in Lane-Donovan et al. (2015) GCD formation was not found after conditional Reelin knockout in the adult dentate gyrus (Lane-Donovan et al., 2015). However, in these mice, 5% of the initial Reelin concentration was still present. Given that very low Reelin concentrations (1 nM) were sufficient to produce significant effects in our study and other studies (∼ 0.5 nM; Leemhuis et al., 2010), the incomplete Reelin knockout could explain the controversy.

Localization Matters: Placement of Reelin-Coated Beads Into the Hilus Stops KA Induced Migration

Reelin loss evidently appears to be involved in pathological neuronal migration in the adult hippocampus and substantial evidence supports the relevance of the presence of Reelin in a specific location to exert its function as a positional signal. Previous studies have shown that, during development, the rescue of GC lamination in OHSC prepared from Reelin-deficient *reeler* mice could be achieved when Reelin was present in its normal position, provided by a wild-type co-culture (Zhao et al., 2004, 2006). Here, we show that placement of Reelin-coated beads into the hilus of KA-treated OHSC could stop GC migration in a distance-dependent manner. Our real time microscopy clearly demonstrated a correlation between the localization of the Reelin source and the covered distance of eGFP-positive GCs. Neurons that were closer to the Reelin source did not significantly move away from their initial position, whereas neurons located further away from Reelin had an increased effective migration distance, but showed lower effective distances, when compared to neurons from OHSC treated with KA alone, and a directionality ratio like controls. The placement of a focal Reelin source into the hilus of OHSC was able to rescue the KA-induced movement of mature GCs in a gradient-like manner. One could explain this with the premise that Reelin fragments were produced from the full-length protein by proteolytic cleavage after Reelin was placed into the hilus due to the existence of proteases in the tissue (Jossin et al., 2007; Yasui et al., 2007). Also, the presence of small fragments bound to the beads before placement must be considered. These small Reelin fragments were then able to diffuse away from their original position, activating the Reelin signaling pathway by binding to the receptors located on the membrane of dentate GCs (Clatworthy et al., 1999; Sakai et al., 2009; reviewed in Reddy et al., 2011; Dlugosz and Nimpf, 2018; Liu et al., 2018). It is controversially discussed whether Reelin acts as a stopping signal (Dulabon et al., 2000; Chai et al., 2009; Sekine et al., 2011), as a global and locally active attractant signal (Rice and Curran, 2001; Courtès et al., 2011; Wang et al., 2018) or as a locally active repelling signal (D'Arcangelo and Curran, 1998; Wang et al., 2018) during neuronal migration in development. So far, our present results indicate that Reelin is an instructive factor, acting as a local stopping cue, responsible for maintaining the position of mature GCs and ceasing their aberrant migration under epileptic conditions.

KA Treatment Compromises Reelin Signaling

Since Reelin can be sensed by GCs, the presence of components of the signaling cascade is imperative. To further analyze the effects of KA-induced impairment of Reelin on the behavior of GCs, expression levels of Dab1 and p-cofilin, important downstream signaling molecules of the Reelin pathway, were assessed. Reelin signaling is mediated by the ApoER2, VLDLR and EphB receptors (D'Arcangelo et al., 1999; Hiesberger et al., 1999; Trommsdorff et al., 1999; Kubo et al., 2002; Strasser et al., 2004; Bouché et al., 2013), members of the Src family of tyrosine kinases (SKF) (Arnaud et al., 2003; Kuo et al., 2005) and the neuronal phosphoprotein Dab1 (Howell et al., 1999, 2000). This pathway modulates the activity of downstream protein kinase cascades, many of which target the neuronal cytoskeleton, explaining the pivotal role of Reelin in neuronal migration. Migration involves active cytoskeleton remodeling. It includes actin filaments, microtubules and cofilin, a protein responsible for the reorganization of actin filaments. Previous studies showed that the loss of downstream signaling components lead to severe cortical alterations and perturbed hippocampal lamination, a phenotype indistinguishable from *reeler* mutants (Trommsdorff et al., 1999; Kuo et al., 2005; Bellenchi et al., 2007; Chai et al., 2009). In our study, KA treatment affected the expression of Dab1 and p-cofilin. It induced the accumulation of Dab1 and reduced

phosphorylation of cofilin. However, application of recombinant Reelin fragments to KA-treated OHSC resulted in a significant decrease of Dab1 levels and increased the phosphorylation of cofilin. In a normal setting, the binding of Reelin extracellularly to its receptors induces intracellular tyrosine phosphorylation of Dab1, and thus activates other downstream components. It has been shown that mutations of Dab1 phenocopy and disruption of the Reelin signaling lead to accumulation of Dab1 protein (Howell et al., 1997; Sheldon et al., 1997; Rice et al., 1998; Hiesberger et al., 1999; Trommsdorff et al., 1999; Arnaud et al., 2003; Bock and Herz, 2003; Kuo et al., 2005), similar to what was found here after exposure to KA. Moreover, the studies from Arnaud et al. (2003) and Bock et al. (2004) reported in primary neuronal cultures that expression of Dab1 is reduced through the ubiquitin-proteasome system in the presence of Reelin and that this modification requires tyrosine phosphorylation of Dab1. In addition, Feng et al. (2007) and Franco et al. (2011) demonstrated that terminal translocation of migrating newborn neurons is Dab1-dependent. Dab1 degradation is critical in neurons to properly terminate their migration. Unfortunately, due to technical difficulties, we were not able to properly detect Dab1 phosphorylation in our system. However, these findings agree with our results showing that addition of exogenous Reelin halted neuronal migration, most likely via induction of Dab1 phosphorylation, resulting in the observed downregulation of Dab1. Reelin induces phosphorylation of Dab1, an important step for the activation of LIMK-cofilin axis. Consecutively, phosphorylation (activation) of LIMK1, a kinase that induces phosphorylation of the actin severing protein cofilin, leads to its inactivation and stabilizes the actin cytoskeleton (Arber et al., 1998; Yang et al., 1998; Meng et al., 2004; Chai et al., 2009). In an unphosphorylated state, cofilin acts as an actin-depolymerizing protein that promotes the disassembly of F-actin, leading to migration (reviewed in Frotscher, 2010). Here, p-cofilin levels were reduced in the presence of KA, and recombinant Reelin fragments abolished this effect. It is tempting to conclude that Reelin counteracts cytoskeleton reorganization and in turn stabilizes the actin cytoskeleton, stopping the migration process. In line with this argument, it was previously shown that the amounts of phosphorylated cofilin were significantly reduced in *reeler* mice and that application of recombinant Reelin to *reeler* tissue significantly increased the phosphorylation of cofilin (Chai et al., 2009, 2016; reviewed in Frotscher et al., 2017). Also, changes in cell shape during neuronal migration are associated with cytoskeletal remodeling (Rivas and Hatten, 1995; Rakic et al., 1996; Nadarajah et al., 2001; Nadarajah and Parnavelas, 2002; Miyata and Ogawa, 2007; Cooper, 2013), being characterized by well-coordinated consecutive periods of cytoskeletal stability. The reduction of phosphorylation levels of cofilin might explain the morphological changes in the soma of mature GCs observed after KA treatment in our live cell imaging experiments. Taken together, the evidences so far suggest the following scenario: after secretion, Reelin is chained to the extracellular matrix where it remains inactive until its proteolysis allows for the initiation of the downstream signaling (Lambert de Rouvroit et al., 1999; Jossin et al., 2007; Trotter et al., 2014). Reelin fragments can act locally or diffuse away from the site of secretion (Jossin et al., 2007), activating Dab1 phosphorylation by binding to its receptors present in GCs and recruiting SKFs (Howell et al., 1997; Strasser et al., 2004; Morimura et al., 2005). Phosphorylation of cofilin at serine3 renders the protein unable to depolymerize actin, thereby stabilizing the actin cytoskeleton. In the adult hippocampus, defects in Reelin-Dab1-dependent signaling caused by KA accounts for the migration of mature GCs, by somatic translocation, toward the Reelin-free hilar area, and this can be explained by the accumulation of Dab1 and the decreased phosphorylation levels of cofilin. These results point to an important role of cofilin and its coordinated regulation by Reelin-dependent phosphorylation steps in the lamination of the mature hippocampus.

Neutralization of Reelin in the Healthy Hippocampus Dissolves GC Lamination

Additional evidence linking Reelin with the maintenance of GC lamination in the adult dentate gyrus was given by our use of the CR-50 antibody in naïve OHSC. The neutralizing antibody CR-50 can block Reelin function *in vivo* and *in vitro* (Ogawa et al., 1995; del Río et al., 1997; Miyata et al., 1997; Nakajima et al., 1997; Utsunomiya-Tate et al., 2000) and infusion of CR-50 into the hippocampus of normal adult mice induced GCD locally (Heinrich et al., 2006). Its epitope in the Reelin structure is located near the N-terminal, between the amino acids 251 and 407, important for protein homopolymerization and signaling. Mutated Reelin, which lacks a CR-50 epitope, fails to form homopolymers, and is therefore unable to transduce the Reelin signal (D'Arcangelo et al., 1997). Incubating OHSC with CR-50 caused a considerable displacement of eGFP-positive GCs in the healthy hippocampus, similar to the KA-induced phenotype. Our live cell imaging revealed that GCs migrated also by somatic translocation but, contrarily to neurons in KA-treated OHSC, in a non-meander manner, straight into one direction without significant changes in directionality, independently from their initial position within the GCL. Here, Reelin was blocked all over the OHSC. Since a positional cue was missing, the GCs immediately started to migrate without any preference in direction. These findings suggest the importance of endogenous Reelin expression and its normal topographical position for proper brain lamination. Accordingly, as previously postulated (Haas et al., 2002; Frotscher et al., 2003; Heinrich et al., 2006), Reelin is not only important for the formation but also relevant for the maintenance of GCL lamination in the adult hippocampus.

DATA AVAILABILITY STATEMENT

The raw data supporting the conclusions of this article will be made available by the authors, without undue reservation.

ETHICS STATEMENT

The animal study was reviewed and approved by the Regierungspräsidium Freiburg.

AUTHOR CONTRIBUTIONS

CO performed the experiments, data analysis, and manuscript writing. AK developed the MATLAB® script for data analysis. MF and EP contributed with input on data analysis. CH designed research and wrote the manuscript together with CO. All authors contributed to the article and approved the submitted version.

FUNDING

This work was supported by BrainLinks-BrainTools, which is funded by the Federal Ministry of Economics, Science and Arts of Baden-Württemberg within the sustainability program for projects of the Excellence Initiative II. The article processing charge was funded by the Baden-Württemberg Ministry of Science, Research and Art and the University of Freiburg within the funding program Open Access Publishing.

ACKNOWLEDGMENTS

We are very grateful to Riko Moroni for his input on data analysis, to Susanne Huber and Andrea Djie-Maletz for excellent technical assistance and to Hans Bock, University of Düsseldorf, for plasmids and reagents.

SUPPLEMENTARY MATERIAL

The Supplementary Material for this article can be found online at: https://www.frontiersin.org/articles/10.3389/fnmol.2021.730811/full#supplementary-material

REFERENCES

Alcántara, S., Ruiz, M., D'Arcangelo, G., Ezan, F., De Lecea, L., Curran, T., et al. (1998). Regional and cellular patterns of reelin mRNA expression in the forebrain of the developing and adult mouse. *J. Neurosci.* 18, 7779–7799. doi: 10.1523/jneurosci.18-19-07779.1998

Antonucci, F., Di Garbo, A., Novelli, E., Manno, I., Sartucci, F., Bozzi, Y., et al. (2008). Botulinum neurotoxin E (BoNT/E) reduces CA1 neuron loss and granule cell dispersion, with no effects on chronic seizures, in a mouse model of temporal lobe epilepsy. *Exp. Neurol.* 210, 388–401. doi: 10.1016/j.expneurol.2007.11.012

Arber, S., Barbayannis, F. A., Hanser, H., Schnelder, C., Stanyon, C. A., Bernards, O., et al. (1998). Regulation of actin dynamics through phosphorylation of cofilin by LIM- kinase. *Nature* 393, 805–809. doi: 10.1038/31729

Armstrong, N. C., Anderson, R. C., and McDermott, K. W. (2019). Reelin: Diverse roles in central nervous system development, health and disease. *Int. J. Biochem. Cell Biol.* 112, 72–75. doi: 10.1016/j.biocel.2019.04.009

Arnaud, L., Ballif, B. A., Förster, E., and Cooper, J. A. (2003). Fyn tyrosine kinase is a critical regulator of Disabled-1 during brain development. *Curr. Biol.* 13, 9–17. doi: 10.1016/S0960-9822(02)01397-0

Bellenchi, G. C., Gurniak, C. B., Perlas, E., Middei, S., Ammassari-Teule, M., and Witke, W. (2007). N-cofilin is associated with neuronal migration disorders and cell cycle control in the cerebral cortex. *Genes Dev.* 21, 2347–2357. doi: 10.1101/gad.434307

Bock, H. H., and Herz, J. (2003). Reelin activates Src family tyrosine kinases in neurons. *Curr. Biol.* 13, 18–26. doi: 10.1016/S0960-9822(02)01403-3

Bock, H. H., Jossin, Y., May, P., Bergner, O., and Herz, J. (2004). Apolipoprotein E receptors are required for reelin-induced proteasomal degradation of the neuronal adaptor protein disabled-1. *J. Biol. Chem.* 279, 33471–33479. doi: 10.1074/jbc.M401770200

Bock, H. H., and May, P. (2016). Canonical and non-canonical reelin signaling. *Front. Cell. Neurosci.* 10:166. doi: 10.3389/fncel.2016.00166

Bouché, E., Romero-Ortega, M. I., Henkemeyer, M., Catchpole, T., Leemhuis, J., Frotscher, M., et al. (2013). Reelin induces EphB activation. *Cell Res.* 23, 473–490. doi: 10.1038/cr.2013.7

Bouilleret, V., Ridoux, V., Depaulis, A., Marescaux, C., Nehlig, A., and Le Gal La Salle, G. (1999). Recurrent seizures and hippocampal sclerosis following intrahippocampal kainate injection in adult mice: Electroencephalography, histopathology and synaptic reorganization similar to mesial temporal lobe epilepsy. *Neuroscience* 89, 717–729. doi: 10.1016/S0306-4522(98)00401-1

Burry, R. W. (2011). Controls for immunocytochemistry: an update. *J. Histochem. Cytochem.* 59, 6–12. doi: 10.1369/jhc.2010.956920

Chai, X., Förster, E., Zhao, S., Bock, H. H., and Frotscher, M. (2009). Reelin stabilizes the actin cytoskeleton of neuronal processes by inducing n-cofilin phosphorylation at serine. *J. Neurosci.* 29, 288–299. doi: 10.1523/JNEUROSCI.2934-08.2009

Chai, X., Münzner, G., Zhao, S., Tinnes, S., Kowalski, J., Häussler, U., et al. (2014). Epilepsy-induced motility of differentiated neurons. *Cereb. Cortex* 24, 2130–2140. doi: 10.1093/cercor/bht067

Chai, X., Zhao, S., Fan, L., Zhang, W., Lu, X., Shao, H., et al. (2016). Reelin and cofilin cooperate during the migration of cortical neurons: a quantitative morphological analysis. *Devlopment* 143, 1029–1040. doi: 10.1242/dev.134163

Clatworthy, A. E., Stockinger, W., Christie, R. H., Schneider, W. J., Nimpf, J., Hyman, B. T., et al. (1999). Expression and alternate splicing of apolipoprotein E receptor 2 in brain. *Neuroscience* 90, 903–911. doi: 10.1016/S0306-4522(98)00489-8

Cooper, J. A. (2013). Mechanisms of cell migration in the nervous system. *J. Cell Biol.* 202, 725–734. doi: 10.1083/jcb.201305021

Courtès, S., Vernerey, J., Pujadas, L., Magalon, K., Cremer, H., Soriano, E., et al. (2011). Reelin controls progenitor cell migration in the healthy and pathological adult mouse brain. *PLoS One* 6:e20430. doi: 10.1371/journal.pone.0020430

D'Arcangelo, G. (2014). Reelin in the years: controlling neuronal migration and maturation in the mammalian brain. *Adv. Neurosci.* 2014, 1–19. doi: 10.1155/2014/597395

D'Arcangelo, G., and Curran, T. (1998). Reeler: new tales on an old mutant mouse. *BioEssays* 20, 235–244. doi: 10.1002/(sici)1521-1878(199803)20:3<235::aid-bies7>3.0.co;2-q

D'Arcangelo, G., Homayouni, R., Keshvara, L., Rice, D. S., Sheldon, M., and Curran, T. (1999). Reelin is a ligand for lipoprotein receptors. *Neuron* 24, 471–479. doi: 10.1016/S0896-6273(00)80860-0

D'Arcangelo, G., Miao, G. G., Chen, S. C., Scares, H. D., Morgan, J. I., and Curran, T. (1995). A protein related to extracellular matrix proteins deleted in the mouse mutant reeler. *Nature* 374, 719–723. doi: 10.1038/374719a0

D'Arcangelo, G., Nakajima, K., Miyata, T., Ogawa, M., Mikoshiba, K., and Curran, T. (1997). Reelin is a secreted glycoprotein recognized by the CR-50 monoclonal antibody. *J. Neurosci.* 17, 23–31. doi: 10.1523/jneurosci.17-01-00023.1997

del Río, J. A., Heimrich, B., Borrell, V., Förster, E., Drakew, A., Alcántara, S., et al. (1997). A role for Cajal-retzius cells and reelin in the development of hippocampal connections. *Nature* 385, 70–74. doi: 10.1038/385070a0

Devinsky, O., Vezzani, A., O'Brien, T. J., Jette, N., Scheffer, I. E., De Curtis, M., et al. (2018). Epilepsy. *Nat. Rev. Dis. Prim.* 4:18024. doi: 10.1038/nrdp.2018.24

Dlugosz, P., and Nimpf, J. (2018). The reelin receptors apolipoprotein e receptor 2 (ApoER2) and VLDL receptor. *Int. J. Mol. Sci.* 19, 1–22. doi: 10.3390/ijms19103090

Dulabon, L., Olson, E. C., Taglienti, M. G., Eisenhuth, S., McGrath, B., Walsh, C. A., et al. (2000). Reelin binds α3β1 integrin and inhibits neuronal migration. *Neuron* 27, 33–44. doi: 10.1016/S0896-6273(00)00007-6

Duveau, V., Madhusudan, A., Caleo, M., Knuesel, I., and Fritschy, J. M. (2011). Impaired reelin processing and secretion by Cajal-Retzius cells contributes to granule cell dispersion in a mouse model of temporal lobe epilepsy. *Hippocampus* 21, 935–944. doi: 10.1002/hipo.20793

Fahrner, A., Kann, G., Flubacher, A., Heinrich, C., Freiman, T. M., Zentner, J., et al. (2007). Granule cell dispersion is not accompanied by enhanced neurogenesis in temporal lobe epilepsy patients. *Exp. Neurol.* 203, 320–332. doi: 10.1016/j.expneurol.2006.08.023

Feng, G., Mellor, R. H., Bernstein, M., Keller-Peck, C., Nguyen, Q. T., Wallace, M., et al. (2000). Imaging neuronal subsets in transgenic mice expressing multiple spectral variants of GFP. *Neuron* 28, 41–51. doi: 10.1016/S0896-6273(00)00084-2

Feng, L., Allen, N. S., Simo, S., and Cooper, J. A. (2007). Cullin 5 regulates Dab1 protein levels and neuron positioning during cortical development. *Genes Dev.* 21, 2717–2730. doi: 10.1101/gad.1604207

Franco, S. J., Martinez-Garay, I., Gil-Sanz, C., Harkins-Perry, S. R., and Müller, U. (2011). Reelin regulates cadherin function via dab1/rap1 to control neuronal migration and lamination in the neocortex. *Neuron* 69, 482–497. doi: 10.1016/j.neuron.2011.01.003

Frotscher, M. (2010). Role for Reelin in stabilizing cortical architecture. *Trends Neurosci.* 33, 407–414. doi: 10.1016/j.tins.2010.06.001

Frotscher, M., Haas, C. A., and Förster, E. (2003). Reelin controls granule cell migration in the dentate gyrus by acting on the radial glial scaffold. *Cereb. Cortex* 13, 634–640. doi: 10.1093/cercor/13.6.634

Frotscher, M., Zhao, S., Wang, S., and Chai, X. (2017). Reelin signaling inactivates cofilin to stabilize the cytoskeleton of migrating cortical neurons. *Front. Cell. Neurosci.* 11:148. doi: 10.3389/fncel.2017.00148

Gerlach, J., Donkels, C., Münzner, G., and Haas, C. A. (2016). Persistent gliosis interferes with neurogenesis in organotypic hippocampal slice cultures. *Front. Cell. Neurosci.* 10:131. doi: 10.3389/fncel.2016.00131

Gong, C., Wang, T. W., Huang, H. S., and Parent, J. M. (2007). Reelin regulates neuronal progenitor migration in intact and epileptic hippocampus. *J. Neurosci.* 27, 1803–1811. doi: 10.1523/JNEUROSCI.3111-06.2007

Gorelik, R., and Gautreau, A. (2014). Quantitative and unbiased analysis of directional persistence in cell migration. *Nat. Protoc.* 9, 1931–1943. doi: 10.1038/nprot.2014.131

Haas, C. A., Dudeck, O., Kirsch, M., Huszka, C., Kann, G., Pollak, S., et al. (2002). Role for reelin in the development of granule cell dispersion in temporal lobe epilepsy. *J. Neurosci.* 22, 5797–5802. doi: 10.1523/jneurosci.22-14-05797.2002

Häussler, U., Bielefeld, L., Froriep, U. P., Wolfart, J., and Haas, C. A. (2012). Septotemporal position in the hippocampal formation determines epileptic and neurogenic activity in temporal lobe epilepsy. *Cereb. Cortex* 22, 26–36. doi: 10.1093/cercor/bhr054

He, M., Zhang, Z. H., Guan, C. B., Xia, D., and Yuan, X. B. (2010). Leading tip drives soma translocation via forward F-actin flow during neuronal migration. *J. Neurosci.* 30, 10885–10898. doi: 10.1523/JNEUROSCI.0240-10.2010

Heinrich, C., Nitta, N., Flubacher, A., Müller, M., Fahrner, A., Kirsch, M., et al. (2006). Reelin deficiency and displacement of mature neurons, but not neurogenesis, underlie the formation of granule cell dispersion in the epileptic hippocampus. *J. Neurosci.* 26, 4701–4713. doi: 10.1523/JNEUROSCI.5516-05.2006

Herz, J., and Chen, Y. (2006). Reelin, lipoprotein receptors and synaptic plasticity. *Nat. Rev. Neurosci.* 7, 850–859. doi: 10.1038/nrn2009

Hiesberger, T., Trommsdorff, M., Howell, B. W., Goffinet, A., Mumby, M. C., Cooper, J. A., et al. (1999). Direct binding of Reelin to VLDL receptor and ApoE receptor 2 induces tyrosine phosphorylation of Disabled-1 and modulates tau phosphorylation. *Neuron* 24, 481–489. doi: 10.1016/S0896-6273(00)80861-2

Hirota, Y., and Nakajima, K. (2017). Control of neuronal migration and aggregation by reelin signaling in the developing cerebral cortex. *Front. cell Dev. Biol.* 5:40. doi: 10.3389/fcell.2017.00040

Hirotsune, S., Takahara, T., Sasaki, N., Hirose, K., Yoshiki, A., Ohashi, T., et al. (1995). The reeler gene encodes a protein with an EGF–like motif expressed by pioneer neurons. *Nat. Genet.* 10, 77–83. doi: 10.1038/ng0595-77

Houser, C. R. (1990). Granule cell dispersion in the dentate gyrus of humans with temporal lobe epilepsy. *Brain Res.* 535, 195–204. doi: 10.1016/0006-8993(90)91601-C

Howell, B. W., Hawkes, R., Soriano, P., and Cooper, J. A. (1997). Neuronal position in the developing brain is regulated by mouse disabled-1. *Nature* 389, 733–737. doi: 10.1038/39607

Howell, B. W., Herrick, T. M., and Cooper, J. A. (1999). Reelin-induced tyrosine phosphorylation of Disabled 1 during neuronal positioning. *Genes Dev.* 13, 643–648. doi: 10.1101/gad.13.6.643

Howell, B. W., Herrick, T. M., Hildebrand, J. D., Zhang, Y., and Cooper, J. A. (2000). Dab1 tyrosine phosphorylation sites relay positional signals during mouse brain development. *Curr. Biol.* 10, 877–885. doi: 10.1016/S0960-9822(00)00608-4

Ishii, K., Kubo, K. I., and Nakajima, K. (2016). Reelin and neuropsychiatric disorders. *Front. Cell. Neurosci.* 10:229. doi: 10.3389/fncel.2016.00229

Janz, P., Savanthrapadian, S., Häussler, U., Kilias, A., Nestel, S., Kretz, O., et al. (2017). Synaptic remodeling of entorhinal input contributes to an aberrant hippocampal network in temporal lobe epilepsy. *Cereb. Cortex* 27, 2348–2364. doi: 10.1093/cercor/bhw093

Jossin, Y. (2020). Reelin functions, mechanisms of action and signaling pathways during brain development and maturation. *Biomolecules* 10, 1–31. doi: 10.3390/BIOM10060964

Jossin, Y., and Goffinet, A. M. (2007). Reelin signals through phosphatidylinositol 3-kinase and Akt to control cortical development and through mtor to regulate dendritic growth. *Mol. Cell. Biol.* 27, 7113–7124. doi: 10.1128/mcb.00928-07

Jossin, Y., Gui, L., and Goffinet, A. M. (2007). Processing of Reelin by embryonic neurons is important for function in tissue but not in dissociated cultured neurons. *J. Neurosci.* 27, 4243–4252. doi: 10.1523/JNEUROSCI.0023-07.2007

Jossin, Y., Ignatova, N., Hiesberger, T., Herz, J., Lambert De Rouvroit, C., and Goffinet, A. M. (2004). The central fragment of reelin, generated by proteolytic processing in vivo, is critical to its function during cortical plate development. *J. Neurosci.* 24, 514–521. doi: 10.1523/JNEUROSCI.3408-03.2004

Koie, M., Okumura, K., Hisanaga, A., Kamei, T., Sasaki, K., Deng, M., et al. (2014). Cleavage within reelin repeat 3 regulates the duration and range of the signaling activity of reelin protein. *J. Biol. Chem.* 289, 12922–12930. doi: 10.1074/jbc.M113.536326

Kralic, J. E., Ledergerber, D. A., and Fritschy, J. M. (2005). Disruption of the neurogenic potential of the dentate gyrus in a mouse model of temporal lobe epilepsy with focal seizures. *Eur. J. Neurosci.* 22, 1916–1927. doi: 10.1111/j.1460-9568.2005.04386.x

Kubo, K. I., Mikoshiba, K., and Nakajima, K. (2002). Secreted reelin molecules form homodimers. *Neurosci. Res.* 43, 381–388. doi: 10.1016/S0168-0102(02)00068-8

Kuo, G., Arnaud, L., Kronstad-O'Brien, P., and Cooper, J. A. (2005). Absence of Fyn and Src causes a Reeler-like phenotype. *J. Neurosci.* 25, 8578–8586. doi: 10.1523/JNEUROSCI.1656-05.2005

Lambert de Rouvroit, C., De Bergeyck, V., Cortvrindt, C., Bar, I., Eeckhout, Y., and Goffinet, A. M. (1999). Reelin, the extracellular matrix protein deficient in reeler mutant mice, is processed by a metalloproteinase. *Exp. Neurol.* 156, 214–217. doi: 10.1006/exnr.1998.7007

Lane-Donovan, C., Philips, G. T., Wasser, C. R., Durakoglugil, M. S., Masiulis, I., Upadhaya, A., et al. (2015). Reelin protects against amyloid β toxicity in vivo. *Sci. Signal* 8, ra67. doi: 10.1126/scisignal.aaa6674

Lee, G. H., and D'Arcangelo, G. (2016). New insights into reelin-mediated signaling pathways. *Front. Cell. Neurosci.* 10:122. doi: 10.3389/fncel.2016.00122

Leemhuis, J., and Bock, H. H. (2011). Reelin modulates cytoskeletal organization by regulating Rho GTPases. *Commun. Integr. Biol.* 4, 254–257. doi: 10.4161/cib.4.3.14890

Leemhuis, J., Bouché, E., Frotscher, M., Henle, F., Hein, L., Herz, J., et al. (2010). Reelin signals through apolipoprotein E receptor 2 and Cdc42 to increase growth cone motility and filopodia formation. *J. Neurosci.* 30, 14759–14772. doi: 10.1523/JNEUROSCI.4036-10.2010

Liu, J. Y. W., Dzurova, N., Al-Kaaby, B., Mills, K., Sisodiya, S. M., and Thom, M. (2020). Granule cell dispersion in human temporal lobe epilepsy: proteomics investigation of neurodevelopmental migratory pathways. *Front. Cell. Neurosci.* 14:53. doi: 10.3389/fncel.2020.00053

Liu, T. T., Li, Y., Shu, Y., Xiao, B., and Feng, L. (2018). Ephrin-B3 modulates hippocampal neurogenesis and the reelin signaling pathway in a pilocarpine-induced model of epilepsy. *Int. J. Mol. Med.* 41, 3457–3467. doi: 10.3892/ijmm.2018.3543

Martini, F. J., and Valdeolmillos, M. (2010). Actomyosin contraction at the cell rear drives nuclear translocation in migrating cortical interneurons. *J. Neurosci.* 30, 8660–8670. doi: 10.1523/JNEUROSCI.1962-10.2010

Meng, Y., Takahashi, H., Meng, J., Zhang, Y., Lu, G., Asrar, S., et al. (2004). Regulation of ADF/cofilin phosphorylation and synaptic function by LIM-kinase. *Neuropharmaco*logy 47, 746–754. doi: 10.1016/j.neuropharm.2004.06.030

Métin, C., Vallee, R. B., Rakic, P., and Bhide, P. G. (2008). Modes and mishaps of neuronal migration in the mammalian brain. *J. Neurosci.* 28, 11746–11752. doi: 10.1523/JNEUROSCI.3860-08.2008

Miyata, T., Kawaguchi, A., Okano, H., and Ogawa, M. (2001). Asymmetric inheritance of radial glial fibers by cortical neurons. *Neuron* 31, 727–741. doi: 10.1016/S0896-6273(01)00420-2

Miyata, T., Nakajima, K., Mikoshiba, K., and Ogawa, M. (1997). Regulation of Purkinje cell alignment by Reelin as revealed with CR-50 antibody. *J. Neurosci.* 17, 3599–3609. doi: 10.1523/jneurosci.17-10-03599.1997

Miyata, T., and Ogawa, M. (2007). Twisting of neocortical progenitor cells underlies a spring-like mechanism for daughter-cell migration. *Curr. Biol.* 17, 146–151. doi: 10.1016/j.cub.2006.11.023

Morest, D. K., and Silver, J. (2003). Precursors of neurons, neuroglia, and ependymal cells in the CNS: what are they? Where are they from? How do they get where they are going? *Glia* 43, 6–18. doi: 10.1002/glia.10238

Morimura, T., Hattori, M., Ogawa, M., and Mikoshiba, K. (2005). Disabled1 regulates the intracellular trafficking of reelin receptors. *J. Biol. Chem.* 280, 16901–16908. doi: 10.1074/jbc.M409048200

Müller, M. C., Osswald, M., Tinnes, S., Häussler, U., Jacobi, A., Förster, E., et al. (2009). Exogenous reelin prevents granule cell dispersion in experimental epilepsy. *Exp. Neurol.* 216, 390–397. doi: 10.1016/j.expneurol.2008.12.029

Murphy, B. L., and Danzer, S. C. (2011). Somatic translocation: a novel mechanism of granule cell dendritic dysmorphogenesis and dispersion. *J. Neurosci.* 31, 2959–2964. doi: 10.1523/JNEUROSCI.3381-10.2011

Nadarajah, B., Brunstrom, J. E., Grutzendler, J., Wong, R. O. L., and Pearlman, A. L. (2001). Two modes of radial migration in early development of the cerebral cortex. *Nat. Neurosci.* 4, 143–150. doi: 10.1038/83967

Nadarajah, B., and Parnavelas, J. G. (2002). Modes of neuronal migration in the developing cerebral cortex. *Nat. Rev. Neurosci.* 3, 423–432. doi: 10.1038/nrn845

Nakajima, K., Mikoshiba, K., Miyata, T., Kudo, C., and Ogawa, M. (1997). Disruption of hippocampal development in vivo by CR-50 mAB against reelin. *Proc. Natl. Acad. Sci. U.S.A.* 94, 8196–8201. doi: 10.1073/pnas.94.15.8196

Nakano, Y., Kohno, T., Hibi, T., Kohno, S., Baba, A., Mikoshiba, K., et al. (2007). The extremely conserved c-terminal region of reelin is not necessary for secretion but is required for efficient activation of downstream signaling. *J. Biol. Chem.* 282, 20544–20552. doi: 10.1074/jbc.M702300200

Niethamer, T. K., and Bush, J. O. (2019). Getting direction(s): the Eph/ephrin signaling system in cell positioning. *Dev. Biol.* 447, 42–57. doi: 10.1016/j.ydbio.2018.01.012

Nitta, N., Heinrich, C., Hirai, H., and Suzuki, F. (2008). Granule cell dispersion develops without neurogenesis and does not fully depend on astroglial cell generation in a mouse model of temporal lobe epilepsy. *Epilepsia* 49, 1711–1722. doi: 10.1111/j.1528-1167.2008.01595.x

Ogawa, M., Miyata, T., Nakajima, K., Yagyu, K., Seike, M., Ikenaka, K., et al. (1995). The reeler gene-associated antigen on cajal-retzius neurons is a crucial molecule for laminar organization of cortical neurons. *Neuron* 14, 899–912. doi: 10.1016/0896-6273(95)90329-1

Orcinha, C., Münzner, G., Gerlach, J., Kilias, A., Follo, M., Egert, U., et al. (2016). Seizure-induced motility of differentiated dentate granule cells is prevented by the central reelin fragment. *Front. Cell. Neurosci* 10:183. doi: 10.3389/fncel.2016.00183

Pahle, J., Muhia, M., Wagener, R. J., Tippmann, A., Bock, H. H., Graw, J., et al. (2020). Selective inactivation of reelin in inhibitory interneurons leads to subtle changes in the dentate gyrus but leaves cortical layering and behavior unaffected. *Cereb. Cortex* 30, 1688–1707. doi: 10.1093/cercor/bhz196

Pesold, C., Impagnatiello, F., Pisu, M. G., Uzunov, D. P., Costa, E., Guidotti, A., et al. (1998). Reelin is preferentially expressed in neurons synthesizing γ-aminobutyric acid in cortex and hippocampus of adult rats. *Proc. Natl. Acad. Sci. U.S.A.* 95, 3221–3226. doi: 10.1073/pnas.95.6.3221

Rakic, P. (1972). Mode of cell migration to the superficial layers of fetal monkey neocortex. *J. Comp. Neurol.* 145, 61–83. doi: 10.1002/cne.901450105

Rakic, P., Knyihar-Csillik, E., and Csillik, B. (1996). Polarity of microtubule assemblies during neuronal cell migration. *Proc. Natl. Acad. Sci. U.S.A.* 93, 9218–9222. doi: 10.1073/pnas.93.17.9218

Reddy, S. S., Connor, T. E., Weeber, E. J., and Rebeck, W. (2011). Similarities and differences in structure, expression, and functions of VLDLR and ApoER2. *Mol. Neurodegener.* 6, 1–10. doi: 10.1186/1750-1326-6-30

Rice, D. S., and Curran, T. (2001). Role of the Reelin signaling pathway in central nervous system development. *Annu. Rev. Neurosci.* 24, 1005–1039. doi: 10.1146/annurev.neuro.24.1.1005

Rice, D. S., Sheldon, M., D'Arcangelo, G., Nakajima, K., Goldowitz, D., and Curran, T. (1998). Disabled-1 acts downstream of Reelin in a signaling pathway that controls laminar organization in the mammalian brain. *Development* 125, 3719–3729. doi: 10.1242/dev.125.18.3719

Rivas, R. J., and Hatten, M. E. (1995). Motility and cytoskeletal organization of migrating cerebellar granule neurons. *J. Neurosci.* 15, 981–989. doi: 10.1523/jneurosci.15-02-00981.1995

Sakai, K., Tiebel, O., Ljungberg, M. C., Sullivan, M., Lee, H. J., Terashima, T., et al. (2009). A neuronal VLDLR variant lacking the third complement-type repeat exhibits high capacity binding of apoE containing lipoproteins. *Brain Res.* 1276, 11–21. doi: 10.1016/j.brainres.2009.04.030

Sato, Y., Kobayashi, D., Kohno, T., Kidani, Y., Prox, J., Becker-Pauly, C., et al. (2016). Determination of cleavage site of Reelin between its sixth and seventh repeat and contribution of meprin metalloproteases to the cleavage. *J. Biochem.* 159, 305–312. doi: 10.1093/jb/mvv102

Sekine, K., Honda, T., Kawauchi, T., Kubo, K. I., and Nakajima, K. (2011). The outermost region of the developing cortical plate is crucial for both the switch of the radial migration mode and the dab1-dependent "inside-out" lamination in the neocortex. *J. Neurosci.* 31, 9426–9439. doi: 10.1523/JNEUROSCI.0650-11.2011

Sentürk, A., Pfennig, S., Weiss, A., Burk, K., and Acker-Palmer, A. (2011). Ephrin Bs are essential components of the Reelin pathway to regulate neuronal migration. *Nature* 472, 356–360. doi: 10.1038/nature09874

Sheldon, M., Rice, D. S., D'Arcangelo, G., Yoneshima, H., Nakajima, K., Mikoshiba, K., et al. (1997). Scrambler and yotari disrupt the disabled gene and produce a reeler- like phenotype in mice. *Nature* 389, 730–733. doi: 10.1038/39601

Shieh, J. C., Schaar, B. T., Srinivasan, K., Brodsky, F. M., and McConnell, S. K. (2011). Endocytosis regulates cell soma translocation and the distribution of adhesion proteins in migrating neurons. *PLoS One* 6:e17802. doi: 10.1371/journal.pone.0017802

Stolt, P. C., and Bock, H. H. (2006). Modulation of lipoprotein receptor functions by intracellular adaptor proteins. *Cell. Signal.* 18, 1560–1571. doi: 10.1016/j.cellsig.2006.03.008

Stoppini, L., Buchs, P. A., and Muller, D. (1991). A simple method for organotypic cultures of nervous tissue. *J. Neurosci. Methods* 37, 173–182. doi: 10.1016/0165-0270(91)90128-M

Strasser, V., Fasching, D., Hauser, C., Mayer, H., Bock, H. H., Hiesberger, T., et al. (2004). Receptor clustering is involved in reelin signaling. *Mol. Cell. Biol.* 24, 1378–1386. doi: 10.1128/mcb.24.3.1378-1386.2004

Thom, M. (2014). Review: hippocampal sclerosis in epilepsy: a neuropathology review. *Neuropathol. Appl. Neurobiol.* 40, 520–543. doi: 10.1111/nan.12150

Tinnes, S., Ringwald, J., and Haas, C. A. (2013). TIMP-1 inhibits the proteolytic processing of Reelin in experimental epilepsy. *FASEB J.* 27, 2542–2552. doi: 10.1096/fj.12-224899

Tinnes, S., Schäfer, M. K. E., Flubacher, A., Münzner, G., Frotscher, M., and Haas, C. A. (2011). Epileptiform activity interferes with proteolytic processing of Reelin required for dentate granule cell positioning. *FASEB J.* 25, 1002–1013. doi: 10.1096/fj.10-168294

Tissir, F., and Goffinet, A. M. (2003). Reelin and brain development. *Nat. Rev. Neurosci.* 4, 496–505. doi: 10.1038/nrn1113

Trommsdorff, M., Gotthardt, M., Hiesberger, T., Shelton, J., Stockinger, W., Nimpf, J., et al. (1999). Reeler/disabled-like disruption of neuronal migration in knockout mice lacking the VLDL receptor and ApoE receptor 2. *Cell* 97, 689–701. doi: 10.1016/S0092-8674(00)80782-5

Trotter, J. H., Lussier, A. L., Psilos, K. E., Mahoney, H. L., Sponaugle, A. E., Hoe, H. S., et al. (2014). Extracellular proteolysis of reelin by tissue plasminogen activator following synaptic potentiation. *Neuroscience* 274, 299–307. doi: 10.1016/j.neuroscience.2014.05.046

Utsunomiya-Tate, N., Kubo, K. I., Tate, S. I., Kainosho, M., Katayama, E., Nakajima, K., et al. (2000). Reelin molecules assemble together to form a large protein complex, which is inhibited by the function-blocking CR-50 antibody. *Proc. Natl. Acad. Sci. U.S.A.* 97, 9729–9734. doi: 10.1073/pnas.160272497

Wang, S., Brunne, B., Zhao, S., Chai, X., Li, J., Lau, J., et al. (2018). Trajectory analysis unveils Reelin's role in the directed migration of granule cells in the

dentate gyrus. *J. Neurosci.* 38, 137–148. doi: 10.1523/JNEUROSCI.0988-17.2017

Yang, N., Higuchi, O., Ohashi, K., Nagata, K., Wada, A., Kangawa, K., et al. (1998). Cofilin phosphorylation by LIM-kinase 1 and its role in Rac-mediated actin reorganization. *Nature* 393, 809–812. doi: 10.1038/31735

Yasui, N., Nogi, T., Kitao, T., Nakano, Y., Hattori, M., and Takagi, J. (2007). Structure of a receptor-binding fragment of reelin and mutational analysis reveal a recognition mechanism similar to endocytic receptors. *Proc. Natl. Acad. Sci. U.S.A.* 104, 9988–9993. doi: 10.1073/pnas.0700438104

Zhao, S., Chai, X., Bock, H. H., Brunne, B., Förster, E., and Frotscher, M. (2006). Rescue of the reeler phenotype in the dentate gyrus by wild-type coculture is mediated by lipoprotein receptors for Reelin and disabled 1. *J. Comp. Neurol.* 495, 1–9. doi: 10.1002/cne.20846

Zhao, S., Chai, X., Förster, E., and Frotscher, M. (2004). Reelin is a potential signal for the lamination of dentate granule cells. *Development* 131, 5117–5125. doi: 10.1242/dev.01387

Conflict of Interest: The authors declare that the research was conducted in the absence of any commercial or financial relationships that could be construed as a potential conflict of interest.

Publisher's Note: All claims expressed in this article are solely those of the authors and do not necessarily represent those of their affiliated organizations, or those of the publisher, the editors and the reviewers. Any product that may be evaluated in this article, or claim that may be made by its manufacturer, is not guaranteed or endorsed by the publisher.

frontiers in Molecular Neuroscience

REVIEW
published: 07 January 2022
doi: 10.3389/fnmol.2021.797253

Roles of N-Methyl-D-Aspartate Receptors (NMDARs) in Epilepsy

*Shuang Chen†, Da Xu†, Liu Fan†, Zhi Fang, Xiufeng Wang and Man Li**

Department of Neurology, Union Hospital, Tongji Medical College, Huazhong University of Science and Technology, Wuhan, China

Epilepsy is one of the most common neurological disorders characterized by recurrent seizures. The mechanism of epilepsy remains unclear and previous studies suggest that N-methyl-D-aspartate receptors (NMDARs) play an important role in abnormal discharges, nerve conduction, neuron injury and inflammation, thereby they may participate in epileptogenesis. NMDARs belong to a family of ionotropic glutamate receptors that play essential roles in excitatory neurotransmission and synaptic plasticity in the mammalian CNS. Despite numerous studies focusing on the role of NMDAR in epilepsy, the relationship appeared to be elusive. In this article, we reviewed the regulation of NMDAR and possible mechanisms of NMDAR in epilepsy and in respect of onset, development, and treatment, trying to provide more evidence for future studies.

Keywords: N-methyl-D-aspartate receptor, epilepsy, anti-NMDAR encephalitis, D-serine, glutamate, excitotoxicity, CREB, epigenomics

OPEN ACCESS

Edited by:
Tobias Engel, Royal College of Surgeons in Ireland, Ireland

Reviewed by:
Hermona Soreq, Hebrew University of Jerusalem, Israel
Nichol Dale, Independent Researcher, Warwick, United Kingdom

****Correspondence:***
Man Li
mmllsy@126.com

†These authors have contributed equally to this work

Specialty section:
This article was submitted to Brain Disease Mechanisms, a section of the journal Frontiers in Molecular Neuroscience

Received: *18 October 2021*
Accepted: *29 November 2021*
Published: *07 January 2022*

Citation:
Chen S, Xu D, Fan L, Fang Z, Wang X and Li M (2022) Roles of N-Methyl-D-Aspartate Receptors (NMDARs) in Epilepsy. Front. Mol. Neurosci. 14:797253. doi: 10.3389/fnmol.2021.797253

INTRODUCTION

Epilepsy is one of the most common neurological disorders characterized by recurrent seizures. Long-term recurrent seizures could lead to cognitive impairment and mental disorders, which severely affect the social interaction level and employment ability of epileptic patients, and result in a decline in the quality of life (Chen et al., 2020a). At present, antiepileptic drugs (AEDs) remain the main therapy of epilepsy, despite no response in about 1/3 patients with epilepsy (Moshé et al., 2015). The mechanism of epilepsy remains unclear but it is generally regarded as a self-facilitated pathological process triggered by brain injury, ultimately resulting in nerve damage, mossin fibrosis, synaptic plasticity, inflammatory response, and ionic pathway dysfunction (Gan et al., 2015). It is widely acknowledged that abnormal excessive synchronous discharge, i.e., the imbalance between excitation and inhibition of neurons, plays an essential role in epileptogenesis. However, the factors affecting this imbalance were sophisticated, and excitatory amino acids were supposed to participate in this imbalance (Bonansco and Fuenzalida, 2016).

In the central nervous system (CNS), N-methyl-D-aspartate receptor (NMDAR) is one of the main excitatory receptors on the synapses of neurons including glutamatergic neurons and GABAergic interneurons, which regulate the balance between neuronal excitation and inhibition (Hendry et al., 1987; Hanada, 2020). Meanwhile, NMDARs, the ionotropic glutamate receptors in the brain, are involved in neuroplasticity, excitatory neurotransmission, and neurotoxicity (Fricker et al., 2018; Horak et al., 2021). Related studies have shown that overexcitation of NMDAR leads to neuronal death in neurological diseases such as epilepsy, stroke, Alzheimer's disease (AD), and Parkinson's disease (PD; Essiz et al., 2021).

In the brain, NMDARs are hetero-tetramers generally composed of two GluN1 subunits and four distinct GluN2 (GluN2A-D) or a mixture of GluN2 with two different GluN3 (GluN3A and 3B) subunits. The GluN1 subunit is required for NMDAR activation and binds to the necessary co-agonists through the amino-terminal domain of the extracellular region. GluN2 subunits are able to bind glutamate specifically and these subunits are different from each other by providing different functional properties of NMDAR. In the NMDAR, *GRIN1* codes for GluN1 subunit, *GRIN2* codes for GluN2 subunit, and *GRIN3* codes for GluN3 subunit (Beesley et al., 2020). Meanwhile, the triheteromer (GluN1/GluN2A/GluN2B) is the main subtype of NMDAR and is widely expressed in the cortex and hippocampus (Luo et al., 1997; Tovar et al., 2013).

Previous studies have shown that glutamate levels increase in the extracellular fluid during seizures in temporal lobe epilepsy (TLE) and glutamate can directly activate NMDAR and induce neuroexcitatory toxicity (Albrecht and Zielińska, 2017). Meanwhile, it has been reported that NMDA, AMPA, and kainite (KA) can induce seizures in animal models, and glutamate receptor antagonists inhibit seizures in animals (Celli and Fornai, 2020). In the PTZ-induced status epilepticus (SE), GluN1, GluN2A, and GluN2B subunits are increased and synaptic plasticity impairs in the hippocampus of rats. Meanwhile, the increase in the GluN2B subunit may result in the decrease of long-term potentiation (LTP; Postnikova et al., 2017). Related studies have shown that *GRIN1*, *GRIN2A*, and *GRIN2B* mutations can lead to epilepsy. In all mutations, *GRIN2A* variants are associated with neurological diseases including developmental and epileptic encephalopathy, which may be manifested as seizures, mild speech and language delay, and cognitive impairment (Lemke et al., 2013, 2014; Fry et al., 2018). In addition, anti-NMDAR encephalitis, a major type of autoimmune encephalitis (AE), has been reported to be an entity of epilepsy (Leypoldt et al., 2015). In addition to neurotoxicity, NMDARs can also participate in neuroprotection by activating cAMP response element-binding protein (CREB) signals in epilepsy (Wang et al., 2020b).

Owing to its role in brain functional plasticity and neuroexcitatory, the regulation of NMDAR in epilepsy has attracted extensive attention. As noted above, NMDARs have been shown to involve in seizures, but functions and mechanisms of NMDARs in epilepsy appear to be elusive. In clinical study, understanding the function of NMDAR is of great significance for the treatment of epilepsy and AEDs selection. This article reviews the regulatory mechanism of NMDAR and the progress of NMDAR in the occurrence, development, and treatment of epilepsy from various points of view (**Figure 1**).

NMDAR AND EPILEPSY

Anti-NMDAR Encephalitis

Anti-NMDAR encephalitis is a major type of AE in which the over-production of NMDAR autoantibodies results in profound neurotransmitter dysregulation, causing seizures and other symptoms such as dysautonomia, orofacial dyskinesia, psychosis, mental status changes, hallucinations, and headaches (Tong et al., 2020). Related studies have shown that approximately 75% of patients with anti-NMDAR encephalitis develop seizures, and refractory status epilepticus (RSE) can lead to neuronal death (Geis et al., 2019). However, the mechanism of anti-NMDAR encephalitis leading to seizures is not fully understood.

NMDARs have been reported to play a role in synaptic homeostasis. Related studies have found that NMDAR autoantibodies could increase extracellular glutamate levels in the brain (Manto et al., 2010). Some findings also have confirmed that NMDAR autoantibodies can result in the internalization of surface NMDARs and the decreasing of receptor density in the patients with anti-NMDAR encephalitis (Hughes et al., 2010; Takahashi et al., 2020). In the patients, NMDAR autoantibodies bind and cross-link to a specific region of NMDARs GluN1, then internalize NMDARs (Gleichman et al., 2012). NMDAR-EphB2 interaction plays a key role in the NMDAR autoantibody-mediated NMDAR internalization. When autoantibodies bind to endogenous NMDARs, the interaction between NMDAR and EphB2 is disrupted, thereby leading to NMDAR internalization and dysfunction, and the reduction of NMDAR-mediated synaptic currents (Hughes et al., 2010; Mikasova et al., 2012). After activation of EphB2, the extracellular domain of EphB2 interacts directly with the GluN1 subunit, thereby stabilizing NMDARs in the synapse (Dalva et al., 2000; Washburn et al., 2020). Meanwhile, a related report has indicated that NMDAR autoantibody interferes with the interaction between NMDARs and EphB2 in cultured hippocampal neurons (Mikasova et al., 2012). In addition, cerebrospinal fluid (CSF) of the patient with anti-NMDAR encephalitis can also result in the reduction of both GluN2A and GluN2B on the synaptic surface and prevent a chemically induced LTP of glutamate synapses (Mikasova et al., 2012). Similar to the anti-NMDAR antibodies-mediated effect, the amino terminal domain (ATD) peptide of GluN1 subunit can also actively immunize against NMDARs and induce anti-NMDAR encephalitis in a mouse model (Ding et al., 2021). A study shows that a single injection of anti-NMDAR antibodies from the patient with anti-NMDAR encephalitis into mice does not induce seizures (Wright et al., 2015). However, injection of anti-NMDAR antibodies *in vivo* can increase the number of seizures in the PTZ induced-mice model. Moreover, about 75–93% of mice developed epilepsy after long-term infusion of CSF or purified anti-NMDAR antibodies from patients with anti-NMDAR encephalitis (Wright et al., 2015). It is puzzling that the function reduction of NMDAR is more likely to activate the persistent abnormal discharge of neurons, but a specific inhibition of the NMDARs in the GABAergic interneurons can also explain this phenomenon (Manto et al., 2010). NMDAR autoantibodies reduce the excitability of GABAergic interneurons through the interaction with NMDAR, thereby weakening the inhibitory effect on excitatory transduction of glutamatergic neurons (Geis et al., 2019). The disinhibition of excitatory glutamatergic neurons may also account for seizures in anti-NMDAR encephalitis. In addition, it has been found that ketamine, an NMDAR

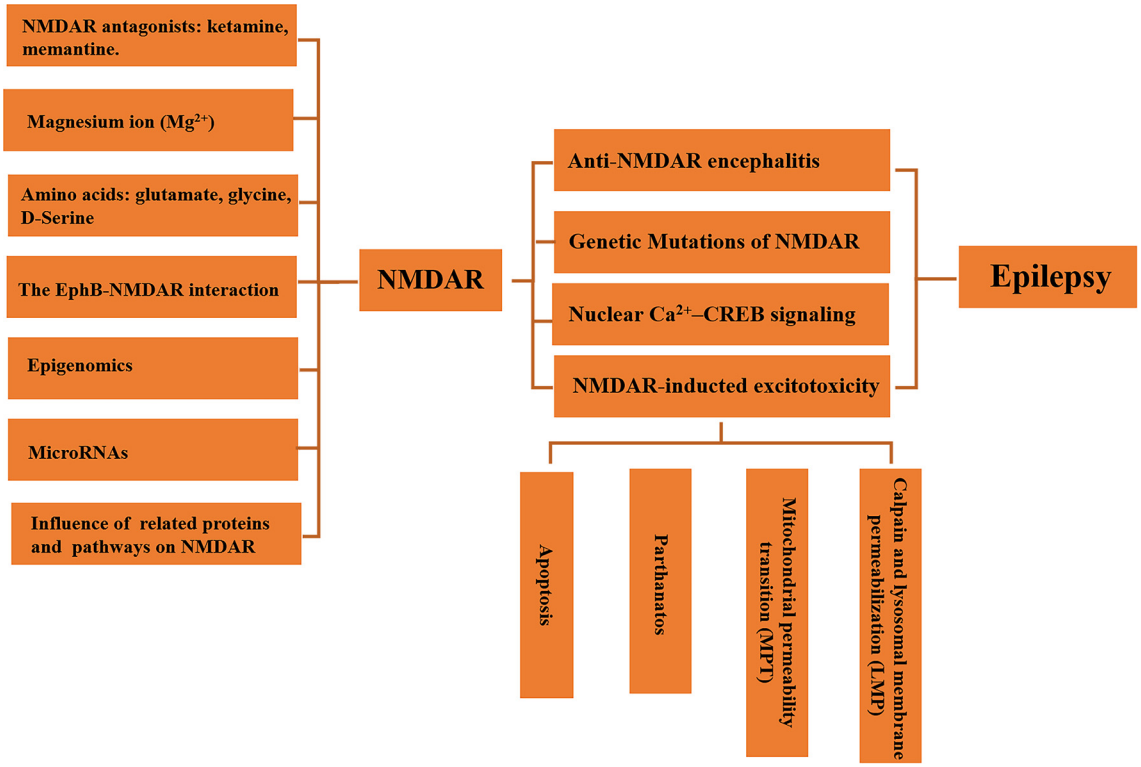

FIGURE 1 | Regulation of neuroexcitatory receptor N-Methyl-D-Aspartate Receptor (NMDAR) in epilepsy.

antagonist, may be useful in super-refractory status epilepticus (SRSE) developed in patients with anti-NMDAR encephalitis (Santoro et al., 2019). Despite the profound effect on NMDARs, there is no evidence that NMDAR autoantibodies can alter the localization and expression of other glutamate receptors such as AMPARs, the synaptic protein PSD-95, as well as the number of synapses, or affect the survival of nerve cells *in vitro* or *in vivo* models (Huang and Xiong, 2021). In a word, both the activation of NMDARs in glutamatergic neurons and the inhibition of NMDARs in GABAergic interneurons may participate in epileptogenesis and more researches are urgently needed.

NMDAR in Epilepsy

In recent years, NMDAR subunit-encoding genes have been confirmed to be involved in epilepsy and the genetic mutations in NMDARs may cause epilepsy in humans, suggesting that NMDAR is closely related to epilepsy (Xu and Luo, 2018). Besides, impairment of NMDAR signals as a result of genetic or environmental insults leads to a variety of neurodevelopmental disorders, including epilepsy, schizophrenia, intellectual disability, or autism (Mielnik et al., 2021). Meanwhile, NMDAR-mediated excitotoxicity was supposed to participate in neuronal death induced by high levels of glutamate and aspartate in neurological diseases such as epilepsy, stroke, AD, and PD (Fricker et al., 2018; Essiz et al., 2021). This article will review genetic mutations of NMDAR, signaling pathways of NMDAR-mediated excitotoxicity, and NMDAR-dependent neuroprotection in epilepsy.

Genetic Mutations of NMDAR in Epilepsy

GluN1 subunit, the essential subunit of functional NMDAR is encoded by GRIN1, and *GRIN1* mutations have a significant effect on neuronal activity, causing various types of epilepsy, including SE, focal dyscognitive seizures, myoclonic seizures, febrile seizures, spasms, hypermotor seizures, tonic and atonic seizures, generalized seizures, etc (Wyllie et al., 2013; Fry et al., 2018). Besides, the epileptic phenotype may contribute to the p. Met641Leu *de novo* variant in *GRIN1* gene, and *de novo GRIN1* mutations were gradually recognized to be in association with severe early infantile encephalopathy (Pironti et al., 2018). The common characteristics are extensive bilateral polymicrogyria with intractable epilepsy, cortical visual impairment, postnatal microcephaly, and severe developmental delay in patients with *de novo GRIN1* mutations (Fry et al., 2018). Extensive bilateral polymicrogyria is associated with severe developmental delay and intractable epilepsy. At present, a variety of polymicrogyria-associated mutations have been found, including p.Asn674Ile, p.Arg794Gln, p.Arg659Trp, p.Asp789Asn, p.Tyr647Cys, p.Asn650Ile, p.Ala653Gly, p.Leu551Pro, p.Ser553Leu, etc (Fry et al., 2018). In *GRIN1* mutations, the mechanisms remained unclear but disrupted gating of the ion channel by p.Gly827Arg mutation and disruption of NMDAR ligand binding by p.Ser688Tyr mutation may be concerned (Zehavi et al., 2017).

Current studies have found that GluN2 subunits may control epileptiform events in the hippocampus (Punnakkal and Dominic, 2018). *GRIN2A*, which encodes the GluN2A subunits, is widely considered to be epileptogenic. The most common types of seizure caused by *GRIN2A* mutations include atypical benign partial epilepsy, Landau–Kleffner syndrome (LKS), and benign epilepsy with centro-temporal spikes (BECT; Hanada, 2020). GluN2 subunits mainly regulate the open/close of the NMDARs. GluN2A-containing receptors have a reversible calcium-dependent inactivation, whereas GluN2B does not (Franchini et al., 2020). Meanwhile, GluN2A subunits can regulate neuronal NMDAR-induced microglia-neuron physical interactions (Eyo et al., 2018). Related studies have shown that voltage-independent GluN2A-related NMDAR-Ca^{2+} signaling is related to audiogenic seizures, attentional and cognitive deficits in mice (Bertocchi et al., 2021). A rare variant of *GRIN2A* associated with epilepsy disrupts CaMKIIα phosphorylation of GluN2A and NMDAR trafficking, which demonstrates a role of GluN2A for CaMKIIα phosphorylation in receptor targeting and suggests that the defects of NMDAR trafficking are related to epilepsy (Mota Vieira et al., 2020). There were defects of GRIN2A related to epileptiform discharges and transient microstructural brain abnormalities in mice with epilepsy (Salmi et al., 2018). The mutant GluN2A (p.Met817Val)-containing receptors decreased sensitivity to endogenous negative inhibitors (Mg, zinc), prolonged the time of synaptic response, increased the time of single-channel mean open, and the probability of channel open. These acquired *GRIN2A* mutations lead to overactivation of NMDAR and increase neuronal excitability, which may be related to epileptogenesis observed in patients (Chen et al., 2017). A *de novo GRIN2A* missense mutation (p.Asp731Asn) in a child with focal epilepsy and acquired epileptic aphasia was reported. However, this mutant reduced NMDAR activation, suggesting that NMDAR hypofunction may also be related to epilepsy pathogenesis (Gao et al., 2017).

GRIN2B mutation is a rare cause of severe epileptic encephalopathy (Sharawat et al., 2019). A related study demonstrated that *GRIN2B, BDNF*, and *IL-1β* gene significantly were upregulated and *GRIN2B* was positively correlated with the expressions of *BDNF* and *IL-1β* gene in people with epilepsy (Zhand et al., 2018). Some *GRIN2B* mutations (p.Val618Gly and p.Asn615Ile) were found in patients with early-onset epilepsy and epileptic encephalopathy (Lemke et al., 2014; Smigiel et al., 2016). Those GluN2B heteromers showed a significant loss of ion-channel block by extracellular Mg^{2+} and a significant increase of Ca^{2+} permeability (Lemke et al., 2014). Meanwhile, blocking GluN2B-containing NMDARs can reduce short-term brain injury caused by early-life SE (Loss et al., 2019).

In addition, *GRIN2C* expression is limited to astrocytes whereas *GRIN2D* are expressed at high levels in GABAergic interneurons in the hippocampus (Shelkar et al., 2019; Dubois and Liu, 2021). These specific distributions are likely to be highly relevant to mechanisms of epilepsy and dysregulation of glutamatergic signaling. Some *GRIN2D* variants (p. Thr674Lys, p.Met681Ile, p.Ser694Arg, p, Asp449Asn, p.Val667Ile, p.Ser573Phe, p.Leu670Phe, p.Ala675Thr, p.Ala678Asp, p.Ser1271Leu, and p.Arg1313Trp) have been found in developmental and epileptic encephalopathy (Tsuchida et al., 2018; Jiao et al., 2021). In a novel *GRIN2D* variant with epileptic encephalopathy, *GRIN2D* mutation-related epilepsy is found to be refractory to conventional AEDs (Camp and Yuan, 2020; Jiao et al., 2021). However, *GRIN2D* dominant mutations can cause severe epileptic encephalopathy, which can be treated with NMDAR channel blockers (Li et al., 2016). In epilepsy, we need to further understand the unique characteristics of *GRIN2D* mutations in neurological function and pathology, which is conducive to the treatment of refractory epilepsy.

NMDAR Mediates Excitotoxicity in Epilepsy

In the CNS, high levels of glutamate induce neuronal death by NMDAR-mediated excitotoxicity (Olney, 1971). Glutamate-induced excitotoxicity is mainly attributed to apoptosis, autophagy, parthanatos, phagocytosis, ferroptosis, apoptosis-inducing factor (AIF), calpain I, mitochondrial permeability transformation (MPT), lysosomal membrane permeability (LMP), and RNS and ROS production (**Figure 2**; Fricker et al., 2018). Activated NMDARs lead to neuronal depolarization and calcium (Ca^{2+}) loading. The increasing of cytoplasmic Ca^{2+} can cause the activation of nNOS, calpain I, and MPT pore, eventually leading to neuronal death (**Figure 2**; Fricker et al., 2018). Overexcitation of NMDAR leads to neuronal death in neurological diseases such as epilepsy, stroke, AD, and PD, and blockade of NMDARs can reduce neuronal death in the brain (Essiz et al., 2021).

Calpain and Lysosomal Membrane Permeabilization (LMP)

Activated NMDAR leads to Ca^{2+} influx, which activates calpain. Calpain I is involved in the late phase of neuronal death caused by mitochondrial dysfunction. Calpain I, a cysteine protease highly expressed in neurons, is activated by high levels of Ca^{2+} in the cytoplasm and can cleave Bid and Bax, leading to the release of AIF and cytochrome C from the mitochondria (Wang, 2000; D'Orsi et al., 2012). Meanwhile, the release of cytochrome C can induce the activation of caspases, and activated calpain I can also directly cleave and activate caspases, thus resulting in apoptosis (Wang, 2000). However, AIF is cleaved by calpain I to a truncated AIF (tAIF), which translocates to the nucleus and induces DNA cleavage, thereby leading to apoptosis and parthanatos (Fricker et al., 2018). In addition, GluN2A subunit-containing synaptic NMDARs preferentially activates calpain I, which is conducive to neuronal survival by selectively degrading the protein phosphatase PHLPP1α and PHLPP1*β* (Wang Y. et al., 2013). On the contrary, calpain II is selectively activated by GluN2B subunit-containing extrasynaptic NMDARs and calpain II participates in neuronal death by degrading the protein tyrosine phosphatase STEP (Hoque et al., 2016). Further studies are needed to clarify the role of these two isoforms of calpains in excitotoxic neuronal death.

Activated calpain can also cause LMP, thereby releasing the toxic cathepsin into the cytoplasm and leading to lysosomal cell death (LCD), also known as autolysis in neurodegenerative diseases (Fricker et al., 2018). It has been found that ischemia

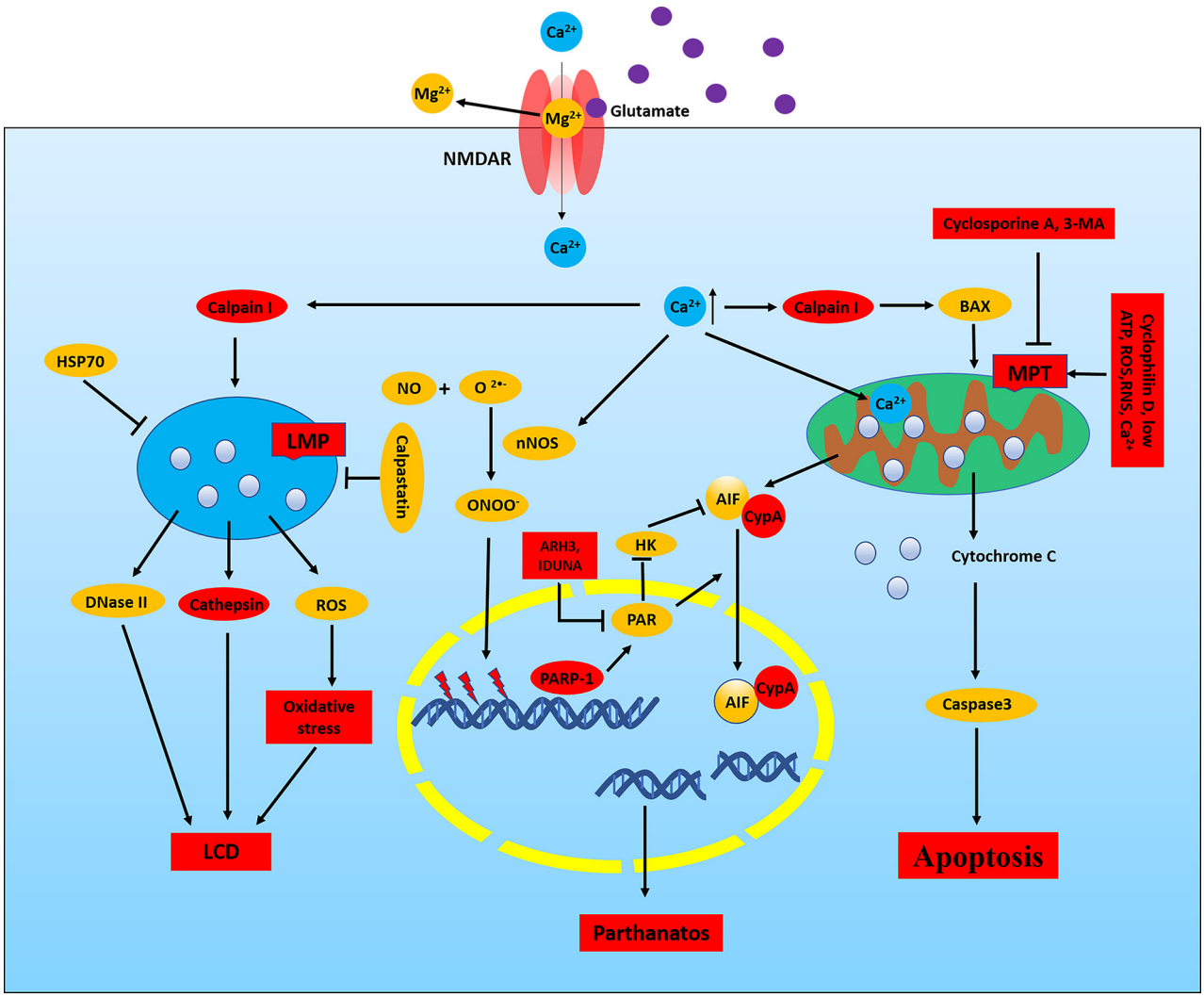

FIGURE 2 | NMDAR-mediated excitotoxicity in epilepsy. In neurons, the NMDAR channel is blocked by Mg^{2+} at neuronal resting membrane potential, and Mg^{2+} is removed when the membrane is depolarized. Activated NMDAR leads to calcium loading which will cause the activation of nNOS, calpain I, and mitochondrial permeability transformation (MPT) pore and eventually lead to neuronal death. Calpain I can cleave Bid and Bax, leading to the release of apoptosis-inducing factor (AIF) and cytochrome C from the mitochondria. Meanwhile, cytochrome C can induce the activation of caspase, and calpain I can also directly cleave and activate caspases, thus resulting in apoptosis. In addition, AIF is cleaved by calpain I to a tAIF, which translocates to the nucleus and induces DNA cleavage, thereby leading to apoptosis and parthanatos. Activation of calpain can cause lysosomal membrane permeability (LMP), which releases the toxic cathepsin, DNase II, and ROS, thereby resulting in LCD. Meanwhile, HSP70 and calpastatin can resist LMP. Increased Ca^{2+}, ROS, RNS, and low ATP in mitochondrial matrix results in MPT which depends on the opening of mPTP. Cyclosporine A and 3-MA can block MPT. Ca^{2+} directly activates nNOS, which can catalyze NO and O_2^- to form $ONOO^-$. $ONOO^-$ damages DNA, thereby activating PARP1, resulting in parthanatos. PARP1 is involved in chromosomal stability, DNA repair, and inflammatory responses. PAR, the product of PARP1 activity, induces nuclear translocation of AIF and inhibits HK. Nuclear translocation of AIF requires the involvement of CypA, which binds to AIF and forms CypA-AIF complex after the release from mitochondria, thereby participating in DNA degradation and leading to parthanatos. ARH3 reduces PAR levels in the nucleus and cytoplasm and IDUNA reduces the release of AIF by binding to the PAR polymers and prevents PARP1-induced cell death. LCD, lysosomal cell death; HSP70, heat shock protein 70; HK, hexokinase.

can induce calpain I to be localized in lysosomes and cause neuronal LMP (Yamashima et al., 1998; Windelborn and Lipton, 2008). Meanwhile, multiple stimuli can also induce LMP, release cathepsin, and induce cell death through a variety of pathways. However, activated NMDAR may also lead to LMP, which is dependent on the activation of calpain (Yan et al., 2016). Activated calpain I can also cleave and inactivate Na^+/Ca^{2+} exchangers in the plasma membrane of the nerve cells during neuroexcitatory toxicity, thereby leading to calcium overload and necrosis (Bano et al., 2005). Thus, calcium overload and neuronal death can be effectively inhibited by inhibiting calpain. In addition, the absence of calpastatin, a natural calpain inhibitor expressed in neurons, makes neurons more susceptible to excitotoxicity, and its overexpression inhibits neuronal death attributed to excitotoxicity (Descloux et al., 2015). Meanwhile, heat shock protein 70 (HSP70) also stabilizes lysosomes to

resist LMP (Aits and Jäättelä, 2013). In conclusion, NMDAR can promote activation of calpain and LMP, while inhibition of calpain and LMP may be an effective method to reduce neuronal death caused by NMDAR-mediated excitotoxicity in epilepsy.

Mitochondrial Permeability Transition (MPT)

Activated NMDARs can also result in MPT by Ca^{2+} influx, involved in neuronal death. MPT is characterized by a significant increase in the permeability of the inner mitochondrial membrane with increased Ca^{2+} concentration, which eventually leads to oxidative phosphorylation decoupling, depletion of cell energy, and necrotic cell death. MPT largely depends on the opening of mitochondrial permeability transition pore (mPTP; Fricker et al., 2018). However, increased Ca^{2+} concentration in the mitochondrial matrix is an important factor leading to the opening of mPTP. In addition, it is also closely associated with ROS and RNS, the decreasing of ATP, the decreasing of mitochondrial membrane potential, and intracellular acidification (Fricker et al., 2018). The opening of mPTP leads to the depolarization of the inner mitochondrial membrane, the reduction of ATP production and the increasing of ATP consumption, the rupture of the mitochondrial membrane and the release of cytochrome C and cytochrome G, eventually causing irreversible cellular respiratory arrest and cell death (El-Mir et al., 2008; Fricker et al., 2018). Activated NMDARs can induce MPT by increasing Ca^{2+}, ROS, and RNS in neurons, while cyclosporine A can reduce neuronal death by blocking MPT (Schinder et al., 1996). Meanwhile, MPT is also inhibited by 3-methyladenine (3-MA), an inhibitor of autophagosome formation, which can inhibit kinases to regulate neuronal survival and death (Xue et al., 2002). Correlative experimental data showed that cyclosporine A had different protective effects on excitotoxicity induced hippocampal nerve cell death (Santos and Schauwecker, 2003). Thus, blocking the opening of mPTP by cyclosporine A or the gene knockout of cyclophilin D can partially prevent neuronal death caused by excitotoxicity. In addition, studies have shown that high levels of Ca^{2+}, ROS, and low levels of ATP in the cytoplasm can promote MPT in the brain of epilepsy, and ketone bodies also mediate antiepileptic effects through MPT (Kim et al., 2015). These studies suggest that MPT may play an important role in the occurrence and treatment of epilepsy.

Parthanatos

Ca^{2+} enters the cytoplasm by activating NMDARs and directly activates nNOS which is significantly expressed in the cytoplasm of some GABAergic neurons of the hippocampus and cortex. Activated nNOS can catalyze the reaction of NO with O_2^-, thereby producing peroxynitrite ($ONOO^-$), which interacts with DNA, lipids, and proteins through a direct oxidative stress response, leading to parthanatos or apoptosis (**Figure 2**; Conrad et al., 2016; Ivanova V. et al., 2020). Parthanatos is an important form of cell death, characterized by dependence on the overactivation of the nuclear protein PARP1 after DNA damage and ROS production (Virág et al., 2013). Related studies have shown that glutamate is involved in inducing neuronal injury through the activation of PARP-1 and generation of poly-ADP-ribose (PAR) polymer, thereby participating in parthanatos (Andrabi et al., 2011). In brief, activated NMDARs can promote $ONOO^-$ production by activating nNOS, which damages DNA and activates PARP, eventually resulting in parthanatos.

As is well-known, PARP1 and PARP2 are involved in chromosomal stability, DNA repair, and inflammatory responses (Curtin and Szabo, 2013). In PARP-dependent death, activated PARP1 results in production and NAD^+ depletion. The direct interaction between AIF and PAR promotes the nuclear translocation of AIF, which leads to chromatin degradation (Andrabi et al., 2008; Wang et al., 2011). Meanwhile, PAR is the product of PARP1 activity and also induces nuclear translocation of AIF by inhibiting hexokinase (HK; Wang et al., 2009). Overactivated PARP1 leads to NAD^+ depletion that further disrupts cellular metabolic processes and promotes cell death (Alano et al., 2010). Nuclear translocation of AIF also requires the involvement of cyclophilin A (CypA), which binds to AIF after the release from mitochondria and forms CypA-AIF complex, thereby participating in DNA degradation under various cellular stress conditions, such as cerebral hypoxia-ischemia and traumatic brain injury (TBI; Zhu et al., 2007; Farina et al., 2017). Related studies have shown that inhibiting the formation of the CypA-AIF complex can reduce glutamate-induced HT22 hippocampal cell death (Doti et al., 2014). The release of AIF in mitochondria may also be associated with calpain, BH3-only protein Bid, and BNIP3 (Fricker et al., 2018). In addition, PAR levels are also regulated by the ADP-ribosyl-acceptor hydrolase 3 (ARH3), which reduces PAR levels in the nucleus and cytoplasm (Mashimo et al., 2013). Meanwhile, the protein IDUNA, also known as E3 ubiquitin protein ligase RNF146, binds to the PAR polymers, thereby reducing the release of AIF and preventing PARP1-induced cell death (Andrabi et al., 2011).

Glutamate acting on NMDAR induces neuronal injury through activation of PARP-1 and generation of PAR polymer (Andrabi et al., 2011). There is currently considerable evidence supporting the role of parthanatos in a variety of neurological disorders including epilepsy, stroke, PD, and TBI, and the inhibition of PARP-1 and PARP-2 can reduce nuclear translocation of AIF and increase neuroprotection (D'Orsi et al., 2016; Xu H. et al., 2019; Dionísio et al., 2021; Koehler et al., 2021). Related studies have found that the formation of the neuronal AIF-CypA complex is considered to be the main target for the recovery of ischemia-stroke injury (Farina et al., 2018). However, in the hippocampal neuronal culture (HNC) model of acute acquired epilepsy, activation of PARP-1 is thought to be a major cause of caspase-independent cell death (Wang S. et al., 2013). Meanwhile, PARP-1-mediated mitochondrial dysfunction promotes neuronal damage in the hippocampus after SE (Lai et al., 2017). In addition, inhibition of PARP-dependent cell death pathways has been shown to prevent seizure-induced neuronal damage (D'Orsi et al., 2016). In epilepsy, activated NMDAR may damage DNA and activate PARP. Thus, blocking PARP-dependent cell death pathways may be a way to mitigate NMDAR-mediated excitotoxicity in epilepsy.

Other Signaling Pathways in NMDAR-Mediated Excitotoxicity

In addition to the signaling pathways described above, NMDAR regulates nerve cell death through other pathways. Activated NMDAR can promote the NADPH oxidase (NOX) to produce O_2^- in neurons, leading to neuronal death. A related study has shown that seizures are induced by NMDAR-mediated activation of NOX-induced oxidative stress and can be arrested by NOX inhibition (Malkov et al., 2019). Meanwhile, activated NMDAR increases c-Jun abundance in several neurodegenerative disorders and following ischemia and SE. Phosphorylated c-Jun is transcriptionally active and can induce apoptosis by upregulation of cell death-inducing genes or by downregulating anti-apoptotic genes (Kravchick et al., 2016). In addition, NMDAR overactivation activates NF-κB signaling to promote IL-1β and IL-6 macrophage marker expression. NMDAR silencing and calpain inhibition reduce inflammatory responses (Cheng et al., 2020). It has been reported that glutamate can reduce the insulin-like growth factor-1 (IGF-1) signal through GluN2B-containing NMDAR in cultured cortical neurons, which is considered to be a new mechanism of glutamate-induced neurotoxicity (Zhao et al., 2020). In epilepsy, increased IGF-1 levels after recurrent hippocampal neuronal discharges might promote seizure by IGF-1R-dependent signaling pathways (Jiang et al., 2015). However, the previous role of the NMDAR-IGF-1 signal is unappreciated in the development of seizure activity.

NMDAR-Dependent Neuroprotection in Epilepsy

Ca^{2+} influx could stimulate and induce cell death, but it is also in association with NMDAR-dependent neuroprotection (Wang et al., 2020b). Ca^{2+} entering the cytoplasm *via* synaptic NMDAR causes an increase of nuclear Ca^{2+} (Wang et al., 2020b). Nuclear Ca^{2+} is one of the most effective activators of neuronal gene expression, and nuclear Ca^{2+} can regulate about 200 neuronal genes in hippocampal neurons (Zhang et al., 2007, 2009). The CREB is a signal-regulating transcription factor that plays a critical role in neuronal survival, synaptic plasticity, neurogenesis, learning, and memory. Activated NMDAR results in translocation of CREB regulators from synapse to nucleus (Hardingham and Bading, 2010). In hippocampal neurons, CREB-dependent gene expression was associated with neuroprotection against apoptosis and excitatory damage, which depends on the nuclear Ca^{2+} signaling (Papadia et al., 2005). However, some studies have also shown that activated extrasynaptic NMDARs can promote the shutdown of CREB, thereby causing mitochondrial membrane potential loss and cell death. Meanwhile, activated synaptic NMDARs activate only the CREB pathway and do not activate apoptosis (Hardingham and Bading, 2010; Franchini et al., 2020).

Synaptic NMDAR activity can activate CREB-dependent gene expression by a variety of signal pathways (**Figure 3**). CREB phosphorylates at serine-133 in order to recruit its co-activator CREB binding protein (CBP). Phosphorylation of CREB is mediated by the fast-acting nuclear Ca^{2+}/CaMK pathway and the slower acting, longer lasting Ras-ERK1/2 pathway, both of them are promoted by activation of synaptic NMDARs (Hardingham and Bading, 2010). Nuclear Ca^{2+}-dependent CaMKIV/CaMKII phosphorylates CBP at serine-301. Meanwhile, CBP is also phosphorylated by the Ras-MEK-ERK1/2 pathway or the CaMKII/PKC/PKA-ERK1/2 pathway (Cortés-Mendoza et al., 2013; Lyu et al., 2020). Nuclear translocation of the transducer of regulated CREB (TORC) activity is a key step in CREB activation. Synaptic NMDAR-induced Ca^{2+} signals promote TORC import into the nucleus by calcineurin (CaN)-dependent dephosphorylation (Screaton et al., 2004; Kovács et al., 2007). TORC also acts at least in part by assisting in the recruitment of CBP to CREB. Meanwhile, CREB-regulated transcription coactivator 1(CRTC1) can also dephosphorylate at Ser-151 and is recruited from cytoplasm to the nucleus, where it competes with FXR (fed-state sensing nuclear receptor) for binding to CREB and drives autophagy gene expression (Pan et al., 2021). Some studies have shown that Ca^{2+} influx activates CREB through TRPC6, which is an important transcription factor linked to neuronal survival. Activated TRPC6 may inhibit neuronal NMDAR activity through the post-translational means to combat glutamate-induced excitotoxic damage (Shekhar et al., 2021). Finally, CREB can also be activated through the PI3K-AKT-GSK3β pathway and play a neuroprotective role in the hippocampus. GSK-3β deletion also inhibits the activity-dependent neural activation and Ca^{2+}/CaMKIV/CaMKII-CREB signaling (Liu et al., 2017; Srivastava et al., 2018). Related studies have shown that the epileptogenesis of pilocarpine-induced medial temporal lobe epilepsy (MTLE) is associated with abnormal regulation of NMDAR-mediated excitatory neuronal mechanisms and neuronal activity regulated by Ca^{2+}/CaMK signaling (Canto et al., 2021).

The gene of neurotrophin BDNF is regulated by nuclear Ca^{2+}-CREB signaling (Favaron et al., 1993; Hardingham and Bading, 2010). NMDAR activation increases the release of BDNF, which protects neurons from damage caused by NMDAR blockade (Fabbrin et al., 2020; Lian et al., 2021). Some studies have shown that improving mitochondrial dynamics and increasing the activity of the NMDAR-CREB-BDNF pathway could ameliorate synaptic function and neuronal survival in SAMP8 mice (Lian et al., 2021). Synaptic NMDARs and extrasynaptic NMDARs have different physiological functions. Activated synaptic NMDARs lead to phosphorylation and activation of CREB, while activated extrasynaptic NMDARs inhibit CREB pathway (Hardingham and Bading, 2010). ERK1/2 pathway also promotes CREB activation and inactivates the pre-death protein BAD, which is associated with NMDAR-dependent neuroprotection (Hetman and Kharebava, 2006). In addition, nuclear factor I subtype A (NFIA), an NMDAR-dependent activation of other neuroprotective factors, may not be associated with the increase of nuclear Ca^{2+}, but its activation depends on the ERK1/2 pathway and nNOS (Zheng et al., 2010).

The NMDAR-CREB-BDNF pathway plays an important role in inhibiting epileptic seizures (Yu et al., 2019; Sharma et al., 2021). Recent studies have indicated that CREB is involved in the etiology of epilepsy (Wang G. et al., 2020). In the KA-induced epilepsy model, CREB is considered to be one of the main upstream transcription factors regulating gene expression and is closely related to the severity of

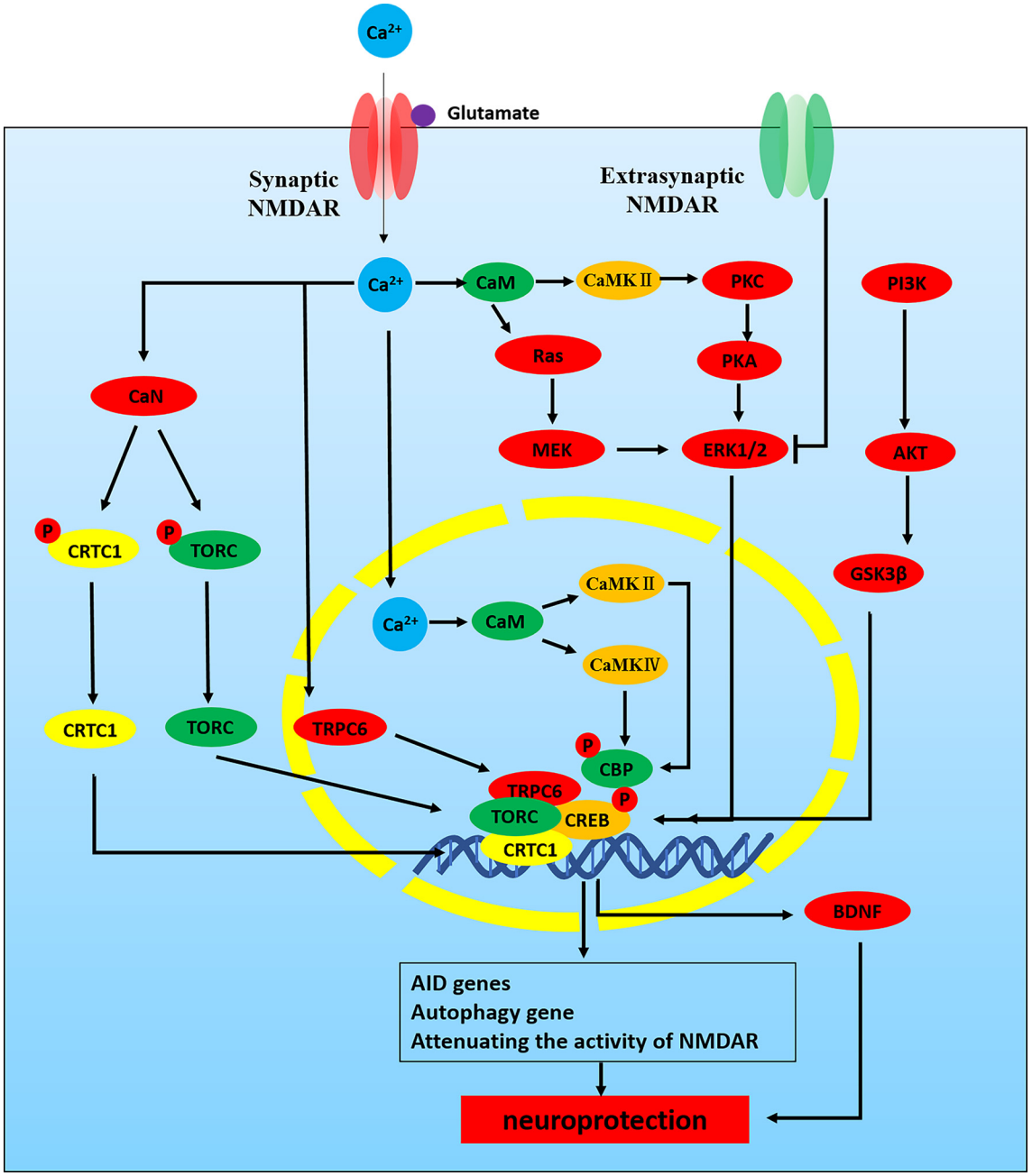

FIGURE 3 | NMDAR -Ca^{2+}-CREB signaling pathways in neuroprotection. NMDAR activity can activate CREB-dependent gene expression. CREB must be phosphorylated at serine-133 in order to recruit its co-activator CREB binding protein (CBP). Phosphorylation of CREB is mediated by the fast-acting nuclear Ca^{2+}/CaMK pathway and the slower acting, longer lasting Ras-ERK1/2 pathway, both of which are promoted by activation of synaptic NMDARs. (1) Nuclear Ca^{2+}-CaM-CaMKIV/CaMKII-CREB: nuclear Ca^{2+}-dependent CaMKIV/CaMKII phosphorylates CBP at serine-301. (2) ERK1/2-CREB: CBP is also phosphorylated by Ras-MEK-ERK1/2 pathway or CaMKII/PKC/PKA-ERK1/2 pathway. CREB phosphorylated at serine-133 recruits its CBP. In addition, nuclear translocation of TORC activity is a key step in CREB activation. (3) Ca^{2+}-TORC-CREB: synaptic NMDAR-induced Ca^{2+} signals promote TORC import into the nucleus by CaN-dependent dephosphorylation. TORC acts at least in part by assisting in the recruitment of CBP to CREB. (4) Ca^{2+}-CRTC1-CREB: CRTC1 dephosphorylates at Ser-151 and is recruited from cytoplasm to the nucleus, where it competes with FXR for binding to CREB and drives autophagy gene expression. (5) Ca^{2+}-TRPC6-CREB: Ca^{2+} influx through TRPC6 activates CREB, an important transcription factor linked to neuronal survival. (6) PI3K-AKT-GSK3β-CREB.

epilepsy (Conte et al., 2020). Meanwhile, recent studies have shown that CREB reduces oxidative neuronal damage in TLE associated with cognitive impairment (Xing et al., 2019). In addition, microRNA-204 also inhibits the epileptiform discharge of hippocampal neurons *in vitro* by regulating TrkB-ERK1/2-CREB signaling (Xiang et al., 2016). NMDAR mediates

CREB-dependent gene expression, which is closely associated with neuroprotection against apoptosis and excitatory damage, so the study of the regulatory mechanism of the NMDAR-CREB pathway in epilepsy is conducive to the neuroprotection of the epileptic brain. However, the regulatory mechanism of the NMDAR-CREB pathway in epilepsy is not entirely clear and needs further exploration.

THE REGULATION OF NMDAR IN EPILEPSY

Although NMDAR affects the occurrence of epilepsy through a variety of mechanisms, it is also regulated by a variety of factors. Activation of the NMDAR is a cooperative process, which depends on: (1) the relief of Mg^{2+} block of the ion channel pore; (2) depolarization of the postsynaptic membrane; and (3) the agonist glutamate, and co-agonists (glycine, D-serine; Jorratt et al., 2021). In addition, the expression and function of NMDAR are also affected by the expression and transcription process of related NMDAR genes, microRNAs, related proteins, and signaling pathways. On this basis, we will discuss a variety of factors for the regulation of NMDARs in the occurrence, development, and treatment of epilepsy (**Tables 1**, **2**).

NMDAR Antagonists

NMDAR antagonists play an important role in the treatment of epilepsy. NMDAR antagonists enhance the anticonvulsant effect of lithium chloride on PTZ-induced clonic seizures in mouse (Ghasemi et al., 2010). Animal studies have suggested NMDAR antagonists may become more effective with seizures lasting longer after the failure of the first line therapies (Sánchez Fernández et al., 2019). In addition, the latter epilepsy patients might respond to positive allosteric modulators of the NMDARs (Zhu and Paoletti, 2015).

Ketamine

Ketamine is a noncompetitive NMDAR antagonist and blocks Ca^{2+} influx by binding to phencyclidine-binding sites of NMDAR. Meanwhile, it is used for evidence of clinically RSE and SRSE (Borsato et al., 2020). Ketamine induces developmental neurotoxicity by inhibiting the expression of NMDAR and increasing the sensitivity of neurons to glutamate excitotoxicity, thereby leading to deregulation of Ca^{2+} signaling and triggering oxidative stress and even mitochondrial apoptosis pathways in neurons. Ketamine significantly upregulates the GluN1 subunit of NMDAR in the frontal cortex, thereby triggering neuronal apoptosis (Liu et al., 2011). Meanwhile, mitochondrial dysfunction and oxidative stress in the hippocampus of rats exposed to ketamine are associated with down-regulation of the ERK signaling cascade (Huang et al., 2012; Li et al., 2017). In addition, ketamine induces apoptosis through the mechanism associated with caspase-1-dependent pyroptosis in the hippocampus (Ye et al., 2018). Ketamine also aggravated cognitive impairment and hippocampal neurodegeneration through the ROS/HIF-1α pathway (Yan et al., 2014). However, ketamine inhibits lipopolysaccharide-mediated BV2 microglia inflammation by blocking NMDARs (Lu et al., 2020). It has been shown that ketamine inhibits the NOX2 activation to produce ROS of the mice brain in pilocarpine-induced epilepsy (Tannich et al., 2021). Ketamine-midazolam therapy can reduce the severity of seizures and improve brain pathology in plasma carboxylesterase knockout mice (Marrero-Rosado et al., 2020). A low dose of ketamine can reduce the behavioral changes in pilocarpine-induced epilepsy mice (Tannich et al., 2020).

In clinical studies, ketamine was used in the treatment of RSE and SRSE (Samanta, 2020). Ketamine treatment is associated with a decrease in seizure burden in patients with SRSE (Alkhachroum et al., 2020). Midazolam-ketamine-valproate therapy is significantly more effective than midazolam-fosphenytoin-valproate therapy in seizure reduction (Niquet et al., 2017). Meanwhile, the combination of ketamine-midazolam can reduce the severity of epilepsy, epileptogenesis, and neuropathology in cholinergic-induced SE (Lumley et al., 2021). And ketamine is also used in anti-NMDAR encephalitis-associated RSE (Santoro et al., 2019). Severe epileptic encephalopathy caused by *GRIN2D* mutations can be treated with NMDAR channel blockers (ketamine, magnesium; Li et al., 2016).

Memantine

Different NMDAR subunit gene mutations also have different responses to NMDAR antagonists. it was reported that a 9-year-old boy with severe early-onset epileptic encephalopathy caused by a GRIN2A missense mutation was trialed on memantine and a significant reduction in seizure frequency was revealed (Pierson et al., 2014). Whereas, another study showed that no seizure reduction was found in patients with *GRIN2B* mutation-related encephalopathy treated by memantine despite improved consciousness, behavior, and sleep (Platzer et al., 2017). In addition, a combination of memantine and cathodal direct current stimulation (cDCS) suppressed KA-induced seizures (Sun et al., 2020). Thus, early identifying the location and type of NMDAR subunit gene mutation in epilepsy has guiding significance for the selection of AEDs.

Magnesium (Mg)

The NMDAR ion channel pores are permeable to Ca^{2+} but can be blocked by Magnesium ion (Mg^{2+}) in a strongly voltage-dependent manner, which makes them largely inactive at resting voltages, even in the presence of agonists (Mayer et al., 1984; Nikolaev et al., 2021). Activation of the NMDAR is a cooperative process, which depends on the relief of the Mg^{2+} block of the ion channel pore (Mg^{2+} is removed into the extracellular compartment from the channel pore; Hou et al., 2020; Jorratt et al., 2021). The NMDAR channel is blocked by Mg^{2+} at neuronal resting membrane potential, and Mg^{2+} is removed when the membrane is depolarized (Jorratt et al., 2021; Li et al., 2021). In addition, non-competitive NMDAR ion channel blockers such as MK-801 mainly bind to ion channels of TMD. Since Mg^{2+} normally blocks this channel, the binding of MK-801 requires NMDAR activation and depolarization to release Mg^{2+} (Wong et al., 2021). A relevant study has shown that Mg^{2+} influx, dependent on NMDAR opening, can transduce a signaling pathway to activate CREB in neurons (Hou et al.,

TABLE 1 | The regulation of NMDAR in epilepsy.

Factors		Mechanisms	References
NMDAR antagonists	Ketamine	Ketamine inhibited the expression of NMDAR and increased the sensitivity of neurons to excitotoxicity. Ketamine use in the treatment of RSE and SRSE.	Liu et al. (2011), Huang et al. (2012), Yan et al. (2014), Li et al. (2016, 2017), Niquet et al. (2017), Ye et al. (2018), Santoro et al. (2019), Alkhachroum et al. (2020), Borsato et al. (2020), Lu et al. (2020), Marrero-Rosado et al. (2020), Samanta (2020), Tannich et al. (2020, 2021), and Lumley et al. (2021)
	Memantine	*GRIN2A* missense mutation retained sensitivity to memantine, and memantine test results showed a significant reduction in seizure frequency. The patients with *GRIN2B* mutation-related encephalopathy treated with memantine had improved consciousness, behavior and sleep, but none showed a reduction in seizure frequency.	Pierson et al. (2014), Platzer et al. (2017), and Sun et al. (2020)
	Allosteric modulators	The latter epilepsy patients might respond to positive allosteric modulators of the NMDARs	Zhu and Paoletti (2015)
Amino acids	Glutamate	NMDAR is one of the excitatory receptors that glutamate acts on directly and may lead to diseases such as epilepsy, stroke, AD, and PD.	Alcoreza et al. (2021) and Essiz et al. (2021)
	Glycine	Glycine binds to glycine binding sites on NMDAR to regulate the function of NMDAR.	Mothet et al. (2015)
	D-serine	D-serine regulates NMDAR by binding to the receptor's glycine binding site. The expression of D-serine and NMDAR was significantly increased in patients with intractable epilepsy. The expression of D-serine depends on the regulation of SR and DAAO.	Mothet et al. (2015), Zhu and Paoletti (2015), Ploux et al. (2020), Beesley et al. (2021), Takagi et al. (2021) and Zhang et al. (2021)
	Cysteine/Homocysteine (HCY)	Redox modulation of cysteine residues is one of the post-translational modifications of NMDAR. HCY activates GluN2 subunit-dependent redox regulation of NMDAR by the reduction of NMDAR disulfide.	Kim et al. (2017), Ivanova M. et al. (2020), and Sibarov et al. (2020)
Magnesium (Mg)		NMDAR channel is blocked by Mg^{2+} at neuronal resting membrane potential, and Mg^{2+} is removed when the membrane is depolarized. Magnesium sulfate can inhibit glutamatergic signaling, thereby altering Ca^{2+} influx, leading to reduced excitotoxicity. TLE cell model is often established by magnesium-free extracellular fluid. Transient culture of hippocampal neurons in magnesium-free induces rhythmic and synchronous epileptiform-like activity.	Mayer et al. (1984), Wang et al. (2020b), Elsayed et al. (2021), Jorratt et al. (2021), Li et al. (2021), Mele et al. (2021), Nikolaev et al. (2021), and Zhou et al. (2021)
The EphB-NMDAR interaction		In epilepsy, the interaction of NMDAR-EphB2 was found in anti-NMDAR encephalitis.	Dalva et al. (2000), Henderson et al. (2001), Hughes et al. (2010), Nolt et al. (2011), Gleichman et al. (2012), Mikasova et al. (2012), Geng et al. (2013), Planagumà et al. (2016), Hu et al. (2017), Ernst et al. (2019), Wang et al. (2020a), Washburn et al. (2020), and Ma et al. (2021)
Epigenomics		DNMT3A1 is controlled by activated NMDAR and the expression of NMDAR is also mediated by epigenomics. In epilepsy, *GRIN2B* DNA methylation levels were increased and *BDNF* DNA methylation levels were decreased, which leading to decreased mRNA and protein expression of GluN2B and increased mRNA and protein expression of BDNF. Suppressive DNMT can increase excitatory postsynaptic potential in hippocampal slices of epileptic rats. Increased TBR1 expression in AF9 mutants is associated with increased expression of GluN1 subunit which is regulated by TBR1.	Büttner et al. (2010), Jiang et al. (2010), D'Aiuto et al. (2011), Ryley Parrish et al. (2013), Kiese et al. (2017), Fachim et al. (2019), Li et al. (2019), Bayraktar et al. (2020), and de Sousa Maciel et al. (2020)

(Continued)

TABLE 1 | Continued

Factors		Mechanisms	References
Proteins and signaling pathways	SPARCL-1	SPARCL-1 localizes to excitatory synapses after SE; SPARCL-1 is involved in synaptic modifications underlying epileptogenesis and remodeling events associated with neuronal degeneration following neural injury.	Chen et al. (2020b) and Gan and Südhof (2020)
	SPDI	SPDI knockdown inhibit seizure activity by nitrososylation-independent thiolation on NMDAR in acute and chronic epileptic model.	Jeon and Kim (2018)
	POSH	POSH is involved in epilepsy by increasing surface NMDAR expression.	Wang X. et al. (2017)
	Nwd1	Inhibition of Nwd1 activity can reduce the hyperexcitability and GluN2B phosphorylation of hippocampal neurons.	Yang et al. (2019)
	TMEM25	TMEM25 modulates the degradation of GluN2B subunits and neuronal excitability.	Zhang et al. (2019)
	DAPK1	DAPK1 interacts with NMDAR and involves in glutamate-induced neurological events, such as stroke. Inhibiting DAPK1 can lead to phosphorylation and surface normalization of GluN2B expression outside the synapse.	DeGregorio-Rocasolano et al. (2020), Schmidt et al. (2020), and Liu et al. (2021)
	PDI	PDI binds to NMDAR in chronic epileptic rats and increases the mercaptan content on recombinant GluN1. PDI can catalyze disulfide bond formation, reduction, and isomerization.	Kim et al. (2017)
	CyclinB/CDK1	CyclinB/CDK1 mediates NMDAR phosphorylation and regulates calcium kinetics and mitosis.	Rosendo-Pineda et al. (2020)
	NSPA	NSPA regulates the postsynaptic stability of NMDAR by ubiquitination of tyrosine phosphatase PTPMEG.	Espinoza et al. (2020)
	SULT4A1	SULT4A1 promotes the formation of PSD-95/NMDAR complex to modulate synaptic development and function.	Culotta et al. (2020)
	PCDH7	PCDH7 interacts with GluN1 subunit to regulate the dendritic spine morphology and synaptic function.	Wang Y. et al. (2020)
	Leptin	Leptin resists to glutamate-induced excitotoxicity in HT22 hippocampal neurons and leptin also increases postsynaptic NMDAR currents to sensitize NTS neurons to vagal input	Jin et al. (2018) and Neyens et al. (2020)
	P2X2 and P2X4	Both P2X2 and P2X4 interact with NMDAR in an inhibitory manner.	Rodriguez et al. (2020)
	NRG1-ErbB4 signaling	NRG1-ErbB4 signaling inhibits phosphorylation of GluN2B at position 1472 by Src kinase. NRG1-ErbB4 signaling may act as a homeostasis regulator, which can protect the brain from the seizure-like activity aggravation.	Zhu et al. (2017)
	ERK1/2 signals	CCL2 rapidly enhances NMDA-induced neuronal electrical currents through the ERK-Glun2B pathway. CXCR7 regulates GluN2A expression by activating ERK1/2, thereby modulating NMDAR-mediated synaptic neurotransmission in hippocampal granulosa cells. Icaritin (ICT) has a neuroprotective effect on glutamate-induced neuronal damage and its mechanism may be associated with inactivating GluN2B-containing NMDAR by ERK/DAPK1 pathway.	Xu T. et al. (2019), Zhang H. et al. (2020), and Liu et al. (2021)
	Cholinergic signals	ACh potentiates NMDARs through muscarinic receptors in CA1 neurons of the hippocampus. Nicotinic α7-nAChR is enriched in the glutamate network synapses in the dorsolateral PFC (dlPFC) and is required for NMDAR action.	Markram and Segal (1990), Flores-Hernandez et al. (2009), and Yang et al. (2013).
	Redox modulation	Cysteine, HCY and PDI are involved in redox modulation of NMDAR. H_2S blocks the enhancement of neuronal excitability in the early hippocampal network by inhibiting voltage-gated sodium channels and NMDARs.	Kim et al. (2017), Yakovlev et al. (2017), Ivanova M. et al. (2020), and Sibarov et al. (2020)
β-hydroxybutyrate and acetone		The inhibitory effect of β-hydroxybutyrate and acetone in NMDARs may be the basis for the therapeutic benefits of ketogenic diet in epilepsy.	Pflanz et al. (2019)

TABLE 2 | Regulation of microRNAs on NMDARs in nervous system.

MicroRNAs	Mechanisms	References
MicroRNA-219, MicroRNA-219a-2	MicroRNA-219 has a regulatory effect on NMDAR in the amygdala and hippocampus of patients with mesial TLE microRNA-219 protects against seizure in the KA-induced epilepsy model. MicroRNA-219a-2 can reduce calcium overload and apoptosis by HIF1α/NMDAR pathway.	Zheng et al. (2016), Hamamoto et al. (2020), and Hu et al. (2020)
microRNA-139-5P	MicroRNA-139-5P has a negative regulatory effect on GluN2A-NMDAR in pilocarpine-induced epilepsy model and TLE patients.	Alsharafi et al. (2016)
MicroRNA-34c	MicroRNA-34c plays a negative role in epileptic seizure cognitive function, by regulating NMDARs and AMPARs associated with LTP.	Huang et al. (2018)
microRNA-15a-5p	Both in hippocampal tissues of SE rats and low Mg-induced hippocampal neurons, propofol can inhibit apoptosis of hippocampal neurons by microRNA-15a-5p/GluN2B/ERK1/2 pathway	Liu et al. (2020)
MicroRNA-124	MicroRNA-124 suppresses seizure and regulates CREB1 activity. Inhibition of neuronal firing by microRNA-124 is associated with the suppression of AMPAR- and NMDAR-mediated currents, accompanied by decreased expression of NMDAR	Wang et al. (2016)
MicroRNA-211, microRNA-128	microRNA-211 or microRNA-128 transgenic mice displayed seizures.	Feng et al. (2020)
MicroRNA-223	MicroRNA-223 regulates the expression of GluN2B subunit, plays a therapeutic role in stroke and other excitotoxic neuronal disorders.	Harraz et al. (2012)
MicroRNA-132, microRNA-107	MicroRNA-132 and microRNA-107 could involve in NMDAR signaling by influencing the expression of pathway genes or the signaling transmission.	Zhang et al. (2015)
MicroRNA-19a, microRNA-539	MicroRNA-19a and microRNA-539 can influence the levels of NMDARs subunits by targeting the mRNAs encoding GluN2A and GluN2B subunits respectively.	Corbel et al. (2015)
MicroRNA-125, microRNA-132	FMRP is an RNA-binding protein responsible for interacting with microRNA-125 and microRNA-132 to regulate NMDAR, and consequently affecting synaptic plasticity	Lin (2015)
MicroRNA-204	EphB2 is a direct target of microRNA-204 and microRNA-204 downregulates EphB2 in hippocampal neurons. EphB2 regulates the surface expression of the NMDAR GluN1 subunit.	Mohammed et al. (2016)
MicroRNA-182-5p	MicroRNA-182-5p regulates nerve injury-induced nociceptive hypersensitivity by targeting EphB1 which interacts with the NMDAR	Zhou et al. (2017)

2020). Magnesium sulfate is a neuroprotective agent in clinical practice. By noncompetitively blocking NMDARs, magnesium sulfate can inhibit glutamatergic signaling, thereby altering Ca^{2+} influx, leading to reduced excitotoxicity (Elsayed et al., 2021). *In vitro*, TLE cell model is often established by treating primary hippocampal cells with magnesium-free extracellular fluid. Transient culture of hippocampal neurons in magnesium-free induces rhythmic and synchronous epileptiform-like activity (Mele et al., 2021).

The low-affinity binding site of Mg^{2+} is located deep in the ion channel and is modulated by the NMDAR subunit. Related studies have shown that NMDAR complexes formed by GluN2A or GluN2B subunits have a higher affinity for Mg^{2+} than those containing GluN2C or GluN2D (Monyer et al., 1994). Due to different GluN2 subunits, NMDAR has different sensitivity to Mg^{2+} (Valdivielso et al., 2020). An important feature of the GluN2 subunits is that GluN2A and GluN2B subunits are more sensitive to voltage-dependent Mg^{2+} blocking than GluN2C and GluN2D subunits (Qian et al., 2005). Meanwhile, the GluN2C subunit contributes to a lower threshold for Mg^{2+} block and influences NMDAR agonist activity (Intson et al., 2020). Compared to GluN1/GluN2D receptors or other NMDAR subtypes, GluN1/GluN2C receptors exhibit higher blockade with ketamine in the presence of Mg^{2+}(Shelkar et al., 2019). The human NMDAR GluN2A variant influences channel blocker potency. A novel genetic variant of *GRIN2A* has been identified in patients with epileptic encephalopathy altering residues located in the NMDAR ion channel pore and significantly reducing Mg^{2+} blockade and channel conductance (Marwick et al., 2019). In functional studies, the *GRIN2A* mutation decreased the potency of endogenous negative modulators, including magnesium and zinc (Fernández-Marmiesse et al., 2018). In addition, missense mutations of *GRIN2B* also alter NMDAR ligand binding and ion channel properties. *GRIN2B* mutants showed decreased glutamate potency, increased NMDAR desensitization, and disappearance of voltage-dependent Mg^{2+} block (Fedele et al., 2018). Meanwhile, Mg^{2+} deficiency down-regulated GluN2B subunits expression in cultured hippocampal slices (Zhou et al., 2021). In addition, presynaptic release and postsynaptic transporter transport zinc (Zn) to different microdomains to regulate NMDAR neurotransmission. Meanwhile, zinc inhibits synaptic NMDARs, which depend on the binding of GluN2A to zinc transporter ZnT1(Krall et al., 2020). In conclusion, Mg^{2+} plays an important role in the pathogenesis of epilepsy. The most prominent of these is voltage-dependent block of the NMDAR channel by Mg^{2+}.

Amino Acids

Glutamate

It is widely believed that the imbalance between excitatory and inhibitory neurotransmission leads to hyperexcitability

of neuronal circuits, which is the basis of the process of epileptogenesis (Alcoreza et al., 2021). Glutamate is an excitatory neurotransmitter in the brain involved in various neural functions and metabolic processes of the CNS (Wang et al., 2020b). NMDAR is one of the excitatory receptors that glutamate acts on directly and may lead to diseases such as epilepsy, stroke, AD, and PD (Essiz et al., 2021). On the one hand, glutamate can be directly synthesized *de novo* by astrocytes in the brain. On the other hand, glutamate can also be produced indirectly with glucose molecules through the action of pyruvate dehydrogenase and pyruvate carboxylase in astrocytes (Schousboe et al., 2014). Meanwhile, extracellular glutamate can be transferred to astrocytes by excitatory amino acid transporter 2 (EAAT2) and then converted to glutamine by glutamine synthetase (GS). Glutamine is transported by astrocytic glutamine transporter-5 (SNAT-5) to the extracellular environment, where it can then be transferred to neurons by astrocytic glutamine transporter-1 (SNAT-1; Danbolt, 2001). In the pre-synaptic neurons, phosphate-activated glutaminase (PAG/GLS-1) converts inactive glutamine to glutamate, which is repackaged into synaptic vesicles and released into the synaptic cleft and directly acts on the NMDAR in the post-synaptic neurons, thus activating NMDAR (Limón et al., 2021). In a word, the glutamate and glutamine cycle in astrocytes and neurons is called the glutamate-glutamine cycle (**Figure 4**).

Astrocyte dysfunction can alter glutamate homeostasis, leading to neuroexcitatory toxicity (Niciu et al., 2012). Excessive glutamate can cause neuroexcitatory toxicity after being released into the synaptic cleft, and excess glutamate needs to be cleared quickly in the brain (Schousboe et al., 2014). However, due to the absence of extracellular enzymes, the uptake of extracellular glutamate mainly relies on EAATs which are located in the plasma membranes of neurons and glia (Zhang et al., 2016). Meanwhile, astrocytes can also completely enclose the glutamate synapse to quickly clear glutamate from the synaptic cleft (Alcoreza et al., 2021). Once glutamate enters the astrocyte, it is converted to glutamine and returned to the neuron by the glutamate-glutamine cycle (Alcoreza et al., 2021). In addition, over-activated astrocytic NMDARs could lead to the release of many other molecules that are likely to be relevant. Astrocyte GluN2A regulates nerve growth factor β (β-NGF) synthesis, maturation, and secretion by regulating pNF-κB, Furin, and VAMP3. It is found that the neuroprotective role of astrocytic GluN2A in the promotion of synapse survival is by regulating these molecules (Du et al., 2021). Both glutamate and quinolinic acid (QUIN) could activate astrocytic NMDARs, which stimulate Ca^{2+} influx into the cell and can result in dysfunction and death of astrocytes (Lee et al., 2010).

D-Serine

In addition to glutamate, the activation of NMDAR also requires the binding of a co-agonist at the glycine binding site. Originally similar to glycine, D-serine can also control the activation of NMDAR by binding to the receptor's glycine binding site in the brain (**Figure 4**; Mothet et al., 2015). Recent studies have indicated that the expression of D-serine and NMDAR is closely related to intractable epilepsy (Zhu and Paoletti, 2015). The review investigated the regulation of NMDAR by D-serine in CNS diseases, including epilepsy.

D-serine is the main endogenous co-agonist of NMDARs, which is significantly dependent on the activity of the metabolic enzyme d-amino acid oxidase (DAAO) and serine racemase (SR). In the brain, DAAO catalyzes the decomposition of D-serine, while the cytoplasmic enzyme SR converts L-serine to D-serine (Takagi et al., 2021). SR is mainly found in neurons, that catalyzes the reversible racemization of L-serine and D-serine (Raboni et al., 2019). On the one hand, D-serine is released from the neuron *via* a plasma membrane transporter (ASC-1/SLC7A10), which mediates D-serine efflux. On the other hand, astrocytes synthesize SR substrate L-serine, which is transferred to neurons through a mechanism of serine shuttle to participate in neuronal D-serine synthesis. L-serine synthesized by astrocytes is dependent on the activity of 3-phosphoglycerate dehydrogenase (PHGDH), which is the key to *de novo* synthesis of L-serine and activation of NMDAR (Neame et al., 2019). Clinically, serine deficiency patients present with severe neurological symptoms, including intractable epilepsy, which suggests the relevance of serine to brain development and morphogenesis (Murtas et al., 2020). Although the activity of SR and DAAO is important for the regulation of D-serine levels, the regulatory mechanisms of SR and DAAO are not fully understood in epilepsy.

DAAO selectively catalyzes the oxidative deamination of natural D-serine to produce imino acid, which is naturally hydrolyzed to the corresponding α-keto acids and ammonia (Pollegioni et al., 2018). Related research has confirmed that inhibition of DAAO can lead to increased D-serine in the brain, thereby regulating a variety of neurophysiological functions including cognitive behavior (Nagy et al., 2020). Meanwhile, it was also found that NMDAR antagonists (MK801 and cocaine) could increase the release of glutamate and decrease the expression of SR and DAAO. However, D-serine and antipsychotics did not modulate the levels of SR and DAAO (Takagi et al., 2021). In addition, the neuroprotective effect of DAAO is also mediated by the ERK1/2 signal pathway (Zhang X. et al., 2020).

In the brain, SR is mainly in excitatory neurons and GABAergic inhibitory interneurons, and is only weakly expressed in astrocytes (Billard, 2018). Through the coordinated activities of ASC-1 and ASCT1 subtypes, D-serine is released and binds with NMDAR to perform neurophysiological functions (Sason et al., 2017; Billard, 2018; Kaplan et al., 2018). The deletion of SR affects the balance of excitatory and inhibitory in the hippocampal CA1 network (Ploux et al., 2020). In addition, related research has found that PKC phosphorylates SR on serine residues and reduces the activity of SR *in vitro*. Similarly, activated PKC also increases SR phosphorylation and decreases the levels of D-serine in the rat frontal cortex (Vargas-Lopes et al., 2011). Therefore, PKC-mediated SR phosphorylation may be important for the activation of NMDARs.

In fact, the specific degradation of D-serine by the enzyme DAAO and the genetic deletion of SR significantly altered the activation of NMDAR. D-serine plays a key role in regulating the functional plasticity of many synapses in the brain (Billard, 2018). Related studies have found that the

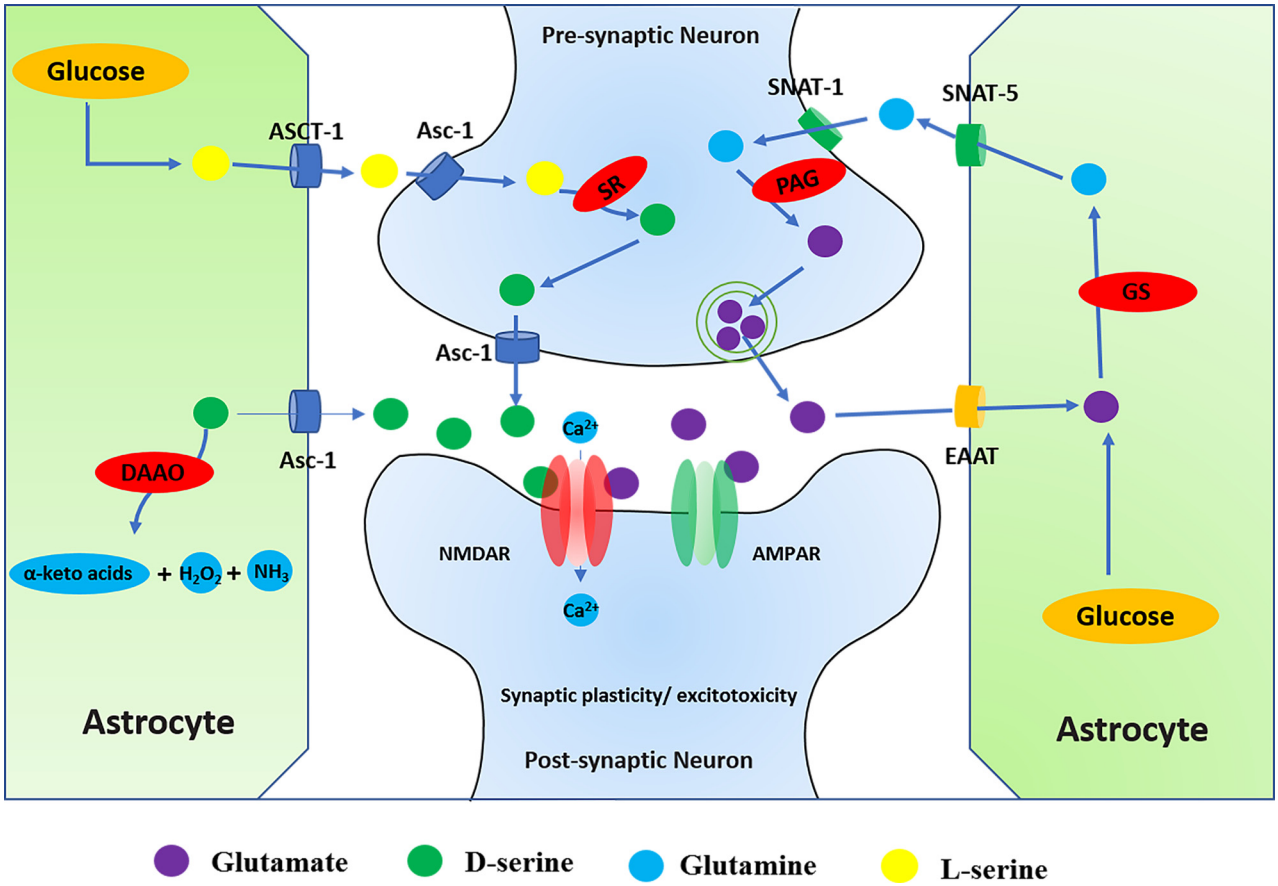

FIGURE 4 | Regulation of NMDARs by D-serine and glutamate. (1) Glutamate can directly act on NMDAR, and the glutamate-glutamine cycle is involved in the regulation of NMDAR. Glutamate-glutamine cycle: glutamate can be directly synthesized *de novo* by astrocytes or indirectly produced from glucose molecules through the actions of pyruvate dehydrogenase and astrocyte-specific enzyme pyruvate carboxylase in the brain. Meanwhile, extracellular glutamate can be transferred to astrocytes by ETTA2 (GLT-1) and then converted to glutamine by glutamine synthetase (GS). Glutamine is transported by SNAT-5 to the extracellular environment, where it can then be transferred to neurons by SNAT-1. In the neuron, glutamine is degraded by PAG into glutamate and ammonia. Glutamate enters the synaptic vesicles in the pre-synaptic neurons and then is released from the pre-synaptic membrane into the synaptic cleave. It directly acts on the NMDAR in the post-synaptic neurons, thus activating NMDAR. (2) In addition to glutamate, activation of NMDAR also requires the binding of D-serine at the glycine binding site. SR converts L-serine to D-serine in the neuron, while DAAO catalyzes the breakdown of d-serine in the astrocyte. D-serine is released from neurons by Asc-1, which mediates D-serine efflux in exchange for external amino acid substrates. L-serine can be directly synthesized *de novo* in astrocytes. Through orchestrated Asc-1 and ASCT1 subtypes, L-serine from astrocytes enters the neuron and is catalyzed by SR to produce D-serine.

beneficial effects of D-serine supplementation may reflect that D-serine levels decreased significantly with age, as supported in the hippocampal trial. Interestingly, this decline of D-serine is also found in human plasma levels (Potier et al., 2010). In addition, in addition to affecting synaptic plasticity and synaptogenesis, dysregulation of D-serine metabolism may also enhance NMDAR-dependent excitotoxicity and promote cognitive impairment and neurodegeneration (Beltrán-Castillo et al., 2018). Therefore, the synaptic availability of D-serine and the preservation of SR activity are critical for maintaining strong cognitive abilities in the brain.

D-serine and NMDAR were found to be significantly upregulated in patients with intractable epilepsy (Zhang et al., 2021). Therefore, the D-serine signal pathway may be a potential target for epilepsy therapy. Endogenous D-serine deficiency may lead to decreased inhibition of the hippocampal CA1 network and altered excitatory/inhibitory balance. besides, D-serine contributes to maintaining cognitive abilities and functional plasticity of synapses (Ploux et al., 2020). Related studies have shown that intracranial injection of D-serine into the medial entorhinal area (MEA) in the TLE is beneficial to prevent neuronal loss and epileptogenesis by rescuing hippocampal CA1 neurons in the epileptic brain and reducing the number of astrocytes and microglia, thus alleviating the effect of neuroinflammation (Beesley et al., 2021). Therefore, D-serine might be a potential therapy target *via* regulating NMDAR in epilepsy, and more studies are needed in the future.

Epigenomics

DNA methylation is a crucial epigenetic mark for activity-dependent gene expression in neurons. It has been shown that the levels of DNA methyltransferase 3A1 (DNMT3A1)

in neurons are closely controlled by the activation of NMDAR-containing GluN2A subunits (Bayraktar et al., 2020). Interestingly, synaptic NMDARs drive methyltransferase degradation in a ubiquitin-like dependent manner. The binding of NEDD8 ubiquitin-like protein to lysine residues inhibits ubiquitination, thereby blocking DNMT3A1 degradation (Bayraktar et al., 2020). Defects in promoter methylation of these activity-dependent genes may be related to synaptic plasticity and memory formation (Bayraktar et al., 2020). Overall, the activity-dependent DNA methylation is regulated by GluN2A-containing NMDAR signals to participate in memory formation. Meanwhile, NO produced by NMDAR activation can also up-regulated DNA methyltransferase 3B (DNMT3B) in the hippocampus (de Sousa Maciel et al., 2020). A related analysis showed that both GluN2B expression levels and histone H3K9 acetylation of *GRIN2B* gene promoter were positively correlated with ethanol withdrawal syndrome (EWS; Li et al., 2019). In addition, the changes of *GRIN2B* promoter methylation may be associated with cognition reduction and glutamatergic dysfunction in schizophrenia (Fachim et al., 2019). Meanwhile, this epigenetic change leads to upregulation of functional NMDAR and abnormal neuronal differentiation (D'Aiuto et al., 2011). In addition, NMDAR expression is also regulated by histone methylation in the brain. Histone methyltransferases targeting histone H3-lysine 9 residues, including Setdb1 (Set domain, bifurcated1)/Eset/Kmt1e, are closely related to inhibition of chromatin remodeling in the adult brain. Meanwhile, the inhibition of Setdb1-mediated histone methylation at *GRIN2B* is associated with decreased expression of GluN2B (Jiang et al., 2010).

In epilepsy, control of epigenetic of epilepsy target genes contributes to cellular memory of epileptogenesis in cultured rat hippocampal neurons (Kiese et al., 2017). In cultured neurons, the altered gene expression and epigenetic modifications can be rescued by blocking action potential propagation or inhibiting glutamatergic activation (Kiese et al., 2017). The epigenetic modification of epileptic target genes and cellular memory of epileptogenesis, which can transform normal neurons and circuits into pro-epileptic neurons and neural circuits (Kiese et al., 2017). SE can also lead to abnormal expression of *GRIN2B* and *BDNF* genes in the hippocampus in TLE (Ryley Parrish et al., 2013). In the epileptic hippocampus, *GRIN2B* DNA methylation levels were increased and *BDNF* DNA methylation levels were decreased, which led to decreased mRNA and protein expression of GluN2B and increased mRNA and protein expression of BDNF. Meanwhile, suppressive DNMT can increase excitatory postsynaptic potential in hippocampal slices of epileptic rats (Ryley Parrish et al., 2013). Therefore, GluN2B DNA methylation may be an early SE-induced event that persists into late epilepsy in the hippocampus and promotes changes of gene expression in TLE. In addition, leukemia-related AF9/MLLT3 mutations are involved in neurodevelopmental disorders such as epilepsy and ataxia (Büttner et al., 2010). Meanwhile, AF9 is found to be an active epigenetic modifier by increasing the expression of GluN1 subunits during the generation of cortical projection neurons (Büttner et al., 2010).

In conclusion, the epigenetic regulation of NMDAR and epilepsy target genes by NMDAR play an important role in the onset and development of seizures. Whereas, the mechanism remains unclear and more studies are urgently needed.

MicroRNA and NMDAR

In recent years, researchers have found a link between microRNAs and NMDARs-mediated neurological diseases (**Table 2**; Alsharafi et al., 2017). A growing body of evidence indicates that microRNAs regulate synaptic homeostasis and plasticity processes, suggesting that they may be involved in synaptic dysfunction during epilepsy, stroke, and AD (Alsharafi et al., 2017). MicroRNA-34a deficiency promotes cognitive function by regulating AMPARs and NMDARs to increase synaptic plasticity (Xu et al., 2018). MicroRNA-219-5p alleviates morphine tolerance by inhibiting the CaMKII/NMDAR pathway (Wang J. et al., 2017). Meanwhile, microRNA-219a-2 has been reported to reduce calcium overload and apoptosis through HIF1α/NMDAR pathway, thus alleviating myocardial ischemia-reperfusion injury (Hu et al., 2020). MicroRNA-182-5p regulates nerve injury-induced nociceptive hypersensitivity by targeting Ephrin type-b receptor 1 (EphB1) which interacts with the NMDAR (Zhou et al., 2017). EphB2 is a direct target of microRNA-204 and microRNA-204 downregulates EphB2 in hippocampal neurons. EphB2 is a known regulator of synaptic plasticity and regulates the surface expression of the NMDAR GluN1 subunit (Mohammed et al., 2016). Thus, microRNA-204 may play an important role in anti-NMDAR encephalitis by regulating EphB2-NMDAR, which remains to be explored. In normal neuronal development, FMRP is an RNA-binding protein responsible for interacting with microRNA-125 and microRNA-132 to regulate NMDAR and consequently affecting synaptic plasticity (Lin, 2015). MicroRNA-19a and microRNA-539 can influence the levels of NMDARs subunits by targeting the mRNAs encoding GluN2A and GluN2B subunits respectively (Corbel et al., 2015). MicroRNA-219, microRNA-132, and microRNA-107 could be involved in NMDAR signaling by influencing the expression of pathway genes or the signaling transmission (Zhang et al., 2015). MicroRNA-223 as a major regulator of the expression of the GluN2B subunit, plays a therapeutic role in stroke and other excitotoxic neuronal disorders (Harraz et al., 2012). These microRNAs provide an entry point for affecting neural plasticity and abnormal nerve firing and provide a new approach for the treatment of NMDAR-related neurological diseases.

In epilepsy, some microRNAs (microRNA-34, microRNA-124, microRNA-146a, microRNA-135a, microRNA-23a, microRNA-132, microRNA-234-5p, microRNA-203, microRNA-181b, microRNA-155 microRNA-219, microRNA-211, microRNA-128, microRNA-23) have been reported and each microRNA has limitations as a potential epilepsy target (Feng et al., 2020). Importantly, microRNA-211 or microRNA-128 transgenic mice displayed seizures (Feng et al., 2020). However, some microRNAs play an important role in epilepsy by regulating NMDARs. MicroRNA-219 had a regulatory effect on NMDAR in the amygdala and hippocampus of patients with mesial TLE and microRNA-219

protects against seizure in the KA-induced epilepsy model (Zheng et al., 2016; Hamamoto et al., 2020). Meanwhile, microRNA-139-5P has a negative regulatory effect on GluN2A-NMDAR in pilocarpine-induced epileptic rat models and TLE patients (Alsharafi et al., 2016). MicroRNA-34c has also been found to play a negative role in seizure and cognitive function, possibly by regulating NMDARs and AMPARs associated with LTP (Huang et al., 2018). Both in hippocampal tissues of SE rats and low Mg-induced hippocampal neurons, propofol can inhibit apoptosis of hippocampal neurons by microRNA-15a-5p/GluN2B/ERK1/2 pathway, which provides theoretical support for propofol treatment of SE (Liu et al., 2020). MicroRNA-124 suppresses seizure and regulates CREB1 activity. Inhibition of neuronal firing by microRNA-124 is associated with the suppression of mEPSC, AMPAR- and NMDAR-mediated currents, which are accompanied by decreased surface expression of NMDAR (Wang et al., 2016). However, many microRNAs have not been confirmed to function in epilepsy by regulating NMDAR. The discovery of various microRNA is also beneficial for the treatment of epilepsy and reducing the occurrence of epilepsy.

The EphB2-NMDAR Interaction

The interaction between NMDAR and EphB2 was found in anti-NMDAR encephalitis (Hughes et al., 2010; Mikasova et al., 2012). It is reported that transcranial direct current stimulation promotes hippocampal neurogenesis in mice with cerebral ischemia by activation of Ephrinb1/EphB2/MAP-2/NMDAR pathway (Ma et al., 2021). Meanwhile, activated EphB receptors promote the excitability of primary sensory neurons either directly through Ca^{2+} influx or by phosphorylation of Src kinase-mediated NMDAR (Washburn et al., 2020). In the acute phase of ischemic stroke, EphB2-dependent signal pathways are found to promote neuronal NMDAR-induced excitotoxicity and inflammation (Ernst et al., 2019). In AD models, overexpression of EphB2 in hippocampal neurons improved impaired NMDAR and cognitive dysfunction (Hu et al., 2017). In addition, EphB2 has a positive protective effect on Aβ1-42 oligomer-induced neurotoxicity by synaptic NMDAR signal pathway in hippocampal neurons (Geng et al., 2013). EphB2 can also prevent the effects of NMDAR antibodies on memory and neuroplasticity (Planagumà et al., 2016). EphB2 regulates NMDAR function and synaptic targeting. In mature neurons, EphB2 regulates the number of synaptic NMDAR, while activated EphB2 reduces desensitization of Ca^{2+}-dependent NMDAR and is required for enhanced synaptic localization of GluN2B-containing NMDAR. EphB knockout mice showed the homeostatic upregulation of NMDAR expression (Nolt et al., 2011). Synaptic plasticity is regulated by the EphB2-GluN2A-AKT cascade, which might be a potential pathogenesis of depression and potential therapeutic target of glutamatergic transmission dysfunction (Wu et al., 2019). Meanwhile, EphrinB/EphB signaling is conducive to synaptic plasticity by GluN2B phosphorylation in chronic migraine (Wang et al., 2020a). In dentate granular neurons of EphB2-deficient mouse, synaptic NMDAR-mediated current was reduced (Henderson et al., 2001). These findings suggest that EphB is a key regulator of NMDAR synaptic localization and NMDAR-dependent synaptic function in the CNS. Together, the regulation of synaptic function may be closely related to EphB2-NMDAR interaction in epilepsy.

Influence of Related Proteins and Signaling Pathways on NMDAR

In addition to the above regulation mechanisms, NMDAR is also modulated by other pathways. Related studies have demonstrated that both purinergic P2X receptors (P2X2) and P2X4 interact with NMDAR in an inhibitory manner (Rodriguez et al., 2020). Meanwhile, SULT4A1 promotes the formation of the PSD-95/NMDAR complex to modulate synaptic development and function (Culotta et al., 2020). It is also found that S-PrP interacts with LRP1/NMDAR system to activate ERK1/2, thereby promoting cell migration in Schwann cells (Mantuano et al., 2020). Neuronal surface P antigen (NSPA) regulates the postsynaptic stability of NMDAR by ubiquitination of tyrosine phosphatase PTPMEG (Espinoza et al., 2020). In addition, Cyclin B/CDK1 mediates NMDAR phosphorylation and regulates calcium kinetics and mitosis (Rosendo-Pineda et al., 2020). Neuroinflammation modulation is known to be controlled by cholinergic signals (Mizrachi et al., 2021). However, ACh potentiates NMDARs through muscarinic receptors in CA1 neurons of the hippocampus (Markram and Segal, 1990). Nicotinic α7-nAChR is enriched in the glutamate network synapses in the dorsolateral PFC (dlPFC) and is required for NMDAR action (Yang et al., 2013). LTP can be induced by exposure to the cholinergic receptor agonist carbachol in the hippocampus, which depends on NMDAR activation (Flores-Hernandez et al., 2009).

In addition, NMDAR is also regulated by ERK signaling pathway. In the spinal cord, CCL2 rapidly enhances NMDAR-induced neuronal electrical currents through the ERK-Glun2B pathway, thereby promoting pain sensitivity (Zhang H. et al., 2020). Related studies have found that CXCR7 can control the synaptic activity of hippocampal granular cells to regulate seizures. CXCR7 regulates GluN2A expression on the cell membrane by activating ERK1/2, thereby selectively modulating NMDAR-mediated synaptic neurotransmission in hippocampal granular cells (Xu T. et al., 2019). Therefore, CXCR7 may regulate seizures and become a new target for antiepileptic therapy by regulating the cell membrane expression of NMDAR. Some studies find that icaritin (ICT) has a neuroprotective effect on glutamate-induced neuronal damage and its mechanism may be associated with inactivating GluN2B-containing NMDAR by ERK/DAPK1 pathway (Liu et al., 2021). Meanwhile, DAPK1 interacts with NMDAR involved in glutamate-induced neurological events during sudden physiopathologic conditions in the brain (DeGregorio-Rocasolano et al., 2020). Inhibition of DAPK1 results in the phosphorylation and surface normalization of GluN2B expression outside the synapse (Schmidt et al., 2020).

Redox modulation of cysteine residues is one of the post-translational modifications of NMDAR. HCY accumulation in the human plasma, known as hyperhomocysteinemia, can exacerbate neurodegenerative diseases and act as a persistent NMDAR agonist (Ivanova M. et al., 2020). Meanwhile, HCY activates GluN2 subunit-dependent redox regulation of NMDAR

by the reduction of NMDAR disulfide (Sibarov et al., 2020). The protein disulfide isomerase (PDI) binds to NMDAR in chronic epileptic rats and increases the mercaptan content on recombinant GluN1 protein (Kim et al., 2017). In fact, PDI plays a crucial role in catalyzing disulfide bond formation, reduction, and isomerization (Kim et al., 2017). Besides, H_2S blocks the enhancement of neuronal excitability in the early hippocampal network by inhibiting voltage-gated sodium channels and NMDARs (Yakovlev et al., 2017). Thus, redox regulation of NMDAR may affect the occurrence and development of epilepsy and provide a new way for reducing the occurrence of epilepsy.

In epilepsy, some proteins and organisms can also affect NMDAR activity. As shown in the treatment of epilepsy, the inhibitory effect of β-hydroxybutyrate and acetone on NMDARs may underlie the therapeutic effects of the ketogenic diet in epilepsy (Pflanz et al., 2019). The interaction between the PCDH7 and the GluN1 subunit regulates the dendritic spine morphology and synaptic function, and it is associated with several CNS diseases including epilepsy (Wang Y. et al., 2020). In acute and chronic epileptic models, SPDI knockdown can inhibit seizure activity by nitrosylation-independent thiolation on NMDAR (Jeon and Kim, 2018). Inhibition of Nwd1 activity can reduce the hyperexcitability and phosphorylation of GluN2B in hippocampal neurons (Yang et al., 2019). Meanwhile, TMEM25 can also modulate the degradation of the GluN2B subunit and neuronal excitability (Zhang et al., 2019). Inhibition of acid-sensing ion channel 3 can regulate NMDAR function, thereby aggravating seizure severity (Cao et al., 2018). POSH could be a potential therapeutic target for epilepsy *via* increasing surface expression of NMDAR (Wang X. et al., 2017). Previous studies have shown that neuregulin1(NRG1)-ErbB4 signaling pathway may regulate the excitability of neurons and participate in primary epilepsy. NRG1-ErbB4 signaling can inhibit the phosphorylation of GluN2B, which has been detected in symptomatic human epileptic tissue (Zhu et al., 2017). In addition, the extracellular matrix protein SPARCL-1 also directly promotes synapse formation and NMDAR recruitment. In addition, SPARCL-1 might directly increase branches of dendrites, augment the numbers of synapse, and induce the formation of NMDARs, thereby increasing synaptic connectivity and reducing the risk for neurodegenerative disease (Chen et al., 2020b; Gan and Südhof, 2020). Leptin resists glutamate-induced excitotoxicity in HT22 hippocampal neurons and leptin also increases postsynaptic NMDAR currents to sensitize the nucleus of the solitary tract (NTS) neurons to vagal input (Jin et al., 2018; Neyens et al., 2020).

CONCLUSION

In this review, we reviewed and elucidated the regulatory mechanisms of NMDAR and its role in the onset, development, and treatment of epilepsy. Increasing evidence suggests that NMDAR is closely related to epilepsy and the autoimmune encephalopathy. Synaptic NMDARs mainly mediate pro-survival and synaptic plasticity pathways, whereas extrasynaptic NMDARs are mostly responsible for glutamate-induced excitotoxicity. Meanwhile, different NMDAR subunit also has different physiological functions in epilepsy. Studying the role of various NMDAR subunits in epilepsy may be beneficial to understand epileptogenesis. At present, there are many ways to regulate NMDAR, but the regulatory mechanism of NMDAR in the onset and development of epilepsy is not fully understood. Therefore, targeting upstream and downstream signal pathways of NMDAR may be a new approach to inhibit seizures and slow the progression of epilepsy. This type of treatment is yet to be discovered and explored.

AUTHOR CONTRIBUTIONS

SC participated in experimental studies. SC and LF searched and sorted out the references and participated in drafting the manuscript. DX and ML coordinated and supervised the work, provided research direction, designed research plans, and modified the final drafts. All authors have carefully read and confirmed the final manuscript. All authors contributed to the article and approved the submitted version.

FUNDING

This study was supported by grants from the National Natural Science Foundation of China (No. 82171315).

ACKNOWLEDGMENTS

We thank for the support of Department of Neurology, Wuhan Union hospital.

REFERENCES

Aits, S., and Jäättelä, M. (2013). Lysosomal cell death at a glance. *J. Cell Sci.* 126, 1905–1912. doi: 10.1242/jcs.091181

Alano, C., Garnier, P., Ying, W., Higashi, Y., Kauppinen, T., and Swanson, R. (2010). NAD+ depletion is necessary and sufficient for poly(ADP-ribose) polymerase-1-mediated neuronal death. *J. Neurosci.* 30, 2967–2978. doi: 10.1523/JNEUROSCI.5552-09.2010

Albrecht, J., and Zielińska, M. (2017). Mechanisms of excessive extracellular glutamate accumulation in temporal lobe epilepsy. *Neurochem. Res.* 42, 1724–1734. doi: 10.1007/s11064-016-2105-8

Alcoreza, O., Patel, D., Tewari, B., and Sontheimer, H. (2021). Dysregulation of ambient glutamate and glutamate receptors in epilepsy: an astrocytic perspective. *Front. Neurol.* 12:652159. doi: 10.3389/fneur.2021.652159

Alkhachroum, A., Der-Nigoghossian, C., Mathews, E., Massad, N., Letchinger, R., Doyle, K., et al. (2020). Ketamine to treat super-refractory status epilepticus. *Neurology* 95, e2286–e2294. doi: 10.1212/WNL.0000000000010611

Alsharafi, W., Luo, Z., Long, X., Xie, Y., and Xiao, B. (2017). MicroRNA in glutamate receptor-dependent neurological diseases. *Clin. Sci. (London)* 131, 1591–1604. doi: 10.1042/CS20170964

Alsharafi, W., Xiao, B., and Li, J. (2016). MicroRNA-139–5p negatively regulates NR2A-containing NMDA receptor in the rat pilocarpine model and patients with temporal lobe epilepsy. *Epilepsia* 57, 1931–1940. doi: 10.1111/epi.13568

Andrabi, S., Dawson, T., and Dawson, V. (2008). Mitochondrial and nuclear cross talk in cell death: parthanatos. *Ann. N Y Acad. Sci.* 1147, 233–241. doi: 10.1196/annals.1427.014

Andrabi, S., Kang, H., Haince, J., Lee, Y., Zhang, J., Chi, Z., et al. (2011). Iduna protects the brain from glutamate excitotoxicity and stroke by interfering with poly(ADP-ribose) polymer-induced cell death. *Nat. Med.* 17, 692–699. doi: 10.1038/nm.2387

Bano, D., Young, K., Guerin, C., Lefeuvre, R., Rothwell, N., Naldini, L., et al. (2005). Cleavage of the plasma membrane Na+/Ca2+ exchanger in excitotoxicity. *Cell* 120, 275–285. doi: 10.1016/j.cell.2004.11.049

Bayraktar, G., Yuanxiang, P., Confettura, A., Gomes, G., Raza, S., Stork, O., et al. (2020). Synaptic control of DNA methylation involves activity-dependent degradation of DNMT3A1 in the nucleus. *Neuropsychopharmacology* 45, 2120–2130. doi: 10.1038/s41386-020-0780-2

Beesley, S., Sullenberger, T., Ailani, R., D'Orio, C., Crockett, M., and Kumar, S. (2021). d-Serine intervention in the medial entorhinal area alters TLE-related pathology in CA1 hippocampus *via* the temporoammonic pathway. *Neuroscience* 453, 168–186. doi: 10.1016/j.neuroscience.2020.10.025

Beesley, S., Sullenberger, T., and Kumar, S. (2020). The GluN3 subunit regulates ion selectivity within native N-methyl-d-aspartate receptors. *IBRO Rep.* 9, 147–156. doi: 10.1016/j.ibror.2020.07.009

Beltrán-Castillo, S., Eugenín, J., and von Bernhardi, R. (2018). Impact of aging in microglia-mediated D-serine balance in the CNS. *Mediators Inflamm.* 2018:7219732. doi: 10.1155/2018/7219732

Bertocchi, I., Eltokhi, A., Rozov, A., Chi, V., Jensen, V., Bus, T., et al. (2021). Voltage-independent GluN2A-type NMDA receptor Ca signaling promotes audiogenic seizures, attentional and cognitive deficits in mice. *Commun. Biol.* 4:59. doi: 10.1038/s42003-020-01538-4

Billard, J. (2018). Changes in serine racemase-dependent modulation of NMDA receptor: impact on physiological and pathological brain aging. *Front. Mol. Biosci.* 5:106. doi: 10.3389/fmolb.2018.00106

Bonansco, C., and Fuenzalida, M. (2016). Plasticity of hippocampal excitatory-inhibitory balance: missing the synaptic control in the epileptic brain. *Neural Plast.* 2016:8607038. doi: 10.1155/2016/8607038

Borsato, G., Siegel, J., Rose, M., Ojard, M., Feyissa, A., Quinones-Hinojosa, A., et al. (2020). Ketamine in seizure management and future pharmacogenomic considerations. *Pharmacogenomics J.* 20, 351–354. doi: 10.1038/s41397-019-0120-2

Büttner, N., Johnsen, S., Kügler, S., and Vogel, T. (2010). Af9/Mllt3 interferes with Tbr1 expression through epigenetic modification of histone H3K79 during development of the cerebral cortex. *Proc. Natl. Acad. Sci. U S A* 107, 7042–7047. doi: 10.1055/a-1651-7450

Camp, C., and Yuan, H. (2020). GRIN2D/GluN2D NMDA receptor: unique features and its contribution to pediatric developmental and epileptic encephalopathy. *Eur. J. Paediatr. Neurol.* 24, 89–99. doi: 10.1016/j.ejpn.2019.12.007

Canto, A., Matos, A., Godoi, A., Vieira, A., Aoyama, B., Rocha, C., et al. (2021). Multi-omics analysis suggests enhanced epileptogenesis in the cornu ammonis 3 of the pilocarpine model of mesial temporal lobe epilepsy. *Hippocampus* 31, 122–139. doi: 10.1002/hipo.23268

Cao, Q., Xiao, Z., Wang, X., Weng, C., Ding, M., Zhu, F., et al. (2018). Inhibition of acid sensing ion channel 3 aggravates seizures by regulating NMDAR function. *Neurochem. Res.* 43, 1227–1241. doi: 10.1007/s11064-018-2540-9

Celli, R., and Fornai, F. (2020). Targeting ionotropic glutamate receptors in the treatment of epilepsy. *Curr. Neuropharmacol.* 19, 747–765. doi: 10.2174/1570159X18666200831154658

Chen, S., Chen, Y., Zhang, Y., Kuang, X., Liu, Y., Guo, M., et al. (2020a). Iron Metabolism and ferroptosis in epilepsy. *Front. Neurosci.* 14:601193. doi: 10.3389/fnins.2020.601193

Chen, W., Tankovic, A., Burger, P., Kusumoto, H., Traynelis, S., and Yuan, H. (2017). GRIN2AFunctional evaluation of a *de novo* mutation identified in a patient with profound global developmental delay and refractory epilepsy. *Mol. Pharmacol.* 91, 317–330. doi: 10.1124/mol.116.106781

Chen, S., Zou, Q., Chen, Y., Kuang, X., Wu, W., Guo, M., et al. (2020b). Regulation of SPARC family proteins in disorders of the central nervous system. *Brain Res. Bull.* 163, 178–189. doi: 10.1016/j.brainresbull.2020.05.005

Cheng, H., Cheng, Q., Bao, X., Luo, Y., Zhou, Y., Li, Y., et al. (2020). Over-activation of NMDA receptors promotes ABCA1 degradation and foam cell formation. *Biochim. Biophys. Acta Mol. Cell Biol. Lipids* 1865:158778. doi: 10.1016/j.bbalip.2020.158778

Conrad, M., Angeli, J., Vandenabeele, P., and Stockwell, B. (2016). Regulated necrosis: disease relevance and therapeutic opportunities. *Nat. Rev. Drug Discov.* 15, 348–366. doi: 10.1038/nrd.2015.6

Conte, G., Parras, A., Alves, M., Ollà, I., De Diego-Garcia, L., Beamer, E., et al. (2020). High concordance between hippocampal transcriptome of the mouse intra-amygdala kainic acid model and human temporal lobe epilepsy. *Epilepsia* 61, 2795–2810. doi: 10.1111/epi.16714

Corbel, C., Hernandez, I., Wu, B., and Kosik, K. (2015). Developmental attenuation of N-methyl-D-aspartate receptor subunit expression by microRNAs. *Neural Dev.* 10:20. doi: 10.1186/s13064-015-0047-5

Cortés-Mendoza, J., Díaz de León-Guerrero, S., Pedraza-Alva, G., and Pérez-Martínez, L. (2013). Shaping synaptic plasticity: the role of activity-mediated epigenetic regulation on gene transcription. *Int J. Dev. Neurosci.* 31, 359–369. doi: 10.1016/j.steroids.2021.108947

Culotta, L., Scalmani, P., Vinci, E., Terragni, B., Sessa, A., Broccoli, V., et al. (2020). SULT4A1 modulates synaptic development and function by promoting the formation of PSD-95/NMDAR complex. *J. Neurosci.* 40, 7013–7026. doi: 10.1523/JNEUROSCI.2194-19.2020

Curtin, N., and Szabo, C. (2013). Therapeutic applications of PARP inhibitors: anticancer therapy and beyond. *Mol. Aspects Med.* 34, 1217–1256. doi: 10.1016/j.mam.2013.01.006

D'Aiuto, L., Di Maio, R., Mohan, K., Minervini, C., Saporiti, F., Soreca, I., et al. (2011). Mouse ES cells overexpressing DNMT1 produce abnormal neurons with upregulated NMDA/NR1 subunit. *Differentiation* 82, 9–17. doi: 10.1016/j.diff.2011.03.003

Dalva, M., Takasu, M., Lin, M., Shamah, S., Hu, L., Gale, N., et al. (2000). EphB receptors interact with NMDA receptors and regulate excitatory synapse formation. *Cell* 103, 945–956. doi: 10.1016/s0092-8674(00)00197-5

Danbolt, N. (2001). Glutamate uptake. *Prog. Neurobiol.* 65, 1–105. doi: 10.1016/s0301-0082(00)00067-8

de Sousa Maciel, I., Sales, A., Casarotto, P., Castrén, E., Biojone, C., and Joca, S. (2020). Nitric Oxide Synthase inhibition counteracts the stress-induced DNA methyltransferase 3b expression in the hippocampus of rats. *Eur. J. Neurosci.* [Online ahead of print]. doi: 10.1111/ejn.15042

DeGregorio-Rocasolano, N., Guirao, V., Ponce, J., Melià-Sorolla, M., Aliena-Valero, A., García-Serran, A., et al. (2020). Comparative proteomics unveils LRRFIP1 as a new player in the DAPK1 interactome of neurons exposed to oxygen and glucose deprivation. *Antioxidants (Basel)* 9:1202. doi: 10.3390/antiox9121202

Descloux, C., Ginet, V., Clarke, P., Puyal, J., and Truttmann, A. (2015). Neuronal death after perinatal cerebral hypoxia-ischemia: focus on autophagy-mediated cell death. *Int. J. Dev. Neurosci.* 45, 75–85. doi: 10.1016/j.ijdevneu.2015.06.008

Ding, Y., Zhou, Z., Chen, J., Peng, Y., Wang, H., Qiu, W., et al. (2021). Anti-NMDAR encephalitis induced in mice by active immunization with a peptide from the amino-terminal domain of the GluN1 subunit. *J. Neuroinflammation* 18:53. doi: 10.1186/s12974-021-02107-0

Dionísio, P., Amaral, J., and Rodrigues, C. (2021). Oxidative stress and regulated cell death in Parkinson's disease. *Ageing Res. Rev.* 67:101263. doi: 10.1016/j.arr.2021.101263

D'Orsi, B., Bonner, H., Tuffy, L., Düssmann, H., Woods, I., Courtney, M., et al. (2012). Calpains are downstream effectors of bax-dependent excitotoxic apoptosis. *J. Neurosci.* 32, 1847–1858. doi: 10.1523/JNEUROSCI.2345-11.2012

D'Orsi, B., Engel, T., Pfeiffer, S., Nandi, S., Kaufmann, T., Henshall, D., et al. (2016). Bok is not pro-apoptotic but suppresses poly ADP-ribose polymerase-dependent cell death pathways and protects against excitotoxic and seizure-induced neuronal injury. *J. Neurosci.* 36, 4564–4578. doi: 10.1523/JNEUROSCI.3780-15.2016

Doti, N., Reuther, C., Scognamiglio, P., Dolga, A., Plesnila, N., Ruvo, M., et al. (2014). Inhibition of the AIF/CypA complex protects against intrinsic death

pathways induced by oxidative stress. *Cell Death Dis.* 5:e993. doi: 10.1038/cddis.2013.518

Du, Z., Song, Y., Chen, X., Zhang, W., Zhang, G., Li, H., et al. (2021). Knockdown of astrocytic Grin2a aggravates β-amyloid-induced memory and cognitive deficits through regulating nerve growth factor. *Aging Cell* 20:e13437. doi: 10.1111/acel.13437

Dubois, C., and Liu, S. (2021). GluN2D NMDA receptors gate fear extinction learning and interneuron plasticity. *Front. Synaptic Neurosci.* 13:681068. doi: 10.3389/fnsyn.2021.681068

El-Mir, M., Detaille, D., R-Villanueva, G., Delgado-Esteban, M., Guigas, B., Attia, S., et al. (2008). Neuroprotective role of antidiabetic drug metformin against apoptotic cell death in primary cortical neurons. *J. Mol. Neurosci.* 34, 77–87. doi: 10.1007/s12031-007-9002-1

Elsayed, N., Boyer, T., and Burd, I. (2021). Fetal neuroprotective strategies: therapeutic agents and their underlying synaptic pathways. *Front. Synaptic Neurosci.* 13:680899. doi: 10.3389/fnsyn.2021.680899

Ernst, A., Böhler, L., Hagenston, A., Hoffmann, A., Heiland, S., Sticht, C., et al. (2019). EphB2-dependent signaling promotes neuronal excitotoxicity and inflammation in the acute phase of ischemic stroke. *Acta Neuropathol. Commun.* 7:15. doi: 10.1186/s40478-019-0669-7

Espinoza, S., Arredondo, S., Barake, F., Carvajal, F., Guerrero, F., Segovia-Miranda, F., et al. (2020). Neuronal surface P antigen (NSPA) modulates postsynaptic NMDAR stability through ubiquitination of tyrosine phosphatase PTPMEG. *BMC Biol.* 18:164. doi: 10.1186/s12915-020-00877-2

Essiz, S., Gencel, M., Aktolun, M., Demir, A., Carpenter, T., and Servili, B. (2021). Correlated conformational dynamics of the human GluN1-GluN2A type N-methyl-D-aspartate (NMDA) receptor. *J. Mol. Model.* 27:162. doi: 10.1007/s00894-021-04755-8

Eyo, U., Bispo, A., Liu, J., Sabu, S., Wu, R., DiBona, V., et al. (2018). The GluN2A subunit regulates neuronal NMDA receptor-induced microglia-neuron physical interactions. *Sci. Rep.* 8:828. doi: 10.1038/s41598-018-19205-4

Fabbrin, S., Girardi, B., de Lorena Wendel, A., Coelho Ilha Valin, C., Pillat, M., Viero, F., et al. (2020). Spermidine-induced improvement of memory consolidation involves PI3K/Akt signaling pathway. *Brain Res. Bull.* 164, 208–213. doi: 10.1016/j.brainresbull.2020.08.018

Fachim, H., Loureiro, C., Corsi-Zuelli, F., Shuhama, R., Louzada-Junior, P., Menezes, P., et al. (2019). GRIN2B promoter methylation deficits in early-onset schizophrenia and its association with cognitive function. *Epigenomics* 11, 401–410. doi: 10.2217/epi-2018-0127

Farina, B., Di Sorbo, G., Chambery, A., Caporale, A., Leoni, G., Russo, R., et al. (2017). Structural and biochemical insights of CypA and AIF interaction. *Sci. Rep.* 7:1138. doi: 10.1038/s41598-017-01337-8

Farina, B., Sturlese, M., Mascanzoni, F., Caporale, A., Monti, A., Di Sorbo, G., et al. (2018). Binding mode of AIF(370–394) peptide to CypA: insights from NMR, label-free and molecular docking studies. *Biochem. J.* 475, 2377–2393. doi: 10.1042/BCJ20180177

Favaron, M., Manev, R., Rimland, J., Candeo, P., Beccaro, M., and Manev, H. (1993). NMDA-stimulated expression of BDNF mRNA in cultured cerebellar granule neurones. *Neuroreport* 4, 1171–1174.

Fedele, L., Newcombe, J., Topf, M., Gibb, A., Harvey, R., and Smart, T. (2018). Disease-associated missense mutations in GluN2B subunit alter NMDA receptor ligand binding and ion channel properties. *Nat. Commun.* 9:957. doi: 10.1038/s41467-018-02927-4

Feng, Y., Yang, H., Yue, Y., and Tian, F. (2020). MicroRNAs and target genes in epileptogenesis. *Epilepsia* 61, 2086–2096. doi: 10.1111/epi.16687

Fernández-Marmiesse, A., Kusumoto, H., Rekarte, S., Roca, I., Zhang, J., Myers, S., et al. (2018). A novel missense mutation in GRIN2A causes a nonepileptic neurodevelopmental disorder. *Mov. Disord.* 33, 992–999. doi: 10.1111/cla.12461

Flores-Hernandez, J., Salgado, H., De La Rosa, V., Avila-Ruiz, T., Torres-Ramirez, O., Lopez-Lopez, G., et al. (2009). Cholinergic direct inhibition of N-methyl-D aspartate receptor-mediated currents in the rat neocortex. *Synapse* 63, 308–318. doi: 10.1002/syn.20609

Franchini, L., Carrano, N., Di Luca, M., and Gardoni, F. (2020). Synaptic GluN2A-containing NMDA receptors: from physiology to pathological synaptic plasticity. *Int. J. Mol. Sci.* 21:1538. doi: 10.3390/ijms21041538

Fricker, M., Tolkovsky, A., Borutaite, V., Coleman, M., and Brown, G. (2018). Neuronal cell death. *Physiol. Rev.* 98, 813–880. doi: 10.1152/physrev.00011.2017

Fry, A., Fawcett, K., Zelnik, N., Yuan, H., Thompson, B., Shemer-Meiri, L., et al. (2018). *De novo* mutations in GRIN1 cause extensive bilateral polymicrogyria. *Brain* 141, 698–712. doi: 10.1093/brain/awx358

Gan, J., Qu, Y., Li, J., Zhao, F., and Mu, D. (2015). An evaluation of the links between microRNA, autophagy and epilepsy. *Rev. Neurosci.* 26, 225–237. doi: 10.1515/revneuro-2014-0062

Gan, K., and Südhof, T. (2020). SPARCL1 promotes excitatory but not inhibitory synapse formation and function independent of neurexins and neuroligins. *J. Neurosci.* 40, 8088–8102. doi: 10.1523/JNEUROSCI.0454-20.2020

Gao, K., Tankovic, A., Zhang, Y., Kusumoto, H., Zhang, J., Chen, W., et al. (2017). A *de novo* loss-of-function GRIN2A mutation associated with childhood focal epilepsy and acquired epileptic aphasia. *PLoS One* 12:e0170818. doi: 10.1371/journal.pone.0170818

Geis, C., Planagumà, J., Carreño, M., Graus, F., and Dalmau, J. (2019). Autoimmune seizures and epilepsy. *J. Clin. Invest.* 129, 926–940. doi: 10.1172/JCI125178

Geng, D., Kang, L., Su, Y., Jia, J., Ma, J., Li, S., et al. (2013). Protective effects of EphB2 on Aβ1–42 oligomer-induced neurotoxicity and synaptic NMDA receptor signaling in hippocampal neurons. *Neurochem. Int.* 63, 283–290. doi: 10.1016/j.neuint.2013.06.016

Ghasemi, M., Shafaroodi, H., Nazarbeiki, S., Meskar, H., Heydarpour, P., Ghasemi, A., et al. (2010). Voltage-dependent calcium channel and NMDA receptor antagonists augment anticonvulsant effects of lithium chloride on pentylenetetrazole-induced clonic seizures in mice. *Epilepsy Behav.* 18, 171–178. doi: 10.1016/j.yebeh.2010.04.002

Gleichman, A., Spruce, L., Dalmau, J., Seeholzer, S., and Lynch, D. (2012). Anti-NMDA receptor encephalitis antibody binding is dependent on amino acid identity of a small region within the GluN1 amino terminal domain. *J. Neurosci.* 32, 11082–11094. doi: 10.1523/JNEUROSCI.0064-12.2012

Hamamoto, O., Tirapelli, D., Lizarte Neto, F., Freitas-Lima, P., Saggioro, F., Cirino, M., et al. (2020). Modulation of NMDA receptor by miR-219 in the amygdala and hippocampus of patients with mesial temporal lobe epilepsy. *J. Clin. Neurosci.* 74, 180–186. doi: 10.1016/j.jocn.2020.02.024

Hanada, T. (2020). Ionotropic glutamate receptors in epilepsy: a review focusing on AMPA and NMDA receptors. *Biomolecules* 10:464. doi: 10.3390/biom10030464

Hardingham, G., and Bading, H. (2010). Synaptic versus extrasynaptic NMDA receptor signalling: implications for neurodegenerative disorders. *Nat. Rev. Neurosci.* 11, 682–696. doi: 10.1038/nrn2911

Harraz, M., Eacker, S., Wang, X., Dawson, T., and Dawson, V. (2012). MicroRNA-223 is neuroprotective by targeting glutamate receptors. *Proc. Natl. Acad. Sci. U S A* 109, 18962–18967. doi: 10.1073/pnas.1121288109

Henderson, J., Georgiou, J., Jia, Z., Robertson, J., Elowe, S., Roder, J., et al. (2001). The receptor tyrosine kinase EphB2 regulates NMDA-dependent synaptic function. *Neuron* 32, 1041–1056. doi: 10.1016/s0896-6273(01)00553-0

Hendry, S., Schwark, H., Jones, E., and Yan, J. (1987). Numbers and proportions of GABA-immunoreactive neurons in different areas of monkey cerebral cortex. *J. Neurosci.* 7, 1503–1519. doi: 10.1523/JNEUROSCI.07-05-01503.1987

Hetman, M., and Kharebava, G. (2006). Survival signaling pathways activated by NMDA receptors. *Curr. Top. Med. Chem.* 6, 787–799. doi: 10.2174/156802606777057553

Hoque, A., Hossain, M., Ameen, S., Ang, C., Williamson, N., Ng, D., et al. (2016). A beacon of hope in stroke therapy-Blockade of pathologically activated cellular events in excitotoxic neuronal death as potential neuroprotective strategies. *Pharmacol. Ther.* 160, 159–179. doi: 10.1016/j.pharmthera.2016.02.009

Horak, M., Barackova, P., Langore, E., Netolicky, J., Rivas-Ramirez, P., and Rehakova, K. (2021). The extracellular domains of GluN subunits play an essential role in processing NMDA receptors in the ER. *Front. Neurosci.* 15:603715. doi: 10.3389/fnins.2021.603715

Hou, H., Wang, L., Fu, T., Papasergi, M., Yule, D., and Xia, H. (2020). Magnesium acts as a second messenger in the regulation of NMDA

receptor-mediated CREB signaling in neurons. *Mol. Neurobiol.* 57, 2539–2550. doi: 10.1007/s12035-020-01871-z

Hu, R., Wei, P., Jin, L., Zheng, T., Chen, W., Liu, X., et al. (2017). Overexpression of EphB2 in hippocampus rescues impaired NMDA receptors trafficking and cognitive dysfunction in Alzheimer model. *Cell Death Dis.* 8:e2717. doi: 10.1038/cddis.2017.140

Hu, F., Zhang, S., Chen, X., Fu, X., Guo, S., Jiang, Z., et al. (2020). MiR-219a-2 relieves myocardial ischemia-reperfusion injury by reducing calcium overload and cell apoptosis through HIF1α/ NMDAR pathway. *Exp. Cell Res.* 395:112172. doi: 10.1016/j.yexcr.2020.112172

Huang, L., Liu, Y., Jin, W., Ji, X., and Dong, Z. (2012). Ketamine potentiates hippocampal neurodegeneration and persistent learning and memory impairment through the PKCγ-ERK signaling pathway in the developing brain. *Brain Res.* 1476, 164–171. doi: 10.1016/j.brainres.2012.07.059

Huang, Y., Liu, X., Liao, Y., Liao, Y., Zou, D., Wei, X., et al. (2018). Role of miR-34c in the cognitive function of epileptic rats induced by pentylenetetrazol. *Mol. Med. Rep.* 17, 4173–4180. doi: 10.3892/mmr.2018.8441

Huang, Y., and Xiong, H. (2021). Anti-NMDA receptor encephalitis: a review of mechanistic studies. *Int. J. Physiol. Pathophysiol. Pharmacol.* 13, 1–11.

Hughes, E., Peng, X., Gleichman, A., Lai, M., Zhou, L., Tsou, R., et al. (2010). Cellular and synaptic mechanisms of anti-NMDA receptor encephalitis. *J. Neurosci.* 30, 5866–5875. doi: 10.1523/JNEUROSCI.0167-10.2010

Intson, K., Geissah, S., McCullumsmith, R., and Ramsey, A. (2020). A role for endothelial NMDA receptors in the pathophysiology of schizophrenia. *Schizophr. Res.* doi: 10.1016/j.schres.2020.10.004. [Online ahead of print].

Ivanova, V., Balaban, P., and Bal, N. (2020). Modulation of AMPA receptors by nitric oxide in nerve cells. *Int. J. Mol. Sci.* 21:981. doi: 10.3390/ijms21030981

Ivanova, M., Kokorina, A., Timofeeva, P., Karelina, T., Abushik, P., Stepanenko, J., et al. (2020). Calcium export from neurons and multi-kinase signaling cascades contribute to ouabain neuroprotection in hyperhomocysteinemia. *Biomolecules* 10:1104. doi: 10.3390/biom10081104

Jeon, A., and Kim, J. (2018). SPDI knockdown inhibits seizure activity in acute seizure and chronic epilepsy rat models *via* S-nitrosylation-independent thiolation on NMDA receptor. *Front. Cell. Neurosci.* 12:438. doi: 10.3389/fncel.2018.00438

Jiang, Y., Jakovcevski, M., Bharadwaj, R., Connor, C., Schroeder, F., Lin, C., et al. (2010). Setdb1 histone methyltransferase regulates mood-related behaviors and expression of the NMDA receptor subunit NR2B. *J. Neurosci.* 30, 7152–7167. doi: 10.1523/JNEUROSCI.1314-10.2010

Jiang, G., Wang, W., Cao, Q., Gu, J., Mi, X., Wang, K., et al. (2015). Insulin growth factor-1 (IGF-1) enhances hippocampal excitatory and seizure activity through IGF-1 receptor-mediated mechanisms in the epileptic brain. *Clin. Sci. (London)* 129, 1047–1060. doi: 10.1042/CS20150312

Jiao, J., Li, L., Sun, M., Fang, J., Meng, L., Zhang, Y., et al. (2021). Identification of a novel GRIN2D variant in a neonate with intractable epileptic encephalopathy-a case report. *BMC Pediatr.* 21:5. doi: 10.1186/s12887-020-02462-6

Jin, M., Ni, H., and Li, L. (2018). Leptin maintained zinc homeostasis against glutamate-induced excitotoxicity by preventing mitophagy-mediated mitochondrial activation in HT22 hippocampal neuronal cells. *Front. Neurol.* 9:322. doi: 10.3389/fneur.2018.00322

Jorratt, P., Hoschl, C., and Ovsepian, S. (2021). Endogenous antagonists of N-methyl-d-aspartate receptor in schizophrenia. *Alzheimer's Dement.* 17, 888–905. doi: 10.1002/alz.12244

Kaplan, E., Zubedat, S., Radzishevsky, I., Valenta, A., Rechnitz, O., Sason, H., et al. (2018). ASCT1 (Slc1a4) transporter is a physiologic regulator of brain d-serine and neurodevelopment. *Proc. Natl. Acad. Sci. U S A* 115, 9628–9633. doi: 10.1073/pnas.1722677115

Kiese, K., Jablonski, J., Hackenbracht, J., Wrosch, J., Groemer, T., Kornhuber, J., et al. (2017). Epigenetic control of epilepsy target genes contributes to a cellular memory of epileptogenesis in cultured rat hippocampal neurons. *Acta Neuropathol. commun.* 5:79. doi: 10.1186/s40478-017-0485-x

Kim, J., Ko, A., Hyun, H., Min, S., and Kim, J. (2017). PDI regulates seizure activity *via* NMDA receptor redox in rats. *Sci. Rep.* 7:42491. doi: 10.1038/srep42491

Kim, D., Simeone, K., Simeone, T., Pandya, J., Wilke, J., Ahn, Y., et al. (2015). Ketone bodies mediate antiseizure effects through mitochondrial permeability transition. *Ann. Neurol.* 78, 77–87. doi: 10.1002/ana.24424

Koehler, R., Dawson, V., and Dawson, T. (2021). Targeting parthanatos in ischemic stroke. *Front. Neurol.* 12:662034. doi: 10.3389/fneur.2021.662034

Kovács, K., Steullet, P., Steinmann, M., Do, K., Magistretti, P., Halfon, O., et al. (2007). TORC1 is a calcium- and cAMP-sensitive coincidence detector involved in hippocampal long-term synaptic plasticity. *Proc. Natl. Acad. Sci. U S A* 104, 4700–4705. doi: 10.1073/pnas.0607524104

Krall, R., Moutal, A., Phillips, M., Asraf, H., Johnson, J., Khanna, R., et al. (2020). Synaptic zinc inhibition of NMDA receptors depends on the association of GluN2A with the zinc transporter ZnT1. *Sci. Adv.* 6:eabb1515. doi: 10.1126/sciadv.abb1515

Kravchick, D., Karpova, A., Hrdinka, M., Lopez-Rojas, J., Iacobas, S., Carbonell, A., et al. (2016). Synaptonuclear messenger PRR7 inhibits c-Jun ubiquitination and regulates NMDA-mediated excitotoxicity. *EMBO J.* 35, 1923–1934. doi: 10.15252/embj.201593070

Lai, Y., Baker, J., Donti, T., Graham, B., Craigen, W., and Anderson, A. (2017). Mitochondrial dysfunction mediated by poly(ADP-Ribose) polymerase-1 activation contributes to hippocampal neuronal damage following status epilepticus. *Int. J. Mol. Sci.* 18:1502. doi: 10.3390/ijms18071502

Lee, M., Ting, K., Adams, S., Brew, B., Chung, R., and Guillemin, G. (2010). Characterisation of the expression of NMDA receptors in human astrocytes. *PLoS One* 5:e14123. doi: 10.1371/journal.pone.0014123

Lemke, J., Hendrickx, R., Geider, K., Laube, B., Schwake, M., Harvey, R., et al. (2014). GRIN2B mutations in west syndrome and intellectual disability with focal epilepsy. *Ann. Neurol.* 75, 147–154. doi: 10.1002/ana.24073

Lemke, J., Lal, D., Reinthaler, E., Steiner, I., Nothnagel, M., Alber, M., et al. (2013). Mutations in GRIN2A cause idiopathic focal epilepsy with rolandic spikes. *Nat. Genet.* 45, 1067–1072. doi: 10.1038/ng.2728

Leypoldt, F., Armangue, T., and Dalmau, J. (2015). Autoimmune encephalopathies. *Ann. N Y Acad. Sci.* 1338, 94–114. doi: 10.1111/nyas.12553

Li, X., Guo, C., Li, Y., Li, L., Wang, Y., Zhang, Y., et al. (2017). Ketamine administered pregnant rats impair learning and memory in offspring *via* the CREB pathway. *Oncotarget* 8, 32433–32449. doi: 10.18632/oncotarget.15405

Li, S., Raychaudhuri, S., Lee, S., Brockmann, M., Wang, J., Kusick, G., et al. (2021). Asynchronous release sites align with NMDA receptors in mouse hippocampal synapses. *Nat. Commun.* 12:677. doi: 10.1038/s41467-021-21004-x

Li, D., Yuan, H., Ortiz-Gonzalez, X., Marsh, E., Tian, L., McCormick, E., et al. (2016). GRIN2D recurrent *de novo* dominant mutation causes a severe epileptic encephalopathy treatable with NMDA receptor channel blockers. *Am. J. Hum. Genet.* 99, 802–816. doi: 10.1016/j.ajhg.2016.07.013

Li, D., Zhang, Y., Zhang, Y., Wang, Q., Miao, Q., Xu, Y., et al. (2019). Correlation between the epigenetic modification of histone H3K9 acetylation of NR2B gene promoter in rat hippocampus and ethanol withdrawal syndrome. *Mol. Biol. Rep.* 46, 2867–2875. doi: 10.1007/s11033-019-04733-7

Lian, W., Zhou, W., Zhang, B., Jia, H., Xu, L., Liu, A., et al. (2021). DL0410 ameliorates cognitive disorder in SAMP8 mice by promoting mitochondrial dynamics and the NMDAR-CREB-BDNF pathway. *Acta Pharmacol. Sin.* 42, 1055–1068. doi: 10.1038/s41401-020-00506-2

Limón, I., Angulo-Cruz, I., Sánchez-Abdon, L., and Patricio-Martínez, A. (2021). Disturbance of the glutamate-glutamine cycle, secondary to hepatic damage, compromises memory function. *Front. Neurosci.* 15:578922. doi: 10.3389/fnins.2021.578922

Lin, S. (2015). microRNAs and fragile X syndrome. *Adv. Exp. Med. Biol.* 888, 107–121. doi: 10.1007/978-3-319-22671-2_7

Liu, X., Geng, J., Guo, H., Zhao, H., and Ai, Y. (2020). Propofol inhibited apoptosis of hippocampal neurons in status epilepticus through miR-15a-5p/NR2B/ERK1/2 pathway. *Cell Cycle* 19, 1000–1011. doi: 10.1080/15384101.2020.1743909

Liu, S., Liu, C., Xiong, L., Xie, J., Huang, C., Pi, R., et al. (2021). Icaritin alleviates glutamate-induced neuronal damage by inactivating GluN2B-containing NMDARs through the ERK/DAPK1 pathway. *Front. Neurosci.* 15:525615. doi: 10.3389/fnins.2021.525615

Liu, F., Paule, M., Ali, S., and Wang, C. (2011). Ketamine-induced neurotoxicity and changes in gene expression in the developing rat brain. *Curr. Neuropharmacol.* 9, 256–261. doi: 10.2174/157015911795017155

Liu, E., Xie, A., Zhou, Q., Li, M., Zhang, S., Li, S., et al. (2017). GSK-3β deletion in dentate gyrus excitatory neuron impairs synaptic plasticity and memory. *Sci. Rep.* 7:5781. doi: 10.1038/s41598-017-06173-4

Loss, C., da Rosa, N., Mestriner, R., Xavier, L., and Oliveira, D. (2019). Blockade of GluN2B-containing NMDA receptors reduces short-term brain damage induced by early-life status epilepticus. *Neurotoxicology* 71, 138–149. doi: 10.1016/j.neuro.2019.01.002

Lu, Y., Ding, X., Wu, X., and Huang, S. (2020). Ketamine inhibits LPS-mediated BV2 microglial inflammation *via* NMDA receptor blockage. *Fundam. Clin. Pharmacol.* 34, 229–237. doi: 10.1111/fcp.12508

Lumley, L., Niquet, J., Marrero-Rosado, B., Schultz, M., Rossetti, F., de Araujo Furtado, M., et al. (2021). Treatment of acetylcholinesterase inhibitor-induced seizures with polytherapy targeting GABA and glutamate receptors. *Neuropharmacology* 185:108444. doi: 10.1016/j.neuropharm.2020.108444

Luo, J., Wang, Y., Yasuda, R., Dunah, A., and Wolfe, B. (1997). The majority of N-methyl-D-aspartate receptor complexes in adult rat cerebral cortex contain at least three different subunits (NR1/NR2A/NR2B). *Mol. Pharmacol.* 51, 79–86. doi: 10.1124/mol.51.1.79

Lyu, Y., Ren, X., Zhang, H., Tian, F., Mu, J., and Zheng, J. (2020). Sub-chronic administration of benzo[a]pyrene disrupts hippocampal long-term potentiation *via* inhibiting CaMK II/PKC/PKA-ERK-CREB signaling in rats. *Environ. Toxicol.* 35, 961–970. doi: 10.1002/tox.22932

Ma, X., Cheng, O., Jiang, Q., Yang, J., Xiao, H., and Qiu, H. (2021). Activation of ephrinb1/EPHB2/MAP-2/NMDAR mediates hippocampal neurogenesis promoted by transcranial direct current stimulation in cerebral-ischemic mice. *Neuromol. Med.* 23, 521–530. doi: 10.1007/s12017-021-08654-2

Malkov, A., Ivanov, A., Latyshkova, A., Bregestovski, P., Zilberter, M., and Zilberter, Y. (2019). Activation of nicotinamide adenine dinucleotide phosphate oxidase is the primary trigger of epileptic seizures in rodent models. *Ann. Neurol.* 85, 907–920. doi: 10.1002/ana.25474

Manto, M., Dalmau, J., Didelot, A., Rogemond, V., and Honnorat, J. (2010). *in vivo* effects of antibodies from patients with anti-NMDA receptor encephalitis: further evidence of synaptic glutamatergic dysfunction. *Orphanet J. Rare Dis.* 5:31. doi: 10.1186/1750-1172-5-31

Mantuano, E., Azmoon, P., Banki, M., Lam, M., Sigurdson, C., and Gonias, S. (2020). A soluble derivative of PrP activates cell-signaling and regulates cell physiology through LRP1 and the NMDA receptor. *J. Biol. Chem.* 295, 14178–14188. doi: 10.1074/jbc.RA120.013779

Markram, H., and Segal, M. (1990). Acetylcholine potentiates responses to N-methyl-D-aspartate in the rat hippocampus. *Neurosci. Lett.* 113, 62–65. doi: 10.1016/0304-3940(90)90495-u

Marrero-Rosado, B., de Araujo Furtado, M., Kundrick, E., Walker, K., Stone, M., Schultz, C., et al. (2020). Ketamine as adjunct to midazolam treatment following soman-induced status epilepticus reduces seizure severity, epileptogenesis and brain pathology in plasma carboxylesterase knockout mice. *Epilepsy Behav.* 111:107229. doi: 10.1016/j.yebeh.2020.107229

Marwick, K., Hansen, K., Skehel, P., Hardingham, G., and Wyllie, D. (2019). Functional assessment of triheteromeric NMDA receptors containing a human variant associated with epilepsy. *J. Physiol.* 597, 1691–1704. doi: 10.1113/JP277292

Mashimo, M., Kato, J., and Moss, J. (2013). ADP-ribosyl-acceptor hydrolase 3 regulates poly (ADP-ribose) degradation and cell death during oxidative stress. *Proc. Natl. Acad. Sci. U S A* 110, 18964–18969. doi: 10.1073/pnas.1312783110

Mayer, M., Westbrook, G., and Guthrie, P. (1984). Voltage-dependent block by Mg2+ of NMDA responses in spinal cord neurones. *Nature* 309, 261–263. doi: 10.1038/309261a0

Mele, M., Vieira, R., Correia, B., De Luca, P., Duarte, F., Pinheiro, P., et al. (2021). Transient incubation of cultured hippocampal neurons in the absence of magnesium induces rhythmic and synchronized epileptiform-like activity. *Sci. Rep.* 11:11374. doi: 10.1038/s41598-021-90486-y

Mielnik, C., Binko, M., Chen, Y., Funk, A., Johansson, E., Intson, K., et al. (2021). Consequences of NMDA receptor deficiency can be rescued in the adult brain. *Mol. Psychiatry* 26, 2929–2942. doi: 10.1038/s41380-020-00859-4

Mikasova, L., De Rossi, P., Bouchet, D., Georges, F., Rogemond, V., Didelot, A., et al. (2012). Disrupted surface cross-talk between NMDA and Ephrin-B2 receptors in anti-NMDA encephalitis. *Brain* 135, 1606–1621. doi: 10.1093/brain/aws092

Mizrachi, T., Vaknin-Dembinsky, A., Brenner, T., and Treinin, M. (2021). Neuroinflammation modulation *via* α7 nicotinic acetylcholine receptor and its chaperone, RIC-3. *Molecules* 26:6139. doi: 10.3390/molecules26206139

Mohammed, C., Rhee, H., Phee, B., Kim, K., Kim, H., Lee, H., et al. (2016). miR-204 downregulates EphB2 in aging mouse hippocampal neurons. *Aging cell* 15, 380–388. doi: 10.1111/acel.12444

Monyer, H., Burnashev, N., Laurie, D., Sakmann, B., and Seeburg, P. (1994). Developmental and regional expression in the rat brain and functional properties of four NMDA receptors. *Neuron* 12, 529–540. doi: 10.1016/0896-6273(94)90210-0

Moshé, S., Perucca, E., Ryvlin, P., and Tomson, T. (2015). Epilepsy: new advances. *Lancet* 385, 884–898. doi: 10.1016/S0140-6736(14)60456-6

Mota Vieira, M., Nguyen, T., Wu, K., Badger, J., Collins, B., Anggono, V., et al. (2020). An epilepsy-associated GRIN2A rare variant disrupts CaMKIIα phosphorylation of GluN2A and NMDA receptor trafficking. *Cell Rep.* 32:108104. doi: 10.1016/j.celrep.2020.108104

Mothet, J. P., Le Bail, M., and Billard, J. (2015). Time and space profiling of NMDA receptor co-agonist functions. *J. Neurochem.* 135, 210–225. doi: 10.1111/jnc.13204

Murtas, G., Marcone, G., Sacchi, S., and Pollegioni, L. (2020). L-serine synthesis *via* the phosphorylated pathway in humans. *Cell. Mol. Life Sci.* 77, 5131–5148. doi: 10.1007/s00018-020-03574-z

Nagy, L. V., Bali, Z., Kapus, G., Pelsöczi, P., Farkas, B., Lendvai, B., et al. (2020). Converging evidence on D-amino acid oxidase-dependent enhancement of hippocampal firing activity and passive avoidance learning in rats. *Int. J. Neuropsychopharmacol.* 24, 434–445. doi: 10.1093/ijnp/pyaa095

Neame, S., Safory, H., Radzishevsky, I., Touitou, A., Marchesani, F., Marchetti, M., et al. (2019). The NMDA receptor activation by d-serine and glycine is controlled by an astrocytic Phgdh-dependent serine shuttle. *Proc. Natl. Acad. Sci. U S A* 116, 20736–20742. doi: 10.1073/pnas.1909458116

Neyens, D., Zhao, H., Huston, N., Wayman, G., Ritter, R., and Appleyard, S. (2020). Leptin sensitizes NTS neurons to vagal input by increasing postsynaptic NMDA receptor currents. *J. Neurosci.* 40, 7054–7064. doi: 10.1523/JNEUROSCI.1865-19.2020

Niciu, M., Kelmendi, B., and Sanacora, G. (2012). Overview of glutamatergic neurotransmission in the nervous system. *Pharmacol. Biochem. Behav.* 100, 656–664. doi: 10.1016/j.pbb.2011.08.008

Nikolaev, M., Chizhov, A., and Tikhonov, D. (2021). Molecular mechanisms of action determine inhibition of paroxysmal depolarizing shifts by NMDA receptor antagonists in rat cortical neurons. *Neuropharmacology* 184:108443. doi: 10.1016/j.neuropharm.2020.108443

Niquet, J., Baldwin, R., Norman, K., Suchomelova, L., Lumley, L., and Wasterlain, C. (2017). Simultaneous triple therapy for the treatment of status epilepticus. *Neurobiol. Dis.* 104, 41–49. doi: 10.1016/j.nbd.2017.04.019

Nolt, M., Lin, Y., Hruska, M., Murphy, J., Sheffler-Colins, S., Kayser, M., et al. (2011). EphB controls NMDA receptor function and synaptic targeting in a subunit-specific manner. *J. Neurosci.* 31, 5353–5364. doi: 10.1523/JNEUROSCI.0282-11.2011

Olney, J. (1971). Glutamate-induced neuronal necrosis in the infant mouse hypothalamus. An electron microscopic study. *J. Neuropathol. Exp. Neurol.* 30, 75–90. doi: 10.1097/00005072-197101000-00008

Pan, Y., He, X., Li, C., Li, Y., Li, W., Zhang, H., et al. (2021). Neuronal activity recruits the CRTC1/CREB axis to drive transcription-dependent autophagy for maintaining late-phase LTD. *Cell Rep.* 36:109398. doi: 10.1016/j.celrep.2021.109398

Papadia, S., Stevenson, P., Hardingham, N., Bading, H., and Hardingham, G. (2005). Nuclear Ca2+ and the cAMP response element-binding protein family mediate a late phase of activity-dependent neuroprotection. *J. Neurosci.* 25, 4279–4287. doi: 10.1523/JNEUROSCI.5019-04.2005

Pflanz, N., Daszkowski, A., James, K., and Mihic, S. (2019). Ketone body modulation of ligand-gated ion channels. *Neuropharmacology* 148, 21–30. doi: 10.1016/j.neuropharm.2018.12.013

Pierson, T., Yuan, H., Marsh, E., Fuentes-Fajardo, K., Adams, D., Markello, T., et al. (2014). GRIN2A mutation and early-onset epileptic encephalopathy: personalized therapy with memantine. *Ann. Clin. Transl. Neurol.* 1, 190–198. doi: 10.1002/acn3.39

Pironti, E., Granata, F., Cucinotta, F., Gagliano, A., Efthymiou, S., Houlden, H., et al. (2018). Electroclinical history of a five-year-old girl with GRIN1-related early-onset epileptic encephalopathy: a video-case study. *Epileptic Disord.* 20, 423–427. doi: 10.1684/epd.2018.0992

Planagumà, J., Haselmann, H., Mannara, F., Petit-Pedrol, M., Grünewald, B., Aguilar, E., et al. (2016). Ephrin-B2 prevents N-methyl-D-aspartate receptor antibody effects on memory and neuroplasticity. *Ann. Neurol.* 80, 388–400. doi: 10.1002/ana.24721

Platzer, K., Yuan, H., Schütz, H., Winschel, A., Chen, W., Hu, C., et al. (2017). GRIN2B encephalopathy: novel findings on phenotype, variant clustering, functional consequences and treatment aspects. *J. Med. Genet.* 54, 460–470. doi: 10.1136/jmedgenet-2016-104509

Ploux, E., Bouet, V., Radzishevsky, I., Wolosker, H., Freret, T., and Billard, J. (2020). Serine racemase deletion affects the excitatory/inhibitory balance of the hippocampal CA1 network. *Int. J. Mol. Sci.* 21:9447. doi: 10.3390/ijms21249447

Pollegioni, L., Sacchi, S., and Murtas, G. (2018). Human D-amino acid oxidase: structure, function and regulation. *Front. Mol. Biosci.* 5:107. doi: 10.3389/fmolb.2018.00107

Postnikova, T., Zubareva, O., Kovalenko, A., Kim, K., Magazanik, L., and Zaitsev, A. (2017). Status epilepticus impairs synaptic plasticity in rat hippocampus and is followed by changes in expression of NMDA receptors. *Biochemistry (Mosc)* 82, 282–290. doi: 10.1134/S0006297917030063

Potier, B., Turpin, F., Sinet, P., Rouaud, E., Mothet, J., Videau, C., et al. (2010). Contribution of the d-serine-dependent pathway to the cellular mechanisms underlying cognitive aging. *Front. Aging Neurosci.* 2:1. doi: 10.3389/neuro.24.001.2010

Punnakkal, P., and Dominic, D. (2018). NMDA receptor GluN2 subtypes control epileptiform events in the hippocampus. *Neuromol. Med.* 20, 90–96. doi: 10.1007/s12017-018-8477-y

Qian, A., Buller, A., and Johnson, J. (2005). NR2 subunit-dependence of NMDA receptor channel block by external Mg2+. *J. Physiol.* 562, 319–331. doi: 10.1113/jphysiol.2004.076737

Raboni, S., Marchetti, M., Faggiano, S., Campanini, B., Bruno, S., Marchesani, F., et al. (2019). The energy landscape of human serine racemase. *Front. Mol. Biosci.* 5:112. doi: 10.3389/fmolb.2018.00112

Rodriguez, L., Yi, C., Chu, C., Duriez, Q., Watanabe, S., Ryu, M., et al. (2020). Cross-talk between P2X and NMDA receptors. *Int. J. Mol. Sci.* 21:7187. doi: 10.3390/ijms21197187

Rosendo-Pineda, M., Vicente, J., Vivas, O., Pacheco, J., Loza-Huerta, A., Sampieri, A., et al. (2020). Phosphorylation of NMDA receptors by cyclin B/CDK1 modulates calcium dynamics and mitosis. *Commun. Biol.* 3:665. doi: 10.1038/s42003-020-01393-3

Ryley Parrish, R., Albertson, A., Buckingham, S., Hablitz, J., Mascia, K., Davis Haselden, W., et al. (2013). Status epilepticus triggers early and late alterations in brain-derived neurotrophic factor and NMDA glutamate receptor Grin2b DNA methylation levels in the hippocampus. *Neuroscience* 248, 602–619. doi: 10.1016/j.neuroscience.2013.06.029

Salmi, M., Bolbos, R., Bauer, S., Minlebaev, M., Burnashev, N., and Szepetowski, P. (2018). Transient microstructural brain anomalies and epileptiform discharges in mice defective for epilepsy and language-related NMDA receptor subunit gene Grin2a. *Epilepsia* 59, 1919–1930. doi: 10.1111/epi.14543

Samanta, D. (2020). Ketamine infusion for super refractory status epilepticus in alternating hemiplegia of childhood. *Neuropediatrics* 51, 225–228. doi: 10.1055/s-0039-3402005

Sánchez Fernández, I., Goodkin, H., and Scott, R. (2019). Pathophysiology of convulsive status epilepticus. *Seizure* 68, 16–21. doi: 10.1016/j.seizure.2018.08.002

Santoro, J., Filippakis, A., and Chitnis, T. (2019). Ketamine use in refractory status epilepticus associated with anti-NMDA receptor antibody encephalitis. *Epilepsy Behav. Rep.* 12:100326. doi: 10.1016/j.ebr.2019.100326

Santos, J., and Schauwecker, P. (2003). Protection provided by cyclosporin A against excitotoxic neuronal death is genotype dependent. *Epilepsia* 44, 995–1002. doi: 10.1046/j.1528-1157.2003.66302.x

Sason, H., Billard, J., Smith, G., Safory, H., Neame, S., Kaplan, E., et al. (2017). Asc-1 transporter regulation of synaptic activity *via* the tonic release of d-serine in the forebrain. *Cereb. Cortex* 27, 1573–1587. doi: 10.1093/cercor/bhv350

Schinder, A., Olson, E., Spitzer, N., and Montal, M. (1996). Mitochondrial dysfunction is a primary event in glutamate neurotoxicity. *J. Neurosci.* 16, 6125–6133. doi: 10.1523/JNEUROSCI.16-19-06125.1996

Schmidt, M., Caron, N., Aly, A., Lemarié, F., Dal Cengio, L., Ko, Y., et al. (2020). DAPK1 promotes extrasynaptic glun2b phosphorylation and striatal spine instability in the YAC128 mouse model of huntington disease. *Front. Cell. Neurosci.* 14:590569. doi: 10.3389/fncel.2020.590569

Schousboe, A., Scafidi, S., Bak, L., Waagepetersen, H., and McKenna, M. (2014). Glutamate metabolism in the brain focusing on astrocytes. *Adv. Neurobiol.* 11, 13–30. doi: 10.1007/978-3-319-08894-5_2

Screaton, R., Conkright, M., Katoh, Y., Best, J., Canettieri, G., Jeffries, S., et al. (2004). The CREB coactivator TORC2 functions as a calcium- and cAMP-sensitive coincidence detector. *Cell* 119, 61–74. doi: 10.1016/j.cell.2004.09.015

Sharawat, I., Yadav, J., and Saini, L. (2019). GRIN2BNovel mutation: a rare cause of severe epileptic encephalopathy. *Neurol. India* 67, 562–563. doi: 10.4103/0028-3886.257986

Sharma, P., Kumari, S., Sharma, J., Purohit, R., and Singh, D. (2021). Hesperidin interacts With CREB-BDNF signaling pathway to suppress pentylenetetrazole-induced convulsions in zebrafish. *Front. Pharmacol.* 11:607797. doi: 10.3389/fphar.2020.607797

Shekhar, S., Liu, Y., Wang, S., Zhang, H., Fang, X., Zhang, J., et al. (2021). Novel mechanistic insights and potential therapeutic impact of TRPC6 in neurovascular coupling and ischemic stroke. *Int. J. Mol. Sci.* 22:2074. doi: 10.3390/ijms22042074

Shelkar, G., Pavuluri, R., Gandhi, P., Ravikrishnan, A., Gawande, D., Liu, J., et al. (2019). Differential effect of NMDA receptor GluN2C and GluN2D subunit ablation on behavior and channel blocker-induced schizophrenia phenotypes. *Sci. Rep.* 9:7572. doi: 10.1038/s41598-019-43957-2

Sibarov, D., Boikov, S., Karelina, T., and Antonov, S. (2020). GluN2 subunit-dependent redox modulation of nmda receptor activation by homocysteine. *Biomolecules* 10:1441. doi: 10.3390/biom10101441

Smigiel, R., Kostrzewa, G., Kosinska, J., Pollak, A., Stawinski, P., Szmida, E., et al. (2016). Further evidence for GRIN2B mutation as the cause of severe epileptic encephalopathy. *Am. J. Med. Genet. A* 170, 3265–3270. doi: 10.1002/ajmg.a.37887

Srivastava, P., Dhuriya, Y., Kumar, V., Srivastava, A., Gupta, R., Shukla, R., et al. (2018). PI3K/Akt/GSK3β induced CREB activation ameliorates arsenic mediated alterations in NMDA receptors and associated signaling in rat hippocampus: Neuroprotective role of curcumin. *Neurotoxicology* 67, 190–205. doi: 10.1016/j.neuro.2018.04.018

Sun, Y., Dhamne, S., Carretero-Guillén, A., Salvador, R., Goldenberg, M., Godlewski, B., et al. (2020). Drug-responsive inhomogeneous cortical modulation by direct current stimulation. *Ann. Neurol.* 88, 489–502. doi: 10.1002/ana.25822

Takagi, S., Balu, D., and Coyle, J. (2021). Factors regulating serine racemase and d-amino acid oxidase expression in the mouse striatum. *Brain Res.* 1751:147202. doi: 10.1016/j.brainres.2020.147202

Takahashi, Y., Nishimura, S., Takao, E., Kasai, R., Enokida, K., Ida, K., et al. (2020). Characteristics of internalization of NMDA-type GluRs with antibodies to GluN1 and GluN2B. *J. Neuroimmunol.* 349:577427. doi: 10.1016/j.jneuroim.2020.577427

Tannich, F., Barhoumi, K., Rejeb, A., Aouichri, M., and Souilem, O. (2020). Ketamine, at low dose, decrease behavioural alterations in epileptic diseases induced by pilocarpine in mice. *Int. J. Neurosci.* 130, 1118–1124. doi: 10.1080/00207454.2020.1730363

Tannich, F., Tlili, A., Pintard, C., Chniguir, A., Eto, B., Dang, P., et al. (2021). Correction to: activation of the phagocyte NADPH oxidase/NOX2 and myeloperoxidase in the mouse brain during pilocarpine-induced temporal lobe epilepsy and inhibition by ketamine. *Inflammopharmacology* 29, 333–334. doi: 10.1007/s10787-020-00779-3

Tong, L., Yang, X., Zhang, S., Zhang, D., Yang, X., Li, B., et al. (2020). Clinical and EEG characteristics analysis of autoimmune encephalitis in children with positive and negative anti-N-methyl- D-aspartate receptor antibodies. *Ann. Palliat. Med.* 9, 2575–2585. doi: 10.21037/apm-19-484

Tovar, K., McGinley, M., and Westbrook, G. (2013). Triheteromeric NMDA receptors at hippocampal synapses. *J. Neurosci.* 33, 9150–9160. doi: 10.1523/JNEUROSCI.0829-13.2013

Tsuchida, N., Hamada, K., Shiina, M., Kato, M., Kobayashi, Y., Tohyama, J., et al. (2018). GRIN2D variants in three cases of developmental and epileptic encephalopathy. *Clin. Genet.* 94, 538–547. doi: 10.1111/cge.13454

Valdivielso, J., Eritja, à., Caus, M., and Bozic, M. (2020). Glutamate-gated NMDA receptors: insights into the function and signaling in the kidney. *Biomolecules* 10:1051. doi: 10.3390/biom10071051

Vargas-Lopes, C., Madeira, C., Kahn, S., Albino do Couto, I., Bado, P., Houzel, J., et al. (2011). Protein kinase C activity regulates D-serine availability in the brain. *J. Neurochem.* 116, 281–290. doi: 10.1111/j.1471-4159.2010.07102.x

Virág, L., Robaszkiewicz, A., Rodriguez-Vargas, J., and Oliver, F. (2013). Poly(ADP-ribose) signaling in cell death. *Mol. Aspects Med.* 34, 1153–1167. doi: 10.1016/j.mam.2013.01.007

Wang, K. (2000). Calpain and caspase: can you tell the difference? *Trends Neurosci.* 23, 20–26. doi: 10.1016/s0166-2236(99)01479-4

Wang, Y., Briz, V., Chishti, A., Bi, X., and Baudry, M. (2013). Distinct roles for μ-calpain and m-calpain in synaptic NMDAR-mediated neuroprotection and extrasynaptic NMDAR-mediated neurodegeneration. *J. Neurosci.* 33, 18880–18892. doi: 10.1523/JNEUROSCI.3293-13.2013

Wang, Y., Dawson, V., and Dawson, T. (2009). Poly(ADP-ribose) signals to mitochondrial AIF: a key event in parthanatos. *Exp. Neurol.* 218, 193–202. doi: 10.1016/j.expneurol.2009.03.020

Wang, Y., Kerrisk Campbell, M., Tom, I., Foreman, O., Hanson, J., and Sheng, M. (2020). PCDH7 interacts with GluN1 and regulates dendritic spine morphology and synaptic function. *Sci. Rep.* 10:10951. doi: 10.1038/s41598-020-67831-8

Wang, Y., Kim, N., Haince, J., Kang, H., David, K., Andrabi, S., et al. (2011). Poly(ADP-ribose) (PAR) binding to apoptosis-inducing factor is critical for PAR polymerase-1-dependent cell death (parthanatos). *Sci. Signal.* 4:ra20. doi: 10.1126/scisignal.2000902

Wang, X., Tian, X., Yang, Y., Lu, X., Li, Y., Ma, Y., et al. (2017). POSH participates in epileptogenesis by increasing the surface expression of the NMDA receptor: a promising therapeutic target for epilepsy. *Expert Opin. Ther. Targets* 21, 1083–1094. doi: 10.1080/14728222.2017.1394456

Wang, W., Wang, X., Chen, L., Zhang, Y., Xu, Z., Liu, J., et al. (2016). The microRNA miR-124 suppresses seizure activity and regulates CREB1 activity. *Expert Rev. Mol. Med.* 18:e4. doi: 10.1017/erm.2016.3

Wang, J., Xu, W., Shao, J., He, Z., Ding, Z., Huang, J., et al. (2017). miR-219-5p targets CaMKIIγ to attenuate morphine tolerance in rats. *Oncotarget* 8, 28203–28214. doi: 10.18632/oncotarget.15997

Wang, S., Yang, X., Lin, Y., Qiu, X., Li, H., Zhao, X., et al. (2013). Cellular NAD depletion and decline of SIRT1 activity play critical roles in PARP-1-mediated acute epileptic neuronal death *in vitro*. *Brain Res.* 1535, 14–23. doi: 10.1016/j.brainres.2013.08.038

Wang, G., Zhu, Z., Xu, D., and Sun, L. (2020). Advances in understanding CREB signaling-mediated regulation of the pathogenesis and progression of epilepsy. *Clin. Neurol. Neurosurg.* 196:106018. doi: 10.1016/j.clineuro.2020.106018

Wang, J., Wang, F., Mai, D., and Qu, S. (2020a). Molecular mechanisms of glutamate toxicity in Parkinson's disease. *Front. Neurosci.* 14:585584. doi: 10.3389/fnins.2020.585584

Wang, J., Fei, Z., Liang, J., Zhou, X., Qin, G., Zhang, D., et al. (2020b). EphrinB/EphB signaling contributes to the synaptic plasticity of chronic migraine through NR2B phosphorylation. *Neuroscience* 428, 178–191. doi: 10.1016/j.neuroscience.2019.12.038

Washburn, H., Xia, N., Zhou, W., Mao, Y., and Dalva, M. (2020). Positive surface charge of GluN1 N-terminus mediates the direct interaction with EphB2 and NMDAR mobility. *Nat. Commun.* 11:570. doi: 10.1038/s41467-020-14345-6

Windelborn, J., and Lipton, P. (2008). Lysosomal release of cathepsins causes ischemic damage in the rat hippocampal slice and depends on NMDA-mediated calcium influx, arachidonic acid metabolism and free radical production. *J. Neurochem.* 106, 56–69. doi: 10.1111/j.1471-4159.2008.05349.x

Wong, H. H.-W., Rannio, S., Jones, V., Thomazeau, A., and Sjöström, P. (2021). NMDA receptors in axons: there's no coincidence. *J. Physiol.* 599, 367–387. doi: 10.1113/JP280059

Wright, S., Hashemi, K., Stasiak, L., Bartram, J., Lang, B., Vincent, A., et al. (2015). Epileptogenic effects of NMDAR antibodies in a passive transfer mouse model. *Brain* 138, 3159–3167. doi: 10.1093/brain/awv257

Wu, Y., Wei, Z., Li, Y., Wei, C., Li, Y., Cheng, P., et al. (2019). Perturbation of ephrin receptor signaling and glutamatergic transmission in the hypothalamus in depression using proteomics integrated with metabolomics. *Front. Neurosci.* 13:1359. doi: 10.3389/fnins.2019.01359

Wyllie, D., Livesey, M., and Hardingham, G. (2013). Influence of GluN2 subunit identity on NMDA receptor function. *Neuropharmacology* 74, 4–17. doi: 10.1016/j.neuropharm.2013.01.016

Xiang, L., Ren, Y., Li, X., Zhao, W., and Song, Y. (2016). MicroRNA-204 suppresses epileptiform discharges through regulating TrkB-ERK1/2-CREB signaling in cultured hippocampal neurons. *Brain Res.* 1639, 99–107. doi: 10.1016/j.brainres.2016.02.045

Xing, J., Han, D., Xu, D., Li, X., and Sun, L. (2019). CREB protects against temporal lobe epilepsy associated with cognitive impairment by controlling oxidative neuronal damage. *Neurodegener. Dis.* 19, 225–237. doi: 10.1159/000507023

Xu, Y., Chen, P., Wang, X., Yao, J., and Zhuang, S. (2018). miR-34a deficiency in APP/PS1 mice promotes cognitive function by increasing synaptic plasticity *via* AMPA and NMDA receptors. *Neurosci. Lett.* 670, 94–104. doi: 10.1016/j.neulet.2018.01.045

Xu, H., Li, X., Wu, X., Yang, Y., Dai, S., Lei, T., et al. (2019). Iduna protects HT22 cells by inhibiting parthanatos: the role of the p53-MDM2 pathway. *Exp. Cell Res.* 384:111547. doi: 10.1016/j.yexcr.2019.111547

Xu, X., and Luo, J. (2018). Mutations of N-methyl-D-aspartate receptor subunits in epilepsy. *Neurosci. Bull.* 34, 549–565. doi: 10.1007/s12264-017-0191-5

Xu, T., Yu, X., Deng, J., Ou, S., Liu, X., Wang, T., et al. (2019). CXCR7 regulates epileptic seizures by controlling the synaptic activity of hippocampal granule cells. *Cell Death Dis.* 10:825. doi: 10.1038/s41419-019-2052-9

Xue, L., Borutaite, V., and Tolkovsky, A. (2002). Inhibition of mitochondrial permeability transition and release of cytochrome c by anti-apoptotic nucleoside analogues. *Biochem. Pharmacol.* 64, 441–449. doi: 10.1016/s0006-2952(02)01181-4

Yakovlev, A., Kurmasheva, E., Giniatullin, R., Khalilov, I., and Sitdikova, G. (2017). Hydrogen sulfide inhibits giant depolarizing potentials and abolishes epileptiform activity of neonatal rat hippocampal slices. *Neuroscience* 340, 153–165. doi: 10.1016/j.neuroscience.2016.10.051

Yamashima, T., Kohda, Y., Tsuchiya, K., Ueno, T., Yamashita, J., Yoshioka, T., et al. (1998). Inhibition of ischaemic hippocampal neuronal death in primates with cathepsin B inhibitor CA-074: a novel strategy for neuroprotection based on 'calpain-cathepsin hypothesis'. *Eur. J. Neurosci.* 10, 1723–1733. doi: 10.1046/j.1460-9568.1998.00184.x

Yan, J., Huang, Y., Lu, Y., Chen, J., and Jiang, H. (2014). Repeated administration of ketamine can induce hippocampal neurodegeneration and long-term cognitive impairment *via* the ROS/HIF-1α pathway in developing rats. *Cell. Physiol. Biochem.* 33, 1715–1732. doi: 10.1159/000362953

Yan, M., Zhu, W., Zheng, X., Li, Y., Tang, L., Lu, B., et al. (2016). Effect of glutamate on lysosomal membrane permeabilization in primary cultured cortical neurons. *Mol. Med. Rep.* 13, 2499–2505. doi: 10.3892/mmr.2016.4819

Yang, Q., Huang, Z., Luo, Y., Zheng, F., Hu, Y., Liu, H., et al. (2019). Inhibition of Nwd1 activity attenuates neuronal hyperexcitability and GluN2B phosphorylation in the hippocampus. *EBioMedicine* 47, 470–483. doi: 10.1016/j.ebiom.2019.08.050

Yang, Y., Paspalas, C., Jin, L., Picciotto, M., Arnsten, A., and Wang, M. (2013). Nicotinic α7 receptors enhance NMDA cognitive circuits in dorsolateral prefrontal cortex. *Proc. Natl. Acad. Sci. U S A* 110, 12078–12083. doi: 10.1073/pnas.1307849110

Ye, Z., Li, Q., Guo, Q., Xiong, Y., Guo, D., Yang, H., et al. (2018). Ketamine induces hippocampal apoptosis through a mechanism associated with the caspase-1 dependent pyroptosis. *Neuropharmacology* 128, 63–75. doi: 10.1016/j.neuropharm.2017.09.035

Yu, X., Guan, Q., Wang, Y., Shen, H., Zhai, L., Lu, X., et al. (2019). Anticonvulsant and anti-apoptosis effects of salvianolic acid B on pentylenetetrazole-kindled rats *via* AKT/CREB/BDNF signaling. *Epilepsy Res.* 154, 90–96. doi: 10.1016/j.eplepsyres.2019.05.007

Zehavi, Y., Mandel, H., Zehavi, A., Rashid, M., Straussberg, R., Jabur, B., et al. (2017). *De novo* GRIN1 mutations: an emerging cause of severe early infantile encephalopathy. *Eur. J. Med. Genet.* 60, 317–320. doi: 10.1016/j.ejmg.2017.04.001

Zhand, A., Sayad, A., Ghafouri-Fard, S., Arsang-Jang, S., Mazdeh, M., and Taheri, M. (2018). Expression analysis of GRIN2B, BDNF and IL-1β genes in the whole blood of epileptic patients. *Neurol. Sci.* 39, 1945–1953. doi: 10.1007/s10072-018-3533-9

Zhang, Y., Fan, M., Wang, Q., He, G., Fu, Y., Li, H., et al. (2015). Polymorphisms in microRNA genes and genes involving in NMDAR signaling and schizophrenia: a case-control study in chinese han population. *Sci. Rep.* 5:12984. doi: 10.1038/srep12984

Zhang, X., Hu, B., Lu, L., Xu, D., Sun, L., and Lin, W. (2021). D-serine and NMDA receptor 1 expression in patients with intractable epilepsy. *Turk. Neurosurg.* 31, 76–82. doi: 10.5137/1019-5149.JTN.28138-19.2

Zhang, H., Ma, S., Gao, Y., Xing, J., Xian, H., Li, Z., et al. (2020). Spinal CCL2 promotes pain sensitization by rapid enhancement of NMDA-induced currents through the ERK-GluN2B pathway in mouse lamina II neurons. *Neurosci. Bull.* 36, 1344–1354. doi: 10.1007/s12264-020-00557-9

Zhang, S., Steijaert, M., Lau, D., Schütz, G., Delucinge-Vivier, C., Descombes, P., et al. (2007). Decoding NMDA receptor signaling: identification of genomic programs specifying neuronal survival and death. *Neuron* 53, 549–562. doi: 10.1016/j.neuron.2007.01.025

Zhang, Y., Tan, F., Xu, P., and Qu, S. (2016). Recent advance in the relationship between excitatory amino acid transporters and Parkinson's disease. *Neural Plast.* 2016:8941327. doi: 10.1155/2016/8941327

Zhang, H., Tian, X., Lu, X., Xu, D., Guo, Y., Dong, Z., et al. (2019). TMEM25 modulates neuronal excitability and NMDA receptor subunit NR2B degradation. *J. Clin. Invest.* 129, 3864–3876. doi: 10.1172/JCI122599

Zhang, X., Zhang, R., Chen, J., and Wu, J. (2020). Neuroprotective effects of DAAO are mediated *via* the ERK1/2 signaling pathway in a glaucomatous animal model. *Exp. Eye Res.* 190:107892. doi: 10.1016/j.exer.2019.107892

Zhang, S., Zou, M., Lu, L., Lau, D., Ditzel, D., Delucinge-Vivier, C., et al. (2009). Nuclear calcium signaling controls expression of a large gene pool: identification of a gene program for acquired neuroprotection induced by synaptic activity. *PLoS Genet.* 5:e1000604. doi: 10.1371/journal.pgen.1000604

Zhao, X., Han, C., Zeng, Z., Liu, L., Wang, H., Xu, J., et al. (2020). Glutamate attenuates the survival property of IGFR through NR2B containing N-methyl-D-aspartate receptors in cortical neurons. *Oxid. Med. Cell. Longev.* 2020:5173184. doi: 10.1155/2020/5173184

Zheng, S., Eacker, S., Hong, S., Gronostajski, R., Dawson, T., and Dawson, V. (2010). NMDA-induced neuronal survival is mediated through nuclear factor I-A in mice. *J. Clin. Invest.* 120, 2446–2456. doi: 10.1172/JCI33144

Zheng, H., Tang, R., Yao, Y., Ji, Z., Cao, Y., Liu, Z., et al. (2016). MiR-219 protects against seizure in the kainic acid model of epilepsy. *Mol. Neurobiol.* 53, 1–7. doi: 10.1007/s12035-014-8981-5

Zhou, X., Huang, Z., Zhang, J., Chen, J., Yao, P., Mai, C., et al. (2021). Chronic oral administration of magnesium-L-threonate prevents oxaliplatin-induced memory and emotional deficits by normalization of TNF-α/NF-κB signaling in rats. *Neurosci. Bull.* 37, 55–69. doi: 10.1007/s12264-020-00563-x

Zhou, X., Zhang, C., Zhang, C., Peng, Y., Wang, Y., and Xu, H. (2017). MicroRNA-182-5p regulates nerve injury-induced nociceptive hypersensitivity by targeting ephrin type-b receptor 1. *Anesthesiology* 126, 967–977. doi: 10.1097/ALN.0000000000001588

Zhu, J., Li, K., Cao, S., Chen, X., Shen, C., Zhang, Y., et al. (2017). Increased NRG1-ErbB4 signaling in human symptomatic epilepsy. *Sci. Rep.* 7:141. doi: 10.1038/s41598-017-00207-7

Zhu, S., and Paoletti, P. (2015). Allosteric modulators of NMDA receptors: multiple sites and mechanisms. *Curr. Opin. Pharmacol.* 20, 14–23. doi: 10.1016/j.coph.2014.10.009

Zhu, C., Wang, X., Deinum, J., Huang, Z., Gao, J., Modjtahedi, N., et al. (2007). Cyclophilin A participates in the nuclear translocation of apoptosis-inducing factor in neurons after cerebral hypoxia-ischemia. *J. Exp. Med.* 204, 1741–1748. doi: 10.1084/jem.20070193

Conflict of Interest: The authors declare that the research was conducted in the absence of any commercial or financial relationships that could be construed as a potential conflict of interest.

Publisher's Note: All claims expressed in this article are solely those of the authors and do not necessarily represent those of their affiliated organizations, or those of the publisher, the editors and the reviewers. Any product that may be evaluated in this article, or claim that may be made by its manufacturer, is not guaranteed or endorsed by the publisher.

frontiers | Frontiers in Molecular Neuroscience

REVIEW
published: 07 April 2022
doi: 10.3389/fnmol.2022.863003

DREADDs in Epilepsy Research: Network-Based Review

*John-Sebastian Mueller†, Fabio Cesar Tescarollo† and Hai Sun**

Department of Neurosurgery, Robert Wood Johnson Medical School, New Brunswick, NJ, United States

Epilepsy can be interpreted as altered brain rhythms from overexcitation or insufficient inhibition. Chemogenetic tools have revolutionized neuroscience research because they allow "on demand" excitation or inhibition of neurons with high cellular specificity. Designer Receptors Exclusively Activated by Designer Drugs (DREADDs) are the most frequently used chemogenetic techniques in epilepsy research. These engineered muscarinic receptors allow researchers to excite or inhibit targeted neurons with exogenous ligands. As a result, DREADDs have been applied to investigate the underlying cellular and network mechanisms of epilepsy. Here, we review the existing literature that has applied DREADDs to understand the pathophysiology of epilepsy. The aim of this review is to provide a general introduction to DREADDs with a focus on summarizing the current main findings in experimental epilepsy research using these techniques. Furthermore, we explore how DREADDs may be applied therapeutically as highly innovative treatments for epilepsy.

Keywords: DREADD = designer receptor exclusively activated by designer drugs, epileptogenesis, epilepsy, ictogenesis, seizure, chemogenetic, pharmaco-genetic

OPEN ACCESS

Edited by:
Tobias Engel,
Royal College of Surgeons in Ireland, Ireland

Reviewed by:
Ilse Julia Smolders,
Vrije University Brussel, Belgium
Rochelle Marie Hines,
University of Nevada, Las Vegas, United States

***Correspondence:**
Hai Sun
hs925@rwjms.rutgers.edu

†These authors have contributed equally to this work

Specialty section:
This article was submitted to Brain Disease Mechanisms, a section of the journal Frontiers in Molecular Neuroscience

Received: *26 January 2022*
Accepted: *17 March 2022*
Published: *07 April 2022*

Citation:
Mueller J-S, Tescarollo FC and Sun H (2022) DREADDs in Epilepsy Research: Network-Based Review. Front. Mol. Neurosci. 15:863003. doi: 10.3389/fnmol.2022.863003

INTRODUCTION

Epilepsy is a disorder that is generally perceived as an imbalance between excitation and inhibition in the brain. According to the International League Against Epilepsy, this disorder affects approximately 65 million people worldwide (Devinsky et al., 2018). Epilepsy leads to physical, cognitive, psychological, and social impairments (Fisher et al., 2014; Falco-Walter et al., 2018), and is a major risk factor for sudden unexpected death in epilepsy (Saetre and Abdelnoor, 2018). Historically, epilepsy research has yielded significant drug discoveries driven by the fields of biochemistry and pharmacology. These anti-seizure drugs (ASDs) have helped patients by eliminating or reducing seizures. Unfortunately, ASDs have rarely been able to provide the ideal effect of immediately nullifying seizures with minimal adverse effects in all patients (Engel, 2016). Despite the continuous development of ASDs, more than 30% of patients continue to have seizures after attempted treatment with multiple ASDs; a condition defined as drug refractory epilepsy (Kwan and Brodie, 2000; Sheng et al., 2017). When drug refractory epilepsies have a focal onset, surgical resection of the epileptic foci can be efficacious in rendering patients seizure free (Sheng et al., 2017). Other approaches for the treatment of drug refractory epilepsies include neuromodulation such as vagal nerve stimulation (Morris et al., 2013) and the ketogenic diet (Kossoff et al., 2018). There is a continuing need to develop new interventions to treat drug refractory epilepsies by advancing our current understanding of the pathophysiology of epilepsy. New and exciting research tools such as chemogenetics provide innovative approaches in epilepsy research to meet these challenges. We begin with a history of chemogenetics followed

by a description of the development of Designer Receptors Exclusively Activated by Designer Drugs (DREADDs) to provide a review on how these techniques are applied in epilepsy research.

Chemogenetics Development

Chemogenetics can be defined as a method that confers cells with a pharmacological response to an engineered receptor (Lieb et al., 2019). The concept that a drug binds to specific sites or receptors on cell surfaces originates from Paul Ehrlich (1854 to 1915; Hill, 2006). Examples of modulating ion channels on the cell membrane of neurons date back to the same period (Cox and Gosling, 2014). In 1959, Nachmansohn isolated a protein identified as the first receptor activated by a neurotransmitter, the acetylcholine nicotinic receptor (Changeux, 2012; Cox and Gosling, 2014). Additional important pharmacological advancements included the development of methods to quantitatively measure affinity, efficacy, and the properties of agonists, partial agonists, and antagonists by the evaluation of functional responses in isolated tissues (Hill, 2006). These discoveries facilitated the development of the first chemogenetic tools. In 2001, Scearce-Levie et al. (2001) published an initial report of chemogenetics involving a receptor activated by an exogenous ligand. This was termed as receptors activated solely by synthetic ligands (Scearce-Levie et al., 2001). By genetically modifying an inhibitory κ-opioid receptor, they were able to generate two κ-opioid receptors, named Ro1 or Ro2, that no longer showed affinity to their endogenous ligand in heart tissue, dynorphin, but responded only to spiradoline, a selective κ-opioid agonist. The administration of spiradoline to mice expressing receptors activated solely by synthetic ligands in cardiac cells resulted in a decreased heart rate while having no effect in wild-type animals. The selectivity of spiradoline in activating only receptors activated solely by synthetic ligands in cardiac tissue may be explained by extremely low expression of endogenous κ-opioid receptors in the heart. In endogenous κ-opioid receptor-rich tissues such as the brain, the administration of spiradoline resulted in sedation of the animals and masked behavioral responses generated by the activation of Ro1 (Redfern et al., 1999; Scearce-Levie et al., 2001). The markedly sedative side effect of receptors activated solely by synthetic ligands precluded its application in neuroscience research and alternative chemogenetics methods were then developed.

To overcome the cross-reaction of the ligand with other endogenous receptors, Lechner et al. (2002) introduced a new approach in which cortical neurons were transfected with *Drosophila* allatostatin receptors. The allatostatin receptor is a non-mammalian G protein-coupled receptor (GPCR) that is solely activated by the insect peptide allatostatin. Delivery of allatostatin to *ex vivo* ferret brain slices induced hyperpolarization of mammalian cortical neurons expressing allatostatin receptors in a reversible manner without endogenous receptor cross-reaction (Lechner et al., 2002). However, allatostatin is a neuropeptide, so it likely does not cross the blood-brain barrier (BBB) when delivered systemically. This would require it to be delivered *via* intracerebroventricular injection for its application *in vivo*. Finally, Lerchner et al. (2007) demonstrated the viability of chemogenetics in freely moving animals by delivering a viral vector encoding for a modified heteromeric ivermectin gated chloride channel from *C. elegans*. Neuronal activity in the striatum of naïve mice was reversibly suppressed upon activation by ivermectin, a synthetic ligand that crosses the BBB (Lerchner et al., 2007).

DREADDs Development

The predominant chemogenetic tools in epilepsy research are DREADDs (Lieb et al., 2019). Armbruster et al. (2007) introduced the concept of DREADDs by generating a family of GPCRs based on the human muscarinic acetylcholine receptor DREADD (hM_xD_y). GPCRs are the largest group of cell surface receptors in the central nervous system (Yang et al., 2021) and the Human Genome Project has identified more than 800 different GPCR genes (Hill, 2006). GPCRs are seven-transmembrane highly selective receptors that trigger intracellular signaling cascades through coupling to a range of intracellular proteins (G-proteins, β-arrestins, and kinases; Yang et al., 2021), and are grouped into four main families: $G_{i/o}$, G_s, G_q, and $G_{12/13}$ (Glukhova et al., 2018). GPCRs significantly contribute to regulation of neuronal excitability, and abnormalities in expression and activity of this class of receptors have been associated with different neuropathological processes including epilepsy (Yu et al., 2019). Therefore, GPCRs provided a logical platform for the development of DREADDs.

The commonly used DREADDs in epilepsy research are hM3Dq and hM4Di. hM3Dq is an engineered muscarinic receptor coupled to a $G_{\alpha q}$ signaling cascade leading to neuronal excitation (Alexander et al., 2009) whereas hM4Di is coupled to $G_{\alpha i}$ and mediates neuronal inhibition (Armbruster et al., 2007; Stachniak et al., 2014). Both hM3Dq and hM4Di are irresponsive to their native ligand, acetylcholine, but have their intracellular signaling cascades mediated and activated solely by a pharmacologically inert and bioavailable compound, which is usually clozapine-N-oxide (CNO; **Figure 1**; Roth, 2016). Furthermore, DREADDs should have a minimal response in the absence of ligand binding. DREADDs activity typically relies upon a dose of CNO, which is usually in nanomolar concentrations.

However, CNO does not generate a cellular response in brain tissue when delivered systemically *in vivo*. Instead, CNO is reverse metabolized into clozapine that can cross the BBB and possesses high affinity to muscarinic DREADDs (Gomez et al., 2017). Despite the low concentrations of clozapine required to activate DREADDs, it is an atypical antipsychotic so CNO-derived clozapine may exert pharmacological effects in non-DREADDs targets that may result in undesirable behavioral changes. Therefore, the dose of the ligand must be titrated to control efficacy of treatment with DREADDs while mitigating potential side effects. When designing experiments, it is important to include appropriate control groups to assess for both: (*i*) potential side effects of CNO in non-DREADD-expressing animals; and (*ii*) the injection of a vehicle, such as saline, within DREADD-expressing subjects (MacLaren et al., 2016; Manvich et al., 2018). An alternative to relying on reverse metabolization of CNO is to inject clozapine at its much smaller reverse metabolized equivalent dose. Additionally, different

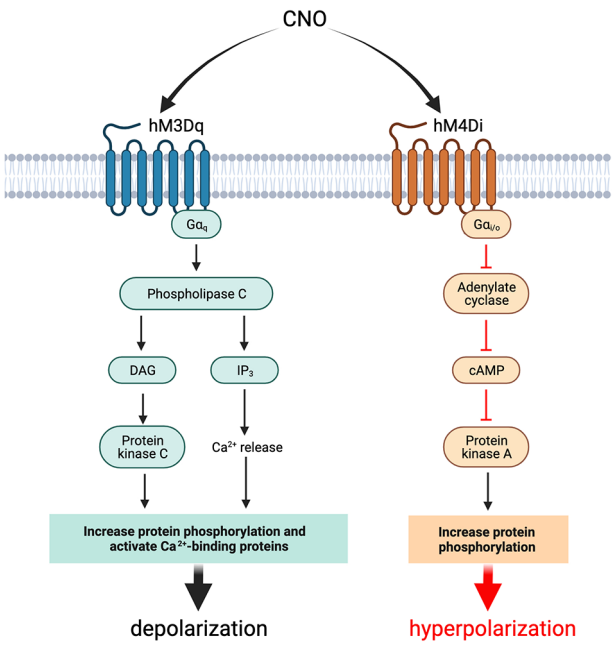

FIGURE 1 | Effects of activation of hM3Dq and hM4Di with CNO in neurons and interneurons. Activation of the DREADD probe hM3Dq with CNO in neurons and interneurons results in cellular depolarization while activation of hM4Di results in hyperpolarization. The net effect of activation of the DREADD construct is dependent on whether inhibitory or excitatory chemogenetics are used and which cell populations are targeted. cAMP, cyclic adenosine monophosphate; CNO, clozapine-N-oxide; DAG, diacylglycerol; DREADDs, designer receptors exclusively activated by designer drugs; hM3Dq, G_q-coupled human M3 muscarinic DREADD; hM4Di, G_i-coupled human M4 muscarinic DREADD; IP_3, inositol 1,4,5-trisphosphate.

ligands that possess higher affinity to DREADDs and reduced side effect profiles may be used, such as olanzapine, which is a second-generation atypical antipsychotic drug approved for use in humans by the Food and Drug Administration (Weston et al., 2019; Goossens et al., 2021).

Methods Used to Drive DREADDs Expression

Selective expression of the engineered receptors in cell populations can be achieved by two main techniques: (*i*) intracerebral injection of adeno-associated virus (AAV) vectors encoding the engineered receptors to a genomic sequence, with the genomic sequence linked to cell-type specific transcription factors, which results in receptor expression in a targeted subset of cells; and (*ii*) using transgenic mice that express the engineered receptors in cell populations genetically defined by the Cre-driver mouse line (Alexander et al., 2009; Farrell and Roth, 2013). These two methods have been used to deliver DREADDs to targeted cell populations in a specific brain region. This allows the neuroscientists to investigate the role of these cells in seizure generation and propagation. The goal of this review is to summarize the existing literature where DREADDs are employed to improve our understanding of the pathophysiology of human epilepsy. The remainder of this review focuses on the application of DREADDs in epilepsy research.

MATERIALS AND METHODS

A PubMed-, Scopus-/ScienceDirect-, and Web of Science-based scoping review of chemogenetics in epilepsy research was performed. Combinations of queries used for searches were ("chemogenetic" OR "pharmaco-genetic" OR "DREADD" OR "hM4Di" OR "hM3Dq") AND ("epilepsy" OR "seizure" OR "spasm" OR "epileptogenesis"). Publications that were classified as reviews were excluded. References were screened for additional relevant articles. Title/abstract and full text screenings were performed. Articles used for full text analysis were those using chemogenetics to investigate the pathophysiology of epilepsy.

RESULTS

Only primary or original research was considered in scope of this review. Our initial search returned 34 publications from PubMed, 385 from Scopus, 124 from ScienceDirect, and 30 from Web of Science. After removal of duplicates, 470 articles were included in our review. Publications were included if DREADDs were used to evaluate mechanisms of epileptogenesis or the epileptic phenotype. Additionally, publications were included if DREADDs were used to analyze biochemical and molecular mechanisms involved in epilepsy, even if results did not directly demonstrate seizure induction or seizure control. Publications were excluded if they evaluated seizures or spasms unrelated to epilepsy (e.g., alcohol withdrawal seizures) or focused purely on chemogenetics development (e.g., alternative ligands). After reading the abstract and applying inclusion and exclusion criteria, we identified 63 articles. After reading the full text and applying the same criteria, we included 25 articles in our analysis. Two (2) additional articles were identified by reference mining (i.e., citation chaining) resulting in a total of 27 articles. See **Figure 2** for PRISMA flow diagram (Page et al., 2021). The information about the studies included in this review is summarized in **Table 1** and reflects the structure of the sections on hippocampal and extrahippocampal networks. For each article in **Table 1**, we listed the DREADD construct, how cellular and regional specificity was controlled, target cell type, neuronal pathway investigated, animal model employed, and citation for the publication. The pathways were then illustrated in **Figures 3**, **4**. Four (4) studies that used DREADDs *in vitro* were excluded from the table but are included in the text. Three (3) publications on chemogenetics with potential for additional development were included in the "Discussion" Section.

We divided the articles included in this review into two main categories, i.e., those investigating hippocampal and extrahippocampal networks. Within the section on hippocampal networks, examples of seizure potentiation and induction by DREADDs are reviewed, followed by studies demonstrating seizure reduction using hM3Dq and then studies describing seizure reduction using hM4Di. A similar structure is used for the section on extrahippocampal targets, with examples of

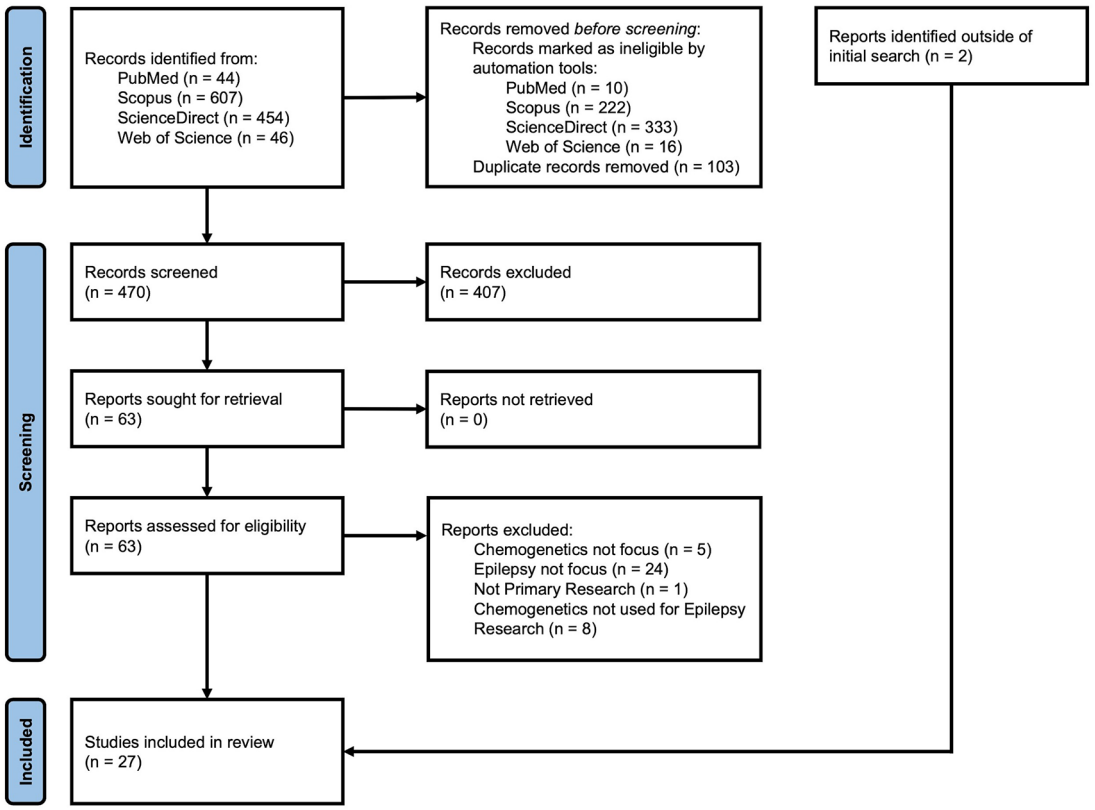

FIGURE 2 | PRISMA flow diagram of record identification, screening, and inclusion process for this review.

seizure induction described, followed by seizures reduced by hM3Dq and then by hM4Di. Finally, we discuss the experiments that use DREADDs to evaluate biochemical changes and then comorbidities associated with epilepsy.

DREADDs Targeted to Hippocampal Networks

Seizure Induction by Targeting Hippocampal Networks

The most common form of seizure disorder in adults is temporal lobe epilepsy (TLE), which is characterized by a seizure onset zone located in the temporal lobe (Navidhamidi et al., 2017). The hippocampus contains excitatory networks that are important for many cognitive functions such as spatial learning and memory (Jokeit and Ebner, 2002; Sweatt, 2004; Strien et al., 2009; Buzsáki and Moser, 2013) and serve as a network substrate for the onset of TLE (Lothman et al., 1991; Chatzikonstantinou, 2014). Three primary excitatory loops, which connect hippocampal and parahippocampal structures, exist. A long trisynaptic loop from the entorhinal cortex (EC) to the dentate gyrus (DG) to area Cornu Ammonis (CA) 3 to area CA1 loops back to different layers of the EC *via* the subiculum. Two other loops that bypass the dentate gyrus are an intermediate-length loop from EC to CA3 to CA1 to subiculum/EC; and a short loop that projects directly from EC to CA1 (Ang et al., 2006; Coulter et al., 2011). In the normal condition, most of the afferent inputs from the cortex are filtered and tightly regulated by cells in the DG (granule cells) and/or area CA1 (pyramidal cells) which are thought to be the two most potent "inhibitory hubs" in the network (Ang et al., 2005; Coulter et al., 2011).

The publications reviewed in this section are summarized in **Figure 3**, which includes hippocampal networks with a key provided in **Table 1** (figure reference designation of 1). The strategic location of the DG at the start of the trisynaptic pathway and the relative reluctance of dentate granule cells (DGCs) of the DG to fire led to postulation of the dentate "gate" hypothesis (Krook-Magnuson et al., 2015). Kahn et al. (2019) demonstrated the capability of DREADDs to induce seizures by providing evidence that non-epileptic mice expressing hM3Dq in calcium/calmodulin-dependent protein kinase II (CaMKIIα)-positive or excitatory neurons in the dorsal DG had variable behavioral seizures after administration of high doses of CNO (≥10 mg/kg). Although their report did not focus on seizure induction, their results provide a concept for further mechanistic studies.

An important means to investigate the role of a certain group of neuronal cells in generating seizures is to ask whether a change of their activities may potentiate seizures, i.e., increasing seizure probability when combined with a chemoconvulsant dose that does not cause seizures. Several groups have potentiated

TABLE 1 | Responses of DREADDs targeted to hippocampal and extrahippocampal networks.

Probe	Cellular specificity	Regional specificity	Cell type/Pathway	Animal model	Ligand	Figure Ref.	Reference
DREADDs Targeted to Hippocampal Networks							
Seizure Potentiation or Induction							
hM3Dq	CaMKIIα promoter	AAV5 into DG bilaterally	DGC	C57BL/6 mice	CNO	1a (3)	Kahn et al. (2019)
	DrD2-Cre mice	AAV2 into HPC bilaterally	Mossy cells	Pilocarpine	CNO	1b (3)	Botterill et al. (2019)
	-	RV into DG bilaterally	Ectopic DGC	Pilocarpine C57BL/6 mice	CNO	1c (3)	Zhou et al. (2019)
hM4Di	AAV-Vgat-Cre	AAV2/8 into CA1	CA1 PV/SOM INs	HPC kindled ChAT-ChR2-YFP mice with CA1 fiber	CNO	1d (3)	Wang et al. (2020)
	PV-Cre mice	AAV2 into Sub	Sub PV-INs	Pentylenetetrazol	CNO	1e (3)	Drexel et al. (2017)
hM3Dq	CaMKIIα promoter	AAV into Sub	Sub PNs	Phenytoin-responsive amygdala kindled Wistar rats	CNO	1f (3)	Xu et al. (2019)
Excitation to Decrease Seizures							
hM3Dq	PV-Cre mice	AAV8 into HPC Bilaterally	HPC PV-INs	4-aminopyridine	CNO	2a (3)	Călin et al. (2018)
	PV-Cre mice	AAV into HPC	DG + CA3 PV-INs	Acute/chronic IHKA, and HPC kindled	CNO	2b (3)	Wang et al. (2018)
	SOM-Cre mice	AAV into CA1	CA1 PV/SOM-INs	Acute IHKA	CNO	2c (3)	Wang et al. (2020)
	Vgat-Cre mice	AAV into Sub	Sub PV/SOM-INs	Acute/chronic IHKA, and HPC kindled	CNO	2d (3)	Wang et al. (2017)
Inhibition to Decrease Seizures							
hM4Di	CaMKIIα promoter	AAV2/7 into HPC	HPC PNs	IPKA Sprague Dawley rats	Clozapine and Olanzapine	3a (3)	Goossens et al. (2021)
	CaMKIIα-Cre mice	AAV into HPC	DG-CA3 microcircuit	Acute/chronic IHKA, and HPC kindled	CNO	3b (3)	Wang et al. (2018)
	CaMKIIα-Cre mice	AAV into HPC	DG-CA3 microcircuit	HPC kindled	CNO	3b (3)	Chen L. et al. (2020)
	hSyn promoter	AAV8 into contralateral HPC	DG-CA3 microcircuit	CaMKIIa-ChR2 mice with DG diode	CNO	3b (3)	Berglind et al. (2018)
	CaMKIIα promoter	Recombinant AAV2/7 into ipsilateral HPC	DGC	IHKA C57BL/6 mice	CNO and Clozapine	3c (3)	Desloovere et al. (2019)
	POMC-Cre mice	-	DGC	Pilocarpine	CNO	3c (3)	Zhou et al. (2019)
	Nestin-CreER mice	-	Adult born DGC	TAM at 6 weeks and pilocarpine 2 weeks later	CNO	3c (3)	Zhou et al. (2019)
	-	RV into DG bilaterally	Ectopic DGC	Pilocarpine C57BL/6 mice	CNO	3d (3)	Zhou et al. (2019)
	-	RV into HPC	Ectopic DGC	Pilocarpine C57BL/6 mice	CNO	3d (3)	Lybrand et al. (2021)
	DrD2-Cre mice	AAV2 into HPC bilaterally	Mossy cells	Pilocarpine	CNO	3e (3)	Botterill et al. (2019)
	CaMKIIα promoter	AAV into Sub	Sub	Phenytoin-unresponsive amygdala kindled Wistar rats	CNO	3f (3)	Xu et al. (2019)

(Continued)

TABLE 1 | Continued

Probe	Cellular specificity	Regional specificity	Cell type/Pathway	Animal model	Ligand	Figure Ref.	Reference
DREADDs Targeted to Extrahippocampal Networks							
Seizure Potentiation or Induction							
hM3Dq	CaMKIIα-tTA in TRE mice	-	HPC and cortex PNs	-	CNO	4a (4)	Alexander et al. (2009)
hM4Di	PV-Cre mice	-	HPC, somatosensory cortex, RTN, and cerebellar cortex PV-INs	-	-	4b (4)	Panthi and Leitch (2019)
Excitation to Decrease Seizures							
hM3Dq	PV-Cre mice	AAV into Motor cortex	Motor cortex PV-INs	Acute IHKA	CNO	5a (4)	Wang et al. (2018)
	ChAT-Cre mice	AAV2/8 into medial septum	Medial septum cholinergic neurons	Acute IHKA	CNO and Clozapine	5b (4)	Wang et al. (2020)
	Vgat-Cre mice	AAV into parafascicular nucleus of thalamus	Parafascicular nucleus INs	ChR2 right SNr with CA3 kindling	CNO	5c (4)	Chen B. et al. (2020)
Inhibition to Decrease Seizures							
hM4Di	CaMKIIα promoter	AAV into motor cortex	Motor cortex PNs	Pilocarpine and picrotoxin seizures, and tetanus toxin Epileptic rats	CNO	6a (4)	Kätzel et al. (2014)
	hSyn promoter	Recombinant AAV8 into midline thalamus bilaterally	Intralaminar thalamus neurons	Amygdala kindled Sprague Dawley rats	CNO	6b (4)	Wicker and Forcelli (2016)
	PV-Cre mice	AAV into SNr	SNr PV-INs	Acute/chronic IHKA	CNO	6c (4)	Chen B. et al. (2020)
	CRH-Cre mice	AAV into PVH bilaterally	PVH CRH neurons	Pilocarpine	CNO	6d (4)	Hooper et al. (2018)

Table 1 *reflects the structure of the sections on hippocampal and extrahippocampal networks. For each article, we listed DREADDs construct, how cellular and regional specificity was controlled, target cell type, neuronal pathway investigated, animal model employed and citation for the publication. The figure reference column contains a key to hippocampal and extrahippocampal networks depicted in* ***Figures 3***, ***4****, respectively. For example, a figure reference of 1 refers to publications that used DREADDs to potentiate or induce seizures by targeting networks within the HPC and has a 3 in parenthesis because it is depicted in* ***Figure 3****. Publications that targeted similar cells or networks have the same alphabetical designation in the figure reference column. The cellular specificity column includes the viral promoter if it was used to drive cellular specificity rather than Cre driver mouse lines. AAV, adeno associated virus; CA, Cornu Ammonis; CaMKII, calcium/calmodulin-dependent protein kinase II; ChAT, choline acetyl-transferase; ChR2, channelrhodopsin-2; CNO, clozapine-N-oxide; CRH, corticotropin-releasing hormone; DG, dentate gyrus; DGC, dentate granule cells; DrD2, dopamine receptor D2; DREADDs, designer receptors exclusively activated by designer drugs; eDGC, ectopic dentate granule cell; ER, estrogen receptor; hM3Dq, G_q-coupled human M3 muscarinic DREADD; hM4Di, G_i-coupled human M4 muscarinic DREADD; HPC, hippocampus; hSyn, human synapsin 1; IHKA, intrahippocampal kainic acid; INs, interneurons; IPKA, intraperitoneal kainic acid; PN, pyramidal neuron; POMC, proopiomelanocortin; PV, parvalbumin; PVH, paraventricular hypothalamic nucleus; RTN, reticular thalamic nucleus; RV, retrovirus; SNr, Substantia nigra; SOM, somatostatin; Sub, subiculum; TA, temporoammonic; TAM, tamoxifen; TRE, tet response element; tTa, tet transactivator; Vgat; vesicular GABA transporter.*

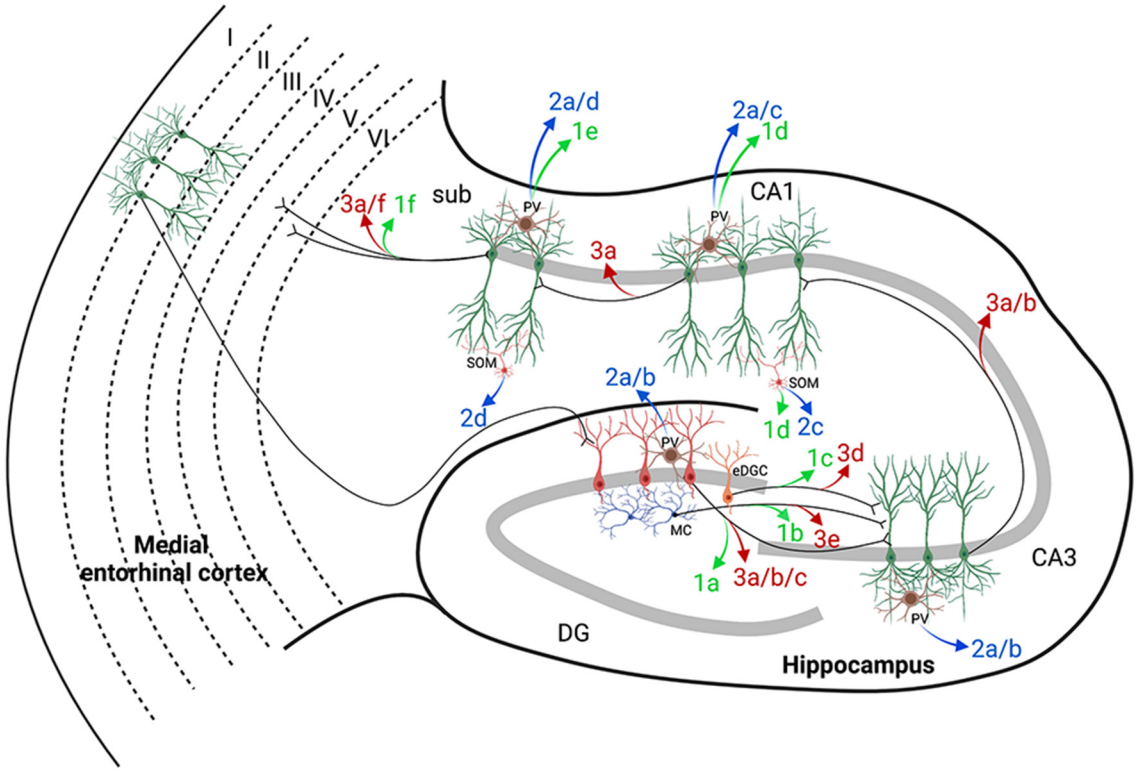

FIGURE 3 | Hippocampal targets of chemogenetics interrogated by each of the authors cited. The two classically defined inputs from the entorhinal cortex (EC) to the hippocampus are the perforant pathway (PP; EC to DG) and the temporoammonic pathway (EC to CA1). A long excitatory synaptic loop (EC to DG to CA3 to CA1 to subiculum and EC) receives inputs from the PP by innervation of the dentate gyrus (DG) and is known as the trisynaptic pathway. **Table 1** provides a key to the denoted projections and is organized by where each of the authors are cited in this review. Projections denoted in green were used by the authors cited to either potentiate or induce seizures with DREADDs (figure reference designation of 4). Blue labels indicate where hM3Dq was used to decrease seizures (figure reference designation of 5). Red labels indicate where hM4Di was used to decrease seizures (figure reference designation of 6). Projections labeled in black indicate connectivity that may contribute to the circuits evaluated. Created in BioRender.com. CA, Cornu Ammonis; DG, dentate gyrus; DREADDs, designer receptors exclusively activated by designer drugs; EC, entorhinal cortex; eDGC, ectopic dentate granule cells; hM3Dq, G_q-coupled human M3 muscarinic DREADD; hM4Di, G_i-coupled human M4 muscarinic DREADD; MC, mossy cells; PV, parvalbumin interneurons; SOM, somatostatin interneurons; Sub, subiculum.

seizures resembling TLE by manipulating a subset of cells with hM3Dq or hM4Di. This has elucidated pathological mechanisms that contribute to the breakdown of the dentate gate. In addition to the classic DG to CA3 microcircuit, another target of DGCs is glutamatergic neurons located in the DG hilus adjacent to DGCs. These cells are known as mossy cells and have been demonstrated to innervate both DGCs and parvalbumin-expressing basket cells, which are inhibitory γ-aminobutyric acid-releasing (GABAergic) interneurons (INs) in the DG (Scharfman and Myers, 2013). To explore the excitatory role of mossy cells in epileptogenesis, Botterill et al. (2019) selectively expressed hM3Dq in dopamine receptor D2-Cre$^{+/-}$ mice. These animals preferentially expressed Cre recombinase in mossy cells. They showed that activation of hM3Dq in mossy cells decreased latency to convulsive seizures after pilocarpine injection (Botterill et al., 2019). Contrary to the prior hypothesis that mossy cells prevent epilepsy, these results suggested that mossy cells become seizure inducing during pathological conditions by increasing excitation of DGCs while not changing their innervation of basket cells. Alternatively, basket cells like other GABAergic INs may become dysfunctional upon sustained excitation.

Another group of cells in the DG that have been investigated for their role in seizure generation are newborn DGCs, which are developed from neural stem cells. In the granular cell layer of the DG, neurogenesis persists throughout life in the adult hippocampus. In physiological conditions, newborn DGCs integrate into existing hippocampal circuitry, which is necessary for hippocampus-dependent learning and memory processes (Parent, 2007). These newborn DGCs may contribute to the breakdown of the dentate gate in TLE. To investigate this, Zhou et al. (2019) expressed hM3Dq in DGCs born 3 days after pilocarpine-induced status epilepticus (SE). They demonstrated that CNO-mediated activation of newborn DGCs two and a half months after transfection with hM3Dq resulted in epileptic spikes and spontaneous recurrent seizures, which are characteristics of chronic epilepsy. Furthermore, they demonstrated that newborn DGCs ectopically integrated into the trisynaptic pathway forming recurrent excitatory loops and contributed to increases in DG excitability (Zhou et al., 2019).

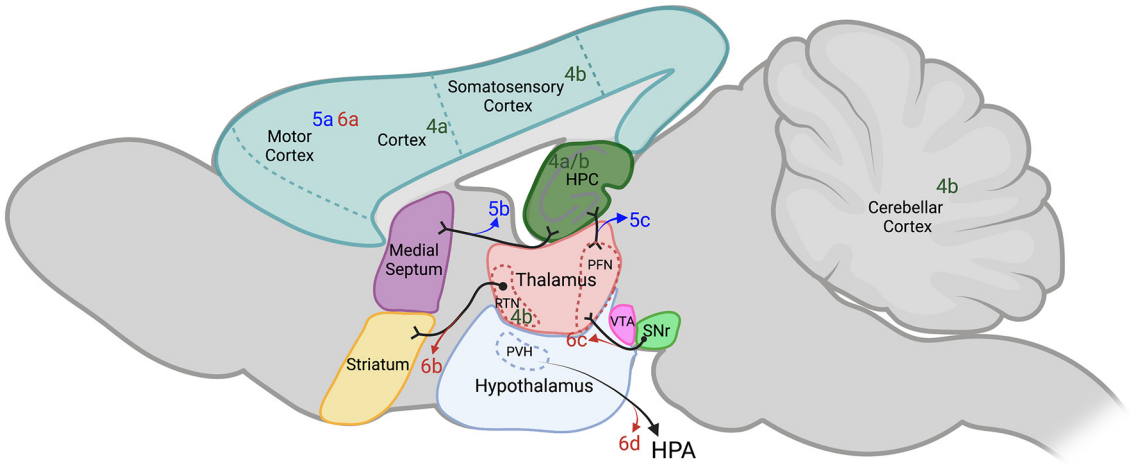

FIGURE 4 | Extrahippocampal targets of chemogenetics interrogated by each of the authors cited. Sagittal section of adult rodent brain. **Table 1** provides a key to the denoted publications and is organized by where each of the authors are cited in this review. Publications denoted in green were used by the authors cited to either potentiate or induce seizures with DREADDs (figure reference designation of 4). Blue labels indicate where hM3Dq was used to decrease seizures (figure reference designation of 5). Red labels indicate where hM4Di was used to decrease seizures (figure reference designation of 6). Projections labeled in black indicate connectivity that may contribute to the circuits evaluated. Dotted lines indicate structures outside of the plane depicted. Created in BioRender.com. DREADDs, designer receptors exclusively activated by designer drugs; hM3Dq, G_q-coupled human M3 muscarinic DREADD; hM4Di, G_i-coupled human M4 muscarinic DREADD; HPA, hypothalamic-pituitary-adrenal axis; HPC, hippocampus; PFN, parafascicular nucleus; PVH, paraventricular hypothalamic nucleus; RTN, reticular thalamic nucleus; SNr, substantia nigra pars reticulata; VTA, ventral tegmental area.

Another means to potentiate TLEs is to directly target the main source of inhibitory signaling in the brain, GABAergic INs. GABAergic INs discussed in this review may be further categorized as parvalbumin (PV)-, somatostatin (SOM)-, cholecystokinin-, and vasointestinal peptide-expressing INs (Pelkey et al., 2017; Marafiga et al., 2020). Under physiological conditions, GABAergic INs function to restrain excessive excitation in principal neurons *via* feedforward, feedback, or tonic inhibitory mechanisms (Marafiga et al., 2020). The breakdown of this inhibition results in a disturbance of the excitation/inhibition balance that contributes to the generation of seizures (Magloire et al., 2019). Wang et al. (2020) used hM4Di to block inhibition mediated by optogenetic stimulation of cholinergic neurons in the medial septum in intrahippocampal kainic acid (IHKA)-treated mice. The hM4Di-mediated inhibition of PV- or SOM-INs in CA1 resulted in increased seizures, suggesting that these INs were the downstream effectors of medial septum cholinergic neurons (Wang et al., 2020). These results suggest a possible involvement of dysfunctional PV- and SOM-INs in contributing to the generation of seizures and demonstrate the ability to target specific subsets of INs with a DREADD construct.

While the dentate gate restrains excitatory input, the other "gate" of the hippocampus is the subiculum which receives information from hippocampal area CA1 by both the trisynaptic pathway and temporoammonic pathway (Coulter et al., 2011). To evaluate the effect of the loss of inhibition at this node, Drexel et al. (2017) evaluated the transient inhibition of PV-INs in the subiculum using hM4Di. While transient inhibition of PV-INs did not generate seizures in non-epileptic mice, the injection of CNO combined with a sub-convulsant dose of pentylenetetrazol induced mice to show clusters of spike-wave discharges (Drexel et al., 2017). Similarly, Xu et al. (2019) used a DREADD construct to increase phenytoin resistance in epileptic mice by activating hM3Dq expressed in subicular pyramidal neurons (PNs). Contrary to phenytoin increasing afterdischarge threshold in wild-type mice, CNO in combination with phenytoin resulted in decreased afterdischarge threshold. These studies support a critical role of the subiculum in gating excitatory transmission.

Seizure Control by hM3Dq Targeted to Hippocampal Networks

In contrast to the previous subsection where we described publications that used DREADDs to induce or potentiate seizures, this section presents *in vitro* and *in vivo* experiments where researchers targeted hM3Dq to hippocampal networks to suppress epileptic seizures by increasing inhibitory signaling. The publications reviewed in this section are summarized in **Figure 3**, which includes hippocampal networks with a key provided in **Table 1** (figure reference designation of 2). A common strategy to suppress seizures has been the potentiation of GABAergic signaling (Perucca and Mula, 2013). The $GABA_A$ receptor is a common target of ASDs and it has been demonstrated that the antiseizure mechanism of benzodiazepines and barbiturates is by direct action on $GABA_A$ receptors (Greenfield, 2013). Therefore, selective targeting of INs to constrain hyperexcited networks is a logical choice for the application of hM3Dq. Several groups have demonstrated the feasibility of harnessing GABAergic INs to suppress seizure activity in models of TLE (Wang et al., 2017, 2018, 2020; Călin et al. 2018).

Since there are different subtypes of GABAergic INs, it is likely important to determine which class of INs promote the

most efficacious inhibitory effect on excitatory neurons in the hippocampus. To evaluate this, Călin et al. (2018) selectively targeted PV-, SOM-, and vasointestinal peptide-INs with hM3Dq *in vitro* using organotypic hippocampal slice cultures. Their data suggested that when targeting the entire hippocampus, PV-INs are more efficacious in suppressing epileptiform activity than other types of INs. Furthermore, the selective activation of hippocampal PV-INs with hM3Dq reduced the severity of systemic 4-aminopyridine-induced seizures in mice (Călin et al. 2018). This report demonstrated the relative difference in the effect of hM3Dq when manipulating subpopulations of INs, which is an important tool in investigating the role of specific cells in controlling seizures.

Since hyperexcitability of DGCs is associated with the emergence of seizures in TLE (Kahn et al., 2019), activating PV-INs within DG and CA3 subfields may also be efficacious in controlling seizures. In addition to confirming this hypothesis, Wang et al. (2018) showed that the anti-seizure effect of hM3Dq occurred in a CNO dose-dependent manner in PV-Cre mice treated with IHKA. An increased dose of CNO activated hM3Dq-expressing PV-INs in the DG and CA3 resulting in increased latency to SE, and decreased duration of chronic seizures and animal mortality. Furthermore, they demonstrated that activation of ventral hippocampal PV-INs reduced the number and duration of generalized seizures in mice during an 8-h measurement window following each dose of CNO for three consecutive days. The authors then applied the same technique to electrically kindled animals and showed that the CNO delayed seizure progression and decreased the duration of generalized seizures among these animals (Wang et al., 2018). In a later study, Wang et al. (2020) provided evidence in their supplemental data comparing direct hM3Dq-mediated activation of PV- and SOM-INs located in CA1. In CA1, these INs receive excitatory inputs from EC through the temporoammonic pathway and from CA3 through Schaffer collaterals, so area CA1 may also be an ideal node for targeting with hM3Dq to control seizures. In addition to decreasing seizures in an acute IHKA model, the study revealed that SOM-INs in CA1 have a greater inhibitory effect on this circuit than PV-INs (Wang et al., 2020).

In the subiculum, Wang et al. (2017) demonstrated that selective hM3Dq-mediated activation of GABAergic INs of vesicular GABA transporter-Cre mice resulted in delayed generalization of IHKA induced SE and reduced episodes of generalized seizures. Vesicular GABA transporter-Cre mice express Cre recombinase under control of the vesicular GABA transporter promoter in both PV- and SOM-INs. Interestingly, the excitation of these INs during the chronic phase of IHKA-induced epilepsy resulted in a transient twofold increase in the duration of generalized seizures during the 3-day CNO treatment window as compared to 3 days prior and post treatment (Wang et al., 2017). Their results suggest the involvement of a phenomenon known as ionic plasticity that may occur during epileptogenesis. This phenomenon refers to a shift from an inhibitory to an excitatory signaling profile of GABA in principal neurons by the modulation of neuronal functions through changes in GABAergic driving forces caused by long-term impairments of ion-regulatory molecules such as cation-chloride cotransporters (K-Cl cotransporter—KCC2, Na-K-2Cl cotransporter—NKCC1), Na-K ATPase, and carbonic anhydrase (Kaila et al., 2014). This early finding suggests that inhibitory neurons in the subiculum may display different roles in seizure generation and modulation in the different phases of epileptogenesis.

Seizure Control by hM4Di Targeted to Hippocampal Networks

Since the potentiation of GABA signaling with hM3Dq was demonstrated to be effective in constraining seizures in the previous section, in this section we address whether directly targeting hM4Di to PNs within a hippocampal seizure onset zone is as efficient in preventing and stopping seizures. This method was pioneered in epilepsy research by Armbruster et al. (2007) when they expressed hM4Di in hippocampal neurons in culture and demonstrated that administration of CNO induced selective membrane hyperpolarization and neuronal inhibition. Later, Avaliani et al. (2016) used a valproate-refractory model of epilepsy to provide evidence that inhibition of PNs of brain slices in organotypic culture could reduce electrically evoked seizure activity. They demonstrated that hyperpolarization of CA3 excitatory neurons by hM4Di was sufficient to suppress DG-initiated stimulus train-induced bursting (Avaliani et al., 2016). These *in vitro* studies represent proof-of-concept models that may be used prior to moving hM4Di to *in vivo* models. The studies presented here on in this section are summarized in **Figure 3**, which includes hippocampal networks with a key provided in **Table 1** (figure reference designation of 3).

Goossens et al. (2021) expanded upon the *in vitro* experiment introduced by Armbruster et al. (2007) by targeting all hippocampal excitatory neurons *in vivo*. They demonstrated that hM4Di-mediated inhibition of these neurons by a single or repetitive (6-h interval) subcutaneous clozapine injection resulted in decreased acute seizure frequency in rats with epilepsy induced by systemic KA. Additionally, clozapine or olanzapine were infused continuously for 7 days using osmotic minipumps, which resulted in significant seizure suppression during the first 4–5 days of treatment. However, seizure frequency increased to pre-treatment levels in the last 2 days of treatment with seizure duration exceeding baseline 3–4 days into treatment. Furthermore, after the removal of the minipumps, the animals showed a rebound effect both in seizure frequency and duration, reaching levels above the baseline observed before the onset of the treatment with CNO (Goossens et al., 2021). This phenomenon is comparable to tolerance effects observed with ASD usage in treating patients with seizure disorders. Tolerance effects of DREADDs should be considered when applying them to epilepsy research in general. Tapering the dosage of ligand instead of abrupt discontinuation could potentially reduce the rebound effect observed by Goossens et al. (2021). Alternatively, targeting DREADDs to more specific subsets of neurons in the hippocampus may remove the observed desensitization, which is similar to the "honeymoon effect" (i.e., loss of efficacy of ASD) observed in some patients after continued treatment with an ASD (Löscher and Schmidt, 2006). Regardless, the results of Goossens et al. (2021) highlight the importance of non-DREADD

expressing controls treated with ligand for interpretation of results.

More anatomically specific inhibition was demonstrated by Wang et al. (2018) when they directly inhibited hippocampal PNs expressing hM4Di in the DG and CA3 ipsilateral to IHKA injection in urethane-anesthetized mice. This led to decreased neuronal firing. Subsequently, they showed that the administration of CNO once per day for 3 days in freely moving mice induced the inhibition of PNs in the DG and area CA3, which in turn resulted in increased latency to seizure progression, decreased seizure duration, and decreased number of generalized seizures during the 8 h of recording after CNO treatment. Although no statistic was provided, a trend toward rebound hyperexcitation after CNO treatment was discontinued was presented in their data. Furthermore, the receptor desensitization described by Goossens et al. (2021) was not observed, which may be due to differences in regional specificity of hM4Di expression, ligand dosing schemes, or lengths of experiments. Additional experiments are necessary to determine the source of the variability in results (Wang et al., 2018). Similar results on seizure progression were reproduced by Chen L. et al. (2020) using the electrical kindling model.

CA3 neurons may project directly (Witter, 2007) or secondarily from mossy cells (Scharfman and Myers, 2013) to the contralateral CA3 and CA1, and it has previously been demonstrated that bilateral DG activation is required for progression of afterdischarge durations (Stringer and Lothman, 1992). hM4Di has also been employed to investigate the role of excitatory neurons and their implications in pathological changes in transhemispheric neuronal networks. Berglind et al. (2018) employed optogenetics to generate focal afterdischarges and expressed hM4Di among PNs in the contralateral DG and CA3. The activation of these PNs by CNO decreased the duration of afterdischarges (Berglind et al., 2018). However, Krook-Magnuson et al. (2015) previously demonstrated that optogenetic inhibition of contralateral DGCs was insufficient to inhibit seizures, so additional experiments are necessary to determine if persistent manipulation of contralateral DG and CA3 neurons with hM4Di would reduce seizures.

Since optogenetic inhibition of DGCs ipsilateral to IHKA was previously demonstrated to inhibit seizures (Krook-Magnuson et al., 2015), prolonged suppression of DGCs expressing hM4Di may result in a similar inhibitory effect. Desloovere et al. (2019) evaluated inhibition of CaMKIIα PNs in the DG. They suggested that DGCs ipsilateral to IHKA injection were predominantly transfected, demonstrated modulatory results of hM4Di on inhibiting seizures, and evaluated long-term effects of inhibition. Specifically, they used either 3 or 10 mg/kg of CNO, or the CNO equivalent doses of clozapine (0.03 or 0.1 mg/kg respectively) to inhibit these DGCs. Their results showed that similar relative ligand concentrations resulted in similar levels of inhibition on seizures. Furthermore, their results revealed that the seizure suppressive effect of these doses of clozapine had a duration of action greater than 8 h. In a subsequent experiment, they demonstrated that chronic repeated administration of the same doses of clozapine once every 8 h for 3 days was capable of near complete suppression of seizure activity during the previously established duration of effect. However, a trend toward rebound hyperexcitability was observed a day after the last dose (Desloovere et al., 2019).

As described previously, newborn DGCs are derived from neural stem cells and integrate ectopically into the trisynaptic pathway forming excitatory loops, contributing to breakdown of the dentate gate. Therefore, hM4Di may be used to control seizures by inhibiting cells derived from neural stem cells. First, Zhou et al. (2019) replicated the anti-seizure effect of inhibiting all DGCs. They then demonstrated that long-term inhibition of neural stem cells that integrate into hippocampal networks could reduce pilocarpine-induced recurrent seizures. Next, they used double-transgenic mice that expressed Cre recombinase fused to an estrogen receptor only in Nestin-positive neural stem cells. Tamoxifen was administered to the mice 2 weeks prior to pilocarpine injection resulting in the expression of hM4Di in the cells derived from these stem cells. Upon development of spontaneous seizures two and half months later, the inhibition of these hM4Di-expressing cells with CNO injected every 8 h for 3 days resulted in decreased frequency of epileptic spikes and spontaneous recurrent seizures. This effect on seizures receded after the completion of treatment with CNO. They suggested that only neural stem cells that have differentiated into DGCs contribute to anti-seizure effects; however, neural stem cells integrate into regions other than the DG hilus so they performed an additional experiment to specifically inhibit newborn DGCs. They injected a retrovirus coding for hM4Di 3 days after pilocarpine injection. Upon development of spontaneous seizures, they observed a reduction in seizure frequency on the day of CNO injection (Zhou et al., 2019). Lybrand et al. (2021) further investigated this mechanism by examining the anatomic changes associated with manipulations of newborn DGCs and their correlations to the occurrence of spontaneous seizures. To do this, animals expressing hM4Di in newborn DGCs were injected intraperitoneally with pilocarpine, followed by CNO administered once daily for the 2 weeks following SE. Eight weeks after the last CNO injection, they observed a significant reduction in ectopic newborn DGCs and reduced seizure frequency. Furthermore, area CA3 back-projections, a part of newborn DGC networks, were reduced while EC projections were increased from non-hM4Di controls toward non-pilocarpine controls (Lybrand et al., 2021). Botterill et al. (2019) harnessed another pathophysiological mechanism when they selectively inhibited hM4Di-expressing mossy cells in the DG of dopamine receptor D2-Cre$^{+/-}$ mice with CNO prior to inducing SE with pilocarpine. Their results demonstrated that, in addition to attenuating SE and decreasing neurodegeneration in the hilus and CA3, the inhibition of mossy cells in the DG resulted in reduced number, frequency, and severity of recurrent seizures during the chronic seizure phase (Botterill et al., 2019).

Previously in this review, we discussed results obtained by Xu et al. (2019) that showed that epileptic mice had increased resistance to phenytoin after activation of hM3Dq-expressing PNs in the subiculum. However, in the same publication, Xu et al. (2019) also decreased phenytoin resistance in the same phenytoin-resistant mouse model by expressing hM4Di in subicular PNs. Specifically, their results demonstrated

that the administration of CNO along with phenytoin raised the afterdischarge threshold in mice that were kindled by the electrical stimulation of the amygdala. Interestingly, the inhibitory effect of hM4Di did not increase the afterdischarge threshold in the absence of phenytoin (Xu et al., 2019). Since phenytoin was administered intraperitoneally, it likely affected cells outside of the hippocampus. The requisite of systemic phenytoin for efficacy of specific inhibition of the subiculum suggests a more complex circuit interaction involving global networks when the seizure focus is located outside of the hippocampus. Targeting a single node within an excited network may not be sufficient to abrogate seizures. Furthermore, choke points distal to the focus may be more efficient in gating excessive network activity (Paz and Huguenard, 2015). For this reason, other researchers have focused their efforts on evaluating the impact of extrahippocampal networks and nodes on epileptic activity. In the next section, we present publications that used DREADDs to investigate extrahippocampal networks.

DREADDs Targeted to Extrahippocampal Networks

Seizures Induced by Targeting Extrahippocampal Networks

To begin, we will describe studies where extrahippocampal networks were manipulated using DREADDs to create new seizure models. Despite the prevalence of using chemoconvulsants in seizure models, they have several drawbacks including lack of control over the interval between the administration of chemoconvulsants and seizure onset, variability in the drug metabolism, and possible off-target and unintended side effects (Cela and Sjöström, 2019). The use of DREADDs to develop seizure animal models may mitigate these drawbacks. **Figure 4** and **Table 1** (figure reference designation of 4) summarize extrahippocampal circuits discussed in this section.

The first example of the use of DREADDs to induce seizures with probes targeted to extrahippocampal networks was demonstrated by Alexander et al. (2009) when they developed a mutant mouse line that expressed hM3Dq in CaMKIIα-positive neurons in the hippocampus and throughout the cortex. The systemic administration of at least 1 mg/kg of CNO in this mutant mouse line induced neuronal activation and generalized seizures similarly observed in chemoconvulsant-induced animal models of acute epilepsy. Additionally, the authors showed that there is a dose dependent response to CNO in seizure severity and the percentage of animals reaching SE (Alexander et al., 2009).

One third of all epilepsies have a genetic origin known as idiopathic generalized epilepsies. Treatment of idiopathic generalized epilepsies with ASDs may be ineffective. Additionally, patients with idiopathic generalized epilepsies often present with a structurally normal brain on imaging studies and have no focal seizure onset zone. This in turn renders the patient ineligible for resective surgery [Engel and International League Against Epilepsy (ILAE), 2001; Mullen et al., 2018]. Absence epilepsy is a non-convulsive idiopathic generalized epilepsy believed to arise from cortico-thalamocortical circuitry and is characterized by spike-wave discharges (McCormick and Contreras, 2001). Panthi and Leitch evaluated the effect of global and focal inhibition of hM4Di-expressing extrahippocampal PV-INs in double transgenic non-epileptic mice. They achieved network-wide inhibition of all cortico-thalamocortical PV-INs by intraperitoneal injection of CNO doses of 5.0 mg/kg or greater. The inhibition induced paroxysmal oscillatory activity known as afterdischarges. Inhibition of somatosensory cortex or reticular thalamic nucleus PV-INs was also achieved by focal injection to the somatosensory cortex or reticular thalamic nucleus, respectively. This approach required lower CNO doses of approximately 2.5 mg/kg and resulted in afterdischarges, spike wave discharges, and behavioral changes characteristic of absence seizures. The study suggested that the somatosensory cortex and reticular thalamic nucleus PV-INs restrained cortical pyramidal cells and thalamic cortical cells, respectively (Panthi and Leitch, 2019).

Although the CNO doses required to generate seizures are much higher than the normal effective doses (≅1 mg/kg) for DREADDs activation, these results show the potential of generating acute generalized seizures in an "on demand" way with high cellular selectivity. By targeting hM3Dq or hM4Di to specific regions and subsets of cells, DREADDs reduce off-target effects of chemoconvulsants since CNO is inert to receptors other than the expressed DREADD. Furthermore, the effect of DREADDs may be titrated both at the level of receptor expression and dose of ligand administered, which may allow for tighter control over the severity and duration of seizures produced in animals.

Seizure Control by hM3Dq Targeted to Extrahippocampal Networks

In addition to activating cells within the hippocampus, hM3Dq-mediated excitation has allowed for evaluation of extrahippocampal neuronal circuits on seizures originating from within the hippocampus. The studies presented in this section are summarized in **Figure 4** and **Table 1** (figure reference designation of 5). Wang et al. (2018) evaluated hM3Dq-mediated activation of motor cortex PV-INs in the same IHKA epilepsy model presented previously. Their data shows that direct activation of motor cortex PV-INs increased the latency to SE but did not reduce the number of generalized seizures. This may suggest that hippocampal inhibitory cells are a better target for reducing TLE progression than cortical areas (Wang et al., 2018). In another study, the same investigators shifted their attention to activation of another extrahippocampal network, the medial septum to hippocampus cholinergic circuit. They demonstrated that administration of CNO to choline acetyl-transferase-Cre mice expressing hM3Dq in medial septum cholinergic neurons resulted in reduced number and duration of spontaneous seizures in epileptic mice subjected to the same IHKA model of TLE. Since the muscarinic agonist pilocarpine is a commonly used chemoconvulsant, exciting cholinergic neurons to inhibit seizures is potentially counterintuitive. Therefore, Wang et al. (2020) used retroviral tracing to demonstrate that most of these cholinergic neurons projected directly to PV- and SOM-INs in the hippocampus. We have previously described that activation

of hippocampal PV- and SOM-INs with hM3Dq has an inhibitory effect on seizures. However, they found that in these choline acetyl-transferase-Cre mice expressing hM3Dq in the medial septum, the sustained antiseizure effect generated by the administration of a daily single dose of CNO for 7 days was maintained for the 7 days following the end of CNO treatment. This may suggest that synaptic plasticity was induced from the sustained modulation of cholinergic signaling (Wang et al., 2020).

The parafascicular nucleus of the thalamus is known to be involved in the generation of physiological oscillatory rhythms and in the control of epileptic seizures due to its projections from and to areas implicated in seizure generation such as the cortex, thalamus, hippocampus, and especially the striatum (Vuong and Devergnas, 2018). In an elegant study using the IHKA animal model of spontaneous seizures in vesicular GABA transporter-Cre mice, Chen B. et al. (2020) demonstrated that the activation of parafascicular nucleus GABAergic neurons with hM3Dq prior to the injection of KA nearly doubled the latency to seizure generalization and decreased the number of generalized seizures. Mortality was also reduced in these mice. Furthermore, retrograde tracing provided evidence that GABAergic neurons in the substantia nigra pars reticulata were upstream of the parafascicular nucleus GABAergic neurons. Optogenetic activation of GABAergic neurons expressing channelrhodopsin-2 in the substantia nigra of vesicular GABA transporter-Cre mice potentiated kindling effects from electrical stimulation of CA3. Activation of hM3Dq-expressing GABAergic neurons in the parafascicular nucleus with CNO prior to kindling events removed this optogenetic pro-kindling effect. This suggests that GABAergic neurons in the substantia nigra modulate the antiseizure effect of parafascicular nucleus GABAergic neurons (Chen B. et al., 2020).

Seizure Control by hM4Di Targeted to Extrahippocampal Networks

For the motor component of a seizure to manifest, it most likely must generalize to regions of the brain that control movement. Additionally, extrahippocampal systems may alter hippocampal excitability through direct or indirect connections. We now present publications that constrained extrahippocampal cells or networks with hM4Di to control seizures (summarized in **Figure 4** and **Table 1**—reference designation of 6). Evidence suggests that seizure control can be achieved by the direct inhibition of motor neurons. Kätzel et al. (2014) demonstrated that direct inhibition of PNs of the motor cortex by hM4Di reduced acute motor seizures induced by pilocarpine and picrotoxin. In their experiments, picrotoxin-induced behavioral seizures were reduced only after 3 months which allowed for maximal hM4Di expression. Additionally, they demonstrated the capability of inhibition of motor neurons in reducing seizure severity over an extended course of more than 3 h in the tetanus-toxin model of neocortical epilepsy (Kätzel et al., 2014).

Since the epileptic focus is not always defined, hM4Di was also employed to evaluate if the thalamus could act as a chokepoint to networks involved in epilepsy. In a study performed by Wicker and Forcelli, the inhibition of thalamic neurons by hM4Di resulted in limbic seizure attenuation in rats submitted to electrical kindling in the amygdala. Furthermore, they showed that the level of reduction in seizure severity and duration of electrographic activity was dependent on the CNO dose administered. Additionally, higher doses of CNO (10 mg/kg) completely blocked seizure activity in a subset of animals (Wicker and Forcelli, 2016). In another previously discussed thalamic interface, the direct inhibition of PV-INs expressing hM4Di in the substantia nigra pars reticulata of PV-Cre mice resulted in prolonged latency to KA-induced SE and seizure generalization, while chronic treatment was able to reduce the number and severity of spontaneous seizures (Chen B. et al., 2020).

The hypothalamic-pituitary-adrenal axis is under control of the paraventricular nucleus of the hypothalamus. Corticotropin-releasing hormone neurons in the paraventricular nucleus of the hypothalamus may provide a link between increased corticosteroid levels and seizure susceptibility (Herman et al., 2003). Previous publications have demonstrated that increased corticotropin-releasing hormone increased PN excitability in the hippocampus (Aldenhoff et al., 1983; Hollrigel et al., 1998; Maguire and Salpekar, 2013). To further investigate the connection between stress and seizures, Hooper et al. (2018) bilaterally inhibited corticotropin-releasing hormone neurons in the paraventricular nucleus of the hypothalamus by expressing hM4Di in transgenic corticotropin-releasing hormone-Cre mice. Orally administered CNO led to a reduction in pilocarpine-induced seizures while also reducing behaviors associated with depression (Hooper et al., 2018). Corticotropin-releasing hormone neurons are under tight control of $GABA_A$ INs from multiple limbic brain regions including the hippocampus and thalamus (Cullinan et al., 1993). However, balanced levels of corticosterone are required for physiological function of the hippocampus (Diamond et al., 1992). Therefore, an abnormal hippocampus may lead to hyperactivity of the hypothalamic-pituitary-adrenal axis and amplify the pro-ictal effect of corticotropin-releasing hormone, further propagating the breakdown of homeostatic mechanisms.

The Use of DREADDs to Understand Biochemical Mechanisms of Epilepsy

In addition to anatomical/network changes, one critical characteristic of epilepsy that results from a persistent hyperexcitable network is the induction of maladaptive responses at the cellular level (Queenan et al., 2018). One of the most important cellular alterations is known as Hebbian plasticity, which comprises mechanisms of long-term potentiation and long-term depression. These mechanisms drive long-lasting alterations in synaptic strength to ensure network stability, providing feedback to unrestrained network hyperactivation (Lignani et al., 2020). Pathological mossy fiber sprouting may occur after death of DGC terminals (Cavarsan et al., 2018) and is assumed to contribute to recurrent closed-loop circuitry of excitatory synapses between the DG and CA3 (Santhakumar et al., 2005; Buckmaster, 2010). To better understand the synaptic homeostatic mechanisms between the hippocampal layers CA3 and DG, Queenan et al. (2018) investigated the synaptic homeostatic plasticity resulting from epileptogenesis

in mice. In their report, they focused on hM4Di-expressing DGCs with mossy fibers that targeted CA3 neurons that were not transfected with hM4Di. Chronic inactivation of this subset of DGCs with CNO was associated with cellular changes in these untransfected CA3 neurons including large increases in presynaptic bouton size, containing increased synaptoporin, and tripled the postsynaptic accumulation of the major scaffolding protein of mature glutamate synapses, postsynaptic density protein-95. Their results suggest that presynaptic mechanisms drive both pre-and postsynaptic expansion of DG-CA3 synapses (Queenan et al., 2018). In addition to a key role in epileptogenesis, these synaptic mechanisms associated with the accumulation of postsynaptic density protein-95 have been described to be fundamental to cognitive and behavioral functions in both healthy and pathological conditions (Yao et al., 2004; Delint-Ramírez et al., 2008; Keith and El-Husseini, 2008; Sun et al., 2009; Coley and Gao, 2019).

As discussed previously, DGCs have low excitability, which contributes to the gating function of the DG. In excitatory neurons, the KCC2 channel is necessary for proper function of postsynaptic $GABA_A$ receptor signaling and hyperpolarizing GABAergic transmission. KCC2 functions by maintaining low intracellular Cl^- concentration in normal conditions through inward K^+ gradients for the extrusion of Cl^- (Cristo et al., 2018). The downregulation of KCC2 can lead to increased neuronal excitability associated with numerous psychiatric and neurologic disorders including epilepsy (Kahle et al., 2016; Chen et al., 2017; Duy et al., 2019; Goutierre et al., 2019). Therefore, the downregulation of KCC2 may lead to increased excitability in DGCs and the breakdown of the dentate gate. First, to test whether the downregulation of KCC2 can be reversed or attenuated, Goutierre et al. (2019) used KCC2-directed small hairpin RNA to downregulate KCC2 expression in the hippocampus of rats expressing hM4Di in DGCs. Their data suggests that the knockdown of KCC2 in DGCs (with similar results in CA1) resulted in reduced potassium conductance due to diminished expression of outward rectifying Task-3 potassium channels, leading to strengthened EC afferents and hippocampal hyperexcitability. After treatment of these rats with CNO, the researchers observed a restoration in DGC membrane properties, which reversed the hyperexcitability generated by KCC2 knockdown. However, selective KCC2 knockdown in the DG of rats did not result in spontaneous recurrent seizures and did not potentiate the effects of pilocarpine induced SE (Goutierre et al., 2019).

The dysregulation of glial cells, specifically astrocytes, has also been implicated in the generation and worsening of epileptiform activity by the release of excitatory gliotransmitters including glutamate, D-serine, and ATP (Robel et al., 2015; Vargas-Sánchez et al., 2018). Therefore, an application of hM3Dq was to modulate astrocytes to investigate both the intrinsic mechanisms of reactive astrogliosis and their influence on surrounding neurons. Durkee et al. (2019) expressed hM3Dq in astrocytes of the hippocampus by using a glial fibrillary acidic protein promoter. The selective activation of these astrocytes increased extracellular Ca^{2+} and facilitated glutamate release, which activated N-methyl-D-aspartate receptors and induced slow inward currents in surrounding neurons. Interestingly, selective activation of both hM3Dq and hM4Di in astrocytes in the primary somatosensory cortex of mouse brain slices generated increased glutamate release resulting in enhanced neuronal excitability (Durkee et al., 2019).

Using DREADDs to Investigate the Comorbidities of Epilepsy

Since the progression of epilepsy exposes the brain to prolonged abnormal electrical activity, it may lead to cognitive and psychosocial impairments (Fisher et al., 2014; Falco-Walter et al., 2018). The most prominent cognitive problems found in TLE patients are mental slowness, memory impairments, and attention deficits (Rijckevorsel, 2006). These cognitive impairments are also found in chemically induced animal models of TLE. The administration of pilocarpine in mice generates chronic hyperexcitability of glutamatergic DGCs increasing seizure susceptibility. These animals also exhibit impairments in spatial and discriminative memory (Kalemenev et al., 2015; Kahn et al., 2019; Smolensky et al., 2019; Park et al., 2020). To minimize the cognitive impairments that result from the progression of epilepsy, Kahn et al. (2019) expressed hM4Di in DGCs of mice with chronic epilepsy, induced by systemic administration of pilocarpine. They demonstrated that the administration of CNO reduced DG hyperexcitability, which led to the recovery of memory impairments in these epileptic mice while having no effect in green fluorescence protein-expressing controls. In a separate cohort of non-epileptic mice, they then showed that hyperexcitability induced in DGCs by hM3Dq led to spatial memory deficits comparable to epileptic mice (Kahn et al., 2019).

DISCUSSION

In this review, we presented examples of the application of DREADDs to epilepsy research. DREADDs has been used to manipulate a subset of cells to potentiate seizures. Additionally, groups have demonstrated DREADDs as a technique to create a seizure focus and to elucidate cellular and network mechanisms underlying seizures. Both hM3Dq and hM4Di have been used to control seizures. Several groups explored ligand dosing strategies for controlling seizures and identified important considerations for designing regimens for future experiments. Furthermore, DREADDs have been used along with other techniques to identify pathological changes in biochemistry that may lead to epilepsy. Finally, DREADDs can be used to investigate comorbidities associated with epilepsy. These experiments may help identify therapeutic targets for future treatment strategies.

Comparison Between DREADDs and Optogenetics

There are other tools that have been used to manipulate cells to evaluate the pathophysiology of epilepsy. Optogenetics is a powerful tool for modulating neuronal activity. Cela and Sjostrom provided a thorough review of its application in epilepsy research (Cela and Sjöström, 2019). A review by Forcelli provided comparisons between optogenetics and chemogenetics in epilepsy research (Forcelli, 2017). Briefly, optogenetics allows

for both the activation (e.g., channelrhodopsins) and inhibition (e.g., halorhodopsin) of neurons by light induced ion channel opening (Nagel et al., 2002; Krook-Magnuson et al., 2015; Cela et al., 2019). Optogenetics has an immediate effect on neuronal activity upon light stimulation and its stimulus has temporal resolution of milliseconds (Boyden et al., 2005; Gunaydin et al., 2010). Despite its high temporal resolution, optogenetics requires hardware implantation for light delivery (Cook et al., 2013; Krook-Magnuson et al., 2013; Paz et al., 2013). In addition, the effect of optogenetics depends on the penetration of light into the brain (Yizhar et al., 2011), which is confined to a small region around the light source. The required light stimulation when using optogenetics has posed challenges for its implementation in larger brains such as nonhuman primates due to the skull's thickness (Herculano-Houzel, 2009; Watanabe et al., 2020). Additionally, the increased intensities necessary to activate larger regions may lead to heat generation from the fibers (Yizhar et al., 2011) which may alter the physiological properties of surrounding brain tissue (Kim and Connors, 2012). Unlike optogenetics, the actions of DREADDs are mediated either by the adenylyl cyclase signaling pathway (hM4Di) or inositol 1,4,5-trisphosphate-mediated Ca^{2+} release (hM3Dq), which results in much slower onset of their effect (Alexander et al., 2009; Forcelli, 2017; Atasoy and Sternson, 2018). The effects of DREADDs on neuronal activity start approximately 30 min after ligand administration and can last up to several hours.

An interesting solution for the limitation of optogenetics was demonstrated by Tung et al. (2018) when they combined optogenetics with chemogenetics to remove the necessity of an implanted light source. Specifically, inhibitory luminopsin, a protein resulting from the fusion of an inhibitory halorhodopsin and luciferase probe, allowed the cells that express inhibitory luminopsins to have an optogenetic-induced response by their own light-source when activated by the ligand coelenterazine. This resulted in inhibitory effects with temporal resolution comparable to external light-activated halorhodopsin, but activated by a chemical ligand. This also allows receptors in spatially distinct locations to be activated by systemic administration of a ligand. By targeting both the dentate gyrus and anterior nucleus of the thalamus, Tung et al. (2018) demonstrated the inhibitory effects of luminopsins in reducing seizures induced by pentylenetetrazol in rats.

Challenges for Clinical Translation of DREADDs

Having presented applications of DREADDs to epilepsy research, we now consider their potential to be used in treating patients with seizure disorders. DREADDs-based therapies are promising treatment strategies to address the need for effective epilepsy treatments. The fact that the exogenous ligands of DREADDs are largely inert toward other receptors and tissues is a desirable attribute of this technique when being considered for therapeutic applications. Here, we have identified a few challenges to be met before the implementation of a DREADD construct as a form of ASD.

First, to apply one of the described DREADDs as an intervention for patients with epilepsy, the utilization of gene therapy is likely needed. Even though several gene therapies have been validated in preclinical models, the concern for untoward effects associated with the use of viral vectors to deliver gene therapies persists. Recent advancements in gene therapies are focused on minimizing potential side effects by engineering vectors with high selectivity for the targeted cells of the brain (Wang et al., 2019).

Second, since the genetic modification of neurons is likely irreversible, an optimal viral dosage to achieve the desired therapeutic effect without compromising normal brain function must be identified. The dosage of viral vectors is dependent on the number of viral copies per infected neurons, number of cells infected, and resultant level of receptor reserve in the target tissue. This requires a precise strategy to ensure that the epileptic zone is effectively transfected with minimal spread to neighboring regions (Lieb et al., 2019).

Third, decisions for current therapies that alter the genome to enter human trials are made restrictively in cases where the diseases are reported to be untreatable, or when conventional therapies are no longer effective (Lowenstein, 2008). Along with the possible safety issues and technical considerations described above, a therapy that modifies the human genome needs to take into consideration the patient's privacy, free will, and personal identity. The legal and social implications of altering the human genome are complex (Canli, 2015).

Fourth, another challenge in applying chemogenetics to treat the diseases that affect the central nervous system is how to deliver the construct across the BBB. For this reason, the AAV carrying the DREADD viral construct has predominantly been delivered to the target brain region *via* stereotaxic surgery. The use of AAVs in neural tissue presents a safe and reliable profile with high specificity of viral vectors to infect specific subsets of cells (McCown, 2005; Bowers et al., 2011; High and Aubourg, 2011; Weinberg et al., 2013; Canli, 2015). However, the limited capacity of AAVs to cross the BBB requires intravenous delivery of different serotypes of AAV. New tools, such as drugs that transiently increase BBB permeability may overcome this problem. An alternative is the development of new AAV serotypes with higher crossing capacities, such as recombinant AAVs or human recombinant AAVs (Jackson et al., 2016; Goertsen et al., 2022). These technologies would need to be combined with more specific cellular promoters to maintain the regional specificity driven by stereotaxic injection (Hudry and Vandenberghe, 2019). Another option is intrathecal injections, either cisternal or lumbar, of the viral vectors (Hocquemiller et al., 2016).

Fifth, ligands for DREADDs activation will also need to cross the BBB. Recent publications provided evidence that CNO is reverse metabolized peripherally into clozapine and N-desmethylclozapine. Instead of CNO, these metabolites cross the BBB and possess higher binding affinity to muscarinic DREADDs than CNO (Nawaratne et al., 2008; Hellman et al., 2016; Gomez et al., 2017; Manvich et al., 2018). A potential alternative to requiring ligand delivery was made by Lieb et al. (2018) when they engineered an antiepileptic autoregulatory chemogenetic therapy. Their technique consisted of genetically modifying a glutamate-gated chloride channel gene found in

round worms (*Caenorhabditis elegans*) to have higher sensitivity to glutamate. Pilocarpine-induced epileptic mice that had these enhanced glutamate-gated chloride channels delivered into cortical pyramidal neurons showed attenuated acute seizures and a progressive decrease in the number and frequency of seizures in the chronic period of epilepsy (Lieb et al., 2018). Most interestingly, despite activity of enhanced glutamate-gated chloride channels being regulated by endogenous glutamate, expression of these modified channels in the brain does not affect normal brain function. This is most likely due to the efficient clearance of glutamate from extrasynaptic spaces by excitatory amino acid transporters (Tzingounis and Wadiche, 2007; Lieb et al., 2018). These results increase the likelihood of finding appropriate ligands for DREADDs as a treatment modality.

Finally, another important consideration when applying DREADDs to treating patients with epilepsy is the longevity of the treatment. The substantial effect and relatively long duration of 8 h after administration of ligand currently make DREADDs an ideal rescue treatment upon administration of the ligand. Long-term dosing of the ligand as a chronic treatment requires further development and consistency across researchers in designing experiments. It is unknown whether the tolerance effect presented by Goossens et al. (2021) above could have been avoided by changing the dosing schedule or increasing the number of expressed receptors since it was originally hypothesized that receptor reserve would protect against tolerance. Furthermore, tolerance effects have not been evaluated when targeting interneurons with DREADDs. An alternative would be to develop a DREADD construct that was resistant to desensitization. Since DREADDs require the same cellular machinery that GPCRs use to mediate their effect, they are also subject to phosphorylation-dependent effects such as desensitization and arrestin-mediated receptor degradation (Yu et al., 1993). These cellular mechanisms can lead to the tolerance effects described above. The neuronal effects of DREADDs are largely thought to be mediated by GPCR mechanisms (Armbruster et al., 2007) so biased receptors may still mediate the intended effect without being desensitized. To evaluate adverse effects that may be associated with the use of cholinesterase inhibitors in Alzheimer's disease, Bradley et al. (2020) developed a phosphorylation-deficient DREADD. Knocking in this DREADD in mice resulted in expression in cells instead of the wild-type receptor. They demonstrated that treatment of these mice with CNO resulted in TLE-like seizures that were comparable to seizures induced by pilocarpine (Bradley et al., 2020). Although they did not show long-term effects of their phosphorylation-deficient DREADD, this DREADD construct or a phosphorylation deficient version of hM3Dq or hM4Di may be resistant to phosphorylation-dependent receptor degradation, and of potential use in chronic treatment for epilepsy.

Prior to clinical use, DREADDs must be demonstrated safe and efficacious in non-human primates. As a first step, researchers investigated whether the use of rodent-optimized viruses can transduce and drive the required levels of DREADD expression in these primates. To evaluate this, Galvan et al. (2019) performed an ultrastructural analysis of DREADD location in non-human primate and mouse neurons to verify whether differences across species might impact the subcellular location and plasma membrane expression of DREADDs. They reasoned that the neurons that express DREADDs in locations other than the plasma membrane would be unable to modulate neural activity. Using the same virus construct to express hM4Di fused to the mCherry fluorescent reporter protein, they showed that individual DREADDs were expressed mainly in the plasma membrane of mice. However, in non-human primate brain tissue, the receptors were found distributed in the intracellular space, where they are not able to perform their modulatory action (Galvan et al., 2019).

CONCLUSION

In summary, DREADDs have proven to be powerful tools for improving our understanding of the pathophysiology of epilepsy. DREADDs have the potential to become new treatment modalities for patients suffering from this disease. Further investigations are needed in order to apply the laboratory findings to improve treatment outcomes for these patients.

AUTHOR CONTRIBUTIONS

All authors contributed equally to the planning, research, writing, review, and development of this work. All authors contributed to the article and approved the submitted version.

FUNDING

HS was supported by the United States Department of Defense (DOD), Congressional Directed Medical Research Program (CDMRP) grant, and Epilepsy Research Program Idea Development Award: #W81XWH-18-1-0655.

REFERENCES

Aldenhoff, J., Gruol, D., Rivier, J., Vale, W., and Siggins, G. (1983). Corticotropin releasing factor decreases postburst hyperpolarizations and excites hippocampal neurons. *Science* 221, 875–877. doi: 10.1126/science.6603658

Alexander, G. M., Rogan, S. C., Abbas, A. I., Armbruster, B. N., Pei, Y., Allen, J. A., et al. (2009). Remote control of neuronal activity in transgenic mice expressing evolved G protein-coupled receptors. *Neuron* 63, 27–39. doi: 10.1016/j.neuron.2009.06.014

Ang, C. W., Carlson, G. C., and Coulter, D. A. (2005). Hippocampal CA1 circuitry dynamically gates direct cortical inputs preferentially at theta frequencies. *J. Neurosci.* 25, 9567–9580. doi: 10.1523/JNEUROSCI.2992-05.2005

Ang, C. W., Carlson, G. C., and Coulter, D. A. (2006). Massive and specific dysregulation of direct cortical input to the hippocampus in temporal lobe epilepsy. *J. Neurosci.* 26, 11850–11856. doi: 10.1523/JNEUROSCI.2354-06.2006

Armbruster, B. N., Li, X., Pausch, M. H., Herlitze, S., and Roth, B. L. (2007). Evolving the lock to fit the key to create a family of G protein-coupled receptors potently activated by an inert ligand. *Proc. Natl. Acad. Sci. U S A* 104, 5163–5168. doi: 10.1073/pnas.0700293104

Atasoy, D., and Sternson, S. M. (2018). Chemogenetic tools for causal cellular and neuronal biology. *Physiol. Rev.* 98, 391–418. doi: 10.1152/physrev.00009.2017

Avaliani, N., Andersson, M., Runegaard, A. H., Woldbye, D., and Kokaia, M. (2016). DREADDs suppress seizure-like activity in a mouse model of pharmacoresistant epileptic brain tissue. *Gene Ther.* 23, 760–766. doi: 10.1038/gt.2016.56

Berglind, F., Andersson, M., and Kokaia, M. (2018). Dynamic interaction of local and transhemispheric networks is necessary for progressive intensification of hippocampal seizures. *Sci. Rep.* 8:5669. doi: 10.1038/s41598-018-23659-x

Botterill, J. J., Lu, Y.-L., LaFrancois, J. J., Bernstein, H. L., Alcantara-Gonzalez, D., Jain, S., et al. (2019). An excitatory and epileptogenic effect of dentate gyrus mossy cells in a mouse model of epilepsy. *Cell Rep.* 29, 2875–2889.e6. doi: 10.1016/j.celrep.2019.10.100

Bowers, W. J., Breakefield, X. O., and Sena-Esteves, M. (2011). Genetic therapy for the nervous system. *Hum. Mol. Genet.* 20, R28–R41. doi: 10.1093/hmg/ddr110

Boyden, E. S., Zhang, F., Bamberg, E., Nagel, G., and Deisseroth, K. (2005). Millisecond-timescale, genetically targeted optical control of neural activity. *Nat. Neurosci.* 8, 1263–1268. doi: 10.1038/nn1525

Bradley, S. J., Molloy, C., Valuskova, P., Dwomoh, L., Scarpa, M., Rossi, M., et al. (2020). Biased M1-muscarinic-receptor-mutant mice inform the design of next-generation drugs. *Nat. Chem. Biol.* 16, 240–249. doi: 10.1038/s41589-019-0453-9

Buckmaster, P. S. (2010). Mossy fiber sprouting in the dentate gyrus. *Epilepsia* 51, 39–39. doi: 10.1111/j.1528-1167.2010.02825.x

Buzsáki, G., and Moser, E. I. (2013). Memory, navigation and theta rhythm in the hippocampal-entorhinal system. *Nat. Neurosci.* 16, 130–138. doi: 10.1038/nn.3304

Călin, A., Stancu, M., Zagrean, A.-M., Jefferys, J. G. R., Ilie, A. S., and Akerman, C. J. (2018). Chemogenetic recruitment of specific interneurons suppresses seizure activity. *Front. Cell Neurosci.* 12:293. doi: 10.3389/fncel.2018.00293

Canli, T. (2015). Neurogenethics: an emerging discipline at the intersection of ethics, neuroscience and genomics. *Appl. Transl. Genom.* 5, 18–22. doi: 10.1016/j.atg.2015.05.002

Cavarsan, C. F., Malheiros, J., Hamani, C., Najm, I., and Covolan, L. (2018). Is mossy fiber sprouting a potential therapeutic target for epilepsy? *Front. Neurol.* 9:1023. doi: 10.3389/fneur.2018.01023

Cela, E., McFarlan, A. R., Chung, A. J., Wang, T., Chierzi, S., Murai, K. K., et al. (2019). An optogenetic kindling model of neocortical epilepsy. *Sci Rep.* 9:5236. doi: 10.1038/s41598-019-41533-2

Cela, E., and Sjöström, P. J. (2019). Novel optogenetic approaches in epilepsy research. *Front. Neurosci.* 13:947. doi: 10.3389/fnins.2019.00947

Changeux, J.-P. (2012). The nicotinic acetylcholine receptor: the founding father of the pentameric ligand-gated ion channel superfamily. *J. Biol. Chem.* 287, 40207–40215. doi: 10.1074/jbc.R112.407668

Chatzikonstantinou, A. (2014). Epilepsy and the hippocampus. *Front. Neurol. Neurosci.* 34, 121–142. doi: 10.1159/000356435

Chen, L., Liang, J., Fei, F., Ruan, Y., Cheng, H., Wang, Y., et al. (2020). Pharmacogenetic inhibition of pyramidal neurons retards hippocampal kindling-induced epileptogenesis. *CNS Neurosci. Ther.* 26, 1111–1120. doi: 10.1111/cns.13434

Chen, L., Wan, L., Wu, Z., Ren, W., Huang, Y., Qian, B., et al. (2017). KCC2 downregulation facilitates epileptic seizures. *Sci. Rep.* 7:156. doi: 10.1038/s41598-017-00196-7

Chen, B., Xu, C., Wang, Y., Lin, W., Wang, Y., Chen, L., et al. (2020). A disinhibitory nigra-parafascicular pathway amplifies seizure in temporal lobe epilepsy. *Nat. Commun.* 11:923. doi: 10.1038/s41467-020-14648-8

Coley, A. A., and Gao, W.-J. (2019). PSD-95 deficiency disrupts PFC-associated function and behavior during neurodevelopment. *Sci. Rep.* 9:9486. doi: 10.1038/s41598-019-45971-w

Cook, M. J., O'Brien, T. J., Berkovic, S. F., Murphy, M., Morokoff, A., Fabinyi, G., et al. (2013). Prediction of seizure likelihood with a long-term, implanted seizure advisory system in patients with drug-resistant epilepsy: a first-in-man study. *Lancet Neurol.* 12, 563–571. doi: 10.1016/S1474-4422(13)70075-9

Coulter, D. A., Yue, C., Ang, C. W., Weissinger, F., Goldberg, E., Hsu, F., et al. (2011). Hippocampal microcircuit dynamics probed using optical imaging approaches. *J. Physiol.* 589, 1893–1903. doi: 10.1113/jphysiol.2010.202184

Cox, B., and Gosling, M. (2014). *Ion Channel Drug Discovery*. Royal Society of Chemistry. doi: 10.1039/9781849735087

Cristo, G. D., Awad, P. N., Hamidi, S., and Avoli, M. (2018). KCC2, epileptiform synchronization and epileptic disorders. *Prog. Neurobiol.* 162, 1–16. doi: 10.1016/j.pneurobio.2017.11.002

Cullinan, W. E., Herman, J. P., and Watson, S. J. (1993). Ventral subicular interaction with the hypothalamic paraventricular nucleus: evidence for a relay in the bed nucleus of the stria terminalis. *J. Comp. Neurol.* 332, 1–20. doi: 10.1002/cne.903320102

Delint-Ramírez, I., Salcedo-Tello, P., and Bermudez-Rattoni, F. (2008). Spatial memory formation induces recruitment of NMDA receptor and PSD-95 to synaptic lipid rafts. *J. Neurochem.* 106, 1658–1668. doi: 10.1111/j.1471-4159.2008.05523.x

Desloovere, J., Boon, P., Larsen, L. E., Merckx, C., Goossens, M., Haute, C. V. den., et al. (2019). Long-term chemogenetic suppression of spontaneous seizures in a mouse model for temporal lobe epilepsy. *Epilepsia* 60, 2314–2324. doi: 10.1111/epi.16368

Devinsky, O., Vezzani, A., O'Brien, T. J., Jette, N., Scheffer, I. E., Curtis, M. de., et al. (2018). Epilepsy. *Nat. Rev. Dis. Primers* 4:18024. doi: 10.1038/nrdp.2018.24

Diamond, D. M., Bennett, M. C., Fleshner, M., and Rose, G. M. (1992). Inverted-U relationship between the level of peripheral corticosterone and the magnitude of hippocampal primed burst potentiation. *Hippocampus* 2, 421–430. doi: 10.1002/hipo.450020409

Drexel, M., Romanov, R. A., Wood, J., Weger, S., Heilbronn, R., Wulff, P., et al. (2017). Selective silencing of hippocampal parvalbumin interneurons induces development of recurrent spontaneous limbic seizures in mice. *J. Neurosci.* 37, 8166–8179. doi: 10.1523/JNEUROSCI.3456-16.2017

Durkee, C. A., Covelo, A., Lines, J., Kofuji, P., Aguilar, J., and Araque, A. (2019). Gi/o protein-coupled receptors inhibit neurons but activate astrocytes and stimulate gliotransmission. *Glia* 67, 1076–1093. doi: 10.1002/glia.23589

Duy, P. Q., David, W. B., and Kahle, K. T. (2019). Identification of KCC2 mutations in human epilepsy suggests strategies for therapeutic transporter modulation. *Front. Cell Neurosci.* 13:515. doi: 10.3389/fncel.2019.00515

Engel, J., Jr. (2016). What can we do for people with drug-resistant epilepsy? The 2016 wartenberg lecture. *Neurology* 87, 2483–2489. doi: 10.1212/WNL.0000000000003407

Engel, J., and International League Against Epilepsy (ILAE). (2001). A proposed diagnostic scheme for people with epileptic seizures and with epilepsy: report of the ILAE task force on classification and terminology. *Epilepsia* 42, 796–803. doi: 10.1046/j.1528-1157.2001.10401.x

Falco-Walter, J. J., Scheffer, I. E., and Fisher, R. S. (2018). The new definition and classification of seizures and epilepsy. *Epilepsy Res.* 139, 73–79. doi: 10.1016/j.eplepsyres.2017.11.015

Farrell, M. S., and Roth, B. L. (2013). Pharmacosynthetics: reimagining the pharmacogenetic approach. *Brain Res.* 1511, 6–20. doi: 10.1016/j.brainres.2012.09.043

Fisher, R. S., Acevedo, C., Arzimanoglou, A., Bogacz, A., Cross, J. H., Elger, C. E., et al. (2014). ILAE official report: a practical clinical definition of epilepsy. *Epilepsia* 55, 475–482. doi: 10.1111/epi.12550

Forcelli, P. A. (2017). Applications of optogenetic and chemogenetic methods to seizure circuits: where to go next? *J. Neurosci. Res.* 95, 2345–2356. doi: 10.1002/jnr.24135

Galvan, A., Raper, J., Hu, X., Paré, J., Bonaventura, J., Richie, C. T., et al. (2019). Ultrastructural localization of DREADDs in monkeys. *Eur. J. Neurosci.* 50, 2801–2813. doi: 10.1111/ejn.14429

Glukhova, A., Draper-Joyce, C. J., Sunahara, R. K., Christopoulos, A., Wootten, D., and Sexton, P. M. (2018). Rules of engagement: GPCRs and G proteins. *ACS Pharmacol. Transl. Sci.* 1, 73–83. doi: 10.1021/acsptsci.8b00026

Goertsen, D., Flytzanis, N. C., Goeden, N., Chuapoco, M. R., Cummins, A., Chen, Y., et al. (2022). AAV capsid variants with brain-wide transgene expression and decreased liver targeting after intravenous delivery in mouse and marmoset. *Nat. Neurosci.* 25, 106–115. doi: 10.1038/s41593-021-00969-4

Gomez, J. L., Bonaventura, J., Lesniak, W., Mathews, W. B., Sysa-Shah, P., Rodriguez, L. A., et al. (2017). Chemogenetics revealed: DREADD occupancy and activation *via* converted clozapine. *Science* 357, 503–507. doi: 10.1126/science.aan2475

Goossens, M., Boon, P., Wadman, W., Haute, C. V. den., Baekelandt, V., Verstraete, A. G., et al (2021). Long-term chemogenetic suppression of seizures

in a multifocal rat model of temporal lobe epilepsy. *Epilepsia* 62, 659–670. doi: 10.1111/epi.16840

Goutierre, M., Awabdh, S. A., Donneger, F., François, E., Gomez-Dominguez, D., Irinopoulou, T., et al. (2019). KCC2 regulates neuronal excitability and hippocampal activity *via* interaction with task-3 channels. *Cell Rep.* 28, 91–103.e7. doi: 10.1016/j.celrep.2019.06.001

Greenfield, L. J. (2013). Molecular mechanisms of antiseizure drug activity at GABAA receptors. *Seizure* 22, 589–600. doi: 10.1016/j.seizure.2013.04.015

Gunaydin, L. A., Yizhar, O., Berndt, A., Sohal, V. S., Deisseroth, K., and Hegemann, P. (2010). Ultrafast optogenetic control. *Nat. Neurosci.* 13, 387–392. doi: 10.1038/nn.2495

Hellman, K., Nielsen, P. A., Ek, F., and Olsson, R. (2016). An *ex vivo* model for evaluating blood-brain barrier permeability, efflux and drug metabolism. *Acs Chem. Neurosci.* 7, 668–680. doi: 10.1021/acschemneuro.6b00024

Herculano-Houzel, S. (2009). The human brain in numbers: a linearly scaled-up primate brain. *Front. Hum. Neurosci.* 3:31. doi: 10.3389/neuro.09.031.2009

Herman, J. P., Figueiredo, H., Mueller, N. K., Ulrich-Lai, Y., Ostrander, M. M., Choi, D. C., et al. (2003). Central mechanisms of stress integration: hierarchical circuitry controlling hypothalamo-pituitary-adrenocortical responsiveness. *Front. Neuroendocrinol.* 24, 151–180. doi: 10.1016/j.yfrne.2003.07.001

High, K. A., and Aubourg, P. (2011). rAAV human trial experience. *Methods Mol. Biol.* 807, 429–457. doi: 10.1007/978-1-61779-370-7_18

Hill, S. J. (2006). G-protein-coupled receptors: past, present and future. *Br. J. Pharmacol.* 147, S27–S37. doi: 10.1038/sj.bjp.0706455

Hocquemiller, M., Giersch, L., Audrain, M., Parker, S., and Cartier, N. (2016). Adeno-associated virus-based gene therapy for CNS diseases. *Hum. Gene Ther.* 27, 478–496. doi: 10.1089/hum.2016.087

Hollrigel, G. S., Chen, K., Baram, T. Z., and Soltesz, I. (1998). The pro-convulsant actions of corticotropin-releasing hormone in the hippocampus of infant rats. *Neuroscience* 84, 71–79. doi: 10.1016/s0306-4522(97)00499-5

Hooper, A., Paracha, R., and Maguire, J. (2018). Seizure-induced activation of the HPA axis increases seizure frequency and comorbid depression-like behaviors. *Epilepsy Behav.* 78, 124–133. doi: 10.1016/j.yebeh.2017.10.025

Hudry, E., and Vandenberghe, L. H. (2019). Therapeutic AAV gene transfer to the nervous system: a clinical reality. *Neuron* 101, 839–862. doi: 10.1016/j.neuron.2019.02.017

Jackson, K. L., Dayton, R. D., Deverman, B. E., and Klein, R. L. (2016). Better targeting, better efficiency for wide-scale neuronal transduction with the synapsin promoter and AAV-PHP.B. *Front. Mol. Neurosci.* 9:116. doi: 10.3389/fnmol.2016.00116

Jokeit, H., and Ebner, A. (2002). Effects of chronic epilepsy on intellectual functions. *Prog. Brain Res.* 135, 455–463. doi: 10.1016/S0079-6123(02)35042-8

Kahle, K. T., Khanna, A. R., Duan, J., Staley, K. J., Delpire, E., and Poduri, A. (2016). The KCC2 cotransporter and human epilepsy: getting excited about inhibition. *Neuroscientist* 22, 555–562. doi: 10.1177/1073858416645087

Kahn, J. B., Port, R. G., Yue, C., Takano, H., and Coulter, D. A. (2019). Circuit-based interventions in the dentate gyrus rescue epilepsy-associated cognitive dysfunction. *Brain* 142, 2705–2721. doi: 10.1093/brain/awz209

Kaila, K., Ruusuvuori, E., Seja, P., Voipio, J., and Puskarjov, M. (2014). GABA actions and ionic plasticity in epilepsy. *Curr. Opin. Neurobiol.* 26, 34–41. doi: 10.1016/j.conb.2013.11.004

Kalemenev, S. V., Zubareva, O. E., Frolova, E. V., Sizov, V. V., Lavrentyeva, V. V., Lukomskaya, N. Ya., et al. (2015). Impairment of exploratory behavior and spatial memory in adolescent rats in lithium-pilocarpine model of temporal lobe epilepsy. *Dokl. Biol. Sci.* 463, 175–177. doi: 10.1134/S0012496615040055

Kätzel, D., Nicholson, E., Schorge, S., Walker, M. C., and Kullmann, D. M. (2014). Chemical-genetic attenuation of focal neocortical seizures. *Nat. Commun.* 5:3847. doi: 10.1038/ncomms4847

Keith, D. J., and El-Husseini, A. (2008). Excitation control: balancing PSD-95 function at the synapse. *Front. Mol. Neurosci.* 1:4. doi: 10.3389/neuro.02.004.2008

Kim, J. A., and Connors, B. W. (2012). High temperatures alter physiological properties of pyramidal cells and inhibitory interneurons in hippocampus. *Front. Cell Neurosci.* 6:27. doi: 10.3389/fncel.2012.00027

Kossoff, E. H., Zupec-Kania, B. A., Auvin, S., Ballaban-Gil, K. R., Bergqvist, A. G. C., Blackford, R., et al. (2018). Optimal clinical management of children receiving dietary therapies for epilepsy: updated recommendations of the international ketogenic diet study group. *Epilepsia Open* 3, 175–192. doi: 10.1002/epi4.12225

Krook-Magnuson, E., Armstrong, C., Bui, A., Lew, S., Oijala, M., and Soltesz, I. (2015). *In vivo* evaluation of the dentate gate theory in epilepsy. *J. Physiol.* 593, 2379–2388. doi: 10.1113/JP270056

Krook-Magnuson, E., Armstrong, C., Oijala, M., and Soltesz, I. (2013). On-demand optogenetic control of spontaneous seizures in temporal lobe epilepsy. *Nat. Commun.* 4:1376. doi: 10.1038/ncomms2376

Kwan, P., and Brodie, M. J. (2000). Early identification of refractory epilepsy. *N. Engl. J. Med.* 342, 314–319. doi: 10.1056/NEJM200002033420503

Lechner, H. A. E., Lein, E. S., and Callaway, E. M. (2002). A genetic method for selective and quickly reversible silencing of mammalian neurons. *J. Neurosci.* 22, 5287–5290. doi: 10.1523/JNEUROSCI.22-13-05287.2002

Lerchner, W., Xiao, C., Nashmi, R., Slimko, E. M., Trigt, L. van., Lester, H. A., et al. (2007). Reversible silencing of neuronal excitability in behaving Mice by a genetically targeted, ivermectin-gated Cl^- channel. *Neuron* 54, 35–49. doi: 10.1016/j.neuron.2007.02.030

Lieb, A., Qiu, Y., Dixon, C. L., Heller, J. P., Walker, M. C., Schorge, S., et al. (2018). Biochemical autoregulatory gene therapy for focal epilepsy. *Nat. Med.* 24, 1324–1329. doi: 10.1038/s41591-018-0103-x

Lieb, A., Weston, M., and Kullmann, D. M. (2019). Designer receptor technology for the treatment of epilepsy. *Ebiomedicine* 43, 641–649. doi: 10.1016/j.ebiom.2019.04.059

Lignani, G., Baldelli, P., and Marra, V. (2020). Homeostatic plasticity in epilepsy. *Front. Cell Neurosci.* 14:197. doi: 10.3389/fncel.2020.00197

Löscher, W., and Schmidt, D. (2006). Experimental and clinical evidence for loss of effect (tolerance) during prolonged treatment with antiepileptic drugs. *Epilepsia* 47, 1253–1284. doi: 10.1111/j.1528-1167.2006.00607.x

Lothman, E. W., Bertram, E. H., and Stringer, J. L. (1991). Functional anatomy of hippocampal seizures. *Prog. Neurobiol.* 37, 1–82. doi: 10.1016/0301-0082(91)90011-o

Lowenstein, P. R. (2008). Clinical trials in gene therapy: ethics of informed consent and the future of experimental medicine. *Curr. Opin. Mol. Ther.* 10, 428–430.

Lybrand, Z. R., Goswami, S., Zhu, J., Jarzabek, V., Merlock, N., Aktar, M., et al. (2021). A critical period of neuronal activity results in aberrant neurogenesis rewiring hippocampal circuitry in a mouse model of epilepsy. *Nat. Commun.* 12:1423. doi: 10.1038/s41467-021-21649-8

MacLaren, D. A. A., Browne, R. W., Shaw, J. K., Radhakrishnan, S. K., Khare, P., España, R. A., et al. (2016). Clozapine N-oxide administration produces behavioral effects in long-evans rats: implications for designing DREADD experiments. *eNeuro* 3:ENEURO.0219-16.2016. doi: 10.1523/ENEURO.0219-16.2016

Magloire, V., Mercier, M. S., Kullmann, D. M., and Pavlov, I. (2019). GABAergic interneurons in seizures: investigating causality with optogenetics. *Neuroscientist* 25, 344–358. doi: 10.1177/1073858418805002

Maguire, J., and Salpekar, J. A. (2013). Stress, seizures and hypothalamic-pituitary-adrenal axis targets for the treatment of epilepsy. *Epilepsy Behav.* 26, 352–362. doi: 10.1016/j.yebeh.2012.09.040

Manvich, D. F., Webster, K. A., Foster, S. L., Farrell, M. S., Ritchie, J. C., Porter, J. H., et al. (2018). The DREADD agonist clozapine N-oxide (CNO) is reverse-metabolized to clozapine and produces clozapine-like interoceptive stimulus effects in rats and mice. *Sci. Rep.* 8:3840. doi: 10.1038/s41598-018-22116-z

Marafiga, J. R., Pasquetti, M. V., and Calcagnotto, M. E. (2020). GABAergic interneurons in epilepsy: more than a simple change in inhibition. *Epilepsy Behav.* 121:106935. doi: 10.1016/j.yebeh.2020.106935

McCormick, D. A., and Contreras, D. (2001). On the cellular and network bases of epileptic seizures. *Annu. Rev. Physiol.* 63, 815–846. doi: 10.1146/annurev.physiol.63.1.815

McCown, T. (2005). Adeno-associated virus (AAV) vectors in the CNS. *Curr. Gene Ther.* 5, 333–338. doi: 10.2174/1566523054064995

Morris, G. L., Gloss, D., Buchhalter, J., Mack, K. J., Nickels, K., and Harden, C. (2013). Evidence-based guideline update: vagus nerve stimulation for the treatment of epilepsy report of the guideline development subcommittee of the american academy of neurology. *Neurology* 81, 1453–1459. doi: 10.1212/WNL.0b013e3182a393d1

Mullen, S. A., Berkovic, S. F., and Commission, the I. G. (2018). Genetic generalized epilepsies. *Epilepsia* 59, 1148–1153. doi: 10.1111/epi.14042

Nagel, G., Ollig, D., Fuhrmann, M., Kateriya, S., Musti, A. M., Bamberg, E., et al. (2002). Channelrhodopsin-1: a light-gated proton channel in green algae. *Science* 296, 2395–2398. doi: 10.1126/science.1072068

Navidhamidi, M., Ghasemi, M., and Mehranfard, N. (2017). Epilepsy-associated alterations in hippocampal excitability. *Rev. Neurosci.* 28, 307–334. doi: 10.1515/revneuro-2016-0059

Nawaratne, V., Leach, K., Suratman, N., Loiacono, R. E., Felder, C. C., Armbruster, B. N., et al. (2008). New insights into the function of M4 muscarinic acetylcholine receptors gained using a novel allosteric modulator and a DREADD (designer receptor exclusively activated by a designer drug). *Mol. Pharmacol.* 74, 1119–1131. doi: 10.1124/mol.108.049353

Page, M. J., McKenzie, J. E., Bossuyt, P. M., Boutron, I., Hoffmann, T. C., Mulrow, C. D., et al. (2021). The PRISMA 2020 statement: an updated guideline for reporting systematic reviews. *BMJ* 372:n71. doi: 10.1136/bmj.n71

Panthi, S., and Leitch, B. (2019). The impact of silencing feed-forward parvalbumin-expressing inhibitory interneurons in the cortico-thalamocortical network on seizure generation and behaviour. *Neurobiol. Dis.* 132:104610. doi: 10.1016/j.nbd.2019.104610

Parent, J. M. (2007). Adult neurogenesis in the intact and epileptic dentate gyrus. *Prog. Brain Res.* 163, 529–540. doi: 10.1016/S0079-6123(07)63028-3

Park, K.-M., Kim, J.-E., Choi, I.-Y., and Cho, K.-O. (2020). Assessment of memory function in pilocarpine-induced epileptic mice. *J. Vis. Exp.* 160:e60751. doi: 10.3791/60751

Paz, J. T., Davidson, T. J., Frechette, E. S., Delord, B., Parada, I., Peng, K., et al. (2013). Closed-loop optogenetic control of thalamus as a tool for interrupting seizures after cortical injury. *Nat. Neurosci.* 16, 64–70. doi: 10.1038/nn.3269

Paz, J. T., and Huguenard, J. R. (2015). Microcircuits and their interactions in epilepsy: is the focus out of focus? *Nat. Neurosci.* 18, 351–359. doi: 10.1038/nn.3950

Pelkey, K. A., Chittajallu, R., Craig, M. T., Tricoire, L., Wester, J. C., and McBain, C. J. (2017). Hippocampal GABAergic inhibitory interneurons. *Physiol. Rev.* 97, 1619–1747. doi: 10.1152/physrev.00007.2017

Perucca, P., and Mula, M. (2013). Antiepileptic drug effects on mood and behavior: molecular targets. *Epilepsy Behav.* 26, 440–449. doi: 10.1016/j.yebeh.2012.09.018

Queenan, B. N., Dunn, R. L., Santos, V. R., Feng, Y., Huizenga, M. N., Hammack, R. J., et al. (2018). Kappa opioid receptors regulate hippocampal synaptic homeostasis and epileptogenesis. *Epilepsia* 59, 106–122. doi: 10.1111/epi.13941

Redfern, C. H., Coward, P., Degtyarev, M. Y., Lee, E. K., Kwa, A. T., Hennighausen, L., et al. (1999). Conditional expression and signaling of a specifically designed Gi-coupled receptor in transgenic mice. *Nat. Biotechnol.* 17, 165–169. doi: 10.1038/6165

Rijckevorsel, K. van. (2006). Cognitive problems related to epilepsy syndromes, especially malignant epilepsies. *Seizure* 15, 227–234. doi: 10.1016/j.seizure.2006.02.019

Robel, S., Buckingham, S. C., Boni, J. L., Campbell, S. L., Danbolt, N. C., Riedemann, T., et al. (2015). Reactive astrogliosis causes the development of spontaneous seizures. *J. Neurosci.* 35, 3330–3345. doi: 10.1523/JNEUROSCI.1574-14.2015

Roth, B. L. (2016). DREADDs for neuroscientists. *Neuron* 89, 683–694. doi: 10.1016/j.neuron.2016.01.040

Saetre, E., and Abdelnoor, M. (2018). Incidence rate of sudden death in epilepsy: a systematic review and meta-analysis. *Epilepsy Behav.* 86, 193–199. doi: 10.1016/j.yebeh.2018.06.037

Santhakumar, V., Aradi, I., and Soltesz, I. (2005). Role of mossy fiber sprouting and mossy cell loss in hyperexcitability: a network model of the dentate gyrus incorporating cell types and axonal topography. *J. Neurophysiol.* 93, 437–453. doi: 10.1152/jn.00777.2004

Scearce-Levie, K., Coward, P., Redfern, C. H., and Conklin, B. R. (2001). Engineering receptors activated solely by synthetic ligands (RASSLs). *Trends Pharmacol. Sci.* 22, 414–420. doi: 10.1016/s0165-6147(00)01743-0

Scharfman, H. E., and Myers, C. E. (2013). Hilar mossy cells of the dentate gyrus: a historical perspective. *Front. Neural Circuits* 6:106. doi: 10.3389/fncir.2012.00106

Sheng, J., Liu, S., Qin, H., Li, B., and Zhang, X. (2017). Drug-resistant epilepsy and surgery. *Curr. Neuropharmacol.* 16, 17–28. doi: 10.2174/1570159X15666170504123316

Smolensky, I. V., Zubareva, O. E., Kalemenev, S. V., Lavrentyeva, V. V., Dyomina, A. V., Karepanov, A. A., et al. (2019). Impairments in cognitive functions and emotional and social behaviors in a rat lithium-pilocarpine model of temporal lobe epilepsy. *Behav. Brain Res.* 372:112044. doi: 10.1016/j.bbr.2019.112044

Stachniak, T. J., Ghosh, A., and Sternson, S. M. (2014). Chemogenetic synaptic silencing of neural circuits localizes a hypothalamus→midbrain pathway for feeding behavior. *Neuron* 82, 797–808. doi: 10.1016/j.neuron.2014.04.008

Strien, N. M. van., Cappaert, N. L. M., and Witter, M. P. (2009). The anatomy of memory: an interactive overview of the parahippocampal-hippocampal network. *Nat. Rev. Neurosci.* 10, 272–282. doi: 10.1038/nrn2614

Stringer, J. L., and Lothman, E. W. (1992). Bilateral maximal dentate activation is critical for the appearance of an afterdischarge in the dentate gyrus. *Neuroscience* 46, 309–314. doi: 10.1016/0306-4522(92)90053-5

Sun, Q.-J., Duan, R.-S., Wang, A.-H., Shang, W., Zhang, T., Zhang, X.-Q., et al. (2009). Alterations of NR2B and PSD-95 expression in hippocampus of kainic acid-exposed rats with behavioural deficits. *Behav. Brain Res.* 201, 292–299. doi: 10.1016/j.bbr.2009.02.027

Sweatt, J. D. (2004). Hippocampal function in cognition. *Psychopharmacology (Berl)* 174, 99–110. doi: 10.1007/s00213-004-1795-9

Tung, J. K., Shiu, F. H., Ding, K., and Gross, R. E. (2018). Chemically activated luminopsins allow optogenetic inhibition of distributed nodes in an epileptic network for non-invasive and multi-site suppression of seizure activity. *Neurobiol. Dis.* 109, 1–10. doi: 10.1016/j.nbd.2017.09.007

Tzingounis, A. V., and Wadiche, J. I. (2007). Glutamate transporters: confining runaway excitation by shaping synaptic transmission. *Nat. Rev. Neurosci.* 8, 935–947. doi: 10.1038/nrn2274

Vargas-Sánchez, K., Mogilevskaya, M., Rodríguez-Pérez, J., Rubiano, M. G., Javela, J. J., and González-Reyes, R. E. (2018). Astroglial role in the pathophysiology of status epilepticus: an overview. *Oncotarget* 9, 26954–26976. doi: 10.1200/JCO.21.02678

Vuong, J., and Devergnas, A. (2018). The role of the basal ganglia in the control of seizure. *J. Neural Transm. (Vienna)* 125, 531–545. doi: 10.1007/s00702-017-1768-x

Wang, Y., Liang, J., Chen, L., Shen, Y., Zhao, J., Xu, C., et al. (2018). Pharmacogenetic therapeutics targeting parvalbumin neurons attenuate temporal lobe epilepsy. *Neurobiol. Dis.* 117, 149–160. doi: 10.1016/j.nbd.2018.06.006

Wang, D., Tai, P. W. L., and Gao, G. (2019). Adeno-associated virus vector as a platform for gene therapy delivery. *Nat. Rev. Drug Discov.* 18, 358–378. doi: 10.1038/s41573-019-0012-9

Wang, Y., Wang, Y., Xu, C., Wang, S., Tan, N., Chen, C., et al. (2020). Direct septum-hippocampus cholinergic circuit attenuates seizure through driving somatostatin inhibition. *Biol. Psychiatry* 87, 843–856. doi: 10.1016/j.biopsych.2019.11.014

Wang, Y., Xu, C., Xu, Z., Ji, C., Liang, J., Wang, Y., et al. (2017). Depolarized GABAergic signaling in subicular microcircuits mediates generalized seizure in temporal lobe epilepsy. *Neuron* 95, 92–105.e5. doi: 10.1016/j.neuron.2017.06.004

Watanabe, H., Sano, H., Chiken, S., Kobayashi, K., Fukata, Y., Fukata, M., et al. (2020). Forelimb movements evoked by optogenetic stimulation of the macaque motor cortex. *Nat. Commun.* 11:3253. doi: 10.1038/s41467-020-16883-5

Weinberg, M. S., Samulski, R. J., and McCown, T. J. (2013). Adeno-associated virus (AAV) gene therapy for neurological disease. *Neuropharmacology* 69, 82–88. doi: 10.1016/j.neuropharm.2012.03.004

Weston, M., Kaserer, T., Wu, A., Mouravlev, A., Carpenter, J. C., Snowball, A., et al. (2019). Olanzapine: a potent agonist at the hM4D(Gi) DREADD amenable to clinical translation of chemogenetics. *Sci. Adv.* 5:eaaw1567. doi: 10.1126/sciadv.aaw1567

Wicker, E., and Forcelli, P. A. (2016). Chemogenetic silencing of the midline and intralaminar thalamus blocks amygdala-kindled seizures. *Exp. Neurol.* 283, 404–412. doi: 10.1016/j.expneurol.2016.07.003

Witter, M. P. (2007). Intrinsic and extrinsic wiring of CA3: indications for connectional heterogeneity. *Learn Mem.* 14, 705–713. doi: 10.1101/lm.725207

Xu, C., Wang, Y., Zhang, S., Nao, J., Liu, Y., Wang, Y., et al. (2019). Subicular pyramidal neurons gate drug resistance in temporal lobe epilepsy. *Ann. Neurol.* 86, 626–640. doi: 10.1002/ana.25554

Yang, D., Zhou, Q., Labroska, V., Qin, S., Darbalaei, S., Wu, Y., et al. (2021). G protein-coupled receptors: structure- and function-based drug discovery. *Signal Transduct. Targeteted Ther.* 6:7. doi: 10.1038/s41392-020-00435-w

Yao, W.-D., Gainetdinov, R. R., Arbuckle, M. I., Sotnikova, T. D., Cyr, M., Beaulieu, J.-M., et al. (2004). Identification of PSD-95 as a regulator of dopamine-mediated synaptic and behavioral plasticity. *Neuron* 41, 625–638. doi: 10.1016/s0896-6273(04)00048-0

Yizhar, O., Fenno, L. E., Davidson, T. J., Mogri, M., and Deisseroth, K. (2011). Optogenetics in neural systems. *Neuron* 71, 9–34. doi: 10.1016/j.neuron.2011.06.004

Yu, S. S., Lefkowitz, R. J., and Hausdorff, W. P. (1993). Beta-adrenergic receptor sequestration. A potential mechanism of receptor resensitization. *J. Biol. Chem.* 268, 337–341. doi: 10.1016/S0021-9258(18)54155-7

Yu, Y., Nguyen, D. T., and Jiang, J. (2019). G protein-coupled receptors in acquired epilepsy: druggability and translatability. *Prog. Neurobiol.* 183:101682. doi: 10.1016/j.pneurobio.2019.101682

Zhou, Q.-G., Nemes, A. D., Lee, D., Ro, E. J., Zhang, J., Nowacki, A. S., et al. (2019). Chemogenetic silencing of hippocampal neurons suppresses epileptic neural circuits. *J. Clin. Invest.* 129, 310–323. doi: 10.1172/JCI95731

Conflict of Interest: The authors declare that the research was conducted in the absence of any commercial or financial relationships that could be construed as a potential conflict of interest.

Publisher's Note: All claims expressed in this article are solely those of the authors and do not necessarily represent those of their affiliated organizations, or those of the publisher, the editors and the reviewers. Any product that may be evaluated in this article, or claim that may be made by its manufacturer, is not guaranteed or endorsed by the publisher.

frontiers | Frontiers in Molecular Neuroscience

ORIGINAL RESEARCH
published: 09 May 2022
doi: 10.3389/fnmol.2022.870947

Anticonvulsant Effect of Carbenoxolone on Chronic Epileptic Rats and Its Mechanism Related to Connexin and High-Frequency Oscillations

*Benke Liu[1,2,3], Xiao Ran[1,2], Yanjun Yi[1,2], Xinyu Zhang[1,2], Hengsheng Chen[1,2] and Yue Hu[1,2]**

[1] Department of Neurology, Children's Hospital of Chongqing Medical University, Chongqing, China, [2] Ministry of Education Key Laboratory of Child Development and Disorders, Chongqing Key Laboratory of Pediatrics, National Clinical Research Center for Child Health and Disorders, China International Science and Technology Cooperation Base of Child Development and Critical Disorders, Chongqing, China, [3] Shenzhen Baoan Women's and Children's Hospital, Jinan University, Shenzhen, China

OPEN ACCESS

Edited by:
Hermona Soreq,
Hebrew University of Jerusalem, Israel

Reviewed by:
Gürsel Caliskan,
Otto von Guericke University Magdeburg, Germany
Edward Haig Beamer,
Nottingham Trent University, United Kingdom

***Correspondence:**
Yue Hu
huyue915@163.com

Specialty section:
This article was submitted to Brain Disease Mechanisms, a section of the journal Frontiers in Molecular Neuroscience

Received: *07 February 2022*
Accepted: *04 April 2022*
Published: *09 May 2022*

Citation:
Liu B, Ran X, Yi Y, Zhang X, Chen H and Hu Y (2022) Anticonvulsant Effect of Carbenoxolone on Chronic Epileptic Rats and Its Mechanism Related to Connexin and High-Frequency Oscillations. Front. Mol. Neurosci. 15:870947. doi: 10.3389/fnmol.2022.870947

Objective: This study was designed to investigate the influence and mechanism of gap junction carbenoxolone (CBX) on dynamic changes in the spectral power of ripples and fast ripples (FRs) in the hippocampus of chronic epileptic rats.

Methods: The lithium-pilocarpine (PILO) status epilepticus (SE) model (PILO group) and the CBX pretreatment model (CBX + PILO group) were established to analyze dynamic changes in the spectral power of ripples and FRs, and the dynamic expression of connexin (CX)26, CX32, CX36, and CX43 in the hippocampus of chronic epileptic rats.

Results: Within 28 days after SE, the number of spontaneous recurrent seizures (SRSs) in the PILO group was significantly higher than that in the CBX + PILO group. The average spectral power of FRs in the PILO group was significantly higher than the baseline level at 1 and 7 days after SE. The average spectral power of FRs in the PILO group was significantly higher than that in the CBX + PILO group at 1, 7, and 14 days after SE. Seizures induced an increase in CX43 expression at 1 and 7 days after SE, but had no significant effect on CX26, CX36, or CX32. CBX pretreatment did not affect the expression of CXs in the hippocampus of normal rats, but it inhibited the expression of CX43 in epileptic rats. The number of SRSs at 2 and 4 weeks after SE had the highest correlation with the average spectral power of FRs; the average spectral power of FRs was moderately correlated with the expression of CX43.

Conclusion: The results of this study indicate that the energy of FRs may be regulated by its interference with the expression of CX43, and thus, affect seizures. Blocking the expression of CX43 thereby reduces the formation of pathological high-frequency oscillations (HFOs), making it a promising strategy for the treatment of chronic epilepsy.

Keywords: carbenoxolone, chronic epilepsy, connexin, ripples, fast ripples

INTRODUCTION

There are extensive high-frequency oscillations (HFOs) in neural networks. The term HFOs refers to electroencephalogram (EEG) activity with a frequency of 40–500 Hz, including γ oscillation (40–80 Hz), ripple oscillation (80–200 Hz), and fast ripple oscillation (250–500 Hz) (Höller et al., 2019). HFOs can be divided into physiological and pathological, which differ in their frequency, location and mechanisms (Le Van Quyen et al., 2006). Physiological HFOs gradually mature with brain development. Ripples (>140 Hz) are observed in the hippocampus of rats during their second week after birth. A vitro hippocampal model has confirmed that physiological HFOs can be controlled by a feedback circuit between GABAergic interneurons and pyramidal cells (Hájos and Paulsen, 2009). In physiological states, HFOs are associated with sensory information processing and hippocampal memory function (Höller et al., 2019); whereas, in pathological states, HFOs are closely related to epilepsy (Frauscher et al., 2017; Velmurugan et al., 2019; Tingley and Buzsáki, 2020).

Our previous study showed that the energy of HFOs in hippocampal regions CA1 and CA3 of the lithium-pilocarpine (PILO) status epilepticus (SE) model was significantly higher than that of physiological HFOs (Song et al., 2016). The spectral power of fast ripples (FRs) during seizures can be used as a quantitative indicator providing an early warning of seizures (Song et al., 2016).

The generation mechanism of HFOs is not completely clear; HFOs may be caused by a variety of mechanisms rather than a single mechanism of neural cells and networks. At present, it is believed that pathological HFOs, whether ripples or FRs, mainly reflect the action potential of principal cells. It may be related to the gap junction (GJ) network (Jiruska et al., 2017). Gap junctions are intercellular channels composed of special transmembrane proteins. These transmembrane protein families are called connexins (CXs) (Beyer and Berthoud, 2018). At present, more than 20 kinds of CXs have been found, and CX26 is expressed in a variety of nerve cells, especially neurons (Su et al., 2017); CX32 is widespread on oligodendrocytes (Men et al., 2019). CX36 is a connexin preferentially expressed by neurons, and it plays an important role in the transmission of electrical signals (Li et al., 2019). CX43 has the highest expression in astrocytes and it may be involved in the regulation of nerve injury, as well as epileptogenesis (Deshpande et al., 2017). The increase in electrical coupling between GJs transforms physiological HFOs into pathological HFOs (Stacey et al., 2011), which induce synaptic plasticity (Jefferys et al., 2012). Our previous study confirmed that in an acute epilepsy rat model, the spectral power of FRs and the degree of seizures can be downregulated by inhibiting the expression of different CXs (Ran et al., 2018).

It is not known whether connexins participate in the occurrence of pathological HFOs, thereby establishing abnormal electrosynaptic transmission and increasing susceptibility to seizure in the chronic phase of epilepsy. Therefore, we established an chronic epilepsy rat model to observe dynamic changes in the energy of HFOs and the expression of CXs in the hippocampus, to explore the role of GJ receptor blockers in the chronic phase of epilepsy, and to clarify whether GJ plays a key role in the occurrence and development of epilepsy, in order to provide a theoretical basis for the selection of new targets for antiepileptic therapy.

MATERIALS AND METHODS

The overall protocol and time-course of the evaluation of various outcomes are shown in **Figure 1A**.

Establishment of the Epilepsy Model and Electroencephalogram Recordings

This study was approved by the Ethics Committee of Chongqing Medical University. The ethical approval number is 2020135. Adult male Sprague–Dawley rats weighing 180–220 g were obtained from the Animal Research Institute of Chongqing Medical University. Before surgery, all the rats were intraperitoneally (IP) injected with penicillin (1 ml/kg, 160,000 U/ml) to prevent intracranial infection. The rats were then anesthetized with 10% chloral hydrate (2 ml/kg, IP) and immobilized in a stereotaxic frame (Shenzhen Reward Life Science Company, Shenzhen, China) to surgically implant the microelectrode (nichrome wires, 0.1 mm in diameter). The recording electrode was implanted as follows: CA1-AP: 3.3–3.7 mm from bregma; ML: 2.0–3.0 mm and DV: 3.0–3.5 mm from the surface of the neocortex; and CA3–AP: 3.3 mm, ML: 3.5–3.7 mm, DV: 3.0–3.5 mm; DG–AP: 5.6 mm, ML: 4.0 mm and DV: 6.0 mm. The reference electrode was implanted on the surface of the neocortex of the bilateral parietal lobe (AP: 7.0 mm; ML: 6.0 mm), and the left forehead was used as the ground (AP: 2.0 mm; ML: 2.0 mm) (Song et al., 2016; Ran et al., 2018). The positions of these electrodes are shown in **Figure 1B** (Bao and Shu, 1991; Zhuge, 2005). Dental cement (Shanghai Medical Equipment Limited by Share Ltd., Shanghai, China) was used to fasten the microelectrode to the skull. After surgery, the rats were housed individually in cages under standard conditions, in a controlled environment (23 ± 2°C, 50–55%) under a 12 h:12 h light/dark cycle (lights on at 08:00 h), and *ad libitum* access to food and water.

Normal intracranial EEG signals (EEG 1200 systems, 32 channels, Nihon Kohden Corporation, Tokyo, Japan) were recorded on the 3rd day after surgery for 5 days (5–8 h/day), and the lithium-pilocarpine SE model was established on the 9th post-operative day (Ran et al., 2018). The rats were injected with pilocarpine (50 mg/kg IP, Sigma, Canada) 18–20 h after an injection of lithium chloride (127 mg/kg IP, Sigma, Canada). If generalized seizures (stage 4 of Racine's criteria) were not elicited within 30 min, a second injection of pilocarpine (10 mg/kg, IP) was administered. SE was defined as the presence of continuous generalized seizures for at least 60 min without returning to normal behavior between seizures. Atropine sulfate (1 mg/kg IP, Shanghai and Feng pharmaceutical companies, Shanghai, China) was injected to limit peripheral cholinergic effects 10 min after the injection of pilocarpine. SE was arrested using diazepam (10 mg/kg IP, Shanghai Asahi Dongpu Pharmaceutical Co. Ltd., Shanghai, China) (Song et al., 2016; Ran et al., 2018). After

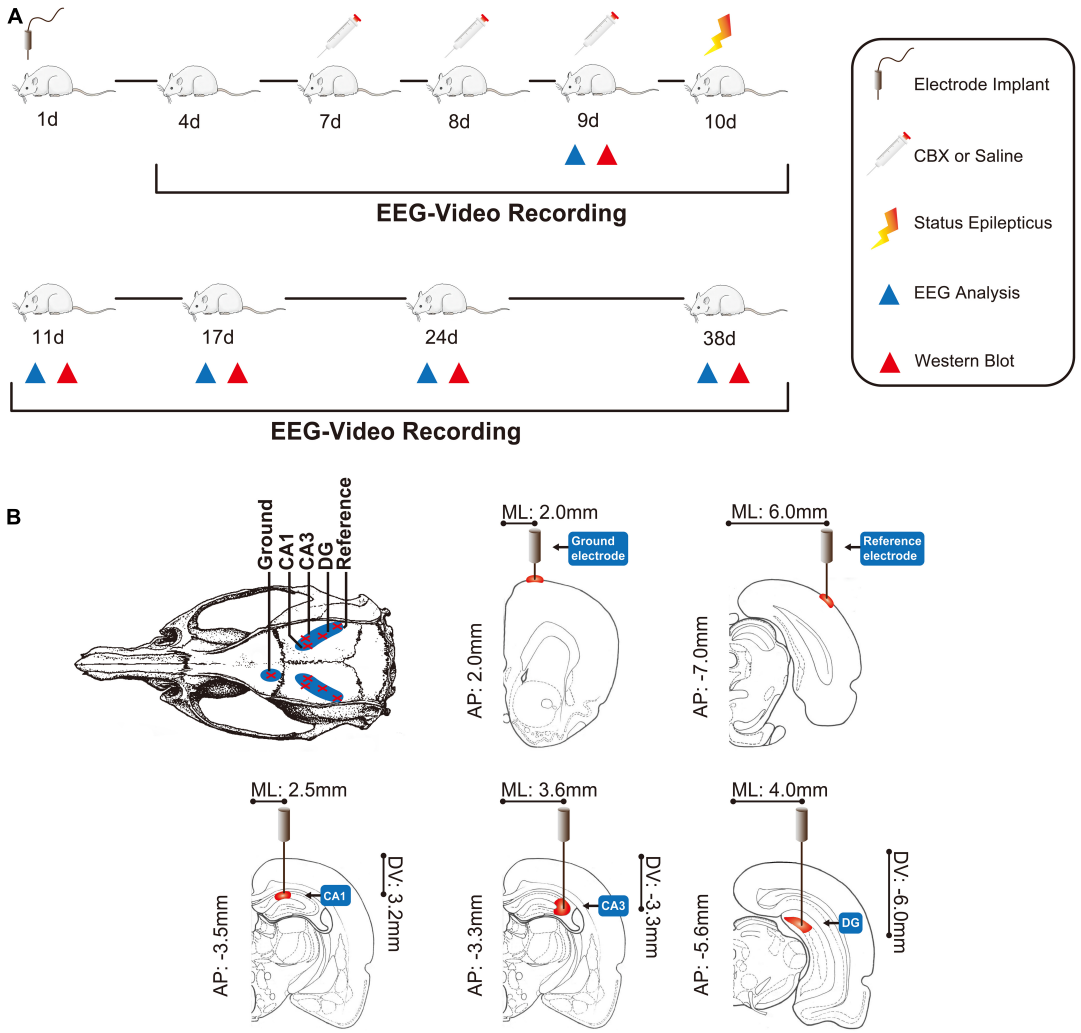

FIGURE 1 | Comprehensive modeling of chronic epilepsy. **(A)** Schematic representation of the overall protocol and various analyses performed in chronic epileptic rats. **(B)** The positions of the EEG recording electrodes. CBX, carbenoxolone; AP, anteroposterior; ML, mediolateral; DV, dorsoventral.

successful modeling, the rats were injected intraperitoneally with glucose saline (2 ml/day for 3 days: 1 ml 10% glucose + 1 ml 0.9% sterile saline) to reduce mortality after SE. At 24 h after SE, EEG signals were recorded for 28 consecutive days. The sampling frequency was 1 kHz, high pass 0.16 Hz, and low pass 500 Hz. Rat seizures were monitored and the number of spontaneous recurrent seizures (SRSs) was recorded.

Forty rats were randomly divided into the lithium-pilocarpine status epileptic model (PILO group) and the carbenoxolone (CBX) pretreatment model (CBX + PILO group), with 20 rats in each group. The PILO group was pretreated with saline [8 ml/kg dose for 3 consecutive days (8:00 am and 8:00 pm) by intraperitoneal injection] before the PILO injection, the CBX + PILO group was injected with CBX [50 mg/kg dose for 3 consecutive days (8:00 am and 8:00 pm) by intraperitoneal injection] before the PILO injection. Of these, 14 rats in the PILO group and 13 rats in the CBX + PILO group were successfully modeled. Due to factors, such as shedding of implanted electrodes and the death of rats, the EEG signals with SRSs of 11 rats in the PILO group and 9 rats in the CBX + PILO group were recorded over 28 consecutive days. One experimenter randomly coded the two groups of rats, and the other experimenter selected 8 rats in each group as the research subjects, using a random coding lottery.

Electroencephalogram Analysis

We selected 10-min samples of the electrical activity of EEG signals for quantitative analysis at 5 time points (1 day before SE, and 1, 7, 14, and 28 days after SE). Quantitative analysis was conducted on the HFOs for the 10 min EEG signals collected at each of the above time points. In this study, the Morlet wavelet algorithm was used to extract ripples and FRs signals, including average and peak spectral power analysis (Song et al., 2016; Ran et al., 2018). The average spectral power of ripples and FRs refers to the average of all spectral power in the entire observation time window; the peak spectral power of ripples and

FRs refers to the spectral power at a certain time point in the entire observation time window, which is the highest spectral power of the observation time window (Song et al., 2016; Ran et al., 2018). The leads where changes in the spectral power of ripples and the FRs were the most significant were defined as responsibility leads (RLs) (Song et al., 2016; Ran et al., 2018).

Western Blot

The rats were sacrificed at 5 time points (1 day before SE, and 1, 7, 14, and 28 days after SE). Western blot was used for the semi-quantitative analysis of CX26 (Sigma-Aldrich, United States; diluted 1:400 dilution), CX32 (Sigma-Aldrich, United States; 1:400), CX36 (Sigma-Aldrich, United States; 1:600), and CX43 (Sigma-Aldrich, United States; 1:8000) expression in the hippocampus. Immunoreactive bands were visualized by the ECL Advance Western blot reagent (Bio-Rad, United States). The optical densities of the immunoreactive bands were quantified by densitometry using Labworks 4.6 software (EC3 Imaging System, UVP Inc., United States). The relative levels of the CX26, CX32, CX36, and CX43 were expressed as ratios (CX26/β-actin, CX32/β-actin, CX36/β-actin, and CX43/β-actin).

Statistical Analysis

SPSS version 23.0 was used for the statistical analysis. Quantitative data are expressed as mean ± SD. A two-way repeated-measures ANOVA was used for the statistical analysis of HFOs' spectral power and connexin expression between the groups, and *t*-tests were used for pairwise comparisons. Pearson's correlations were used to analyze other quantitative data. A bad value refers to a maximum or minimum value that does not conform to the normal distribution. A $p < 0.05$ was considered to be a statistically significant difference.

RESULTS

Behavioral Study

We did not observe any abnormal behaviors during the 18–24 h after lithium chloride injection. All the rats exhibited peripheral cholinergic effects after the pilocarpine injection, including pupil narrowing, piloerection, hemolacria, diarrhea, and wet-dog shakes. Seizures in all the rats were classified as stages IV and V, and all the rats exhibited SE; the peripheral cholinergic effects gradually disappeared after atropine injection. After diazepam injection, the seizures stopped.

After a latent phase lasting approximately 2–10 days (6.25 ± 2.55 days), during which no organized activity was recorded, spontaneous grade I-V SRSs reappeared in the rats in the PILO group, showing no statistical difference from rats in the CBX + PILO group [4–16 days (9.38 ± 4.03 days), $t(14) = 1.852$, $p = 0.085$] (**Figure 2A**). However, the probability of a seizure in the CBX + PILO group was lower than that in the PILO group (**Figure 2B**). Within 4 weeks, the average number of SRSs in the PILO group was significantly higher than that in the CBX + PILO group [58.88 ± 14.32 vs. 43.75 ± 10.39, $t(14) = 2.418$, $p = 0.03$] (**Figure 2C**). The number of SRSs per week after SE in the two groups are shown in **Figure 2D**.

The relationship between the number of SRSs at 2 and 4 weeks after SE and the spectral power of ripples/FRs in the PILO and CBX + PILO groups are shown in **Figures 2E,F**; the bubbles of the two groups that are gathered in **Figure 2E** are separated in **Figure 2F**. The number of SRSs at 2 and 4 weeks after SE had the highest correlation with the average spectral power of FRs ($r = 0.38$, $p = 0.035$). Then, the correlations decreased with the peak spectral power of FRs ($r = 0.23$, $p = 0.213$), the peak spectral power of ripples ($r = 0.11$, $p = 0.593$), and the average spectral power of ripples ($r = 0.10$, $p = 0.621$) (**Figure 2G**).

Quantitative Analysis of High-Frequency Oscillations

Before modeling, ripples and FRs were observed in hippocampal regions CA1, CA3, and DG in normal rats. The most significant dynamic changes in the energy of HFOs were noted in the CA1 and CA3 regions ($n = 6$) and the DG region ($n = 2$) in the PILO group, and the CA1 and CA3 regions ($n = 8$) in the CBX + PILO group. Waveforms and spectrograms showing the spectral and temporal characteristics of lithium-pilocarpine-induced electrographic seizures are shown in **Figure 3**. Further statistical analyses of the average and peak spectral power of ripples and FRs are shown in **Tables 1**, **2**.

There was no significant difference in the average spectral power of ripples in the PILO and CBX + PILO groups before and after SE, nor was there a significant difference in the average spectral power of ripples between the two groups at any time point ($p > 0.05$) (**Table 1**).

The average spectral power of FRs in the PILO group at 1 and 7 days after SE was significantly higher than that at baseline [$F(4,35) = 23.27$, $p < 0.05$], peaking 1 day after SE, then gradually decreasing to baseline until 28 days after SE. There was no significant difference in the average spectral power of FRS in the CBX + PILO group before and after SE ($p > 0.05$) (**Table 2**). The average spectral power of FRs in the PILO group was significantly higher than that in the CBX + PILO group at 1, 7, and 14 days after SE [$F(4,69) = 16.31$, $p < 0.05$] (**Table 2**).

The dynamic changes in the average and peak spectral power of ripples and FRs were similar (**Tables 1**, **2**).

Expression of Connexins

There was no significant difference in the expression of CX26 in the PILO and CBX + PILO groups before and after SE, nor was there a significant difference in the expression of CX26 between the two groups at any time point (**Figure 4A**).

There was no significant difference in the expression of CX32 and CX36 before and after SE in the PILO and CBX + PILO groups, but the expression of CX32 [$t(14) = 2.614$, $p = 0.02$] and CX36 [$t(14) = 3.075$, $p < 0.05$] in the PILO group was significantly higher than that in the CBX + PILO group 1 day after SE (**Figures 4B,C**).

Compared to the expression of CX43 before SE in the PILO group, CX43 expression increased significantly at 1 and 7 days after SE [$F(4,35) = 3.63$, $p < 0.05$], and then returned to baseline. There was no significant difference in the expression of CX43 in the CBX + PILO group before and after SE. The expression of

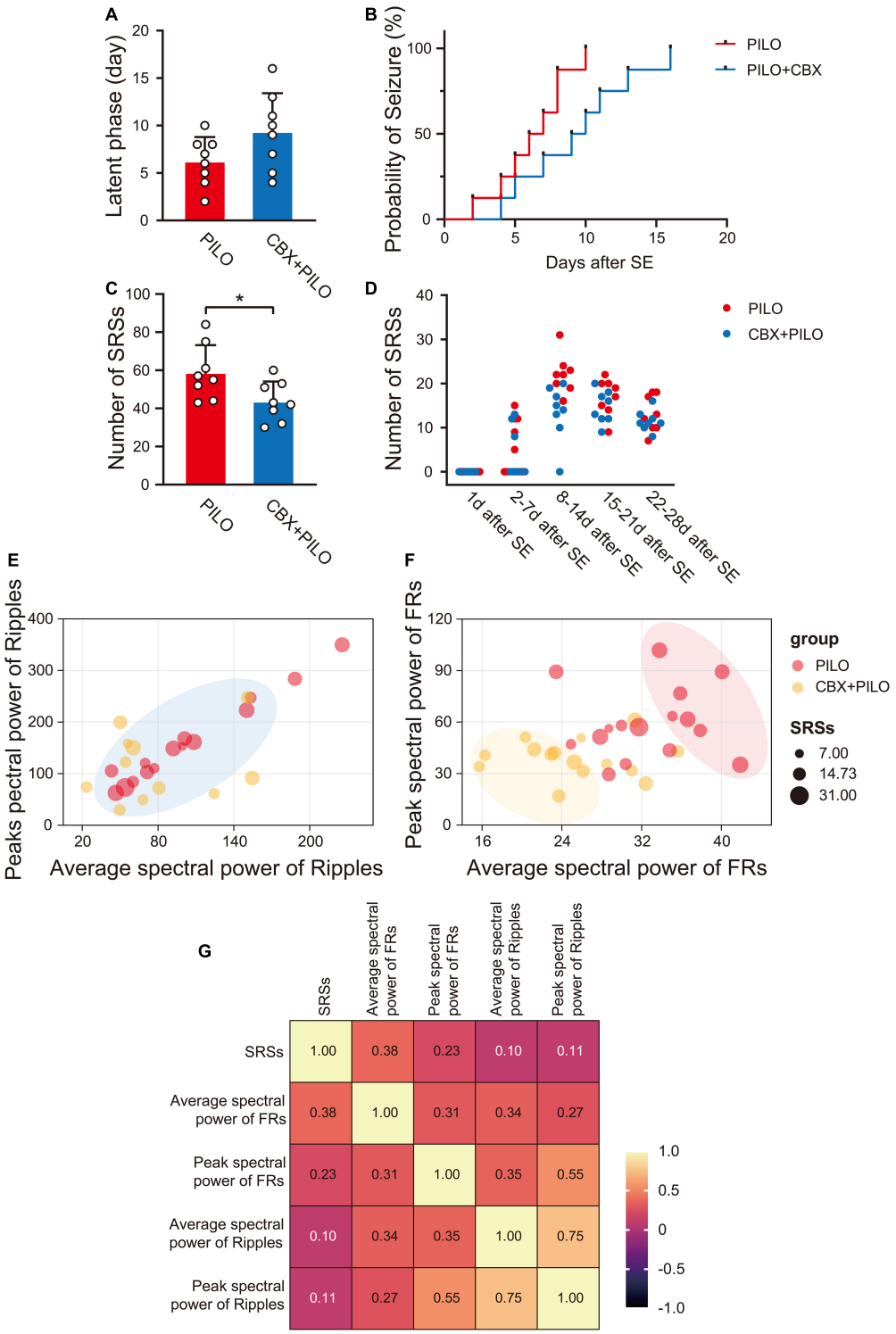

FIGURE 2 | Lithium-pilocarpine produced chronic SRSs in rats. **(A)** Average latent phase in PILO and CBX + PILO groups. **(B)** Incidence curve of epileptic rats over time, showing latent phase to first seizure after SE. **(C)** Average number of SRSs in PILO and CBX + PILO groups during the 4 weeks after SE. **(D)** The number of SRSs per week after SE in PILO and CBX + PILO groups. **(E,F)** Bubble diagram of the relationship between the number of SRSs and the spectral power of ripples/FRs at 2 and 4 weeks after SE in PILO and CBX + PILO groups, the gathered bubbles of the two groups means weak correlation, and the separated bubbles of the two groups means strong correlation. **(G)** The correlation coefficient matrix of the number of SRSs and the spectral power of HFOs at 2 and 4 weeks after SE (average spectral power of FRs, $r = 0.38$; peak spectral power of FRs, $r = 0.23$; peak spectral power of ripples, $r = 0.11$; average spectral power of ripples, $r = 0.10$). *$P < 0.05$; SRSs, spontaneous recurrent seizures; PILO, pilocarpine; SE, status epilepticus; FRs, fast ripples; HFOs, high-frequency oscillations.

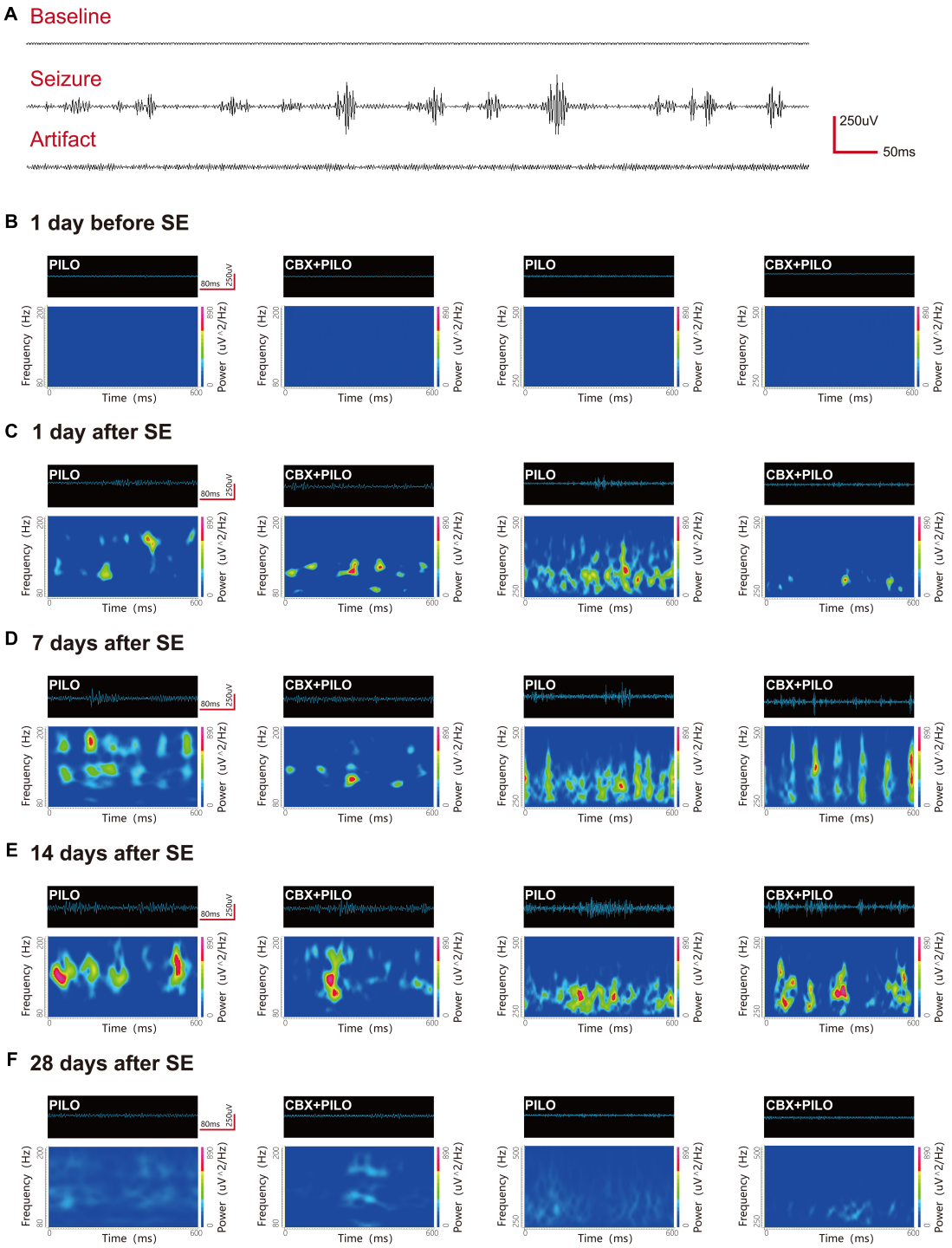

FIGURE 3 | Waveforms and spectrograms features of lithium-pilocarpine-induced electrographic seizures. **(A)** Representative EEG traces of the baseline, epileptic seizure, and an artifact. **(B–F)** Waveforms and spectrograms showing the spectral and temporal characteristics of ripples (80–200 Hz) and FRs (250–500 Hz) in the PILO and CBX + PILO groups at 5 time points [1 day before SE, and 1, 7, 14, and 28 days after SE]. The waveforms were filtered with a band pass filter of 80–200 Hz and 250–500 Hz. The spectrograms reflect the accumulated time-frequency representations of the corresponding waveforms. The data demonstrate that the initiation of seizures was associated with an increase of HFOs energy, and that pretreatment with CBX could reduce HFOs energy and the degree of seizures. The HFOs are characterized by rhythmic bursts, which are significantly different from systematic artifacts, such as power line noise and its harmonics.

TABLE 1 | Dynamic changes in the average and peak spectral power of ripples recorded in RLs in the PILO and CBX + PILO groups at different time points after SE (n = 8).

Time points	Average spectral power of ripples		Peak spectral power of ripples	
	PILO	CBX + PILO	PILO	CBX + PILO
1 day before SE	97.75 ± 39.83*	86.99 ± 27.98#	139.73 ± 62.89#	121.37 ± 37.28*
1 day after SE	108.06 ± 41.1	79.14 ± 54.16*	195.2 ± 69.96*	107.62 ± 55.37a,#
7 days after SE	112.23 ± 66.33	71.16 ± 32.95	206.14 ± 129.92	98.51 ± 58.74
14 days after SE	102.53 ± 61.59	75.66 ± 49.9#	161.56 ± 92.73	116.69 ± 77.09
28 days after SE	94.85 ± 50.5	76.03 ± 40.89#	157.44 ± 77.47*	105.61 ± 41.4#
F	0.141	0.128	0.636	0.189
P	0.965	0.971	0.641	0.942

a$p < 0.05$ *compared to the PILO group at the same time.*
**Eliminated a bad value at this time point.*
#*Eliminated two bad values at this time point.*
RLs, responsibility leads; PILO, pilocarpine; CBX, carbenoxolone; SE, status epilepticus.

TABLE 2 | Dynamic changes in the average and peak spectral power of FRs recorded in RLs in the PILO and CBX + PILO groups at different time points after SE (n = 8).

Time points	Average spectral power of FRs		Peak spectral power of FRs	
	PILO	CBX + PILO	PILO	CBX + PILO
1 day before SE	29.64 ± 6.75	32.19 ± 9.14	55.81 ± 16.67	58.08 ± 26.48
1 day after SE	52.19 ± 9.19b	24.74 ± 4.36a	93.15 ± 44.93b	45.43 ± 20.85a,*
7 days after SE	51.93 ± 5.99b	25.27 ± 6.05a,*	90.44 ± 20.28*	40.1 ± 24.12a
14 days after SE	34.15 ± 6.27	25.85 ± 4.02a	67.6 ± 23.1	38.4 ± 10.59a
28 days after SE	31.05 ± 3.85	25.4 ± 7.31	51.26 ± 15.43	37.24 ± 13.25
F	23.27	1.309	4.127	1.461
P	<0.001	0.286	<0.05	0.236

a$p < 0.05$ *compared to PILO group at the same time.*
b$p < 0.05$ *compared to 1 day before SE in the same group.*
**Eliminated a bad value at this time point.*
#*Eliminated two bad values at this time point.*
FRs, fast ripples; RLs, responsibility leads; PILO, pilocarpine; CBX, carbenoxolone; SE, status epilepticus.

CX43 in the PILO group at 1 and 7 days after SE was significantly higher than that in the CBX + PILO group [$F(4,70) = 5.83$, $p < 0.05$] (**Figure 4D**). The dynamic expression of four kinds of CXs in the hippocampus of chronic epileptic rats are shown in **Figure 4E**.

Correlation Analysis of High-Frequency Oscillations and Connexins

There was no significant correlation between the average spectral power of ripples and the expression of CX26, CX32, CX36, or CX43 ($p > 0.05$) (**Figures 5A–D**). There was no significant correlation between the average spectral power of FRs and the expression of CX26 or CX32 ($p > 0.05$) (**Figures 5E,F**). The average spectral power of FRs was weakly correlated with CX36 expression ($r = 0.37$, $p < 0.05$; **Figure 5G**), and moderately correlated with CX43 expression ($r = 0.42$, $p < 0.05$; **Figure 5H**).

DISCUSSION

Pilocarpine is a post-ganglionic cholinergic drug, which can directly stimulate M-cholinergic receptors to produce a cholinergic effect, thereby inducing seizures by activating central cholinergic receptors. The adult rat lithium-pilocarpine epilepsy model exhibits three periods: an acute phase–6–24 h after SE; a latent phase–no organized activity and EEG for at least 1 day; and a chronic phase–the appearance of SRSs. SRSs are important clinical manifestations of epilepsy. In the rat model of epilepsy, which is created using lithium-pilocarpine, SRSs appear after SE. The damage and manifestations of this model are similar to human temporal lobe epilepsy, and this model is one of the most commonly used experimental epilepsy models (Song et al., 2016). In this study, SRSs occurred within 16 days after SE, indicating entry into the chronic phase of epilepsy in the experimental rats.

Enhanced intercellular GJ communication may be involved in epileptic production (Mylvaganam et al., 2014). CBX is a glycyrrhizonic acid derivative that reduces plasma membrane mobility and inhibits gap junction conductance through multiple pathways, including protein kinase, G protein, transport ATP enzyme, and CX phosphorylation (Walrave et al., 2020). It is a broad-spectrum GJ blocker that acts on a variety of CXs. Whether in cell culture *in vitro*, acute brain slices, or *in vivo* animal experiments, CBX has been proven to block GJ quickly and reversibly, thus, further reducing the number of spontaneous/induced seizures, and reducing the duration, frequency, and amplitude of epileptic discharges (Vincze et al., 2019; Walrave et al., 2020). CBX can reduce the

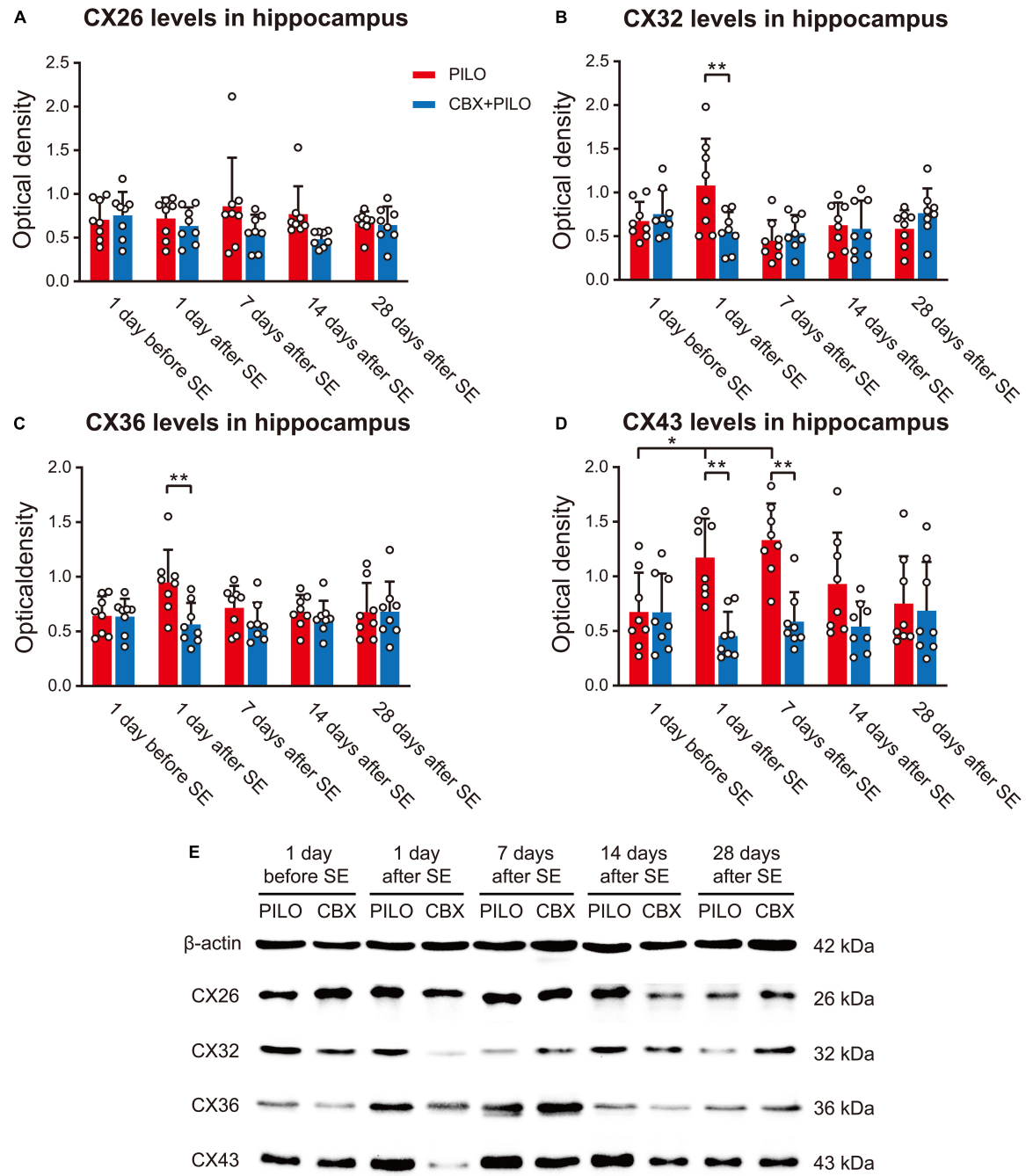

FIGURE 4 | Expression of four kinds of CXs. **(A–D)** Western blot showing the expression of CX26, CX32, CX36, and CX43 in the hippocampus before and after SE in the PILO and CBX + PILO groups. **(E)** β-actin is used as a loading control. Each bar represents the mean ± SD of eight separate assays. *$P < 0.05$, **$P < 0.01$; CX, connexin.

frequency of spontaneous HFOs activity (Naggar et al., 2020). This study confirmed that CBX can reduce the number of SRSs and the average spectral power of FRs in rats, with an antiepileptic effect.

High-frequency oscillations in the human brain are affected by sleep. Studies show that the rate of HFOs is highest during non-rapid eye movement (NREM) sleep and lowest during rapid eye movement (REM) sleep and the waking stage; the area of HFOs during NREM sleep is larger (von Ellenrieder et al., 2017). Our previous study showed that physiological and pathological HFOs have similar sleep balance characteristics (Yan et al., 2021). At present, the correlation between HFOs and sleep in the animal brain is not clear. Therefore, in our study, we selected 10-min samples of EEG signals during the interictal period (waking stage)

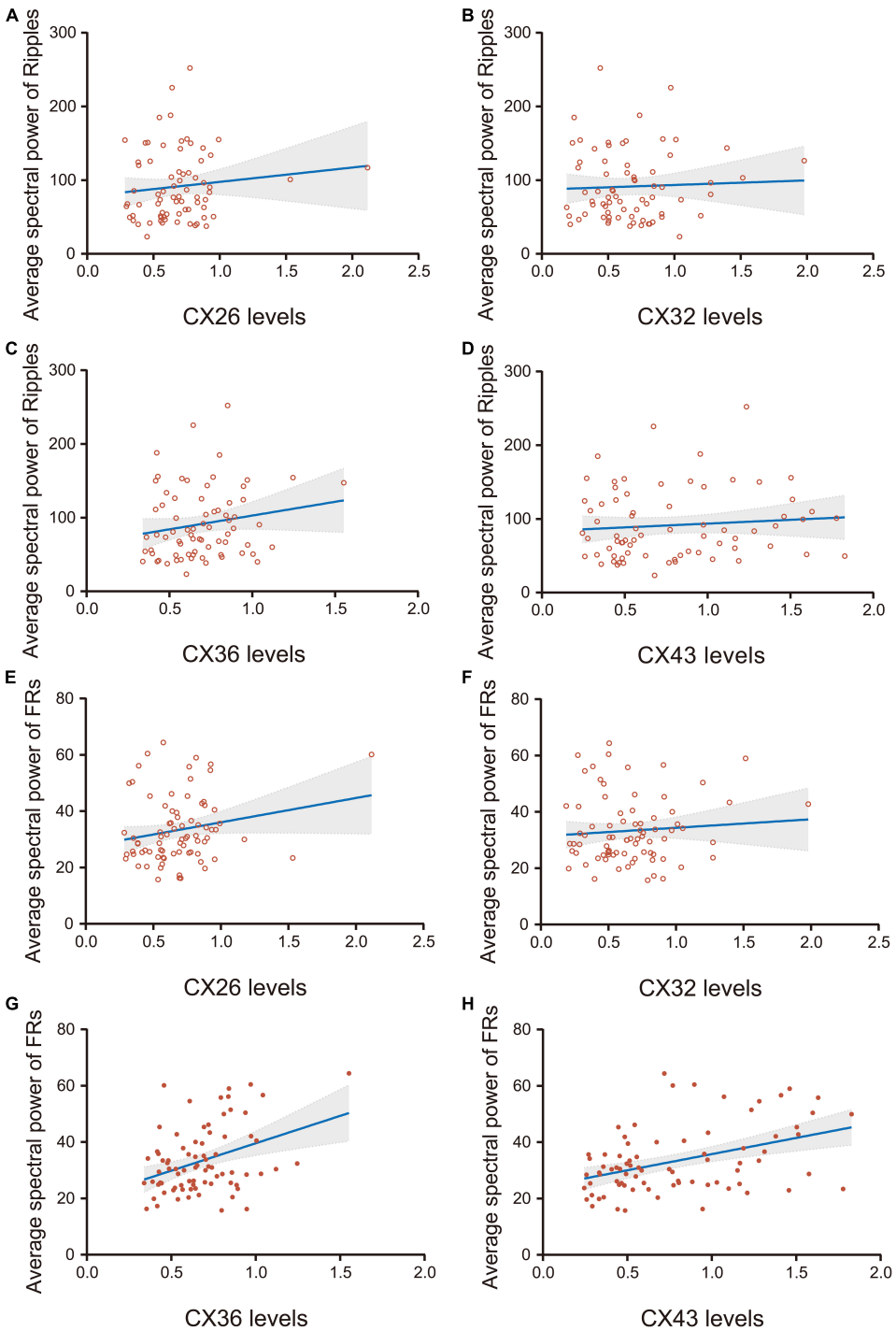

FIGURE 5 | Correlation analysis of the average spectral power of HFOs and the expression of CX26, CX32, CX36, and CX43. **(A–D)** There was no significant correlation between the average spectral power of ripples and the expression of CX26, CX32, CX36, or CX43 ($P > 0.05$). **(E,F)** There was no significant correlation between the average spectral power of FRs and the expression of CX26 or CX32 ($p > 0.05$). **(G)** The average spectral power of FRs was weakly correlated with CX36 expression ($r = 0.37$, $p < 0.05$) and **(H)** moderately correlated with CX43 expression ($r = 0.42$, $p < 0.05$).

to explore the effect of CBX on the energy changes of ripples and FRs in rats with chronic epilepsy.

High-frequency oscillations are generated by multiple mechanisms such as synchronized inhibitory post-synaptic potentials with sparse pyramidal cell firing or principal cell action potentials (Ylinen et al., 1995; Bragin et al., 2011). Synchronization of fast firing within the population of interconnected neurons leads to the formation of an episode

of high-frequency population spikes, which is extracellularly recorded as an HFO event. It requires synchronization on a millisecond time scale, which is achieved *via* fast synaptic transmission or non-synaptic mechanisms like gap-junction coupling or ephaptic interactions–a synchronizing mechanism that depends on specific geometric organization and tight cellular arrangement (Jiruska et al., 2017). Both pyramidal neurons and interneurons are involved in HFO generation, but pyramidal cells fire preferentially at the highest amplitude of the ripples, and interneurons begin to discharge earlier than the pyramidal cells do (Cepeda et al., 2020). The inhibitory effect of the interneurons is maintained in ripples (Jefferys et al., 2012), whereas FRs reflect hypersynchronous population spikes of excitatory pyramidal cells (Kanazawa et al., 2015). The formation mechanism of HFOs with different frequencies may be different. The ripples may be formed by the synchronization of the inhibitory post-synaptic potential generated by excitatory neurons mediated by GABAA receptors, while the FRs may be derived from the field potential formed by transient, highly synchronized and sudden discharges of excitatory neurons with pathological connections (Jacobs et al., 2014; Frauscher et al., 2017). Our previous studies confirmed that the frequency of HFOs is not necessary to distinguish physiological and pathological states, that ripples and FRs can be present in both the normal and the epileptic hippocampus, and that the main difference between the two states is the different energy of HFOs (Ran et al., 2018). This study found that during the chronic phase of epilepsy, the average and/or peak spectral power of ripples did not significantly change before and after SE in the PILO and CBX + PILO groups. However, the average and peak spectral power of FRs in the PILO group were significantly higher at 1 and 7 days after SE than those 1 day before SE, and that the average spectral power of FRs in the PILO group were significantly higher than those in CBX + PILO group at 1, 7, and 14 days after SE. This suggests that in the chronic phase of epilepsy, FRs respond more to the real situation of SRSs than ripples do. In a study of intracranial EEG in epileptic patients, González Otárula et al. (2019) found the distribution of ripples was widespread, while FRs were restricted to the epilepsy initiation region. The association of FRs with seizure onset zone may be stronger than that of ripples (Frauscher et al., 2018). Animal studies suggest that ripples are related to physiological functions, such as the formation of memory and cognition, while FRs are related to the seizure onset zone (Nevalainen et al., 2020). FRs are able to influence the specific synaptic driving function of CA1 pyramidal cells, make neuronal firing randomized, and ultimately lead to the loss of control of selective discharges in the hippocampus (Valero et al., 2017). It has been suggested that an energy analysis of FRs may be a more sensitive and specific biomarker of epilepsy, compared to ripples.

Gap junction is considered to be an important component of the neuronal network, with synchronized neuronal activity and field potential oscillations (Posluszny, 2014). The EEG signals during the seizure and interictal seizure phases are correlated with the degree of electrical coupling to the GJ (Roopun et al., 2010). The upregulation of CX43 by the transient receptor potential vanoxalate-4 (TRPV4) may be involved in the pathophysiological process of epilepsy (Men et al., 2019), and the specific CX43 mimic peptide and TAT-Gap19 can reduce spontaneous seizures by inhibiting the function of GJ channels/hemi-channels of CX43 between astrocytes (Delvaeye et al., 2018; Walrave et al., 2018). We investigated the effects of seizures and CBX intervention on the expression of different CXs in the hippocampus in chronic epilepsy and found that seizures induced an increase in CX43 expression at 1 and 7 days after SE, but had no significant effect on CX26, CX36, or CX32. CBX pretreatment did not affect the expression of CXs in the hippocampus of normal rats, but it inhibited CX43 expression in epileptic rats. Further analyses revealed that the expression of CX43 was more strongly correlated with the spectral power change of FRs than the other three CXs, suggesting that the energy of FRs may be regulated by interfering with the expression of CX43, so as to affect seizures. Therefore, in addition to traditional antiepileptic drugs, drugs should be developed that target blocking the electrical conduction of GJ, thereby reducing pathological HFOs formation, which can provide a new strategy for treating epilepsy. However, the causal relationship between the energy of FRs and the expression of CX43 is still unclear. What specific signaling pathways of connexin regulate HFOs, or how neuroelectrical activity affect connexin expression, remain to be explored in the future.

DATA AVAILABILITY STATEMENT

The raw data supporting the conclusions of this article will be made available by the authors, without undue reservation.

ETHICS STATEMENT

The animal study was reviewed and approved by Ethics Committee of Chongqing Medical University.

AUTHOR CONTRIBUTIONS

YH conceived and designed the experiments and revised the manuscript critically for important intellectual content. BL made acquisition and interpretation of data and was involved in drafting the manuscript. BL, XR, and YY performed the experiments. XZ and HC performed data analysis. All authors wrote the manuscript and approved the submitted version.

FUNDING

This work was supported by the National Natural Science Foundation of China (grant nos. 81971215 and 81301124).

ACKNOWLEDGMENTS

We are deeply grateful to the laboratory researchers who participated in this study.

REFERENCES

Bao, X. M., and Shu, S. Y. (1991). *The Stereotaxic Atlas of the Rat Brian*. Beijing: People's Medical Publishing House.

Beyer, E. C., and Berthoud, V. M. (2018). Gap junction gene and protein families: connexins, innexins, and pannexins. *Biochim. Biophys. Acta Biomembr.* 1860, 5–8. doi: 10.1016/j.bbamem.2017.05.016

Bragin, A., Benassi, S. K., Kheiri, F., and Engel, J. Jr. (2011). Further evidence that pathologic high-frequency oscillations are bursts of population spikes derived from recordings of identified cells in dentate gyrus. *Epilepsia* 52, 45–52. doi: 10.1111/j.1528-1167.2010.02896.x

Cepeda, C., Levinson, S., Nariai, H., Yazon, V. W., Tran, C., Barry, J., et al. (2020). Pathological high frequency oscillations associate with increased GABA synaptic activity in pediatric epilepsy surgery patients. *Neurobiol. Dis.* 134:104618. doi: 10.1016/j.nbd.2019.104618

Delvaeye, T., Vandenabeele, P., Bultynck, G., Leybaert, L., and Krysko, D. V. (2018). Therapeutic targeting of connexin channels: new views and challenges. *Trends Mol. Med.* 24, 1036–1053. doi: 10.1016/j.molmed.2018.10.005

Deshpande, T., Li, T., Herde, M. K., Becker, A., Vatter, H., Schwarz, M. K., et al. (2017). Subcellular reorganization and altered phosphorylation of the astrocytic gap junction protein connexin43 in human and experimental temporal lobe epilepsy. *Glia* 65, 1809–1820. doi: 10.1002/glia.23196

Frauscher, B., Bartolomei, F., Kobayashi, K., Cimbalnik, J., van 't Klooster, M. A., Rampp, S., et al. (2017). High-frequency oscillations: the state of clinical research. *Epilepsia* 58, 1316–1329. doi: 10.1111/epi.13829

Frauscher, B., von Ellenrieder, N., Zelmann, R., Rogers, C., Nguyen, D. K., Kahane, P., et al. (2018). High-Frequency oscillations in the normal human brain. *Ann. Neurol.* 84, 374–385. doi: 10.1002/ana.25304

González Otárula, K. A., von Ellenrieder, N., Cuello-Oderiz, C., Dubeau, F., and Gotman, J. (2019). High-Frequency oscillation networks and surgical outcome in adult focal epilepsy. *Ann. Neurol.* 85, 485–494. doi: 10.1002/ana.25442

Hájos, N., and Paulsen, O. (2009). Network mechanisms of gamma oscillations in the CA3 region of the hippocampus. *Neural Netw.* 22, 1113–1119. doi: 10.1016/j.neunet.2009.07.024

Höller, P., Trinka, E., and Höller, Y. M. E. E. G. I. P. S.-A. (2019). Modular EEG investigation and processing system for visual and automated detection of high frequency oscillations. *Front. Neuroinform.* 13:20. doi: 10.3389/fninf.2019.00020

Jacobs, J., Golla, T., Mader, M., Schelter, B., Dümpelmann, M., Korinthenberg, R., et al. (2014). Electrical stimulation for cortical mapping reduces the density of high frequency oscillations. *Epilepsy Res.* 108, 1758–1769. doi: 10.1016/j.eplepsyres.2014.09.022

Jefferys, J. G., Menendez de la Prida, L., Wendling, F., Bragin, A., Avoli, M., Timofeev, I., et al. (2012). Mechanisms of physiological and epileptic HFO generation. *Prog. Neurobiol.* 98, 250–264. doi: 10.1016/j.pneurobio.2012.02.005

Jiruska, P., Alvarado-Rojas, C., Schevon, C. A., Staba, R., Stacey, W., Wendling, F., et al. (2017). Update on the mechanisms and roles of high-frequency oscillations in seizures and epileptic disorders. *Epilepsia* 58, 1330–1339. doi: 10.1111/epi.13830

Kanazawa, K., Matsumoto, R., Imamura, H., Matsuhashi, M., Kikuchi, T., Kunieda, T., et al. (2015). Intracranially recorded ictal direct current shifts may precede high frequency oscillations in human epilepsy. *Clin. Neurophysiol.* 126, 47–59. doi: 10.1016/j.clinph.2014.05.028

Le Van Quyen, M., Khalilov, I., and Ben-Ari, Y. (2006). The dark side of high-frequency oscillations in the developing brain. *Trends Neurosci.* 29, 419–427. doi: 10.1016/j.tins.2006.06.001

Li, Q., Li, Q. Q., Jia, J. N., Liu, Z. Q., Zhou, H. H., Mao, X. Y., et al. (2019). Targeting gap junction in epilepsy: perspectives and challenges. *Biomed. Pharmacother.* 109, 57–65. doi: 10.1016/j.biopha.2018.10.068

Men, C., Wang, Z., Zhou, L., Qi, M., An, D., Xu, W., et al. (2019). Transient receptor potential vanilloid 4 is involved in the upregulation of connexin expression following pilocarpine-induced status epilepticus in mice. *Brain Res. Bull.* 152, 128–133. doi: 10.1016/j.brainresbull.2019.07.004

Mylvaganam, S., Ramani, M., Krawczyk, M., and Carlen, P. L. (2014). Roles of gap junctions, connexins, and pannexins in epilepsy. *Front. Physiol.* 5:172. doi: 10.3389/fphys.2014.00172

Naggar, I., Stewart, M., and Orman, R. (2020). High frequency oscillations in rat hippocampal slices: origin, frequency characteristics, and spread. *Front. Neurol.* 11:326. doi: 10.3389/fneur.2020.00326

Nevalainen, P., von Ellenrieder, N., Klimeš, P., Dubeau, F., Frauscher, B., and Gotman, J. (2020). Association of fast ripples on intracranial EEG and outcomes after epilepsy surgery. *Neurology* 95, e2235–e2245. doi: 10.1212/WNL.0000000000010468

Posluszny, A. (2014). The contribution of electrical synapses to field potential oscillations in the hippocampal formation. *Front. Neural Circuits* 8:32. doi: 10.3389/fncir.2014.00032

Ran, X., Xiang, J., Song, P. P., Jiang, L., Liu, B. K., and Hu, Y. (2018). Effects of gap junctions blockers on fast ripples and connexin in rat hippocampi after status epilepticus. *Epilepsy Res.* 146, 28–35. doi: 10.1016/j.eplepsyres.2018.07.010

Roopun, A. K., Simonotto, J. D., Pierce, M. L., Jenkins, A., Nicholson, C., Schofield, I. S., et al. (2010). A nonsynaptic mechanism underlying interictal discharges in human epileptic neocortex. *Proc. Natl. Acad. Sci. U.S.A* 107, 338–343. doi: 10.1073/pnas.0912652107

Song, P. P., Xiang, J., Jiang, L., Chen, H. S., Liu, B. K., and Hu, Y. (2016). Dynamic changes in spectral and spatial signatures of high frequency oscillations in rat hippocampi during epileptogenesis in acute and chronic stages. *Front. Neurol.* 7:204. doi: 10.3389/fneur.2016.00204

Stacey, W. C., Krieger, A., and Litt, B. (2011). Network recruitment to coherent oscillations in a hippocampal computer model. *J. Neurophysiol.* 105, 1464–1481. doi: 10.1152/jn.00643.2010

Su, X., Chen, J. J., Liu, L. Y., Huang, Q., Zhang, L. Z., Li, X. Y., et al. (2017). Neonatal CX26 removal impairs neocortical development and leads to elevated anxiety. *Proc. Natl. Acad. Sci. U.S.A* 114, 3228–3233. doi: 10.1073/pnas.1613237114

Tingley, D., and Buzsáki, G. (2020). Routing of hippocampal ripples to subcortical structures *via* the lateral septum. *Neuron* 105, 138.e–149.e. doi: 10.1016/j.neuron.2019.10.012

Valero, M., Averkin, R. G., Fernandez-Lamo, I., Aguilar, J., Lopez-Pigozzi, D., Brotons-Mas, J. R., et al. (2017). Mechanisms for selective single-cell reactivation during offline sharp-wave ripples and their distortion by fast ripples. *Neuron* 94, 1234.e–1247.e. doi: 10.1016/j.neuron.2017.05.032

Velmurugan, J., Nagarajan, S. S., Mariyappa, N., Mundlamuri, R. C., Raghavendra, K., Bharath, R. D., et al. (2019). Magnetoencephalography imaging of high frequency oscillations strengthens presurgical localization and outcome prediction. *Brain* 142, 3514–3529. doi: 10.1093/brain/awz284

Vincze, R., Péter, M., Szabó, Z., Kardos, J., Héja, L., and Kovács, Z. (2019). Connexin 43 differentially regulates epileptiform activity in models of convulsive and non-convulsive epilepsies. *Front. Cell. Neurosci.* 13:173. doi: 10.3389/fncel.2019.00173

von Ellenrieder, N., Dubeau, F., Gotman, J., and Frauscher, B. (2017). Physiological and pathological high-frequency oscillations have distinct sleep-homeostatic properties. *Neuroimage Clin.* 14, 566–573. doi: 10.1016/j.nicl.2017.02.018

Walrave, L., Pierre, A., Albertini, G., Aourz, N., De Bundel, D., Van Eeckhaut, A., et al. (2018). Inhibition of astroglial connexin43 hemichannels with TAT-Gap19 exerts anticonvulsant effects in rodents. *Glia* 66, 1788–1804. doi: 10.1002/glia.23341

Walrave, L., Vinken, M., Leybaert, L., and Smolders, I. (2020). Astrocytic connexin43 channels as candidate targets in epilepsy treatment. *Biomolecules* 10:1578. doi: 10.3390/biom10111578

Yan, L., Li, L., Chen, J., Wang, L., Jiang, L., and Hu, Y. (2021). Application of high-frequency oscillations on scalp EEG in infant spasm: a prospective controlled study. *Front. Hum. Neurosci.* 15:682011. doi: 10.3389/fnhum.2021.682011

Ylinen, A., Bragin, A., Nádasdy, Z., Jandó, G., Szabó, I., Sik, A., et al. (1995). Sharp wave-associated high-frequency oscillation (200-Hz) in the intact hippocampus - network and intracellular mechanisms. *J. Neurosci.* 15, 30–46.

Zhuge, Q. C. (2005). *The Rat Brian in Stereotaxic Coordinates*. Beijing: People's Medical Publishing House.

Conflict of Interest: The authors declare that the research was conducted in the absence of any commercial or financial relationships that could be construed as a potential conflict of interest.

Publisher's Note: All claims expressed in this article are solely those of the authors and do not necessarily represent those of their affiliated organizations, or those of the publisher, the editors and the reviewers. Any product that may be evaluated in this article, or claim that may be made by its manufacturer, is not guaranteed or endorsed by the publisher.

frontiers | Frontiers in Molecular Neuroscience

MINI REVIEW
published: 11 May 2022
doi: 10.3389/fnmol.2022.868531

Gene and Cell Therapy for Epilepsy: A Mini Review

*Alisa A. Shaimardanova[1], Daria S. Chulpanova[1], Aysilu I. Mullagulova[1], Zaid Afawi[2], Rimma G. Gamirova[1], Valeriya V. Solovyeva[1] and Albert A. Rizvanov[1]**

[1] Institute of Fundamental Medicine and Biology, Kazan Federal University, Kazan, Russia, [2] Center for Neuroscience, Ben Gurion University of the Negev, Be'er Sheva, Israel

Epilepsy is a chronic non-infectious disease of the brain, characterized primarily by recurrent unprovoked seizures, defined as an episode of disturbance of motor, sensory, autonomic, or mental functions resulting from excessive neuronal discharge. Despite the advances in the treatment achieved with the use of antiepileptic drugs and other non-pharmacological therapies, about 30% of patients suffer from uncontrolled seizures. This review summarizes the currently available methods of gene and cell therapy for epilepsy and discusses the development of these approaches. Currently, gene therapy for epilepsy is predominantly adeno-associated virus (AAV)-mediated delivery of genes encoding neuro-modulatory peptides, neurotrophic factors, enzymes, and potassium channels. Cell therapy for epilepsy is represented by the transplantation of several types of cells such as mesenchymal stem cells (MSCs), bone marrow mononuclear cells, neural stem cells, and MSC-derived exosomes. Another approach is encapsulated cell biodelivery, which is the transplantation of genetically modified cells placed in capsules and secreting various therapeutic agents. The use of gene and cell therapy approaches can significantly improve the condition of patient with epilepsy. Therefore, preclinical, and clinical studies have been actively conducted in recent years to prove the benefits and safety of these strategies.

Keywords: epilepsy, gene therapy, cell therapy, adeno-associated virus, mesenchymal stem cells, neural stem cells, mononuclear cells, encapsulated cell biodelivery

OPEN ACCESS

Edited by:
Tobias Engel, Royal College of Surgeons in Ireland, Ireland

Reviewed by:
Dinesh Upadhya, Manipal Academy of Higher Education, India

***Correspondence:**
Albert A. Rizvanov
rizvanov@gmail.com

Specialty section:
This article was submitted to Brain Disease Mechanisms, a section of the journal Frontiers in Molecular Neuroscience

Received: *02 February 2022*
Accepted: *30 March 2022*
Published: *11 May 2022*

Citation:
Shaimardanova AA, Chulpanova DS, Mullagulova AI, Afawi Z, Gamirova RG, Solovyeva VV and Rizvanov AA (2022) Gene and Cell Therapy for Epilepsy: A Mini Review. Front. Mol. Neurosci. 15:868531. doi: 10.3389/fnmol.2022.868531

INTRODUCTION

Epilepsy is one of the most common diseases of the nervous system (more than 50 million cases have been reported worldwide). This condition is characterized by recurrent unprovoked seizures that result from abnormally excessive firing of neurons due to an imbalance in levels of excitation and inhibition in the brain (Stafstrom and Carmant, 2015). Epilepsy can have a variety of etiologies: structural, infectious, metabolic, immune, genetic as well as unknown (Perucca et al., 2020). Despite the active research in this area, the causes of the disease are still unclear. Epilepsy is also a group of conditions that are heterogeneous in manifestations and causes, making it difficult to develop unambiguous diagnostic criteria (Thijs et al., 2019). Patients suffer from seizures that often worsen over time and is accompanied by cognitive function deterioration and mental health problems. Patients often become resistant to existing antiepileptic drugs (Sheng et al., 2018).

The production of effective methods of treatment is an urgent problem that requires an immediate solution since epilepsy is a serious medical and social problem.

The risk of premature death in people with epilepsy is three times higher than in the general population (according to WHO[1]).

Currently, gene and cell therapy is being investigated as a way to reduce neuronal loss, inflammation, oxidative stress, and the frequency and duration of epileptic seizures. The new approaches being developed are capable of increasing the survival of neurons, improving neurogenesis, providing neuroprotection and preserving cognitive functions.

Thus, this paper discusses the promising results of gene and cell therapy for epilepsy. **Table 1** and **Figure 1** provide detailed information on existing *in vivo* studies and clinical trials.

GENE THERAPY

The current focus of gene therapy strategies for epilepsy is primarily aimed at reducing neuronal excitability by overexpressing neuro-modulatory peptides such as neuropeptide Y (Dong et al., 2013; Zhang et al., 2013), galanin etc. (McCown, 2006) or by the genetic modification of astrocytes, for example, to suppress adenosine kinase (ADK) expression (Young et al., 2014).

Overexpression of ion channels such as the Kv1 potassium channel, which reduces the intrinsic excitability of neurons, increases the threshold for action potential generation required for neuron firing. Thus, permanent inhibition of the increased internal excitability of neurons inside the epileptic focus may have a long-term antiepileptic effect (Snowball et al., 2019). In a rat model of chronic refractory focal neocortical epilepsy, a lentivirus encoding Kv1.1 was shown to suppress epileptic activity for several weeks upon injection into an epileptic focus (Wykes et al., 2012). In addition, the use of adeno-associated virus (AAV) overexpressing Kv1.1 has resulted in a decrease in both the frequency and duration of seizures in the temporal lobe epilepsy (TLE) model (Snowball et al., 2019). CRISPRa-mediated Kv1.1 upregulation decreased spontaneous generalized seizures in the mouse model of TLE (Colasante et al., 2020).

Another approach in antiepileptic treatment is the suppression of the activity of the excitatory mediator glutamate. Neuropeptide Y (NPY) preferentially binds to three G-protein coupled receptors (Y1, Y2, and Y5). Furthermore, the antiepileptic effect of NPY in the hippocampus is mediated by binding of NPY with presynaptic Y2 or Y5 receptors, which subsequently suppress glutamate release at excitatory synapses (Berglund et al., 2003). Binding of NPY to Y1 receptors leads to an increase in the epileptic activity (Benmaamar et al., 2003). Thus, genetic modification of the hippocampus by viruses with NPY can reduce the frequency of spontaneous seizures by 40% in both the TLE model (Noe et al., 2008) and kainate-induced seizures model (Dong et al., 2013; Zhang et al., 2013). Additionally, AAV-NPY was shown to have therapeutic effects when injected into the thalamus or somatosensory cortex (SC) of genetic epilepsy model rats (Powell et al., 2018). In addition to viruses encoding the NPY, viruses encoding the receptors for this protein have also been administered to suppress seizures, which significantly increased the antiepileptic effect. For example, the injection of AAV1/2 with the NPY and Y5 significantly reduced the number of kainate-induced seizures (Gotzsche et al., 2012). The use of AAV1/2 viral vector encoding the NPY in combination with Y2 resulted in the reduction in the number of kainate-induced seizures by 31–45% (Ledri et al., 2016; Melin et al., 2019). The mechanisms of the antiepileptic effect of NPY are still unclear. However, overexpression of NPY is known to result in the expression of the N-methyl-D-aspartate receptor subunits NR1, NR2A, and NR2B, which plays a critical role in the development of epilepsy (Dong et al., 2013). Moreover, the level of the synaptophysin protein, whose expression increased in the hippocampus of patients with epilepsy, was also decreased in the kainate-induced seizures model (Zhang et al., 2013). Overexpression of NPY has been studied in limited studies. Some studies have shown no effect on short- or long-term memory (Szczygiel et al., 2020), while others have illustrated that NPY decreases synaptic plasticity and negatively affects hippocampal-based spatial discrimination learning (Sorensen et al., 2008).

In addition to the treatment approaches described above, AAVs are actively being used to deliver proteins with therapeutic properties. Nevertheless, these are primarily *in vivo* studies that have not yet been further developed. For example, the introduction of AAV encoding the glial cell line-derived neurotrophic factor (GDNF) gene or the γ-aminobutyric acid decarboxylase 67 (GAD67) gene reduced the seizure frequency in the TLE model (Kanter-Schlifke et al., 2007; Shimazaki et al., 2019). Moreover, promising results were demonstrated for AVVs encoding preprosomatostatin injected into the hippocampus (Natarajan et al., 2017).

Astrocyte transduction using AAV9 differs from the approach based on genetic modification of neurons described above. For example, miR-mediated suppression of ADK expression in astrocytes allowed an increase in the concentration of adenosine, which plays a pivotal role in seizure termination, and led to a decrease in the duration of kainate-induced seizures (Young et al., 2014).

A potential limitation of the viral vectors for the treatment of epilepsy is that viruses can transduce not only the epileptic focus cells, but also surrounding brain areas, so it can be difficult to determine the optimal dosage to achieve a therapeutic effect without impairing normal brain function. These difficulties can be overcome by a new strategy for creating a group of G-protein coupled receptors called designer receptors exclusively activated by designer drugs (DREADDs). DREADD technology is based on mutated human muscarinic receptors, which, when expressed in cells, can only be specifically bound and activated by the pharmacologically inert compounds, such as clozapine-N-oxide (CNO). Systemic administration of CNO leads to the opening of Gi-protein gated inwardly rectifying potassium channels, resulting in membrane hyperpolarization and neuronal inhibition. The efficacy of DREADDs has already been confirmed in a number of therapeutically relevant animal models of epilepsy (Lieb et al., 2019). For example, injection of AAV5 expressing a synthetic receptor hM4Di into the dorsal hippocampus of

[1]https://www.who.int/ru

TABLE 1 | Gene and cell therapy for epilepsy.

Therapeutic agent	Model	Dose and duration	Therapy results	References
GENE THERAPY				
LV encoding potassium channel Kv1.1	Rat model of tetanus toxin-induced epilepsy	Single injection of 1–1.5 mL of LV [2.6×10^9 viral genomes (vg/mL)] into layer 5 of the right motor cortex	Decrease in the frequency of seizures over several weeks	Wykes et al., 2012
AAV encoding potassium channel Kv1.1	Rat model of kainic acid-induced status epilepticus	Single injection of 8.0 μl of AAV (8.3×10^{14} vg/mL) into dorsal and ventral hippocampus	Decrease in the frequency and duration of seizures	Snowball et al., 2019
AAV9 encoding small guide RNAs for Kv1.1 upregulation	Mouse model of kainic acid-induced status epilepticus	Single injection of 300 nL of AAV9 (8×10^{12} vg/ml) into right ventral hippocampus	Decrease in the frequency of spontaneous generalized seizures	Colasante et al., 2020
AAV1/2 encoding NPY	Rat model of kainate-induced seizures	Single injection of 2 μl of AAV2 (10^{12} vg/mL) into dorsal hippocampus	Decrease in the frequency of kainate-induced seizures	Gotzsche et al., 2012
AAV encoding NPY	Rat model of kainate-induced seizures	Single injection of 10 μL of AAV (5×10^{11} vg/mL) into the right lateral ventricle	Decrease in the frequency of kainate-induced seizures	Dong et al., 2013; Zhang et al., 2013
AAV1/2 encoding NPY and Y2	Rat model of kainate-induced seizures	Single injection of 1 μl of AAV-NPY (10^{12} vg/mL) and 1.5 μl of AAV-Y2 (10^{12} vg/mL) into dorsal and ventral hippocampus	Decrease in the frequency of kainate-induced seizures	Ledri et al., 2016
AAV1/2 encoding NPY	Rat model of genetic generalized epilepsy	Single injection of 3 μl of AAV (6.6×10^{12} vg/ml) into thalamus and 1 μl into SC	Decrease in the frequency and duration of seizures in the thalamus, decrease in the frequency of seizures in the SC	Powell et al., 2018
AAV1 encoding NPY and Y2	Rat model of kainate-induced seizures	Single injection of 3 μL of AAV (10^{12} vg/mL) into hippocampus	Decrease in the frequency of seizures	Melin et al., 2019
AAV2 encoding GDNF	Rat model of kindling-induced epilepsy	Single injection of 1 and 2 μl of virus (2.1×10^{12} vg/mL) into dorsal and ventral hippocampus	Decrease in the frequency of seizures, increase in seizure induction threshold	Kanter-Schlifke et al., 2007
AAV9 encoding miR-ADK	Rat model of kainate-induced seizures	Single injection of 3 μL of AAV (9.48×10^{11} vg/mL) vector infused into hippocampus	Decrease in the frequency of seizures, protection of dentate hilar neurons	Young et al., 2014
AAV5 encoding preprosomatostatin	Rat model of kindling-induced epilepsy	Single injection of 2 μL of AAV (4.19×10^{13} vg/mL) into the left and right CA1 region and dentate gyrus	Development of seizure resistance in 50% of animals	Natarajan et al., 2017
AAV8 encoding GAD67	The EL/Suz mouse model of epilepsy	Single injection of 3 μL of AAV (1×10^{10} vg/mL) bilaterally into the CA3 region of hippocampus	Significant reduction in seizure generation	Shimazaki et al., 2019
AAV2 encoding galanin	Rat model of kainate-induced seizures	Single injection of 2 μl of AAV (8×10^{12} vg/mL) into the piriform cortex	Prevention of kainic acid-induced seizures	McCown, 2006
CELL THERAPY				
Nervous system cells				
Intravenous infusion of neurospheres	Rat model of pilocarpine-induced status epilepticus	Single intravenous injection of 2×10^6 cells	Decrease in the oxidative stress damage	de Gois da Silva et al., 2018
Transplantation of medial ganglionic eminence-derived neural stem cell grafts	Rat model of kainic acid-induced status epilepticus	Single transplantation of 4 grafts of 80,000 cells in each side of the hippocampus (640,000 cells/rat)	Suppression of spontaneous recurrent motor seizures, an increase in the number of GABAergic neurons, restoration of GDNF expression. No improvement in cognitive function	Waldau et al., 2010
GABAergic interneuron precursors from the medial ganglionic eminence	Kv1.1 mutant mice	Bilateral transplantation into the deep layers of the cortex at two different sites on the hemisphere (4×10^5 cells/mouse)	Decrease in the duration and frequency of spontaneous electrographic seizures	Baraban et al., 2009
Human iPSCs-derived medial ganglionic eminence cells	Mouse model of pilocarpine-induced status epilepticus	Transplantation of cells in the hippocampus (3×10^5 cells/mouse)	Suppression of seizures, aggressiveness, hyperactivity, improvement of cognitive function	Cunningham et al., 2014

(Continued)

TABLE 1 | (Continued)

Therapeutic agent	Model	Dose and duration	Therapy results	References
Human iPSCs-derived medial ganglionic eminence cells	Rat model of kainic acid-induced status epilepticus	Single transplantation of 3 grafts of 100,000 cells in each side of the hippocampus (600,000 cells/rat)	Relief of spontaneous recurrent seizures, improvement of cognitive function and memory, reduction in the loss of interneurons	Upadhya et al., 2019
MSCs				
Undifferentiated autologous bone marrow-derived MSCs (in combination with anti-epileptic drugs)	Patients with epilepsy	Single intravenous injection of 1–1.5 $\times$ 10^6 cells/kg and single intrathecal injection of 1 $\times$ 10^5 cells/kg after 5–7 days	No serious side effects. Reduction in frequency or complete stop of seizures, improvement of clinical manifestations	Hlebokazov et al., 2017; Hlebokazov et al., 2021 NCT02497443
Adipose derived regenerative cells	Patients with autoimmune refractory epilepsy	Intrathecal injection of 4 ml of stromal fraction, 3 times every 3 months	Complete remission in 1 of 6 patients (within 3 years), mild and short-term reduction in seizure (3 of 6 patients). Improvement in patients' daily functioning. No further regression was observed for 3 years	Szczepanik et al., 2020 NCT03676569
Bone marrow-derived CD271$^+$ MSCs and bone marrow MSCs	Pediatric patients with drug-resistant epilepsy	Combination therapy consisting of single intrathecal (0.5 $\times$ 10^9) and intravenous (0.38 $\times$ 10^9–1.72 $\times$ 10^9) injections of bone marrow-derived CD271$^+$ MSC and four intrathecal injections of bone marrow MSC (18.5 $\times$ 10^6–40 $\times$ 10^6) every 3 months	Neurological and cognitive improvement, decrease in the frequency of seizures	Milczarek et al., 2018
Bone marrow-derived MSCs	Rat model of pilocarpine-induced status epilepticus	Single intravenous injection of 3 $\times$ 10^6 cells/rat	Decrease in the frequency of seizures, increase in the number of neurons	Abdanipour et al., 2011
Bone marrow-derived MSCs	Rat model of lithium-pilocarpine- induced epilepsy	Single intravenous injection of 10^6 cells/rat	Inhibition of epileptogenesis and improvement of cognitive functions	Fukumura et al., 2018
Bone marrow-derived MSCs	Rat model of pilocarpine-induced status epilepticus	Single injection of 100,000 cells in each side of the hippocampus (200,000 cells/rat) or single intravenous injection of 3 $\times$ 10^6 cells/rat	Reduction of oxidative stress in the hippocampus, decrease in the levels of inflammatory cytokines (TNF-α and IL-1β) and an apoptotic marker (caspase 3). Improvement of neurochemical and pathological changes in the brain	Salem et al., 2018
Neural-induced adipose-derived stem cells	Rat model of kainic acid-induced status epilepticus	Single transplantation into the hippocampus (50,000 cells/rat)	Decrease in seizure activity, recovery of memory and learning ability	Wang et al., 2021
Umbilical cord blood MSCs	Rat model of pentylenetetrazole-induced chronic epilepsy	Single intravenous injection (10^6 cells/rat)	Decrease in the severity of seizures and oxidative stress damage, improved motor coordination and cognitive function	Mohammed et al., 2014
Umbilical cord blood MSCs	Rat model of lithium-pilocarpine induced status epilepticus	Single transplantation into the hippocampus (5 $\times$ 10^5 cells/rat)	Partial restoration of glucose metabolism in the hippocampus, seizure frequency did not differ from the control group	Park et al., 2015
Exosomes				
MSC-derived exosomes	Mouse model of pilocarpine-induced status epilepticus	Single intraventricular injection (30 μg)	Reduction in the intensity of manifestation of reactive astrogliosis and inflammatory response, improvement in cognitive functions and memory	Xian et al., 2019
MSC-derived A1-exosomes	Mouse model of pilocarpine-induced status epilepticus	Two intranasal administrations after 18 h (15 μg)	Reduction in the loss of glutamatergic and GABAergic neurons, reduction in the inflammation, support of normal hippocampal neurogenesis, cognitive function, and memory	Long et al., 2017

(Continued)

TABLE 1 | (Continued)

Therapeutic agent	Model	Dose and duration	Therapy results	References
Mononuclear cells				
Bone marrow mononuclear cells	Patients with temporal lobe epilepsy	Single intra-arterial injection ($1.52–10 \times 10^8$ cells/patient)	Decrease in the number of seizures, increase in average memory indicators. Complete disappearance of seizures in 40% of patients	DaCosta et al., 2018 NCT00916266
Bone marrow mononuclear cells	Rat model of lithium-pilocarpine induced status epilepticus	Single intravenous injection (1×10^6 cells/rat)	Prevention of spontaneous recurrent seizures in the early stage of epilepsy, a significant reduction in the frequency and duration of seizures in the chronic phase	Costa-Ferro et al., 2010
Bone marrow mononuclear cells	Mouse model of pilocarpine-induced status epilepticus	Single intravenous injection (2×10^6 cells/mouse)	Neuroprotective and anti-inflammatory effects, decrease in the loss of hippocampal neurons	Leal et al., 2014
Encapsulated cell biodelivery				
Semipermeable capsule containing GDNF-secreting ARPE-19 cells (arising retinal pigment epithelia cells)	Rat model of pilocarpine-induced status epilepticus	Transplantation in the hippocampus (5×10^4 cells/capsule). GDNF concentration up to 566.79 ± 192.47 ng/24 h	Decrease in the frequency of seizures, cognitive function improvement, neuroprotective effect	Paolone et al., 2019
Semipermeable capsule containing GDNF-secreting cells	Rat model of kindling-induced epilepsy	Transplantation in the hippocampus. High GDNF concentration – 150.92 ± 44.51 ng/ml/24 h, low concentration – 0.04 ± 0.88 ng/ml/24 h	Low GDNF levels have an antiepileptic effect compared to elevated levels	Kanter-Schlifke et al., 2009
Semipermeable capsule containing galanin-secreting ARPE-19 cells	Rat model of kindling-induced epilepsy	Transplantation in the hippocampus (6×10^4 cells/capsule) High galanin concentration – 12.6 ng/ml/24 h, low concentration – 8.3 ng/ml/24 h	High doses decrease the duration of focal seizures	Nikitidou et al., 2014
Semipermeable capsule containing BDNF-secreting ARPE-19 cells	Rat model of pilocarpine-induced status epilepticus	Transplantation in the hippocampus (5×10^4 cells/capsule). BDNF concentration – 200–400 ng/24 h	Decrease in the frequency of seizures. Cognitive function improvement	Falcicchia et al., 2018
Semipermeable capsule containing BDNF-secreting baby hamster kidney cells	Rat model of pilocarpine-induced status epilepticus	Transplantation in the hippocampus (10^6 cells/capsule) BDNF concentration – 7.2 ± 1.2 ng/24 h	Injection of low doses had a neuroprotective effect and stimulated neurogenesis	Kuramoto et al., 2011

rats with pilocarpine-induced epilepsy led to a significantly reduction of seizures (Katzel et al., 2014). Another limiting factor is the high invasiveness of virus injection methods. In addition, even the most non-immunogenic AAV-based vectors are capable of inducing both humoral and cellular immune responses, which can greatly influence the outcome of gene therapy, since neutralizing antibodies can bind the viral particles and significantly reduce the transduction efficiency (Ronzitti et al., 2020). Some viral vectors can also lead to insertional mutagenesis due to genome integration (Athanasopoulos et al., 2017). In addition, the capacity of the vector is of great importance. For example, AAVs can only package ∼4.7 kb of DNA (Weinberg and McCown, 2013).

In gene therapy for epilepsy, the use of AAVs encoding potassium channel or NPY genes are the most investigated. However, the evaluation of the effectiveness of these therapeutic agents has not gone beyond *in vivo* animal systems. To date, there are no registered clinical trials aimed at investigating gene drugs for the treatment of epilepsy. In this regard, we can say that gene therapy is at an early stage of development and obviously requires more attention from researchers.

CELL THERAPY

Cell therapy for epilepsy includes a variety of approaches, including the use of MSCs (Abdanipour et al., 2011; Mohammed et al., 2014; Park et al., 2015; Hlebokazov et al., 2017, 2021; Fukumura et al., 2018; Salem et al., 2018; Melin et al., 2019; Szczepanik et al., 2020; Wang et al., 2021), mononuclear cells (Costa-Ferro et al., 2010; Leal et al., 2014; DaCosta et al., 2018), cells of the nervous system (Baraban et al., 2009; Waldau et al., 2010; Cunningham et al., 2014; de Gois da Silva et al., 2018; Upadhya et al., 2019), and encapsulated cells expressing various therapeutic factors (Kanter-Schlifke et al., 2009; Kuramoto et al., 2011; Nikitidou et al., 2014; Falcicchia et al., 2018;

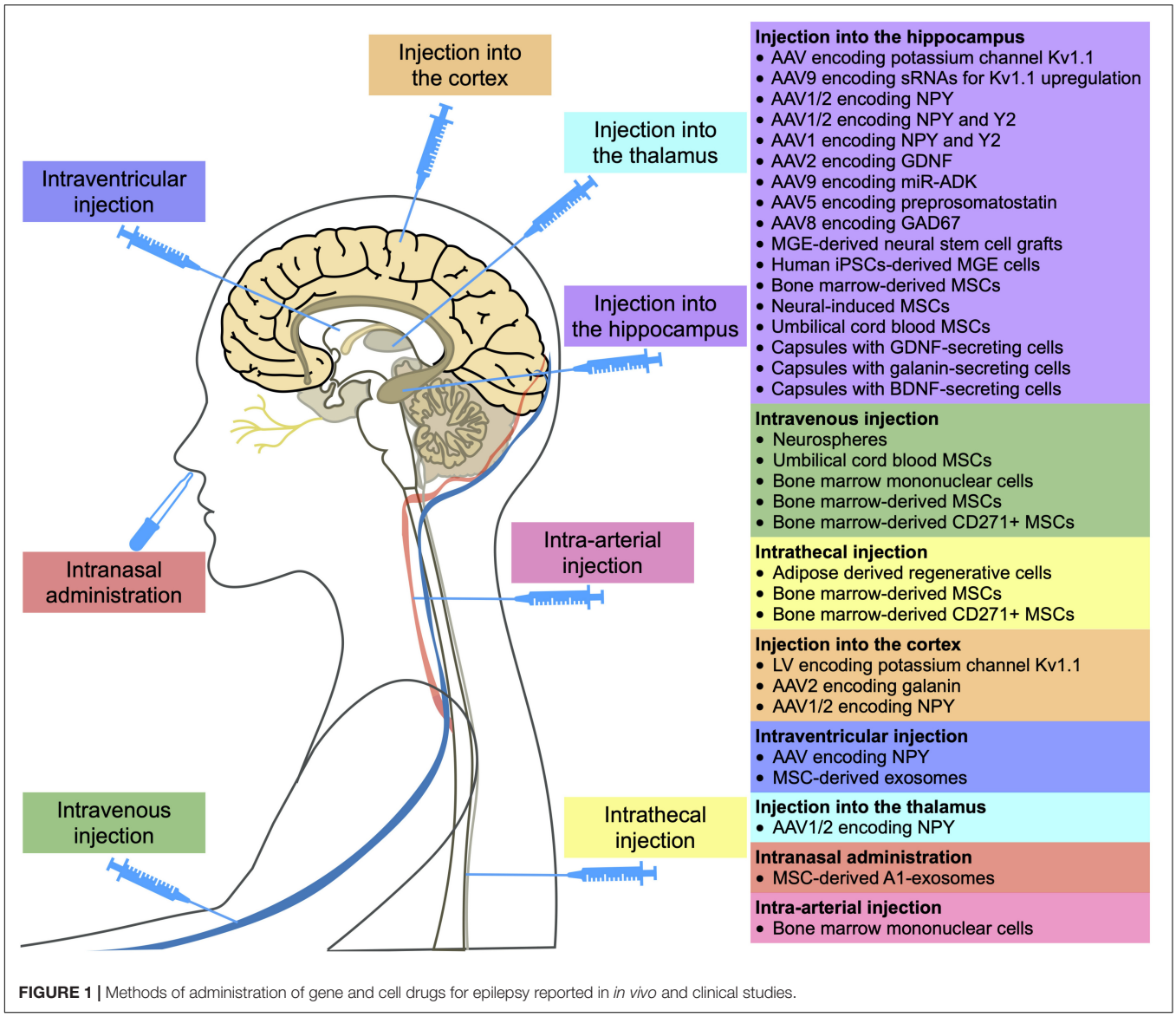

FIGURE 1 | Methods of administration of gene and cell drugs for epilepsy reported in *in vivo* and clinical studies.

Paolone et al., 2019), as well as exosomes (Long et al., 2017; Xian et al., 2019). Cell therapy is an alternative treatment that can be used to reduce the incidence rate of seizures in epilepsy, including drug-resistant epilepsy, as shown in several clinical studies (Hlebokazov et al., 2017, 2021; DaCosta et al., 2018; Milczarek et al., 2018; Szczepanik et al., 2020).

Transplantation of Neural Cells

Promising approaches for epilepsy treatment are aimed at replenishing the neuronal loss in the hippocampus by transplanting cells of the nervous system. The neural stem cell is capable of self-renewal and differentiation into neurons, glial cells, and oligodendrocytes as well as expression of neurotrophic factors. Transplantation of neural stem cells into the hippocampus of epileptic rats led to an increase in the number of GABAergic neurons and cells expressing GDNF, which resulted in the suppression of seizures (Waldau et al., 2010).

The protective role of neurospheres, which are spherical clusters of neural stem cells grown *in vitro*, have also been studied. Intravenous administration of neurospheres into epileptic rats has been shown to reduce oxidative damage by significantly increasing the level of antioxidant enzymes such as glutathione, superoxide dismutase and catalase (de Gois da Silva et al., 2018).

It has been shown that progenitor cells from embryonic medial ganglionic eminence (MGE) can differentiate into functional GABAergic interneurons. Transplantation of MGE precursors into the cortex of model mice with a deletion of potassium channels led to a significant reduction in the duration and frequency of spontaneous electrographic seizures, which is achieved due to GABA-mediated synaptic inhibition (GABA is an inhibitory neurotransmitter) (Baraban et al., 2009).

GABAergic interneurons can be derived from induced pluripotent stem cells (iPSCs). It has been shown that transplantation of pluripotent stem cell-derived GABAergic

interneurons into the hippocampus of model animals led to a decrease in seizures and other behavioral abnormalities (Cunningham et al., 2014; Upadhya et al., 2019).

Mesenchymal Stem Cell Transplantation

Mesenchymal stem cells (MSCs) have many therapeutic properties useful in epilepsy, including neuroprotection, immunomodulation, neurogenesis support, inflammation, and oxidative stress damage suppression. These effects are achieved due to the fact that MSCs secrete various neurotrophic factors, anti-inflammatory cytokines, growth factors and other biologically active molecules (Vizoso et al., 2017; Milczarek et al., 2018). It is also known that MSCs can cross the blood-brain barrier and migrate to the affected area. Even after intravenous administration, MSCs migrate into the hippocampus of model animals with epilepsy and have a therapeutic effect (Abdanipour et al., 2011).

Numerous studies have shown that the administration of undifferentiated MSCs can significantly decrease the frequency of seizures (Hlebokazov et al., 2017, 2021; Milczarek et al., 2018; Szczepanik et al., 2020), improve cognitive (Fukumura et al., 2018; Milczarek et al., 2018; Wang et al., 2021) and motor functions (Mohammed et al., 2014), increase the number of neurons (Abdanipour et al., 2011), reduce oxidative stress (Salem et al., 2018). The introduction of MSCs promotes the survival of GABAergic interneurons (Mohammed et al., 2014; Fukumura et al., 2018).

It has been shown that MSCs begin to secrete BDNF, NT3, and NT4 after neuronal differentiation. Their transplantation into the hippocampus of rats with kainic acid-induced epilepsy led to an increase in the level of BCL-2 and BCL-XL anti-apoptotic proteins and a decrease in the level of BAX pro-apoptotic protein in the hippocampus. Suppression of seizure activity and restoration of learning ability have also been noted (Wang et al., 2021).

The results of clinical studies also confirm benefits of MSC transplantation. For example, phase I/II clinical trials have demonstrated that the administration of antiepileptic drugs along with one or two intravenous and intrathecal administrations of MSCs has been safe and effective in treating patients with drug-resistant epilepsy. Combined use of levetiracetam (an antiepileptic drug) and MSCs led to a decrease in the frequency of seizures, and a repeated course of MSC administration contributed to a further improvement in the patients' condition (NCT02497443) (Hlebokazov et al., 2017, 2021).

A combination therapy has also been used for pediatric patients with drug-resistant epilepsy. The intrathecal and intravenous administration of autologous bone marrow nucleated cells, followed by four intrathecal injections of MSCs every 3 months, resulted in neurological and cognitive improvement in all patients, including a decrease in the number of seizures (Milczarek et al., 2018).

Intrathecal administration of adipose-derived regenerative cells (a heterogeneous population of cells, including multipotent stem cells, fibroblasts, regulatory T-cells, and macrophages) into patients with autoimmune refractory epilepsy (3 times every 3 months) has also been reported. Only 1 out of 6 patients achieved complete remission (there were no seizures for more than 3 years), in 3 out of 6 there was a slight and short-term decrease in the frequency of seizures, and in two out of six no effect was found (Szczepanik et al., 2020). In all these clinical studies, some improvement after the introduction of cells without serious side effects was observed.

Exosome Injection

Not only MSCs, but also exosomes derived from them, exhibit immunoregulatory, anti-inflammatory and trophic effects (Harrell et al., 2019; Ha et al., 2020; Xunian and Kalluri, 2020), which means they also have great potential for the treatment of nervous systems diseases (Gorabi et al., 2019; Guy and Offen, 2020). As a result of intraventricular injection of exosomes, hippocampal astrocytes are able to take up the exosomes and attenuate astrogliosis and inflammation in model mice (Xian et al., 2019). After intranasal administration, exosomes also were able to reach the hippocampus, reduce the loss of glutamatergic and GABAergic neurons, and significantly reduce inflammation in the hippocampus of model animals (Long et al., 2017).

Mononuclear Cell Transplantation

Bone marrow mononuclear cells (BMCs) also possess immunomodulatory and neuroprotective properties (Yoshihara et al., 2007; Shrestha et al., 2014; do Prado-Lima et al., 2019; Wei et al., 2020) due to the secretion of various trophic factors and cytokines (Liu et al., 2004; Wei et al., 2020).

It has been shown that after intravenous administration to animals with status epilepticus, BMCs can migrate to the hippocampus, reduce the frequency and duration of seizures, maintain neuronal density (Costa-Ferro et al., 2010), increase proliferation of neurons, reduce the level of inflammatory cytokines and increase the level of anti-inflammatory cytokines (Leal et al., 2014).

Phase I/II clinical trials have investigated the safety and efficacy of intra-arterial injection of BMCs in TLE patients. Researchers demonstrated safety, improved memory, a decrease in theta activity, and a decrease in spike density (DaCosta et al., 2018).

ENCAPSULATED CELL BIODELIVERY

Despite the proven efficacy, gene and cell therapy methods have a number of known disadvantages and side effects. It should be noted that these methods of therapy are irreversible and unregulated, and some of them can lead to an immune response and malignant transformation.

In the case of cell therapy, as mentioned above for gene therapy, the major limiting factor is safety, specifically the possibility of a significant immune response induction and oncogenic transformation. In some cases, long-term immunosuppressive therapy and monitoring of the cells after the administration are required (Aly, 2020). It is important to select a suitable donor in the case of allogeneic transplantation, not only in terms of HLA compatibility, but also in the heterogeneity of effector molecules secreted by the cells, which

vary considerably between different donors and can lead to a significant variation in the treatment efficacy (Montzka et al., 2009; Mukhamedshina et al., 2019). The migration ability of cells also imposes restrictions on the use of cell-based therapy in clinical practice since highly invasive cell delivery is sometimes required to reach the target area and cross the blood-brain barrier (Issa et al., 2020).

One of the approaches to overcome some of the difficulties of cell-based therapy is encapsulated cell biodelivery (ECB). ECB usually involves the implantation of a capsule with a semipermeable membrane containing genetically modified cells that secrete therapeutic substances. In this case, the cells do not leave the capsule, but the therapeutically active molecules leave and spread in the area of transplantation. This method allows (1) preventing an immune response and transplant rejection, since the cells are physically isolated, (2) locally delivering therapeutic substances, and (3) stopping treatment by removing the capsule from the brain. To suppress epileptic activity, such capsules were designed to contain cells expressing GDNF (Kanter-Schlifke et al., 2009; Paolone et al., 2019), BDNF (Kuramoto et al., 2011; Falcicchia et al., 2018), or galanin (Nikitidou et al., 2014). ECB has shown positive results in epilepsy therapy since these neurotrophic factors and neuropeptide exhibit antiepileptic activity.

CONCLUSION

This review discussed recent developments in gene and cell therapy for epilepsy. To date, *in vivo* models have shown the potential benefit of viral vectors (mainly AAVs, rarely LVs) encoding genes of therapeutic agents. Thus, the effectiveness of viral delivery of (1) neuro-modulatory peptides, such as NPY or galanin, (2) potassium channels to inhibit increased internal excitability of neurons, (3) GDNF, (4) GAD67, (5) preprosomatostatin, as well as (6) miR to suppress ADK expression has been shown.

Cell-based therapy has made more progress with documented clinical trials showing the benefits and safety of MSC or BMC transplantation. The therapeutic effect can be achieved due to the neuroprotective, anti-inflammatory, immunomodulatory properties of these cells, which is also shown for MSC-derived exosomes. Researchers are also focusing on the transplantation of neural stem cells into the hippocampus to reduce neuronal loss in animal models. ECB, which is the injection of capsules with cells expressing BDNF, GDNF or galanin in the hippocampus, has shown an antiepileptic effect.

The majority of gene and cell therapies have not yet reached clinical practice, but they have made significant progress. To date, preclinical studies in animal model are ongoing and new clinical trials are being registered to confirm both the effectiveness and safety of these approaches. Considering the heterogeneous nature of the onset and manifestation of epilepsy, the development of methods of gene and cell therapy can make a significant contribution to progress in the treatment of this disease.

AUTHOR CONTRIBUTIONS

AS, DC, VS, and AR: conceptualization. AS and DC: writing-original draft preparation. VS, AM, RG, ZA, and AR: writing-review and editing. AS: visualization. VS and AR: supervision. All authors have read and agreed to the published version of the manuscript.

FUNDING

This work was funded by the subsidy allocated to KFU for the state assignment 0671-2020-0058 in the sphere of scientific activities.

ACKNOWLEDGMENTS

We thank the Center for Precision Genome Editing and Genetic Technologies for Biomedicine, IGB RAS for scientific advice on development of gene therapy drugs. This article has been supported by the Kazan Federal University Strategic Academic Leadership Program (PRIORITY-2030).

REFERENCES

Abdanipour, A., Tiraihi, T., and Mirnajafi-Zadeh, J. (2011). Improvement of the pilocarpine epilepsy model in rat using bone marrow stromal cell therapy. *Neurol. Res.* 33, 625–632. doi: 10.1179/1743132810Y.0000000018

Aly, R. M. (2020). Current state of stem cell-based therapies: an overview. *Stem Cell Investig.* 7:8. doi: 10.21037/sci-2020-001

Athanasopoulos, T., Munye, M. M., and Yanez-Munoz, R. J. (2017). Nonintegrating Gene Therapy Vectors. *Hematol. Oncol. Clin. North Am.* 31, 753–770. doi: 10.1016/j.hoc.2017.06.007

Baraban, S. C., Southwell, D. G., Estrada, R. C., Jones, D. L., Sebe, J. Y., Alfaro-Cervello, C., et al. (2009). Reduction of seizures by transplantation of cortical GABAergic interneuron precursors into Kv1.1 mutant mice. *Proc. Natl. Acad. Sci. U S A* 106, 15472–15477. doi: 10.1073/pnas.0900141106

Benmaamar, R., Pham-Le, B. T., Marescaux, C., Pedrazzini, T., and Depaulis, A. (2003). Induced down-regulation of neuropeptide Y-Y1 receptors delays initiation of kindling. *Eur. J. Neurosci.* 18, 768–774. doi: 10.1046/j.1460-9568.2003.02810.x

Berglund, M. M., Hipskind, P. A., and Gehlert, D. R. (2003). Recent developments in our understanding of the physiological role of PP-fold peptide receptor subtypes. *Exp. Biol. Med. (Maywood)* 228, 217–244. doi: 10.1177/153537020322800301

Colasante, G., Qiu, Y., Massimino, L., Di Berardino, C., Cornford, J. H., Snowball, A., et al. (2020). *In vivo* CRISPRa decreases seizures and rescues cognitive deficits in a rodent model of epilepsy. *Brain* 143, 891–905. doi: 10.1093/brain/awaa045

Costa-Ferro, Z. S., Vitola, A. S., Pedroso, M. F., Cunha, F. B., Xavier, L. L., Machado, D. C., et al. (2010). Prevention of seizures and reorganization of hippocampal functions by transplantation of bone marrow cells in the acute phase of experimental epilepsy. *Seizure* 19, 84–92. doi: 10.1016/j.seizure.2009.12.003

Cunningham, M., Cho, J. H., Leung, A., Savvidis, G., Ahn, S., Moon, M., et al. (2014). hPSC-derived maturing GABAergic interneurons ameliorate seizures and abnormal behavior in epileptic mice. *Cell Stem Cell* 15, 559–573. doi: 10.1016/j.stem.2014.10.006

DaCosta, J. C., Portuguez, M. W., Marinowic, D. R., Schilling, L. P., Torres, C. M., DaCosta, D. I., et al. (2018). Safety and seizure control in patients with

mesial temporal lobe epilepsy treated with regional superselective intra-arterial injection of autologous bone marrow mononuclear cells. *J. Tiss. Eng. Regen. Med.* 12, e648–e656. doi: 10.1002/term.2334

de Gois da Silva, M. L., da Silva, Oliveira, G. L., de Oliveira Bezerra, D., da Rocha, et al. (2018). Neurochemical properties of neurospheres infusion in experimental-induced seizures. *Tissue Cell* 54, 47–54. doi: 10.1016/j.tice.2018.08.002

do Prado-Lima, P. A. S., Onsten, G. A., de Oliveira, G. N., Brito, G. C., Ghilardi, I. M., de Souza, E. V., et al. (2019). The antidepressant effect of bone marrow mononuclear cell transplantation in chronic stress. *J. Psychopharmacol.* 33, 632–639. doi: 10.1177/0269881119841562

Dong, C., Zhao, W., Li, W., Lv, P., and Dong, X. (2013). Anti-epileptic effects of neuropeptide Y gene transfection into the rat brain. *Neural Regen. Res.* 8, 1307–1315. doi: 10.3969/j.issn.1673-5374.2013.14.007

Falcicchia, C., Paolone, G., Emerich, D. F., Lovisari, F., Bell, W. J., Fradet, T., et al. (2018). Seizure-Suppressant and Neuroprotective Effects of Encapsulated BDNF-Producing Cells in a Rat Model of Temporal Lobe Epilepsy. *Mol. Ther. Methods Clin. Dev.* 9, 211–224. doi: 10.1016/j.omtm.2018.03.001

Fukumura, S., Sasaki, M., Kataoka-Sasaki, Y., Oka, S., Nakazaki, M., Nagahama, H., et al. (2018). Intravenous infusion of mesenchymal stem cells reduces epileptogenesis in a rat model of status epilepticus. *Epilep. Res.* 141, 56–63. doi: 10.1016/j.eplepsyres.2018.02.008

Gorabi, A. M., Kiaie, N., Barreto, G. E., Read, M. I., Tafti, H. A., and Sahebkar, A. (2019). The Therapeutic Potential of Mesenchymal Stem Cell-Derived Exosomes in Treatment of Neurodegenerative Diseases. *Mol. Neurobiol.* 56, 8157–8167. doi: 10.1007/s12035-019-01663-0

Gotzsche, C. R., Nikitidou, L., Sorensen, A. T., Olesen, M. V., Sorensen, G., Christiansen, S. H., et al. (2012). Combined gene overexpression of neuropeptide Y and its receptor Y5 in the hippocampus suppresses seizures. *Neurobiol. Dis.* 45, 288–296. doi: 10.1016/j.nbd.2011.08.012

Guy, R., and Offen, D. (2020). Promising Opportunities for Treating Neurodegenerative Diseases with Mesenchymal Stem Cell-Derived Exosomes. *Biomolecules* 10:1320. doi: 10.3390/biom10091320

Ha, D. H., Kim, H. K., Lee, J., Kwon, H. H., Park, G. H., Yang, S. H., et al. (2020). Mesenchymal Stem/Stromal Cell-Derived Exosomes for Immunomodulatory Therapeutics and Skin Regeneration. *Cells* 9:1157. doi: 10.3390/cells9051157

Harrell, C. R., Jovicic, N., Djonov, V., Arsenijevic, N., and Volarevic, V. (2019). Mesenchymal Stem Cell-Derived Exosomes and Other Extracellular Vesicles as New Remedies in the Therapy of Inflammatory Diseases. *Cells* 8:1605. doi: 10.3390/cells8121605

Hlebokazov, F., Dakukina, T., Ihnatsenko, S., Kosmacheva, S., Potapnev, M., Shakhbazau, A., et al. (2017). Treatment of refractory epilepsy patients with autologous mesenchymal stem cells reduces seizure frequency: An open label study. *Adv. Med. Sci.* 62, 273–279. doi: 10.1016/j.advms.2016.12.004

Hlebokazov, F., Dakukina, T., Potapnev, M., Kosmacheva, S., Moroz, L., Misiuk, N., et al. (2021). Clinical benefits of single vs repeated courses of mesenchymal stem cell therapy in epilepsy patients. *Clin. Neurol. Neurosurg.* 207:106736. doi: 10.1016/j.clineuro.2021.106736

Issa, S., Shaimardanova, A., Valiullin, V., Rizvanov, A., and Solovyeva, V. (2020). Mesenchymal Stem Cell-Based Therapy for Lysosomal Storage Diseases and Other Neurodegenerative Disorders. *Front. Pharmacol.* 13:859516. doi: 10.3389/fphar.2022.859516

Kanter-Schlifke, I., Fjord-Larsen, L., Kusk, P., Angehagen, M., Wahlberg, L., and Kokaia, M. (2009). GDNF released from encapsulated cells suppresses seizure activity in the epileptic hippocampus. *Exp. Neurol.* 216, 413–419. doi: 10.1016/j.expneurol.2008.12.021

Kanter-Schlifke, I., Georgievska, B., Kirik, D., and Kokaia, M. (2007). Seizure suppression by GDNF gene therapy in animal models of epilepsy. *Mol. Ther.* 15, 1106–1113. doi: 10.1038/sj.mt.6300148

Katzel, D., Nicholson, E., Schorge, S., Walker, M. C., and Kullmann, D. M. (2014). Chemical-genetic attenuation of focal neocortical seizures. *Nat. Commun.* 5:3847. doi: 10.1038/ncomms4847

Kuramoto, S., Yasuhara, T., Agari, T., Kondo, A., Jing, M., Kikuchi, Y., et al. (2011). BDNF-secreting capsule exerts neuroprotective effects on epilepsy model of rats. *Brain Res.* 1368, 281–289. doi: 10.1016/j.brainres.2010.10.054

Leal, M. M., Costa-Ferro, Z. S., Souza, B. S., Azevedo, C. M., Carvalho, T. M., Kaneto, C. M., et al. (2014). Early transplantation of bone marrow mononuclear cells promotes neuroprotection and modulation of inflammation after status epilepticus in mice by paracrine mechanisms. *Neurochem. Res.* 39, 259–268. doi: 10.1007/s11064-013-1217-7

Ledri, L. N., Melin, E., Christiansen, S. H., Gotzsche, C. R., Cifra, A., Woldbye, D. P., et al. (2016). Translational approach for gene therapy in epilepsy: Model system and unilateral overexpression of neuropeptide Y and Y2 receptors. *Neurobiol. Dis.* 86, 52–61. doi: 10.1016/j.nbd.2015.11.014

Lieb, A., Weston, M., and Kullmann, D. M. (2019). Designer receptor technology for the treatment of epilepsy. *EBioMedicine* 43, 641–649. doi: 10.1016/j.ebiom.2019.04.059

Liu, Y., Guo, J., Zhang, P., Zhang, S., Chen, P., Ma, K., et al. (2004). Bone marrow mononuclear cell transplantation into heart elevates the expression of angiogenic factors. *Microvasc. Res.* 68, 156–160. doi: 10.1016/j.mvr.2004.06.008

Long, Q., Upadhya, D., Hattiangady, B., Kim, D. K., An, S. Y., Shuai, B., et al. (2017). Intranasal MSC-derived A1-exosomes ease inflammation, and prevent abnormal neurogenesis and memory dysfunction after status epilepticus. *Proc. Natl. Acad. Sci. U S A* 114, E3536–E3545. doi: 10.1073/pnas.1703920114

McCown, T. J. (2006). Adeno-associated virus-mediated expression and constitutive secretion of galanin suppresses limbic seizure activity *in vivo*. *Mol. Ther.* 14, 63–68. doi: 10.1016/j.ymthe.2006.04.004

Melin, E., Nanobashvili, A., Avdic, U., Gotzsche, C. R., Andersson, M., Woldbye, D. P. D., et al. (2019). Disease Modification by Combinatorial Single Vector Gene Therapy: A Preclinical Translational Study in Epilepsy. *Mol. Ther. Methods Clin. Dev.* 15, 179–193. doi: 10.1016/j.omtm.2019.09.004

Milczarek, O., Jarocha, D., Starowicz-Filip, A., Kwiatkowski, S., Badyra, B., and Majka, M. (2018). Multiple Autologous Bone Marrow-Derived CD271(+) Mesenchymal Stem Cell Transplantation Overcomes Drug-Resistant Epilepsy in Children. *Stem Cells Transl. Med.* 7, 20–33. doi: 10.1002/sctm.17-0041

Mohammed, A. S., Ewais, M. M., Tawfik, M. K., and Essawy, S. S. (2014). Effects of intravenous human umbilical cord blood mesenchymal stem cell therapy versus gabapentin in pentylenetetrazole-induced chronic epilepsy in rats. *Pharmacology* 94, 41–50. doi: 10.1159/000365219

Montzka, K., Lassonczyk, N., Tschoke, B., Neuss, S., Fuhrmann, T., Franzen, R., et al. (2009). Neural differentiation potential of human bone marrow-derived mesenchymal stromal cells: misleading marker gene expression. *BMC Neurosci.* 10:16. doi: 10.1186/1471-2202-10-16

Mukhamedshina, Y., Shulman, I., Ogurcov, S., Kostennikov, A., Zakirova, E., Akhmetzyanova, E., et al. (2019). Mesenchymal Stem Cell Therapy for Spinal Cord Contusion: A Comparative Study on Small and Large Animal Models. *Biomolecules* 9:811. doi: 10.3390/biom9120811

Natarajan, G., Leibowitz, J. A., Zhou, J., Zhao, Y., McElroy, J. A., King, M. A., et al. (2017). Adeno-associated viral vector-mediated preprosomatostatin expression suppresses induced seizures in kindled rats. *Epilepsy Res* 130, 81–92. doi: 10.1016/j.eplepsyres.2017.01.002

Nikitidou, L., Torp, M., Fjord-Larsen, L., Kusk, P., Wahlberg, L. U., and Kokaia, M. (2014). Encapsulated galanin-producing cells attenuate focal epileptic seizures in the hippocampus. *Epilepsia* 55, 167–174. doi: 10.1111/epi.12470

Noe, F., Pool, A. H., Nissinen, J., Gobbi, M., Bland, R., Rizzi, M., et al. (2008). Neuropeptide Y gene therapy decreases chronic spontaneous seizures in a rat model of temporal lobe epilepsy. *Brain* 131(Pt 6), 1506–1515. doi: 10.1093/brain/awn079

Paolone, G., Falcicchia, C., Lovisari, F., Kokaia, M., Bell, W. J., Fradet, T., et al. (2019). Long-Term, Targeted Delivery of GDNF from Encapsulated Cells Is Neuroprotective and Reduces Seizures in the Pilocarpine Model of Epilepsy. *J. Neurosci.* 39, 2144–2156. doi: 10.1523/JNEUROSCI.0435-18.2018

Park, G. Y., Lee, E. M., Seo, M. S., Seo, Y. J., Oh, J. S., Son, W. C., et al. (2015). Preserved Hippocampal Glucose Metabolism on 18F-FDG PET after Transplantation of Human Umbilical Cord Blood-derived Mesenchymal Stem Cells in Chronic Epileptic Rats. *J. Kor. Med. Sci.* 30, 1232–1240. doi: 10.3346/jkms.2015.30.9.1232

Perucca, P., Bahlo, M., and Berkovic, S. F. (2020). The Genetics of Epilepsy. *Annu. Rev. Genom. Hum. Genet.* 21, 205–230. doi: 10.1146/annurev-genom-120219-074937

Powell, K. L., Fitzgerald, X., Shallue, C., Jovanovska, V., Klugmann, M., Von Jonquieres, G., et al. (2018). Gene therapy mediated seizure suppression in Genetic Generalised Epilepsy: Neuropeptide Y overexpression in a rat model. *Neurobiol. Dis.* 113, 23–32. doi: 10.1016/j.nbd.2018.01.016

Ronzitti, G., Gross, D. A., and Mingozzi, F. (2020). Human Immune Responses to Adeno-Associated Virus (AAV) Vectors. *Front. Immunol.* 11:670. doi: 10.3389/fimmu.2020.00670

Salem, N. A., El-Shamarka, M., Khadrawy, Y., and El-Shebiney, S. (2018). New prospects of mesenchymal stem cells for ameliorating temporal lobe epilepsy. *Inflammopharmacology* 26, 963–972. doi: 10.1007/s10787-018-0456-2

Sheng, J., Liu, S., Qin, H., Li, B., and Zhang, X. (2018). Drug-Resistant Epilepsy and Surgery. *Curr. Neuropharmacol.* 16, 17–28. doi: 10.2174/1570159X15666170504123316

Shimazaki, K., Kobari, T., Oguro, K., Yokota, H., Kasahara, Y., Murashima, Y., et al. (2019). Hippocampal GAD67 Transduction Using rAAV8 Regulates Epileptogenesis in EL Mice. *Mol. Ther. Methods Clin. Dev.* 13, 180–186. doi: 10.1016/j.omtm.2018.12.012

Shrestha, R. P., Qiao, J. M., Shen, F. G., Bista, K. B., Zhao, Z. N., and Yang, J. (2014). Intra-Spinal Bone Marrow Mononuclear Cells Transplantation Inhibits the Expression of Nuclear Factor-kappaB in Acute Transection Spinal Cord Injury in Rats. *J. Kor. Neurosurg. Soc.* 56, 375–382. doi: 10.3340/jkns.2014.56.5.375

Snowball, A., Chabrol, E., Wykes, R. C., Shekh-Ahmad, T., Cornford, J. H., Lieb, A., et al. (2019). Epilepsy Gene Therapy Using an Engineered Potassium Channel. *J. Neurosci.* 39, 3159–3169. doi: 10.1523/JNEUROSCI.1143-18.2019

Sorensen, A. T., Kanter-Schlifke, I., Carli, M., Balducci, C., Noe, F., During, M. J., et al. (2008). NPY gene transfer in the hippocampus attenuates synaptic plasticity and learning. *Hippocampus* 18, 564–574. doi: 10.1002/hipo.20415

Stafstrom, C. E., and Carmant, L. (2015). Seizures and epilepsy: an overview for neuroscientists. *Cold Spring Harb. Perspect. Med.* 5:a022426. doi: 10.1101/cshperspect.a022426

Szczepanik, E., Mierzewska, H., Antczak-Marach, D., Figiel-Dabrowska, A., Terczynska, I., Tryfon, J., et al. (2020). Intrathecal Infusion of Autologous Adipose-Derived Regenerative Cells in Autoimmune Refractory Epilepsy: Evaluation of Safety and Efficacy. *Stem Cells Int.* 2020:7104243. doi: 10.1155/2020/7104243

Szczygiel, J. A., Danielsen, K. I., Melin, E., Rosenkranz, S. H., Pankratova, S., Ericsson, A., et al. (2020). Gene Therapy Vector Encoding Neuropeptide Y and Its Receptor Y2 for Future Treatment of Epilepsy: Preclinical Data in Rats. *Front. Mol. Neurosci.* 13:232. doi: 10.3389/fnmol.2020.603409

Thijs, R. D., Surges, R., O'Brien, T. J., and Sander, J. W. (2019). Epilepsy in adults. *Lancet* 393, 689–701. doi: 10.1016/S0140-6736(18)32596-0

Upadhya, D., Hattiangady, B., Castro, O. W., Shuai, B., Kodali, M., Attaluri, S., et al. (2019). Human induced pluripotent stem cell-derived MGE cell grafting after status epilepticus attenuates chronic epilepsy and comorbidities *via* synaptic integration. *Proc. Natl. Acad. Sci. U S A* 116, 287–296. doi: 10.1073/pnas.1814185115

Vizoso, F. J., Eiro, N., Cid, S., Schneider, J., and Perez-Fernandez, R. (2017). Mesenchymal Stem Cell Secretome: Toward Cell-Free Therapeutic Strategies in Regenerative Medicine. *Int. J. Mol. Sci.* 18, 1852. doi: 10.3390/ijms18091852

Waldau, B., Hattiangady, B., Kuruba, R., and Shetty, A. K. (2010). Medial ganglionic eminence-derived neural stem cell grafts ease spontaneous seizures and restore GDNF expression in a rat model of chronic temporal lobe epilepsy. *Stem Cells* 28, 1153–1164. doi: 10.1002/stem.446

Wang, L., Zhao, Y., Pan, X., Zhang, Y., Lin, L., Wu, Y., et al. (2021). Adipose-derived stem cell transplantation improves learning and memory *via* releasing neurotrophins in rat model of temporal lobe epilepsy. *Brain Res.* 1750:147121. doi: 10.1016/j.brainres.2020.147121

Wei, W., Li, L., Deng, L., Wang, Z. J., Dong, J. J., Lyu, X. Y., et al. (2020). Autologous Bone Marrow Mononuclear Cell Transplantation Therapy Improved Symptoms in Patients with Refractory Diabetic Sensorimotor Polyneuropathy *via* the Mechanisms of Paracrine and Immunomodulation: A Controlled Study. *Cell Transplant.* 29:963689720949258. doi: 10.1177/0963689720949258

Weinberg, M. S., and McCown, T. J. (2013). Current prospects and challenges for epilepsy gene therapy. *Exp. Neurol.* 244, 27–35. doi: 10.1016/j.expneurol.2011.10.003

Wykes, R. C., Heeroma, J. H., Mantoan, L., Zheng, K., MacDonald, D. C., Deisseroth, K., et al. (2012). Optogenetic and potassium channel gene therapy in a rodent model of focal neocortical epilepsy. *Sci. Transl. Med.* 4:161ra152. doi: 10.1126/scitranslmed.3004190

Xian, P., Hei, Y., Wang, R., Wang, T., Yang, J., Li, J., et al. (2019). Mesenchymal stem cell-derived exosomes as a nanotherapeutic agent for amelioration of inflammation-induced astrocyte alterations in mice. *Theranostics* 9, 5956–5975. doi: 10.7150/thno.33872

Xunian, Z., and Kalluri, R. (2020). Biology and therapeutic potential of mesenchymal stem cell-derived exosomes. *Cancer Sci.* 111, 3100–3110. doi: 10.1111/cas.14563

Yoshihara, T., Ohta, M., Itokazu, Y., Matsumoto, N., Dezawa, M., Suzuki, Y., et al. (2007). Neuroprotective effect of bone marrow-derived mononuclear cells promoting functional recovery from spinal cord injury. *J. Neurotrauma* 24, 1026–1036. doi: 10.1089/neu.2007.132R

Young, D., Fong, D. M., Lawlor, P. A., Wu, A., Mouravlev, A., McRae, M., et al. (2014). Adenosine kinase, glutamine synthetase and EAAT2 as gene therapy targets for temporal lobe epilepsy. *Gene Ther.* 21, 1029–1040. doi: 10.1038/gt.2014.82

Zhang, F., Zhao, W., Li, W., Dong, C., Zhang, X., Wu, J., et al. (2013). Neuropeptide Y gene transfection inhibits post-epileptic hippocampal synaptic reconstruction. *Neural Regen. Res.* 8, 1597–1605. doi: 10.3969/j.issn.1673-5374.2013.17.008

Conflict of Interest: The authors declare that the research was conducted in the absence of any commercial or financial relationships that could be construed as a potential conflict of interest.

Publisher's Note: All claims expressed in this article are solely those of the authors and do not necessarily represent those of their affiliated organizations, or those of the publisher, the editors and the reviewers. Any product that may be evaluated in this article, or claim that may be made by its manufacturer, is not guaranteed or endorsed by the publisher.

frontiers | Frontiers in Molecular Neuroscience

TYPE Original Research
PUBLISHED 13 October 2022
DOI 10.3389/fnmol.2022.974784

OPEN ACCESS

EDITED BY
Gary Patrick Brennan,
University College Dublin, Ireland

REVIEWED BY
Casper René Gøtzsche,
University of Copenhagen, Denmark
Mitesh Dwivedi,
Uka Tarsadia University, India
Maria Concetta Geloso,
Catholic University of the Sacred Heart, Rome, Italy

*CORRESPONDENCE
Meinrad Drexel
meinrad.drexel@i-med.ac.at
Günther Sperk
guenther.sperk@i-med.ac.at

SPECIALTY SECTION
This article was submitted to Brain Disease Mechanisms, a section of the journal Frontiers in Molecular Neuroscience

RECEIVED 21 June 2022
ACCEPTED 26 September 2022
PUBLISHED 13 October 2022

CITATION
Drexel M and Sperk G (2022) Seizure-induced overexpression of NPY induces epileptic tolerance in a mouse model of spontaneous recurrent seizures.
Front. Mol. Neurosci. 15:974784.
doi: 10.3389/fnmol.2022.974784

Seizure-induced overexpression of NPY induces epileptic tolerance in a mouse model of spontaneous recurrent seizures

Meinrad Drexel* and Günther Sperk*

Department of Pharmacology, Medical University Innsbruck, Innsbruck, Austria

Epileptic seizures result in pronounced over-expression of neuropeptide Y (NPY). *In vivo* and *in vitro* studies revealed that NPY exerts potent anticonvulsive actions through presynaptic Y2 receptors by suppressing glutamate release from principal neurons. We now investigated whether seizure-induced over-expression of NPY contributes to epileptic tolerance induced by preceding seizures. We used a previously established animal model based on selective inhibition of GABA release from parvalbumin (PV)-containing interneurons in the subiculum in mice. The animals present spontaneous recurrent seizures (SRS) and clusters of interictal spikes (IS). The frequency of SRS declined after five to six weeks, indicating development of seizure tolerance. In interneurons of the subiculum and sector CA1, SRS induced over-expression of NPY that persisted there for a prolonged time despite of a later decrease in SRS frequency. In contrast to NPY, somatostatin was not overexpressed in the respective axon terminals. Contrary to interneurons, NPY was only transiently expressed in mossy fibers. To demonstrate a protective function of endogenous, over-expressed NPY, we injected the selective NPY-Y2 receptor antagonist JNJ 5207787 simultaneously challenging the mice by a low dose of pentylenetetrazol (PTZ, 30 or 40 mg/kg, i.p.). In control mice, neither PTZ nor PTZ plus JNJ 5207787 induced convulsions. In mice with silenced GABA/PV neurons, PTZ alone only modestly enhanced EEG activity. When we injected JNJ 5207787 together with PTZ (either dose) the number of seizures, however, became significantly increased. In addition, in the epileptic mice CB1 receptor immunoreactivity was reduced in terminal areas of basket cells pointing to reduced presynaptic inhibition of GABA release from these neurons. Our experiments demonstrate that SRS result in overexpression of NPY in hippocampal interneurons. NPY overexpression persists for several weeks and may be related to later decreasing SRS frequency. Injection of the Y2 receptor antagonist JNJ 5207787 prevents this protective action of NPY only

when release of the peptide is triggered by injection of PTZ and induces pronounced convulsions. Thus, over-expressed NPY released "on demand" by seizures may help terminating acute seizures and may prevent from recurrent epileptic activity.

KEYWORDS

neuropeptide Y, somatostatin, CB1 receptor, subiculum, hippocampus, ischemic tolerance, parvalbumin, O-LM cells

Introduction

Ischemic or epileptic tolerance are mechanisms contributing to termination of seizures and protect from exacerbation of epilepsy (Gidday, 2006; Simon et al., 2007). Epileptic tolerance may be caused by reorganization of neuronal circuitries or expression of endogenous anticonvulsive compounds. For example, erythropoietin (Sakanaka et al., 1998), adenosine (Schubert and Kreutzberg, 1993), neurosteroids (Biagini et al., 2010; Lawrence et al., 2010) and heat shock proteins (HSP) over-expressed after ischemia or epileptic seizures protect from subsequent seizures (Chang et al., 2014). Seizures also significantly activate GABA-ergic interneurons and induce augmented expression of the GABA synthesizing enzyme glutamate decarboxylase 67 (GAD-1) and of neuropeptides contained in GABA neurons (Houser et al., 1986; Marksteiner and Sperk, 1988; Feldblum et al., 1990; Sperk et al., 1992).

Particularly the expression of neuropeptide Y (NPY) is strongly enhanced in animal models of epilepsy and human temporal lobe epilepsy (TLE). Kainic acid (KA)-induced seizures or kindling induce a widespread and lasting over-expression of NPY in the hippocampus and in cortical areas (Marksteiner and Sperk, 1988; Schwarzer et al., 1996; Drexel et al., 2012). In the dentate gyrus of the hippocampus, its expression is transient in granule cells but lasting in interneurons (Gruber et al., 1994) and associated with transient upregulation of Y2 but not Y1 receptors in mossy fibers (Röder et al., 1996; Kofler et al., 1997; Schwarzer et al., 1998; Furtinger et al., 2001). Seizures markedly enhance expression of the peptide also in interneurons of the hippocampus proper and in the subiculum (Vezzani and Sperk, 2004; Drexel et al., 2012). NPY and Y2 receptor agonists, like NPY (3-36) as well as viral vectors expressing NPY are strongly anticonvulsive when applied *in vitro* or in living animals (Woldbye et al., 1996, 2010; Richichi et al., 2004; El Bahh et al., 2005; Ledri et al., 2015). This activity is mediated by potent inhibition of glutamate release through NPY-Y2 receptors located presynaptically on glutamate neurons (Colmers et al., 1991; Greber et al., 1994). There is also evidence that endogenous NPY may be involved in seizure control. Knock out of NPY or of Y2 receptors makes mice more susceptible to epileptic seizures (Baraban et al., 1997; El Bahh et al., 2005) and, in reverse, transgenic rats over-expressing NPY are less susceptible to convulsant drugs or kindling (Vezzani et al., 2002). A protective role of endogenous, over-expressed NPY has been documented in seizures induced by elevated temperatures in 10–11 days old rat pups (Dubé et al., 2005). Whereas in naïve rat pups seizures were induced by rising the surrounding temperature to 41°C, the threshold for initiating seizures increased by one and two°C when hyperthermia was repeated after 4 and 8 h, respectively, indicating that the rats became somewhat resistant to the rise in temperature. Concomitantly with the first exposure to hyperthermia, an increase of NPY mRNA expression was observed in interneurons of the dentate hilus, and pretreatment with the Y2 receptor antagonist BIIE0246 antagonized the NPY mediated epileptic tolerance (Dubé et al., 2005).

We now investigated whether endogenous NPY released after its over-expression during spontaneous recurrent seizures (SRS) may protect from subsequent seizures and thereby may induce epileptic tolerance. We used an animal model of increased seizure susceptibility after silencing parvalbumin (PV) interneurons in the subiculum and show increased expression of NPY and precipitation of acute seizures by antagonizing NPY-Y2 receptors. The experiments indicate that NPY over-expressed by SRS contributes to epileptic tolerance by activating Y2 receptors. Analogous to our previous studies (Drexel et al., 2012, 2017) we focused also in our present study on the ventral subiculum/hippocampus. We aimed to target the subiculum as the primary output region of the hippocampus, which is anatomically closely related to the ventral hippocampus in rodents and better accessible for the required vector injections. In addition is the ventral hippocampus a primary epileptogenic zone in rat models with high relevance for human TLE (Buckmaster et al., 2022).

Besides NPY a variety of other parameters of GABA-ergic neurons, e.g., glutamate decarboxylase (GAD1 and 2), somatostatin (SOM) or cholecystokinin (CCK-8) are dynamically altered in animal models of epilepsy (Schwarzer et al., 1996). A loss of dynorphin contained in mossy fibers is associated with the seizure presentation which can be

overcome by substitution of the peptide by kappa opioid agonists (Solbrig et al., 2006a,b). Another possible mechanism for an endogenous adaptive and anticonvulsive mechanism may be down-regulation of the cannabinoid receptor CB1. Endocannabinoids are released by CCK-8 containing basket cells and can retrogradely inhibit GABA release through presynaptic CB1 receptors and thereby have pro-convulsive effect (Katona et al., 1999). After KA-induced epilepsy that is associated with a loss of subicular PV neurons, we observed sprouting of SOM neurons in the outer molecular layer of the subiculum (Drexel et al., 2017), which may serve an endogenous anticonvulsive function (Vezzani and Hoyer, 1999). Thus, in the search of possible alternative mechanisms mediating epileptic tolerance we investigated VGAT-, SOM-IR and mRNA expression, dynorphin-IR and CB1-IR in the hippocampus of mice injected with AAV-*TeLC* or AAV-*GFP*.

Materials and methods

Mice

Animal experiments were conducted according to national guidelines and European Community laws and were approved by the Committee for Animal Protection of the Austrian Ministry of Science. PV-cre transgenic mice [Pvalb$^{TM1(cre)Arbr}$; Jackson Laboratories, Farmington, CT, United States, obtained through Charles River, Sulzfeld, Germany], expressing Cre-recombinase under the PV promoter, were maintained on a C57BL/6N background. All mice were housed in groups of 3–5 in single ventilated cages under standard laboratory conditions (12/12 h light/dark cycle, light turns on at 06:30 AM) and had free access to food and water. For the experiments, 10–14 weeks old heterozygous male mice [Pvalb$^{TM1(cre)Arbr\pm}$] were used.

Vectors

Adenovirus associated virus vector (AAV1/2) containing either the gene for tetanus toxin light chain (TeLC) fused with a green fluorescence protein (GFP) tag or GFP alone, with the reading frames inverted in a flip-excision (FLEX) cassette (AAV-*TeLC* and AAV-*GFP*, respectively) and a cytomegalovirus (CMV) immediate early enhancer/chicken β-actin promoter were prepared as described (Murray et al., 2011; Drexel et al., 2017).

Surgery and vector injection

Anesthesia and stereotaxic surgeries were performed as described in detail previously (Drexel et al., 2017). One hour prior to surgery, the mice were injected with the analgesic drug carprofen (5 mg/kg, s.c.; Rimadyl, Pfizer, United States). They were then anesthetized with 150 mg/kg i.p. ketamine (Ketasol, stock solution 50 mg/ml, Ogris Pharma Vertriebs-GmbH, Wels, Austria) and maintained anesthetized under 1–3% sevoflurane (Sevorane, Abbott, Vienna, Austria) applied through a veterinary anesthesia mask with oxygen (400 ml/min) as a carrier gas. For surgery, the anesthetized mice were placed into a stereotaxic frame (David-Kopf Instruments, Tujunga, CA, United States) and the skin above the skull was opened. A telemetric EEG transmitter (TA10EA-F20, Data Sciences International, Arden Hills, MN, United States) was inserted into a subcutaneous pocket at the abdominal wall and the electrode wires were pulled through a subcutaneous channel from the pocket to the skull, and the pocket was sutured. Bilateral holes were drilled for AAV-vector injection and insertion of a depth-electrode (coordinates from bregma in mm: posterior, 3.8; lateral, 3.5) and for the epidural reference electrode (posterior, 2.0; lateral, 1.6).

We injected the AAV vectors (1.5 μl), AAV-*TeLC* (titer: 2.4×10^{10}/ml) or AAV-*GFP* (1.4×10^{11}/ml for pAM-FLEX-*GFP*, for controls) unilaterally at the above coordinates into the left ventral CA1/subiculum (3.5 mm deep). For telemetric EEG recordings, we implanted a tungsten depth electrode (Cat. no 577100; Science Products GmbH, Hofheim, Germany) into the left ventral subiculum (3.0 mm deep) and attached, as reference electrode, a stainless-steel screw (M1*2, Hummer und Rieß GmbH, Nürnberg, Germany) epidurally to the skull (posterior, 2.0, right, 1.6). Electrodes were fixed to the skull with dental cement (Paladur, Heraeus Kulzer, Henry Schein, Innsbruck, Austria). After surgery and during EEG recording, the mice were single housed.

C57BL/6N wild-type mice (Charles River, Sulzfeld, Germany) or PV-cre transgenic mice injected with AAV-*GFP* into CA1/subiculum were used as controls.

EEG recordings and video monitoring

EEGs were recorded continuously using a telemetry system (Dataquest A.R.T. Gold 4.33 Acquisition, Data Sciences International, Arden Hills, MN, United States). For recording motor seizures in addition to EEG seizures, continuous video recordings were performed with Axis 221 network cameras (Axis communications AB, Lund, Sweden) and, during darkness, under infrared illumination (Conrad Electronic GmbH, Wels, Austria). EEGs were recorded at a sampling rate of 1,000 Hz without *a priori* filter cut-off and saved on external hard disk drives.

EEG traces of local field potentials were visually inspected by two independent observers using the Dataquest A.R.T. Gold 4.33 Analysis software. We defined seizures as EEG segments with continuous high frequency activity with an amplitude of at least twice the baseline amplitude, a duration of at least

10 s, and the presence of a post-ictal depression (EEG-signal below baseline amplitude). Clusters of interictal spikes (IS) were defined as a series of at least 5 high amplitude (at least 2 times baseline) discharges not more than 60 s apart.

After terminating EEG recordings 42 (Experiment 1) or 102 days (Experiment 2) after vector injection, the mice were deeply anesthetized with thiopental (150 mg/kg; Sandoz, Austria) and perfused *via* the left ventricle of the heart with 25 ml 50 mM phosphate-buffered saline (PBS, room temperature) followed by 100 ml ice-cold 4% paraformaldehyde (PFA). The brains were then removed from the skulls, post-fixed in 4% PFA/PBS (cold room, 90 min) and then transferred to 20% sucrose/PBS (cold room, over-night). The brains were then snap-frozen in −70°C isopentane (Merck, Darmstadt, Germany, 3 min) and kept in sealed vials at −70°C until they were cut in a cryostat-microtome (Carl Zeiss AG, Vienna, Austria). Microtome sections (40 μm) were maintained in PBS/0.01% sodium azide at cold room temperature (4°C) until they were processed.

Evaluation of motor seizures

All seizures observed by EEG were investigated by video recordings for their behavioral correlate. Seizure rating was done in accordance with that used for KA-injected rats (Sperk et al., 1983). All EEG seizures corresponded to limbic motor seizures (rating 3–4; data not shown).

Experimental approach

The goal of the experiments was to induce spontaneous seizures by selective, locally restricted silencing of PV containing interneurons by unilateral, local injection of AAV-*TeLC* into the ventral subiculum/CA1 area. We investigated two primary parameters in these mice: 1. Temporal patterns of SRS and of IS clusters, and 2. Expression of NPY-immunoreactivity (IR) in interneurons of the hippocampus and in mossy fibers of the dentate gyrus.

We performed three principal experiments (focused on NPY expression in relation to SRS) and one experiment investigating the role of the Y2 receptor antagonist JNJ 5207787.

Experiment 1

We injected 22 mice with the AAV-*TeLC* vector into the ventral subiculum/CA1, monitored EEG and behavioral activity for 42 days (experimental details see below), sacrificed the mice and processed their brains for NPY-IR. Three mice lost their electrodes at earlier intervals and were therefore sacrificed at these points (**Figure 1A** shows 12 representative AAV-*TeLC* mice). Five mice were injected with AAV-*GFP* as controls and treated in the same way. They did not develop SRS or IS clusters. The numbers of animals are based on our previous experiments (Drexel et al., 2017) taking in account that about one third of mice will not show SRS.

Experiment 2

In the first experiment, we suspected that the frequency of SRS and IS clusters declined at later intervals after vector injection. For investigating this more closely, we performed a second experiment also silencing PV neurons in the ventral subiculum/CA1 by local AAV-*TeLC* injections. We injected six mice with AAV-*TeLC* and, according to our previous protocol (Drexel et al., 2017), triggered the development of SRS and IS clusters by a single low dose injection of PTZ (40 mg/kg, i.p.) 7 days after AAV-injection. All AAV-*TeLC*-injected mice developed SRS and IS (see **Figure 1B**). Five AAV-*GFP* injected mice were included as controls. None of them developed acute seizures upon PTZ application, SRS or IS. All mice were sacrificed after 102 days and their brains were processed for immunohistochemistry. The numbers of animals had been chosen according to our previous experiment using PTZ challenge after AAV-*TeLC* injection, resulting in 100% of mice developing SRS (Drexel et al., 2017).

Experiment 3

This experiment was performed for examining NPY mRNA by *in situ*-hybridization in the brains. Nine mice were injected with AAV-*TeLC* and with 40 mg/kg PTZ after 7 days. All mice developed SRS and IS clusters (not shown) and were sacrificed after 42 days. Eight mice were injected with AAV-*GFP* as controls; none of these mice developed acute seizures after PTZ injection, SRS or IS. The brains were snap frozen and processed for NPY mRNA *in situ* hybridization. The numbers of mice were chosen according to our previous experiments on NPY expression after KA-induced seizures (Drexel et al., 2012).

Experiment 4: Injection of the Y2 receptor antagonist JNJ 5207787

Mice were injected with the AAV-*TeLC* (n = 16) or with the AAV-*GFP* (n = 8) into sector CA1/subiculum. Recording electrodes were *placed* as described above and EEG recordings were started immediately after vector injection. One group of AAV-*TeLC*-injected mice received the non-peptidergic Y2 receptor antagonist JNJ 5207787 (30 mg/kg; Tocris, *N*-(1-Acetyl-2,3-dihydro-1H-indol-6-yl)-3-(3-cyano-phenyl)-*N*-[1-(2-cyclopentyl-ethyl)-piperidin-4yl]-acrylamide, Cat. No. 4018/10, Biotechne, Abingdon, United Kingdom) dissolved in 0.5 ml 2-hydroxy propyl-β-cyclodextrin (20%) in saline (80%) i.p. (n = 4) or 0.5 ml solvent alone i.p. (n = 3), and (after 30 min) 30 mg/kg i.p. PTZ in saline. A second group was injected with 0.5 ml solvent (n = 4) or with JNJ 5207787 (n = 5) followed by 40 mg/kg i.p. PTZ after 30 min. We injected also untreated controls (n = 8) and AAV-*GFP*-injected mice (n = 8) with JNJ 5207787 followed by 30 mg/kg PTZ and 40 mg/kg

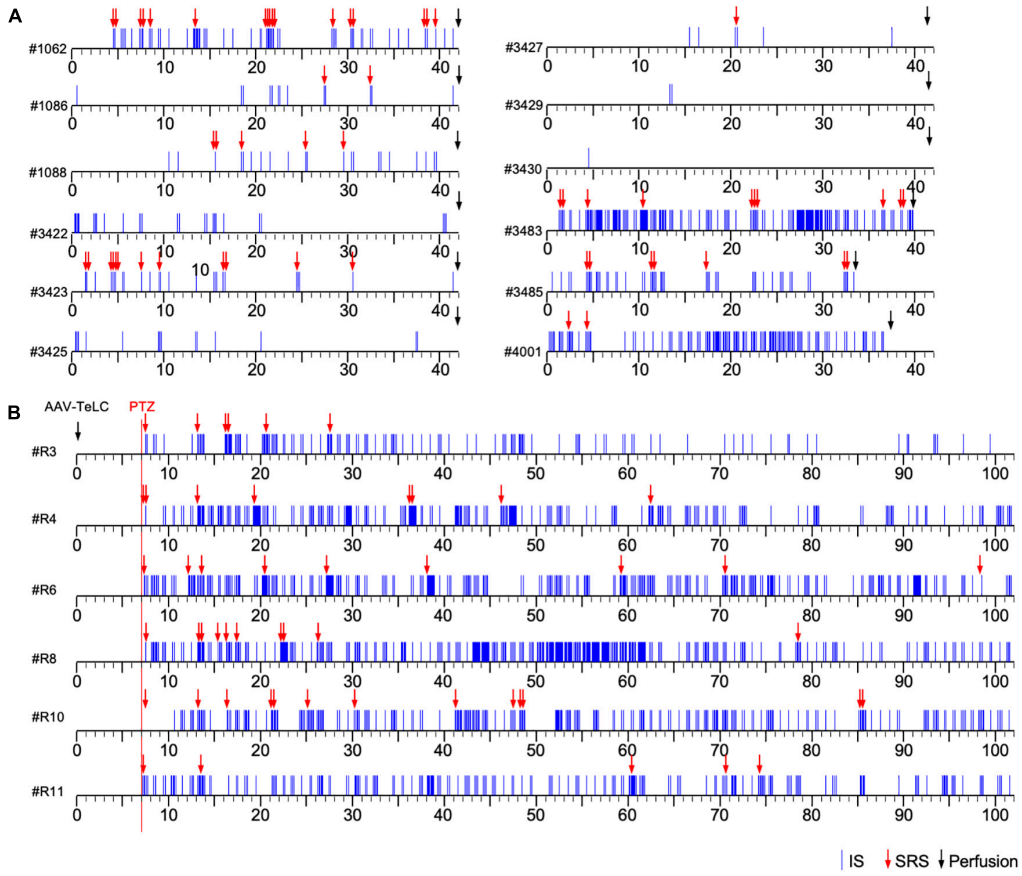

FIGURE 1
Development of clusters of interictal spikes (IS) and spontaneous recurrent seizures (SRS) in PV-cre mice after unilateral injection of AAV-*TeLC* into the ventral subiculum/area CA1. **(A)** Events of IS clusters (blue lines) and of SRS (red arrows) are listed for twelve representative mice; the respective identification code is shown left to the time scale. Panels **(A,B)** show the results of Experiments 1 and 2, respectively (see section "Experimental approach"). In contrast to Experiment 1 **(A)**, in Experiment 2 **(B)** EEG recordings were started at day seven after vector injection (red vertical line). About 30 min later, mice were injected with a low dose of PTZ (40 mg/kg; red arrows indicate acute PTZ-induced seizures). Besides acute seizures, PTZ induced development of SRS and IS clusters in all AAV-*TeLC*-injected mice but not in AAV-*GFP*-injected mice (not shown). In Experiment 1, mice were sacrificed after 42 days (except three mice that lost their electrodes earlier; **(A)**. In Experiment 2, mice were monitored for 102 days **(B)**. Both groups of mice were sacrificed immediately after terminating EEG recordings and their brains were processed for NPY-IR. Five AAV-*GFP*-injected mice were included as controls in each experiment. They developed no SRS or IS clusters (not shown).

PTZ, respectively. EEG recordings were continued immediately after PTZ injections. JNJ 5207787 was injected 30 min prior to PTZ due to its much slower uptake to the brain compared to PTZ. JNJ 5207787 has been developed by Bonaventure et al. It is more than 100 times more active toward Y2 than Y1, Y4 or Y5 receptors *in vitro* and penetrates the brain at the dose applied (Bonaventure et al., 2004). The doses for PTZ have been optimized recently (Drexel et al., 2017).

Immunohistochemistry

Immunohistochemistry for NPY was performed on free-floating, 40 µm thick horizontal 4% PFA-fixed sections (obtained in Experiment 1) using indirect peroxidase labeling as described before (Sperk et al., 2012; Wood et al., 2016). In brief, horizontal sections were incubated free-floating with 10% normal goat or horse serum (Biomedica, Vienna, Austria) in Tris–HCl buffered saline (TBS; 50 mM, pH = 7.2) containing 0.4% Triton X-100 (TBS-Triton) for 90 min and then incubated with a rabbit NPY antiserum raised toward the peptide coupled to ovalbumin (1: 1,000; (Marksteiner and Sperk, 1988) at room temperature for 16 h) and subsequently washed with TBS-Triton. The reaction product was visualized by incubation with a horseradish peroxidase (HRP)-coupled secondary antibody (1:250, goat anti-rabbit P0448; Dako, Vienna, Austria; 1:500; room temperature for 150 min). After washing with TBS, HRP bound to the secondary antibodies was reacted with 0.05% diaminobenzidine tetrahydrochloride dihydrate (DAB, Fluka, Sigma-Aldrich Handels GmbH, Vienna, Austria) and 0.005% H_2O_2 as substrate. Sections were then washed in TBS, mounted on gelatin-coated glass slides in 55% ethanol and allowed to dry

overnight. After dehydration in ethanol and clearing in butyl-acetate, they were coverslipped using Eukitt mounting medium (Gröpl, Vienna, Austria).

Using sections obtained in Experiment 1, we furthermore studied possible changes in the expression of VGAT, SOM, dynorphin and CB1. Immunohistochemistry for SOM and dynorphin was performed as described previously using the same antibodies (Schwarzer et al., 1996; Pirker et al., 2001). VGAT-IR and CB1-IR were assessed by immunofluorescence using respective antibodies [VGAT (rabbit), donated by Prof. R. Edwards, University of California San Francisco, CA; 1:2,500 dilution (Sperk et al., 2003); CB1, CB1-Rb-Af380 (rabbit, RRID:AB_2571591, Hölzel Diagnostika Handels GmbH, Köln, Germany), dilution 1:1,000].

In situ hybridization

NPY *in situ* hybridization was done in 20 μm thick horizontal microtome sections obtained from snap frozen sections. Tissue preparation and *in situ* hybridization was performed as described in detail previously (Drexel et al., 2012). Densitometry was done as described in detail before (Drexel et al., 2013). *In situ* hybridization for SOM and VGAT mRNAs was performed as described previously (Schwarzer et al., 1996; Sperk et al., 2003).

Semi-quantitative analysis of NPY-IR in the molecular layer of the subiculum

Densitometry of NPY-IR was performed in microphotographs of 40 μm thick horizontal sections labeled by NPY immunohistochemistry. The sections were photographed at 10-fold magnification under consistent camera settings (including illumination times) with a black and white camera (Orca II, Hamamatsu Photonics, Hamamatsu City, Japan) attached to a Zeiss Axiophot microscope (Carl Zeiss GmbH, Jena, Germany). Two matched sections per mouse were used and values obtained from left and right hemispheres and from different sections were averaged.

Microphotographs (8 bit) were imported into NIH ImageJ (v. 1.53q[1]; NIH, Bethesda, MD, United States). To measure gray scale values of NPY-IR in mossy fibers, a line scan (width: 150 μm) through the mossy fibers in stratum lucidum of sector CA3a was performed. Gray scale values were converted to relative optical density (ROD)-values by the following formula: ROD = log [256/(255 - gray value)]. Section background-labeling was measured in the thalamus and subtracted from the values obtained in stratum lucidum. To measure NPY-IR in the molecular layer of the ventral subiculum, a line scan (width: 400 μm) was performed extending from the fissure between the dentate gyrus and the subiculum to the pyramidal cell layer of the subiculum. The resulting gray scale values were converted to ROD-values (see above), the curve was plotted, and the area under the curve above the molecular layer of the subiculum was calculated. The intensity of NPY-IR in the molecular layer of the subiculum was then given as arbitrary units (a.u., see graphs in **Figures 4E**, **5E**).

False color images

Microphotographs of NPY-immunolabeled sections were opened in NIH ImageJ and the image type was changed to 8 bit. "Spectrum" was selected as the lookup table and the colors of the lookup table were adjusted as follows: Black was selected for the bottom 4 rows of the lookup table and blue for the 5th row from the bottom. Brightness and contrast were optimized using identical values for all microphotographs.

Statistical analyses

All statistical analyses were performed using GraphPad Prism statistical software (version 5.0f; GraphPad Software). The Fisher's exact test was used for analysis to compare the number of SRS in mice 15–50 and 65–100 days after vector

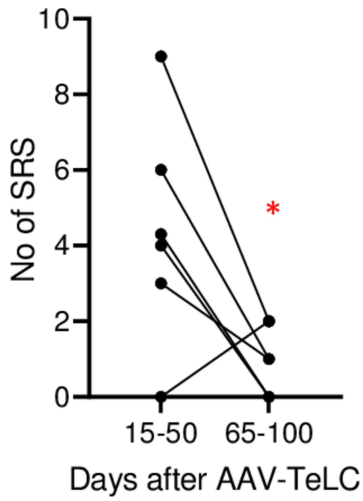

FIGURE 2
Decline in SRS frequency. The analysis was done for animals in Experiment 2 (monitored for 102 days). The graph shows the number of SRS for each mouse during days 15–50 and during days 65–100, respectively. The mean numbers of seizures were 4.3 ± 1.23 and 1.0 ± 0.37, respectively. At the 65–100 days interval, seizure frequency was significantly lower ($P = 0.0452$) in paired Student's *t*-test (*). The data indicate development of induced epileptic tolerance.

1 http://imagej.nih.gov/ij

injection. Two-way repeated-measures ANOVA with Dunnett's multiple-comparison *post hoc* test were used for comparing multiple groups differences in NPY-IR. A p value of < 0.05 was considered as statistically significant.

Results

Induction of spontaneous recurrent seizures (SRS) and interictal spike (IS) clusters by injection of AAV-*TeLC* into the subiculum/CA1

Unilateral injection of the AAV-vectors into the ventral subiculum/sector CA1 resulted in selective silencing of PV-containing basket and axo-axonic cells, as characterized in detail previously (Drexel et al., 2017). The ventral extension of the subiculum had been chosen as target for the vector injections because it is better accessible compared to the dorsal subiculum. **Figures 1A,B** show representative time courses of IS clusters and of SRS presented after injection of AAV-*TeLC* into the subiculum/CA1 (Experiments 1 and 2). As shown in **Figure 1A** (Experiment 1), most AAV-*TeLC*-injected mice experienced between one and 17 SRS and all mice exposed at least one IS cluster during the of 42 days period investigated. The first SRS was observed on day two after AAV-*TeLC* injection. IS clusters developed in all mice at considerably different frequencies; the first IS clusters were observed between days 1 and 14 after AAV-*TeLC*. None of the AAV-*GFP*-injected mice showed SRS or IS. The frequency of SRS appeared to decline gradually after around day 25.

In Experiment 2 (**Figure 1B**), we triggered SRS by injecting the convulsive $GABA_A$ receptor antagonist PTZ 7 days after AAV-*TeLC* injection. The mice experienced between four to twelve SRS and numerous IS during the 102 days of EEG recording (**Figure 1B**). To determine whether the frequency of SRS declined at prolonged intervals after vector injection, we determined the mean seizure frequency at an early interval (15–50 days) after vector injection and compared it with that at a late interval (65–100 days; **Figure 2**). Between 15 and 50 days after AAV-*TeLC* injection, the mean number of seizures was 4.3 ± 1.23 and after 65–100 days (1.0 ± 0.37) it was significantly lower ($P = 0.0452$) indicating seizure-induced epileptic tolerance (see **Figure 2**).

Differential increases of NPY expression in interneurons and in mossy fibers are related to SRS but not IS

We observed marked increases in NPY-IR throughout the brains of all mice with previous SRS and IS clusters (**Figures 3C,D,F,H,J,L**, **4C,D**), but not in AAV-GFP-injected mice (**Figure 3A**) or in mice that had presented IS clusters alone (**Figure 3B**). The increases in NPY-IR were especially prominent in interneurons of the subiculum especially including their axon terminals in the outer molecular layer of the subiculum (**Figures 3C,D,F,L**). Increased NPY-IR was also observed in the cerebral cortex (**Figures 3C,D**, **4C,D**, **5C**) and in interneurons of the dentate gyrus (**Figures 3H**, **4C**). Expression of NPY-IR in interneurons (of the subiculum/sector CA1 and of the dentate gyrus) was high, independently of the interval between the last seizure and sacrificing (**Figures 5C,E**); in contrast, in mossy fibers NPY-IR increased only in mice that experienced their last seizure during the last 5 days before sacrificing (**Figures 5D,F**; compare **Figures 5E,F**). In mice with longer intervals (7–15 days after last seizure) between the last seizure and sacrificing, NPY-IR had faded away in mossy fibers during the succeeding seizure-free interval (**Figures 3C**, **5C,F**).

Thus, in the molecular layer of the subiculum (representing axon terminals of interneurons; see **Figures 3F,L**), NPY-IR was increased in mice that had experienced their last seizure already 10–21 days before sacrificing ($179.6 \pm 16.50\%$; $P < 0.05$ vs. controls) as well as in mice that had their last seizure within the last 5 days before sacrificing ($181.6 \pm 17.87\%$; $P < 0.05$ vs. controls) (**Figure 4E**). In contrast, in the dentate gyrus, NPY-IR was increased ($207.5 \pm 17.91\%$; $P < 0.001$ vs. controls) only in the four mice that experienced their last seizure within the last 5 days before sacrificing (**Figure 4F**) but not in the ones that experienced their last seizure more than 10 days before sacrificing (**Figure 4E**).

Like in axon terminals of subicular interneurons, also in interneurons of the dentate hilus (**Figures 3G,H**, **6B**) and in the cerebral cortex (insular, perirhinal, entorhinal cortices; see **Figure 6**) the increases in NPY-IR appeared to be independent from the duration of the seizure-free interval before sacrificing. Thus, the persisting increase in NPY-IR in interneurons (notably of the subiculum), but not its transient increase in mossy fibers, may be causatively related to the subsequent decline in seizure frequency (epileptic tolerance).

Injection of the NPY-Y2 receptor antagonist JNJ 5207787 facilitates PTZ-induced seizures

All mice were injected with PTZ (40 mg/kg, i. p.) 7 days after AAV-*TeLC* injection; as shown previously, this treatment resulted in SRS and NPY over-expression in 100% (Drexel et al., 2017). To demonstrate that over-expressed NPY serves an endogenous protective role, we injected 7 days later the Y2 receptor antagonist JNJ 5207787 (**Figure 7**). Neither controls nor AAV-*TeLC*-injected mice disclosed EEG changes after JNJ 5207787 alone (not shown). No seizures were observed in untreated controls or AAV-*GFP*-injected mice after injection of PTZ (30 or with 40 mg/kg) or

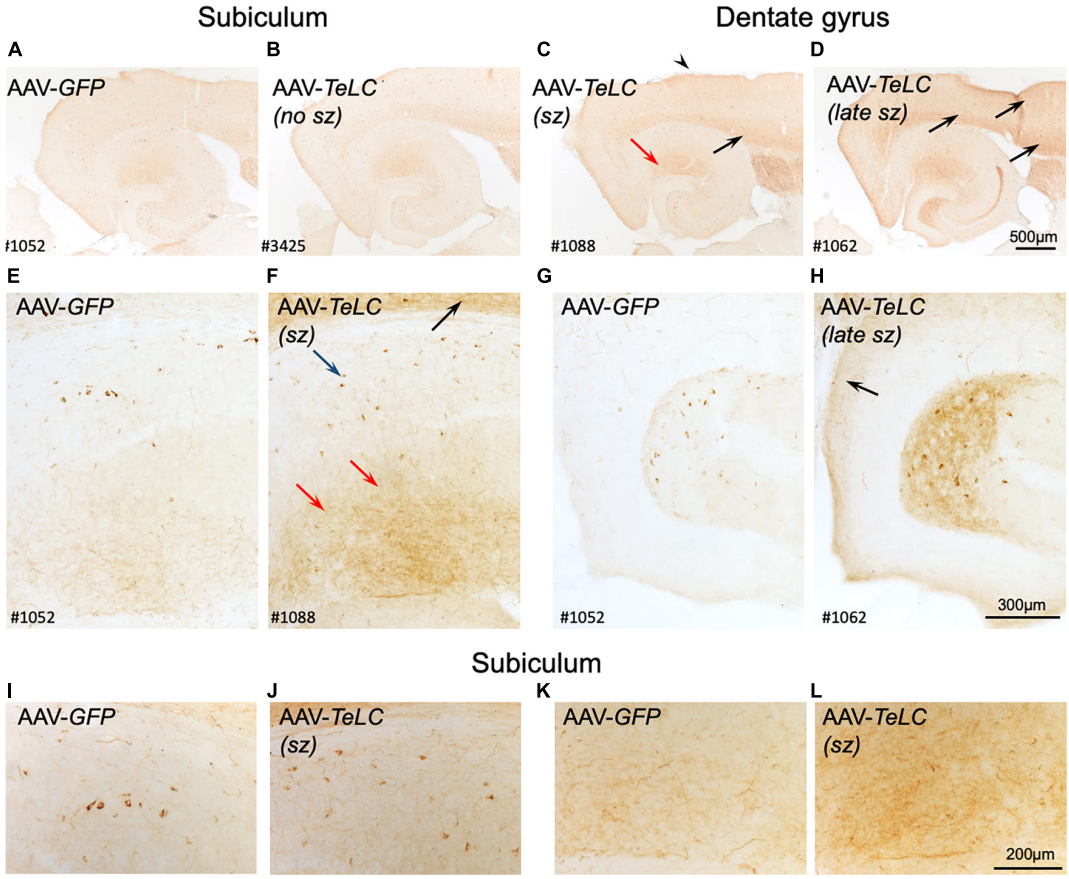

FIGURE 3
Expression of NPY-IR in the cortical areas, the subiculum and in the dentate gyrus 42 days after vector injection. Panels **(A,E,G)** show images from horizontal sections at the level of the of the ventral subiculum/hippocampus obtained from an AAV-*GFP*-injected mouse and show basal NPY expression. Panel **(B)** is taken from an AAV-*TeLC*-injected mouse without spontaneous seizures. In panel **(C)**, a mouse that had experienced 5 seizures between days 16 and 29 is shown ("sz"; see **Figure 1A**). Slightly increased expression of NPY-IR is seen in the outer molecular layer of the subiculum, in cortical layers [black arrows in panels **(C,D,F)**] and in hilar interneurons. Panels **(D,F,H)** derive from an AAV-*TeLC*-injected mouse that had experienced seven SRS during days 30–42 after vector injection (last 12 days before sacrificing, "late sz"). Note the pronounced increases in NPY-IR in cortical areas [arrows in panels **(D,F,H)**], in interneurons (blue arrow) and their fibers (red arrows) in the molecular layer of the subiculum **(D,F)**, and in interneurons and their fibers in the hilus of the dentate gyrus **(H)**; compare AAV-*GFP*-injected control **(G)**. Note that NPY-IR is lastingly up-regulated, both in interneurons and axon terminals of the subiculum [blue and red arrows in panel **(F)**] and of the dentate hilus **(H)**. Furthermore, panels **(I–L)** show larger magnification aspects of the subiculum highlighting the seizure-induced increased number of NPY-positive interneurons **(J)** and fibers **(L)** after AAV-*TeLC* injection compared to AAV-*GFP*-injected controls **(I,K)**. Numbers (#) in the left lower corners of the images refer to numbers of individual animals; the time course of their seizure spells and of IS clusters is shown in **Figure 1A**. sz, seizures between days 16 and 29 (seizure-free for last 13 days before sacrificing; sz +, strong seizures within 12 days before sacrificing.

PTZ plus JNJ 5207787 (black traces in **Figure 7A** and black filled circles in **Figure 7B**). Treating AAV-*TeLC*-injected mice with PTZ (30 mg/kg) alone revealed IS activity but no convulsions (EEG-trace not shown) and, after 40 mg/kg PTZ, in average one convulsion (**Figures 7A,B**; red traces and red filled circles, respectively). In mice injected with the Y2 receptor antagonist together with PTZ, we observed significant increases in EEG activity, including IS clusters and increased numbers of convulsions after 30 mg/kg PTZ + JNJ 5207787 (1.3 ± 0.25 convulsions vs. zero) and after 40 mg/kg PTZ + JNJ 5207787 (increase from 1.0 ± 0.00 to 2.6 ± 0.40 convulsions); one and two mice died in seizures after 30 and 40 mg/kg PTZ plus JNJ 5207787, respectively [**Figure 7A** blue trace (40 mg/kg PTZ); **Figure 7B** blue filled circles].

VGAT, SOM, dynorphin and CB1 expression after SRS induced by AAV-*TeLC* injections

Dynorphin-IR

Dynorphin is highly expressed in mossy fibers and has been considered to act anticonvulsive through kappa receptors (Solbrig et al., 2006b; Loacker et al., 2007). As shown in **Supplementary Image 1**, we observed no change in

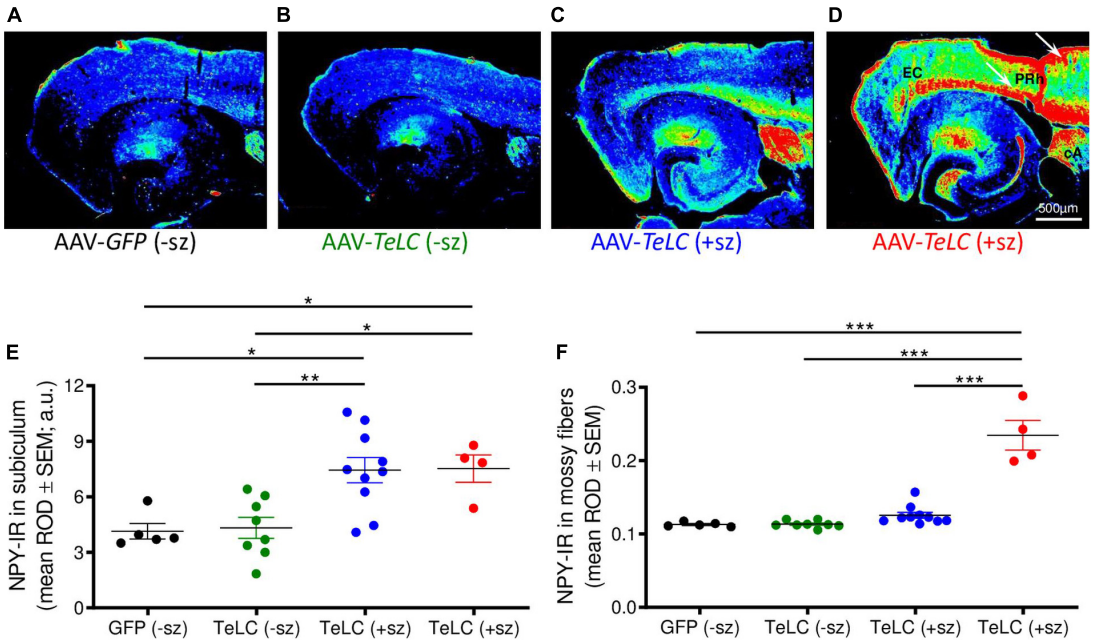

FIGURE 4
NPY overexpression in mice experiencing SRS but not in mice with clusters of IS. NPY-IR was assessed in horizontal brain slices at the level of the ventral subiculum/hippocampus in mice 42 days after injection with AAV-*GFP* or AAV-*TeLC*, respectively (Experiment 1). Panels **(A–D)** show false color images of NPY-IR representative for: **(A)** a control (AAV-*GFP*-injected, black); **(B)** representative mouse presenting only IS clusters after AAV-*TeLC* injection (green, mouse #3425); **(C)** a mouse that experienced SRS during days 10–30 (blue, mouse #1088); and **(D)** a mouse with seizures (3) after day 32 (red, mouse #1062). **(E,F)** Corresponding to the labeling of the images above, the first column in panels **(E,F)** shows data of control mice without SRS. Note the pronounced increase in NPY-IR in the subiculum, both in mice with seizures up to day 30 **(C)** and during 10 days before sacrificing **(D)**. Note also the strong increases in NPY-IR in cortical areas in epileptic mice [**(C)**, white arrows in panel **(D)**]. Black: AAV-*GFP*-injected controls (n = 5); green: AAV-*TeLC*-injected mice with IS only (n = 8); blue: mice that experienced SRS only in the first 32 days after AAV-*TeLC* injection (thus, were at least 10 days seizure-free before sacrificing) (n = 10); red: mice that experienced SRS within 5 days before sacrificing (n = 4). Note that the increase in NPY-IR persists in the subiculum of mice that experienced SRS only at earlier intervals [up to day 32 after vector injection; filled blue circles in panel **(E)**]. In contrast, increased expression of NPY-IR was observed in the dentate gyrus only in mice that showed SRS also within the last 5 days before sacrificing [filled red circles in panel **(F)**]. Letters in panel **(D)**: EC, entorhinal cortex, PRh, perirhinal cortex, cA, central amygdala. Statistical analysis was done by two-way repeated-measures ANOVA with Dunnett's multiple-comparison *post hoc* test; ***$p < 0.001$; **$p < 0.01$; *$p < 0.05$.

dynorphin-IR in mossy fiber terminals in the stratum lucidum and in the dentate hilus of mice that had experienced series of SRS (see Figure 1). Interestingly, the mice revealed no sprouting of mossy fibers to the inner molecular layer of the dentate gyrus in spite of SRS, confirming that the mice had no loss in hilar interneurons.

VGAT-IR

The vesicular GABA transporter VGAT is a valid marker for GABA-ergic axon terminals. We investigated VGAT-IR in the hippocampus/subiculum for obtaining a possible indication for sprouting of GABA neurons. We observed, however, no change in the density or distribution of VGAT-IR 42 days after AAV-TeLC injection into the subiculum (Supplementary Image 2).

SOM mRNA and IR

We previously obtained indication for sprouting of SOM neurons in the molecular layer of the subiculum after KA-induced seizures in the rat (Drexel et al., 2012). Since this may represent an endogenous anticonvulsive mechanism, we investigated SOM mRNA and IR in our SRS prone mice (42 days after AAV-*TeLC* injection). In spite of the strong increases in SOM mRNA and IR previously observed in KA treated rats and after kindling (Sperk et al., 1992; Schwarzer et al., 1996), we detected no change in SOM mRNA expression in the hippocampus (Supplementary Image 3). There was also no correlation between SOM mRNA levels and the number of SRS experienced by the mice. Similarly, SRS did also not induce an increase in SOM-IR in the molecular layer of the subiculum (Figure 8).

Cannabinoid receptor CB1

CB1-IR was highly expressed in the pyramidal layers of CA1, CA3 and the subiculum, and in the inner molecular layer of the dentate gyrus. These are terminal areas of CCK-8 (and vesicular glutamate transporter, vGLUT3) positive basket cells containing the presynaptic CB1 receptors. As shown in

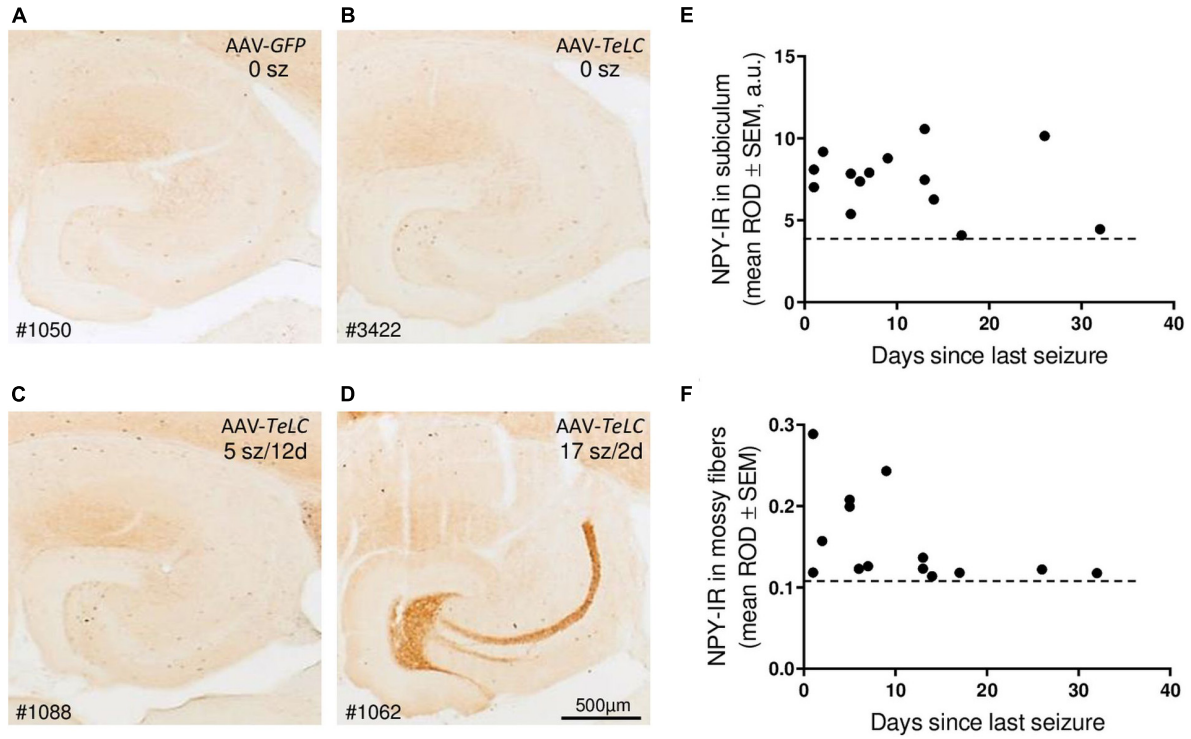

FIGURE 5
Seizure-induced over-expression of NPY-IR persists in interneurons of the subiculum but in mossy fibers is restricted to mice with frequent SRS close to sacrificing. NPY-IR in the ventral hippocampus at different intervals between last SRS and sacrificing. **(A)** AAV-*GFP*-injected control mouse (no seizures); **(B)** mouse that experienced IS only; **(C)** mouse that had expressed five SRS up to 12 days before sacrificing (last seizure on day 12; note increased NPY-IR in the inner molecular layer of the subiculum and in interneurons of the dentate gyrus) and **(D)** mouse that had 17 seizures in total, including three severe seizures two and three days before sacrificing (note the pronounced expression of NPY-IR in mossy fibers). **(E,F)** NPY-IR in relation of the time of last SRS to time of sacrificing in the subiculum **(E)** and in mossy fibers as determined in the stratum lucidum, the terminal area of mossy fibers **(F)**. Horizontal dotted lines indicate the background of NPY-IR. Note that in mossy fibers increased NPY-IR was detected only in mice that had experienced their last seizure 1–5 days prior to sacrificing **(F)**, whereas in interneurons of the subiculum the SRS-induced increase in NPY-IR persisted for up to 25 days **(E)**. Optic density is given in arbitrary units (a.u.).

Figure 9, we observed modest decreases in CB1-IR throughout the ventral hippocampal formation of mice that had experienced SRS during the 42 days observation period (see **Figure 1**). Since this decrease affects different parts of the hippocampus and is also present on the contralateral side it may be related to the SRS experienced and not directly to the unilateral vector injection.

Discussion

Plasticity of the NPY system

In the brain, the 36 amino acid-containing neuropeptide NPY is contained in large dense core vesicles of GABA-ergic interneurons. Whereas the classical transmitter GABA is already released after low frequency stimulation, neuropeptides like NPY are generally released only after sustained, high frequency stimulation (Hökfelt, 1991). In animal models of epilepsy and in human TLE, recurrent seizures cause marked overexpression of NPY in GABA-ergic interneurons and in glutamatergic mossy fibers (Sperk et al., 1992; Gruber et al., 1994; Mathern et al., 1995; Furtinger et al., 2001; Drexel et al., 2012). Together with the augmented expression of the GABA synthesizing enzyme GAD-1, overexpression of NPY indicates that the activity of the respective neurons persists beyond the acute seizures. It has also been suggested that high frequency stimulation during subsequent seizures may lead to enhanced release of NPY together with that of GABA (Gruber et al., 1994; Vezzani and Sperk, 2004). NPY is mostly released to extra-synaptic sites and inhibits glutamate release also through distant presynaptic Y2 receptors (Colmers et al., 1991; Greber et al., 1994). We therefore speculated that over-expressed NPY may serve as an endogenous anticonvulsive and protective mechanism (Marksteiner and Sperk, 1988; Vezzani and Sperk, 2004). Upon sustained neuronal stimulation during acute seizures, release of NPY may occur, so to say "on demand" and may dampen glutamate release and contribute to termination of seizures.

Here, we studied NPY expression in an animal model with rare but recurrent seizures (SRS) induced by selective silencing of GABA/PV containing interneurons in sector CA1

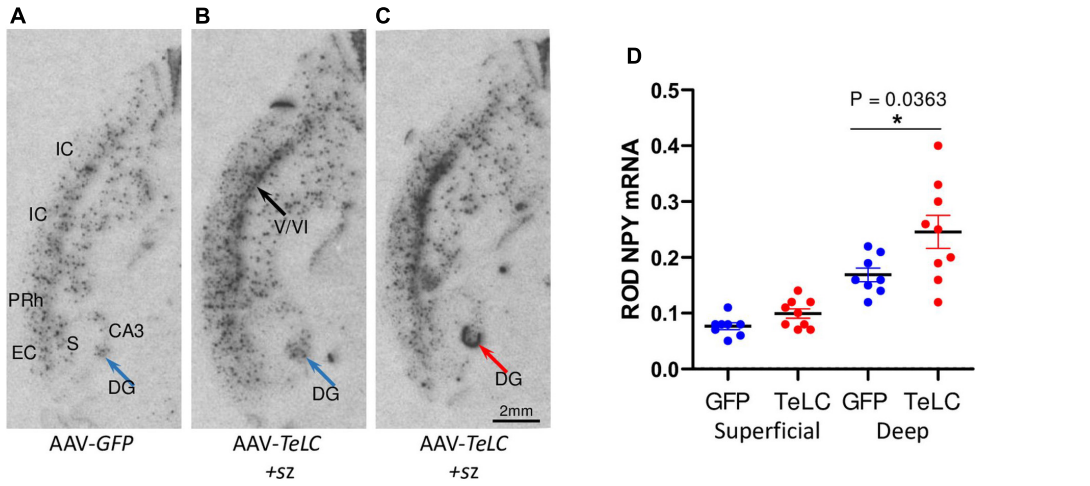

FIGURE 6
NPY mRNA expression in the deep layers of the cerebral cortex. Mice injected with AAV-*GFP* or AAV-*TeLC* were sacrificed after 6 weeks and brains were subjected to *in situ* hybridization. The images were obtained in horizontal sections showing the ventral hippocampus and adjacent limbic cortex areas (insular, perirhinal, entorhinal cortices). **(A)** AAV-*GFP*-injected control; **(B)** AAV-*TeLC*-injected mouse that exposed five SRS between days 6–25; **(C)** AAV-*TeLC*-injected mouse that exposed four SRS on days 3 and 2 before sacrificing (day 42). Black arrow in panel **(B)** denotes NPY mRNA expression in the deep cortical layers; blue arrow in panel **(B)** points to interneurons in the dentate hilus expressing NPY mRNA; red arrow in panel **(C)** denotes massive *de novo* NPY mRNA expression in the granule cell layer. **(D)** Quantification of NPY mRNA in the deep and superficial cortical layers 6 weeks after AAV-*GFP* and AAV-*TeLC* injection. Data are shown as mean ± SEM. Statistics (Student's *t*-test) was performed using the GraphPad Prism program. In interneurons of the deep layers (V/VI) but not in the superficial layers (layers II/III) of the insular, perirhinal and entorhinal cortices, NPY mRNA was significantly increased ($P = 0.0363$, *). Abbreviations: DG, dentate gyrus (hilus); CA3, hippocampal subfield CA3; S, subiculum; IC, insular cortex; PRh, perirhinal cortex; EC, entorhinal cortex.

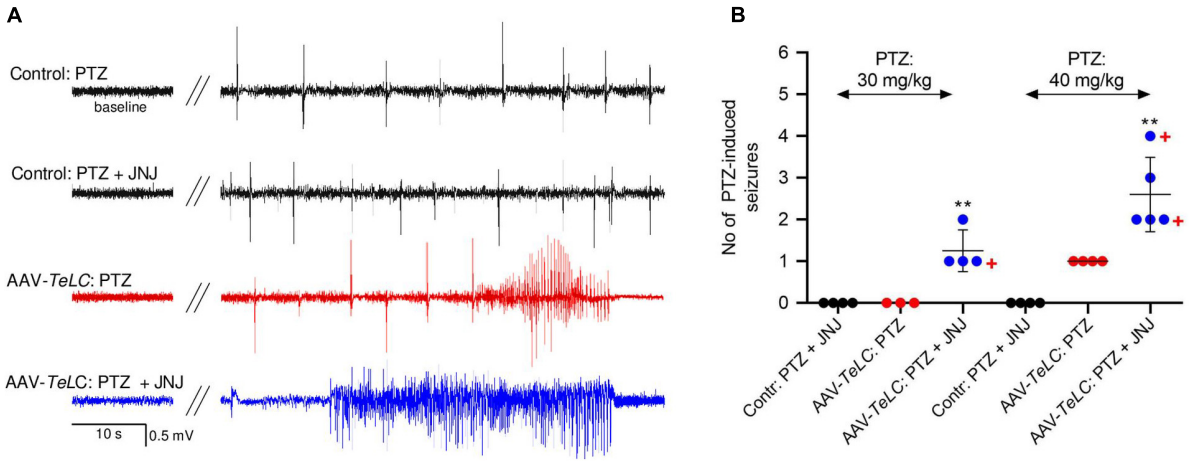

FIGURE 7
The Y2 receptor antagonist JNJ 5207787 potentiates PTZ-induced seizures in AAV-*TeLC*-injected epileptic mice. **(A)** EEG traces after injection of 40 mg/kg PTZ i.p. or injection of the Y2 receptor antagonist JNJ 5207787 (20 mg/kg, i.p.) followed by PTZ (40 mg/kg, i.p.). Note that neither the low dose of PTZ nor PTZ + JNJ 5207787 induced seizures in naïve controls (black traces) nor in AAV-*GFP*-injected mice (not shown). PTZ induced significant convulsions in AAV-*TeLC*-injected mice (red trace) that were markedly augmented by prior 20 mg/kg JNJ 5207787 injection (blue trace). **(B)** Numbers of PTZ-induced seizures with and without JNJ 5207787 injection. Neither naïve controls (black circles) nor AAV-*GFP*-injected mice (not shown; together $n = 8$) presented epileptic spells after 30 or after 40 mg/kg PTZ without JNJ 5207787 ($n = 3$ and 4, respectively; black filled circles). Mice previously injected with AAV-*TeLC* responded with no seizure (0/3) after 30 mg/kg PTZ; after 40 mg/kg PTZ all four mice responded modestly with 1 seizure (red filled circles). At both doses of PTZ, the number of seizures markedly increased when injected together with JNJ 5207787 (blue filled circles). Neither control mice ($n = 4$) nor AAV-*GFP*-injected mice ($n = 3$) showed changes in the EEG after JNJ 5207787 injection (not shown). +, indicate mice that died in seizures. Statistics (Student's *t*-test): $^{**}p < 0.01$, respective AAV-*TeLC* and PTZ-injected with vs. without prior injection of JNJ 5207787. The important message of this experiment is that the Y2 antagonist is inactive in naïve mice and in mice without acute seizures. However, in mice with seizures, it augments the epileptic activity presumably by inhibiting the protective action of NPY (released primarily during seizures) on Y2 receptors.

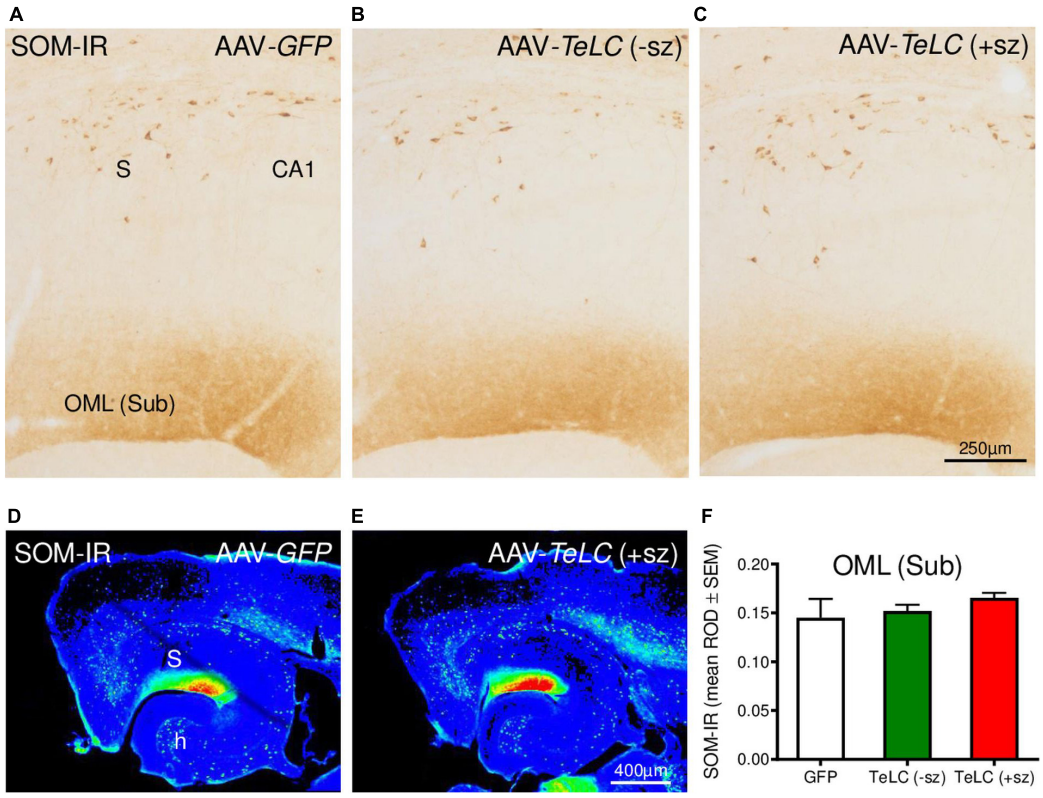

FIGURE 8
SOM-IR after AAV-*TeLC* injection. SOM-IR in sector CA1 and subiculum of mice injected with AAV-*GFP* **(A)** or AAV-*TeLC* that were seizure-free **(B)** or had experienced SRS **(C)**. Note that neither the number of SOM-positive interneurons in the pyramidal layers of the subiculum (S) and sector CA1 nor the density of SOM-positive axon terminals in the outer molecular layer (OML) of the subiculum was altered. Panels **(D,E)** show false color images of panels **(A,C)**, respectively. **(F)** Mean ROD values of the molecular layer were not altered by previous SRS. +sz, mouse with previous seizures; -sz, mouse was seizure-free.

and subiculum (Drexel et al., 2017). This animal model is based on unilateral injection of small amounts of an AAV vector into transgenic PV-cre mice, resulting in local expression of tetanus toxin light chain only in PV containing cells. In the hippocampus and the subiculum, PV-containing basket cells and axo-axonic cells exert potent somatic and perisomatic inhibition of pyramidal cells. The toxin locally inhibits vesicular GABA release from the affected interneurons. Consequently, the mice develop SRS and IS clusters but show no neurodegeneration (Drexel et al., 2017). It is also important to note that only SRS but not recurrent clusters of IS caused increased NPY expression. Whereas expression of the peptide was transient in mossy fibers, it persisted in interneurons. This is consistent with our previous finding showing that after KA-induced seizures over-expression of NPY lasted for a prolonged time in interneurons, whereas it was limited to a few days in mossy fibers (Gruber et al., 1994). Interestingly, in our present experiments, the increase in NPY-IR in subicular interneurons (not in mossy fibers) persisted, although the frequency of SRS appeared to decline 4–6 weeks after initial silencing of GABA/PV neurons.

Evidence for an endogenous protective effect of NPY

To demonstrate that endogenous over-expressed NPY serves a protective role, we injected the Y2 receptor antagonist JNJ 5207787 to our seizure prone mice. The mice had been injected with the AAV-*TeLC* into the sector CA1/subiculum before and SRS were triggered additionally by a low dose of PTZ after 7 days. After this treatment, all mice experienced SRS leading to upregulation of NPY (Drexel et al., 2017). Notably, these mice did not respond to injection of JNJ 5207787 alone, indicating that Y2 receptors were not occupied by NPY (NPY is almost not released prior to seizures). Thus, to induce NPY release in the mice, we challenged them by injecting once more a low dose of PTZ. Since the AAV-*TeLC*-injected mice (due to silencing of PV neurons) have a lowered seizure threshold (Drexel et al., 2017), the otherwise not convulsive dose of PTZ induced modest convulsions (**Figure 7A**). When applying the Y2 receptor antagonist in addition, we observed significant increases in PTZ-induced epileptic activity (**Figures 7A,B**). It is important again to point

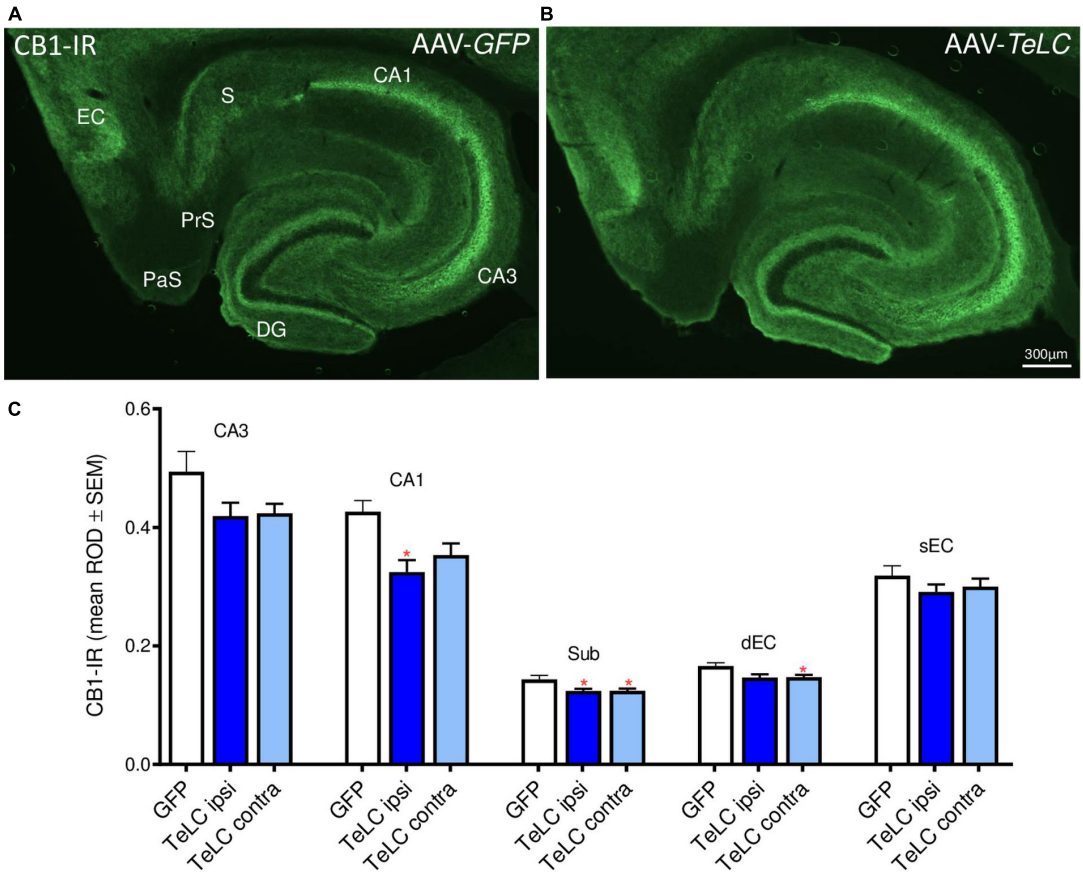

FIGURE 9
CB1-IR after AAV-*TeLC* injection. Immunofluorescence of horizontal sections on the level of the ventral hippocampus of mice injected into the subiculum with **(A)** AAV-*GFP* or **(B)** AAV-*TeLC*. CB1-IR is highly expressed in pyramidal layers of CA3, CA1, the subiculum and in the inner molecular layer of the dentate gyrus, layers that are innervated by basket cells. CB1-IR is presumably located presynaptically on these GABA-ergic terminals mediating inhibition of GABA release. **(C)** Optic density of CB1-IR is modestly reduced in sectors CA3 (statistically not significant) and CA1 ($p < 0.05$, ipsilateral side), in the subiculum ($p < 0.05$, *) and in the deep layers of the entorhinal cortex ($p < 0.05$, contralateral side). Note that the ROD values were not significantly different in the AAV-*TeLC*-injected side versus the not-injected contralateral area. Abbreviations in panels **(A,C)**: DG, dentate gyrus; EC, entorhinal cortex; dEC, deep entorhinal cortex; sEC, superficial entorhinal cortex; S, Sub, subiculum; PaS, parasubiculum; PrS, presubiculum.

out that JNJ 5207787 *per se* did not evoke seizures, although the AAV-*TeLC*-injected mice had a lowered seizure threshold. Only triggering convulsions and thereby also the release of NPY disclosed the activity of the Y2 antagonist. This finding clearly suggests that over-expressed NPY is released during seizures and then exerts its anticonvulsive activity (antagonized by JNJ 5207787).

Seizures induce release of NPY

The fact that seizures can induce NPY release has been shown using another experimental approach long ago. Measuring NPY levels in brain areas after a KA-induced status epilepticus revealed an initial drop in the levels of the peptide due to its extensive release and degradation during and after the acute seizures (Bellmann et al., 1991). This initial drop in NPY levels is overcome after 1–3 days and is followed by re-synthesis and marked over-expression of the neuropeptide (Marksteiner et al., 1990; Bellmann et al., 1991). Upregulation of the NPY, however, seems to require recurrent seizures or kindling (Schwarzer et al., 1996). Early anticonvulsant treatment with MK-801 or thiopental after the initial KA-induced status epilepticus prevented the subsequent increases in NPY and somatostatin levels (Marksteiner et al., 1990; Vezzani and Sperk, 2004).

Earlier evidence for epileptic tolerance mediated by NPY expression

An association between epileptic tolerance and NPY upregulation has also been reported by El Bahh et al. (2001, 2005). They observed that intrahippocampal injection of a

low dose of KA can prevent pyramidal cell loss that had been induced by subsequent intraventricular injection of the toxin, and that this effect correlated with increased NPY-IR in CA1 interneurons. Interestingly, this "preconditioning" lasted for seven but not for 15 days, again supporting the idea that NPY-induced epileptic tolerance may be limited in time and may require repeated convulsions for its persistence. Previous experiments demonstrating that febrile seizures induce tolerance to subsequent thermal induction of seizures indicate fast development of epileptic tolerance (Dubé et al., 2005). Also in these experiments, the inhibition of epileptic tolerance by application of a Y2 receptor antagonist suggested a crucial role of NPY over-expressed by the preceding seizures (Dubé et al., 2005).

The role of interneurons vs. granule cells/mossy fibers

Over-expression of NPY in interneurons of the subiculum (possibly also of the cortex and dentate hilus) may lead to a lasting seizure protection. On the other hand, both NPY and Y2 receptors are also ectopically expressed in granule cells/mossy fibers after severe seizures (Gruber et al., 1994; Röder et al., 1996; Sadamatsu et al., 1998). Expression of the peptide as well of its Y2 receptors, however, is short-lived and wanes after a few days. It may, however, represent an immediate anticonvulsive mechanism protecting from acute epileptic activity that often persists even for several days after the initial status epilepticus. The underlying mechanism for NPY's anticonvulsive activity is a potent inhibition of glutamate release from mossy fibers mediated by presynaptic NPY-Y2 receptors (Colmers et al., 1991; Greber et al., 1994). Interestingly, the anticonvulsive action of brain derived neurotrophic factor (BDNF) has been suggested to be mediated by inducing NPY expression (Reibel et al., 2000). The mechanisms underlying the different durations of expression in interneurons vs. granule cells are not known.

Expression of VGAT, SOM, dynorphin and CB1 receptor after silencing PV neurons

In addition to NPY-IR, we investigated the expression of VGAT, SOM, dynorphin and CB1 receptor in the subiculum and hippocampus of mice that had experienced SRS and IS during a period of 42 days (Experiment 1). VGAT-, SOM- and dynorphin-IR and SOM mRNA were not altered indicating that there is no sprouting of the respective GABA neurons and of mossy fibers. In contrast, we observed a modest decrease of the endocannabinoid receptor CB1. This change could be associated with reduced inhibition of GABA release from basket cells and, thus, could also represent an endogenous anticonvulsive mechanism. In a preliminary experiment we also applied the CB1 agonist WIN55,212 to AAV-*TeLC*-injected mice. If the reduction in CB1 receptors would have an anticonvulsive effect, the CB1 agonist should be proconvulsive (in the same way as the Y2 antagonist). We, however, observed no effect of WIN55,212.

A key finding of the model of KA-induced recurrent seizures was the selective degeneration of PV-containing basket cells in the subiculum (Drexel et al., 2011) that may be causatively related to the subsequent development of SRS. This finding is supported by the present model showing that already unilateral silencing of PV-interneurons in the subiculum (without degeneration of the affected neurons) leads to SRS (Drexel et al., 2017). In the KA model, fibers of SOM neurons sprout in the subiculum [and even beyond to the molecular layer of the dentate gyrus (Peng et al., 2013)] whereas they do not in our present experiments after only silencing PV basket cells. SOM is primarily contained in oriens-lacunosum moleculare (O-LM) cells projecting from the stratum oriens to the stratum lacunosum moleculare in CA1 (and from the pyramidal cell layer to the molecular layer of the subiculum) and mediate feed-back inhibition upon pyramidal cells (Klausberger, 2009). NPY is mainly contained in bistratified cells and in Ivy cells also exerting feed-back inhibition upon pyramidal cell dendrites (Klausberger, 2009). It is interesting to note that NPY-containing axon terminals over-express the peptide (or even sprout) already after silencing of PV neurons (without neurodegeneration) and resulting SRSs, whereas SOM-containing O-LM cells only sprout after degeneration of PV neurons in the subiculum (KA model). Sprouted O-LM cells may mediate augmented feed-back inhibition after the loss of PV cell mediated feed-forward inhibition. As discussed above, in the present model over-expressed NPY may primarily act by presynaptic inhibition of glutamate release.

Does NPY-induced epileptic tolerance also play a role in human TLE?

In specimens of TLE patients, less prominent expression of NPY was seen in granule cells/mossy fibers, possibly due to a prolonged interval between the last seizure and surgery in the patients (Furtinger et al., 2001). Expression of Y2 receptors—in contrast to Y1 receptors—however, was increased throughout the hippocampus including mossy fibers, and increased expression of NPY was observed in axons of interneurons of the subiculum and other parts of the hippocampus (Furtinger et al., 2001). In hippocampal slices obtained from TLE patients, NPY prominently inhibits glutamate release (Ledri et al., 2015). Thus, also in humans NPY may mediate epileptic tolerance, and enhancing NPY-Y2 receptor mediated transmission may be an effective strategy for antiepileptic treatment for epilepsies in humans (Cattaneo et al., 2020).

Conclusion

In conclusion, we provided evidence that NPY overexpressed by SRS and released "on demand" by acute seizures may contribute to epileptic tolerance by stimulating Y2 receptors and inhibiting glutamate release. On the other hand, also increased release of GABA and NO from the same neurons could take part in this mechanism. The site of the anticonvulsive activity of endogenous NPY, however, may not only be limited to the hippocampus and subiculum since SRS cause lasting overexpression of NPY also in other cortical areas such as the perirhinal and entorhinal cortex (Drexel et al., 2012).

Data availability statement

The raw data supporting the conclusions of this article will be made available by the authors, without undue reservation.

Ethics statement

This animal study was reviewed and approved by Committee for Animal Protection of the Austrian Ministry of Science.

Author contributions

MD performed the experiments in part assisted by technical personnel. GS planned the study. GS and MD prepared the manuscript. Both authors contributed to the article and approved the submitted version.

Funding

This work was supported by the Austrian Science Fund (Projects: P 26680 and P 31777).

Acknowledgments

We thank Dr. Ramon Tasan and Dr. Peer Wulff (University Kiel) for preparation of the vectors and Mrs. Annelise Bukovac for assistance with immunohistochemistry.

Conflict of interest

The authors declare that the research was conducted in the absence of any commercial or financial relationships that could be construed as a potential conflict of interest.

Publisher's note

All claims expressed in this article are solely those of the authors and do not necessarily represent those of their affiliated organizations, or those of the publisher, the editors and the reviewers. Any product that may be evaluated in this article, or claim that may be made by its manufacturer, is not guaranteed or endorsed by the publisher.

Supplementary material

The Supplementary Material for this article can be found online at: https://www.frontiersin.org/articles/10.3389/fnmol.2022.974784/full#supplementary-material

SUPPLEMENTARY IMAGE 1
Dynorphin-IR is not altered in mossy fibers. Dynorphin-IR was assessed in the terminal field of mossy fibers in the stratum lucidum 42 days after AAV-*GFP* **(A)** or AAV-*TeLC* injection **(B)**. **(C)** Dentate hilus of the same section as in panel **(B)**; note the absence of mossy fiber sprouting proving that there is no neurodegeneration. **(D)** Relative optic densities (ROD) in the strata lucidum of AAV-*GFP*-injected controls (GFP) and of AAV-*TeLC*-injected mice without [TeLC (-sz)] and with previous SRS [TeLC (+sz)].

SUPPLEMENTARY IMAGE 2
VGAT-IR in mice with previous SRS. VGAT immunofluorescence in horizontal sections on the level of the ventral hippocampus of mice injected with AAV-*GFP* **(A)** or AAV-*TeLC* **(B)**. **(C)** Mean VGAT-immunofluorescence levels were not altered in the outer molecular layer of the subiculum (OML) 42 days after AAV-*TeLC* injection and did not correlate with the number of previous seizures **(D)**. DG, dentate gyrus; EC, entorhinal cortex; PaS, parasubiculum; PrS, presubiculum; S, subiculum; OML, outer molecular layer.

SUPPLEMENTARY IMAGE 3
SOM mRNA in mice with SRS. Horizontal sections on the level of the ventral hippocampus of mice injected with AAV-*GFP* **(A,C)** or AAV-*TeLC* **(B,D)** were subjected to *in situ* hybridization of SOM mRNA. **(E)** Mean SOM mRNA levels were not altered in interneurons located in the hilus of the dentate gyrus 42 days after AAV-*TeLC* injection. **(F)** SOM mRNA expression also did not correlate with the numbers of previous SRS.

References

Baraban, S. C., Hollopeter, G., Erickson, J. C., Schwartzkroin, P. A., and Palmiter, R. D. (1997). Knock-out mice reveal a critical antiepileptic role for neuropeptide Y. *J. Neurosci.* 17, 8927–8936. doi: 10.1523/JNEUROSCI.17-23-08927.1997

Bellmann, R., Widmann, R., Olenik, C., Meyer, D. K., Maas, D., Marksteiner, J., et al. (1991). Enhanced rate of expression and biosynthesis of neuropeptide Y after kainic acid-induced seizures. *J. Neurochem.* 56, 525–530. doi: 10.1111/j.1471-4159.1991.tb08181.x

Biagini, G., Panuccio, G., and Avoli, M. (2010). Neurosteroids and epilepsy. *Curr. Opin. Neurol.* 23, 170–176.

Bonaventure, P., Nepomuceno, D., Mazur, C., Lord, B., Rudolph, D. A., Jablonowski, J. A., et al. (2004). Characterization of N-(1-Acetyl-2,3-dihydro-1H-indol-6-yl)-3-(3-cyano-phenyl)-N-[1-(2-cyclopentyl-ethyl)-piperidin-4yl]acrylamide (JNJ-5207787), a small molecule antagonist of the neuropeptide Y Y2 receptor. *J. Pharmacol. Exp. Ther.* 308, 1130–1137.

Buckmaster, P. S., Reyes, B., Kahn, T., and Wyeth, M. (2022). Ventral hippocampal formation is the primary epileptogenic zone in a rat model of temporal lobe epilepsy. *J. Neurosci.* 42, 7482–7495. doi: 10.1523/JNEUROSCI.0429-22.2022

Cattaneo, S., Verlengia, G., Marino, P., Simonato, M., and Bettegazzi, B. (2020). NPY and Gene Therapy for Epilepsy: How When. and Y. *Front. Mol. Neurosci.* 13:608001. doi: 10.3389/fnmol.2020.608001

Chang, C. C., Chen, S. D., Lin, T. K., Chang, W. N., Liou, C. W., Chang, A. Y., et al. (2014). Heat shock protein 70 protects against seizure-induced neuronal cell death in the hippocampus following experimental status epilepticus via inhibition of nuclear factor-κB activation-induced nitric oxide synthase II expression. *Neurobiol. Dis.* 62, 241–249. doi: 10.1016/j.nbd.2013.10.012

Colmers, W. F., Klapstein, G. J., Fournier, A., St-Pierre, S., and Treherne, K. A. (1991). Presynaptic inhibition by neuropeptide Y in rat hippocampal slice in vitro is mediated by a Y2 receptor. *Br. J. Pharmacol.* 102, 41–44.

Drexel, M., Kirchmair, E., and Sperk, G. (2013). Changes in the expression of GABAA receptor subunit mRNAs in parahippocampal areas after kainic acid induced seizures. *Front. Neural Circuits* 7:142. doi: 10.3389/fncir.2013.00142

Drexel, M., Kirchmair, E., Wieselthaler-Hölzl, A., Preidt, A. P., and Sperk, G. (2012). Somatostatin and neuropeptide Y neurons undergo different plasticity in parahippocampal regions in kainic acid-induced epilepsy. *J. Neuropathol. Exp. Neurol.* 71, 312–329. doi: 10.1097/NEN.0b013e31824d9882

Drexel, M., Preidt, A. P., Kirchmair, E., and Sperk, G. (2011). Parvalbumin interneurons and calretinin fibers arising from the thalamic nucleus reuniens degenerate in the subiculum after kainic acid-induced seizures. *Neuroscience* 189, 316–329. doi: 10.1016/j.neuroscience.2011.05.021

Drexel, M., Romanov, R. A., Wood, J., Weger, S., Heilbronn, R., Wulff, P., et al. (2017). Selective Silencing of Hippocampal Parvalbumin Interneurons Induces Development of Recurrent Spontaneous Limbic Seizures in Mice. *J. Neurosci.* 37, 8166–8179. doi: 10.1523/JNEUROSCI.3456-16.2017

Dubé, C., Brunson, K. L., Eghbal-Ahmadi, M., Gonzalez-Vega, R., and Baram, T. Z. (2005). Endogenous neuropeptide Y prevents recurrence of experimental febrile seizures by increasing seizure threshold. *J. Mol. Neurosci.* 25, 275–284. doi: 10.1385/JMN:25:3:275

El Bahh, B., Auvergne, R., Leré, C., Brana, C., Le Gal La Salle, G., and Rougier, A. (2001). Decreased epileptic susceptibility correlates with neuropeptide Y overexpression in a model of tolerance to excitotoxicity. *Brain Res.* 894, 209–217. doi: 10.1016/s0006-8993(01)02027-3

El Bahh, B., Balosso, S., Hamilton, T., Herzog, H., Beck-Sickinger, A. G., Sperk, G., et al. (2005). The anti-epileptic actions of neuropeptide Y in the hippocampus are mediated by Y and not Y receptors. *Eur. J. Neurosci.* 22, 1417–1430. doi: 10.1111/j.1460-9568.2005.04338.x

Feldblum, S., Ackermann, R. F., and Tobin, A. J. (1990). Long-term increase of glutamate decarboxylase mRNA in a rat model of temporal lobe epilepsy. *Neuron* 5, 361–371. doi: 10.1016/0896-6273(90)90172-c

Furtinger, S., Pirker, S., Czech, T., Baumgartner, C., Ransmayr, G., and Sperk, G. (2001). Plasticity of Y1 and Y2 receptors and neuropeptide Y fibers in patients with temporal lobe epilepsy. *J. Neurosci.* 21, 5804–5812. doi: 10.1523/JNEUROSCI.21-15-05804.2001

Gidday, J. M. (2006). Cerebral preconditioning and ischaemic tolerance. *Nat. Rev. Neurosci.* 7, 437–448.

Greber, S., Schwarzer, C., and Sperk, G. (1994). Neuropeptide Y inhibits potassium-stimulated glutamate release through Y2 receptors in rat hippocampal slices in vitro. *Br. J. Pharmacol.* 113, 737–740. doi: 10.1111/j.1476-5381.1994.tb17055.x

Gruber, B., Greber, S., Rupp, E., and Sperk, G. (1994). Differential NPY mRNA expression in granule cells and interneurons of the rat dentate gyrus after kainic acid injection. *Hippocampus* 4, 474–482. doi: 10.1002/hipo.450040409

Hökfelt, T. (1991). Neuropeptides in perspective: The last ten years. *Neuron* 7, 867–879.

Houser, C. R., Harris, A. B., and Vaughn, J. E. (1986). Time course of the reduction of GABA terminals in a model of focal epilepsy: A glutamic acid decarboxylase immunocytochemical study. *Brain Res.* 383, 129–145. doi: 10.1016/0006-8993(86)90014-4

Katona, I., Sperlágh, B., Sík, A., Käfalvi, A., Vizi, E. S., Mackie, K., et al. (1999). Presynaptically located CB1 cannabinoid receptors regulate GABA release from axon terminals of specific hippocampal interneurons. *J. Neurosci.* 19, 4544–4558. doi: 10.1523/JNEUROSCI.19-11-04544.1999

Klausberger, T. (2009). GABAergic interneurons targeting dendrites of pyramidal cells in the CA1 area of the hippocampus. *Eur. J. Neurosci.* 30, 947–957.

Kofler, N., Kirchmair, E., Schwarzer, C., and Sperk, G. (1997). Altered expression of NPY-Y1 receptors in kainic acid induced epilepsy in rats. *Neurosci. Lett.* 230, 129–132. doi: 10.1016/s0304-3940(97)00492-8

Lawrence, C., Martin, B. S., Sun, C., Williamson, J., and Kapur, J. (2010). Endogenous neurosteroid synthesis modulates seizure frequency. *Ann. Neurol.* 67, 689–693.

Ledri, M., Sørensen, A. T., Madsen, M. G., Christiansen, S. H., Ledri, L. N., Cifra, A., et al. (2015). Differential Effect of Neuropeptides on Excitatory Synaptic Transmission in Human Epileptic Hippocampus. *J. Neurosci.* 35, 9622–9631.

Loacker, S., Sayyah, M., Wittmann, W., Herzog, H., and Schwarzer, C. (2007). Endogenous dynorphin in epileptogenesis and epilepsy: Anticonvulsant net effect via kappa opioid receptors. *Brain* 130, 1017–1028. doi: 10.1093/brain/awl384

Marksteiner, J., Prommegger, R., and Sperk, G. (1990). Effect of anticonvulsant treatment on kainic acid-induced increases in peptide levels. *Eur. J. Pharmacol.* 181, 241–246.

Marksteiner, J., and Sperk, G. (1988). Concomitant increase of somatostatin, neuropeptide Y and glutamate decarboxylase in the frontal cortex of rats with decreased seizure threshold. *Neuroscience* 26, 379–385. doi: 10.1016/0306-4522(88)90155-8

Mathern, G. W., Babb, T. L., Pretorius, J. K., and Leite, J. P. (1995). Reactive synaptogenesis and neuron densities for neuropeptide Y, somatostatin, and glutamate decarboxylase immunoreactivity in the epileptogenic human fascia dentata. *J. Neurosci.* 15, 3990–4004. doi: 10.1523/JNEUROSCI.15-05-03990.1995

Murray, A. J., Sauer, J. F., Riedel, G., McClure, C., Ansel, L., Cheyne, L., et al. (2011). Parvalbumin-positive CA1 interneurons are required for spatial working but not for reference memory. *Nat. Neurosci.* 14, 297–299. doi: 10.1038/nn.2751

Peng, Z., Zhang, N., Wei, W., Huang, C. S., Cetina, Y., Otis, T. S., et al. (2013). A reorganized GABAergic circuit in a model of epilepsy: Evidence from optogenetic labeling and stimulation of somatostatin interneurons. *J. Neurosci.* 33, 14392–14405. doi: 10.1523/JNEUROSCI.2045-13.2013

Pirker, S., Czech, T., Baumgartner, C., Maier, H., Novak, K., Fürtinger, S., et al. (2001). Chromogranins as markers of altered hippocampal circuitry in temporal lobe epilepsy. *Ann. Neurol.* 50, 216–226. doi: 10.1002/ana.1079

Reibel, S., Larmet, Y., Carnahan, J., Marescaux, C., and Depaulis, A. (2000). Endogenous control of hippocampal epileptogenesis: A molecular cascade involving brain-derived neurotrophic factor and neuropeptide Y. *Epilepsia* 41, S127–S133. doi: 10.1111/j.1528-1157.2000.tb01571.x

Richichi, C., Lin, E. J., Stefanin, D., Colella, D., Ravizza, T., Grignaschi, G., et al. (2004). Anticonvulsant and antiepileptogenic effects mediated by adeno-associated virus vector neuropeptide Y expression in the rat hippocampus. *J. Neurosci.* 24, 3051–3059. doi: 10.1523/JNEUROSCI.4056-03.2004

Röder, C., Schwarzer, C., Vezzani, A., Gobbi, M., Mennini, T., and Sperk, G. (1996). Autoradiographic analysis of neuropeptide Y receptor binding sites in the rat hippocampus after kainic acid-induced limbic seizures. *Neuroscience* 70, 47–55. doi: 10.1016/0306-4522(95)00332-d

Sadamatsu, M., Tsunashima, K., Schwarzer, C., Takahashi, Y., Kato, N., and Sperk, G. (1998). Trimethyltin-induced expression of neuropeptide Y Y2 receptors in rat dentate gyrus. *Neurotoxicol. Teratol.* 20, 607–610. doi: 10.1016/s0892-0362(98)00022-1

Sakanaka, M., Wen, T. C., Matsuda, S., Masuda, S., Morishita, E., Nagao, M., et al. (1998). In vivo evidence that erythropoietin protects neurons from ischemic damage. *Proc. Natl. Acad. Sci. U.S.A.* 95, 4635–4640.

Schubert, P., and Kreutzberg, G. W. (1993). Cerebral protection by adenosine. *Acta Neurochir. Suppl.* 57, 80–88.

Schwarzer, C., Kofler, N., and Sperk, G. (1998). Up-regulation of neuropeptide Y-Y2 receptors in an animal model of temporal lobe epilepsy. *Mol. Pharmacol.* 53, 6–13.

Schwarzer, C., Sperk, G., Samanin, R., Rizzi, M., Gariboldi, M., and Vezzani, A. (1996). Neuropeptides-immunoreactivity and their mRNA expression in kindling: Functional implications for limbic epileptogenesis. *Brain Res. Brain Res. Rev.* 22, 27–50.

Simon, R., Henshall, D., Stoehr, S., and Meller, R. (2007). Endogenous mechanisms of neuroprotection. *Epilepsia* 48, 72–73.

Solbrig, M. V., Adrian, R., Baratta, J., Lauterborn, J. C., and Koob, G. F. (2006a). Kappa opioid control of seizures produced by a virus in an animal model. *Brain* 129, 642–654. doi: 10.1093/brain/awl008

Solbrig, M. V., Adrian, R., Chang, D. Y., and Perng, G. C. (2006b). Viral risk factor for seizures: Pathobiology of dynorphin in herpes simplex viral (HSV-1) seizures in an animal model. *Neurobiol. Dis.* 23, 612–620. doi: 10.1016/j.nbd.2006.05.014

Sperk, G., Lassmann, H., Baran, H., Kish, S. J., Seitelberger, F., and Hornykiewicz, O. (1983). Kainic acid induced seizures: Neurochemical and histopathological changes. *Neuroscience* 10, 1301–1315.

Sperk, G., Marksteiner, J., Gruber, B., Bellmann, R., Mahata, M., and Ortler, M. (1992). Functional changes in neuropeptide Y- and somatostatin-containing neurons induced by limbic seizures in the rat. *Neuroscience* 50, 831–846. doi: 10.1016/0306-4522(92)90207-i

Sperk, G., Schwarzer, C., Heilman, J., Furtinger, S., Reimer, R. J., Edwards, R. H., et al. (2003). Expression of plasma membrane GABA transporters but not of the vesicular GABA transporter in dentate granule cells after kainic acid seizures. *Hippocampus* 13, 806–815.

Sperk, G., Wieselthaler-Hölzl, A., Pirker, S., Tasan, R., Strasser, S. S., Drexel, M., et al. (2012). Glutamate decarboxylase 67 is expressed in hippocampal mossy fibers of temporal lobe epilepsy patients. *Hippocampus* 22, 590–603.

Vezzani, A., and Hoyer, D. (1999). Brain somatostatin: A candidate inhibitory role in seizures and epileptogenesis. *Eur. J. Neurosci.* 11, 3767–3776.

Vezzani, A., Michalkiewicz, M., Michalkiewicz, T., Moneta, D., Ravizza, T., Richichi, C., et al. (2002). Seizure susceptibility and epileptogenesis are decreased in transgenic rats overexpressing neuropeptide Y. *Neuroscience* 110, 237–243. doi: 10.1016/s0306-4522(01)00581-4

Vezzani, A., and Sperk, G. (2004). Overexpression of NPY and Y2 receptors in epileptic brain tissue: An endogenous neuroprotective mechanism in temporal lobe epilepsy. *Neuropeptides* 38, 245–252. doi: 10.1016/j.npep.2004.05.004

Woldbye, D. P., Angehagen, M., Gøtzsche, C. R., Elbrønd-Bek, H., Sørensen, A. T., Christiansen, S. H., et al. (2010). Adeno-associated viral vector-induced overexpression of neuropeptide Y Y2 receptors in the hippocampus suppresses seizures. *Brain* 133, 2778–2788.

Woldbye, D. P., Madsen, T. M., Larsen, P. J., Mikkelsen, J. D., and Bolwig, T. G. (1996). Neuropeptide Y inhibits hippocampal seizures and wet dog shakes. *Brain Res.* 737, 162–168.

Wood, J., Verma, D., Lach, G., Bonaventure, P., Herzog, H., Sperk, G., et al. (2016). Structure and function of the amygdaloid NPY system: NPY Y2 receptors regulate excitatory and inhibitory synaptic transmission in the centromedial amygdala. *Brain Struct. Funct.* 221, 3373–3391. doi: 10.1007/s00429-015-1107-7

frontiers | Frontiers in Molecular Neuroscience

TYPE Original Research
PUBLISHED 17 October 2022
DOI 10.3389/fnmol.2022.954167

OPEN ACCESS

EDITED BY
Tobias Engel,
Royal College of Surgeons in Ireland, Ireland

REVIEWED BY
Miao He,
Fudan University, China
Misha Zilberter,
Gladstone Institutes, United States

*CORRESPONDENCE
Guojun Zhang
zgj62051@163.com
Xiaofeng Yang
xiaofengyang@yahoo.com

SPECIALTY SECTION
This article was submitted to Brain Disease Mechanisms, a section of the journal Frontiers in Molecular Neuroscience

RECEIVED 27 May 2022
ACCEPTED 27 September 2022
PUBLISHED 17 October 2022

CITATION
Liu R, Xing Y, Zhang H, Wang J, Lai H, Cheng L, Li D, Yu T, Yan X, Xu C, Piao Y, Zeng L, Loh HH, Zhang G and Yang X (2022) Imbalance between the function of Na^+-K^+-2Cl and K^+-Cl impairs Cl^- homeostasis in human focal cortical dysplasia. *Front. Mol. Neurosci.* 15:954167. doi: 10.3389/fnmol.2022.954167

Imbalance between the function of Na^+-K^+-2Cl and K^+-Cl impairs Cl^- homeostasis in human focal cortical dysplasia

Ru Liu[1,2,3,4], Yue Xing[1], Herui Zhang[1], Junling Wang[1,2,3,4], Huanling Lai[1], Lipeng Cheng[1,3,4], Donghong Li[5], Tao Yu[6], Xiaoming Yan[6], Cuiping Xu[6], Yueshan Piao[7], Linghui Zeng[8], Horace H. Loh[1], Guojun Zhang[6]* and Xiaofeng Yang[1,4]*

[1]Guangzhou Laboratory, Guangzhou, China, [2]Beijing Tiantan Hospital, Capital Medical University, Beijing, China, [3]Beijing Institute of Brain Disorders, Capital Medical University, Beijing, China, [4]Neuroelectrophysiological Laboratory, Xuanwu Hospital, Capital Medical University, Beijing, China, [5]Department of Neurology, The Third Affiliated Hospital of Sun Yat-sen University, Guangzhou, Guangdong, China, [6]Department of Functional Neurosurgery, Xuanwu Hospital, Capital Medical University, Beijing, China, [7]Department of Pathology, Xuanwu Hospital, Capital Medical University, Beijing, China, [8]Department of Pharmacology, Zhejiang University City College, Hangzhou, China

Objective: Altered expression patterns of Na^+-K^+-$2Cl^-$ (NKCC1) and K^+-Cl^- (KCC2) co-transporters have been implicated in the pathogenesis of epilepsy. Here, we assessed the effects of imbalanced NKCC1 and KCC2 on γ-aminobutyric acidergic (GABAergic) neurotransmission in certain brain regions involved in human focal cortical dysplasia (FCD).

Materials and methods: We sought to map a micro-macro neuronal network to better understand the epileptogenesis mechanism. In patients with FCD, we resected cortical tissue from the seizure the onset zone (SOZ) and the non-seizure onset zone (non-SOZ) inside the epileptogenic zone (EZ). Additionally, we resected non-epileptic neocortical tissue from the patients with mesial temporal lobe epilepsy (MTLE) as control. All of tissues were analyzed using perforated patch recordings. NKCC1 and KCC2 co-transporters expression and distribution were analyzed by immunohistochemistry and western blotting.

Results: Results revealed that depolarized GABAergic signals were observed in pyramidal neurons in the SOZ and non-SOZ groups compared with the control group. The total number of pyramidal neurons showing GABAergic spontaneous postsynaptic currents was 11/14, 7/17, and 0/12 in the SOZ, non-SOZ, and control groups, respectively. The depolarizing GABAergic response was significantly dampened by the specific NKCC1 inhibitor bumetanide (BUM). Patients with FCD exhibited higher expression and internalized distribution of KCC2, particularly in the SOZ group.

Conclusion: Our results provide evidence of a potential neurocircuit underpinning SOZ epileptogenesis and non-SOZ seizure susceptibility.

Imbalanced function of NKCC1 and KCC2 may affect chloride ion homeostasis in neurons and alter GABAergic inhibitory action, thereby contributing to epileptogenesis in FCDs. Maintaining chloride ion homeostasis in the neurons may represent a new avenue for the development of novel anti-seizure medications (ASMs).

KEYWORDS

epilepsy, focal cortical dysplasia, cation-chloride cotransporters, pyramidal neurons, seizure onset zone

Introduction

Focal cortical dysplasia (FCD) is a common cause of refractory epilepsy (Blumcke et al., 2011). Histological features have shed light on the cytoarchitectural differences and underpinning developmental pathogenic mechanisms allowing for a more detailed categorization of FCD. However, from a functional perspective, the electrophysiological changes corresponding to these pathological changes and precise epileptogenic mechanisms of FCD remain unknown (Muhlebner et al., 2019).

Epilepsy results from an imbalance between excitatory and inhibitory synaptic transmission in the brain (Palma et al., 2017). Previous studies have documented decreased expression of γ-aminobutyric acid (GABA) receptor subunits, reduced γ-aminobutyric acidergic (GABAergic) interneuron, and decreased spontaneous postsynaptic GABA currents in pyramidal neurons. This may underpin the epileptogenic mechanisms of FCD (Talos et al., 2012; Zhou and Roper, 2014; Medici et al., 2016). FCD patients with epilepsy typically exhibit resistance to conventional anti-seizure medications (ASMs), especially $GABA_A$ receptor agonists; this remains a clinical challenge. Recent studies have demonstrated that the Na^+-K^+-$2Cl^-$ (NKCC1) and K^+-Cl^- (KCC2) cotransporters alter GABAergic inhibitory function by regulating intracellular chloride concentration ($[Cl^-]_i$) (Doyon et al., 2016; Liu et al., 2019). Histological and molecular studies have revealed altered expression and distribution patterns of NKCC1 and KCC2 in the dysplastic neurons of patients with FCD exhibiting epilepsy (Aronica et al., 2007; Munakata et al., 2007; Sen et al., 2007). In addition, bumetanide (BUM), a specific blocker of NKCC1, has been reported to exhibit antiepileptic effects in several preclinical and clinical studies (Dzhala et al., 2005; Beleza, 2009; Eftekhari et al., 2013; Gharaylou et al., 2019; Ragot et al., 2021). This suggests that the expression and function changes in the chloride co-transporter play important roles in epileptogenesis. However, electrophysiological studies of the functional alterations underlying these changes remain limited. Cepeda et al. (2007) reported the depolarized equilibrium potential of GABA (E_{GABA}) and prominent $GABA_A$ receptor ($GABA_AR$)-mediated spontaneous and evoked depolarizing responses in pediatric patients with severe FCD exhibiting epilepsy. Blauwblomme et al. (2019) demonstrated that the abnormal function and expression of the chloride transporter in neurons of patients with FCD exhibiting epilepsy may lead to the paradoxical depolarization of pyramidal neurons. However, these studies have inherent limitations, such as inevitable disputed $[Cl^-]_i$ caused by whole-cell recordings or the lack of intracellular recordings.

At the macroscopic level, based on electrocorticography (ECoG) data Rosenow and Luders (2001) defined the epileptogenic zone (EZ) as the area of the cortex necessary for the generation of recurrent seizures that needs to be removed to achieve seizure freedom. Recently, under diverse macroscopic diagnostic tools, different cortical zones have been conceptualized, such as the seizure onset zone (SOZ), which has been found to be characterized by anomalous EEG signals compared with the surrounding tissues (Jehi, 2018; Zijlmans et al., 2019). Although the temporal dynamics of epileptiform synchronization and epileptogenic networks are well described at the macroscopic level, the key features at the cellular and microcircuit levels cannot be captured by macroscopic evaluation. Therefore, little remains known about the microscopic characteristics and network changes of the EZ (Farrell et al., 2019). Clinicians were determined to gain a comprehensive understanding of epileptic mechanisms through multi-scale evaluations. Therefore, in this study, we selected the SOZ and non-seizure onset zone (non-SOZ) in the EZ of patients with FCD exhibiting epilepsy to assess disease-related changes at the cellular and microcircuit levels.

This study sought to compare the detailed electrophysiological characterization of GABAergic neurotransmission in pyramidal neurons in the SOZ and non-SOZ inside the EZ of patients with FCD with non-epileptic temporal neocortex and to correlate these features with the patterns of NKCC1 and KCC2. We probed whether depolarizing GABAergic action caused by the imbalanced function of NKCC1 and KCC2 cotransporters would perturb chloride ion homeostasis in neurons and contribute to the generation and propagation of epilepsy in patients with FCD.

TABLE 1 Patients characteristics.

Patient/Sex/Age	Histology	Onset age; frequency	Sz types	ASMs, n; Name	EEG	MRI; PET	Surgery	Regions	Groups
FCD									
1/M/18.5 years	FCD Ia	15 years; 2–3 Sz/day	Focal impaired awareness seizure	2; OXC, LEV	Abnormal spikes in RT	Normal MRI; hypometabolism in RT	RT + RI cortectomy	RIT	SOZ
2/M/34 years	FCD Ia	7 years; NA	Focal impaired awareness seizure, GTCS	2; CBZ, VPA	Abnormal spikes in LT	Normal MRI; hypometabolism in LT	LT lesion- ectomy after SEEG	LT	SOZ non-SOZ
3/F/22.1 years	FCD IIa	10 years; NA	Focal aware/impaired awareness seizure	NA	Abnormal spikes in RF	Abnormal signals in RA; hypometabolism in RF and RT	RF cortectomy after SEEG	RMF	SOZ
4/F/28.8 years	FCD IIa	9 years; 1 Sz/several days	Focal aware/impaired awareness seizure, GTCS	2; LEV, LTG	Rhythmic posterior RMF spikes and waves	NA; hypometabolism in RF and RIT	RF and RT lesionectomy	RSF	SOZ
5/M/31 years	FCD IIa	2 years; 10 Sz/month	Focal impaired awareness seizure	2; OXC, VPA	Abnormal spikes in LF	Mild LH swelling; hypometabolism in LF, LT, and LP	LF, LT, LH lesionectomy after SEEG	LMF	SOZ
6/F/7 years	FCD IIb	4 years; 2 Sz/day	Focal aware seizure	2; OXC, LEV	Abnormal spikes in LF	NA	LF lesion-ectomy	LMF	SOZ
7/F/11.9 years	FCD IIIa	5 years; 1–2 Sz/week	Focal impaired awareness seizure	3; VPA, OXC, CBZ	Abnormal spikes in LT	LH abnormal signals; hypo-metabolism in LT, LP, LO	LATL after SEEG	LTP	SOZ
8/M/31.3 years	FCD IIIa	24 years; 3–5 Sz/month	AS	2; LTG, VPA	Rhythmic LT spikes and slow waves	Bilateral mild HS; hypometabolism in LT, LH	Mesial LT lobectomy after SEEG	LTP	SOZ
9/M/27.6 years	FCD IIIb + CG	9 years; 2 Sz/month	Focal impaired awareness seizure	2; CBZ, VPA	RP, RT slow waves	Encephalomalacia foci in RP; NA	RT + RP lesionectomy after SEEG	RIP	SOZ
10/M/11.1 years	CD	2 years; NA	Focal impaired awareness seizure, GTCS, SE	NA	Abnormal spikes in RF, RMT	R cerebral hemisphere malformation; NA	Lesion-ectomy + hemispherectomy	RT	SOZ
11/F/12 years	CD	2 years; >2 Sz/six months	Focal impaired awareness seizure, GTCS	2; OXC, LEV	Rhythmic RP, RO, RT, central gyrus spikes and waves	RSF, RP G/W matter blur-ring; hypometabolism in RSP, RIT	Lesionectomy	RT	SOZ
12/F/35 years	FCD Ia	20 years; 1–2 Sz/day	Focal impaired awareness seizure	1; CBZ	Rhythmic RF, RT spikes	Hypersignal in RH; hypo-metabolism in RT, RH	RATL after SEEG	RMT	non-SOZ

(Continued)

10.3389/fnmol.2022.954167

TABLE 1 (Continued)

Patient/Sex/Age	Histology	Onset age; frequency	Sz types	ASMs, n; Name	EEG	MRI; PET	Surgery	Regions	Groups
13/M/22.8 years	FCD Ib	11 years; >10 Sz/month	focal impaired awareness seizure	2; CBZ, PB	Abnormal spikes in RT	FLAIR hyper-signal in RH; hypometabo-lism in RT	RATL	RMT	non-SOZ
14/M/24.3 years	FCD IIa	10 years; 1–2 Sz/day	Focal impaired awareness seizure, GTCS	2; TPA, CBZ	RF spikes and waves	Normal MRI; hypometabo-lism in RF	RF cortectomy	RSF	non-SOZ
15/F/15 years	FCD IIb	5 years; 10–20 Sz/month	Focal impaired awareness seizure, GTCS	2; VPA, TPM	Rhythmic LF, LT spikes, and slow waves	FLAIR hypersignal in LF; NA	LF + LCC cortectomy after SEEG	LSF	non-SOZ
16/F/12 years	FCD IIb	5 years; 4 Sz/week	Focal impaired awareness seizure	2; OXC, LEV	Rhythmic RT spikes and slow waves	RT abnormal signals; NA	RT cortectomy after SEEG	RT	non-SOZ
17/F/11 years	FCD IIb	6 years; 1–2 Sz/week	Focal impaired awareness seizure	4; OXC, VPA, LTG, CLZ	Spikes and slow waves in LF, central area and LT	LACC G/W blurring; hypometabo-lism in LF and LP	LF + LCC cortectomy after SEEG	LSF	non-SOZ
18/M/26 years	FCD IIIb + CG	1 year; 1 Sz/month	Focal impaired awareness seizure	2; CBZ, VPA	Abnormal spikes in RF	Encephalomalacia in RF and RI	RF cortectomy after SEEG	RIF	non-SOZ
19/M/31.7 years	CD	29 years; 2–3 Sz/day	GTCS	1; CBZ	RT and RF slow waves	R cerebral hemisphere malformation; hypometa-bolism in RT, RH, and RIF	RF + RT cortectomy	RT	non-SOZ
20/F/34.1 years	CD	13 years; 4–5 Sz/week	Focal aware/impaired awareness seizure, GTCS	1; CBZ	Rhythmic RF and RT waves and spikes.	RHS and RF G/W blurring; hypometabo-lism in RF and posterior RIT	RF + RT cortectomy after SEEG	RIF	non- SOZ
Con									
21/F/30 years	HS	23 years; 1–2 Sz/day	Focal impaired awareness seizure	2;LEV, VPA	RT spike (or sharp) slow wave	RHS; hypo-metabolism in RT	RATL	RTP	Con
22/F/21 years	HS (WHO I)	1 year; 4–5 Sz/month	Focal impaired awareness seizure	4; LTP, PB,VPA, CBZ	LT spike (or sharp) slow wave	LHS; hypo-metabolism in LH	LATL	LTP	Con
23/F/32 years	HS (WHO I)	2 years; NA	Focal impaired awareness seizure GTCS	3; PB, LTG, CBZ	Rhythmic LT spikes	LHS; hypo-metabolism in LT and LH	LATL	LTP	Con
24/F/33 years	HS	26 years; NA	Focal impaired awareness seizure GTCS	2; OXC, TPM	Rhythmic RH spikes	RHS; hypo-metabolism in RH	RATL	RTP	Con
25/M/48.5 years	HS (WHO I)	30 years; 1–3 Sz/day	Focal impaired awareness seizure GTCS	NA	LT slow waves and spikes	LT abnormal signals; NA	LATL	LTP	Con

(Continued)

10.3389/fnmol.2022.954167

TABLE 1 (Continued)

Patient/Sex/Age	Histology	Onset age; frequency	Sz types	ASMs, n; Name	EEG	MRI; PET	Surgery	Regions	Groups
26/M/45.7 years	GG	18 years; >3 Sz/week	Focal impaired awareness seizure, GTCS	2; CBZ, LEV	Rhythmic RT spikes	Hypersignal in RH; hypometabolism in RMT	RATL	RTP	Con
27/M/27 years	HGM	16 years; 1–2 Sz/week	Focal impaired awareness seizure	3; TPM, VPA, CBZ	Rhythmic RT spikes and slow waves	Normal MRI; hypometabolism in RP and RT	RATL	RTP	Con
28/M/39.3 years	HGM	24 years; 1–2 Sz/day	Focal impaired awareness seizure, GTCS	1;OXC	Abnormal spikes in LT	Bilateral mild HS; NA	LATL	LTP	Con
29/F/38 years	HS	23 years; 3–4 Sz/day	Focal aware/impaired awareness seizure	1;CBZ	Abnormal spikes in LT	Reduced LT; hypometabolism in LP, LF, LT	LATL	LT	Con
30/M/6 years	CG	4 years; 3–4 Sz/day	Focal aware/impaired awareness seizure	1;VPA	Abnormal spikes in LT	Reduced volume of LH; NA	LATL	LT	Con

ACC, anterior cingulate; ASM, antiseizure medicine; AS, atypical seizure; ATL, anterior temporal lobectomy; CBZ, carbamazepine; CG, cicatricial gyrus; CLZ, clonazepam; EEG, electroencephalography; F, female; FCD, focal cortical dysplasia; F, frontal lobe; GTCS, generalized tonic-clonic seizures; GG, ganglioglioma; G/W, gray/white; H, hippocampus; HGM: heterotopic gray matter; HS, hippocampal sclerosis; I, insular; L, left; LCM, lacosamide; LEV, levetiracetam; IF, inferior frontal gyrus; LRZ, lorazepam; LTG, lamotrigine; M, male; MF, middle frontal lobe; MT, middle temporal gyrus; NA, information not available; O, occipital lobe; OXC, oxcarbazepine; PB, Phenobarbital; PHT, phenytoin; RA, right amygdaloid nucleus; PPA, para-hippocampal place area; RB, right parietal lobe; RT, right temporal lobe; SE, status epilepticus; SF, superior frontal gyrus; Sz, seizure(s); T, temporal lobe; TP, temporal pole; TPM, topiramate; VPA, valproic acid.

Materials and methods

Patient selection and cortical tissue acquisition

In this study, 30 patients with intractable epilepsy were enrolled at Xuanwu Hospital of Capital Medical University from June 2018 to December 2019. Following a standardized preoperative evaluation, all patients underwent surgery to remove the EZ. Neocortical tissues were obtained from 20 patients with FCD and epilepsy. In addition, 10 patients with mesial temporal lobe epilepsy (MTLE) were chosen as the control group because of their relatively non-epileptic neocortical tissue, as suggested by previous studies (D'Antuono et al., 2004; Palma et al., 2006). The temporal neocortex of these patients with MTLE was characterized by no obvious structural aberration and minimal epileptic discharge based on intraoperative ECoG recording. The detailed clinical information and pathological characteristics of the enrolled patients are summarized in **Table 1**. Our research protocol was approved by the Medical Ethics Committee of Xuanwu Hospital, Capital Medical University. All patients were well informed about the study, and consents were obtained from them.

Each patient recruited in the study underwent standardized preoperative evaluation procedures to delineate the EZ and locate the SOZ, including detailed clinical history, neurological examinations, video-electroencephalographic recordings (vEEG), neuropsychological examinations, and neuroimaging studies, etc. Neuroimaging studies include high-resolution magnetic resonance imaging (MRI, 3T), magnetoencephalography, and 18-fluorodeoxyglucose positron emission tomography (FDG-PET). As mentioned above, Rosenow and Luders (2001) defined the EZ as the area of cortex that is indispensable for the generation of epileptic seizures. An integral component for the delineation of the EZ is the seizure onset zone (SOZ): the area of cortex that initiates clinical seizures as determined predominantly by intracranial investigations. Inside the EZ, two blocks of neocortical tissue (1 cm × 1 cm × 1 cm) were defined as SOZ and non-SOZ. However, there is currently no clear definition of "non-SOZ." In this study, SOZ is confirmed as the area of cortex that initiates clinical seizures by combining presurgical intracranial investigations and symptomatology (**Figure 1A**, electrode B). For the other area expect SOZ in the surgical resection, as our previous study, we choose "non-SOZ" as one of brain tissue which is also located in the area to be excised but showing the least abnormal electrophysiological recordings under subdural recording (**Figure 1B**; Cheng et al., 2022).

Given that the brain tissue is taken during surgery, the surgeon cannot cut off the blood supply in order to keep the brain tissue alive before collecting the brain tissue. When we collected the first two samples (SOZ and non-SOZ) from the first patient, it was shown that collecting two brain

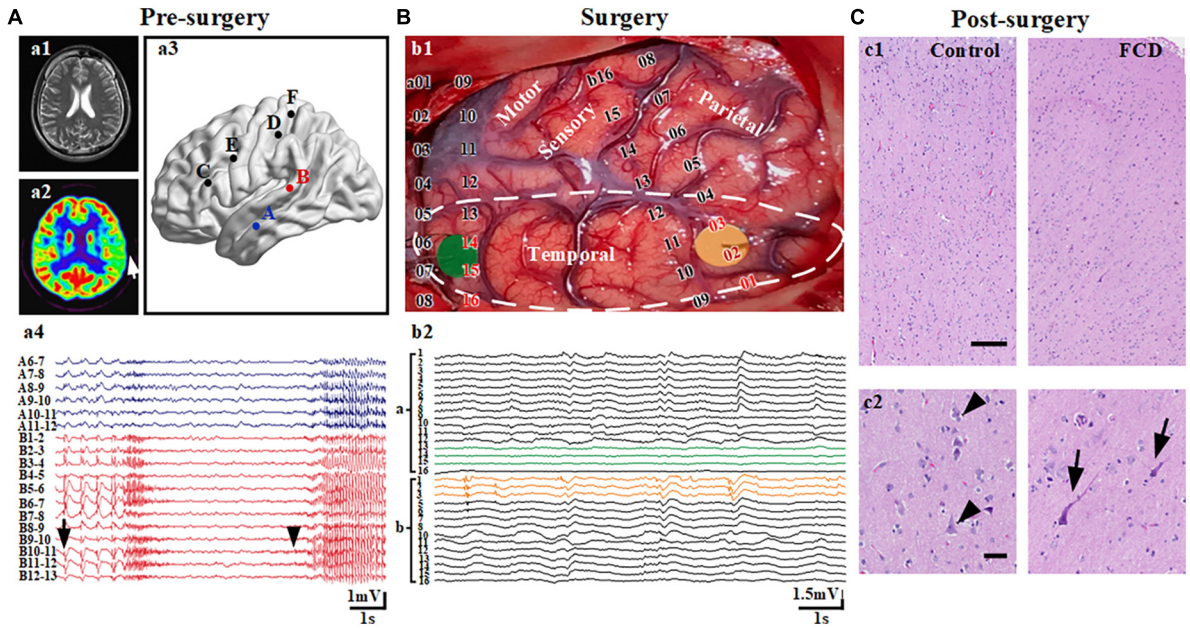

FIGURE 1
Localization of the seizure onset zone (SOZ) and non-seizure onset zone (non-SOZ). **(A)** Presurgical evaluation and confirmation of SOZ. **(a1,2)** Represents an area of hypometabolism in the left middle temporal lobe (arrow) in a PET scan of the patient with focal cortical dysplasia (FCD) having a negative MRI. **(a3,4)** Represents spontaneous recurrent rhythmic interictal spikes (arrow) and ictal discharges (arrowhead) restricted to the region in the left middle temporal gyrus from electrode B in the stereo-electroencephalograph recordings. **(B)** Reconfirmation of neocortical samples during surgery. **(b1)** The yellow and green areas reflect the areas of tissue samples used for electrophysiological recording. **(b2)** Recordings based on electrocorticography (ECoG) showed continuous epileptiform discharges (yellow line) and normal background activity (green line) in the temporal region. The area surrounded by a white dotted line is the region being removed. **(C)** Post-surgery histological examination with FCD IIa. **(c1)** Hematoxylin and eosin (H and E)-stained section of brain tissues of control and FCD groups. **(c2)** The left section shows relative normal shaped and arranged neurons (arrowheads) in the lateral neocortex from patients with mesial temporal lobe epilepsy. The right section represents the extension of the area in the first panel showing dysmorphic neurons with disrupted cortical lamination (arrows). Scale bars represent 500 and 100 μm for the first and second panels, respectively.

tissues at the same time would cause more serious bleeding which did inevitable damages to the patient. Therefore, from the second patient, we adopted a double-blind and random sampling method, and each patient randomly collected one piece of brain tissue. All patients with FCD were confirmed by a postoperative histological examination (Figure 1C). In summary, we divided our experiment into three groups: the SOZ, non-SOZ, and control groups.

Brain tissue slice preparation

After being obtained in the operating room, neocortical tissues were immediately placed into an ice-cooled and oxygenated (95% O_2 and 5% CO_2) cutting solution containing 220 mM sucrose, 2.5 mM KCl, 1.25 mM NaH_2PO_4, 25 mM $NaHCO_3$, 0.5 mM $CaCl_2$, 7 mM $MgCl_2$, and 10 mM D-glucose (pH 7.4; osmolarity maintained at 340 mOsm/kg), and transferred to our electrophysiological laboratory within 5–10 min. Subsequently, meninges and blood clots were gently removed, and 400 μm neocortical transverse slices were cut using a vibratome (VT 1000S; Leica Microsystems, Wetzlar, Germany) and incubated in oxygenated (95% O_2 and 5% CO_2) artificial cerebrospinal fluid (ACSF) containing (in mM) 125 NaCl, 2.5 KCl, 1.25 NaH_2PO_4, 26 $NaHCO_3$, 2 $CaCl_2$, 2 $MgCl_2$, and 10 D-glucose (pH 7.3; osmolarity maintained at 300–310 mOsm/kg) at room temperature for at least 1 h before recording.

Perforated patch-clamp recording and data analysis

Following incubation, the brain slices were submerged in a recording chamber perfused with oxygenated ACSF at a rate of 2–2.5 mL/min at room temperature. Perforated patch-clamp recordings were performed on pyramidal neurons in the neocortex and viewed under an infrared differential interference contrast microscope with a Nikon 40 water immersion lens (ECLIPSE FN1, Nikon Corp., Tokyo, Japan). Recordings were performed in layers III and IV in the non-SOZ and control groups. In the SOZ group, in which the lamina was not clearly defined, layers III and IV were generally located according to the non-SOZ lamina in the middle region of the dysplastic cortex

(Figure 2A). Pyramidal neurons were identified based on their triangular-shaped cell bodies and relatively simple axons and were confirmed by electrophysiological recordings as displaying longer action potential (AP) half-widths and lower peak AP frequency (Avermann et al., 2012). Recording electrodes (resistance, 4–6 MΩ) were prepared from borosilicate glass capillaries (B15014F, Vital Sense Scientific Instruments Co., Ltd., Wuhan, China) using a horizontal pipette puller (P-1000 Next Generation Micropipette Puller, Sutter Instrument, CA, USA). The pipette solution contained (in mM) 135 KCl, 10 HEPES, 0.5 $CaCl_2$, 2 $MgCl_2$, and 5 EGTA (pH 7.3 adjusted with KOH; osmolarity maintained at 290–300 mOsm/kg). Gramicidin was stocked at an initial concentration of 16 mg/ml and then diluted with pipette solution to reach a final concentration of 80 μg/ml. The electrode tip and barrel were backfilled with pipette solution and gramicidin-containing pipette solution, respectively. Following the formation of a tight seal and after the series resistance (Rs) decreased and stabilized at 30–110 MΩ, we started recording. Recordings were ended when a rapid decrease in Rs and a "leak-like" current were observed, indicating that the cell had entered the conventional whole-cell configuration by rupture of the membrane seal. The resistance and capacitance of the pipette have been compensated. Liquid junction potential was not corrected.

We first recorded the resting membrane potential (V_m), membrane conductance, and firing properties to identify pyramidal neurons in the current-clamp mode. Next, we recorded spontaneous excitatory postsynaptic currents (sEPSCs) for 3 min at a holding potential of −70 mV in the voltage-clamp mode. Subsequently, we acquired pharmacologically isolated GABAergic sPSCs by applying 6-cyano-7-nitroquinoxaline-2,3-dione (CNQX, 10 μM) and DL-2-amino-5-phosphonopentanoic acid (DL-AP5, 100 μM) to block α-amino-3-hydroxy-5-methylisoxazole-4-propionic acid (AMPA) and *N*-methyl-D-aspartate (NMDA) receptors. BUM (10 μM) was then added to assess its effects on GABAergic sPSCs. The sEPSCs were automatically detected at amplitude adjusted above the root 2 mean square noise level using Clampfit 10.5 (Molecular Devices, CA, USA). Cumulative amplitudes were calculated by summating amplitudes of all events within 180 s periods.

In this study, to probe the E_{GABA} of pyramidal neurons, we first determined the neuronal firing patterns in response to depolarizing current injections prior to perfusion with tetrodotoxin. We applied GABA in the chamber with a pulsed fashion immediately during the ramp test. A hand-made fast drug delivery systems was used to apply GABA (100 μM, containing: CGP 35348, 1 μM; TTX, 1 μM) from a pipette resting 10 –20 μm above the slice at the position of the recorded soma. The system enabled quick fluid changes with a speed of 1 ml/min and a diameter of about 20 μm for its tip. Voltage ramps −80 to + 10 mV over 100 ms applied from a holding potential of −70 mV in the absence and presence of GABA were used to determine E_{GABA}. The membrane voltage at which the current traces, obtained in the presence and absence of GABA, crossed was measured as the apparent E_{GABA}. Then, voltage ramps were repeated following the addition of BUM (10 μM). The membrane voltage at which the current traces, obtained in the presence and absence of BUM, crossed was measured as the apparent E_{BUM}. In addition, the driving force for GABA production ($DF_{GABA} = E_{GABA} - Vm$) was measured.

Immunohistochemistry

The brain tissue was fixed in 10% formalin and embedded in paraffin. Paraffin-embedded tissues were sectioned at 6 μm and heated in a microwave oven (60°C for 60 min). The sections were thereafter deparaffinized in xylene and rehydrated sequentially in graded concentrations of alcohol. Sections from the SOZ, non-SOZ, and control groups were probed with an anti-KCC2 antibody (Millipore, #07-432, Boston, MA, USA, 1:200) overnight at 4°C. The slides were then incubated with horseradish peroxidase-conjugated secondary antibodies at room temperature for 1 h. Immunolabeling was visualized using the avidin-biotin conjugation method and 3,3′-diaminobenzidine. The sections were next counterstained with hematoxylin.

Immunofluorescence staining

Brain slices were post-fixed with 10% formalin, washed three times with PBS, incubated for 30 min with 0.3% Triton, and then blocked with 1% goat serum for 1 h to avoid binding of non-specific antibodies. Sections were then incubated at 4°C overnight with the following primary antibodies: anti-NKCC1 (Millipore, PA5-118800, Boston, MA, USA, 1:200), anti-NeuN (Sigma-Aldrich, St. Louis, MO, USA, MAB377, 1:200). Secondary antibodies conjugated to Alexa Fluor 488 or 594 (1:1,000; Invitrogen) were applied for 1.5 h at room temperature. Slides were mounted with Fluoroshield containing DAPI (Ab104139; Abcam) and observed with a confocal microscope (LSM710; Zeiss, Oberkochen, Germany).

Western blot analysis

Total protein was quantified using a BCA Protein Assay Kit (Solarbio, Beijing, China). Samples were electrophoresed on 5 and 10% Tris–HCl gels, transferred onto polyvinylidene difluoride membranes, and incubated with primary antibodies (anti-KCC2, Millipore, 1:1,000). GAPDH (mouse monoclonal IgG, CST, Danvers, MO, USA 1:5,000) was used as the reference protein. Horseradish peroxidase-conjugated secondary antibodies (anti-rabbit IgG and anti-mouse IgG; LI-COR, USA) were used to bind the primary antibodies. The bands were visualized using a two-channel infrared (IR) scanner

(Odyssey, NE, USA). Densitometric analysis of the protein signals was carried out using the ImageJ software (version 6.0; NIH, Bethesda, MD, USA). The target protein levels were normalized to internal control.

Statistical analysis

All data distributions were assessed with the Shapiro–Wilk test. For the normal distribution, data were analyzed using Student's *t*-test or one-way ANOVA with *post-hoc* tests. Results were expressed as mean ± standard error of the mean (SEM), with significance set at $p < 0.05$. For the skewed distribution, analysis was carried out using the non-parametric Kruskal–Wallis test followed by Dunn's multiple comparisons or Mann–Whitney *U*-test. Results were expressed as medians and interquartile range (IQR), with significance set at $p < 0.05$.

Results

Clinical information

First, we analyzed the clinical characteristics of the patients included in this study. No significant differences in the mean duration of epilepsy were observed across the groups. Briefly, the male/female ratio of patients with FCD exhibiting epilepsy enrolled in the study was 1:1, the mean duration of epilepsy being 13.5 ± 1.8 years and the average age at surgery being 22.9 ± 2.1 years old. The EZ in the FCD was localized in frontal ($n = 9$), temporal ($n = 10$), or posterior quadrants ($n = 1$).

Comparison of electrophysiological properties in pyramidal neurons among seizure the onset zone, non-seizure the onset zone, and control groups

Using perforated patch-clamp recording, we first compared the basic electrophysiological properties of pyramidal neurons across the three groups in the current-clamp mode. No significant differences were observed across the groups in terms of average V_m, cell capacitance (C_m), input resistance (R_N), or membrane time constant (**Table 2**). No significant differences were observed across the pyramidal neurons of the three groups regarding the characteristics of the action potentials induced by the injection of a + 300 pA current (**Figures 2B,C** and **Supplementary Figure 1**).

Next, we recorded the sEPSCs of pyramidal neurons in the SOZ, non-SOZ, and control groups held at −70 mV. The average frequency of sEPSCs on pyramidal neurons was significantly lower in the control group than in the SOZ group (median = 0.25 Hz, IQR = 0.1–0.28 Hz, $n = 17$ vs. median = 0.36 Hz, IQR = 0.22–0.85 Hz, $n = 20$, p = 0.02) and non-SOZ group (median = 0.53 Hz, IQR = 0.28–1.05 Hz, $n = 16$, $p = 0.003$). However, no significant difference was observed between the SOZ and non-SOZ groups. The median amplitude of sEPSCs on pyramidal neurons was not significantly different among the three groups. The decay time was smaller in the non-SOZ group (median = 17.02 ms, IQR = 15.95–18.54 ms) than in the control group (median = 23.11 ms, IQR = 19.61–47.29 ms, $p = 0.0001$) and the SOZ group (median = 19.73 ms, IQR = 18.62–31.47 ms, $p = 0.02$). In addition, no significant differences in the sEPSC rise time were observed across the groups (**Figures 2D,E**).

In a previous study, Talos et al. applied glutamatergic receptor antagonists to isolate and confirm the GABAergic components ($GABA_A$ receptor-mediated spontaneous postsynaptic currents, $GABA_A$R-mediated sPSCs) with picrotoxin at a holding potential close to RMP in patients with tuberous sclerosis (Talos et al., 2012). Based on their study's results, we assessed the effects of GABAergic neurotransmission on sPSCs after blocking glutamatergic receptors to investigate the alterations in GABAergic neurotransmission in human dysplastic epileptic tissues. We first recorded sEPSCs in pyramidal neurons under normal ACSF perfusion in the SOZ, non-SOZ, and control groups, followed by the complete blockade of AMPA and NMDA receptors with CNQX and DL-AP5. Consistent with a previous study, under conditions of complete AMPA and NMDA receptor blockade, residual $GABA_A$R-mediated sPSCs disappeared completely in the control group. However, $GABA_A$R-mediated sPSCs remained present in the SOZ and non-SOZ groups, although they were significantly reduced (**Figure 3A**).

We assessed the effects of BUM, a NKCC1 blocker, on $GABA_A$R-mediated sPSCs. We first probed how BUM would affect sPSCs by regulating neuronal action potentials. Results demonstrated that BUM did not change the frequency, peak amplitude, threshold, or half-width of the neuronal action potential (data not shown). We normalized $GABA_A$R-mediated sPSCs before and after the application of BUM (10 μM). BUM reduced $GABA_A$R-mediated sPSCs frequency (from 1 to 0.25; $n = 10$, $p = 0.002$) and cumulative amplitude (from 1 to 0.24, $n = 10$, $p = 0.004$) in FCD patients (**Figure 3B**). No significant effect of BUM was observed on $GABA_A$R-mediated sPSCs amplitude (**Figure 3B**).

Features of γ-aminobutyric acidergic transmission

We found no $GABA_A$R-mediated sPSCs on pyramidal neurons in the control group. However, $GABA_A$R-mediated

TABLE 2 Comparison of the intrinsic membrane properties of pyramidal neurons among different groups.

	FCD (SOZ, $N = 20$)	FCD (non-SOZ, $N = 18$)	Control ($N = 16$)
RMP (mV)	−74.4 (−64.1 to −78.3)	−76.5 (−72.0 to −79.8)	−73.1 (−69.9 to −78.1)
Cm (pF)	109.3 (81.2 to 129.9)	88.7 (83.25 to 104.8)	99.1 (77.2 to 119.2)
R_N (MΩ)	226.2 ± 26.4	189.4 ± 20.9	229.9 ± 22.0
Time constant (ms)	5.0 ± 0.5	4.2 ± 0.5	5.0 ± 0.4

RMP, resting membrane potential; Cm, membrane capacitance; R_N, input resistance. Values are reported as mean ± SEM; medians and interquartile range (IQR), with significance set at $p < 0.05$. There was no significant difference among three groups in the above parameters.

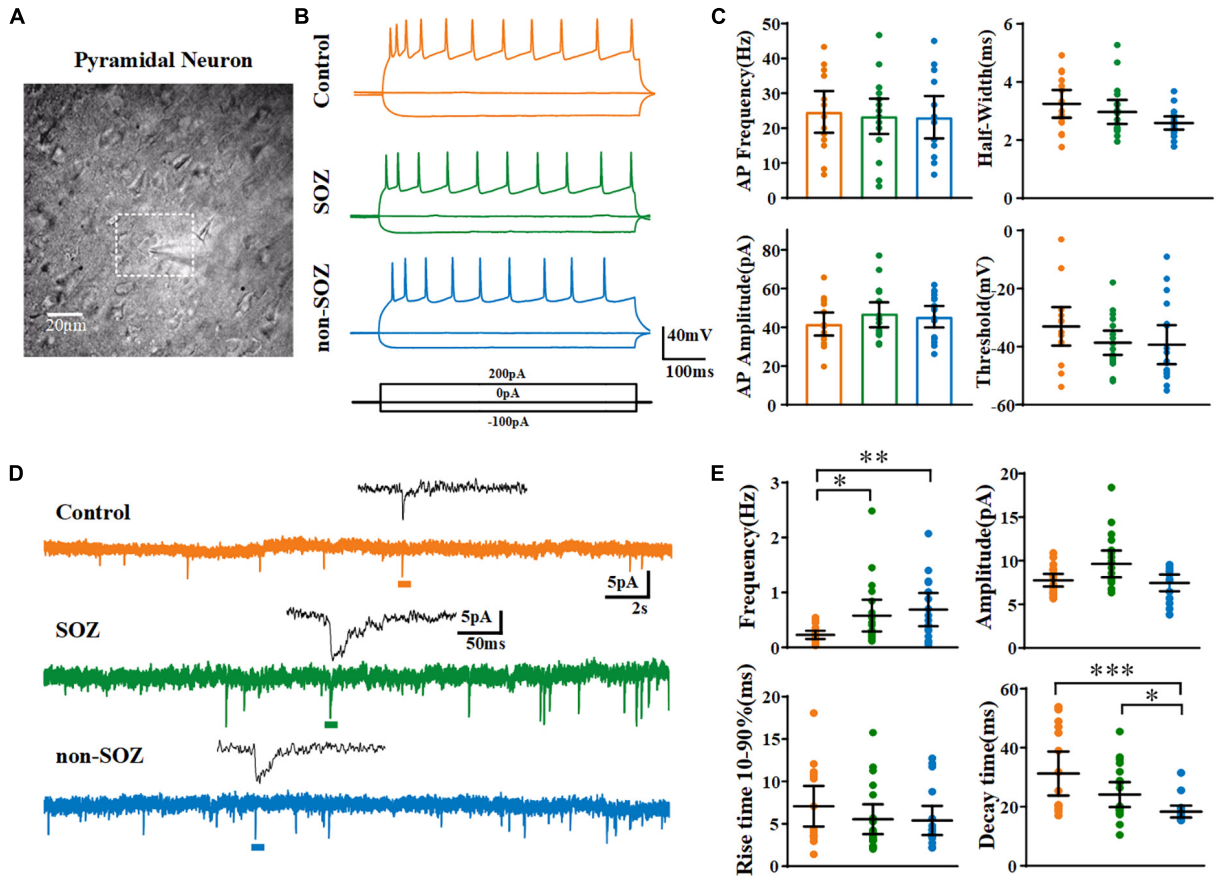

FIGURE 2
Electrophysiological characteristics and spontaneous excitatory postsynaptic currents of pyramidal neurons (PN) among groups. **(A)** Photomicrographs of individual PN within the dysplastic cortex. **(B)** Representative traces and action potential firing of pyramidal neurons from the SOZ, non-SOZ, and control groups with −100, 0, 200 pA injection at the resting membrane potential. **(C)** Representative traces of spontaneous excitatory postsynaptic currents obtained in the three groups. **(D)** Comparison of the electrophysiological characteristics of pyramidal neurons across the three groups $N = 19, 18, 16$ for SOZ, non-SOZ, and control groups, respectively. **(E)** Comparison of spontaneous excitatory postsynaptic currents of pyramidal neurons across the three groups. $N = 20, 18, 16$ for SOZ, non-SOZ, and control groups, respectively. $^*p < 0.05$, $^{**}p < 0.01$, $^{***}p < 0.01$. Data was shown as mean ± SEM.

sPSCs were more common in neurons in the SOZ group (11/18, 61.11%) than in the non-SOZ (7/18, 38.89%). There was no significant difference in the frequency of $GABA_A$R-mediated sPSCs (median = 0.08 Hz, IQR = 0.03–0.17 Hz, $n = 11$ vs. median = 0.07 Hz, IQR = 0.02–0.11 Hz, $n = 7$, $p > 0.05$), the amplitude of $GABA_A$R-mediated sPSCs (median = 7.5 pA, IQR = 6.4–12.0 pA, $n = 11$ vs. median = 7.1 pA, IQR = 6.6–9.6 pA, $n = 7$, $p > 0.05$) and the cumulative amplitude of $GABA_A$R-mediated sPSCs (median = 90.7 pA, IQR = 44.7–360.2 pA, $n = 11$ vs. median = 95.0 pA, IQR = 48.9–125.4 pA,

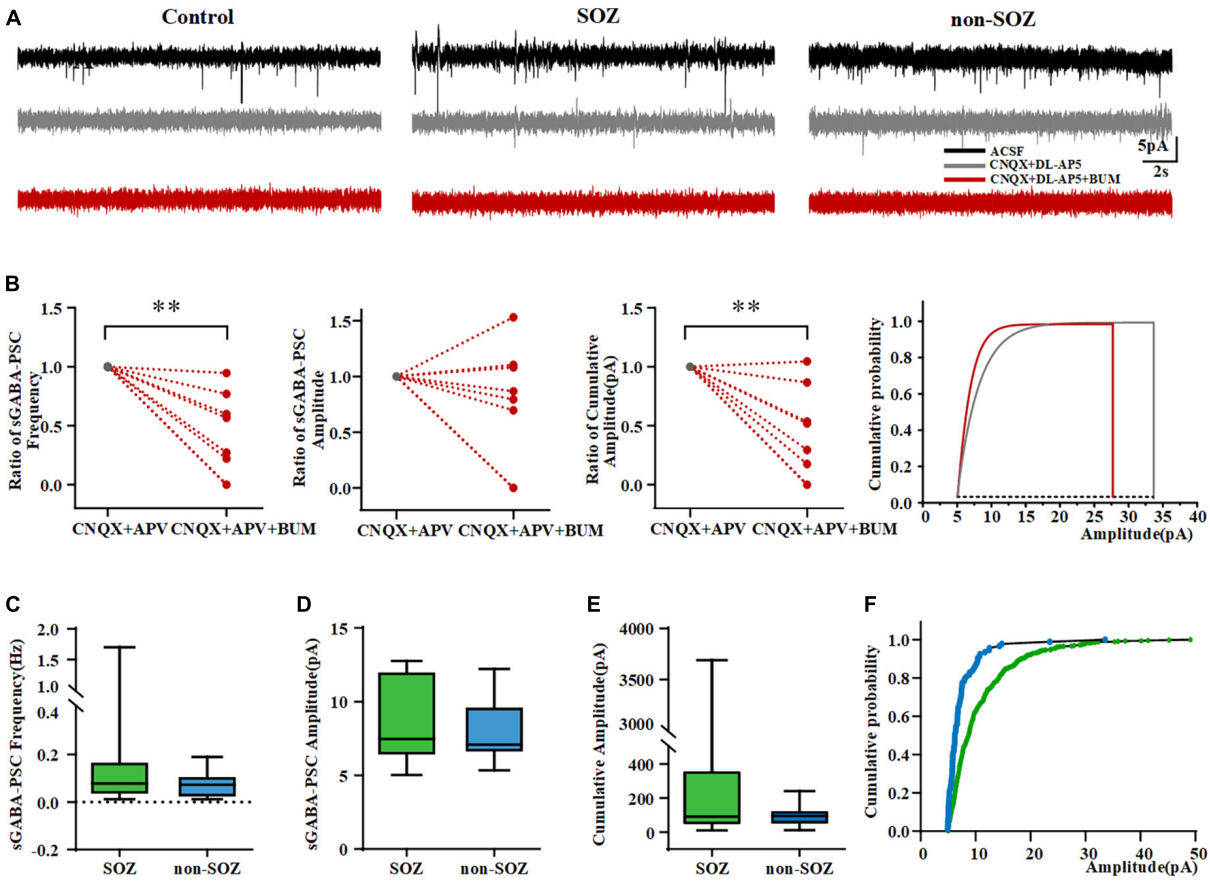

FIGURE 3
Pyramidal neurons in the SOZ and non-SOZ of focal cortical dysplasia (FCD) showing depolarizing bumetanide-sensitive $GABA_A$ receptor responses. **(A)** Altered inhibitory GABAergic signaling in SOZ and non-SOZ groups. **(B)** Bumetanide significantly dampened the frequency and cumulative amplitude of $GABA_AR$-mediated sPSCs in FCD patients $N = 10$. **(C–E)** $GABA_AR$-mediated sPSCs are shown in the SOZ and non-SOZ groups. **(F)** Cumulative $GABA_AR$-mediated sPSCs amplitude probability distributions for pyramidal neurons from SOZ and non-SOZ groups. $^{**}p < 0.01$. Data was shown as medians and interquartile range (IQR).

$n = 7$, Mann–Whitney U-test, $p > 0.05$) in the pyramidal neurons of between SOZ and non-SOZ groups (Figures 3C–E). Cumulative $GABA_AR$-mediated sPSCs amplitude distribution from cells depicted in SOZ showed was significantly higher in SOZ compared with non-SOZ group ($P < 0.001$, Mann–Whitney U-test, Figure 3F).

More depolarized E_{GABA} in seizure the onset zone of focal cortical dysplasia

E_{GABA} reflects the potential at which currents are generated during the voltage ramp in the absence and presence of GABA intersect (Figure 4A). The average E_{GABA} for each neuron measured in the different groups is represented in Figure 4B. The E_{GABA} on pyramidal neurons in the SOZ group (-54.5 ± 6.2 mV, $n = 7$) was significantly shifted to more positive values compared to that in the control group (-73.0 ± 1.0 mV, $n = 7$, $p < 0.05$) and non-SOZ group (-69.2 ± 1.9 mV, $n = 6$, $p < 0.05$, Figure 4B). The polarity of GABAergic response is affected by the driving force of GABA. E_{GABA} (-54.5 ± 6.2 mV, $n = 7$) was more positive than RMP (71.6 ± 2.5 mV, $n = 7$, Student's t-test, $p < 0.05$) in the SOZ group. In contrast, no significant differences were observed between E_{GABA} and RMP in the non-SOZ (-75.2 ± 2.8 mV, $n = 6$ vs. -69.2 ± 1.9 mV, $n = 6$) and control groups (-73.6 ± 2.4 mV, $n = 7$ vs. -73.0 ± 1.0 mV, $n = 7$). DF_{GABA} was significantly higher in the SOZ group than in the control group (median = 17.85 mV, IQR = 8.43–15.55 mV, $n = 7$ vs. median = 4.29 mV, IQR = −8.18-4.617 mV, $n = 7$, $p > 0.05$ Figure 4B). In contrast, no significant difference was observed in the DF_{GABA} of the non-SOZ group compared to the control group. Application of BUM did not alter E_{GABA} in the control group (−75.1 vs. −71.2 mV), but E_{GABA} shifted to more negative values in the SOZ group (−52.9 vs. −75.0 mV) (Figure 4A).

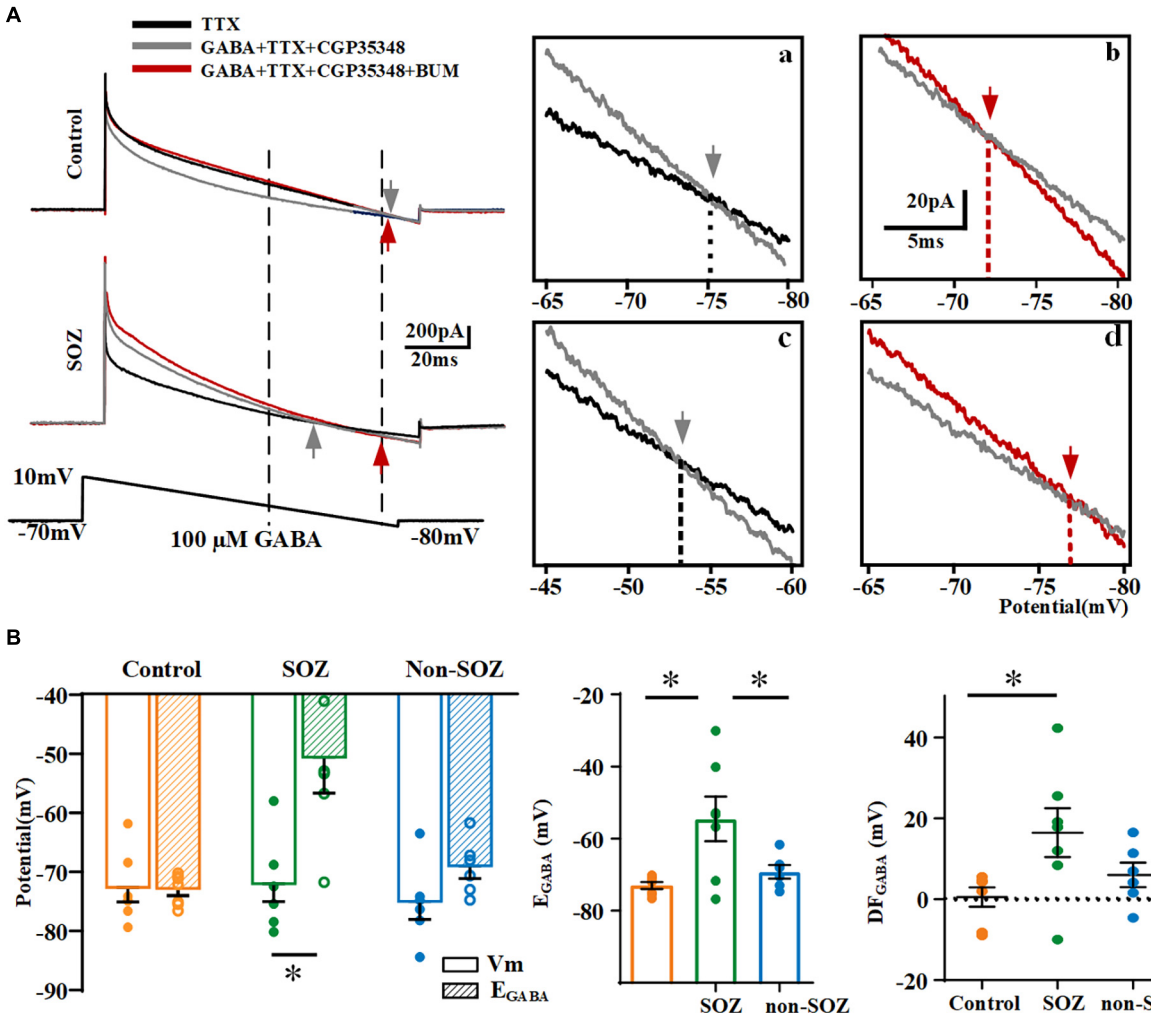

FIGURE 4
Comparison of reversal potentials of GABA (E_{GABA}) across groups. **(A)** Gramicidin-perforated-patch recordings exhibiting current traces of pyramidal neurons from SOZ **(a)** and control groups **(b)** during hyperpolarizing ramps (bottom) in the absence of GABA (black line), with the application of 100 μM GABA (gray line), and with the application of 100 μM GABA and 10 μM BUM (red line). The ramp potential at which the current traces without GABA and with GABA, without BUM and with BUM intersected, represent E_{GABA} (gray arrow in inset) and E_{BUM} (red arrow in inset). Vertical dashed lines intersecting the command potential schematic show the range of command voltage in the boxed area. Insets: expanded traces of boxed regions illustrate the E_{GABA} (gray arrow) and E_{BUM} (red arrow) of a pyramidal neuron in SOZ **(a,c)** and control groups **(b,d)**. **(B)** Summary plot of E_{GABA} and DF_{GABA} across groups. $^*p < 0.05$. Data was shown as mean ± SEM.

Expression and distribution of K^+-Cl^- in human epileptic focal cortical dysplasia and non-epileptic cortical tissues

In addition to the electrophysiological results indicated significant depolarizing GABAergic signaling in neurons in the SOZ group, we assessed the neuronal expression of NKCC1 and KCC2 in the three groups (Figure 5). As previous studies, NKCC1 showed a wide distribution in a variety of tissues and cell types within and outside the nervous system (Virtanen et al., 2020). In our study, we also tried to explore the subcellular distribution of NKCC1 using immunofluorescence but found that no significant differences in the subcellular location of NKCC1 were observed across the groups. Strong NKCC1 immunoreactivity was detected in most NeuN-expressing normal-sized neurons in all the groups. Immunostaining for NKCC1 was present in the soma and dense intra-somatic staining (Supplementary Figure 2).

Diffuse neuropil staining for KCC2 was observed in the FCD cortical tissue as well as in the control temporal neocortex. The neurons in the SOZ showed that KCC2 was internalized into the cells and that its distribution on the cell membrane was significantly reduced. However, there was no obvious KCC2 cell internalization in the non-SOZ and control groups. Histological

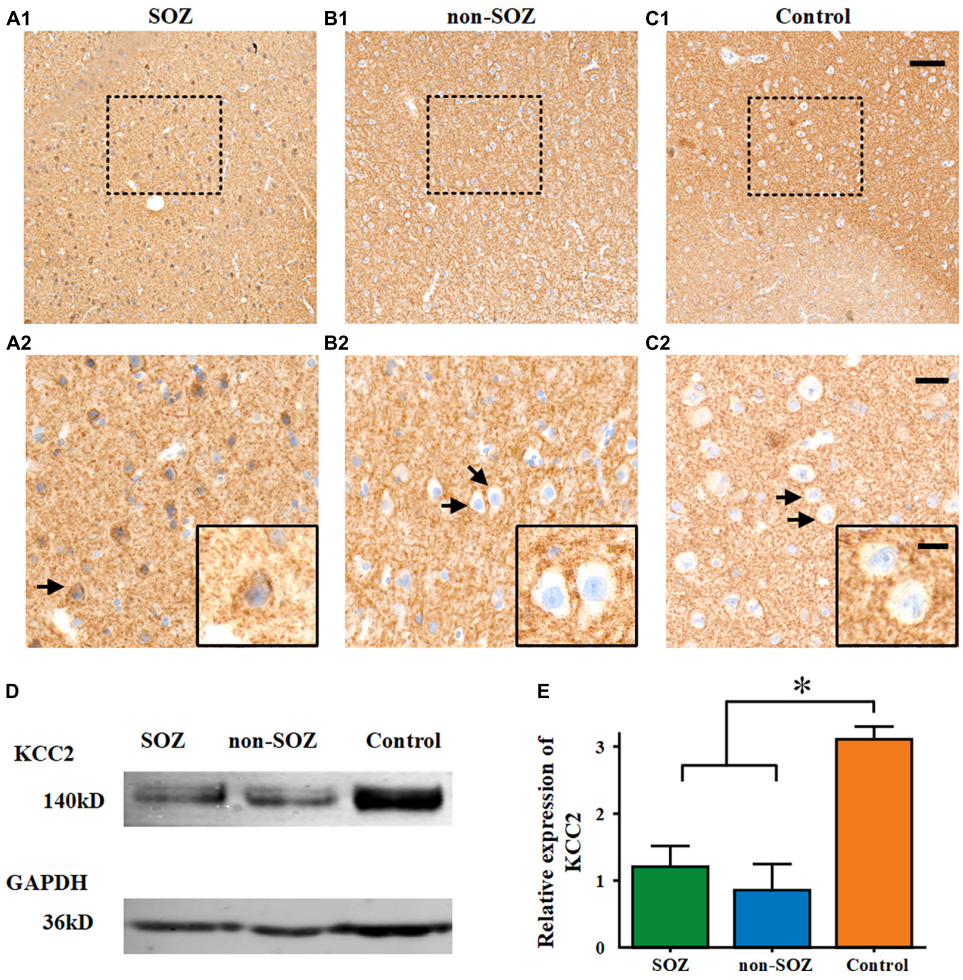

FIGURE 5
Comparison of KCC2 expression across all three groups. A diaminobenzidine reaction product was used for the immunohistochemical detection of KCC2 using a hematoxylin counterstain. **(A–C)** Sub-cellular KCC2 distribution in the three groups. High peri-somatic KCC2 localization was assessed in the SOZ of patients with FCD and epilepsy. Cytoplasmic expression was absent in the non-SOZ of the same patient and the control group. **(A2–C2)** Represent magnified images of the enclosed areas in **(A1–C1)**. Black frames in **(A2–C2)** depict different sub-cellular KCC2 distribution (arrows). Scale bars represent 100 μm for **(A1–C1)**, 30 μm for **(A2–C2)**, and 10 μm for the black frame in **(A2–C2)**. **(D,E)** Expression in total homogenates from specimens in SOZ, non-SOZ, and control groups. Expression of GAPDH (as a reference protein) as seen in the same protein extracts. *$p < 0.05$. Data was shown as mean ± SEM.

analyses revealed cytoplasmic KCC2 accumulation in neurons in the SOZ group, whereas cytoplasmic KCC2 staining was absent in the non-SOZ and control groups (Figures 5A–C). A western blot analysis showed that the expression of KCC2 protein in the SOZ and non-SOZ groups was significantly decreased compared with that in the control group (Figures 5D,E).

Discussion

In this study, we assessed the electrophysiological characteristics and depolarizing synaptic activity of pyramidal neurons in patients with FCD and epilepsy. In particular, we probed the effects of imbalanced function of NKCC1 and KCC2 on GABAergic signaling in pyramidal neurons inside the SOZ, non-SOZ within the EZ of the patients with FCD, and non-epileptic neocortex in patients with MTLE (control). We sought to establish a relationship between macroscopic epileptogenesis and microscopic cell-to-cell communication to better understand the epileptogenic network of FCD through a micro-macro neuro-electrophysiology lens. We observed depolarizing GABAergic signaling in pyramidal neurons located in the SOZ and non-SOZ of the FCD, but not in the control group. Although there is no significant difference between SOZ and non-SOZ in terms of frequency and intensity of depolarizing GABAergic responses at this microscopic level, however, there were more neurons with depolarizing GABAergic responses and higher E_{GABA} in the

SOZ than in the non-SOZ, which may explain the macroscopic differences between the SOZ and non-SOZ in patients with FCD. In addition, we revealed that depolarizing GABAergic neurotransmission in FCD patients, which can be reversed by BUM, is related to the imbalanced function of NKCC1 and KCC2 in the SOZ. This is the first comparative study of depolarizing GABAergic signals in the SOZ, non-SOZ, and non-epileptic cortical regions. Our findings provide important evidence of a potential neurocircuit underlying SOZ epileptogenesis and non-SOZ seizure susceptibility. These results also point to a possible mechanism for epileptogenesis in FCD at the cellular and microcircuit levels, highlighting a novel therapeutic avenue for patients with FCD and epilepsy.x

Establishing micro-macro electrophysiological recordings to gain a better understanding of the epileptogenic network of patients with focal cortical dysplasia exhibiting epilepsy

Accurate delineation of the EZ is critical to determining which patients with refractory epilepsy are appropriate candidates for surgical intervention (Feindel et al., 2009). Although the EZ remains a theoretical concept, five cortical zones (including the SOZ) related to the EZ are roughly defined in presurgical evaluations (Jehi, 2018; Zijlmans et al., 2019). The precise definition of the SOZ has long been thought to accurately delineate the EZ, but it has been found that the EZ is often more extensive than the SOZ, and the precise boundary of the EZ is poorly defined (Rosenow and Luders, 2001). Rasmussen et al. proposed that removing the SOZ was necessary but insufficient to achieve lasting seizure-free survival (Rasmussen, 1983), which indicates the potential involvement of the non-SOZ within the EZ in epileptogenesis. Currently, epilepsy is considered to be a disease of neural networks (Gonzalez Otarula et al., 2019). Successful surgical outcomes depend on the analysis of seizure-generating networks. For a network-based analysis, focusing on regions in the EZ beyond the SOZ to understand the mechanisms of epileptogenesis is crucial (Badier et al., 2015; Paz and Huguenard, 2015; Zijlmans et al., 2019). In addition, a well-recognized, major clinical problem is that most studies locating the SOZ and EZ mainly emphasize the macroscopic level, with little concern over the microscopic changes involved. Given the markedly different EEG signals between the SOZ and non-SOZ in patients with FCD, we assessed the underlying neurotransmission patterns, particularly the depolarizing GABAergic signals, to uncover potential microscopic distinctions that contribute to the macroscopic differences.

Another challenge in human clinical research remains the acquisition of healthy, non-epileptic brain tissue, which would otherwise not warrant surgical resection in a clinical setting. Here, we chose the temporal neocortex from patients with MTLE as our control group for the following reasons: (1) temporal neocortical tissue lies far from the EZ and is not characterized by any obvious structural aberration (D'Antuono et al., 2004); (2) temporal neocortical tissue has been shown to have the least abnormal transcription of Cl^- transporters and highest E_{GABA} compared to the subiculum and hippocampal proper in patients with MTLE, which indicates relatively balanced NKCC1 and KCC2 level (Palma et al., 2006); and (3) temporal neocortical tissue is often resected during operations for such patients with epilepsy.

$GABA_A$ receptor-mediated depolarization caused by imbalanced function of Na^+-K^+-2Cl and K^+-Cl^- promotes epileptogenesis in patients with focal cortical dysplasia exhibiting epilepsy

The recruitment of glutamatergic neurons is a fundamental component of seizures (Farrell et al., 2019). As 80% of neocortical neurons are excitatory glutamatergic pyramidal neurons (with a higher percentage in CD) (Deukmedjian et al., 2004), pyramidal neurons in FCD are maintained in an immature state with hyperexcitable properties in the malformed cortex (George and Jacobs, 2011). Pathologically interconnected neurons have been hypothesized to gather as novel pathological microdomains, leading to interacting networks that generate hypersynchronous discharges that trigger a seizure (Bragin et al., 2000). Previous reports have indicated that the key features of microcircuits captured by microscopic recordings in different brain regions associated with the EZ are significantly different (Stead et al., 2010; Blauwblomme et al., 2019). The heterogeneity of these microcircuits plays an important role in the formation of the macro-networks. Our results demonstrated that the frequency sEPSCs in pyramidal neurons were higher in the patients with FCD than in the non-epileptic cortex. This supports previous findings in animal models of CD (Zhu and Roper, 2000). The increased frequency of sEPSCs in pyramidal neurons is associated with a shorter decay time in the non-SOZ of patients with FCD as compared to that in the non-epileptic cortex, which may reflect a high epileptogenicity in the non-SOZ group. However, recent studies have demonstrated that depolarizing GABA activity, caused by imbalanced function of NKCC1 and KCC2, initiates and propagates hypersynchronous neuronal activity into a larger network (Dzhala and Staley, 2021; Ragot et al., 2021). Consistent with the different patterns of NKCC1 and KCC2 during development, GABA initially depolarized immature neurons and controls the early network activity in the developing neocortex (Dzhala et al., 2005; Kirmse et al., 2018). However, Valeeva et al. found a developmental

excitatory-to-inhibitory switch in GABA actions on pyramidal neurons from P2–P8 and P9-15 mice *in vitro*. In contrast, mainly inhibitory GABA actions was shown in the immature hippocampus and neocortex *in vivo* (Valeeva et al., 2016). It is that whether traumatic injury might affect results obtained from *in vitro* preparations is currently highly debated (Zilberter, 2016). Further research is required to clarify whether or not this is the case. Human FCD, which has many similarities to the immature cortex, may result in epileptiform synchronization, paradoxically initiated by $GABA_A$ activation and $GABA_AR$-mediated synaptic transmission changes from inhibitory to excitatory effects caused by altered NKCC1 and KCC2 (D'Antuono et al., 2004; Blauwblomme et al., 2019). In our study, we provided direct neuro-electrophysiological evidence of $GABA_AR$-mediated postsynaptic responses, depolarized E_{GABA} in pyramidal neurons at the single-cell level, and corresponding changes in NKCC1 and KCC2 in the SOZ and non-SOZ of patients with FCD exhibiting epilepsy, when compared to those obtained from non-epileptic human temporal neocortex from patients with MTLE. Moreover, we found several differences in GABA activity between the SOZ and non-SOZ groups in the EZ of patients with FCD, highlighting the importance of depolarizing GABA within a seizure network.

Studying microcircuits in the seizure the onset zone and non-seizure the onset zone may help reveal the mechanism underpinning the generation and spread of macroscopic epileptic networks

In our study, consistent with previous studies, we observed that KCC2 expression was downregulated and internalized in the EZ of patients with FCD, especially in the SOZ (Talos et al., 2012; Blauwblomme et al., 2019). Although decreased expression of KCC2 was noted in both the SOZ and non-SOZ groups, internalized KCC2 was only observed in the SOZ group. Impaired KCC2 regulation may represent a risk factor for the emergence of neuropathology. Pisella et al. (2019) found that heterozygous phosphomimetic variants of KCC2 exhibit altered GABAergic inhibition, increased glutamate/GABA synaptic ratio, and greater susceptibility to seizures. They deduced that dysregulated KCC2 contributed to pathogenesis by controlling the GABAergic developmental sequence *in vivo*, which has been shown to impair neuronal network formation (Pisella et al., 2019). Moreover, normal GABA receptor-mediated inhibition depends on low levels of intracellular Cl^-, which are modulated by the extrusion of Cl^- by KCC2. Thus, the loss of KCC2 function results in the neuronal accumulation of Cl^-, shifting the direction of ion flow through GABA receptors from hyperpolarizing to depolarizing (Kuchenbuch et al., 2021).

The change of GABA function in the SOZ can strongly affect the microcircuit connection and neuronal network, as well as activate and silence individual neurons. In support of the critical role of KCC2 in postnatal GABAergic inhibition, Kontou et al. (2021) documented rapid mature neuronal apoptosis induced by KCC2 malfunctioning while immature neurons remained mostly intact. This can be explained by the fact that instead of KCC2, NKCC1 is highly expressed in immature neurons and drives Cl^- inward. We found that the imbalanced function of NKCC1 and KCC2 in the EZ resulted in depolarization of GABA receptor function and may underpin the hyperexcitability of FCD brain regions. Compared with the control group, SOZ and non-SOZ of patients with FCD showed depolarizing GABA response on pyramidal neurons. Although there were no significant differences in terms of the frequency and intensity of the depolarizing GABA response across the SOZ and non-SOZ groups, fewer neurons with depolarizing GABAergic responses and higher E_{GABA} were shown in the SOZ than in the non-SOZ of FCD patients. The migration of seizures from one side to the other requires the presence of dynamic depolarizing GABA in the network (Kuchenbuch et al., 2021). Therefore, the non-SOZ may represent a subsequent propagation region involved in FCD epileptogenesis. The non-SOZ, with a higher seizure susceptibility, may represent a potential brain region for the initial propagation of epileptic discharges originating in the SOZ. This is consistent with the macroscopic epileptiform discharges observed on EEG recordings that arise in the SOZ and propagate to the non-SOZ. It has also been suggested that more than one potential SOZ, with different thresholds, may exist in a single EZ (Rosenow and Luders, 2001). Although the SOZ with the lowest threshold typically generates seizures, another area in the non-SOZ with the second-lowest threshold would take over to be the new SOZ if the original SOZ has been resected. We speculate that non-SOZ may represent a potential SOZ capable of generating recurrent seizures upon resection of the previous SOZ, which thereby emphasizes the need to remove the entire EZ for seizure-free survival.

Outlooks and limitations

In our study, we focused on the depolarizing GABA synaptic activity caused by the imbalance of NKCC1 and KCC2 and aimed to build a micro-macro neuronal network to determine the relationship between depolarizing GABA and epileptogenesis in FCD. We observed depolarizing GABAergic signaling among pyramidal neurons in both the SOZ and non-SOZ of the patients with FCD, with a higher number of responsive neurons in the SOZ group. Thus, we speculated that abnormal GABAergic activity might influence epileptogenesis in the SOZ group and seizure susceptibility in the non-SOZ group. The microscopic recordings within areas of macroscopic evaluation and definition, that is, SOZ and non-SOZ, also

pointed to the importance and potential of mapping epileptic activities at multiple scales. In addition, given the effects of BUM, the maintenance of chloride homeostasis in neurons could represent an alternative avenue for developing ASMs. Previous studies have reported that BUM exerted significant seizure control effects in adult patients with temporal lobe epilepsy (Eftekhari et al., 2013; Gharaylou et al., 2019). In our study, a BUM application inhibited $GABA_AR$-mediated postsynaptic responses in cortical slices of patients with FCD and epilepsy at the individual cell level. However, the use of BUM as a potential new antiepileptic drug warrant further examination. Future studies should examine BUM derivatives as novel ASMs. In addition to NKCC1, an inhibitor of KCC2 should be explored for its effect on depolarizing GABA responses.

This study had several inevitable limitations. First, although we found the specific NKCC1 inhibitor BUM significantly reduced the depolarizing GABAergic response, it is hard to figure out why BUM functions as a result from functional upregulation of NKCC1 or decreased expression of KCC2 in FCD. To solve this issue, we think that the single-channel recording and the specific and available blocker of KCC2 is in urgent need. Second, it remained difficult to obtain SOZ and non-SOZ from the same patient with FCD to avoid excess injury and protect important functional brain areas during surgery. Finally, the size of our cohort was relatively small, and we did not take a deeper look into the differences across variable FCD subtypes and neuronal subgroups. In the future, a larger cohort of patients should be recruited to assess the potentially different GABAergic functions across FCD subtypes and other types of neurons, such as interneurons.

Data availability statement

The raw data supporting the conclusions of this article will be made available by the authors, without undue reservation.

Ethics statement

The studies involving human participants were reviewed and approved by the Medical Ethics Committee of Xuanwu Hospital, Capital Medical University. Written informed consent to participate in this study was provided by the participants' legal guardian/next of kin.

Author contributions

GZ and XFY: supervision and conceptualization. RL: methodology and writing – original draft. YX, HZ, JW, HLL, and LC: writing – review and editing. DL: visualization. TY, XMY, CX, YP, and LZ: provide clinical patient data, tissue specimens, and pathological examination. HHL: review and edit the manuscript. All authors contributed to the article and approved the submitted version.

Funding

This work was supported by the National Natural Science Foundation of China (81971202, 81790653, and 81671367).

Acknowledgments

We deeply appreciate the clinical team from the functional neurosurgery department of Xuanwu Hospital of Capital Medical University. We also thank Zhiqian Tong's technical help in the late stage of this work.

Conflict of interest

The authors declare that the research was conducted in the absence of any commercial or financial relationships that could be construed as a potential conflict of interest.

Publisher's note

Supplementary material

The Supplementary Material for this article can be found online at: https://www.frontiersin.org/articles/10.3389/fnmol.2022.954167/full#supplementary-material

SUPPLEMENTARY FIGURE 1
Action potential properties of pyramidal neurons. **(A)** The action potential number of pyramidal neurons (PNs) from control, FCD SOZ, and FCD non-SOZ cortex under a stepped current injection lasting 600 ms. *N* = 16, 19,18 for control and SOZ, non-SOZ groups. **(B)** The first spike latency of PC from control, FCD SOZ, and FCD non-SOZ under a 300 pA injection. *N* = 16, 19, 18 for control and SOZ, non-SOZ groups. Data was shown as mean ± SEM.

SUPPLEMENTARY FIGURE 2
Expression of NKCC1 in neurons from three groups. Double-label immunostaining for NeuN and NKCC1 demonstrated no obvious differences in expression and sub-cellular localization in neurons from SOZ, non-SOZ and control groups. Arrow indicated neurons with intra-somatic expression of NKCC1. Arrowheads indicated neurons with membrane expression of NKCC1. Scale bar represented 20 μm.

References

Aronica, E., Boer, K., Redeker, S., Spliet, W. G., van Rijen, P. C., Troost, D., et al. (2007). Differential expression patterns of chloride transporters, Na+-K+-2Cl–cotransporter and K+-Cl–cotransporter, in epilepsy-associated malformations of cortical development. *Neuroscience* 145, 185–196. doi: 10.1016/j.neuroscience.2006.11.041

Avermann, M., Tomm, C., Mateo, C., Gerstner, W., and Petersen, C. C. (2012). Microcircuits of excitatory and inhibitory neurons in layer 2/3 of mouse barrel cortex. *J. Neurophysiol.* 107, 3116–3134. doi: 10.1152/jn.00917.2011

Badier, J. M., Bartolomei, F., Chauvel, P., Benar, C. G., and Gavaret, M. (2015). Magnetic source imaging in posterior cortex epilepsies. *Brain Topogr.* 28, 162–171. doi: 10.1007/s10548-014-0412-4

Beleza, P. (2009). Refractory epilepsy: A clinically oriented review. *Eur. Neurol.* 62, 65–71. doi: 10.1159/000222775

Blauwblomme, T., Dossi, E., Pellegrino, C., Goubert, E., Iglesias, B. G., Sainte-Rose, C., et al. (2019). Gamma-aminobutyric acidergic transmission underlies interictal epileptogenicity in pediatric focal cortical dysplasia. *Ann. Neurol.* 85, 204–217. doi: 10.1002/ana.25403

Blumcke, I., Thom, M., Aronica, E., Armstrong, D. D., Vinters, H. V., Palmini, A., et al. (2011). The clinicopathologic spectrum of focal cortical dysplasias: A consensus classification proposed by an ad hoc task force of the ILAE diagnostic methods commission. *Epilepsia* 52, 158–174. doi: 10.1111/j.1528-1167.2010.02777.x

Bragin, A., Wilson, C. L., and Engel, J. Jr. (2000). Chronic epileptogenesis requires development of a network of pathologically interconnected neuron clusters: A hypothesis. *Epilepsia* 41, S144–S152. doi: 10.1111/j.1528-1157.2000.tb01573.x

Cepeda, C., Andre, V. M., Wu, N., Yamazaki, I., Uzgil, B., Vinters, H. V., et al. (2007). Immature neurons and GABA networks may contribute to epileptogenesis in pediatric cortical dysplasia. *Epilepsia* 48, 79–85. doi: 10.1111/j.1528-1167.2007.01293.x

Cheng, L., Xing, Y., Zhang, H., Liu, R., Lai, H., Piao, Y., et al. (2022). Mechanistic analysis of micro-neurocircuits underlying the epileptogenic zone in focal cortical dysplasia patients. *Cereb. Cortex* 32, 2216–2230. doi: 10.1093/cercor/bhab350

D'Antuono, M., Louvel, J., Kohling, R., Mattia, D., Bernasconi, A., Olivier, A., et al. (2004). GABAA receptor-dependent synchronization leads to ictogenesis in the human dysplastic cortex. *Brain* 127(Pt 7), 1626–1640. doi: 10.1093/brain/awh181

Deukmedjian, A. J., King, M. A., Cuda, C., and Roper, S. N. (2004). The GABAergic system of the developing neocortex has a reduced capacity to recover from in utero injury in experimental cortical dysplasia. *J. Neuropathol. Exp. Neurol.* 63, 1265–1273. doi: 10.1093/jnen/63.12.1265

Doyon, N., Vinay, L., Prescott, S. A., and De Koninck, Y. (2016). Chloride regulation: A dynamic equilibrium crucial for synaptic inhibition. *Neuron* 89, 1157–1172. doi: 10.1016/j.neuron.2016.02.030

Dzhala, V. I., and Staley, K. J. (2021). KCC2 chloride transport contributes to the termination of ictal epileptiform activity. *eNeuro* 8, 208–220. doi: 10.1523/ENEURO.0208-20.2020

Dzhala, V. I., Talos, D. M., Sdrulla, D. A., Brumback, A. C., Mathews, G. C., Benke, T. A., et al. (2005). NKCC1 transporter facilitates seizures in the developing brain. *Nat. Med.* 11, 1205–1213. doi: 10.1038/nm1301

Eftekhari, S., Mehvari Habibabadi, J., Najafi Ziarani, M., Hashemi Fesharaki, S. S., Gharakhani, M., Mostafavi, H., et al. (2013). Bumetanide reduces seizure frequency in patients with temporal lobe epilepsy. *Epilepsia* 54, e9–e12. doi: 10.1111/j.1528-1167.2012.03654.x

Farrell, J. S., Nguyen, Q. A., and Soltesz, I. (2019). Resolving the micro-macro disconnect to address core features of seizure networks. *Neuron* 101, 1016–1028. doi: 10.1016/j.neuron.2019.01.043

Feindel, W., Leblanc, R., and de Almeida, A. N. (2009). Epilepsy surgery: Historical highlights 1909-2009. *Epilepsia* 50, 131–151. doi: 10.1111/j.1528-1167.2009.02043.x

George, A. L., and Jacobs, K. M. (2011). Altered intrinsic properties of neuronal subtypes in malformed epileptogenic cortex. *Brain Res.* 1374, 116–128. doi: 10.1016/j.brainres.2010.12.020

Gharaylou, Z., Tafakhori, A., Agah, E., Aghamollaii, V., Kebriaeezadeh, A., and Hadjighassem, M. (2019). A preliminary study evaluating the safety and efficacy of bumetanide, an NKCC1 inhibitor, in patients with drug-resistant epilepsy. *CNS Drugs* 33, 283–291. doi: 10.1007/s40263-019-00607-5

Gonzalez Otarula, K. A., von Ellenrieder, N., Cuello-Oderiz, C., Dubeau, F., and Gotman, J. (2019). High-frequency oscillation networks and surgical outcome in adult focal epilepsy. *Ann. Neurol.* 85, 485–494. doi: 10.1002/ana.25442

Jehi, L. (2018). The epileptogenic zone: Concept and definition. *Epilepsy Curr.* 18, 12–16. doi: 10.5698/1535-7597.18.1.12

Kirmse, K., Hubner, C. A., Isbrandt, D., Witte, O. W., and Holthoff, K. (2018). GABAergic transmission during brain development: Multiple effects at multiple stages. *Neuroscientist* 24, 36–53. doi: 10.1177/1073858417701382

Kontou, G., Ng, S. F., Cardarelli, R. A., Howden, J. H., Choi, C., Ren, Q., et al. (2021). KCC2 is required for the survival of mature neurons but not for their development. *J. Biol. Chem.* 296:100364. doi: 10.1016/j.jbc.2021.100364

Kuchenbuch, M., Nabbout, R., Yochum, M., Sauleau, P., Modolo, J., Wendling, F., et al. (2021). In silico model reveals the key role of GABA in KCNT1-epilepsy in infancy with migrating focal seizures. *Epilepsia* 62, 683–697.

Liu, R., Wang, J., Liang, S., Zhang, G., and Yang, X. (2019). Role of NKCC1 and KCC2 in epilepsy: From expression to function. *Front. Neurol.* 10:1407. doi: 10.3389/fneur.2019.01407

Medici, V., Rossini, L., Deleo, F., Tringali, G., Tassi, L., Cardinale, F., et al. (2016). Different parvalbumin and GABA expression in human epileptogenic focal cortical dysplasia. *Epilepsia* 57, 1109–1119. doi: 10.1111/epi.13405

Muhlebner, A., Bongaarts, A., Sarnat, H. B., Scholl, T., and Aronica, E. (2019). New insights into a spectrum of developmental malformations related to mTOR dysregulations: Challenges and perspectives. *J. Anat.* 235, 521–542. doi: 10.1111/joa.12956

Munakata, M., Watanabe, M., Otsuki, T., Nakama, H., Arima, K., Itoh, M., et al. (2007). Altered distribution of KCC2 in cortical dysplasia in patients with intractable epilepsy. *Epilepsia* 48, 837–844. doi: 10.1111/j.1528-1167.2006.00954.x

Palma, E., Amici, M., Sobrero, F., Spinelli, G., Di Angelantonio, S., Ragozzino, D., et al. (2006). Anomalous levels of Cl- transporters in the hippocampal subiculum from temporal lobe epilepsy patients make GABA excitatory. *Proc. Natl. Acad. Sci. U.S.A.* 103, 8465–8468. doi: 10.1073/pnas.0602979103

Palma, E., Ruffolo, G., Cifelli, P., Roseti, C., Vliet, E. A. V., and Aronica, E. (2017). Modulation of GABAA receptors in the treatment of epilepsy. *Curr. Pharm. Des.* 23, 5563–5568. doi: 10.2174/1381612823666170809100230

Paz, J. T., and Huguenard, J. R. (2015). Microcircuits and their interactions in epilepsy: Is the focus out of focus? *Nat. Neurosci.* 18, 351–359.

Pisella, L. I., Gaiarsa, J. L., Diabira, D., Zhang, J., Khalilov, I., Duan, J., et al. (2019). Impaired regulation of KCC2 phosphorylation leads to neuronal network dysfunction and neurodevelopmental pathology. *Sci. Signal* 12:eaay0300. doi: 10.1126/scisignal.aay0300

Ragot, A., Luhmann, H. J., Dipper-Wawra, M., Heinemann, U., Holtkamp, M., and Fidzinski, P. (2021). Pathology-selective antiepileptic effects in the focal freeze-lesion rat model of malformation of cortical development. *Exp. Neurol.* 343:113776. doi: 10.1016/j.expneurol.2021.113776

Rasmussen, T. (1983). Characteristics of a pure culture of frontal lobe epilepsy. *Epilepsia* 24, 482–493. doi: 10.1111/j.1528-1157.1983.tb04919.x

Rosenow, F., and Luders, H. (2001). Presurgical evaluation of epilepsy. *Brain* 124(Pt 9), 1683–1700. doi: 10.1093/brain/124.9.1683

Sen, A., Martinian, L., Nikolic, M., Walker, M. C., Thom, M., and Sisodiya, S. M. (2007). Increased NKCC1 expression in refractory human epilepsy. *Epilepsy Res.* 74, 220–227. doi: 10.1016/j.eplepsyres.2007.01.004

Stead, M., Bower, M., Brinkmann, B. H., Lee, K., Marsh, W. R., Meyer, F. B., et al. (2010). Microseizures and the spatiotemporal scales of human partial epilepsy. *Brain* 133, 2789–2797. doi: 10.1093/brain/awq190

Talos, D. M., Sun, H., Kosaras, B., Joseph, A., Folkerth, R. D., Poduri, A., et al. (2012). Altered inhibition in tuberous sclerosis and type IIb cortical dysplasia. *Ann. Neurol.* 71, 539–551. doi: 10.1002/ana.22696

Valeeva, G., Tressard, T., Mukhtarov, M., Baude, A., and Khazipov, R. (2016). An optogenetic approach for investigation of excitatory and inhibitory network GABA actions in mice expressing channelrhodopsin-2 in GABAergic neurons. *J. Neurosci.* 36, 5961–5973. doi: 10.1523/JNEUROSCI.3482-15.2016

Virtanen, M. A., Uvarov, P., Hubner, C. A., and Kaila, K. (2020). NKCC1, an elusive molecular target in brain development: Making sense of the existing data. *Cells* 9:2607. doi: 10.3390/cells9122607

Zhou, F. W., and Roper, S. N. (2014). Reduced chemical and electrical connections of fast-spiking interneurons in experimental cortical dysplasia. *J. Neurophysiol.* 112, 1277–1290. doi: 10.1152/jn.00126.2014

Zhu, W. J., and Roper, S. N. (2000). Reduced inhibition in an animal model of cortical dysplasia. *J. Neurosci.* 20, 8925–8931.

Zijlmans, M., Zweiphenning, W., and van Klink, N. (2019). Changing concepts in presurgical assessment for epilepsy surgery. *Nat. Rev. Neurol.* 15, 594–606. doi: 10.1038/s41582-019-0224y

Zilberter, M. (2016). Reality of inhibitory GABA in neonatal brain: Time to rewrite the textbooks? *J. Neurosci.* 36, 10242–10244. doi: 10.1523/JNEUROSCI.2270-16.2016

Frontiers in Molecular Neuroscience

Leading research into the brain's molecular structure, design and function

Part of the most cited neuroscience series, this journal explores and identifies key molecules underlying the structure, design and function of the brain across all levels.

Discover the latest Research Topics

See more →

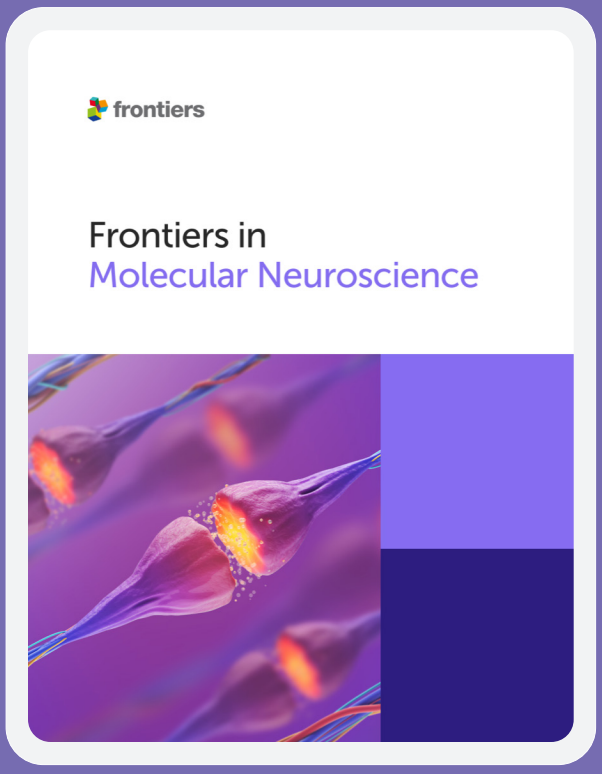

Frontiers

Avenue du Tribunal-Fédéral 34
1005 Lausanne, Switzerland
frontiersin.org

Contact us

+41 (0)21 510 17 00
frontiersin.org/about/contact